

Dissertation zur Erlangung des Doktorgrades

der Fakultät für Chemie und Pharmazie
der Ludwig-Maximilians-Universität München



**Development of novel small molecule modulators of
TRPML ion channels and Sirtuin 6**

Charlotte Sophie Leser

aus

München

2024

Dissertation zur Erlangung des Doktorgrades
der Fakultät für Chemie und Pharmazie
der Ludwig-Maximilians-Universität München

**Development of novel small molecule modulators of
TRPML ion channels and Sirtuin 6**

Charlotte Sophie Leser

aus

München

2024

Erklärung

Diese Dissertation wurde im Sinne von § 7 der Promotionsordnung vom 28. November 2011 von Herrn Prof. Dr. Franz Bracher betreut.

Eidesstattliche Versicherung

Diese Dissertation wurde eigenständig und ohne unerlaubte Hilfe erarbeitet.

Basel, den 19.08.2024

.....
Charlotte Sophie Leser

Dissertation eingereicht am 09.09.2024

1. Gutachter: Prof. Dr. Franz Bracher

2. Gutachter: Prof. Dr. Ivan Huc

Mündliche Prüfung am 11.10.2024

Danksagung

An erster Stelle gilt mein Dank Herrn Prof. Dr. Franz Bracher für die stets wohlwollende Unterstützung und Förderung dieser Arbeit, die interessanten Themen, die ich bearbeiten durfte, sowie die Chance, die er mir gegeben hat.

Auch bei den restlichen Mitgliedern der Prüfungskommission möchte ich mich bedanken, speziell bei Herrn Prof. Dr. Ivan Huc für die freundliche Übernahme des Koreferats.

Des Weiteren danke ich meinen Kooperationspartnern Prof. Dr. Dr. Christian Grimm, Prof. Dr. Michael Schaefer und Nicole Urban, für die Zusammenarbeit bei der pharmakologischen Evaluierung der TRPML Modulatoren. Herrn Prof. Dr. Clemens Steegborn und Dr. Weije You danke ich für die biologische Testung der Sirtuin 6 Modulatoren. Ich bedanke mich bei Martina Stadler für die Durchführung des MTT Assays und Agar-Diffusionstests. Vielen Dank auch an die Kollegen aus den analytischen Abteilungen der Departments Pharmazie und Chemie, Dr. Lars Allmendinger und Claudia Glas für die Messung der NMR-Spektren, Dr. Werner Spahl für die Messung der Massenspektren, sowie Anna Niedrig für die Reinheitsbestimmungen mittels HPLC.

Meiner Masterstudentin Katharina Kriegler und meinem Bachelorstudenten Dominik Ebert danke ich ganz herzlich für die aktive und erfolgreiche Mitarbeit am TRPML Projekt.

Natürlich möchte ich mich auch bei allen aktuellen und ehemaligen Kollegen aus dem Arbeitskreis Bracher für die gute Zusammenarbeit, alles, was ich von euch lernen durfte und die schöne Zeit bedanken. Vor allem bei Susanne, Desirée und Carina möchte ich mich für eure unentwegte Bereitschaft danken, euer Wissen weiterzugeben. Besonders hervorheben möchte ich auch meine beiden langjährigen Laborkolleginnen Angelina und Miriam, vielen Dank für euer offenes Ohr und die gute Atmosphäre in C3.042. Ihr habt diese Zeit zu etwas sehr Besonderem gemacht.

Ein großer Dank gilt auch meiner Familie und meinen Freunden, für die stetige moralische Unterstützung. Ganz besonders möchte ich mich bei Eugen bedanken, der bei allen Höhen und Tiefen an meiner Seite war und immer an mich geglaubt hat, auch in Momenten, in denen ich das selbst nicht konnte.

Ohne euch wäre all das nicht möglich gewesen!

Vielen Dank!

Für meine Familie

Preface

This thesis consists of two independent research topics, representing the two different projects, I had the chance to work on during my doctoral studies.

The first topic of this thesis discusses the lysosomal cation channels TRPML1-3, with focus on their modulation by ML-SI3 and related compounds. The work for this topic was continued by my master and bachelor students Katharina Kriegler and Dominik Ebert under my supervision, whilst I started with the second project. The ML-SI3 related results are mostly published in scientific journals and will be presented in a cumulative manner. Except for the results from Dominik Ebert's bachelor thesis, which are discussed in an extra chapter.

The second topic of this thesis is from the field of epigenetics, where the serendipitous discovery of the promising Sirtuin 6 inhibitor KV-30 prompted the start of an exciting new project. The results of this second project were not yet published by the time this dissertation was submitted and are therefore presented as monograph.

Publications

Peer reviewed journal articles

Leser, C.; Keller, M.; Gerndt, S.; Urban, N.; Chen, C. C.; Schaefer, M.; Grimm, C.; Bracher, F., Chemical and pharmacological characterization of the TRPML calcium channel blockers ML-SI1 and ML-SI3. *Eur J Med Chem* **2021**, *210*, 112966.

Ruhl, P.; Rosato, A. S.; Urban, N.; Gerndt, S.; Tang, R.; Abrahamian, C.; Leser, C.; Sheng, J.; Jha, A.; Vollmer, G.; Schaefer, M.; Bracher, F.; Grimm, C., Estradiol analogs attenuate autophagy, cell migration and invasion by direct and selective inhibition of TRPML1, independent of estrogen receptors. *Sci Rep* **2021**, *11*, 8313.

Kriegler, K.; Leser, C.; Mayer, P.; Bracher, F., Effective chiral pool synthesis of both enantiomers of the TRPML inhibitor trans-ML-SI3. *Arch Pharm (Weinheim)* **2021**, e2100362.

Goretzko, J.; Pauels, I.; Heitzig, N.; Thomas, K.; Kardell, M.; Nass, J.; Krogsaeter, E. K.; Schloer, S.; Spix, B.; Linard Matos, A. L.; Leser, C.; Wegner, T.; Glorius, F.; Bracher, F.; Gerke, V.; Rossaint, J.; Grimm, C.; Rescher, U., P-selectin-dependent leukocyte adhesion is governed by endolysosomal two-pore channel 2. *Cell Rep* **2023**, *42*, 113501.

Book chapters

Rautenberg, S.; Keller, M.; Leser, C.; Chen, C.-C.; Bracher, F.; Grimm, C., Expanding the Toolbox: Novel Modulators of Endolysosomal Cation Channels. In *Endolysosomal Voltage-Dependent Cation Channels*, Wahl-Schott, C.; Biel, M., Eds. Springer International Publishing: Cham, **2023**; pp 249-276.

Table of contents

1	Introduction	1
1.1	Autophagy: efficient cellular recycling	1
1.2	The endolysosomal system	2
1.2.1	Biological functions of the lysosome	2
1.2.2	Lysosomal ion channels TRPML1-3	3
1.3	Epigenetic regulation of gene expression	5
1.3.1	Sirtuins: class III histone deacetylases	6
1.3.2	Sirtuin 6 modulation	7
2	Objectives	12
2.1	TRPML modulators	12
2.2	Sirtuin 6 modulators	13
3	Results and Discussion	15
3.1	TRPML modulators	15
3.1.1	Chemical and pharmacological characterization of ML-SI1 and ML-SI3	15
3.1.2	Chiral pool synthesis of enantiopure <i>trans</i> -ML-SI3	59
3.1.3	Enantiopure variations of <i>trans</i> -ML-SI3	88
3.2	Sirtuin 6 Modulators	110
3.2.1	Co-crystallization of KV-30 and synthesis planning	110
3.2.2	Synthesis of KV-30 by VÖGERL	114
3.2.3	Excursus: Bischler-Napieralski reaction	115
3.2.4	Synthesis of KV-30 analogues with replaced hydroxamic acid	118
3.2.5	Synthesis of variations aimed at the replacement of water	129
3.2.6	Synthesis of potential substrate mimetic analogues	137
3.2.7	Results from biological testing	144
3.2.8	Experimental part for Sirtuin 6 modulators	153
4	Summary	204
4.1	TRPML modulators	205
4.2	Sirtuin 6 modulators	211
5	Appendix	217
5.1	Abbreviations	217
5.2	References	221

1 Introduction

1.1 Autophagy: efficient cellular recycling

In a time of an imminent and life-threatening climate crisis, responsible handling of resources has become the motto of the day. A major part in handling of limited resources, is sustainable waste management by successful recycling. This is reducing the negative impact of waste to the environment and creates valuable materials for the construction of new products. While our society is just at the beginning of learning how important such sustainability is, nature is, as almost always, already one step ahead. Our cells are running a very efficient recycling system, keeping a clean environment and reusing important building blocks.

The process by which the cells are achieving this, is called autophagy and has raised much attention from scientists over the last few decades. The name autophagy comes from the greek word “autophagos”, which means “self-eating” and was first suggested by CHRISTIAN DE DUVE, a biochemist who won the Nobel prize in Physiology in 1972 for the discovery of the lysosome^[1]. Autophagy is the upstream process of lysosomal degradation of biomacromolecules. Cytoplasmic components for degradation, like damaged cell organelles, proteins or lipids are delivered through the autophagic process to the lysosome, where they are broken down to their respective building blocks for reuse. Figure 1 shows the interaction of autophagic vesicles with the lysosome^[2]. Autophagy can be divided in different forms. The most prominent is macroautophagy. Here, the cargo is packed into a double layered membrane (phagophore), which can originate from different locations (e.g. the endoplasmic reticulum,

mitochondria, the Golgi apparatus, endosomes or the plasma membrane). The resulting organelle is called autophagosome, which eventually fuses with the lysosome to build the autolysosome^[3]. Besides macroautophagy, other forms of autophagy exist, like chaperone-mediated autophagy (CMA), RN/DN-autophagy and microautophagy^[4]. For these types of autophagy, the cargo is directly delivered to the lysosome through distinguished recognition patterns between the substrate and the lysosomal membrane^[3-4]. Since macroautophagy is the most prominent of the different

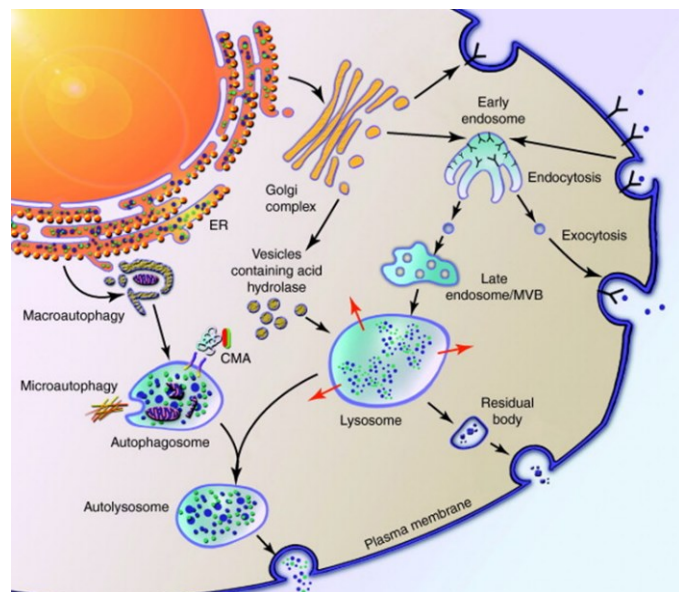


Figure 1 The autophagic process and interaction with the lysosome. Reproduced with permission from Elsevier^[2].

types, only this will be discussed and will henceforth be referred to as autophagy. Autophagy is a highly conserved process which is regulated mainly through nutrient availability. The master regulator of autophagy is mTOR, an enzyme of great importance for signal transduction in growth, cell survival and proliferation^[5]. mTOR acts as a nutrient sensor and the mTORC1 complex, located at the lysosomal membrane, is active in times of normal, nutrient rich conditions. Upon starvation, mTORC1 dissociates from the lysosomal membrane, resulting in the translocation of transcription factor (TF)EB into the nucleus, where it stimulates the expression of autophagy and lysosomal biogenesis genes^[4]. But not only nutrient deprivation is able to activate the autophagic process, other stress cues can have this effect as well. For example, metabolic stress (high ADP levels can activate the AMPK pathway), ER stress, hypoxia, oxidative stress with ROS generation or pathogen infection equally activate autophagy^[6-7]. This helps organisms to adapt to and overcome unfavourable conditions^[8]. In response to these stresses, autophagy genes are transcriptionally regulated. This process is epigenetically controlled by histone deacetylation^[9].

Two different fields of research in the BRACHER group are involved in the regulation of autophagy. The first one, lysosomal ion channels, is linked to autophagy in an obvious way, since the lysosome is highly involved in autophagy and the master regulator mTORC1 is located at the lysosomal membrane. The signal transduction in the lysosomal membrane is mainly controlled through lysosomal ion channels like TRPML1-3 and TPC1-2^[10-11]. The link to autophagic regulation of the second topic about epigenetic enzymes is slightly more in the background, but nevertheless exciting links have been found. Sirtuins belong to the class III of histone deacetylases and are involved in gene transcription regulation and various other chromatin related regulation mechanisms. Especially for Sirtuin 1 and Sirtuin 6 involvement in the autophagic process has been observed, mainly in the context of ageing, ROS regulation and cancer^[12-16].

1.2 The endolysosomal system

1.2.1 Biological functions of the lysosome

The lysosome is one of the two big degradation centres of the cell, besides the proteasome. The proteasome is a protein complex, which degrades ubiquitin marked proteins directly in the cytosol and the importance of successful degradation for cell survival is observed in cancer treatment. Several proteasome inhibitors, like bortezomib or ixazomib are used for cancer treatment, because inefficient degradation and accumulation of defective proteins and peptides can be fatal for cells. In contrast to the proteasome, the lysosome is not a protein complex, but belongs to the cell organelles and the degradation takes place in vesicles.

Activated lysosomes have an acidic luminal acidic pH and over 60 acidic hydrolases ensure a clean breakdown of diverse macromolecules to their corresponding building blocks^[4, 17]. This process delivers valuable amino acids, nucleic acids, sugars, and lipids to the cell. Since the acidic hydrolases require the low pH of the lysosome for their catalytic function, the cell is protected from these aggressive hydrolases in case of leakage to the neutral cytoplasm. The lysosome not only degrades macromolecules, but it is also a major metabolic signalling hub. Several lysosomal membrane proteins are responsible for nutrient sensing and regulate the contents and functions of the lysosome. These proteins comprise the lysosomal V-ATPase, responsible for the H⁺-gradient, transporter proteins for the release of degraded biomolecule building blocks and different ion channels needed for signal transduction. A very important class of lysosomal ion channels are the calcium and sodium permeable TRPMLs. An overview of the lysosomal ion channels and the ion gradients is depicted in Figure 2^[17].

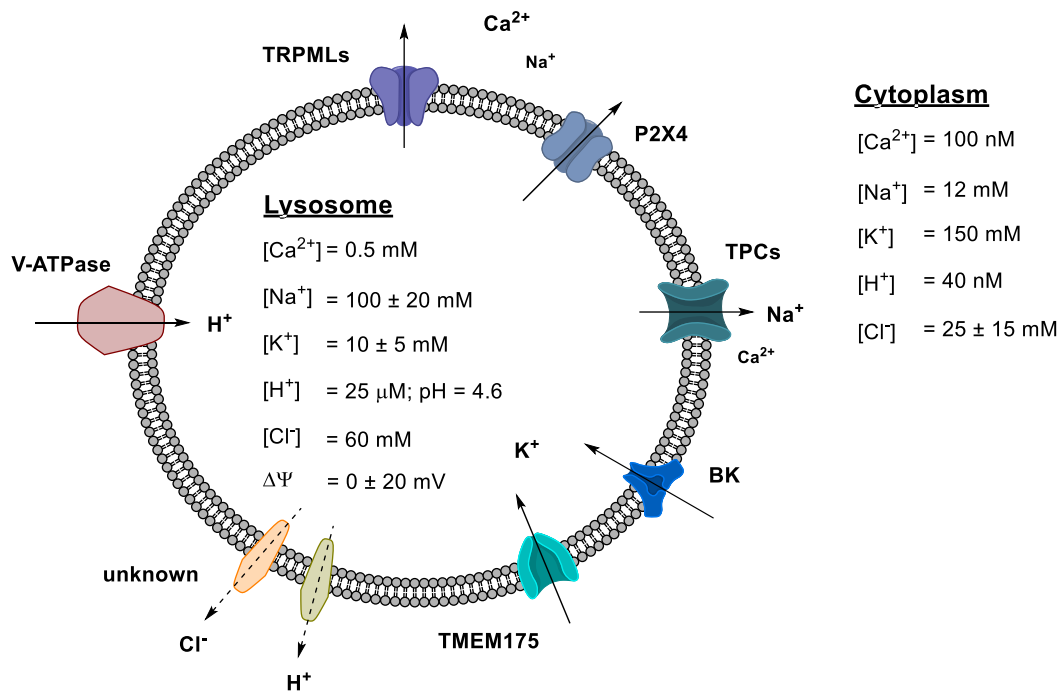


Figure 2 Overview of known and unknown lysosomal ion channels and their respective conductance^[17].

1.2.2 Lysosomal ion channels TRPML1-3

TRPML channels belong to the class of transient receptor potential (TRP) channels, which is a family of highly diverse cation channels. There are six subfamilies in mammals (TRPC, TRPV, TRPM, TRPA, TRPP, and TRPML) and most of them are involved in sensory functions. However, the TRPML subfamily, which consists of three isoforms (TRPML1-3), is not involved in sensory functions, but in the regulation of the endolysosome. These channels are mainly located in the membrane of lysosomes (TRPML1-3), recycling endosomes (TRPML2) and

early endosomes (TRPML3) and are involved in lysosomal ion homeostasis, lysosomal and endosomal trafficking and phagocytosis^[17]. Mutation with loss of function of the TRPML1 channel causes the neurodegenerative lysosomal storage disorder mucopolysaccharidosis type IV, which is characterized by psychomotor retardation, corneal clouding, retinal degeneration and strabismus^[18]. TRPML2 is known to enhance viral entry and viral trafficking of e.g. the yellow fever virus, dengue virus and influenza virus type A, who require transport to late endosomes for infection^[19]. Gain of function mutations of TRPML3 cause the varitint-waddler phenotype in mice, where the affected animals are exhibiting deafness, circling behaviour and coat colour dilution^[20]. Phosphatidylinositol 3,5-bisphosphate (PI(3,5)P₂, Figure 3 left), which is a constituent of the lysosomal membrane, has been identified as endogenous activator of all TRPML channels^[17, 21]. In contrast, phosphatidylinositol 4,5-bisphosphate (PI(4,5)P₂, Figure 3 right), the phosphatidylinositol of the plasma membrane, inhibits TRPML1 and TRPML3^[17].

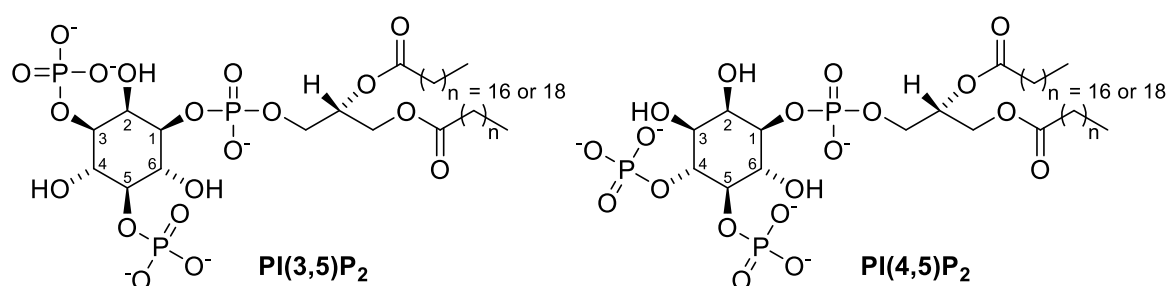


Figure 3 Chemical structures of the lysosomal membrane phosphatidylinositol PI(3,5)P₂ and the plasma membrane phosphatidylinositol PI(4,5)P₂.

Several synthetic activators of the TRPML channels have been discovered in the recent years, e.g. the aryl sulfonamides **SF-22** and **MK6-83**^[22], the amino acetamides **SF-51** and **ML-SA1**^[23] and the TRPML2 selective activator **ML2-SA1** developed from **SN-2**^[24] (Figure 4).

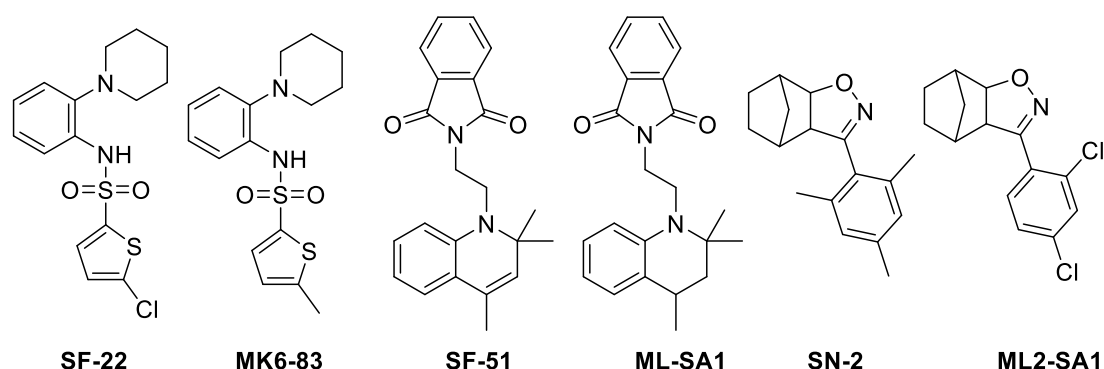


Figure 4 Chemical structures of TRPML activators **SF-22**, **MK6-83**, **SF-51**, **ML-SA1**, **SN-2**, and **ML2-SA1**.

Besides the TRPML channel agonists, there are a few synthetic inhibitors (ML-SI1-3) reported, however they are poorly characterized^[25-26]. Recently 17 β -estradiol methyl ether (EDME) has been identified as partly selective TRPML1 inhibitor^[27]. To further understand the functions and

involvements of these ion channels, there is a huge need for well characterized and readily available small molecule inhibitors of TRPML ion channels.

1.3 Epigenetic regulation of gene expression

Epigenetics has become over the recent years an emerging field of research. The term epigenetics, which essentially means “above genetics”, was coined by CONRAD WADDINGTON, who first discovered the phenomenon in 1942 and was used to describe changes in phenotype without changes in genotype^[28-29]. Nowadays we know that epigenetic mechanisms influence gene expression by modification of the DNA bases (e.g. cytosine methylation) or adapting chromatin^[29].

Chromatin is a complex of DNA and special proteins and influences the physiological form of genetic information. The most important proteins of chromatin are histones. The chromosomal DNA is wrapped around octamers of histone proteins, dimers of H2A, H2B, H3 and H4, forming nucleosomes. Histones are positively charged proteins due to their numerous lysine residues. The under physiological conditions positively charged lysine residues allow the negatively charged DNA to be tightly wrapped around the histone. Chromatin can exist in two different states, euchromatin (gene expression active) and heterochromatin (gene expression repressed). Chromatin state is controlled by the acetylation pattern of histone lysine residues. In euchromatin lysine residues are acetylated, which means, most of the negative charge is neutralized and the DNA is no longer bound as tightly to the histones, which ultimately leads to gene transcription. In heterochromatin acetyl residues are removed and gene transcription is in repressed state, as the DNA is more tightly bound. This process is controlled by writers, which transfer acetyl residues (histone acetyl transferases, HATs) and erasers, who remove acetyl residues (histone deacetylases, HDACs). These acetyl patterns can be recognized by specific reader proteins, transducing relevant epigenetic signals further. An overview of chromatin interaction with writers, erasers and readers is shown in Figure 5^[30].

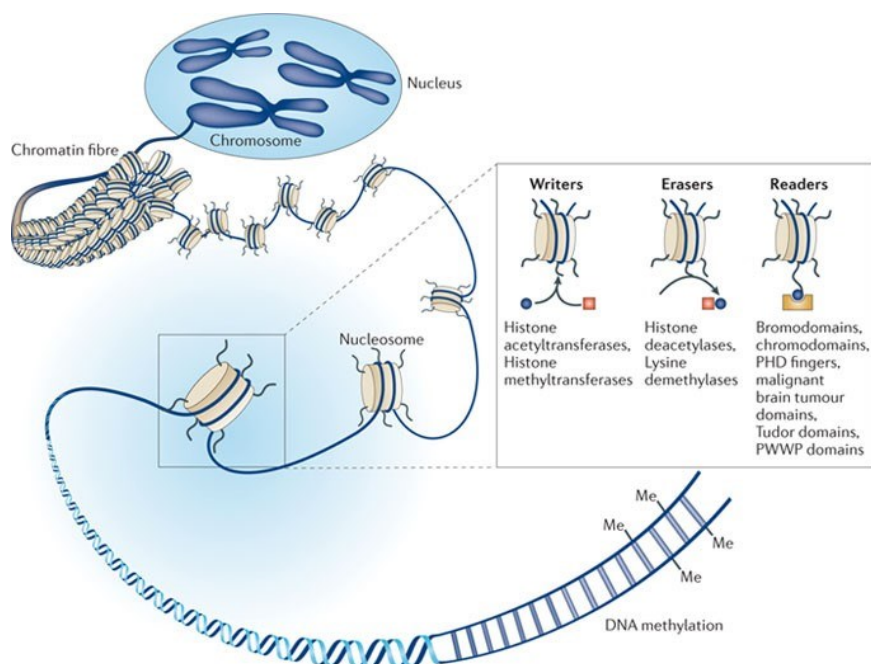


Figure 5 Organisation of DNA in nucleosomes, chromatin and chromosomes. Interactions with the Nucleosome with Writers, Erasers and Readers. Reproduced with permission from Springer Nature^[30].

1.3.1 Sirtuins: class III histone deacetylases

An important class of enzymes in epigenetic regulation are the beforementioned histone deacetylases HDACs (also more generically called lysine deacetylases KDACs). HDACs are divided into four classes. Class I, II and IV are zinc dependent enzymes, whereas class III, the sirtuins, are NAD^+ dependent^[31]. An overview of the different classes of HDACs and the chemical structure of NAD^+ are given in Figure 6.

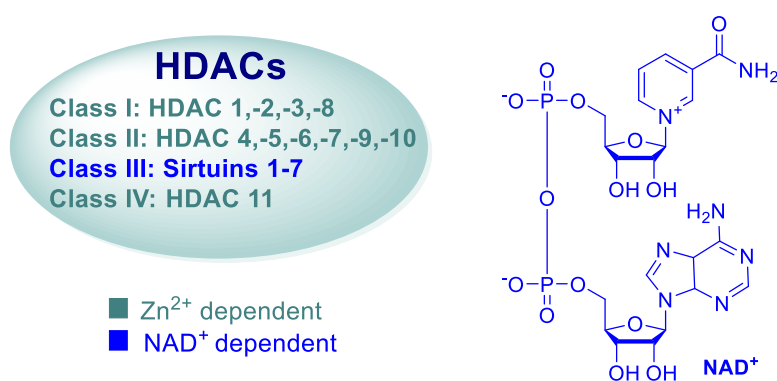


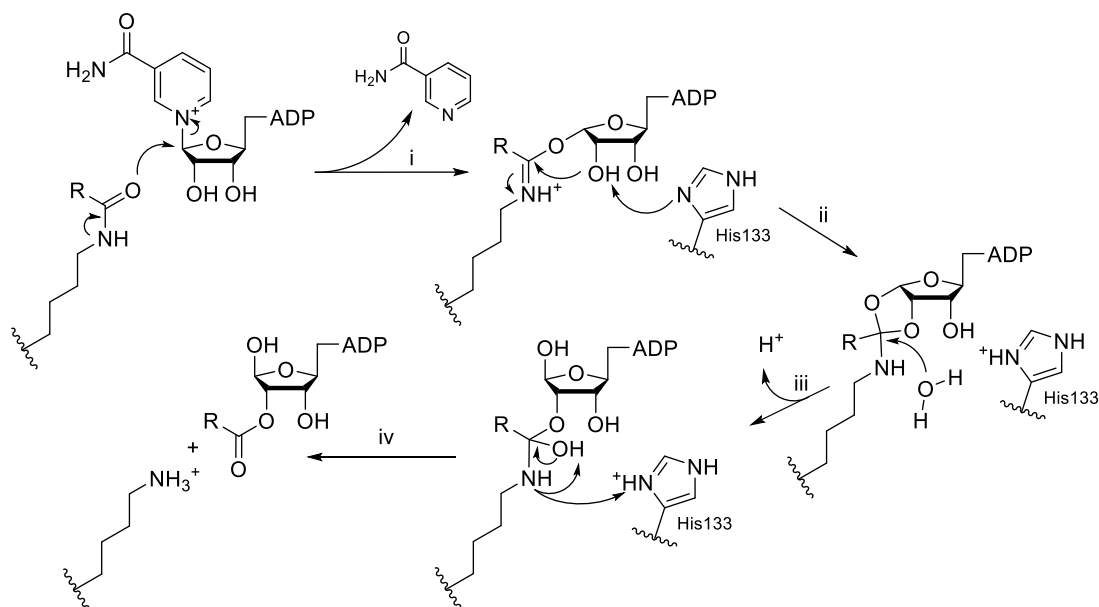
Figure 6 Overview of different HDAC classes. Chemical structure of NAD^+ .

The name sirtuin comes from their homology to the silent information regulator 2 (Sir2), which was the first identified silencing factor member of the yeast sirtuin family. So far, seven mammalian sirtuins have been identified. They can be found at different locations in the cell, where they interact with their respective acylated endogenous substrates. Sirtuins 1 and 2 are

found in the cytoplasm or the nucleus, Sirtuins 3, 4 and 5 in the mitochondria. Sirtuin 6 and Sirtuin 7 are located exclusively in the nucleus^[32].

1.3.2 Sirtuin 6 modulation

Sirtuin 6 has become over the past years an emerging target for investigations in epigenetic processes. Its biological function has been established as important regulator of chromatin signalling and has been linked to genome maintenance (including DNA repair), stem cell differentiation, longevity, cancer, inflammation, and immunity as well as glucose and lipid homeostasis^[32] ^[33] ^[34]. Sirtuin 6 can deacylate histone (e.g. deacetylation of H3K9 and H3K56) and non-histone (e.g. demyristoylation of TNF- α) substrates^[32]. The NAD⁺ dependent catalytic mechanism starts with a nucleophilic attack of the acyl carbonyl at C1' of the ribose, releasing nicotinamide and resulting in an imidate (Scheme 1, step i). The imidate carbon is further attacked by the 2'-OH, facilitated through deprotonation by His133, resulting in a cyclic intermediate (Scheme 1, step ii). This cyclic intermediate is then hydrolysed by a water molecule, leading to a tetrahedral intermediate (Scheme 1, step iii). Upon protonation by the before protonated His133, the C-N bond is cleaved and O-acyl-ADP-ribose as well as the deacylated substrate are released (Scheme 1, step iv).^[35]



Scheme 1 Catalytic mechanism of Sirtuin 6 deacylation^[35].

Sirtuin 6 has compared to other sirtuins a unique structure which allows its NAD⁺ binding site to remain relatively stable, even without substrate, allowing it to bind NAD⁺ independent of the presence of an acylated substrate^[36]. Together with the fact that histone deacetylation of Sirtuin 6 is activated by free fatty acids, it prompts the question whether Sirtuin 6 could act as redox (NAD⁺) and nutrient (FFA) sensor, translating the metabolic condition of a cell into epigenetic signals^[32-33]. Sirtuin 6 is also involved in circadian regulation of fatty acid

metabolism^[37]. But deacetylation isn't Sirtuin 6's only catalytic function, it is also a mono-ADP-ribose transferase (e.g. autoribosylation and PARP1 ribosylation)^[32].

Because of the diverse catalytic activities, targets and biological functions of Sirtuin 6, it is crucial to develop potent and selective modulators for a better in-depth understanding of the role of Sirtuin 6. Several groups have been working on finding small molecule activators of Sirtuin 6. As previously mentioned, long chained FFA like myristic acid, oleic acid and linoleic acid can stimulate Sirtuin 6^[38] and a first class of activators, ethanolamides of the fatty acids, arose from them (Figure 7)^[39]. Interestingly, myristic acid for example, activates Sirtuin 6 deacetylation, but inhibits demyristoylation^[38].

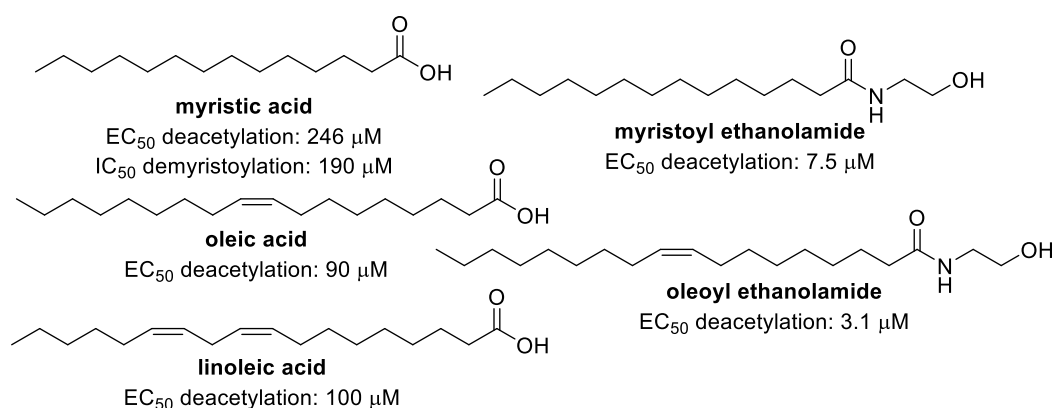


Figure 7 Free fatty acids and fatty acid ethanolamides activating Sirtuin 6 deacetylation.

Quercetin and other flavonoids were found to interact with Sirtuin 6, either activating or inhibiting its activity (Figure 8). In the case of quercetin both effects have been observed. The catechins (-)-catechin gallate and (-)-gallocatechin gallate are potent inhibitors of Sirtuin 6. However, this class of natural products is known to interact with many biological targets and therefore no selectivity can be expected.^[40-42]

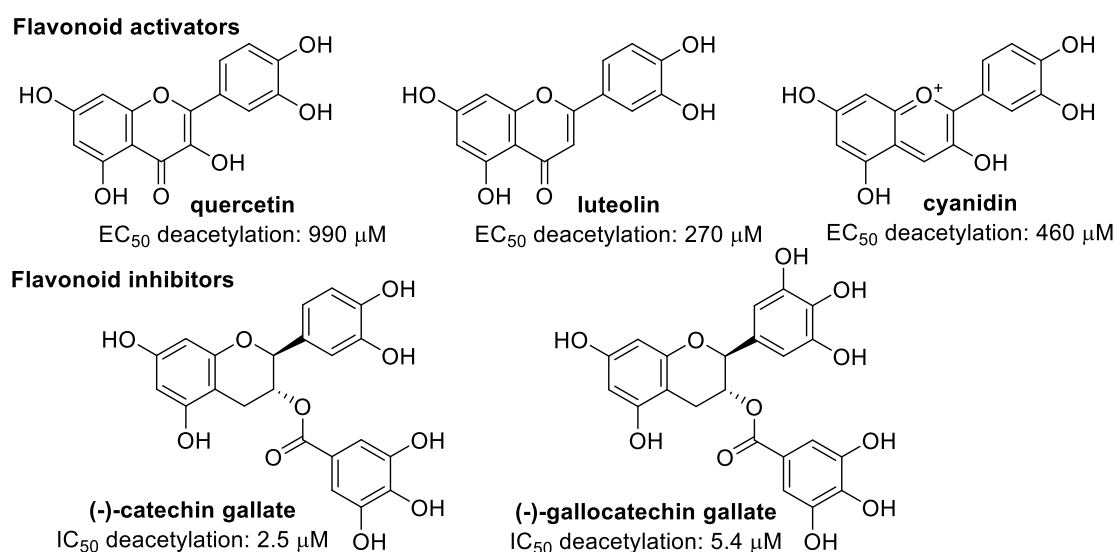


Figure 8 Selection of flavonoids interacting with Sirtuin 6.

The first synthetic activator **UBCS039**, a pyrrolo-[1,2-a]quinoxaline derivative, was discovered in 2017^[43]. **UBCS039** can induce activation of lethal autophagy in several human cancer cells, underlining the involvement of Sirtuin 6 in autophagic processes^[16]. UBCS039 was further developed by XU *et al.* (**Xu compound 36**)^[44]. ZHANG *et al.* found a new inhibitor with a similar heterocycle with improved potency (**Zhang compound 21q**)^[45]. A virtual screening revealed **MDL-800** as a selective activator with a new chemotype^[46]. Furthermore, a screening for drug repurposing showed that fluvastatin, a HMG-CoA reductase inhibitor, activates Sirtuin 6^[47] [48]. Another screening of lipid-like molecules gave the hit compound CL4 and further optimization led to the Sirtuin 6 activator **CL5D**^[49]. In 2020 another compound found by CHEN *et al.* identified a quinolone derivative (**Chen compound 12q**) that emerged from a virtual screening, as potent and selective activator, for which an anti-pancreatic ductal adenocarcinoma activity was shown^[50]. Additionally, in 2021, a 4H-chromen derivative (**Tenhunen compound 1**), which is structurally related to quercetin, was identified as Sirtuin 6 activator and shown to decrease cell proliferation in breast cancer cells^[51]. Sirtuin 6 activators are shown in Figure 9.

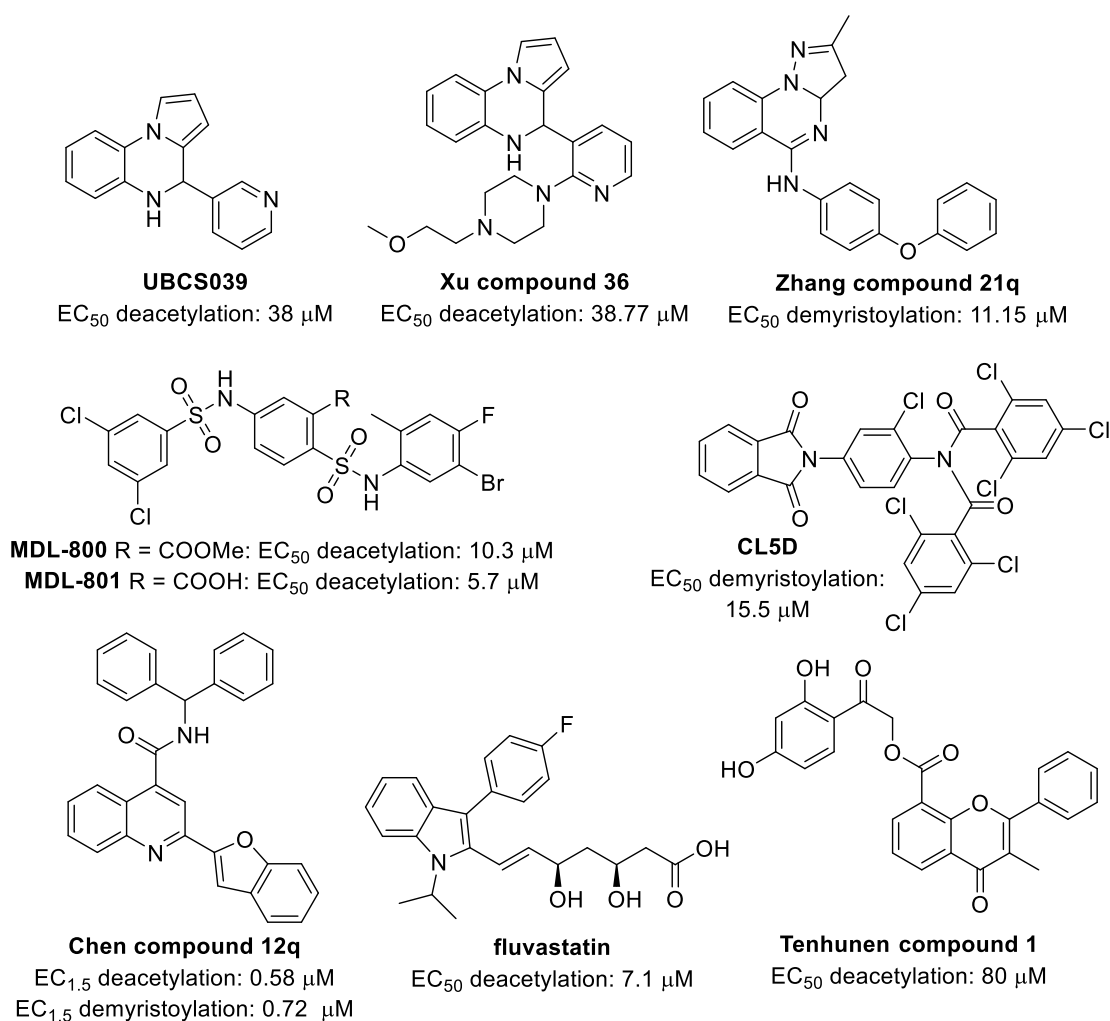


Figure 9 Sirtuin 6 activators.

Inhibition of Sirtuin 6 has been investigated as well, as it could have a positive impact on diseases like cancer and inflammation^[34]. Besides the directly to the enzymatic mechanism linked *N*-thioacyl lysine peptide-based inhibitors^[52-53] and the natural product inhibitors catechine gallate and gallic acid (Figure 8)^[41], there are only few synthetic inhibitors for such purposes. In 2014 PARENTI *et al.* identified the salicylate **Parenti compound 9**, also known as OSS_128167^[54], and a quinazolinone **Parenti compound 5** as Sirtuin 6 inhibitors^[55]. Further improvement of those compounds show increased selectivity for Sirtuin 6 but are still lack sufficient potency^[56-57]. With these compounds however it was shown that pharmacological inhibition of Sirtuin 6 can improve glucose tolerance in a type 2 diabetes mouse model and sensitize several cancer cells to chemotherapeutics^[56, 58]. The nicotinamide relative 5-chloro-pyrazineamide (**5-Cl-PZA**) was reported to inhibit Sirtuin 6 by disturbing the NAD⁺ Sirtuin 6 interaction^[59]. A screening of a DNA-encoded chemical library, designed for NAD⁺ binding pockets, revealed **A127-(CONHPr)-B178** as Sirtuin 6 inhibitor with a 5-carboxamide uracil core^[60]. In 2020, a series of 2-nitroaniline derivatives were reported as Sirtuin 6 inhibitors by SUN *et al.* (**Sun compound 6d**)^[61]. TENHUNEN *et al.* found inhibitors with a 1,4-dihydropyridine scaffold (**Tenhunen compound 1**)^[51]. The HDAC inhibitor Trichostatin A (TSA), inhibits Sirtuin 6 with subtype selectivity^[62]. A co-crystal of TSA and Sirtuin 6 showed the binding mode to the acyl channel, explaining its selectivity^[63]. The thus far most potent inhibitor of Sirtuin 6 is **JYQ-42** with an IC₅₀ of 2.33 μM, published in 2022^[64]. Sirtuin 6 inhibitors are shown in Figure 10.

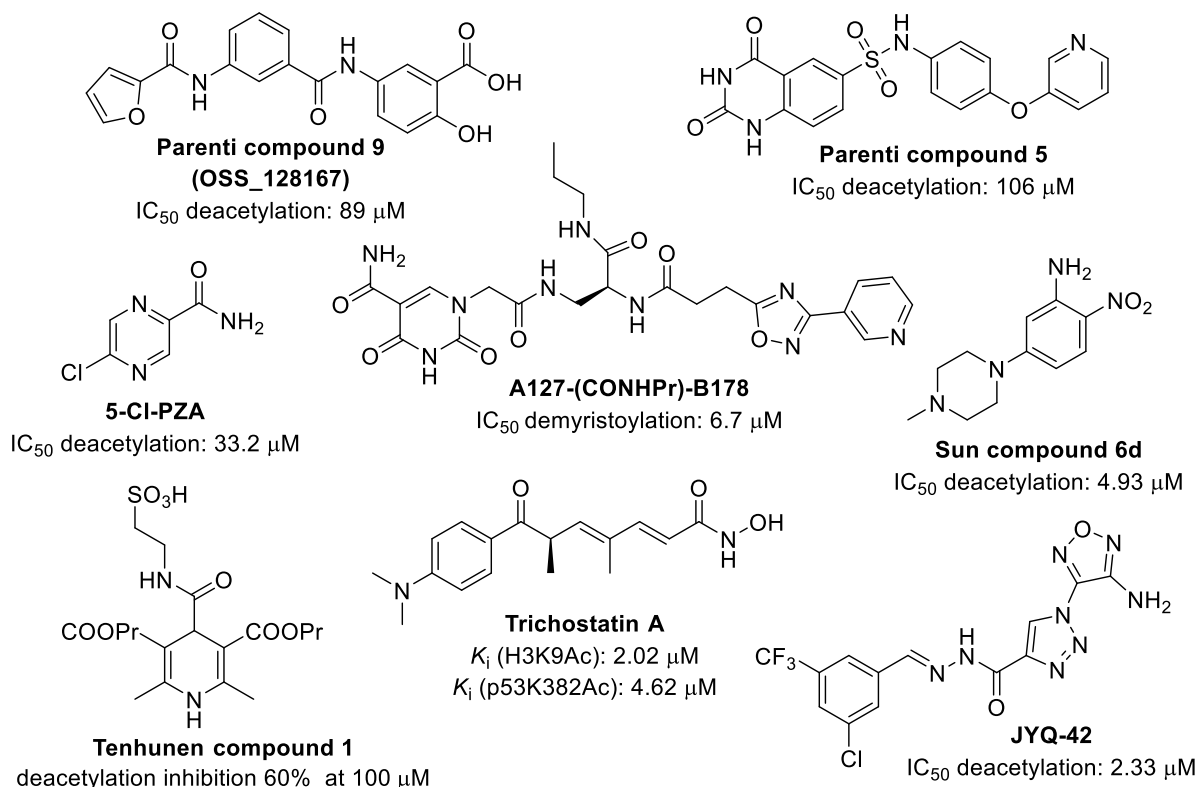


Figure 10 Sirtuin 6 inhibitors

Recently **KV-30**, a compound from the BRACHER group originating from a project designated at the discovery of HDAC 6 inhibitors, was identified as a new chemotype of Sirtuin 6 inhibitors. **KV-30** bears structural features of the Sirtuin 6 activator **UBCS039** (similar heteroaromatic tricyclus) and the Sirtuin 6 inhibitor Trichostatin A (hydroxamic acid). Therefore structure modifications could potentially lead to new compounds inhibiting or activating Sirtuin 6. Structures of **UBCS039**, **KV-30** and Trichostatin A are depicted in Figure 11.

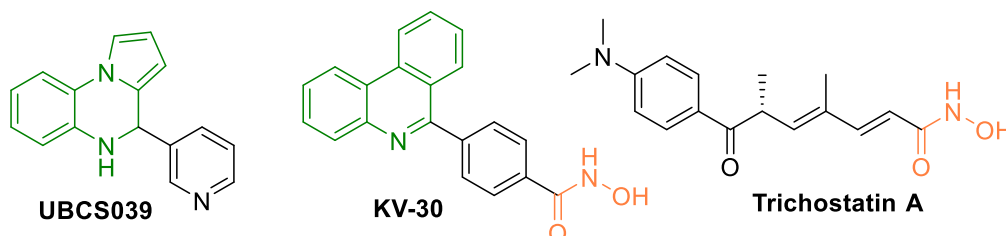


Figure 11 Chemical structures of the Sirtuin 6 modulators **UBCS039**, **KV-30**, and Trichostatin A.

2 Objectives

Small molecule modulators are the gold standard of studying physiological functions of a certain target. To be valuable chemical tools and maybe even future drug candidates, the compounds need strong potency and selectivity for their respective target. Much effort is made in the field of medicinal chemistry research to identify such molecules. The most common way to find a suitable hit compound, is performing a high throughput screening (HTS), where thousands of compounds are screened in order to identify compounds that interact with the target under investigation. Conducting a HTS is a very time-consuming endeavour and often the identified compounds lack potency and selectivity. Extensive development work by medicinal chemists is needed to get suitable lead structures for valuable chemical tools and possible drug candidates. The first in 2013 reported synthetic antagonists of TRPML, **ML-SI1-3**, were most likely identified by a high throughput screening. They were used as identified without further characterization or optimization regarding chemical configuration, potency and selectivity^[25].

Sometimes however, new small molecule modulators are identified by serendipity with a little bit of luck. This is what happened for the second topic of this thesis, Sirtuin 6 modulators. The lead structure **KV-30** was originally designed and synthesized for HDAC 6 inhibition. It was completely inactive towards its intended target but turned out to be a promising Sirtuin 6 inhibitor and therefore an interesting starting point for the development of Sirtuin 6 modulators.

2.1 TRPML modulators

Over the last decade, several small molecule activators of TRPML ion channels have been discovered in the BRACHER group, as well as in other groups (see Chapter 1.2.2, Figure 4).

In contrast to synthetic activators, there was still a lack of well characterized inhibitors. Synthetic inhibitors are urgently needed to study the effects of TRPML modulation, since the endogenous inhibitor PI(4,5)P₂, a phosphatidylinositol, is not membrane permeable and can thus not be used in cellular studies. Small molecule modulators of TRPML channels are not only valuable chemical tools for research but also potential future drug candidates for diseases like cancer or infections^[65]. The synthetic inhibitors from the ML-SI series (mucolipin synthetic inhibitors) mostly have been published without any information about the chemical structure. WANG et al. first showed the chemical structures of **ML-SI1** and **ML-SI3** in the supporting information, but in this depiction however, essential information about the stereochemical configuration of these compounds is missing (Figure 12)^[26].

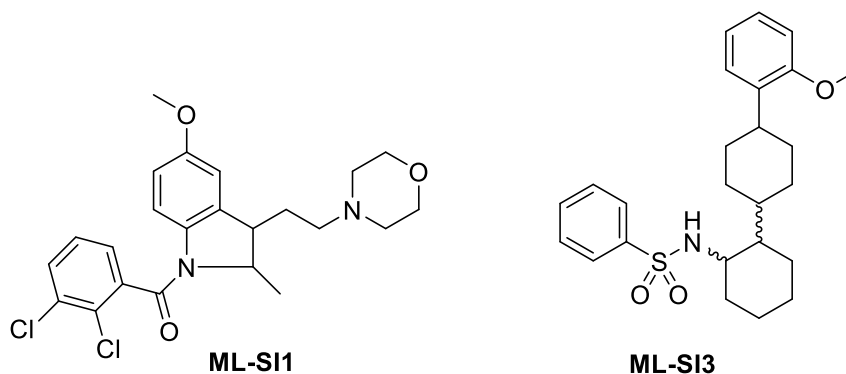


Figure 12 Chemical structures of the TRPML inhibitors ML-SI1 and ML-SI3 as depicted by Wang et al. in the supporting information.

Both structures have two stereocentres, which results in four possible isomers (two respective enantiomers for the two *cis*- and *trans*-diastereomers). Stereochemistry can be crucial for the biological activity of a compound, so elucidation of the exact configuration of these inhibitors was one of the major objectives of this project. Additionally, starting from these structures, the possibility for advanced, more potent, and selective inhibitors should be assessed.

2.2 Sirtuin 6 modulators

Both Sirtuin 6 and HDAC 6, the originally intended target of **KV-30**, are histone deacetylases. **KV-30**, a hydroxamic acid with a phenanthridine scaffold, was originally synthesized in the BRACHER group by DR. KATHARINA VÖGERL for inhibition of HDAC 6. Even though Sirtuin 6 and HDAC 6 are catalysing the same reaction (histone deacetylation), there is one major difference. As a member of the sirtuin family, Sirtuin 6 is NAD⁺, not zinc dependent. In the case of HDAC 6, the hydroxamate of **KV-30** was intended to chelate the zinc and thus inhibit the activity of enzyme, which is the common mode of action for this class of inhibitors (e.g. Vorinostat)^[66]. But **KV-30** turned out to be completely inactive towards HDAC 6. Ongoing investigations of the diverse biological activities of HDAC 6 inhibitors prompted the evaluation of a collection of hydroxamates, including **KV-30**, for protozoal inhibition. Epigenetic enzymes are known to be highly involved in the life cycle development of protozoa. Therefore, **KV-30** was tested together with **KV-46**, a highly potent inhibitor of HDAC 6 (IC₅₀ hHDAC6: 5 nM)^[67], **KV-24** and **KV-50** for their effect towards parasitic single-cell eukaryotes in the group of DE SOUZA in Rio de Janeiro. **KV-46**, **KV-30**, and **KV-24** and showed potent inhibition of *Toxoplasma gondii*. The results obtained are depicted in Figure 13.

Objectives

Compound	IC ₅₀ - 24h	TC ₅₀
KV50	> 10 μ M	2,15 μ M
KV46	0,22 μ M	10,80 μ M
KV30	< 0,11 μ M	9,92 μ M
KV24	0,22 μ M	35,66 μ M

IC₅₀: Inhibitory concentration 50 % (*T. gondii*)

TC₅₀: Toxic concentration 50 % (MTS assay)

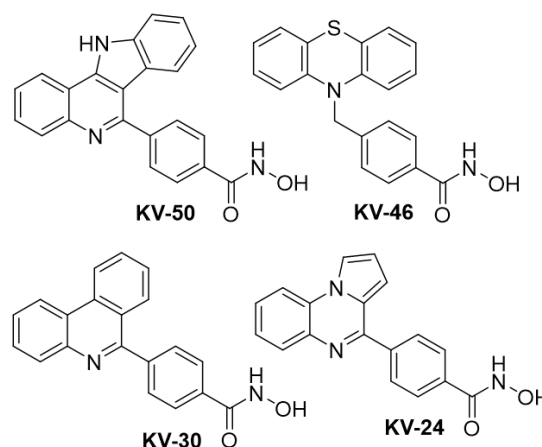


Figure 13 Biological activity of the hydroxamates **KV-50**, **KV-46**, **KV-30**, and **KV-24** towards *Toxoplasma gondii*.

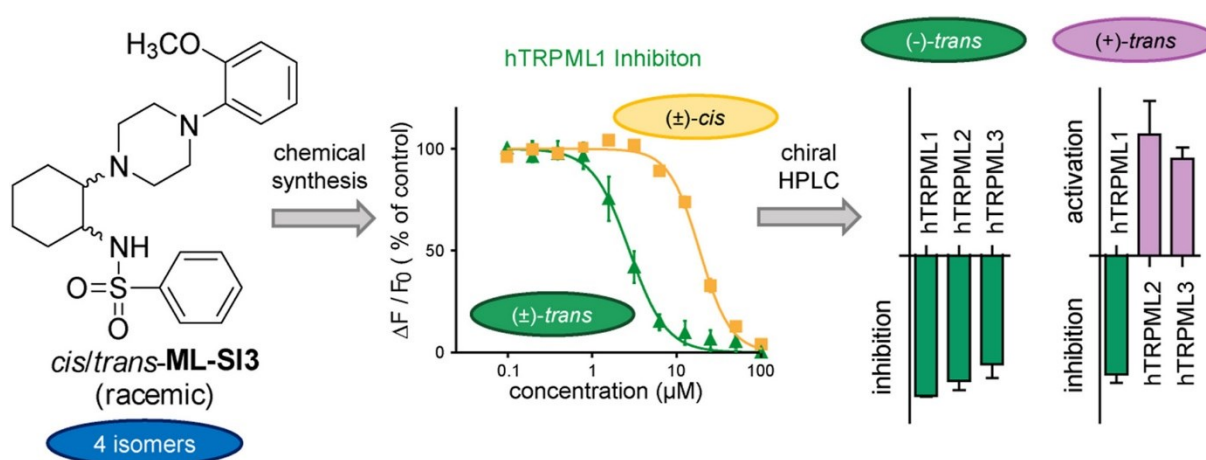
The observed inhibition of *T. gondii* could not be mediated by HDAC 6 inhibition, because of **KV-30**'s proven inactivity on this target. On the search for the biomolecular connection responsible for the antiprotozoal activity, a thorough literature search revealed the chemical similarity of **KV-24** with the recently published Sirtuin 6 activator **UBCS039** from the STEEGBORN group at the University of Bayreuth. The idea came up, that the observed biological activity could be connected to Sirtuin 6 and the compounds were sent to Bayreuth to be tested for their activity towards this supposed target. And indeed, **KV-30** showed activity on Sirtuin 6, surprisingly not Sirtuin 6 activation but potent inhibition. At that time only very few inhibitors of Sirtuin 6 were known, and none of them were subtype-selective for Sirtuin 6. **KV-30** has great potential for the development of highly potent and selective inhibitors, and maybe even for identification of activators, due to the similarity to the know activator **UBCS039**. Since the STEEGBORN group was already working together with the MAI group from the University of Rome on compounds with the pyrrolo[1,2-a]quinoxaline scaffold of **UBCS039** and **KV-24**, it was decided, that the BRACHER group would focus on compounds with phenanthridine scaffold. The aim of this project was to chemically modify the serendipitously found hydroxamic acid inhibitor **KV-30**, to obtain less toxic, druglike, potent, and selective modulators of Sirtuin 6 as chemical tool for the investigation of the physiological functions of this exciting target.

3 Results and Discussion

3.1 TRPML modulators

3.1.1 Chemical and pharmacological characterization of ML-SI1 and ML-SI3

Leser, C.; Keller, M.; Gerndt, S.; Urban, N.; Chen, C. C.; Schaefer, M.; Grimm, C.; Bracher, F., *Chemical and pharmacological characterization of the TRPML calcium channel blockers ML-SI1 and ML-SI3*. *Eur J Med Chem* 2021, 210, 112966.



3.1.1.1 Summary

In 2015 WANG *et al.* published an article about the role of TRPML1 in lysosomal adaptation to nutrient starvation^[26]. For this study the authors used different synthetic TRPML1 activators and inhibitors, but there was no information provided about the actual pharmacological profile of these modulators, regarding potency and selectivity. In addition, the published chemical structure of **ML-SI1** and **ML-SI3**, shown only in the supporting information, did not provide any information about their distinct stereochemistry. Therefore, the aim of the present study was to elucidate the pharmacological and stereochemical properties of **ML-SI1** and **ML-SI3**. As a first step, a synthetic route to **ML-SI1** and **ML-SI3** was developed. Both inhibitors have two stereocentres, and thus there are four possible isomers, two diastereomers (*cis*- and *trans*-configuration) and their respective enantiomers. For **ML-SI1** the synthetic route led to a racemic mixture of diastereomers and for **ML-SI3** the first synthetic approach led to racemic *trans*-**ML-SI3**. In a first screening, **ML-SI3** turned out to be the more potent compound, showing good, activator independent, inhibition of TRPML1. Thus, **ML-SI3** was chosen for further, in-depth characterization and structure-activity relationship analysis. A synthetic route, leading to

racemic *cis*-**ML-SI3**, was developed and the biological activities in single cell calcium imaging of both diastereomers on all three TRPML subtypes were evaluated. The results showed that racemic *trans*-**ML-SI3** is an inhibitor of all three subtypes, while *cis*-**ML-SI3** is only a moderate inhibitor of TRPML1 and a moderate activator of TRPML2 and TRPML3. A series of structure variations of **ML-SI3** with the superior *trans*-configuration was synthesized for structure-activity relationship analysis. Single cell calcium imaging experiments revealed that already small changes to the structure can shift the activity from inhibition to activation, especially for TRPML2 and TRPML3. All compounds were tested at this stage in their racemic form. Since *trans*-**ML-SI3** was still the most promising candidate, a method for enantiomer separation by chiral HPLC was developed, yielding the two enantiomers (-)-*trans*-**ML-SI3** (ee: 99 %) and (+)-*trans*-**ML-SI3** (ee: 96 %). Already the single cell calcium imaging experiments showed, that (-)-*trans*-**ML-SI3** is the most potent TRPML1 inhibitor, while (+)-*trans*-**ML-SI3** is a potent TRPML2 activator. These findings were confirmed by a FLIPR screening of all synthesized and separated compounds for their concentration effect relationship. These experiments provided an IC₅₀ value for TRPML1 inhibition for (-)-*trans*-**ML-SI3** of 1.6 μM and an EC₅₀ value for TRPML2 activation for (+)-*trans*-**ML-SI3** of 2.7 μM, emphasising the importance of stereochemistry in the biological environment.

3.1.1.2 Personal contribution

My contribution to this article was the synthesis and characterization of all compounds from the **ML-SI3** series, as well as the development of the analytical and semipreparative chiral HPLC method for the separation of the enantiomers. Fura-2 single cell calcium imaging experiments for the SAR study of **ML-SI3** were planned, performed and analysed by me. Further, visualisation of the experimental results, writing of the original draft, reviewing and editing were my contributions to the manuscript for this publication.

MARCO KELLER performed the synthesis of **ML-SI1** and contributed to reviewing and editing of the original draft.

SUSANNE RAUTENBERG (née GERNDT) carried out the initial screening of biological activity of **ML-SI1** and commercially available **ML-SI3**, helped with visualisation of the experimental results and contributed to reviewing and editing of the original draft.

NICOLE URBAN performed the FLIPR screening of all compounds and contributed to reviewing and editing of the original draft.

CHENG-CHANG CHEN created the cell lines stably expressing the respective TRPML-YFP channels and reviewed the original draft.

MICHAEL SCHAEFER supervised the FLIPR screening, granted the resources for these experiments and was involved in reviewing and editing of the original draft.

CHRISTIAN GRIMM supervised the single cell calcium imaging experiments, granted resources for these experiments and contributed to reviewing and editing of the original draft.

FRANZ BRACHER supervised and supported all chemical work and was involved in the conceptualization of this project. He provided resources and contributed to writing of the original draft, reviewing and editing.

3.1.1.3 Article

The following article is printed in the original wording. Formatting may vary slightly compared to the original article.



Contents lists available at ScienceDirect

European Journal of Medicinal Chemistry

journal homepage: <http://www.elsevier.com/locate/ejmech>



Chemical and pharmacological characterization of the TRPML calcium channel blockers ML-SI1 and ML-SI3



Charlotte Leser^a, Marco Keller^a, Susanne Gerndt^a, Nicole Urban^c, Cheng-Chang Chen^a, Michael Schaefer^c, Christian Grimm^b, Franz Bracher^{a,*}

^a Department of Pharmacy – Center for Drug Research, Ludwig-Maximilians University, Munich, Germany

^b Walther-Straub-Institute of Pharmacology and Toxicology, Faculty of Medicine, Ludwig-Maximilians University, Munich, Germany

^c Rudolf-Boehm-Institute for Pharmacology and Toxicology, Leipzig University, Leipzig, Germany

ARTICLE INFO

Article history:

Received 18 August 2020

Received in revised form

6 October 2020

Accepted 21 October 2020

Available online 24 October 2020

Keywords:

TRPML calcium Channels

Channel blocker

Indoline

N-arylpiperazine

Stereoselective synthesis

ABSTRACT

The members of the TRPML subfamily of non-selective cation channels (TRPML1–3) are involved in the regulation of important lysosomal and endosomal functions, and mutations in TRPML1 are associated with the neurodegenerative lysosomal storage disorder mucopolipidosis type IV. For in-depth investigation of functions and (patho)physiological roles of TRPMLs, membrane-permeable chemical tools are urgently needed. But hitherto only two TRPML inhibitors, ML-SI1 and ML-SI3, have been published, albeit without clear information about stereochemical details. In this investigation we developed total syntheses of both inhibitors. ML-SI1 was only obtained as a racemic mixture of inseparable diastereomers and showed activator-dependent inhibitory activity. The more promising tool is ML-SI3, hence ML-SI1 was not further investigated. For ML-SI3 we confirmed by stereoselective synthesis that the *trans*-isomer is significantly more active than the *cis*-isomer. Separation of the enantiomers of *trans*-ML-SI3 further revealed that the (–)-isomer is a potent inhibitor of TRPML1 and TRPML2 (IC₅₀ values 1.6 and 2.3 μM) and a weak inhibitor (IC₅₀ 12.5 μM) of TRPML3, whereas the (+)-enantiomer is an inhibitor on TRPML1 (IC₅₀ 5.9 μM), but an activator on TRPML 2 and 3. This renders the pure (–)-*trans*-ML-SI3 more suitable as a chemical tool for the investigation of TRPML1 and 2 than the racemate. The analysis of 12 analogues of ML-SI3 gave first insights into structure–activity relationships in this chemotype, and showed that a broad variety of modifications in both the *N*-arylpiperazine and the sulfonamide moiety is tolerated. An aromatic analogue of ML-SI3 showed an interesting alternative selectivity profile (strong inhibitor of TRPML1 and strong activator of TRPML2).

© 2020 Elsevier Masson SAS. All rights reserved.

1. Introduction

Transient receptor potential (TRP) channels are a family of highly diverse cation channels. There are 6 subfamilies in mammals (TRPC, TRPV, TRPM, TRPA, TRPP and TRPML) and many of these channels are involved in sensory functions [1]. The TRPML subfamily which has three members (TRPML1–3) is an exception to this mutuality within the TRP family. These channels are mainly located in the lysosome (TRPML1–3), recycling endosome (TRPML2) and early endosome (TRPML3). They are involved in the regulation of several lysosomal and endosomal functions such as lysosomal ion homeostasis, lysosomal and endosomal trafficking and

phagocytosis [2]. Mutation with loss of function of the TRPML1 channel causes the neurodegenerative lysosomal storage disorder mucopolipidosis type IV, which is characterized by psychomotor retardation, corneal clouding, retinal degeneration and strabismus [3]. Gain of function mutations of TRPML3 cause the varitint-waddler phenotype in mice, which is characterized by deafness, circling behaviour and coat colour dilution [4–8]. There is no identified TRPML3 associated phenotype in humans [9]. For TRPML2 it is known that it enhances viral entry and trafficking of viruses such as yellow fever virus, dengue virus and influenza virus type A, which require transport to late endosomes for infection [10]. Phosphatidylinositol 3,5-bisphosphate (PI(3,5)P₂) has been identified as endogenous activator of all TRPMLs and is a major constituent of the lysosomal membrane. In contrast, phosphatidylinositol 4,5-bisphosphate (PI(4,5)P₂) inhibits TRPML1 and TRPML3 and is located at the plasma membrane [11]. Bisphosphates are not

* Corresponding author.

E-mail address: Franz.Bracher@cup.uni-muenchen.de (F. Bracher).

membrane permeable and therefore not suitable tools for pharmacological investigations in intact cells.

Thus several synthetic activators of the TRPML channels have been generated in recent years, e.g. the thienylsulfonamide MK6-83 [12], the phthalimidoacetamides SF-51 and ML-SA1 [13], the TRPML2 selective arylisoxazoline-type activator ML2-SA1 and the TRPML3-selective arylisoxazole EVP21 [14], a derivative of the originally identified TRPML3 agonist SN-2 [15]. Besides the many TRPML agonists, only three synthetic inhibitors (ML-S11, ML-S12, ML-S13) have been identified by Samie et al. [16] using a calcium imaging-based high-throughput screening. Though only the chemical structures of ML-S11 and ML-S13 were released by Wang et al. in 2015 in the Supporting Information of their publication [17], ML-S11 is a 2,3-disubstituted *N*-aroylindoline, whereas ML-S13 is a highly functionalized 1,2-diaminocyclohexane containing an *N*-arylpiperazine moiety. Both compounds have two stereocenters, but the authors did not provide any information about the stereochemistry of these inhibitors (Fig. 1).

As TRPML inhibitors are valuable tools required for in-depth characterization of the calcium channels, there is an urgent need to identify the exact structures of the active stereoisomers of ML-S11 and ML-S13. Further, synthetic work on structure-activity relationships (SAR) for both inhibitors was highly attractive, aimed at the possible improvement of both activity and subtype selectivity of these compounds.

2. Results and discussion

2.1. Chemistry

2.1.1. ML-S11

A short synthetic approach to ML-S11 was implemented, as no synthesis of this compound has been published yet. Following work of Li et al. [18], commercially available indole-3-acetic acid **1** was converted into the *N*-acylmorpholine **2** utilizing EDC and DMAP as condensing agents, and subsequent reduction of the amide group with LiAlH₄ gave amine **3** in 50% overall yield. Reduction of indole **3** to the corresponding indoline **4** was unexpectedly challenging. A couple of protocols for reduction of related 2,3-disubstituted indoles, in part even claiming to give *cis*- or *trans*-configured products selectively, have been published in the past [19–21]. The attempted reduction with H₂/Pd to the racemic *cis* compound failed with **3** as substrate. However, reduction with NaBH₃CN [22] gave indoline **4** in 61% yield. Inspection of the NMR data clearly indicated that this product was obtained as a 57:43 mixture of diastereomers. This diastereomeric mixture could not be separated by column chromatography. In a final step, ML-S11 was obtained as a racemic 55:45 mixture of diastereomers with a yield of 67% when reacting **4** with 2,3-dichlorobenzoyl chloride following a procedure of Ohkawa

et al. [23] (Scheme 1). Separation of the racemic diastereomers of ML-S11 was attempted by column chromatography and preparative HPLC on achiral stationary phases, but failed. Even analytical separation on achiral HPLC phases failed, but separation on a chiral analytical Daicel Chiralcel-OD column (for the chromatogram, see Supplementary Information) clearly indicated that the compound is a racemic 55:45 mixture of diastereomers. This was important, as the ¹H and ¹³C NMR spectra of ML-S11 turned out to be quite complex due to the occurrence of rotamers at the amide bond.

2.1.2. ML-S13: identification of the active stereoisomer

As mentioned above (Fig. 1) no information on the relative and absolute stereochemistry of ML-S13 was available from Wang's publication [17], nor from earlier or later scientific work describing the utilization of this inhibitor [16,24–27]. This prompted us to develop synthetic approaches to both *cis*- and *trans*-configured ML-S13 in a first initiative, then to identify the active form (eutomer) of the active diastereomer and finally, perform an analysis of structure-activity relationships by systematic modifications of relevant functional groups in ML-S13. As screening hit ML-S13 arose from a commercial compound library, we speculated that this compound was prepared via a straightforward synthetic path from commercially available building blocks. Inspection of published approaches to related *N*-sulfonyl 1,2-diaminocyclohexane derivatives [28] strongly indicated that *cis*-*N*-phenylsulfonyl cyclohexaneaziridine **7** is a synthetic precursor of ML-S13 and imaginable further synthetic transformations should give the hit compound as the racemic *trans* isomer. In fact, aziridine **7** (conveniently obtained by direct NBS-mediated sulfonylaziridination of cyclohexene **5** with chloramine B **6**) following a protocol of Thakur et al. [29] was reacted with 1-(2-methoxyphenyl)piperazine (**8**) in hexanes containing DMSO to give, under ring opening of the aziridine ring and inversion, pure racemic *trans*-configured product *trans*-ML-S13 in 63% yield (Scheme 2).

For the synthesis of *cis*-ML-S13 we attempted to utilize a protocol published by Labrie et al. [30] for the preparation of closely related products. In this approach, a *trans*-configured *N*-(arylsulfonylamino)cyclohexanol closely related to **10** was converted into the mesyl ester, and then converted into an azidocyclohexane, putatively under complete inversion. Reduction of the azido group followed by *N*-sulfonylation should open an access to *cis*-ML-S13. To our surprise, *O*-mesylation of **10** (prepared by reaction of *cis*-cyclohexene oxide **9** and piperazine **8**), followed by treatment with sodium azide gave a product, which, based on investigation of NMR data (see Supporting Information) was unambiguously identified as the *trans*-configured isomer **11**. Most likely, the intermediate *trans*-configured mesylate underwent, under complete inversion, spontaneous ring closure by attack at the piperazine nitrogen to a *cis*-configured spiroaziridinium intermediate, which in turn then underwent another complete inversion by nucleophilic attack of the azide ion (Scheme 3). Most likely, the same cascade of reactions took place in Labrie's work [30], but was not detected. In a control experiment, we performed reduction of the azido group in **11** to the primary amine (see compound **19** in Scheme 6), and subsequent *N*-sulfonylation with benzenesulfonyl chloride in fact gave pure *trans*-ML-S13. Consequently, this approach did not allow synthesis of *cis*-ML-S13 (see Scheme 3).

Thus, a novel approach to *cis*-ML-S13 had to be worked out. Mono-phenylsulfonylation of commercially available *cis*-1,2-diaminocyclohexane (**12**) gave racemic *cis*-configured sulfonamide **13**. The piperazine moiety was subsequently constructed by reaction of the primary amino group of **13** with *N,N*-bis(2-chloroethyl)-2-methoxyaniline (available from 2-methoxyaniline via bis-hydroxyethylation with oxirane, affording bis(2-hydroxyethyl)-2-aniline **14** and subsequent chlorination with

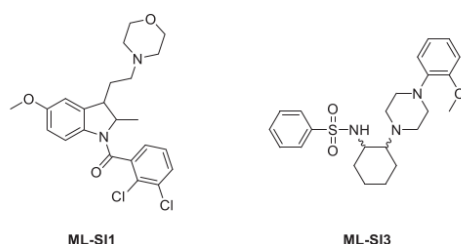
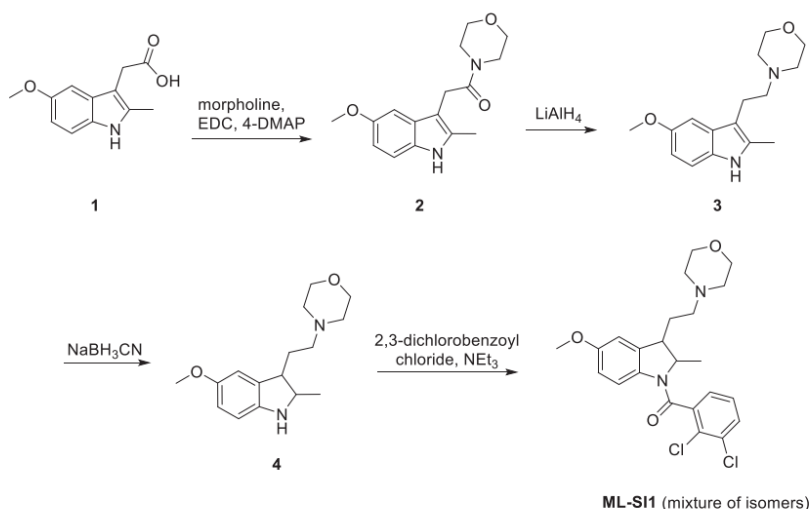
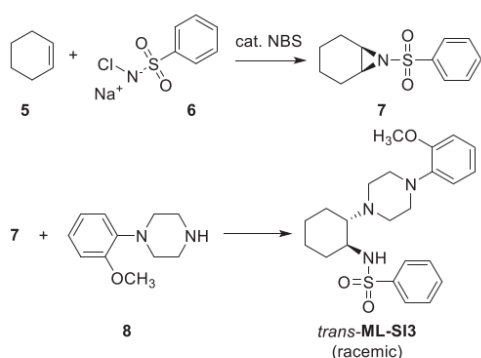


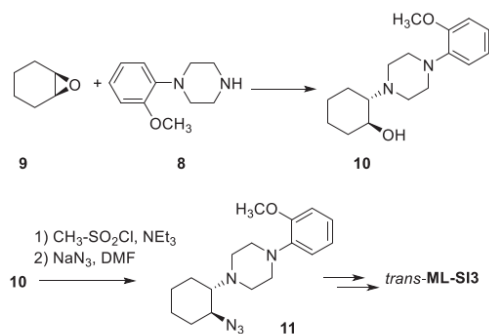
Fig. 1. Structures of the TRPML inhibitors ML-S11 and ML-S13, as depicted by Wang et al. [17].



Scheme 1. Synthesis of ML-SI1 as a racemic mixture of diastereomers.



Scheme 2. Synthesis of racemic *trans*-ML-SI3.



Scheme 3. Attempted synthesis of racemic *cis*-ML-SI3.

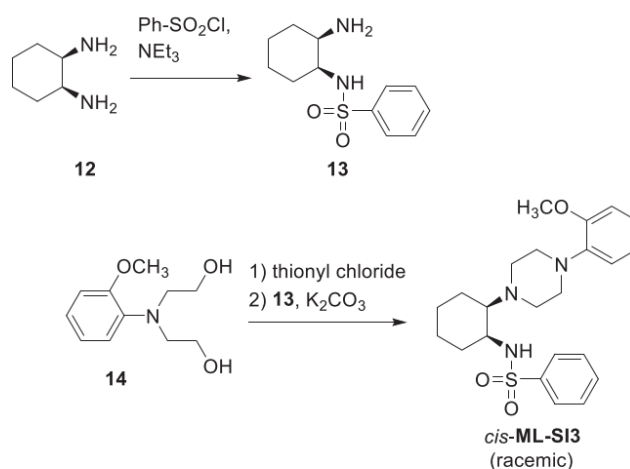
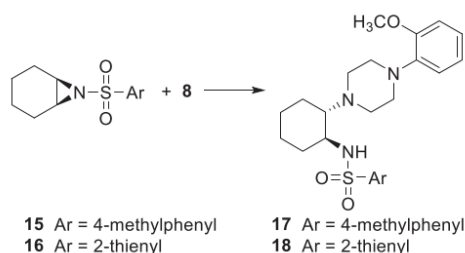
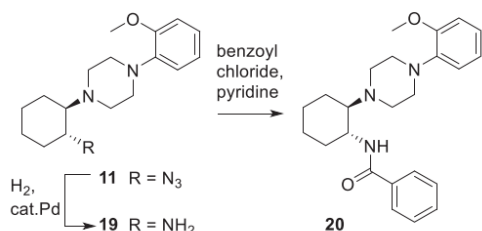
thionyl chloride [31,32]) to give pure racemic *cis*-ML-SI3 (Scheme 4).

Based on the evidence that *trans*-ML-SI3 is superior to its *cis* isomer in blocking TRPML channels (see Chapter 2.2.), we further intended to identify the active enantiomer (eutomer) of *trans*-ML-SI3. Separation of the enantiomers of the racemic inhibitor was attempted *via* chromatographic separation by chiral HPLC. The separation could be achieved on a YMC Chiral Art Cellulose-SB column (250 × 10.0 mm, 5 μm) and both enantiomers were obtained in pure form (ee values: (–)-*trans*-ML-SI3 99%, (+)-*trans*-ML-SI3 96%).

2.1.3. ML-SI3: chemistry aimed at analysis of structure-activity relationships

Systematic investigation of SAR of ML-SI3 included variation of both, the sulfonyl and the *N*-arylpiperazine residue. For replacing the phenylsulfonyl group of ML-SI3 by toluenesulfonyl and thiophene-2-sulfonyl groups the same procedure as described for the synthesis of racemic *trans*-ML-SI3 (Scheme 2) was followed in general. The required *cis*-configured *N*-tosylsulfonylaziridine **15** was obtained directly from cyclohexene and chloramine T hydrate and catalytic NBS, as shown in Scheme 2 for its phenylsulfonyl analogue **7**. The *N*-thiophene-2-sulfonyl analogue **16** [33] was prepared from *cis*-cyclohexene oxide (**9**) in three steps (with two inversions of configuration) involving nucleophilic ring opening with the thiophene-2-sulfonamide under phase-transfer catalysis, *O*-tosylation and subsequent K₂CO₃-mediated aziridine formation [34]. Nucleophilic ring opening of these *N*-sulfonylaziridines with *N*-arylpiperazine **8** gave the desired ML-SI3 analogues **17** and **18** (Scheme 5).

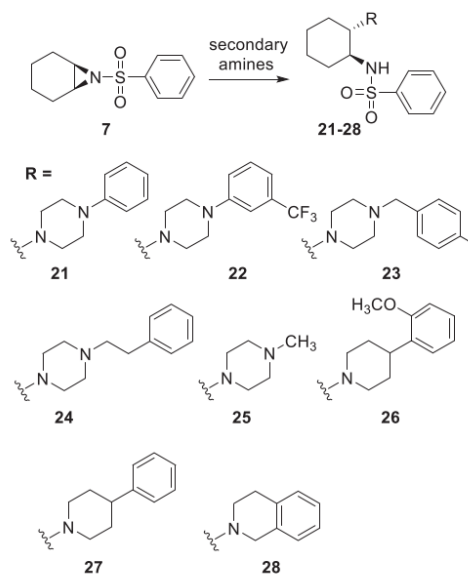
The role of the sulfonamide group in ML-SI3 was analysed by synthesis of the carboxamide analogue **20**. This compound was obtained from the *trans*-configured azido intermediate **11** that was obtained inadvertently in our attempts to synthesize *cis*-ML-SI3 (see Scheme 3). Catalytic hydrogenation of the azido group gave the primary amine **19**, which was directly converted into the benzamide **20** by treatment with benzoyl chloride/pyridine (Scheme 6).


 Scheme 4. Synthesis of racemic *cis*-ML-SI3.

 Scheme 5. Modification of the *N*-sulfonyl residues of ML-SI3.

 Scheme 6. Synthesis of the benzamide analogue **20** of ML-SI3.

For investigation of the role of the 2-methoxyphenyl residue on the piperazine ring of ML-SI3, we prepared, strictly following the chemistry described in Scheme 2 for the synthesis of racemic *trans*-ML-SI3, using *N*-phenylsulfonylaziridine **7** and appropriate *N*-substituted piperazines, analogues bearing modified aromatic residues (phenyl compound **21**, 3-(trifluoromethyl)phenyl compound **22**), homologous compounds in which the *N*-aryl piperazine is replaced by an *N*-arylalkyl piperazine (4-methylbenzyl compound **23**, phenethyl compound **24**) and a truncated analogue **25** in which

the 2-methoxyphenyl residue is replaced by a methyl group. Further, the *N*-aryl piperazine residue was replaced by 4-aryl piperidines (products **26**, **27**) utilizing appropriate piperidine building blocks in combination with *N*-phenylsulfonylaziridine **7**. Replacement of the *N*-aryl piperazine residue by the rigid 1,2,3,4-tetrahydroisoquinoline gave compound **28** (Scheme 7).

Finally, we prepared an analogue **31** in which the 1,2-disubstituted cyclohexane moiety of ML-SI3 is replaced by a 1,2-


 Scheme 7. Modification of the (2-methoxyphenyl)piperazinyl residue of *trans*-ML-SI3.

disubstituted benzene ring. Related compounds were described very recently as TRPML1 activators in a patent [35]. Buchwald-Hartwig amination of 2-bromonitrobenzene (**29**) with 1-(2-methoxyphenyl)piperazine (**8**) under Pd(OAc)₂/BINAP catalysis [36] gave (nitrophenyl)piperazine **30**, which yielded the desired phenylethylamine product **31** upon catalytic hydrogenation of the nitro group and subsequent *N*-sulfonylation with benzenesulfonyl chloride (Scheme 8).

2.2. Biological testing

2.2.1. Pre-screening of the activity of ML-S11 and ML-S13

The synthesized racemic mixture of ML-S11, and a commercially available sample of ML-S13, which was identified as (±)-*trans*-ML-S13, were analysed in Fura-2 and Fluo-4 calcium imaging experiments. Fura-2 based single cell calcium imaging experiments confirmed that the synthesized racemic ML-S11 (mixture of diastereomers) has an inhibitory effect on hTRPML1 (Fig. 2 A, C). Statistical analysis of the three isoforms of the ion channel showed a strong inhibitory effect on hTRPML1, weaker effect on hTRPML2 and (at the test concentration of 10 μM) no effect on hTRPML3, all after activation with ML-SA1 (Fig. 2 A). While inhibition after activation with ML-SA1 showed a robust signal, it was not possible to significantly block MK6-83 induced activation (Fig. 2 B). This indicates an activator dependent inhibition. Comparing the inhibitory effect of ML-S11 and commercially available ML-S13, ML-S13 is able to block hTRPML1 and hTRPML2 around 50%, but not hTRPML3 (Fig. 2 E). Comparing different activators, ML-S13 is able to block both ML-SA1 and MK6-83 induced activation in the same manner (Fig. 2 F, G). Concentration-effect experiments revealed that ML-S13 (IC₅₀: 2.6 μM) is more potent than ML-S11 (IC₅₀: 15 μM) for inhibition of TRPML1. Furthermore, ML-S13 can inhibit TRPML3 as well at higher concentrations (IC₅₀: 17 μM), while ML-S11 has no effect (Fig. 2 D, H). Thus, ML-S13 seemed the more promising antagonist for further investigations. As, in addition, ML-S11 was obtained as an inseparable mixture of diastereomers with unpredictable individual activities, this inhibitor was not further investigated, and no further derivatives of ML-S11 were generated.

2.2.2. Single cell calcium imaging

All compounds of the ML-S13 series were further tested by single cell Ca²⁺-imaging using Fura-2-loaded HEK293 cells stably expressing hTRPML1^{ΔNC}-YFP, hTRPML2-YFP and hTRPML3-YFP (Fig. 3). Activators were tested by adding the compound solution (10 μM) and recording the signals of Ca²⁺-chelated Fura-2 and free Fura-2 for 200 s. For inhibitors, cells were first stimulated with 10 μM of ML-SA1 or MK6-83, the compound solution added after 200 s, and the signals recorded for additional 200 s. All compounds, except *N*-phenethyl piperazine **24**, significantly block TRPML1 (Fig. 3D). Piperazine **24** is the only compound from this series that activates TRPML1, but the effect is not significant at 10 μM (Fig. 3A). Only weak inhibitory effects on TRPML1 were detected for *cis*-ML-

S13, the *N*-methyl piperazine **25** and the benzamide **20** analogue of *trans*-ML-S13. Surprisingly, on TRPML2 the activity is mainly the opposite, most of the compounds are activating this channel (Fig. 3B). Interestingly, the racemic mixture of *trans*-ML-S13 is activating the TRPML2 channel as efficiently as the known activator ML-SA1. Responsible for this activation is exclusively the (+)-*trans*-ML-S13, which activates TRPML2 stronger than ML-SA1, same as the toluenesulfonamide **17**. In contrast, (–)-*trans*-ML-S13, as well as tetrahydroisoquinoline derivative **28**, does not activate but inhibit TRPML2 (Fig. 3E). For TRPML3 the activity largely resembles the activity observed on TRPML2. Here (+)-*trans*-ML-S13, toluenesulfonamide **17**, *N*-(4-methylbenzyl) piperazine **23** and *N*-phenethyl piperazine **24** are strong activators, whereas (–)-*trans*-ML-S13 and thiophenesulfonamide **18** are the best inhibitors.

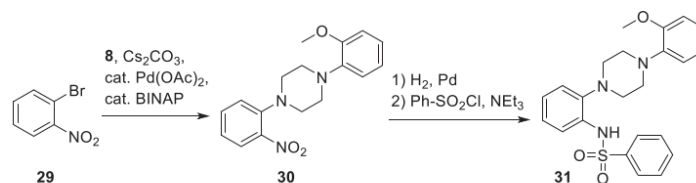
2.2.3. FLIPR screening

A Fluo-4 calcium-imaging based FLIPR-method was used for determination of concentration-effect relationships of the ML-S13-type compounds. First, HEK293 cells stably expressing hTRPML1^{ΔNC}-YFP, hTRPML2-YFP or hTRPML3-YFP were treated with the test compound solutions in final concentrations from 0.098 μM to 100 μM for 10 min, followed by activation with the known activator ML-SA1 (5 μM) for another 10 min. Concentration-effect relationships are shown in Fig. 4, the calculated EC₅₀ and IC₅₀ values are presented in Table 1. These data fully confirm the Fura-2 calcium imaging results shown in Chapter 2.2.2.

2.2.4. Analysis of structure-activity relationships of ML-S13 and its analogues

As evident from Table 1, racemic *trans*-ML-S13 is blocking TRPML1 stronger (factor 6) than its racemic *cis* isomer. The active (±)-*trans*-isomer has some selectivity for blocking TRPML1 (factor 9) over TRPML3, but activates TRPML2. The racemic *cis* isomer is an activator on both TRPML2 and TRPML3. Separation of the more potent racemic *trans*-ML-S13 into the pure enantiomers led to the evidence that the levorotatory form (–)-*trans*-ML-S13 is the eutomer and the only compound from this series that is an inhibitor on all three TRPMLs, being virtually equipotent on TRPML1 and TRPML2 and less potent on TRPML3 (factor of 5–7). The activities of the ML-S13 isomers on hTRPML1 and hTRPML2 are summarized in Fig. 5.

Systematic variation of structural motifs in racemic *trans*-ML-S13 led to identification of the following structure activity relationships: (a) most of the (racemic) analogues of *trans*-ML-S13 (except **20** and **25**) show an activity profile similar to the parent compound; (b) variation of the aromatic moiety of the sulfonamide (**17**, **18**) is well tolerated, whereas replacing the benzenesulfonamide by a benzamide (**20**) leads to dramatic loss of activity; (c) modifications of the substitution pattern of the phenyl ring located at N-4 of the piperazine (**21**, **22**) do not change activity significantly, but introduction of an aliphatic spacer (methylene in **23**, ethylene in **24**) between N-4 and the aromatic ring changes the activity from



Scheme 8. Synthesis of the 1,2-phenylethylamine-based analogue **31** of *trans*-ML-S13.

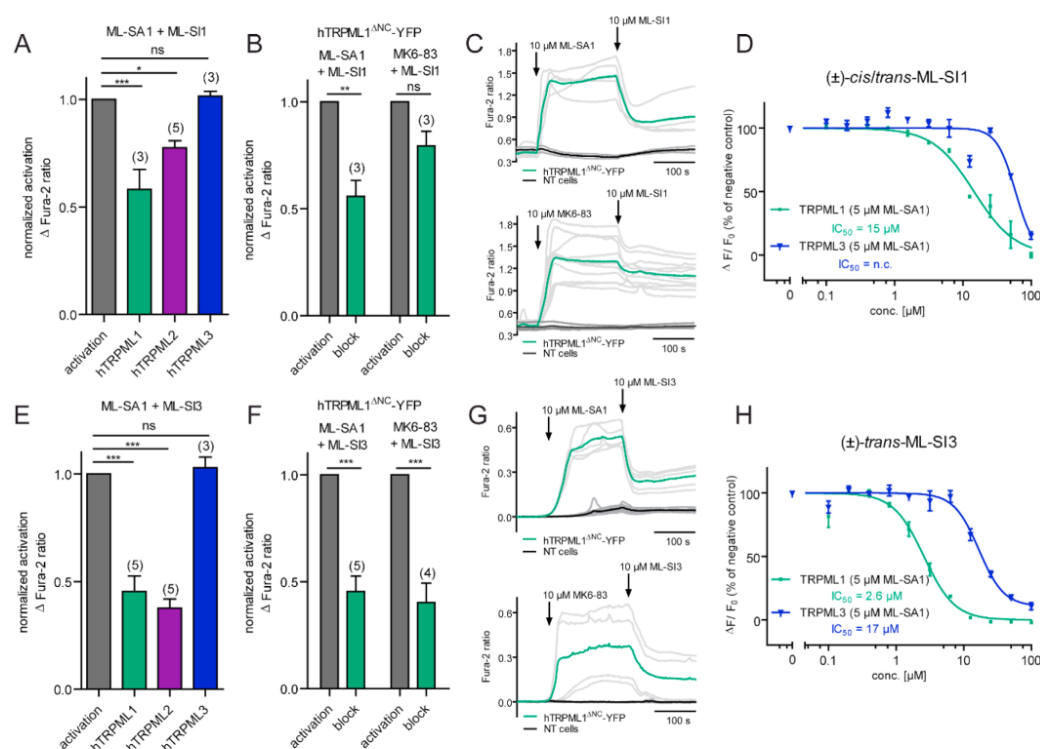


Fig. 2. Pre-screening results for the synthesized ML-SI1 and commercially available ML-SI3. (A) Statistical analysis of the inhibitory effect of ML-SI1 (10 μM) on TRPMLs in Fura-2 Ca²⁺ imaging experiments (normalized activation) after activation with ML-SI1 (10 μM). HEK293 cells stably expressing hTRPML2-YFP or hTRPML3-YFP and transiently transfected hTRPML1^{ΔNC}-YFP cells were used [1]. (B) Statistical analysis as in (A), using ML-SI1 (10 μM) or MK6-83 (10 μM) for activation of hTRPML1^{ΔNC}-YFP transiently transfected HEK293 cells. (C) Representative Ca²⁺ signals recorded from hTRPML1^{ΔNC}-YFP transiently transfected HEK293 cells. Cells were sequentially stimulated with ML-SI1 (10 μM, n = 5 transfected and 2 NT cells) or MK6-83 (10 μM, n = 11 transfected and 3 NT cells) and ML-SI1 (10 μM). Highlighted lines represent the mean response from a population of cells. Shaded traces represent responses of single cells. (D) Concentration-effect measurements on HEK293 cells stably expressing hTRPML1 and hTRPML3. Cells were treated with ML-SI1, followed by activation with ML-SI1 (5 μM). (E) Statistical analysis of the inhibitory effect of ML-SI3 as in (A) using ML-SI1 (10 μM) for activation and ML-SI3 (10 μM) for inhibition. (F) Statistical analysis as in (B) but inhibition with ML-SI3 (10 μM). (G) Representative Ca²⁺ signals as in (C), but performed on a Leica DMI8 live cell microscope and traces are normalized to basal. Cells were treated with ML-SI1 (10 μM, n = 5 transfected and 8 NT cells) or MK6-83 (10 μM, n = 4 transfected and 5 NT cells) and ML-SI3 (10 μM). (H) Concentration-effect measurements as in (D) but using ML-SI3 as inhibitor. *** indicates p < 0.001, ** indicates p < 0.01, * indicates p < 0.05, ns = not significant, one-way ANOVA test followed by Tukey's post-hoc test.

inhibition to activation, for compound **24** on all three subtypes, for compound **23** on TRPML2 and TRPML3; (d) replacement of N-4 of the piperazine by a carbon atom (giving piperidine analogues **26**, **27**) leads only to a slight loss of activity on TRPML1, whereas rigidization (tetrahydroisoquinoline analogue **28**) is more detrimental, including a change on TRPML2 from activation to inhibition; (e) replacement of the N-aryl residue on the piperazine by a methyl group (**25**) leads to a dramatic loss of activity.

In conclusion, the structure-activity relationship seen for the racemic analogues of ML-SI3 is rather flat. Additional work on optimization of the identified eutomer (–)-*trans*-ML-SI3 is only promising when working with pure enantiomers of analogues. This approach is presently hampered by the lacking access to significant amounts of pure enantiomers. Nevertheless, some of the analogues showing in their racemic form comparable activity profiles (potency and subtype-selectivity) as racemic *trans*-ML-SI3 might provide pure enantiomers with a similar gain in selectivity as seen here for *trans*-ML-SI3. Among them are the thiophenesulfonyl

analogue **18** and the 4-arylpiperidine analogues **26** and **27**.

Noteworthy, replacement of the cyclohexane moiety of ML-SI3 by a benzene ring gave interesting results. The resulting achiral phenylenediamine derivative **31** retained inhibitory activity on TRPML1, equipotent to (–)-*trans*-ML-SI3. This was not unexpected, since the overall geometries of *trans*-configured 1,2-disubstituted cyclohexanes like ML-SI3 (in which both substituents are preferentially orientated in equatorial position) and of 1,2-disubstituted benzenes (where both residues are coplanar) are rather similar. However, the activation effect on TRPML2 could not be eliminated for aromatic analogue **31** as it could be for (–)-*trans*-ML-SI3. No activation of TRPML3 was observed for compound **31** and only weak inhibition. This interesting finding is in contrast to a report on closely related compounds, which were claimed (without details about activity) as TRPML1 activators very recently in a patent [35].

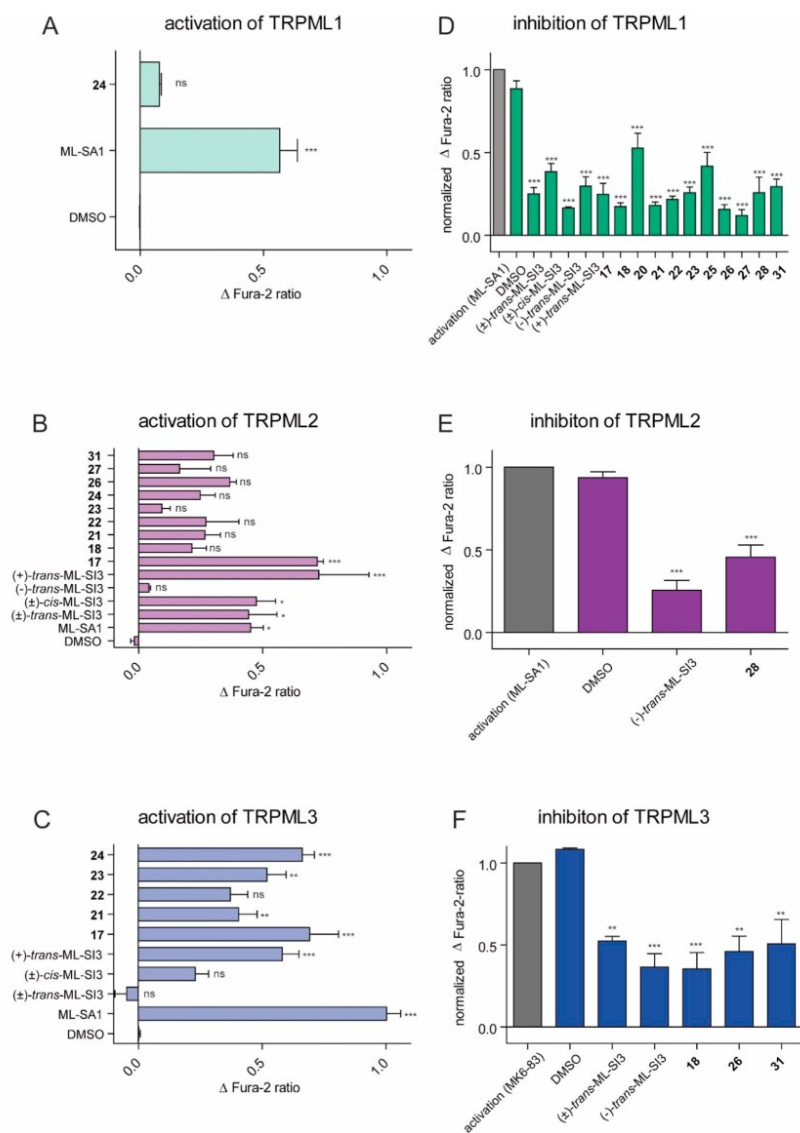


Fig. 3. Statistical analysis of calcium imaging results. (A, B, C) Activation of TRPMLs in Fura-2 single cell calcium imaging experiments. Mean values of at least three independent experiments are shown. (D, E, F) Inhibition of TRPMLs, after activation with ML-SA1 (10 μ M, TRPML1 and 2) or MK6-83 (10 μ M, TRPML3), DMSO was used as negative control. Activation of ML-SA1 or MK6-83 is normalized to 1. All statistical analyses of Ca^{2+} imaging experiments are mean values of $n = 3$ or $n = 4$ independent experiments. Test compounds 17–28 were applied in racemic form. *** indicates $p < 0.001$, ** indicates $p < 0.01$, * indicates $p < 0.05$, ns = not significant, one-way ANOVA test followed by Tukey's post-hoc test, compared to DMSO.

3. Conclusions

For in-depth investigation of functions and (patho)physiological roles of TRPMLs versatile chemical tools are urgently needed. Phosphatidylinositol 3,5-bisphosphate ($\text{PI}(3,5)\text{P}_2$) has been

identified as endogenous activator of all TRPMLs, whereas phosphatidylinositol 4,5-bisphosphate ($\text{PI}(4,5)\text{P}_2$) inhibits TRPML1 and TRPML3. But these physiological compounds are not suitable as chemical tools for cellular assays due to their high polarity and lack of membrane permeability. In the past few years several low-

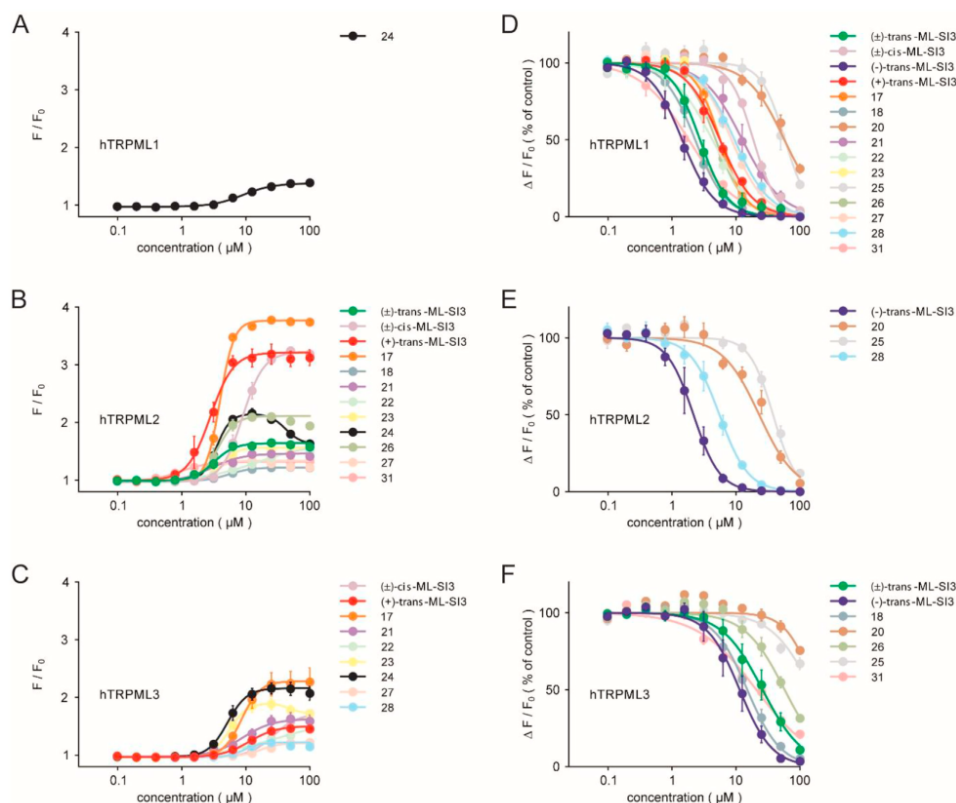


Fig. 4. ML-SI3 and analogues in FLIPR experiments. Shown are concentration-effect relationships for Ca^{2+} increases (Fluo-4) in response to different concentrations of activating ML-SI3 analogues on HEK293 cells stably expressing hTRPML1-YFP (A), hTRPML2-YFP (B) or hTRPML3-YFP (C). After 10 min, cells were activated with 5 μM ML-SA1 to determine half maximal inhibition concentration of non-activating compounds on hTRPML1-YFP (D), hTRPML2-YFP (E) or hTRPML3-YFP (F). Data are calculated from 3 independent experiments, each and represented as means \pm SEM. EC_{50} and IC_{50} values are presented in Table 1.

Table 1

Activation and inhibition of the three subtypes of TRPML by the ML-SI3-type compounds. Mean values \pm SD of at least three independent experiments are shown.

Compound	EC_{50} [μM]		activation		IC_{50} [μM]		inhibition	
	TRPML1	TRPML2	TRPML1	TRPML3	TRPML1	TRPML2	TRPML1	TRPML3
(\pm)-trans-ML-SI3	–	3.3 ± 1.5	–	–	3.1 ± 1.5	–	–	28.5 ± 15.9
(\pm)-cis-ML-SI3	–	9.4 ± 2.7	–	29.0 ± 4.1	18.5 ± 1.9	–	–	–
(–)-trans-ML-SI3	–	–	–	1.6 ± 0.7	1.6 ± 0.7	2.3 ± 1.1	–	12.5 ± 7.6
(+)-trans-ML-SI3	–	2.7 ± 1.4	–	10.8 ± 0.5	5.9 ± 1.7	–	–	–
17	–	4.0 ± 0.4	–	8.5 ± 0.9	5.6 ± 0.5	–	–	–
18	–	6.3 ± 3	–	–	2.3 ± 1.2	–	–	15.9 ± 8.9
20	–	–	–	–	65.1 ± 11.1	26.8 ± 8.7	–	>100
21	–	3.6 ± 1.8	–	9.5 ± 3.9	14.9 ± 10.5	–	–	–
22	–	9.1 ± 4.2	–	14.6 ± 2.2	4.4 ± 2.9	–	–	–
23	–	4.4 ± 1.1	–	5.8 ± 0.9	5.7 ± 0.6	–	–	–
24	9.4 ± 0.6	3.6 ± 0.3	–	5.4 ± 1.1	–	–	–	–
25	–	–	–	–	53.3 ± 15.6	40.2 ± 7.9	–	>100
26	–	3.9 ± 1.6	–	–	4.8 ± 2.0	–	–	56.2 ± 16.2
27	–	3.7 ± 0.8	–	20.7 ± 4.4	8.9 ± 1.5	–	–	–
28	–	–	–	9.5 ± 1.4	9.5 ± 2.0	5.5 ± 2.5	–	–
31	–	1.1 ± 0.5	–	–	1.8 ± 0.9	–	–	21.7 ± 7.7

--: no effect.

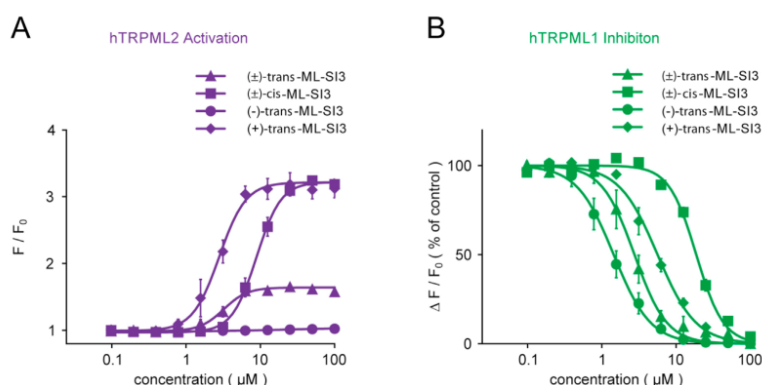


Fig. 5. Summary of the activity of the stereoisomers of ML-SI3. (A) Concentration-effect relationships for activation TRPML2. (B) Concentration-effect relationships for inhibition of TRPML1.

molecular, membrane-permeable activators of TRPMLs have been developed by our and other groups [12–14], but well characterized lipophilic inhibitors are still missing. Recently, three synthetic inhibitors (ML-SI1, ML-SI2, ML-SI3) have been reported by Samie et al. [16], but only the chemical structures of ML-SI1 and ML-SI3 were released by Wang et al. in 2015 [17]. Both, the 2,3-disubstituted *N*-aroylindoline ML-SI1 and the highly functionalized 1,2-diaminocyclohexane ML-SI3 contain two stereocenters, but no information about the stereochemistry of these inhibitors was published (Fig. 1). This prompted us to develop syntheses of these inhibitors for elucidation of the exact structures of the active stereoisomers and for analysis of structure-activity relationships (SAR).

ML-SI1 was obtained as an inseparable racemic mixture of *cis*-/*trans*-isomers (55:45) in a short synthetic sequence and its inhibitory activity on hTRPML1 (and a weak effect on TRPML2) after activation with ML-SA1, but not with the alternative activator MK6-83, was confirmed by calcium imaging experiments. As concentration-effect experiments revealed that ML-SI1 is inferior to the second inhibitor of interest, ML-SI3, and the mixture of isomers could not be separated on a preparative scale for the characterization of the single stereoisomers, ML-SI1 was not further investigated.

For ML-SI3 we developed stereoselective syntheses of both racemic *cis*- and *trans*-isomers and identified *trans*-ML-SI3 as the active TRPML inhibitor. Further, this compound was separated into its enantiomers by semi-preparative chiral HPLC and 12 analogues of *trans*-ML-SI3 were prepared (in racemic form) on different synthetic routes for an analysis of structure-activity relationships. With few exceptions (*N*-methyl derivative **25**, benzamide **20**) these analogues showed a comparable activity profile as racemic *trans*-ML-SI3. However, besides the expected inhibitory activity on subtype TRPML1, racemic *trans*-ML-SI3 and most of the analogues showed significant activating effects on TRPML2 and TRPML3. Finally, detailed characterization of the separated enantiomers of *trans*-ML-SI3 revealed that (–)-*trans*-ML-SI3 is an inhibitor on all three subtypes, namely a potent inhibitor of both TRPML1 and TRPML2 (IC₅₀ values of 1.6 and 2.3 μM) and a weak inhibitor (IC₅₀ 12.5 μM) of TRPML3. In contrast, the (+)-enantiomer is an inhibitor on TRPML1, but an activator on TRPML 2 and TRPML3. This renders the pure (–)-*trans*-ML-SI3 more suitable as a chemical tool for the investigation of TRPML1 and 2 than the racemate. Future work in this field will require efficient enantioselective syntheses of ML-

SI3-related compounds and this will be subject of upcoming investigations.

Further, we identified the achiral aromatic ML-SI3 analogue **31**, which has an uncommon selectivity profile (strong inhibitor of TRPML1 and strong activator of TRPML2).

4. Experimental section

4.1. Chemistry

All chemicals used were of analytical grade and were obtained from abcr (Karlsruhe, Germany), Fischer Scientific (Schwerte, Germany), Sigma-Aldrich (now Merck, Darmstadt, Germany), TCI (Eschborn, Germany) or Th. Geyer (Renningen, Germany). HPLC grade and dry solvents were purchased from VWR (Darmstadt, Germany) or Sigma-Aldrich, all other solvents were purified by distillation. All reactions were monitored by thin-layer chromatography (TLC) using pre-coated plastic sheets POLYGRAM® SIL G/UV254 from Macherey-Nagel and detected by irradiation with UV light (254 nm). Flash column chromatography (FCC) was performed on Merck silica gel Si 60 (0.015–0.040 mm).

NMR spectra (¹H, ¹³C, DEPT, H-H-COSY, HSQC/HMQC, HMBC) were recorded at 23 °C on an Avance III 400 MHz Bruker BioSpin or Avance III 500 MHz Bruker BioSpin instrument. Chemical shifts δ are stated in parts per million (ppm) and are calibrated using residual protic solvent as an internal reference for proton (CDCl₃: δ = 7.26 ppm, CD₂Cl₂: δ = 5.32 ppm) and for carbon the central carbon resonance of the solvent (CDCl₃: δ = 77.16 ppm, CD₂Cl₂: δ = 53.84 ppm). Multiplicity is defined as s = singlet, d = doublet, t = triplet, q = quartet, p = pentet, m = multiplet. NMR spectra were analysed with NMR software MestReNova, version 12.0.1–20560 (Mestrelab Research S.L.). High resolution mass spectra were performed by the LMU Mass Spectrometry Service applying a Thermo Finnigan LTQ FT Ultra Fourier Transform Ion Cyclotron Resonance device at 250 °C for ESI and a Thermo Q Exactive GC Orbitrap device at 250 °C and an electron energy of 70 eV for EI. IR spectra were recorded on a PerkinElmer FT-IR Paragon 1000 instrument as neat materials. Absorption bands were reported in wave number (cm⁻¹) with ATR PRO450-S. Melting points were determined by the open tube capillary method on a Büchi melting point B-540 apparatus and are uncorrected. HPLC purities were determined using an HP Agilent 1100 HPLC with a diode array detector and an Agilent Zorbax Eclipse plus C18 column

(150 × 4.6 mm, 5 μm) with methanol/water in different proportions adjusted to pH = 9 with NaOH or neutral as mobile phase. Determination of ee values was performed using a Daicel Chiralcel-OD column (250 × 4.6 mm, 10 μm). Semi-preparative HPLC was performed on a YMC Chiral Art Cellulose-SB column (250 × 10.0 mm, 5 μm) using a VWR LaPrep P110 system with a UV Detector P311. Values for specific rotation [α] were measured at 23 °C at a wavelength of λ = 589 nm (Na-D-line) using a PerkinElmer 241 Polarimeter instrument. All samples were dissolved in chloroform (layer thickness l = 10 cm), the concentration is stated in g/100 mL.

4.1.1. Synthesis

4.1.1.1. General procedure A: synthesis of aziridines from cyclohexene. According to Thakur et al. [29] the appropriate chloramine hydrate was dried at 60 °C for 24 h and suspended in acetonitrile (~2 M). Cyclohexene (1.0 eq) and NBS (0.2 eq) were added to the suspension and the resulting mixture stirred at rt for 22 h. The solvent was removed *in vacuo* and the residue taken up in ethyl acetate. The organic layer was washed with water and brine, dried over Na₂SO₄ and the solvent removed *in vacuo*. The residue was purified by FCC using petrol ether/ethyl acetate (7:3) as an eluent to afford the desired product.

4.1.1.2. General procedure B: synthesis of trans-1,2-diaminocyclohexanes from aziridines. The aziridine was suspended in dry hexanes (~0.3 M), then DMSO (5 eq) and the appropriate secondary amine were added. The resulting mixture was stirred at rt for 24 h. After completion (TLC control) ethyl acetate was added and the organic layer washed three times with water and dried over Na₂SO₄. The solvent was removed *in vacuo* and the crude product recrystallized from ethanol to afford the desired product.

4.1.1.3. 4-(2-(5-Methoxy-2-methylindolin-3-yl)ethyl)morpholine (4). 4-(2-(5-Methoxy-2-methyl-1H-indol-3-yl)ethyl)morpholine (100 mg, 0.364 mmol) was dissolved in 2.5 mL trifluoroacetic acid and cooled to 0 °C. Then, sodium borohydride (133 mg, 2.00 mmol) was added portionwise. The reaction mixture was stirred for 2 h, then quenched with 2 N NaOH (10 mL) and extracted with ethyl acetate (3 × 70 mL). The combined organic layers were washed with water (100 mL) and brine (100 mL), dried by filtration and the solvent was removed *in vacuo*. Purification by FCC using methylene chloride/methanol (9:1) as an eluent gave **4** (62 mg) as a brown oil (yield: 61%). ¹H NMR (400 MHz, CD₂Cl₂): δ (ppm) = 6.69 (m, 1H, 4-H), 6.59–6.46 (m, 2H, 6-H, 7-H), 3.91 (p, J = 7.6, 6.5 Hz, 0.6H, 2-H), 3.71 (d, J = 0.9 Hz, 3H, O-CH₃), 3.67 (m, 4H, 3'-H, 5'-H), 3.58 (p, J = 6.3 Hz, 0.4H, 2-H), 3.12 (q, J = 7.5 Hz, 0.6H, 3-H), 2.83 (q, J = 6.6 Hz, 0.4H, 3-H), 2.49–2.33 (m, 6H, 2'-H, 2''-H, 6''-H), 1.92–1.70 (m, 2H, 1'-H), 1.23 (d, J = 6.2 Hz, 1.2H, CH₃), 1.12 (d, J = 6.5 Hz, 1.8H, CH₃); ¹³C NMR (101 MHz, CD₂Cl₂): δ (ppm) = 153.7 (C-5), 153.7 (C-5), 145.0 (C-7a), 144.8 (C-7a), 134.6 (C-3a), 134.5 (C-3a), 112.5 (C-6), 112.2 (C-4), 112.0 (C-6), 111.7 (C-4), 109.9 (C-7), 109.9 (C-7), 67.4 (C-3'', C-5''), 61.7 (C-2), 59.3 (C-2), 57.3 (C-1'), 56.8 (C-1'), 56.2 (O-CH₃), 56.2 (O-CH₃), 54.3 (C-2'', C-6''), 48.6 (C-3), 43.7 (C-3), 31.3 (C-1'), 25.1 (C-1'), 22.4 (CH₃), 16.3 (CH₃). IR (ATR): ν̄ [cm⁻¹] = 2956, 1489, 1270, 1230, 1116, 1034, 915; HR-MS (EI): calcd. for C₁₆H₂₄N₂O₂: 276.1838, found 276.1832; purity (HPLC): >96%.

4.1.1.4. (2,3-Dichlorophenyl) (5-methoxy-2-methyl-3-(2-morpholinoethyl)indolin-1-yl)methanone (ML-S11). (racemic mixture of diastereomers) **4** (38 mg, 0.14 mmol) was dissolved in 5 mL dichloromethane and cooled to 0 °C. Triethylamine (20 μL, 0.14 mmol) and 2,3-dichlorobenzoyl chloride (35 mg, 0.17 mmol) were added portionwise. The reaction mixture was stirred at room for 12 h, then poured into brine (30 mL) and extracted with dichloromethane (3 ×, 20 mL). The combined organic layers were

dried by filtration and the solvent was removed *in vacuo*. Purification by FCC using methylene chloride/methanol (9:1) as an eluent gave the product (41 mg) as a yellow solid (yield: 67%). ML-S11 was obtained as a 55:45 mixture of *cis/trans* isomers. In the ¹H and ¹³C NMR spectra we saw a set of signals, caused by the diastereomers and their rotamers. mp: 68–69 °C. ¹H NMR (500 MHz, CD₂Cl₂): δ (ppm) = 8.21–8.02 (m, 0.58H), 7.64–7.54 (m, 1H), 7.51–7.21 (m, 2H), 7.16–7.09 (m, 0.16H), 6.87–6.74 (m, 1.7H), 6.42–6.32 (m, 0.4H), 5.71–5.58 (m, 0.4H), 5.15–5.07 (m, 0.23H), 4.75–4.68 (m, 0.12 H), 4.12–4.05 (m, 0.28H), 3.86–3.49 (m, 8H), 2.09–2.79 (m, 0.51H), 2.61–2.30 (m, 8H), 2.21–2.08 (m, 0.77H), 1.88–1.59 (m, 2.52H), 1.36 (dd, J₁ = 16.1 Hz, J₂ = 6.5 Hz, 0.49H), 1.21 (dd, J₁ = 15.1 Hz, J₂ = 6.5 Hz, 0.79H), 1.08 (d, J = 6.4 Hz, 0.97H), 0.95 (d, J = 6.4 Hz, 0.83H); ¹³C NMR (126 MHz, CD₂Cl₂): δ (ppm) = 164.4, 164.0, 163.7, 163.5, 163.2, 163.2, 162.7, 157.9, 157.6, 157.3, 157.2, 157.0, 156.9, 139.3, 139.2, 139.2, 139.0, 138.9, 138.9, 138.7, 138.6, 138.4, 137.7, 137.6, 137.3, 134.8, 134.5, 134.3, 134.3, 134.2, 134.0, 133.9, 133.7, 133.4, 133.3, 133.0, 133.0, 131.8, 131.7, 131.7, 131.4, 130.2, 130.1, 129.9, 129.1, 129.0, 128.9, 128.9, 128.8, 128.8, 128.7, 128.7, 128.6, 128.4, 127.8, 127.6, 127.2, 127.0, 126.3, 126.0, 126.0, 119.1, 119.0, 115.3, 115.1, 115.1, 114.8, 112.9, 112.8, 112.8, 112.3, 112.3, 112.0, 111.9, 111.9, 111.7, 110.9, 110.8, 110.4, 67.3, 67.3, 67.3, 64.1, 63.0, 62.4, 62.2, 62.0, 61.2, 60.5, 60.1, 57.6, 57.5, 56.8, 56.5, 56.3, 56.2, 56.0, 56.0, 55.9, 55.9, 55.9, 55.8, 54.3, 54.3, 54.2, 54.2, 47.7, 46.1, 45.8, 43.5, 42.9, 42.4, 41.9, 41.5, 33.1, 33.0, 32.9, 32.6, 30.1, 24.3, 24.3, 21.9, 21.3, 20.0, 19.6, 15.2, 14.8, 13.4, 12.8; IR (ATR): ν̄ [cm⁻¹] = 1636, 1485, 1398, 1277, 1115, 1029, 795, 686, 630, 617, 607, 596, 581, 570; HR-MS (ESI): calcd. for C₂₃H₂₆Cl₂N₂O₃: 449.1399 [M+H]⁺, found 449.1389; purity (HPLC): >96%.

4.1.1.5. 7-(Phenylsulfonyl)-7-azabicyclo[4.1.0]heptane (7). Following general procedure A, chloramine B hydrate (6.9 g, 30 mmol), cyclohexene (3.0 mL, 30 mmol) and NBS (1.1 g, 6.0 mmol) were reacted in 150 mL acetonitrile. Purification by FCC gave **7** as a colourless oil (yield: 45%). ¹H NMR (400 MHz, CDCl₃): δ (ppm) = 7.98–7.92 (m, 2H, 2'H, 6'-H), 7.65–7.59 (m, 1H, 4'-H), 7.57–7.51 (m, 2H, 3'-H, 5'-H), 3.01 (p, J = 1.6 Hz, 2H, 1-H, 6-H), 1.79 (tt, J = 6.3, 1.3 Hz, 4H, 2-H, 5-H), 1.46–1.35 (m, 2H, 3-H, 4-H), 1.28–1.17 (m, 2H, 3-H, 4-H); ¹³C NMR (101 MHz, CDCl₃): δ (ppm) = 139.1 (C-1'), 133.3 (C-4'), 129.1 (C-3', C-5'), 127.7 (C-2', C-6'), 40.1 (C-1, C-6), 22.9 (C-2, C-5), 19.5 (C-3, C-4); IR (ATR): ν̄ [cm⁻¹] = 2938, 2862, 1446, 1318, 1153, 1091; HR-MS (ESI): calcd. for C₁₂H₁₆NO₂S⁺: 238.0896 [M+H]⁺, found 238.0897; purity (HPLC): >96%.

4.1.1.6. trans-N-(2-(4-(2-Methoxyphenyl)piperazin-1-yl)cyclohexyl)benzenesulfonamide (trans-ML-S13). Following general procedure B, 7-(phenylsulfonyl)-7-azabicyclo [4.1.0]heptane (**7**, 122 mg, 0.514 mmol) and 1-(2-methoxyphenyl)piperazine (**8**, 119 mg, 0.617 mmol) were reacted to give trans-ML-S13 as a white solid (yield: 63%). mp: 150–151 °C. ¹H NMR (500 MHz, CDCl₃): δ (ppm) = 7.94–7.89 (m, 2H, 2-H, 6-H), 7.60–7.56 (m, 1H, 4-H), 7.53 (ddt, J = 8.4, 6.6, 1.5 Hz, 2H, 3-H, 5-H), 7.02 (td, J = 7.6, 1.7 Hz, 1H, 4''-H), 6.95 (td, J = 7.5, 1.5 Hz, 1H, 5''-H), 6.89 (dd, J = 7.8, 1.7 Hz, 1H, 6''-H), 6.85 (dd, J = 8.0, 1.4 Hz, 1H, 3''-H), 6.11 (s, 1H, NH), 3.83 (s, 3H, OCH₃), 3.12–2.10 (m, 11H), 1.91–1.64 (m, 3H, CH₂ cyclohexane), 1.35–1.04 (m, 4H, CH₂ cyclohexane). ¹³C NMR (126 MHz, CDCl₃): δ (ppm) = 152.3 (C-2'''), 141.2 (C-1'''), 139.9 (C-1), 132.7 (C-4), 129.1 (C-3, C-5), 127.4 (C-2, C-6), 123.3 (C-4'''), 121.2 (C-5'''), 118.4 (C-6'''), 111.3 (C-3'''), 66.8 (C-2'), 55.5 (OCH₃), 53.5 (C-1'), 51.2 (CH₂ piperazine), 33.0 (CH₂ cyclohexane), 25.5 (CH₂ cyclohexane), 24.3 (CH₂ cyclohexane), 23.2 (CH₂ cyclohexane). IR (ATR): ν̄ [cm⁻¹] = 3171, 2932, 2809, 1497, 1447, 1339, 1307, 1021, 757, 725, 690. HR-MS (ESI): calcd. for C₂₃H₃₂N₃O₃S⁺: 430.2159 [M+H]⁺; found: 430.2159. purity (HPLC): >96%.

4.1.1.7. trans-2-(4-(2-Methoxyphenyl)piperazin-1-yl)cyclohexan-1-ol (10). Cyclohexene oxide (0.43 mL, 4.2 mmol) and 1-(2-methoxyphenyl)piperazine (**8**, 0.41 g, 2.1 mmol) were suspended in water (10 mL), heated to reflux for 1 h. After cooling to rt the water was decanted off and the precipitate recrystallized from ethanol to afford **10** as an off-white solid (yield: 85%). mp: 109–110 °C. ¹H NMR (400 MHz, CDCl₃): δ (ppm) = 7.04–6.83 (m, 4H; Ar-H), 4.04 (s, 1H, OH), 3.86 (s, 3H, OCH₃), 3.41 (td, *J* = 9.8, 4.5 Hz, 1H, 2-H), 3.20–2.83 (m, 6H, CH₂ piperazine), 2.62 (dt, *J* = 10.2, 4.7 Hz, 2H, CH₂ piperazine), 2.32–2.22 (m, 1H, 1-H), 2.18–2.10 (m, 1H, CH₂ cyclohexane), 1.92–1.68 (m, 3H, CH₂ cyclohexane), 1.32–1.17 (m, 4H, CH₂ cyclohexane). ¹³C NMR (101 MHz, CDCl₃): δ (ppm) = 152.2 (C-2''), 141.3 (C-1''), 123.0 (C-4''), 121.0 (C-5''), 118.3 (C-6''), 111.1 (C-3''), 70.3 (C-1), 68.6 (C-2), 55.3 (OCH₃), 51.3 (CH₂ piperazine), 48.6 (CH₂ piperazine), 33.3 (CH₂ cyclohexane), 25.6 (CH₂ cyclohexane), 24.1 (CH₂ cyclohexane), 22.5 (CH₂ cyclohexane). IR (ATR): $\tilde{\nu}$ [cm⁻¹] = 3471, 2931, 2838, 2817, 1593, 1499, 1448, 1240, 1121, 1080, 1017, 949, 751, 741. HR-MS (ESI): calcd. for C₁₇H₂₇N₂O₂: 291.2067 [M+H]⁺; found: 291.2066. Purity (HPLC): >96%.

4.1.1.8. trans-1-(2-Azidocyclohexyl)-4-(2-methoxyphenyl)piperazine (11). To a solution of **10** (0.35 g, 1.2 mmol) and triethylamine (0.34 mL, 2.4 mmol) in methylene chloride (12 mL) was added mesyl chloride (0.19 mL, 2.4 mmol) dropwise at 0 °C. After warming up to rt, the solution was stirred for 12 h. After addition of 1 N NaOH (15 mL) the phases were separated and the aqueous layer extracted twice with methylene chloride (20 mL). The combined organic phases were dried over Na₂SO₄ and the solvent removed *in vacuo*. The residue was dissolved in dimethyl formamide (10 mL) and sodium azide (0.39 g, 6.0 mmol) added. The resulting mixture was heated to reflux for 24 h. After cooling to rt 1 N NaOH (50 mL) was added and the aqueous layer extracted with methylene chloride (3 × 50 mL). The combined organic layers were washed with water (100 mL) and brine (100 mL), dried over Na₂SO₄ and the solvent removed *in vacuo*. Purification by FCC using petrol ether/ethyl acetate/triethylamine (7:3:0.1) as an eluent gave **11** as a white solid (yield: 55%). mp: 77–88 °C. ¹H NMR (500 MHz, CDCl₃): δ (ppm) = 7.02–6.89 (m, 3H, 4''-H, 5''-H, 6''-H), 6.85 (dd, *J* = 8.0, 1.4 Hz, 1H, 3''-H), 3.86 (s, 3H, OCH₃), 3.35 (td, *J* = 10.6, 4.4 Hz, 1H, 2'-C), 3.10 (s, 4H; CH₂ piperazine), 2.93 (dt, *J* = 10.1, 4.7 Hz, 2H, CH₂ piperazine), 2.76–2.70 (m, 2H, CH₂ piperazine), 2.46 (ddd, *J* = 11.7, 10.3, 3.7 Hz, 1H, 1'-H), 2.07–1.93 (m, 2H, CH₂ cyclohexane), 1.84–1.66 (m, 2H, CH₂ cyclohexane), 1.32–1.14 (m, 4H, CH₂ cyclohexane). ¹³C NMR (126 MHz, CDCl₃): δ (ppm) = 152.4 (C-1''), 141.7 (C-1''), 122.9 (C-4''), 121.1 (C-5''), 118.5 (C-6''), 111.1 (C-3''), 68.5 (C-1), 60.8 (C-2), 55.4 (OCH₃), 51.0 (CH₂ piperazine), 48.8 (CH₂ piperazine), 32.6 (CH₂ cyclohexane), 25.2 (CH₂ cyclohexane), 24.9 (CH₂ cyclohexane), 24.0 (CH₂ cyclohexane). IR (ATR): $\tilde{\nu}$ [cm⁻¹] = 2924, 2823, 2091, 1593, 1497, 1446, 1265, 1236, 1143, 1113, 1026, 740. HR-MS (ESI): calcd. for C₁₇H₂₆N₅O⁺: 316.2132 [M+H]⁺; found: 316.2130. Purity (HPLC): >96%.

4.1.1.9. cis-N-(2-Aminocyclohexyl)benzenesulfonamide (13). To a solution of cis-1,2-cyclohexanediamine (0.59 g, 5.0 mmol) and triethylamine (2.8 mL, 20 mmol) in methylene chloride (30 mL) was added benzenesulfonyl chloride (0.64 mL, 5.0 mmol) at 0 °C and the solution stirred for 10 min. The solution was concentrated *in vacuo* and the residue taken up in ethyl acetate. The organic layer was washed with sat. aq. NaHCO₃ solution (20 mL), subsequently HCl conc. aq. (approx. 1 mL) added and extracted twice with water (20 mL). The combined aqueous layers were brought to pH 9 with a 50% NaOH in water solution and extracted three times with ethyl acetate (30 mL). The combined organic layers were dried over Na₂SO₄ and the solvent removed *in vacuo*, to afford **13** as a light

brown solid (yield: 81%). mp: 75–76 °C ¹H NMR (400 MHz, CDCl₃): δ (ppm) = 7.93–7.85 (m, 2H, 2-H, 6-H), 7.59–7.53 (m, 1H, 4-H), 7.53–7.47 (m, 2H, 3-H, 5-H), 5.29 (bs, 1H, SO₂NH), 3.16 (dt, *J* = 7.7, 3.8 Hz, 1H, CH cyclohexane), 2.82 (dt, *J* = 7.3, 3.7 Hz, 1H, CH cyclohexane), 1.66–0.99 (m, 10H, CH₂ cyclohexane, NH₂). ¹³C NMR (101 MHz, CDCl₃): δ (ppm) = 141.1 (C-1), 132.5 (C-4), 129.1 (C-3, C-5), 127.2 (C-2, C-6), 54.6 (CH cyclohexane), 50.1 (CH cyclohexane), 31.6 (CH₂), 28.6 (CH₂), 22.1 (CH₂), 21.3 (CH₂). IR (ATR): $\tilde{\nu}$ [cm⁻¹] = 3375, 2931, 1445, 1307, 1151, 1091, 930, 758. HR-MS (ESI): calcd. for C₁₂H₁₉N₂O₂S⁺: 255.1162 [M+H]⁺; found: 255.1161. Purity (NMR): >96%.

4.1.1.10. N,N-Bis(2-hydroxyethyl)-2-methoxyaniline (14). 2-Methoxyaniline (0.37 g, 3.0 mmol) and ethylene oxide (4.6 mL of an approx. 3.3 M solution in THF, ~15 mmol) in 1 N aqueous acetic acid (10 mL) were stirred for 40 h, then the solution poured into brine (15 mL) and extracted three times with ethyl acetate (30 mL). The combined organic layers were dried over Na₂SO₄ and the solvent removed *in vacuo*. The residue was purified by FCC using ethyl acetate as an eluent to afford **14** as a colourless oil (yield: 86%). ¹H NMR (400 MHz, CDCl₃): δ (ppm) = 7.21 (dd, *J* = 7.8, 1.7 Hz, 1H, 6-H), 7.16 (ddd, *J* = 8.2, 7.5, 1.7 Hz, 1H, 4-H), 6.98 (td, *J* = 7.6, 1.4 Hz, 1H, 3-H), 6.93 (dd, *J* = 8.2, 1.4 Hz, 1H, 5-H), 3.88 (s, 3H, OCH₃), 3.52–3.48 (m, 4H, 2 CH₂O), 3.23–3.07 (m, 6H, 2 CH₂N, OH). ¹³C NMR (101 MHz, CDCl₃): δ (ppm) = 155.8 (C-2), 138.2 (C-1), 126.4 (C-4), 125.4 (C-6), 121.9 (C-3), 111.7 (C-5), 59.9 (NCH₂), 57.8 (OCH₂), 55.8 (OCH₃). IR (ATR): $\tilde{\nu}$ [cm⁻¹] = 3359, 2926, 1593, 1497, 1236, 1024, 746. HR-MS (ESI): calcd. for C₁₁H₁₈NO₃: 212.1281 [M+H]⁺; found: 212.1280. Purity (HPLC): >96%.

4.1.1.11. cis-N-(2-(4-(2-Methoxyphenyl)piperazin-1-yl)cyclohexyl)benzenesulfonamide (cis-ML-S13). 14 (450 mg, 2.13 mmol) was dissolved in methylene chloride (5 mL) and a solution of thionyl chloride (0.326 mL, 4.47 mmol) in methylene chloride (4.5 mL) added dropwise. The solution was heated for 1 h at 40 °C, then the solvent and excess of thionyl chloride were removed *in vacuo*. The residue was dissolved in ethanol (5 mL), K₂CO₃ and a solution of compound **13** (1.08 g, 4.26 mmol) in ethanol (10 mL) added. The reaction mixture was heated to reflux for 72 h and then the solvent removed *in vacuo*. The residue was taken up in methylene chloride, the inorganic salts filtered off and the solvent removed *in vacuo*. The residue was purified by FCC using petrol ether/ethyl acetate/triethylamine (6:4:0.1) as an eluent, followed by recrystallization from ethanol to afford cis-ML-S13 as a pale yellow solid (yield: 42%). mp: 129–130 °C. ¹H NMR (500 MHz, CDCl₃): δ (ppm) = 7.95–7.86 (m, 2H, 2-H, 6-H), 7.60–7.56 (m, 1H, 4-H), 7.52 (ddt, *J* = 8.4, 6.5, 1.5 Hz, 2H, 3-H, 5-H), 7.01 (td, *J* = 7.7, 1.7 Hz, 1H, 4''-H), 6.94 (td, *J* = 7.6, 1.5 Hz, 1H, 5''-H), 6.86 (ddd, *J* = 8.5, 7.9, 1.6 Hz, 2H, 6''-H, 3''-H), 5.45 (s, 1H, NH), 3.83 (s, 3H, OCH₃), 3.34 (q, *J* = 3.4 Hz, 1H, 1'-H), 2.83 (s, 4H, CH₂ piperazine), 2.60–2.34 (m, 3H, CH₂ piperazine, 6'-H), 2.23 (dt, *J* = 10.5, 4.8 Hz, 2H, CH₂ piperazine), 2.10 (dt, *J* = 12.0, 3.9 Hz, 1H, 2'-H), 1.84–1.75 (m, 2H, CH₂ cyclohexane), 1.64–1.55 (m, 1H, CH₂ cyclohexane), 1.39–1.15 (m, 4H, CH₂ cyclohexane). ¹³C NMR (126 MHz, CDCl₃): δ (ppm) = 152.4 (C-2'''), 141.1 (C-1'''), 139.6 (C-1), 132.7 (C-4), 129.1 (C-3, C-5), 127.5 (C-2, C-6), 123.3 (C-4''), 121.2 (C-5''), 118.2 (C-6''), 111.3 (C-3''), 63.6 (C-2''), 55.5 (OCH₃), 51.0 (CH₂ piperazine), 49.5 (CH₂ piperazine), 49.1 (C-1'), 28.7 (C-6'), 25.0 (CH₂ cyclohexane), 24.7 (CH₂ cyclohexane), 18.9 (CH₂ cyclohexane). IR (ATR): $\tilde{\nu}$ [cm⁻¹] = 3148, 2808, 1499, 1333, 1168, 1237, 1022, 733. HR-MS (ESI): calcd. for C₂₃H₃₂N₃O₃S⁺: 430.2159 [M+H]⁺; found: 430.2152. Purity (HPLC): >96%.

4.1.1.12. 7-(4-Methylbenzenesulfonyl)-7-azabicyclo[4.1.0]heptane (15). Following general procedure A, chloramine T hydrate (1.2 g, 4.8 mmol), cyclohexene (0.5 mL, 4.8 mmol) and NBS (0.17 g,

0.96 mmol) were reacted in 25 mL acetonitrile. Purification by FCC gave **15** as a white solid (yield: 34%). mp: 56–57 °C (lit.: 55–57 °C [29]). ¹H NMR (400 MHz, CDCl₃): δ (ppm) = 7.86–7.77 (m, 2H, 2-H, 6-H), 7.35–7.29 (m, 2H, 3-H, 5-H), 2.97 (p, *J* = 1.5 Hz, 2H, 1'-H, 2'-H), 2.44 (s, 3H, CH₃), 1.81–1.74 (m, 4H, 2'-H, 5'-H), 1.45–1.34 (m, 2H, 3'-H or 4'-H), 1.27–1.16 (m, 2H, 3'-H or 4'-H). ¹³C NMR (101 MHz, CDCl₃): δ (ppm) = 144.1 (C-4), 136.0 (C-1), 129.7 (C-3, C-5), 127.8 (C-2, C-6), 39.9 (C-1', C-2'), 22.9 (C-3', C-6'), 21.8 (CH₃), 19.6 (C-4', C-5'); IR (ATR): $\bar{\nu}$ [cm⁻¹] = 2946, 2864, 1315, 1288, 1155, 1087, 961, 921, 849, 721, 664; HR-MS (ESI): calcd. for C₁₃H₁₈NO₂S⁺: 252.1053 [M+H]⁺, found 252.1053; purity (HPLC): >96%.

4.1.1.13. *trans-N*-(2-Hydroxycyclohexyl)thiophene-2-sulfonamide.

Cyclohexene oxide (0.30 mL, 3.0 mmol), thiophene-2-sulfonamide (0.59 mg, 3.6 mmol), benzyltriethylammonium chloride (68 mg, 0.30 mmol) and K₂CO₃ (50 mg, 0.30 mmol) were suspended in dioxane (2 mL). The reaction mixture was heated to 90 °C and stirred for 16 h. After cooling to rt the mixture was diluted with methylene chloride, the solids filtered off and the solvent removed *in vacuo*. The residue was purified by FCC using diethyl ether/petrol ether 8:2 as an eluent to give the target compound as a white solid (yield: 100%). mp: 110–111 °C. ¹H NMR (500 MHz, CDCl₃): δ (ppm) = 7.66 (dd, *J* = 3.7, 1.3 Hz, 1H, 3-H), 7.61 (dd, *J* = 5.0, 1.3 Hz, 1H, 5-H), 7.10 (dd, *J* = 5.0, 3.7 Hz, 1H, 4-H), 4.79 (d, *J* = 6.8 Hz, 1H, NH), 3.38–3.29 (m, 1H, 2'-H), 3.00–2.93 (m, 1H, 1'-H), 2.35 (d, *J* = 3.5 Hz, 1H, OH), 2.07–2.00 (m, 1H, CH₂ cyclohexane), 1.90–1.81 (m, 1H, CH₂ cyclohexane), 1.73–1.60 (m, 2H, CH₂ cyclohexane), 1.30–1.13 (m, 4H, CH₂ cyclohexane). ¹³C NMR (126 MHz, CDCl₃): δ (ppm) = 141.3 (C-2), 132.7 (C-3), 132.3 (C-5), 127.6 (C-4), 73.4 (C-2'), 60.3 (C-1'), 33.7 (C-3'), 32.0 (C-6'), 24.8 (C-4' or C-5'), 24.0 (C-4' or C-5'). IR (ATR): $\bar{\nu}$ [cm⁻¹] = 3487, 3141, 2942, 2858, 1449, 1402, 1311, 1150, 1138, 1062, 727, 672. HR-MS (ESI): calcd. for C₁₀H₁₄NO₃S₂: 260.0421 [M-H]⁻, found: 260.0419. purity (HPLC): >96%.

4.1.1.14. 7-(Thiophen-2-ylsulfonyl)-7-azabicyclo[4.1.0]heptane (**16**).

p-Toluenesulfonyl chloride (2.9 g, 15 mmol) was suspended in methylene chloride (15 mL) and pyridine (1.2 mL, 15 mmol) added dropwise at 0 °C. The resulting solution was stirred for 20 min at 0 °C, then a solution of *trans-N*-(2-hydroxycyclohexyl)thiophene-2-sulfonamide in methylene chloride (10 mL) added dropwise. After stirring at 0 °C for 20 min, the solution was heated to 40 °C and stirred at this temperature for 72 h. After cooling to rt, the mixture was washed with 2 N HCl and brine, dried over Na₂SO₄ and the solvent removed *in vacuo*. The residue was purified by FCC and directly used for the next step. The crude tosylate was dissolved in acetonitrile (20 mL), K₂CO₃ (0.70 g, 1.7 mmol) was added and the mixture heated to reflux for 4 h. Acetonitrile was removed *in vacuo*, the residue taken up in methylene chloride, the organic layer washed with water and brine, dried over Na₂SO₄ and the solvent removed *in vacuo*. Purification by FCC using petrol ether/ethyl acetate 7:3 as an eluent gave **16** as a white solid (yield: 59%). mp: 67–68 °C (lit. 71–71.5 °C [33]). ¹H NMR (400 MHz, CDCl₃): δ (ppm) = 7.70 (dd, *J* = 3.7, 1.4 Hz, 1H, 3-H), 7.66 (dd, *J* = 5.0, 1.4 Hz, 1H, 5-H), 7.12 (dd, *J* = 5.0, 3.8 Hz, 1H, 4-H), 3.02 (tt, *J* = 1.9, 1.1 Hz, 2H, 1'-H, 2'-H), 1.90–1.78 (m, 4H, 3'-H, 6'-H), 1.49–1.39 (m, 2H, 4'-H or 5'-H), 1.29–1.19 (m, 2H, 4'-H or 5'-H). ¹³C NMR (101 MHz, CDCl₃): δ (ppm) = 139.1 (C-2'), 133.2 (C-3), 133.0 (C-5), 127.4 (C-4), 40.8 (C-1', C-2'), 22.9 (C-3', C-6'), 19.5 (C-4', C-5'). IR (ATR): $\bar{\nu}$ [cm⁻¹] = 3121, 2949, 1401, 1312, 1143, 1016, 964, 923, 849, 737, 714. HR-MS (ESI): calcd. for C₁₀H₁₄NO₂S₂: 244.0460 [M+H]⁺, found: 244.0460. Purity (NMR): >96%.

4.1.1.15. *trans-N*-(2-(4-(2-Methoxyphenyl)piperazin-1-yl)cyclohexyl)-4-methylbenzenesulfonamide (**17**).

Following general

procedure B, 7-(4-methylbenzenesulfonyl)-7-azabicyclo[4.1.0]heptane (**15**, 139 mg, 0.551 mmol) and 1-(2-methoxyphenyl)piperazine (**8**, 127 mg, 0.662 mmol) were reacted to give **17** (yield: 63%). mp: 132–133 °C. ¹H NMR (400 MHz, CDCl₃): δ (ppm) = 7.81–7.75 (m, 2H, 3-H, H-5), 7.34–7.29 (m, 2H, 2-H, 6-H), 7.02 (ddd, *J* = 7.9, 7.3, 1.8 Hz, 1H, H-4'''), 6.95 (td, *J* = 7.6, 1.5 Hz, 1H, H-5'''), 6.90 (dd, *J* = 7.8, 1.8 Hz, 1H, H-3'''), 6.86 (dd, *J* = 8.0, 1.5 Hz, 1H, H-6'''), 6.08 (s, 1H, NH), 3.84 (s, 3H, OCH₃), 3.06–2.64 (m, 5H), 2.52–2.16 (m, 9H), 1.91–1.64 (m, 3H, CH₂ cyclohexane), 1.35–1.03 (m, 4H, CH₂ cyclohexane). ¹³C NMR (101 MHz, CDCl₃): δ (ppm) = 152.3 (C-2'''), 143.4 (C-4), 141.2 (C-1'''), 136.9 (C-1), 129.7 (C-2, C-6), 127.4 (C-3, C-5), 123.3 (C-4'''), 121.2 (C-5'''), 118.4 (C-3'''), 111.2 (C-6'''), 66.8 (C-2'), 55.5 (OCH₃), 53.5 (C-1'), 51.2 (CH₂ piperazine), 33.0 (CH₂ cyclohexane), 25.5 (CH₂ cyclohexane), 24.3 (CH₂ cyclohexane), 23.2 (CH₂ cyclohexane), 21.7 (CH₃). IR (ATR): $\bar{\nu}$ [cm⁻¹] = 3183, 2933, 2809, 1498, 1448, 1339, 1239, 1167, 1022, 753, 704. HR-MS (ESI): calcd. for C₂₄H₃₄N₃O₃S⁺: 444.2315 [M+H]⁺, found: 444.2316. purity (HPLC): >96%.

4.1.1.16. *trans-N*-(2-(4-(2-Methoxyphenyl)piperazin-1-yl)cyclohexyl)thiophene-2-sulfonamide (**18**).

Following general procedure B, 7-(thiophen-2-ylsulfonyl)-7-azabicyclo[4.1.0]heptane (**16**, 125 mg, 0.514 mmol) and 1-(2-methoxyphenyl)piperazine (**8**, 116 mg, 0.603 mmol) were reacted to give **18** as an off-white solid (yield: 78%). mp: 149–150 °C. ¹H NMR (400 MHz, CDCl₃): δ (ppm) = 7.62 (dd, *J* = 3.7, 1.3 Hz, 1H, 3-H), 7.58 (dd, *J* = 5.0, 1.3 Hz, 1H, 5-H), 7.11 (dd, *J* = 5.0, 3.7 Hz, 1H, 4-H), 7.02 (ddd, *J* = 8.0, 7.2, 1.9 Hz, 1H, 4'''), 6.94 (td, *J* = 7.5, 1.4 Hz, 1H, 5'''), 6.89 (dd, *J* = 7.8, 1.9 Hz, 1H, 6'''), 6.85 (dd, *J* = 8.0, 1.5 Hz, 1H, 3'''), 6.21 (s, 1H, NH), 3.84 (s, 3H, OCH₃), 3.06–2.21 (m, 11H), 1.96–1.66 (m, 3H, CH₂ cyclohexane), 1.39–1.11 (m, 4H, CH₂ cyclohexane). ¹³C NMR (101 MHz, CDCl₃): δ (ppm) = 152.3 (C-2'''), 141.2 (C-1'''), 140.9 (C-1), 132.0 (C-3), 131.7 (C-5), 127.6 (C-4), 123.3 (C-4'''), 121.2 (C-5'''), 118.4 (C-6'''), 111.2 (C-3'''), 66.7 (C-2'), 55.5 (OCH₃), 54.0 (C-1'), 51.2 (CH₂ piperazine), 33.0 (C-6'), 25.5 (CH₂ cyclohexane), 24.4 (CH₂ cyclohexane), 23.2 (CH₂ cyclohexane). IR (ATR): $\bar{\nu}$ [cm⁻¹] = 3159, 2936, 2873, 2831, 1344, 1239, 1227, 1158, 1141, 1032, 1016, 729, 706. HR-MS (ESI): calcd. for C₂₁H₃₀N₃O₃S₂: 436.1723 [M+H]⁺, found: 436.1723. purity (HPLC) > 96%.

4.1.1.17. *trans-N*-(2-(4-(2-Methoxyphenyl)piperazin-1-yl)cyclohexyl)benzamide (**20**).

Azide **11** (0.43 g, 1.5 mmol) was dissolved in ethanol (30 mL), 10% Pd/C (~50 mg) added, and the mixture stirred under hydrogen atmosphere for 72 h. The catalyst was removed by filtration over a pad of Celite and the solvent removed *in vacuo*. A part of the crude product (0.11 g, 0.39 mmol) was dissolved in pyridine (3 mL), cooled to 0 °C and benzoyl chloride (90 μL, 0.76 mmol) added. The solution was stirred and warmed up to rt over 3 h. Satd. aqueous NaHCO₃ solution (15 mL) and ethyl acetate (20 mL) were added and the phases separated. The organic layer was washed with water (15 mL) and brine (15 mL), dried over Na₂SO₄ and the solvent removed *in vacuo*. The crude product was recrystallized from ethanol to afford **20** as a pale yellow solid (yield: 42%). mp: 144–145 °C. ¹H NMR (400 MHz, CDCl₃): δ (ppm) = 7.83–7.78 (m, 2H, 2-H, 6-H), 7.50–7.45 (m, 1H, 4-H), 7.45–7.39 (m, 2H, 3-H, 5-H), 7.04 (d, *J* = 4.1 Hz, 1H, NH), 7.01–6.95 (m, 1H, 4'''), 6.91–6.82 (m, 3H, 6''', 5''', 3'''), 3.85 (s, 3H, OCH₃), 3.70 (tt, *J* = 10.8, 4.0 Hz, 1H, 1'-H), 3.14–2.86 (m, 6H, CH₂ piperazine), 2.73 (d, *J* = 12.6 Hz, 1H, 6'-H), 2.62 (dt, *J* = 10.3, 4.5 Hz, 2H, CH₂ piperazine), 2.49 (td, *J* = 11.0, 3.1 Hz, 1H, 2'-H), 2.02 (d, *J* = 11.4 Hz, 1H, CH₂ cyclohexane), 1.88 (d, *J* = 11.4 Hz, 1H, CH₂ cyclohexane), 1.74 (d, *J* = 13.4 Hz, 1H, CH₂ cyclohexane), 1.48–1.12 (m, 4H, CH₂ cyclohexane). ¹³C NMR (101 MHz, CDCl₃): δ (ppm) = 167.9 (OCNH), 152.3 (C-2''), 141.4 (C-1'''), 135.5 (C-1), 131.3 (C-4), 128.7 (C-3, C-5), 127.0 (C-2, C-6), 123.1 (C-4'''), 121.0 (C-

5^{'''}), 118.3 (C-6^{'''}), 111.3 (C-3^{'''}), 67.5 (C-2'), 55.5 (OCH₃), 51.6 (CH₂ piperazine), 51.3 (C-1'), 48.2 (CH₂ piperazine), 32.8 (CH₂ cyclohexane), 25.8 (CH₂ cyclohexane), 24.8 (CH₂ cyclohexane), 23.5 (CH₂ cyclohexane). IR (ATR): $\bar{\nu}$ [cm⁻¹] = 3310, 2923, 2818, 1626, 1542, 1503, 1240. HR-MS (ESI): calcd. for C₂₄H₃₂N₃O₂: 394.2489 [M+H]⁺; found: 394.2483. Purity (HPLC): >96%.

4.1.1.18. trans-N-(2-(4-Phenylpiperazin-1-yl)cyclohexyl)benzenesulfonamide (21). Following general procedure B, 7-(phenylsulfonyl)-7-azabicyclo[4.1.0]heptane (**7**, 125 mg, 0.527 mmol) and 1-phenylpiperazine (92 μ L, 0.60 mmol) were reacted to give **21** as a white solid (yield: 77%), mp: 154–155 °C. ¹H NMR (500 MHz, CDCl₃): δ (ppm) = 7.96–7.91 (m, 2H, 2-H, 6-H), 7.65–7.61 (m, 1H, 4-H), 7.58–7.53 (m, 2H, 3-H, 5-H), 7.32–7.26 (m, 2H, 3^{'''}-H, 5^{'''}-H), 6.93–6.87 (m, 3H, 2^{''}-H, 4^{''}-H, 6^{''}-H), 6.04 (s, 1H, NH), 3.07–2.92 (m, 4H, CH₂ piperazine), 2.78 (td, *J* = 10.6, 4.1 Hz, 1H, 1[']-H), 2.55–2.50 (m, 1H, 6[']-H), 2.42–2.26 (m, 5H), 1.90–1.69 (m, 3H, CH₂ cyclohexane), 1.37–1.05 (m, 4H, CH₂ cyclohexane). ¹³C NMR (126 MHz, CDCl₃): δ (ppm) = 151.2 (C-1^{'''}), 139.8 (C-1), 132.6 (C-4), 129.2 (C-3^{'''}, C-5^{'''}), 129.1 (C-3, C-5), 127.2 (C-2, C-6), 120.1 (C-4^{'''}), 116.3 (C-2^{''}, C-6^{''}), 66.6 (C-2'), 53.4 (C-1'), 49.7 (CH₂ piperazine), 47.6 (CH₂ piperazine), 32.9 (C-6'), 25.2 (CH₂ cyclohexane), 24.2 (CH₂ cyclohexane), 22.8 (CH₂ cyclohexane). IR (ATR): $\bar{\nu}$ [cm⁻¹] = 3183, 2935, 2852, 1600, 1504, 1449, 1159, 754, 724, 689. HR-MS (ESI): calcd. for C₂₂H₃₀N₃O₂S⁺: 400.2053 [M+H]⁺; found: 400.2053. purity (HPLC): >96%.

4.1.1.19. trans-N-(2-(4-(3-(Trifluoromethyl)phenyl)piperazin-1-yl)cyclohexyl)benzenesulfonamide (22). Following general procedure B, 7-(phenylsulfonyl)-7-azabicyclo[4.1.0]heptane (**7**, 120 mg, 0.506 mmol) and 1-(3-(trifluoromethyl)phenyl)piperazine (140 mg, 0.608 mmol) were reacted to give **22** as a white solid (yield: 77%), mp: 111–112 °C. ¹H NMR (500 MHz, CDCl₃): δ (ppm) = 7.93–7.89 (m, 2H, 2-H, 6-H), 7.64–7.59 (m, 1H, H-4), 7.57–7.51 (m, 2H, 3-H, 5-H), 7.37–7.32 (m, 1H, 5[']-H), 7.11–7.07 (m, 1H, 4[']-H), 7.05–7.02 (m, 1H, 2^{''}-H), 6.99 (dd, *J* = 8.3, 2.6 Hz, 1H, 6[']-H), 5.95 (s, 1H, NH), 3.08–2.92 (m, 4H), 2.80 (td, *J* = 10.5, 4.1 Hz, 1H, 1[']-H), 2.51–2.44 (m, 1H, 6[']-H), 2.41–2.25 (m, 5H), 1.87–1.65 (m, 3H, CH₂ cyclohexane), 1.34–1.04 (m, 4H, CH₂ cyclohexane). ¹³C NMR (126 MHz, CDCl₃): δ (ppm) = 151.2 (C-1^{'''}), 139.9 (C-1), 132.7 (C-4), 131.5 (q, *J* = 31.7 Hz, C-3^{'''}), 129.6 (C-5^{'''}), 129.1 (C-3, C-5), 127.2 (C-2, C-6), 124.3 (q, *J* = 27.2 Hz, CF₃), 118.9 (C-6^{'''}), 116.2 (q, *J* = 3.8 Hz, C-4^{'''}), 112.5 (q, *J* = 3.9 Hz, C-2^{''}), 66.58 (C-2'), 53.4 (C-1'), 49.2 (CH₂ piperazine), 47.4 (CH₂ piperazine), 33.0 (CH₂ cyclohexane), 25.2 (CH₂ cyclohexane), 24.1 (CH₂ cyclohexane), 22.9 (CH₂ cyclohexane). IR (ATR): $\bar{\nu}$ [cm⁻¹] = 2939, 1446, 1346, 1308, 1156, 1119, 1092, 756, 729, 689. HR-MS (ESI): calcd. for C₂₃H₂₉F₃N₃O₂S⁺: 468.1927 [M+H]⁺; found: 468.1928. purity (HPLC): >96%.

4.1.1.20. trans-N-(2-(4-(4-Methylbenzyl)piperazin-1-yl)cyclohexyl)benzenesulfonamide (23). Following general procedure B, 7-(phenylsulfonyl)-7-azabicyclo[4.1.0]heptane (**7**, 125 mg, 0.527 mmol) and 1-(4-methylbenzyl)piperazine (117 mg, 0.615 mmol) were reacted to give **23** as a pale yellow solid (yield: 49%), mp: 97–98 °C. ¹H NMR (400 MHz, CDCl₃): δ (ppm) = 7.90–7.86 (m, 2H, 2-H, 6-H), 7.58–7.53 (m, 1H, 4-H), 7.52–7.47 (m, 2H, 3-H, 5-H), 7.18–7.11 (m, 4H, Ar-H), 6.06 (s, 1H, NH), 3.42 (s, 2H, 1[']-H), 2.65 (td, *J* = 10.5, 4.0 Hz, 1H, 1[']-H), 2.53–1.87 (m, 13H), 1.81–1.64 (m, 3H, CH₂ cyclohexane), 1.35–0.90 (m, 4H, CH₂ cyclohexane). ¹³C NMR (101 MHz, CDCl₃): δ (ppm) = 139.8 (C-1), 136.9 (C-4^{'''}), 134.9 (C-1^{'''}), 132.6 (C-4), 129.3 (C-3, C-5), 129.1 (C-Ar), 127.4 (C-2, C-6), 66.6 (C-2'), 62.9 (C-1^{'''}), 53.5 (C-1'), CH₂ piperazine), 32.9 (C-6'), 25.4 (CH₂ cyclohexane), 24.3 (CH₂ cyclohexane), 23.0 (CH₂ cyclohexane), 21.3 (CH₃). IR (ATR): $\bar{\nu}$ [cm⁻¹] = 3204, 2929, 2817, 1448, 1401, 1332, 1317, 1169, 1098, 1010, 758. HR-MS (ESI): calcd. for C₂₄H₃₄N₃O₂S⁺: 428.2366

[M+H]⁺; found: 428.2366. purity (HPLC): >96%.

4.1.1.21. trans-N-(2-(4-Phenethylpiperazin-1-yl)cyclohexyl)benzenesulfonamide (24). Following general procedure B, 7-(phenylsulfonyl)-7-azabicyclo[4.1.0]heptane (**7**, 130 mg, 0.548 mmol) and 1-phenethylpiperazine (121 mg, 0.636 mmol) were reacted to give **24** as an off-white solid (yield: 45%), mp: 92–93 °C. ¹H NMR (500 MHz, CDCl₃): δ (ppm) = 7.92–7.87 (m, 2H, 2-H, 6-H), 7.59–7.54 (m, 1H, 4-H), 7.52–7.48 (m, 2H, 3-H, 5-H), 7.32–7.27 (m, 2H, 3^{'''}-H, 5^{'''}-H), 7.23–7.18 (m, 3H, 2^{''}-H, 4^{''}-H, 6^{''}-H), 6.04 (s, 1H, NH), 2.83–2.09 (m, 15H), 1.84–1.64 (m, 3H, CH₂ cyclohexane), 1.31–1.00 (m, 4H, CH₂ cyclohexane). ¹³C NMR (126 MHz, CDCl₃): δ (ppm) = 140.2 (C-1^{'''}), 139.7 (C-1), 132.5 (C-4), 128.7 (C-3^{'''}, C-5^{'''}), 128.5 (C-2^{''}, C-6^{''}), 127.2 (C-2, C-6), 126.1 (C-4^{'''}), 66.4 (C-2'), 60.4 (C-1'), 53.6 (CH₂ piperazine), 53.4 (C-1'), 33.7 (C-2^{''}), 32.8 (C-6'), 25.3 (CH₂ cyclohexane), 24.2 (CH₂ cyclohexane), 22.8 (CH₂ cyclohexane). IR (ATR): $\bar{\nu}$ [cm⁻¹] = 3578, 3168, 2827, 1645, 1454, 1336, 1310, 1163, 1089, 1005, 762, 723. HR-MS (ESI): calcd. for C₂₄H₃₄N₃O₂S⁺: 428.2366 [M+H]⁺; found: 428.2366. purity (HPLC): >96%.

4.1.1.22. trans-N-(2-(4-Methylpiperazin-1-yl)cyclohexyl)benzenesulfonamide (25). Following general procedure B, 7-(phenylsulfonyl)-7-azabicyclo[4.1.0]heptane (**7**, 123 mg, 0.518 mmol) and 1-methylpiperazine (69 μ L, 0.62 mmol) reacted and the crude product purified by FCC using methylene chloride/methanol/triethylamine as an eluent to give **25** as a white solid (yield: 57%), mp: 106–107 °C. ¹H NMR (500 MHz, CDCl₃): δ (ppm) = 7.92–7.88 (m, 2H, 3-H, 5-H), 7.61–7.55 (m, 1H, 4-H), 7.52 (dd, *J* = 8.4, 6.6, 1.4 Hz, 2H, 2-H, 6-H), 6.00 (s, 1H, NH), 2.68 (td, *J* = 10.6, 4.1 Hz, 1H, 1[']-H), 2.49–2.04 (m, 12H), 1.82–1.63 (m, 3H, CH₂), 1.30–0.99 (m, 5H, CH₂). ¹³C NMR (126 MHz, CDCl₃): δ (ppm) = 139.9 (C-1), 132.7 (C-4), 129.1 (C-2, C-6), 127.4 (C-3, C-5), 66.6 (C-1'), 55.5 (CH₂ piperazine), 53.5 (C-2'), 46.1 (CH₃), 32.9 (CH₂ cyclohexane), 25.4 (CH₂ cyclohexane), 24.3 (CH₂ cyclohexane), 22.9 (CH₂ cyclohexane). IR (ATR): $\bar{\nu}$ [cm⁻¹] = 2923, 2819, 1448, 1162, 757, 719, 691. HR-MS (ESI): calcd. for C₁₇H₂₈N₃O₂S⁺: 338.1897 [M+H]⁺; found 338.1898. purity (HPLC): >96%.

4.1.1.23. trans-N-(2-(4-(2-Methoxyphenyl)piperidin-1-yl)cyclohexyl)benzenesulfonamide (26). Following general procedure B, 7-(phenylsulfonyl)-7-azabicyclo[4.1.0]heptane (**7**, 121 mg, 0.510 mmol) and 4-(2-methoxyphenyl)piperidine (120 mg, 0.609 mmol) were reacted to give **26** as a white solid (yield: 85%), mp: 131–132 °C. ¹H NMR (400 MHz, CDCl₃): δ (ppm) = 7.94–7.88 (m, 2H, 2-H, 6-H), 7.57–7.47 (m, 3H, 3-H, 4-H, 5-H), 7.23–7.15 (m, 2H, 4[']-H, 6[']-H), 6.98 (td, *J* = 7.5, 1.1 Hz, 1H, 5[']-H), 6.86 (dd, *J* = 8.2, 1.1 Hz, 1H, 3[']-H), 6.21 (s, 1H, NH), 3.81 (s, 3H, OCH₃), 2.79 (tt, *J* = 12.0, 3.7 Hz, 1H, 4[']-H), 2.72–2.57 (m, 3H), 2.55–2.46 (m, 1H, 6[']-H), 2.27–2.18 (m, 1H, 2[']-H), 1.97 (td, *J* = 11.5, 2.5 Hz, 1H, CH₂ piperidine), 1.88–1.63 (m, 6H), 1.51–1.44 (m, 1H, 6[']-H), 1.35–0.99 (m, 5H). ¹³C NMR (101 MHz, CDCl₃): δ (ppm) = 156.9 (C-2^{''}), 139.8 (C-1), 134.2 (C-1^{'''}), 132.6 (C-4), 129.1 (C-3, C-5), 127.4 (C-2, C-6), 127.1 (C-4^{'''} or C-6^{'''}), 126.7 (C-4^{'''} or C-6^{'''}), 120.9 (C-5^{'''}), 110.5 (C-3^{'''}), 67.2 (C-2'), 55.5 (OCH₃), 53.7 (C-1'), 53.1 (CH₂ piperidine), 44.9 (CH₂ piperidine), 35.5 (C-4[']), 33.0 (C-6'), 32.7 (CH₂ piperidine), 32.7 (CH₂ piperidine), 25.5 (CH₂ cyclohexane), 24.4 (CH₂ cyclohexane), 22.9 (CH₂ cyclohexane). IR (ATR): $\bar{\nu}$ [cm⁻¹] = 3167, 2935, 2839, 1493, 1336, 1230, 1163, 1092, 1032, 757, 691. HR-MS (ESI): calcd. for C₂₄H₃₃N₂O₃S⁺: 429.2206 [M+H]⁺; found: 429.2205. purity (HPLC): >96%.

4.1.1.24. trans-N-(2-(4-Phenylpiperidin-1-yl)cyclohexyl)benzenesulfonamide (27). Following general procedure B, 7-(phenylsulfonyl)-7-azabicyclo[4.1.0]heptane (**7**, 120 mg, 0.506 mmol) and 4-phenylpiperidine (99 mg, 0.61 mmol) were reacted to give **27** as

white solid (yield: 72%), mp: 129–130 °C. ^1H NMR (500 MHz, CDCl_3): δ (ppm) = 7.96–7.88 (m, 2H, 2-H, 6-H), 7.58–7.48 (m, 3H, 3-H, 4-H, 5-H), 7.37–7.29 (m, 2H, 3''-H, 5''-H), 7.24–7.14 (m, 3H, 2''-H, 4''-H, 6''-H), 6.14 (s, 1H, NH), 2.74–2.46 (m, 4H), 2.35 (tt, J = 12.1, 3.6 Hz, 1H, 4'-H), 2.23 (td, J = 11.8, 3.2 Hz, 1H, 2'-H), 1.98–1.48 (m, 9H, CH_2), 1.34–1.02 (m, 5H, CH_2). ^{13}C NMR (126 MHz, CDCl_3): δ (ppm) = 146.1 (C-1'''), 139.8 (C-1), 132.7 (C-4), 129.1 (C-3, C-5), 128.6 (C-3'', C5''), 127.3 (C-2, C-6), 126.9 (C-2'', C-6''), 126.4 (C-4''), 67.2 (C-2'), 53.7 (C-1'), 52.9 (CH_2 piperidine), 44.7 (CH_2 piperidine), 42.9 (C-4'), 34.1 (CH_2 piperidine), 34.1 (CH_2 piperidine), 33.0 (CH_2 cyclohexane), 25.5 (CH_2 cyclohexane), 24.4 (CH_2 cyclohexane), 22.9 (CH_2 cyclohexane). IR (ATR): $\bar{\nu}$ [cm^{-1}] = 2932, 1344, 1313, 1164, 1086, 1068, 905, 759, 737, 691. HR-MS (ESI): calcd. for $\text{C}_{23}\text{H}_{31}\text{N}_2\text{O}_2\text{S}^+$: 399.2101 [$\text{M}+\text{H}$] $^+$; found: 399.2099. purity (HPLC): >96%.

4.1.1.25. *trans-N-(2-(1,2,3,4-Tetrahydroisoquinolin-2-yl)cyclohexyl)benzenesulfonamide (28)*. Following general procedure B, 7-(phenylsulfonyl)-7-azabicyclo[4.1.0]heptane (**7**, 122 mg, 0.514 mmol) and 1,2,3,4-tetrahydroisoquinoline (77 μL , 0.62 mmol) were reacted to give **28** as a yellow solid (yield: 24%), mp: 113–114 °C. ^1H NMR (500 MHz, CDCl_3): δ (ppm) = 7.84–7.77 (m, 2H, 2-H, 6-H), 7.62–7.55 (m, 1H, 4-H), 7.46 (t, J = 7.8 Hz, 2H, 3-H, 5-H), 7.12 (pd, J = 7.3, 1.8 Hz, 2H, 6''-H, 7''-H), 7.08–7.05 (m, 1H, 5''-H), 6.80 (d, J = 7.2 Hz, 1H, 8''-H), 6.10 (s, 1H, NH), 3.48–3.29 (m, 2H, 1''-H), 2.83–2.38 (m, 7H), 1.91–1.67 (m, 3H, CH_2 cyclohexane), 1.35–1.11 (m, 4H, CH_2 cyclohexane). ^{13}C NMR (126 MHz, CDCl_3): δ (ppm) = 139.7 (C-1), 134.4 (C-4a'' or C-8a''), 134.2 (C-4a'' or C-8a''), 132.5 (C-4), 129.0 (C-2, C-5), 128.7 (C-5''), 127.2 (C-2, C-6), 126.6 (C-8''), 126.2 (C-6'' or C-7''), 125.5 (C-6'' or C-7''), 66.6 (C-2'), 53.6 (C-1'), 50.3 (C-1''), 32.83 (C-3''), 32.8 (C-6'), 29.8 (C-4'). 25.29 (CH_2 cyclohexane), 24.2 (CH_2 cyclohexane), 22.6 (CH_2 cyclohexane). IR (ATR): $\bar{\nu}$ [cm^{-1}] = 2929, 1446, 1340, 1307, 1159, 1091, 903, 741, 724, 689. HR-MS (ESI): calcd. for $\text{C}_{21}\text{H}_{27}\text{N}_2\text{O}_2\text{S}^+$: 371.1788 [$\text{M}+\text{H}$] $^+$ found: 371.1788. purity (HPLC): >96%.

4.1.1.26. *1-(2-Methoxyphenyl)-4-(2-nitrophenyl)piperazine (30)*. A oven-dried Schlenk tube containing 2-bromonitrobenzene (0.20 g, 1.0 mmol), 1-(2-methoxyphenyl)piperazine (0.27 g, 1.4 mmol), $\text{Pd}(\text{OAc})_2$ (23 mg, 0.10 mmol), BINAP (93 mg, 0.15 mmol) and Cs_2CO_3 (0.46 g, 1.4 mmol) was degassed *in vacuo* and purged with N_2 , then dry toluene (12 mL) was added and the resulting suspension stirred for 30 min at rt, then at 80 °C for 16 h. After completion (TLC control) the mixture was filtered over a pad of Celite and the Celite washed several times with ethyl acetate (~30 mL). The filtrate was washed with water (20 mL) and brine (20 mL), dried over Na_2SO_4 and the solvent removed *in vacuo*. The residue was purified by FCC using petrol ether/ethyl acetate as an eluent to afford **30** as an orange solid (yield: 94%), mp: 117–118 °C. ^1H NMR (500 MHz, CDCl_3): δ (ppm) = 7.78 (dd, J = 8.1, 1.7 Hz, 1H, 3'-H), 7.50 (ddd, J = 8.2, 7.3, 1.6 Hz, 1H, 5'-H), 7.22 (dd, J = 8.3, 1.3 Hz, 1H, 6'-H), 7.08–6.98 (m, 3H, 4'-H, 4''-H, 6''-H), 6.97–6.93 (m, 1H, 5''-H), 6.89 (dd, J = 8.0, 1.4 Hz, 1H, 3''-H), 3.89 (s, 3H, OCH_3), 3.28–3.16 (m, 8H, CH_2). ^{13}C NMR (126 MHz, CDCl_3): δ (ppm) = 152.4 (C-2''), 146.3 (C-1'), 143.8 (C-2'), 141.1 (C-1''), 133.7 (C-5'), 126.0 (C-3'), 123.4 (C-4'), 122.0 (C-5''), 121.2 (C-6'), 118.6 (C-4'', C-6''), 111.4 (C-3''), 55.5 (OCH_3), 52.2 (C-2, C-6), 50.9 (C-3, C-5). IR (ATR): $\bar{\nu}$ [cm^{-1}] = 3373, 2930, 1480, 1444, 1307, 1149, 1090, 930, 717. HR-MS (ESI): calcd. for $\text{C}_{17}\text{H}_{20}\text{N}_2\text{O}_3$: 314.1499 [$\text{M}+\text{H}$] $^+$; found: 314.1496. Purity (HPLC): >96%.

4.1.1.27. *N-(2-(4-(2-methoxyphenyl)piperazin-1-yl)phenyl)benzenesulfonamide (31)*. **30** (0.16 g, 0.50 mmol) was dissolved in methanol

(30 mL), 10% Pd/C (~20 mg) added and the mixture stirred under hydrogen atmosphere for 72h. The catalyst was filtered off over a pad of Celite and the solvent removed *in vacuo*. A part of the crude product (78 mg, 0.27 mmol) was dissolved in methylene chloride (10 mL) containing triethylamine (0.15 mL, 1.1 mmol). Benzenesulfonyl chloride (0.16 mL, 1.25 mmol) was added dropwise and the solution stirred at rt for 16h. Satd. aqueous NaHCO_3 solution (10 mL) was added, the phases separated and the aqueous layer extracted with methylene chloride (2×15 mL). The combined organic layers were dried over Na_2SO_4 and the solvent removed *in vacuo*. The residue was purified by FCC using petrol ether/ethyl acetate as an eluent to afford **31** as a pale yellow solid (yield: 71%), mp: 147–148 °C. ^1H NMR (400 MHz, CDCl_3): δ (ppm) = 8.10 (s, 1H, NH), 7.84–7.78 (m, 2H, 2-H, 6-H), 7.65 (dd, J = 8.0, 1.5 Hz, 1H, 6'-H), 7.54–7.49 (m, 1H, 4-H), 7.42 (t, J = 7.8 Hz, 2H, 3-H, 5-H), 7.20–7.12 (m, 2H, 3'-H, 5'-H), 7.10–6.95 (m, 4H, 4'-H, 4''-H, 6''-H, 5''-H), 6.89 (dd, J = 7.9, 1.3 Hz, 1H, 3''-H), 3.88 (s, 3H, OCH_3), 3.11 (s, 4H, CH_2), 2.70 (s, 4H, CH_2). ^{13}C NMR (101 MHz, CDCl_3): δ (ppm) = 152.3 (C-2''), 142.3 (C-2'), 140.9 (C-1''), 139.6 (C-1), 133.2 (C-1'), 133.0 (C-4), 129.0 (C-3, C-5), 126.9 (C-2, C-6), 126.3 (C-5'), 124.7 (C-4'), 123.4 (C-4''), 122.4 (C-3'), 121.1 (C-5''), 119.1 (C-6'), 118.5 (C-6''), 111.3 (C-3''), 55.4 (OCH_3), 52.9 (CH_2), 51.3 (CH_2). IR (ATR): $\bar{\nu}$ [cm^{-1}] = 3228, 2835, 1495, 1236, 1170, 741. HR-MS (ESI): calcd. for $\text{C}_{23}\text{H}_{26}\text{N}_3\text{O}_3\text{S}^+$: 424.1689 [$\text{M}+\text{H}$] $^+$; found: 424.1684. Purity (HPLC): >96%.

4.1.2. Separation of enantiomers of *trans*-ML-S13

4.1.2.1. *Analytical chiral HPLC*. Stationary phase: Daicel Chiralcel-OD column (250 \times 4.6 mm, 10 μm); mobile phase: heptane/methyl *tert*-butyl ether/2-propanol/ethanolamine (50/48/2/0.1); sample solution: approx. 1 mg in 1 mL methyl *tert*-butyl ether; injection volume: 5 μL ; flow: 1.5 mL/min. Retention times of the enantiomers: 5.8 and 6.5 min.

4.1.2.2. *Semi-preparative chiral HPLC*. Stationary phase: YMC Chiral Art Cellulose-SB column (250 \times 10.0 mm, 5 μm); mobile phase: heptane/methyl *tert*-butyl ether/2-propanol/diethylamine (70/28/2/0.1); sample solution: saturated solution in methyl *tert*-butyl ether; injection volume: 1 mL; flow: 7.0 mL/min.

Analytical data of the separated enantiomers:

(–)-*trans-N-(2-(4-(2-methoxyphenyl)piperazin-1-yl)cyclohexyl)benzenesulfonamide*
ee-value: 99%, optical rotation: $[\alpha]_D^{23} = -19.6$ ($c = 0.103$, CHCl_3),
rt (HPLC): 5.8 min

(+)-*trans-N-(2-(4-(2-methoxyphenyl)piperazin-1-yl)cyclohexyl)benzenesulfonamide*
ee-value: 96%, optical rotation: $[\alpha]_D^{23} = +16.8$ ($c = 0.102$, CHCl_3),
rt (HPLC): 6.5 min

4.2. Biological experiments

4.2.1. Generation of the stably expressing hTRPML2-YFP cell line

Stably expressing hTRPML2-YFP cells were generated as previously described [12] using 400 mg/mL geneticin (G418, Sigma). If G418-resistant foci were not identified after 3–4 days, the concentration of G418 was increased to 800 mg/mL. After 2–3 weeks cells were picked from G418-resistant foci and colonies were expanded in six well plates. YFP expression was assessed using confocal microscopy when cells were >50% confluent. Colonies with more than 95% YFP positive cells were selected, grown to >90% confluency, split and further expanded.

4.2.2. Concentration-effect relationships

Concentration-effect measurements were based on a Fluo-4/AM assay and were performed by using a custom-made fluorescence imaging plate reader (FLIPR) built into a robotic liquid handling station (Freedom Evo 150, Tecan, Männedorf, Switzerland). All imaging experiments were done in a HEPES buffered solution (HBS), containing 132 mM NaCl, 6 mM KCl, 1 mM MgCl₂, 1 mM CaCl₂, 5.5 mM D-glucose, 10 mM HEPES, pH 7.4. Compounds dissolved in DMSO (10 mM) were serially prediluted in HBS (0.98 μM–1 mM). HEK293 cells stably expressing plasma membrane-targeted human TRPML1, TRPML2 or TRPML3 [14] were trypsinized and resuspended in cell culture medium supplemented with 4 μM Fluo-4/AM (Invitrogen, Thermo Fisher Scientific, Waltham, MA, U.S.A.). After incubation at 37 °C for 30 min, the cell suspension was briefly centrifuged, resuspended in HBS and dispensed into black pigmented, clear-bottom 384-well microwell plates (Greiner μClear, Frickenhausen, Germany). Then plates were placed into the FLIPR and fluorescence signals (excitation 470 nm, emission 515 nm) were recorded with a Zyla 5.5 camera (Andor, Belfast, UK) and the μManager software like previously described [37]. In a first step and video, the Tecan 96-tip multichannel arm added a negative HBS control or the prediluted compounds to the cells in final concentrations of 0.098 μM–100 μM. To map antagonistic effects, ML-SA1 (5 μM) was subsequently pipetted in each well and fluorescence signals were recorded for 10 min. Analyses were performed by calculating fluorescence intensities for each well and background areas with ImageJ (National Institutes of Health, Bethesda, MD, U.S.A.). Finally, the background was subtracted and the fluorescence intensities were normalized to initial intensities (F/F_0). For comparing inhibition potency of compounds, a second normalization to the negative control was done. All concentration-effect curves were fitted to a four-parameter Hill equation to obtain I_{min} , I_{max} , IC_{50} and the Hill coefficient n .

4.2.3. Culture of HEK293 cells and calcium imaging

Single cell Ca²⁺ imaging experiments were performed using Fura-2 as previously described [38]. HEK293 cells stably expressing hTRPML1^{ΔNC}-YFP, hTRPML2-YFP or hTRPML3-YFP [14] were cultured at 37 °C with 5% of CO₂ in Dulbecco's modified Eagle medium (Thermo Fisher), supplemented with 10% fetal bovine serum, 100 U/mL penicillin, and 0.1 mg/mL streptomycin. Cells were plated onto poly-L-lysine (sigma)-coated glass coverslips and grown for 2–3 days. For Ca²⁺ imaging experiments cells were loaded for 45 min at 37 °C with Fura-2 AM (4.0 μM) and 0.005% (v/v) pluronic acid (both from Thermo Fisher) in HEPES-buffered solution (HBS) comprising 138 mM NaCl, 6 mM KCl, 2 mM MgCl₂, 2 mM CaCl₂, 10 mM HEPES and 5.5 mM D-glucose (adjusted to pH 7.4 with NaOH). After loading, cells were washed with HBS and mounted in an imaging chamber. Experiments were carried out as previously described [14]. After stimulation with an activator (10 μM) for 200 s, the inhibitor (10 μM) was applied for another 200 s. Activation was normalized to 1. All recordings were performed in HBS on a Leica DMi8 live cell microscope or a Polychrome IV mono-chromator (only for experiments with transiently transfected hTRPML1 HEK293 cells). Fura-2 was excited at 340 nm/380 nm. Emitted fluorescence was captured using 515 nm long-pass filter. Compounds were prediluted in DMSO and stored as 10 mM stock solutions at –20 °C, not exceeding three months. Working solutions were prepared directly before using by dilution with HBS. In all statistical analyses of Ca²⁺ imaging experiments, mean values of at least three independent experiments are shown as indicated. *** indicates $p < 0.001$, ** indicates $p < 0.01$, * indicates $p < 0.05$, ns = not significant, one-way ANOVA test followed by Tukey's post-hoc test.

Declaration of competing interest

The authors declare that they have no known competing financial interests or personal relationships that could have appeared to influence the work reported in this paper.

Acknowledgement

We thank Ms. Hua Yang (Trinity College Dublin, Ireland) for her support on the synthesis of ML-S11 during her Erasmus exchange program.

Appendix A. Supplementary data

Supplementary data to this article can be found online at <https://doi.org/10.1016/j.ejmech.2020.112966>.

Funding sources

We thank the Deutsche Forschungsgemeinschaft, DFG (projects BR-1034/7-1 and GR-4315/2-1) for financial support. Additionally M.S. thanks the DFG for funding SFB-TRR 152 P18 and C.G. for funding SFB/TRR152 P04.

Author contributions

The manuscript was written through contributions of all authors. C.L. performed synthesis of the ML-S13 series, single-cell Ca²⁺ imaging experiments, coordinated data assembly and wrote the manuscript. N.U. performed FLIPR experiments and analysis of concentration effect curves. M.K. performed synthesis of ML-S11. S.G. performed single-cell Ca²⁺ imaging experiments. C.C. prepared the stably expressing TRPML cell lines. M.S. supervised FLIPR experiments. C.G. supervised single cell Ca²⁺ imaging experiments. F.B. designed the project, supervised synthesis and wrote the manuscript. All authors have given approval to the final version of the manuscript.

References

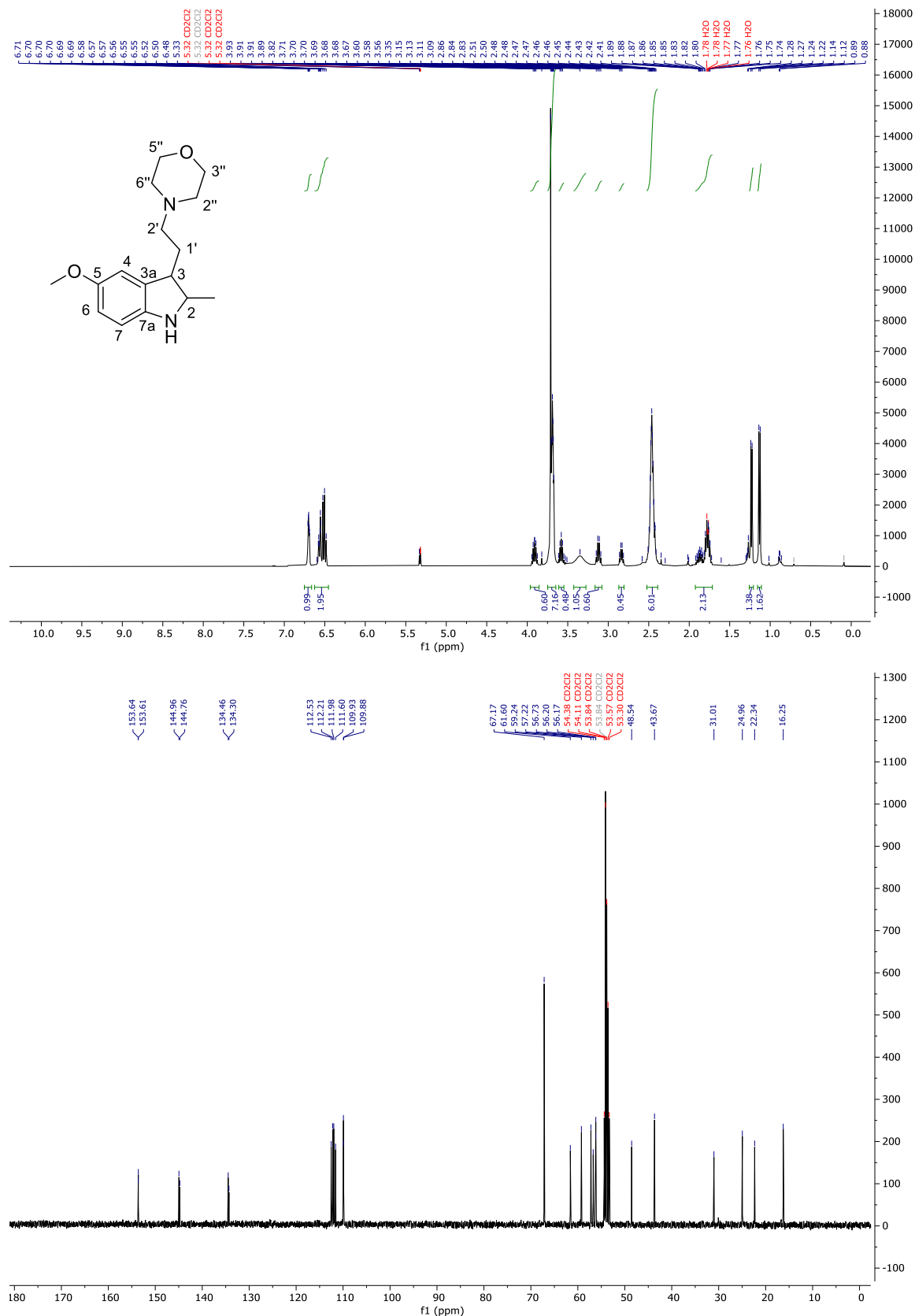
- [1] M.M. Moran, M.A. McAlexander, T. Biro, A. Szallasi, Transient receptor potential channels as therapeutic targets, *Nat. Rev. Drug Discov.* 10 (2011) 601–620.
- [2] K. Venkatachalam, C.O. Wong, M.X. Zhu, The role of TRPMLs in endolysosomal trafficking and function, *Cell Calcium* 58 (2015) 48–56.
- [3] R. Bargal, N. Avidan, E. Ben-Asher, Z. Olender, M. Zeigler, A. Frumkin, A. Raas-Rothschild, G. Glusman, D. Lancet, G. Bach, Identification of the gene causing mucopolidiosis type IV, *Nat. Genet.* 26 (2000) 118–123.
- [4] F. Di Palma, I.A. Belyantseva, H.J. Kim, T.F. Vogt, B. Kachar, K. Noben-Trauth, Mutations in Mcoln3 associated with deafness and pigmentation defects in varitint-waddler (Va) mice, *Proc. Natl. Acad. Sci. U. S. A.* 99 (2002) 14994–14999.
- [5] H. Xu, M. Delling, L. Li, X. Dong, D.E. Clapham, Activating mutation in a mucolipin transient receptor potential channel leads to melanocyte loss in varitint-waddler mice, *Proc. Natl. Acad. Sci. U. S. A.* 104 (2007) 18321–18326.
- [6] K. Nagata, L. Zheng, T. Madathany, A.J. Castiglioni, J.R. Bartles, J. Garcia-Anoveros, The varitint-waddler (Va) deafness mutation in TRPML3 generates constitutive, inward rectifying currents and causes cell degeneration, *Proc. Natl. Acad. Sci. U. S. A.* 105 (2008) 353–358.
- [7] H.J. Kim, Q. Li, S. Tjon-Kon-Sang, I. So, K. Kiselyov, S. Muallem, Gain-of-function mutation in TRPML3 causes the mouse Varitint-Waddler phenotype, *J. Biol. Chem.* 282 (2007) 36138–36142.
- [8] C. Grimm, M.P. Cuajungco, A.F. van Aken, M. Schnee, S. Jors, C.J. Kros, A.J. Ricci, S. Heller, A helix-breaking mutation in TRPML3 leads to constitutive activity underlying deafness in the varitint-waddler mouse, *Proc. Natl. Acad. Sci. U. S. A.* 104 (2007) 19583–19588.
- [9] D.A. Zeevi, A. Frumkin, V. Offen-Glasner, A. Kogot-Levin, G. Bach, A potentially dynamic lysosomal role for the endogenous TRPML proteins, *J. Pathol.* 219 (2009) 153–162.
- [10] N. Rinkenberger, J.W. Schoggins, Mucolipin-2 cation channel increases trafficking efficiency of endocytosed viruses, *mBio* 9 (2018) e02314–17.
- [11] X. Zhang, X. Li, H. Xu, Phosphoinositide isoforms determine compartment-

- specific ion channel activity, *Proc. Natl. Acad. Sci. U. S. A.* 109 (2012) 11384–11389.
- [12] C.C. Chen, M. Keller, M. Hess, R. Schiffmann, N. Urban, A. Wolfgardt, M. Schaefer, F. Bracher, M. Biel, C. Wahl-Schott, C. Grimm, A small molecule restores function to TRPML1 mutant isoforms responsible for mucopolidosis type IV, *Nat. Commun.* 5 (2014) 4681.
- [13] D. Shen, X. Wang, X. Li, X. Zhang, Z. Yao, S. Dibble, X.P. Dong, T. Yu, A.P. Lieberman, H.D. Showalter, H. Xu, Lipid storage disorders block lysosomal trafficking by inhibiting a TRP channel and lysosomal calcium release, *Nat. Commun.* 3 (2012) 731.
- [14] E. Plesch, C.C. Chen, E. Butz, A. Scotto Rosato, E.K. Krogsaeter, H. Yinan, K. Bartel, M. Keller, D. Robaa, D. Teupser, L.M. Holdt, A.M. Vollmar, W. Sippl, R. Puertollano, D. Medina, M. Biel, C. Wahl-Schott, F. Bracher, C. Grimm, Selective agonist of TRPML2 reveals direct role in chemokine release from innate immune cells, *Elife* 7 (2018) e39720.
- [15] C. Grimm, S. Jors, S.A. Saldanha, A.G. Obukhov, B. Pan, K. Oshima, M.P. Cuajungco, P. Chase, P. Hodder, S. Heller, Small molecule activators of TRPML3, *Chem. Biol.* 17 (2010) 135–148.
- [16] M. Samie, X. Wang, X. Zhang, A. Goschka, X. Li, X. Cheng, E. Gregg, M. Azar, Y. Zhuo, A.G. Garrity, Q. Gao, S. Slaughaupt, J. Pickel, S.N. Zolov, L.S. Weisman, G.M. Lenk, S. Titus, M. Bryant-Geneviev, N. Southall, M. Juan, M. Ferrer, H. Xu, A TRP channel in the lysosome regulates large particle phagocytosis via focal exocytosis, *Dev. Cell* 26 (2013) 511–524.
- [17] W. Wang, Q. Gao, M. Yang, X. Zhang, L. Yu, M. Lawas, X. Li, M. Bryant-Geneviev, N.T. Southall, J. Marugan, M. Ferrer, H. Xu, Up-regulation of lysosomal TRPML1 channels is essential for lysosomal adaptation to nutrient starvation, *Proc. Natl. Acad. Sci. U. S. A.* 112 (2015) 1373–1381.
- [18] J. Li, J. Ji, R. Xu, Z. Li, Indole compounds with N-ethyl morpholine moieties as CB2 receptor agonists for anti-inflammatory management of pain: synthesis and biological evaluation, *MedChemComm* 10 (2019) 1935–1947.
- [19] T.C.M.L.S.C. Fanshawe W.J., Clifton N.J., *Cis-mono and disubstituted 2-methyl-3-(piperaziny) and (piperidino)ethylindolines, intermediates for their preparation and methods of preparation*, A.C. Company, 1981, pp. 1–8 USA, US4302589A.
- [20] D.E. Ames, H.R. Ansari, A.D.G. France, A.C. Lovesey, B. Novitt, R. Simpson, Cinnolines. Part XV. Methylation of methoxy- and alkyl-cinnolines and -4(1H)-cinnolones, *J. Chem. Soc. C* (1971) 3088–3097.
- [21] A. Kulkarni, W. Zhou, B. Torok, Heterogeneous catalytic hydrogenation of unprotected indoles in water: a green solution to a long-standing challenge, *Org. Lett.* 13 (2011) 5124–5127.
- [22] M. Lopez-Iglesias, E. Busto, V. Gotor, V. Gotor-Fernandez, Stereoselective synthesis of 2,3-disubstituted indoline diastereoisomers by chemoenzymatic processes, *J. Org. Chem.* 77 (2012) 8049–8055.
- [23] T. Ohkawa, T. Zenkoh, M. Tomita, N. Hosogai, K. Hemmi, H. Tanaka, H. Setoi, Synthesis and characterization of orally active nonpeptide vasopressin V2 receptor antagonists, *Chem. Pharm. Bull. (Tokyo)* 47 (1999) 501–510.
- [24] X. Cheng, X. Zhang, Q. Gao, M. Ali Samie, M. Azar, W.L. Tsang, L. Dong, N. Sahoo, X. Li, Y. Zhuo, A.G. Garrity, X. Wang, M. Ferrer, J. Dowling, L. Xu, R. Han, H. Xu, The intracellular Ca²⁺(+) channel MCOLN1 is required for sarcolemma repair to prevent muscular dystrophy, *Nat. Med.* 20 (2014) 1187–1192.
- [25] B.S. Kilpatrick, E. Yates, C. Grimm, A.H. Schapira, S. Patel, Endo-lysosomal TRP mucolipin-1 channels trigger global ER Ca²⁺ release and Ca²⁺ influx, *J. Cell Sci.* 129 (2016) 3859–3867.
- [26] X. Zhang, X. Cheng, L. Yu, J. Yang, R. Calvo, S. Patnaik, X. Hu, Q. Gao, M. Yang, M. Lawas, M. Delling, J. Marugan, M. Ferrer, H. Xu, MCOLN1 is a ROS sensor in lysosomes that regulates autophagy, *Nat. Commun.* 7 (2016) 12109.
- [27] D. Li, R. Shao, N. Wang, N. Zhou, K. Du, J. Shi, Y. Wang, Z. Zhao, X. Ye, X. Zhang, H. Xu, Sulforaphane Activates a lysosome-dependent transcriptional program to mitigate oxidative stress, *Autophagy* (2020) 1–16.
- [28] T. Isobe, T. Oriyama, Ring-opening reaction of aziridines with amines under the influence of dimethyl sulfoxide, *Tetrahedron Lett.* 57 (2016) 2849–2852.
- [29] V.V. Thakur, A. Sudalai, N-Bromoamides as versatile catalysts for aziridination of olefins using chloramine-T, *Tetrahedron Lett.* 44 (2003) 989–992.
- [30] P. Labrie, S.P. Maddaford, J. Lacroix, C. Catalano, D.K. Lee, S. Rakhit, R.C. Gaudreault, In vitro activity of novel dual action MDR anthranilamide modulators with inhibitory activity on CYP-450 (Part 2), *Bioorg. Med. Chem.* 15 (2007) 3854–3868.
- [31] B.D. Palmer, W.R. Wilson, S.M. Pullen, W.A. Denny, Hypoxia-selective anti-tumor agents. 3. Relationships between structure and cytotoxicity against cultured tumor cells for substituted N,N-bis(2-chloroethyl)anilines, *J. Med. Chem.* 33 (1990) 112–121.
- [32] S.W. Lin, Q. Sun, Z.M. Ge, X. Wang, J. Ye, R.T. Li, Synthesis and structure-analgesic activity relationships of a novel series of monospirocyclopiperazinium salts (MSPZ), *Bioorg. Med. Chem. Lett.* 21 (2011) 940–943.
- [33] S. Nakamura, M. Ohara, M. Koyari, M. Hayashi, K. Hyodo, N.R. Nabisaheb, Y. Funahashi, Desymmetrization of meso-aziridines with TMSNCS using metal salts of novel chiral imidazoline-phosphoric acid catalysts, *Org. Lett.* 16 (2014) 4452–4455.
- [34] D. Albanese, D. Landini, M. Penso, S. Petricci, Synthesis of N-sulfonyl aziridines through regioselective opening of epoxides under solid-liquid PTC conditions, *Tetrahedron* 55 (1999) 6387–6394.
- [35] Congxin L., *Piperazine Derivatives as TRPML Modulators*, 2018 USA, WO2018005713A1.
- [36] J.W. Hubbard, A.M. Piegols, B.C.G. Söderberg, Palladium-catalyzed N-heteroannulation of N-allyl- or N-benzyl-2-nitrobenzenamines: synthesis of 2-substituted benzimidazoles, *Tetrahedron* 63 (2007) 7077–7085.
- [37] N. Urban, M. Schaefer, Direct activation of TRPC3 channels by the antimalarial agent artemisinin, *Cells* 9 (2020) 202.
- [38] C. Grimm, S. Hassan, C. Wahl-Schott, M. Biel, Role of TRPML and two-pore channels in endolysosomal cation homeostasis, *J. Pharmacol. Exp. Therapeut.* 342 (2012) 236–244.

3.1.1.4 Supporting Information

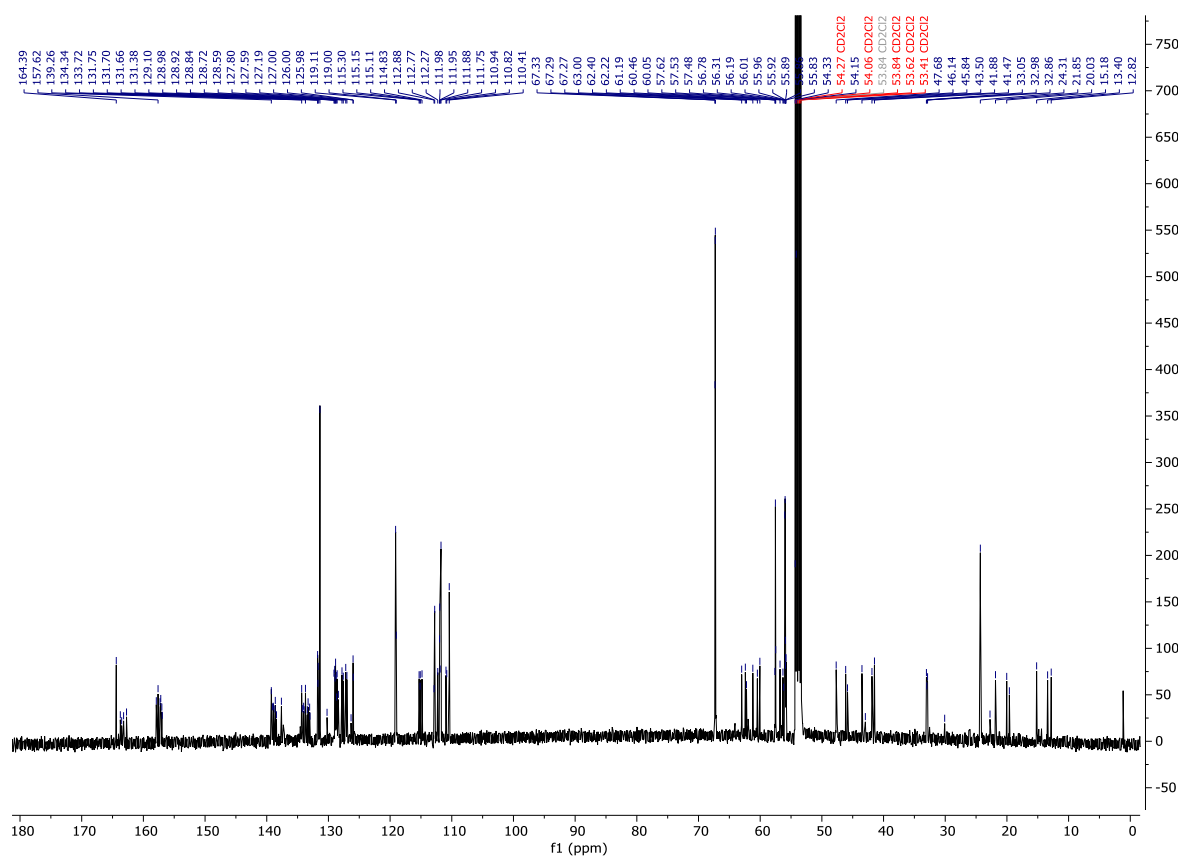
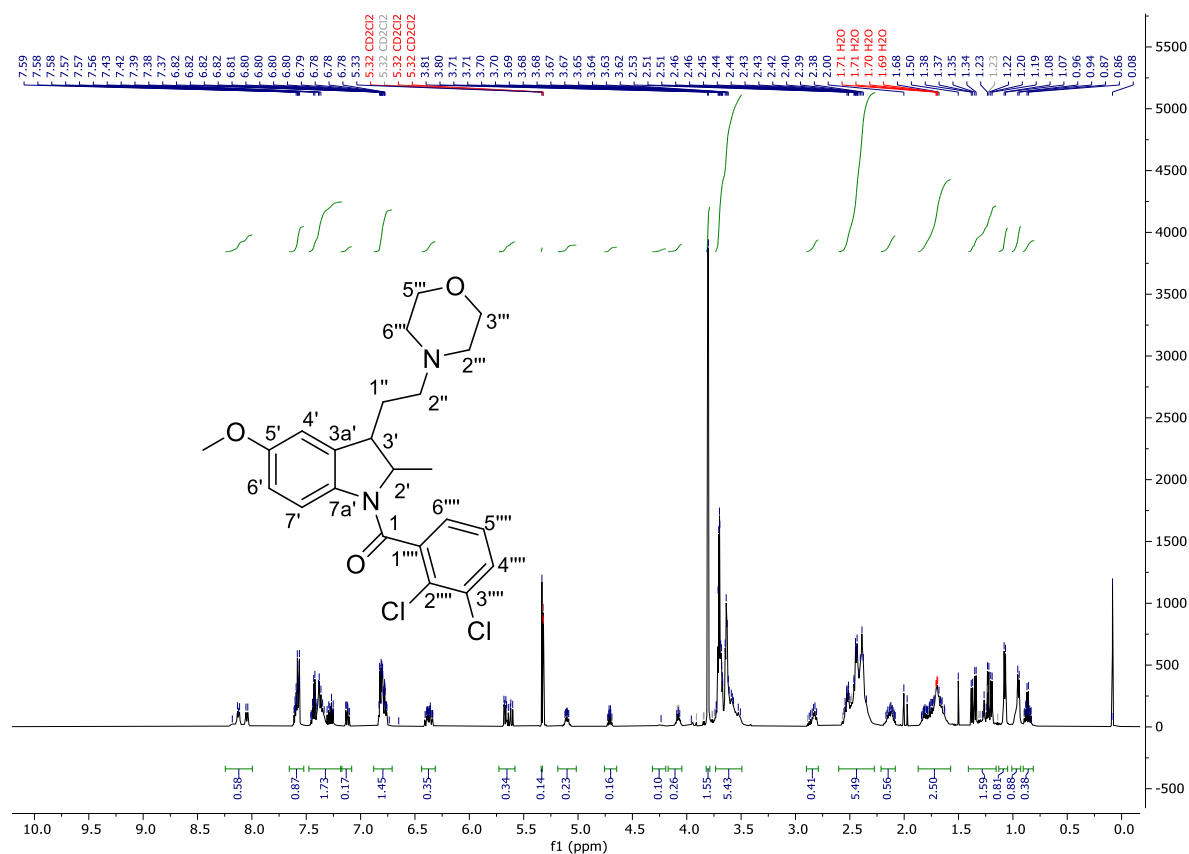
NMR Spectra

EY19 (4-(2-(5-methoxy-2-methylindolin-3-yl)ethyl)morpholine)

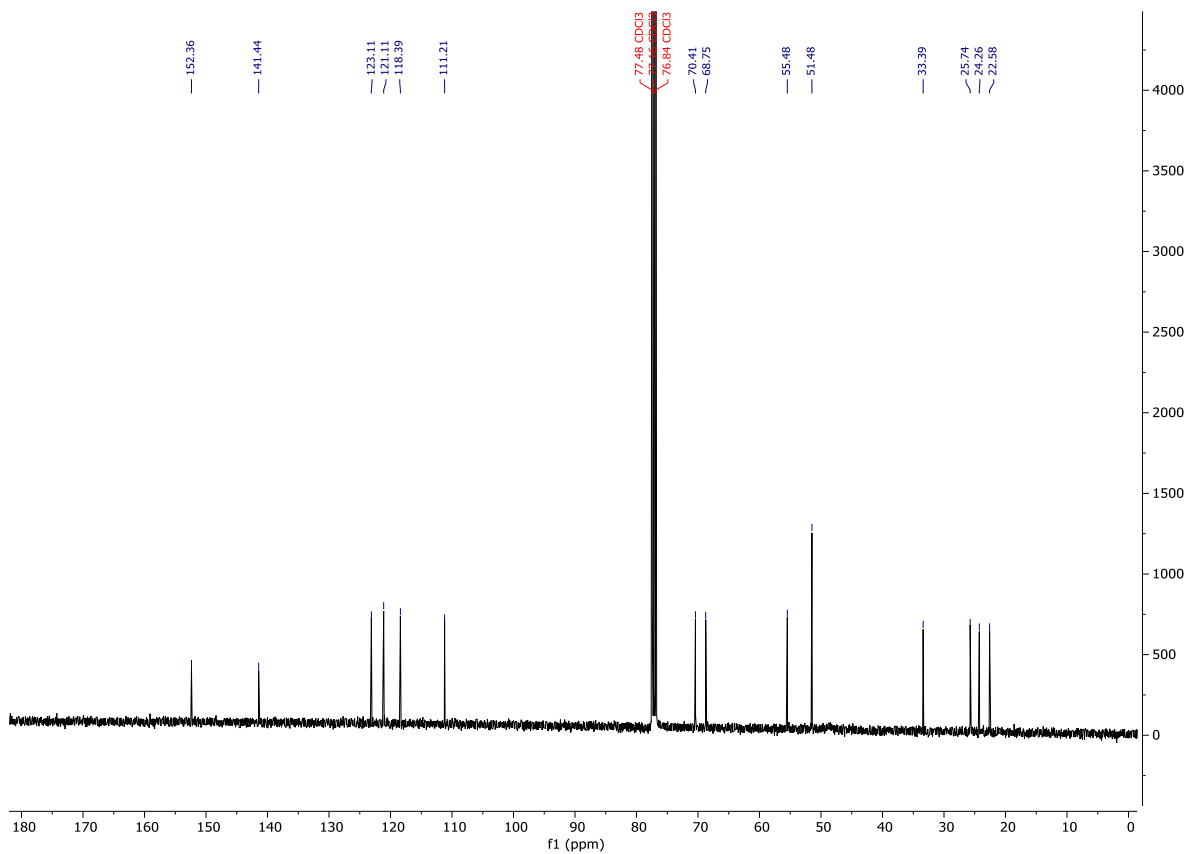
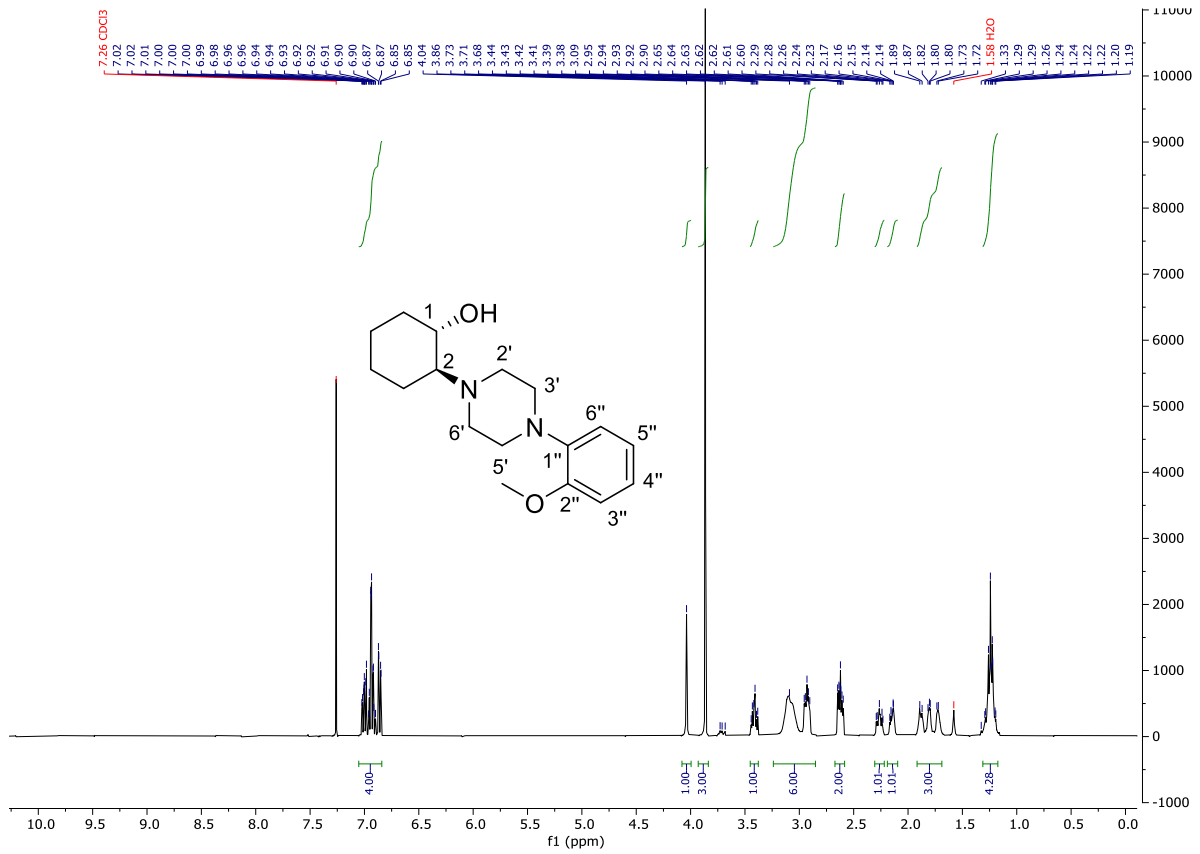


Chemical and pharmacological characterization of ML-S11 and ML-S13

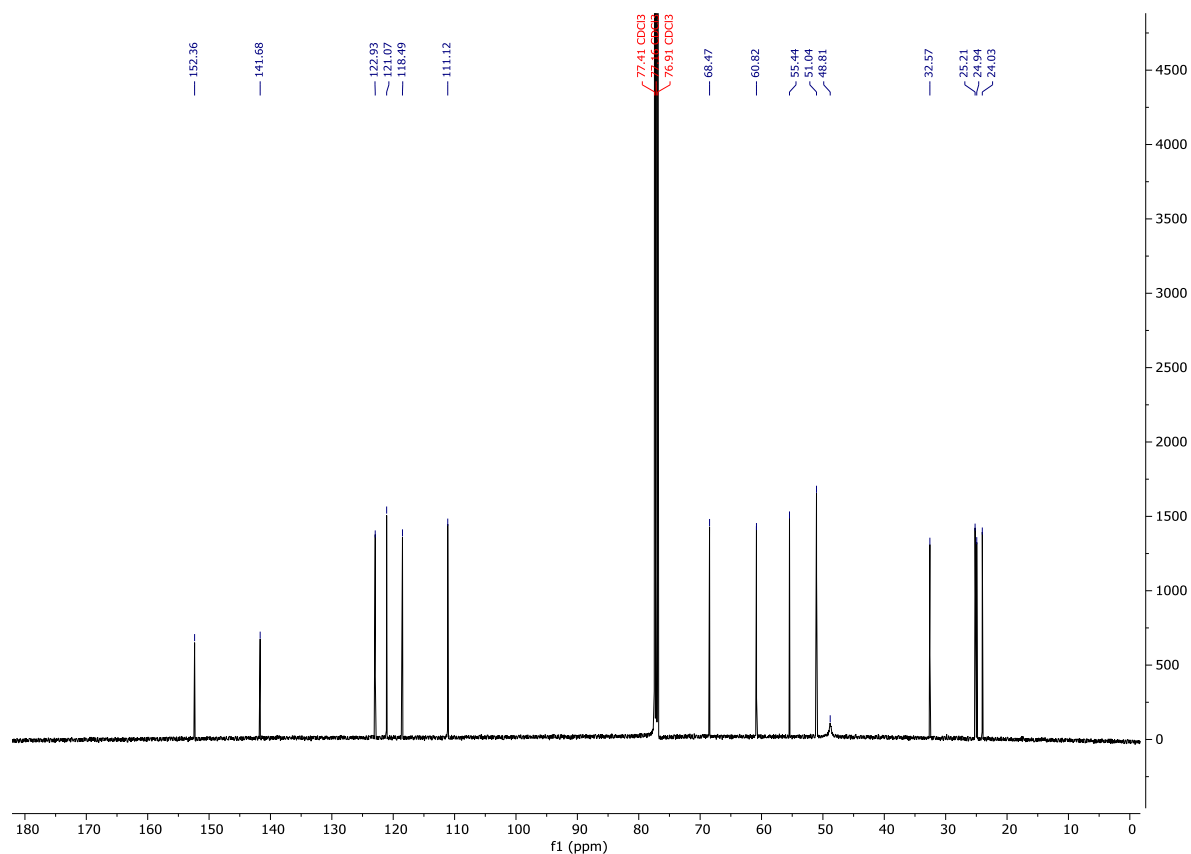
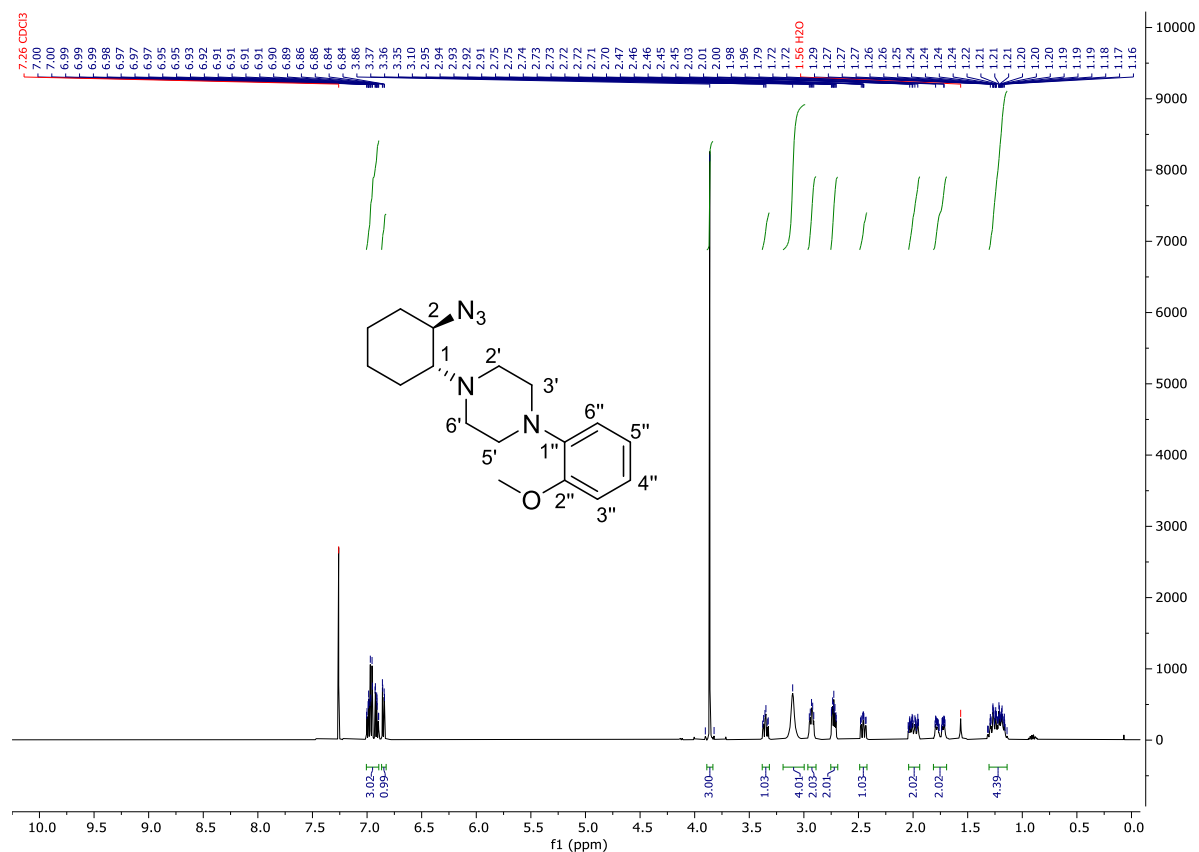
(2,3-dichlorophenyl)(5-methoxy-2-methyl-3-(2-morpholinoethyl)indolin-1-yl)methanone (ML-S11)



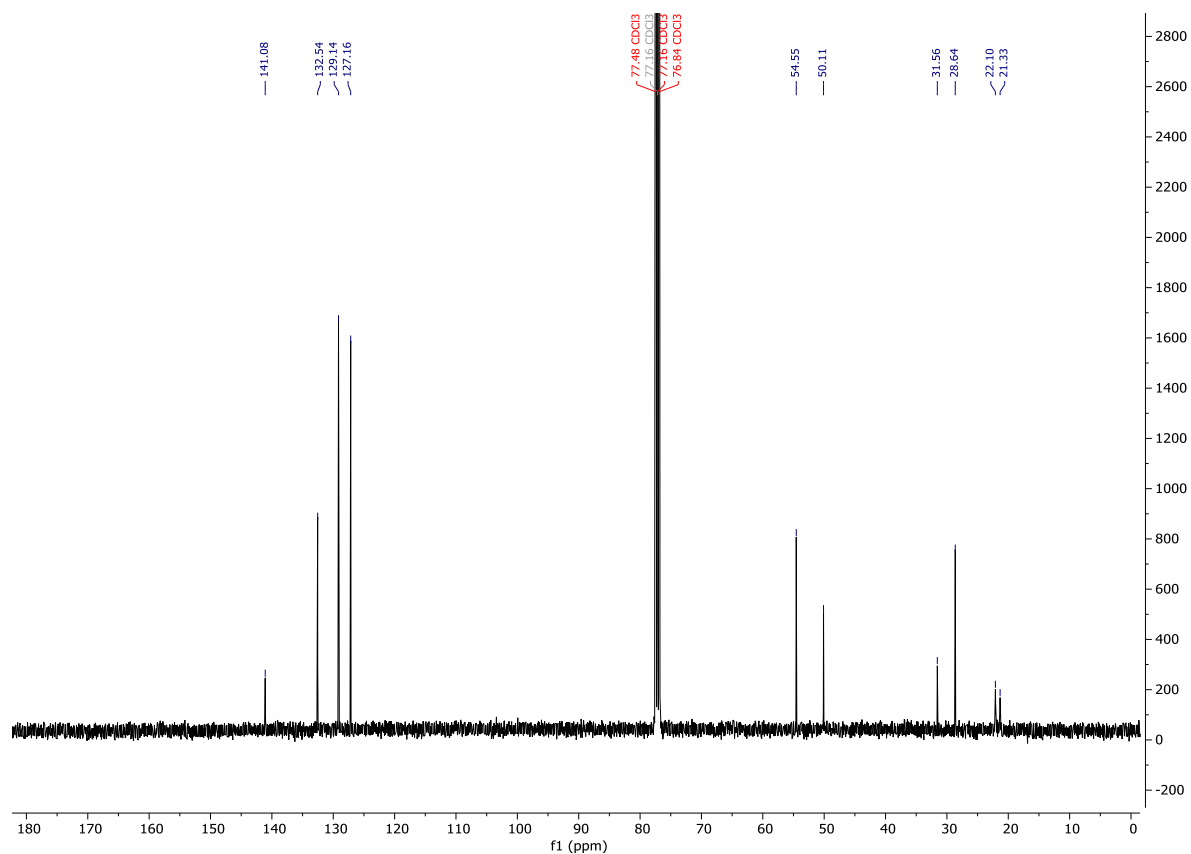
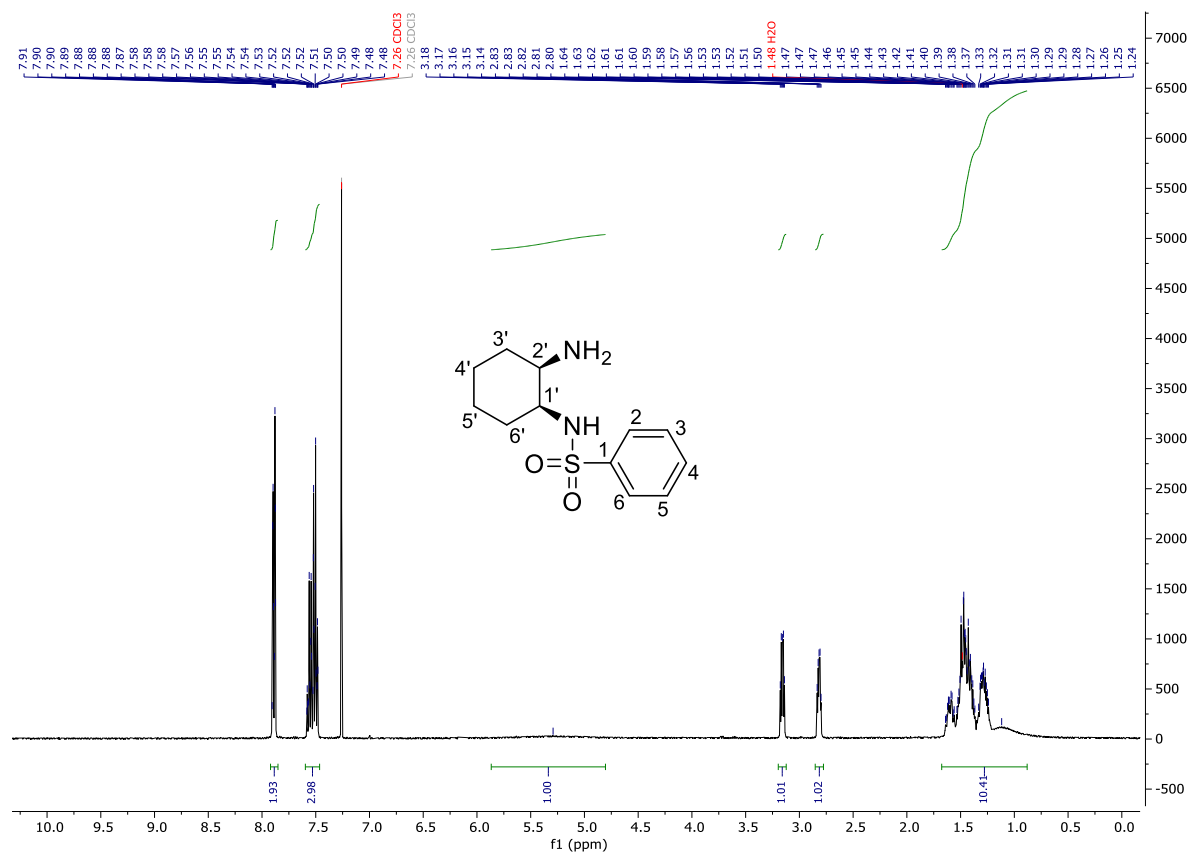
trans-2-(4-(2-Methoxyphenyl)piperazin-1-yl)cyclohexan-1-ol (**10**)



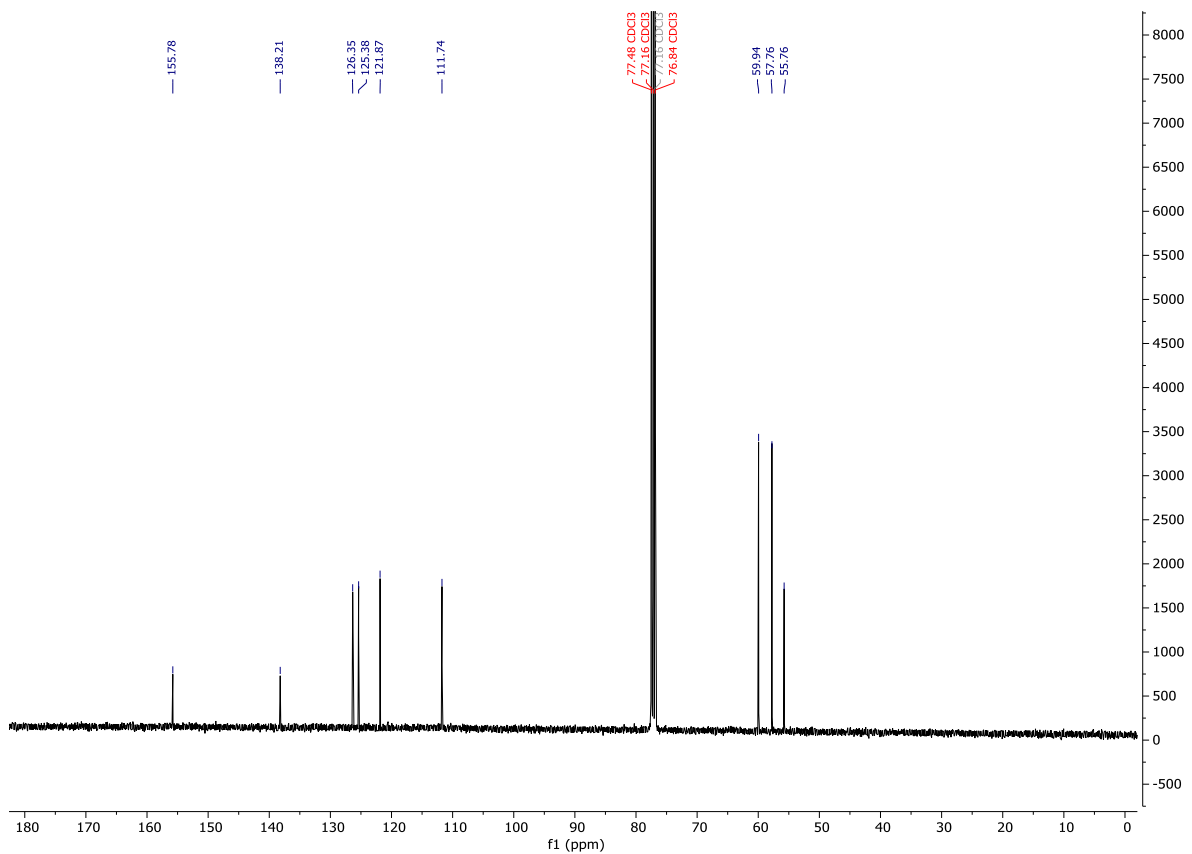
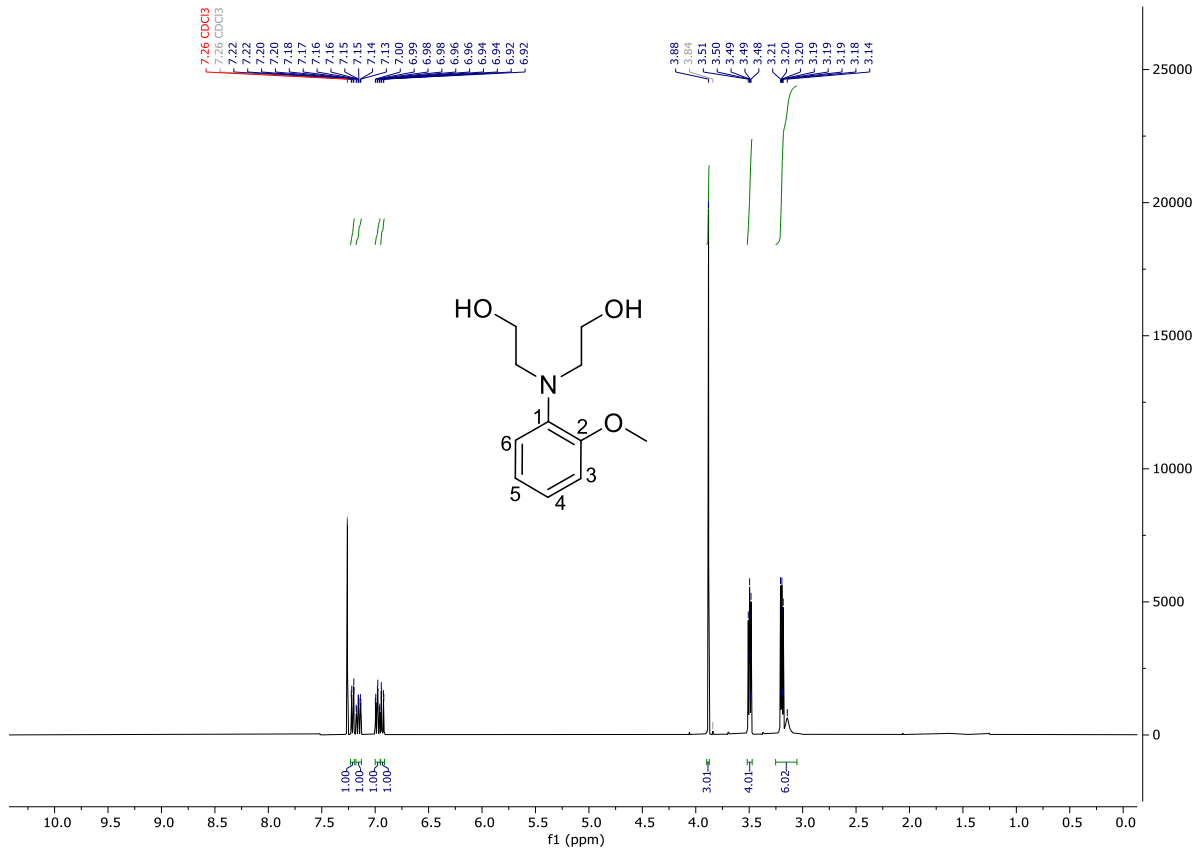
trans-1-(2-azidocyclohexyl)-4-(2-methoxyphenyl)piperazine (11)



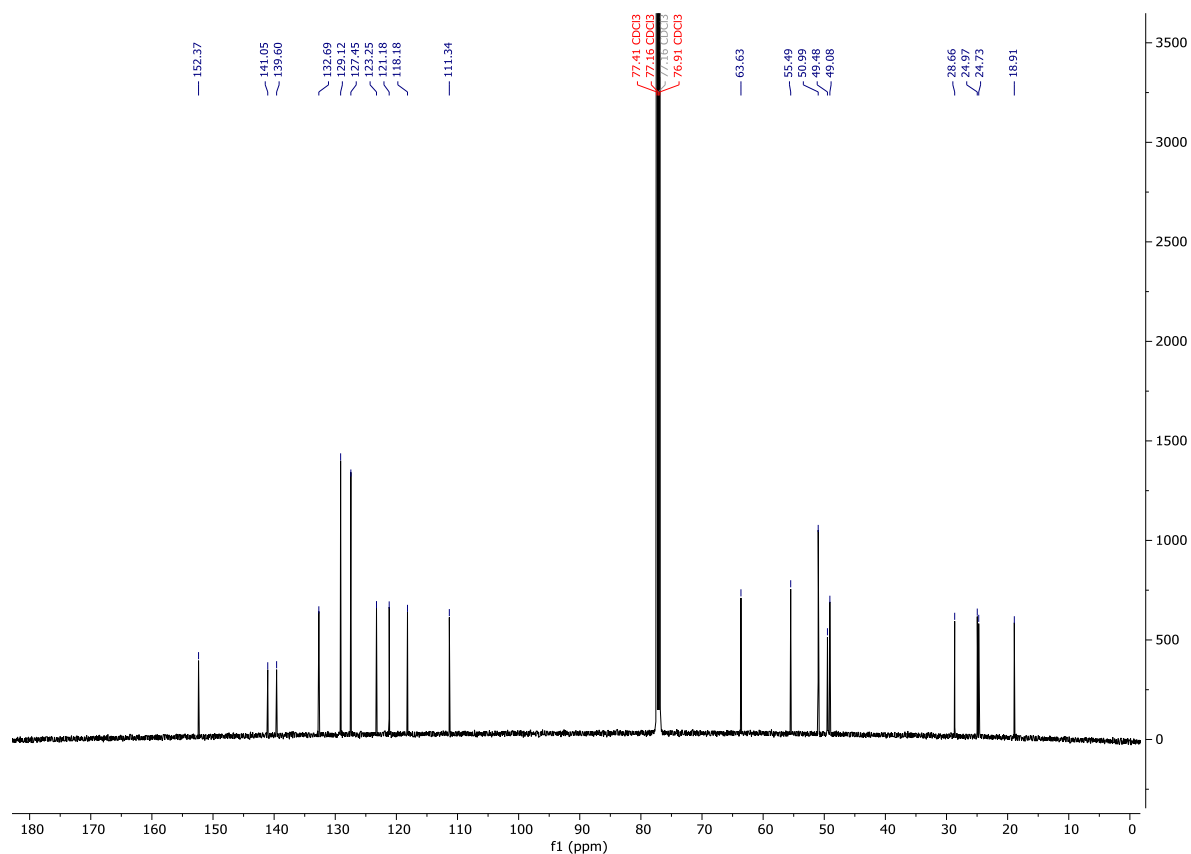
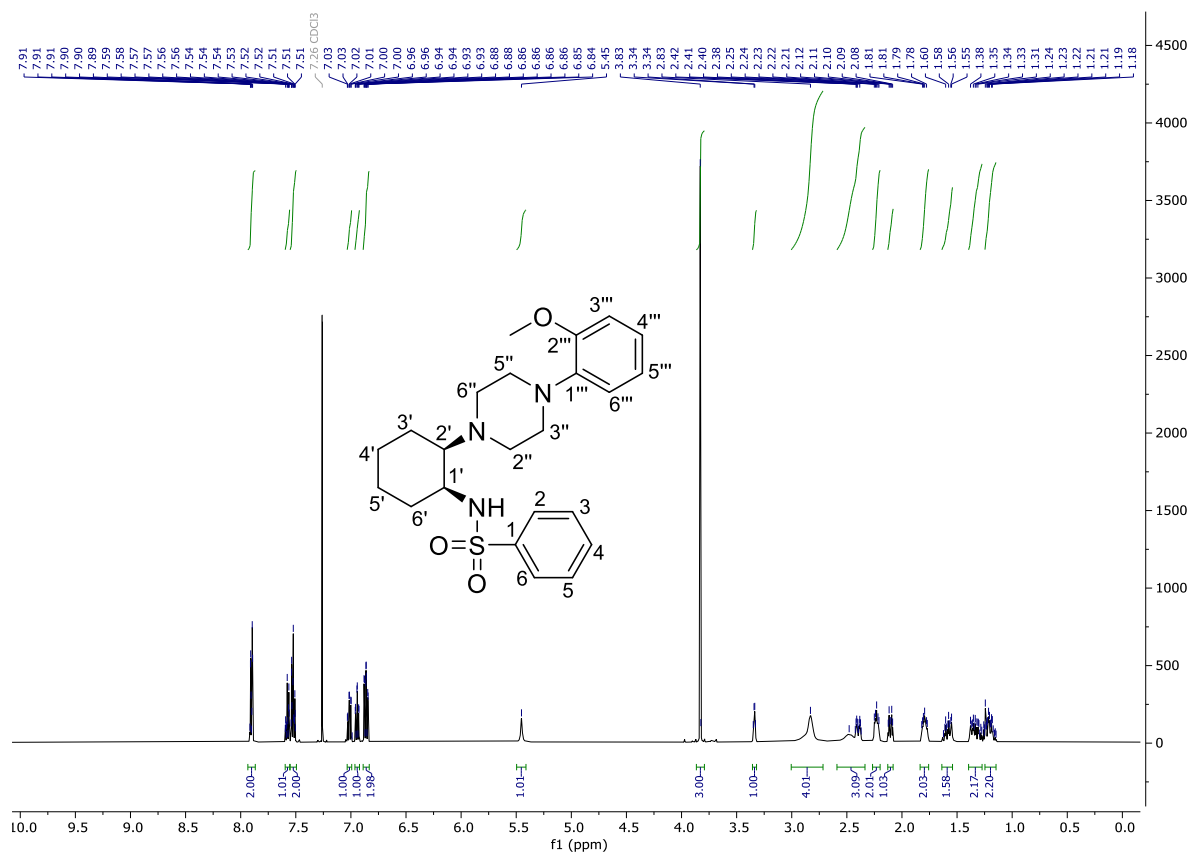
cis-*N*-(2-aminocyclohexyl)benzenesulfonamide (**13**)



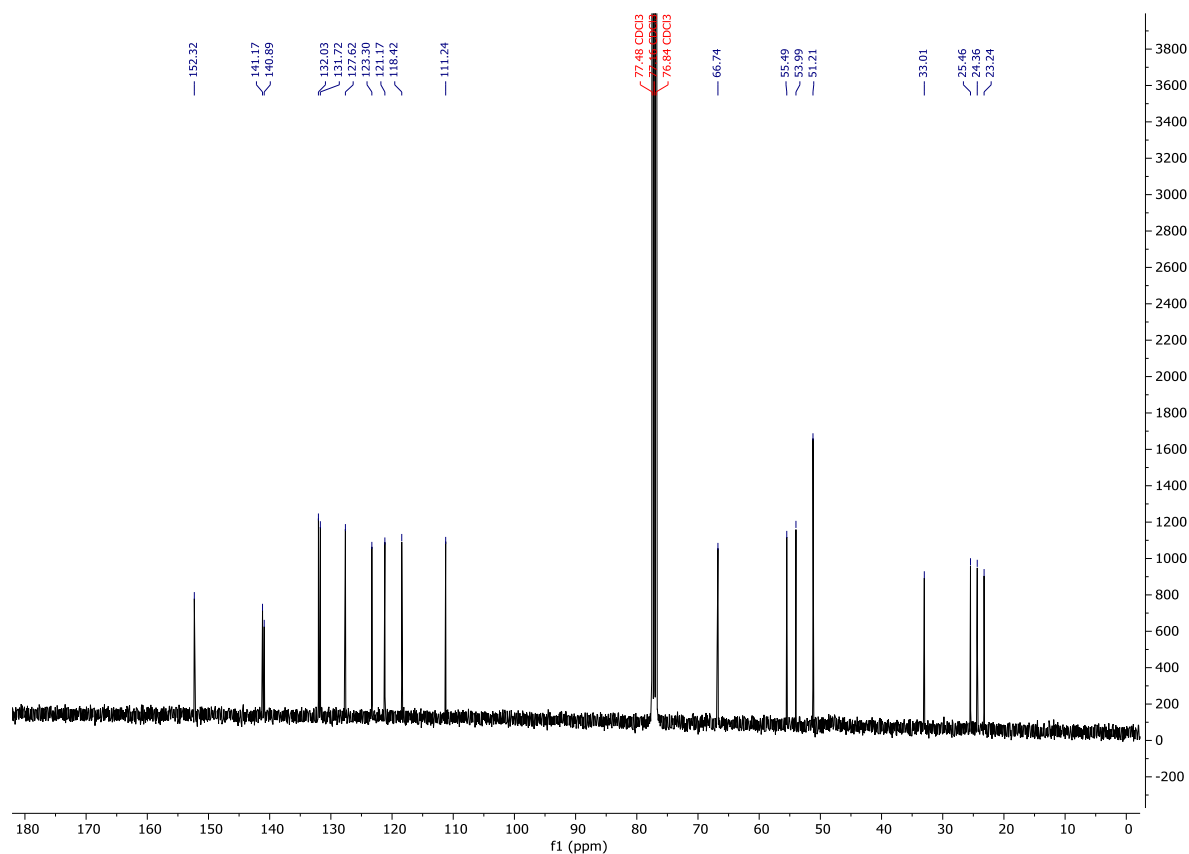
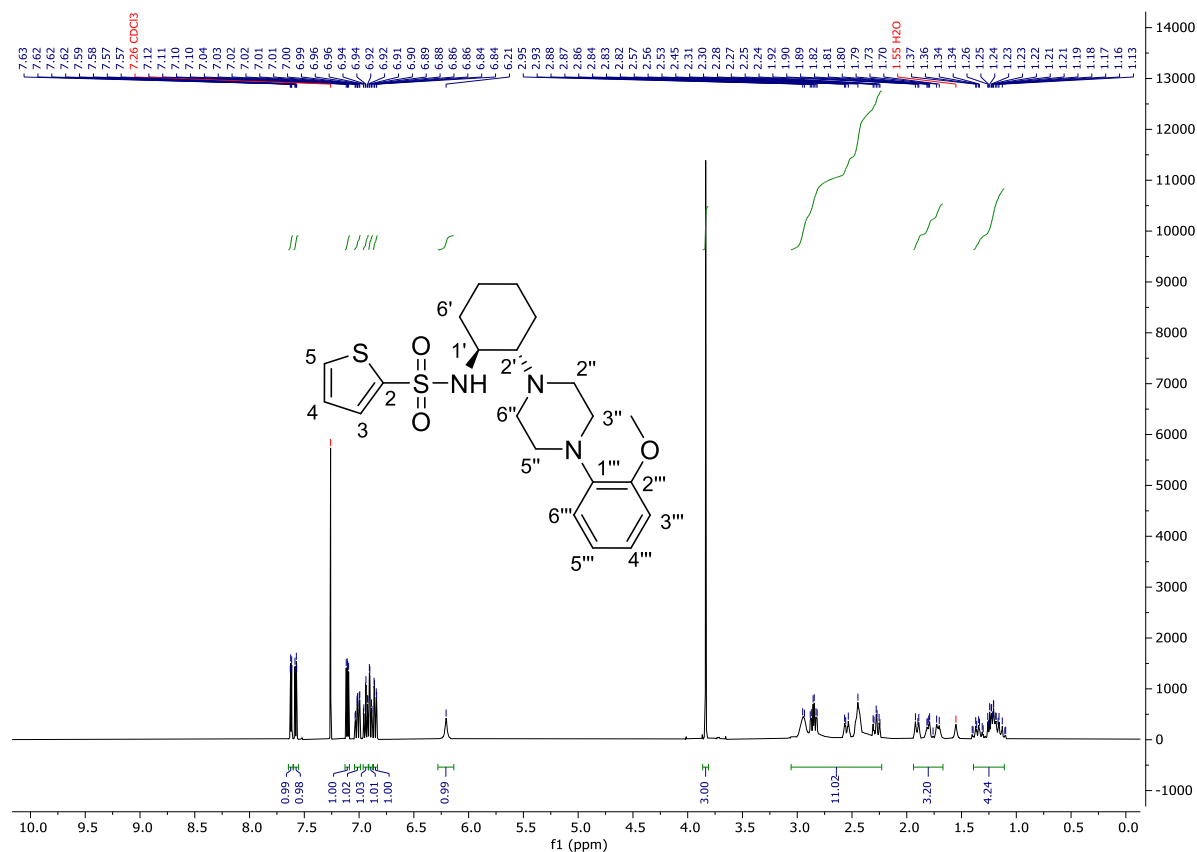
N,N-bis(2-hydroxyethyl)-2-methoxyanilin (**14**)



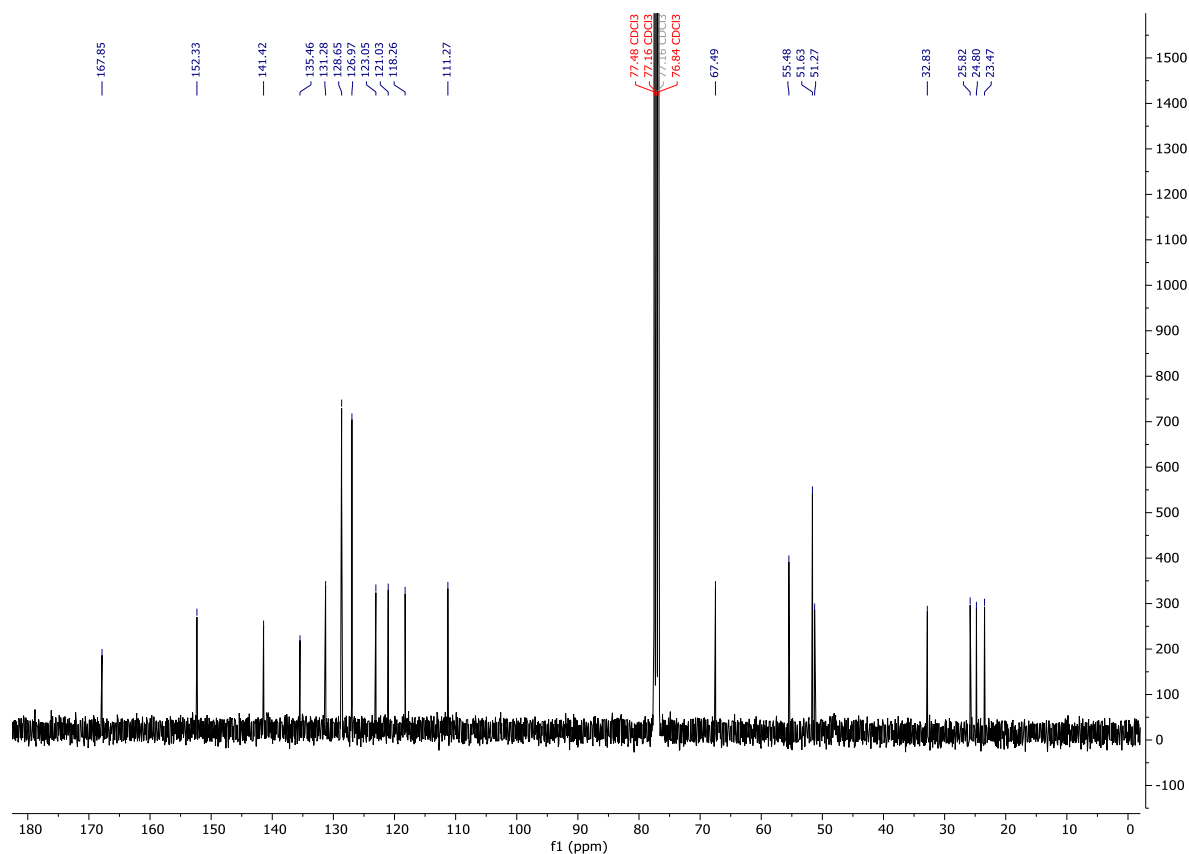
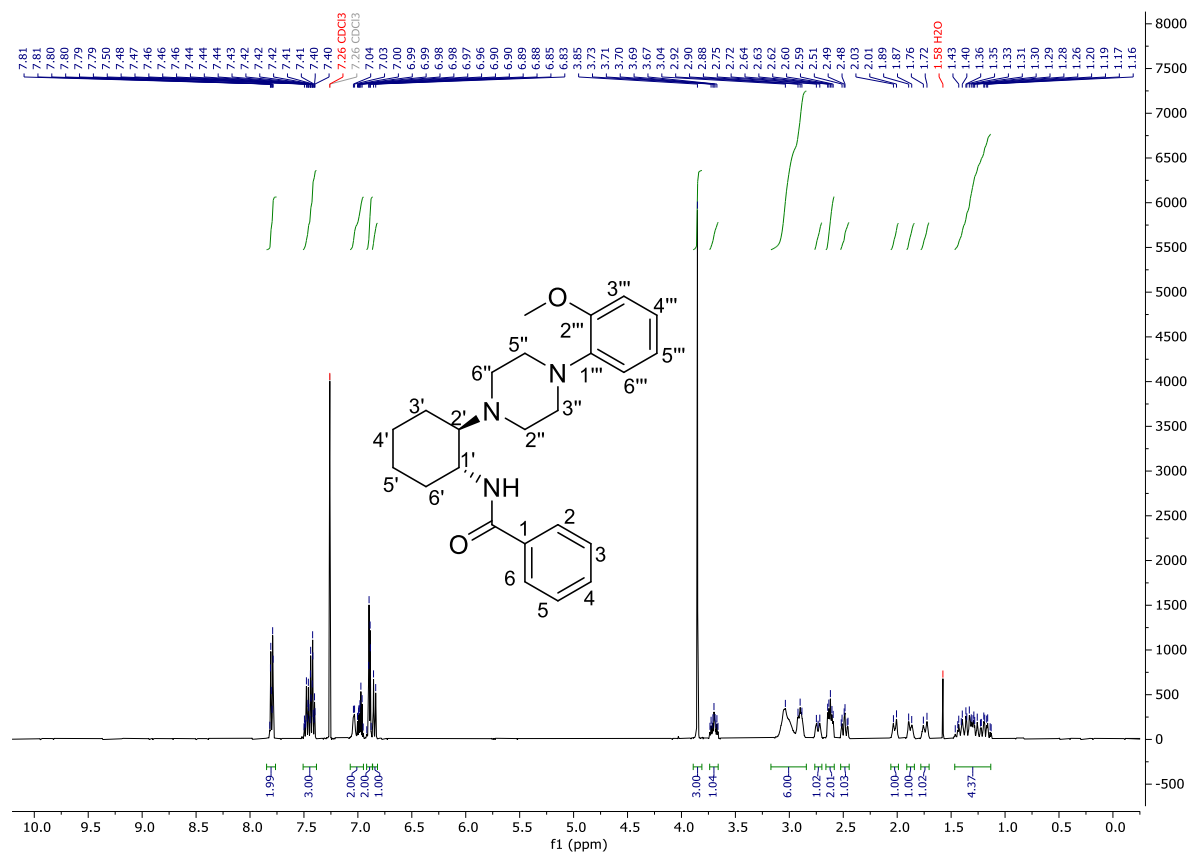
cis-*N*-(2-(4-(2-methoxyphenyl)piperazin-1-yl)cyclohexyl)benzenesulfonamide (*cis* ML-SI3)



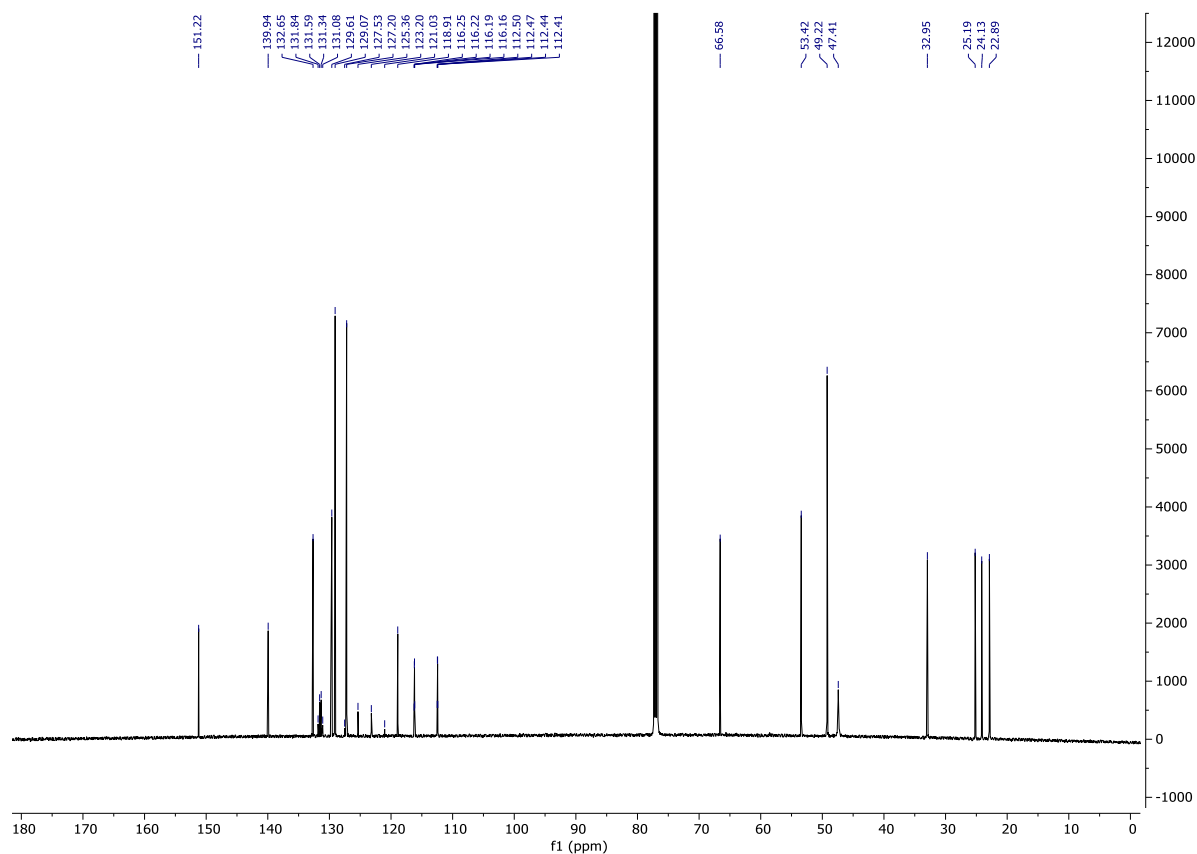
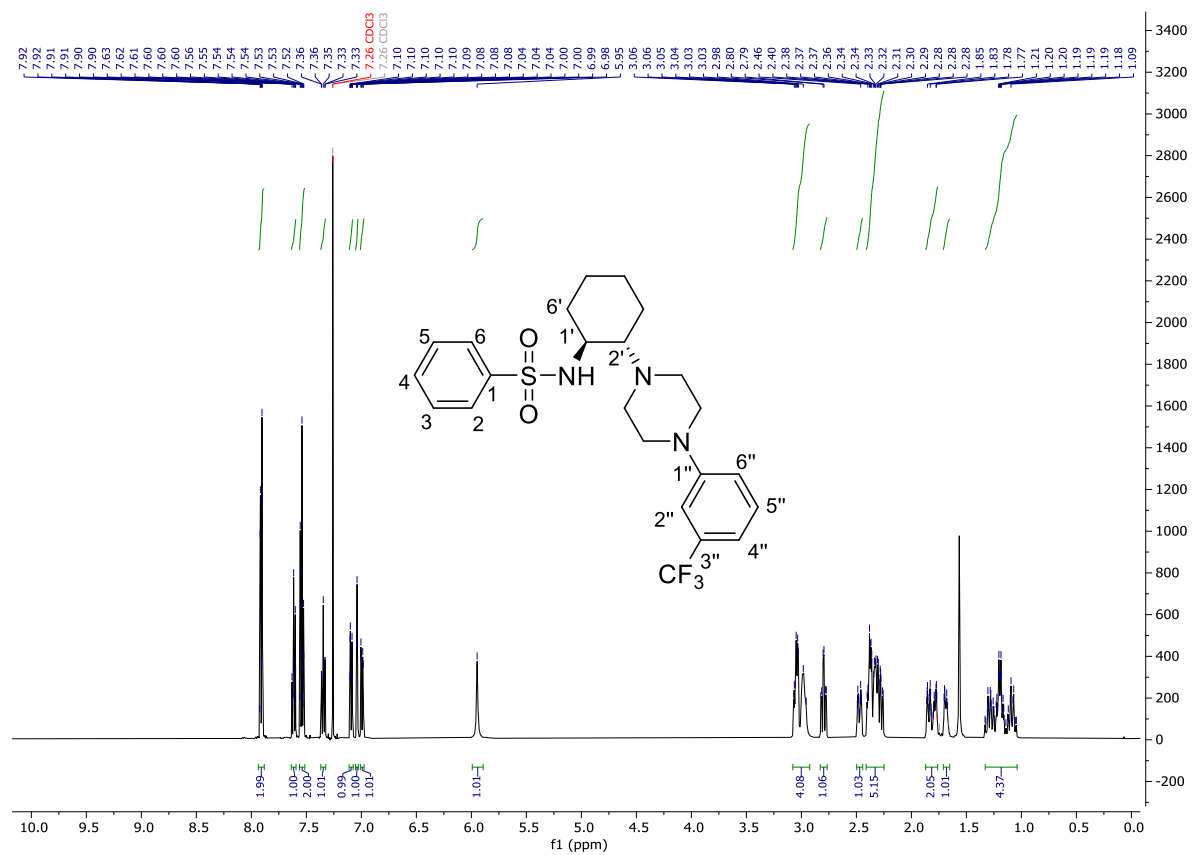
trans-*N*-(2-(4-(2-methoxyphenyl)piperazin-1-yl)cyclohexyl)thiophene-2-sulfonamide (**18**)



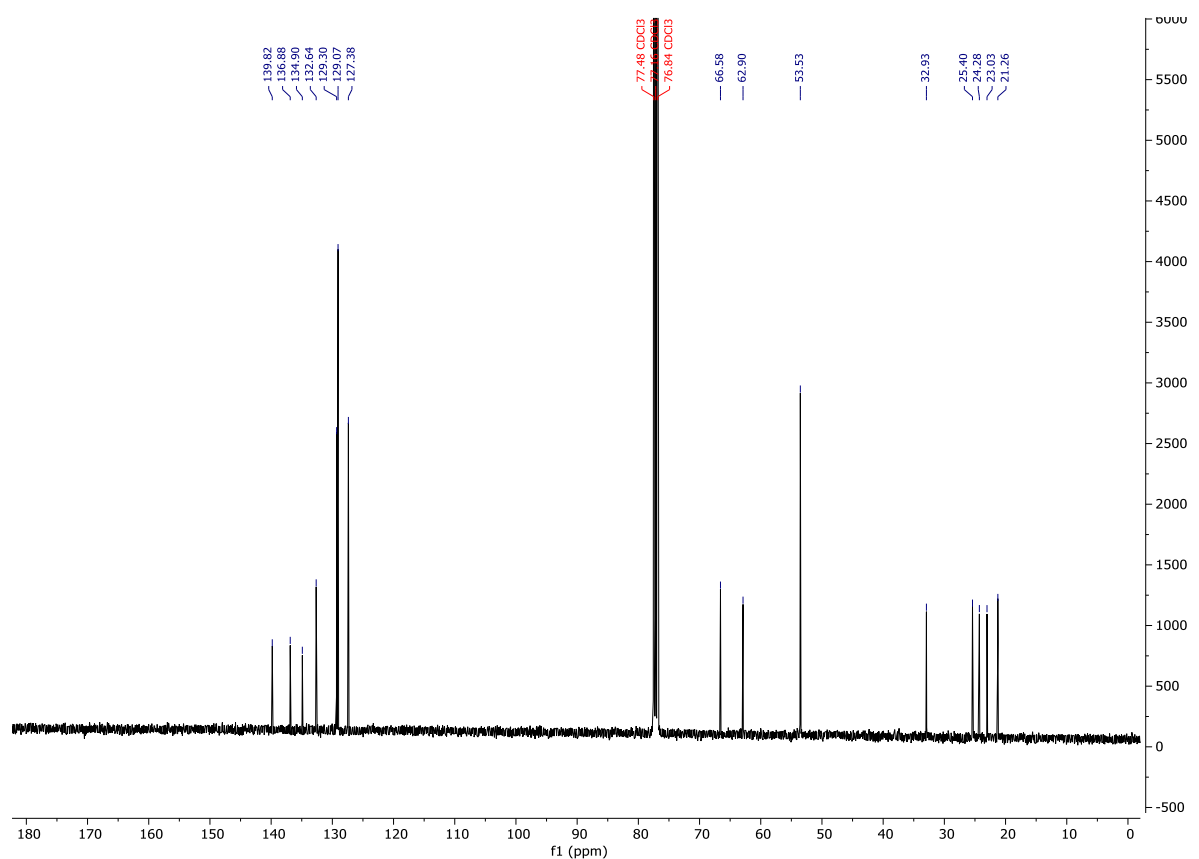
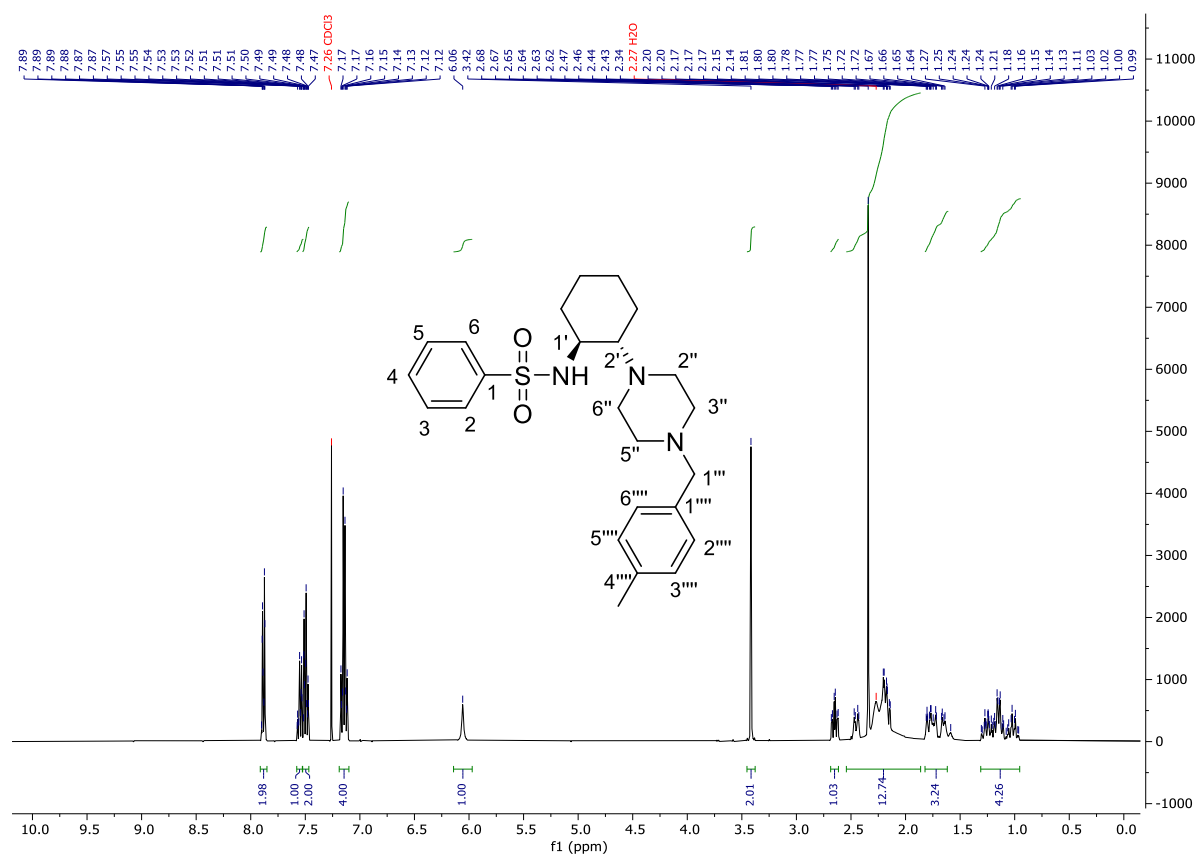
trans-N-(2-(4-(2-methoxyphenyl)piperazin-1-yl)cyclohexyl)benzamide (20)



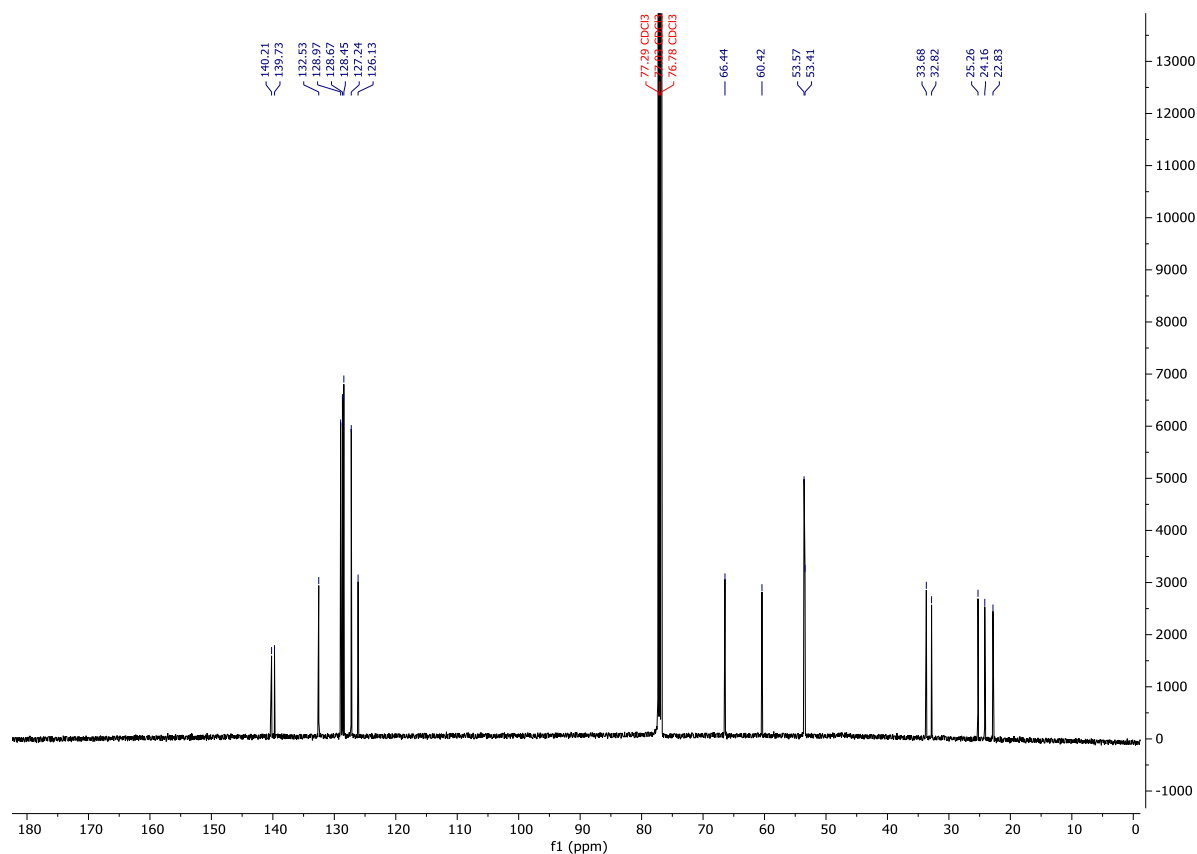
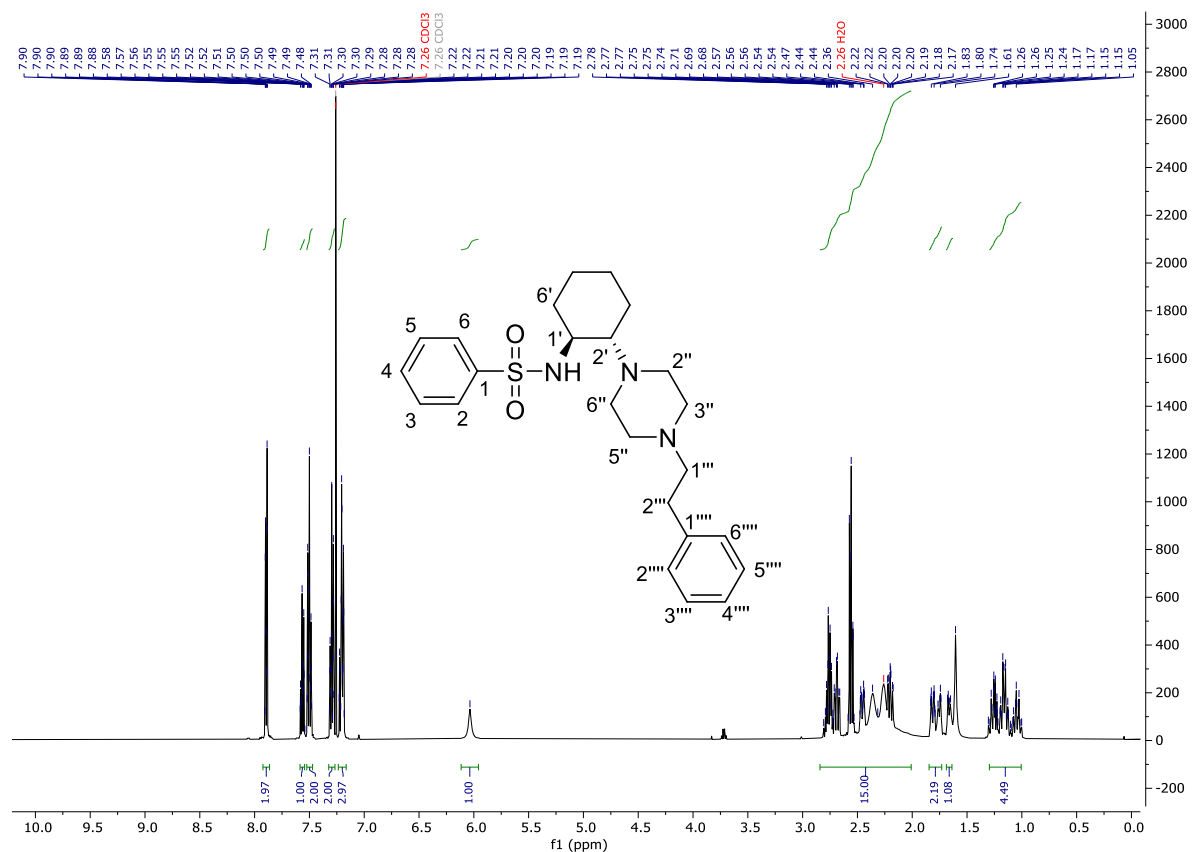
trans-N-(2-(4-(3-(trifluoromethyl)phenyl)piperazin-1-yl)cyclohexyl)benzenesulfonamide (**22**)



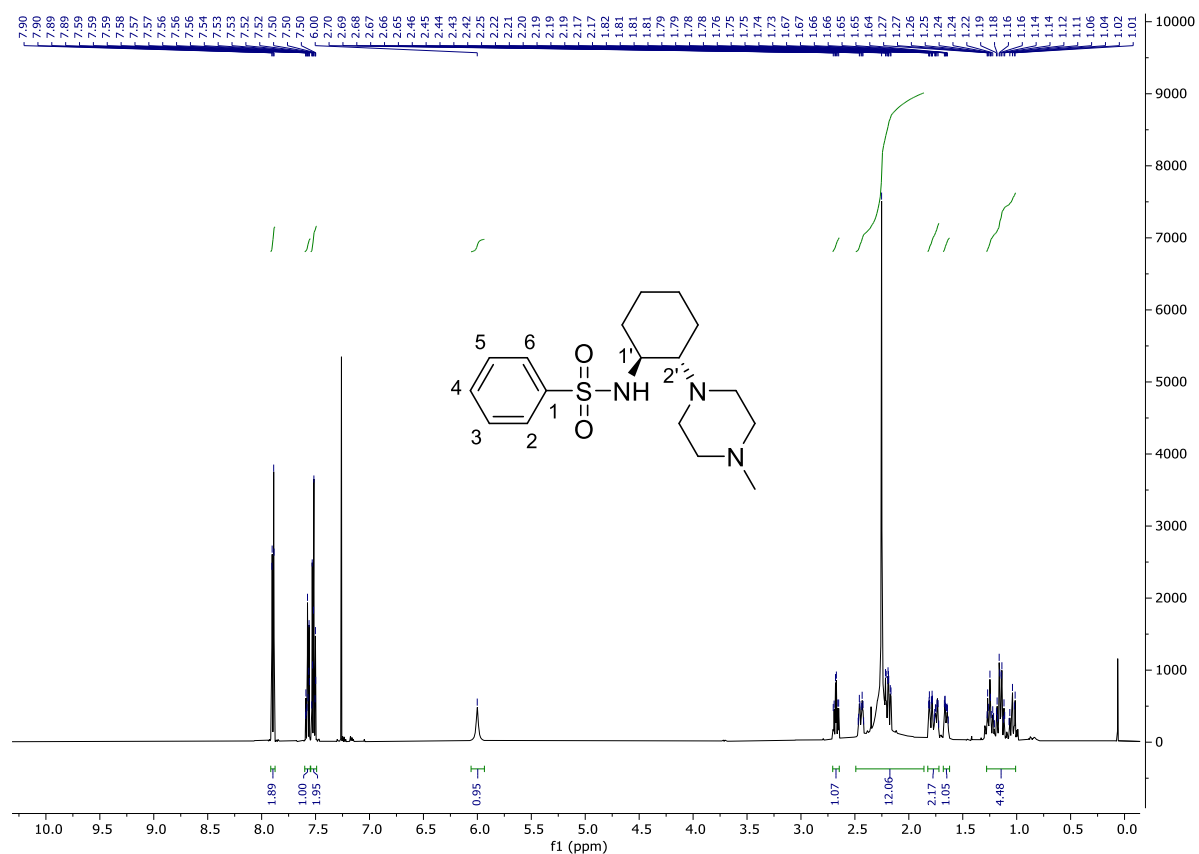
trans-N-(2-(4-(4-methylbenzyl)piperazin-1-yl)cyclohexyl)benzenesulfonamide (**23**)



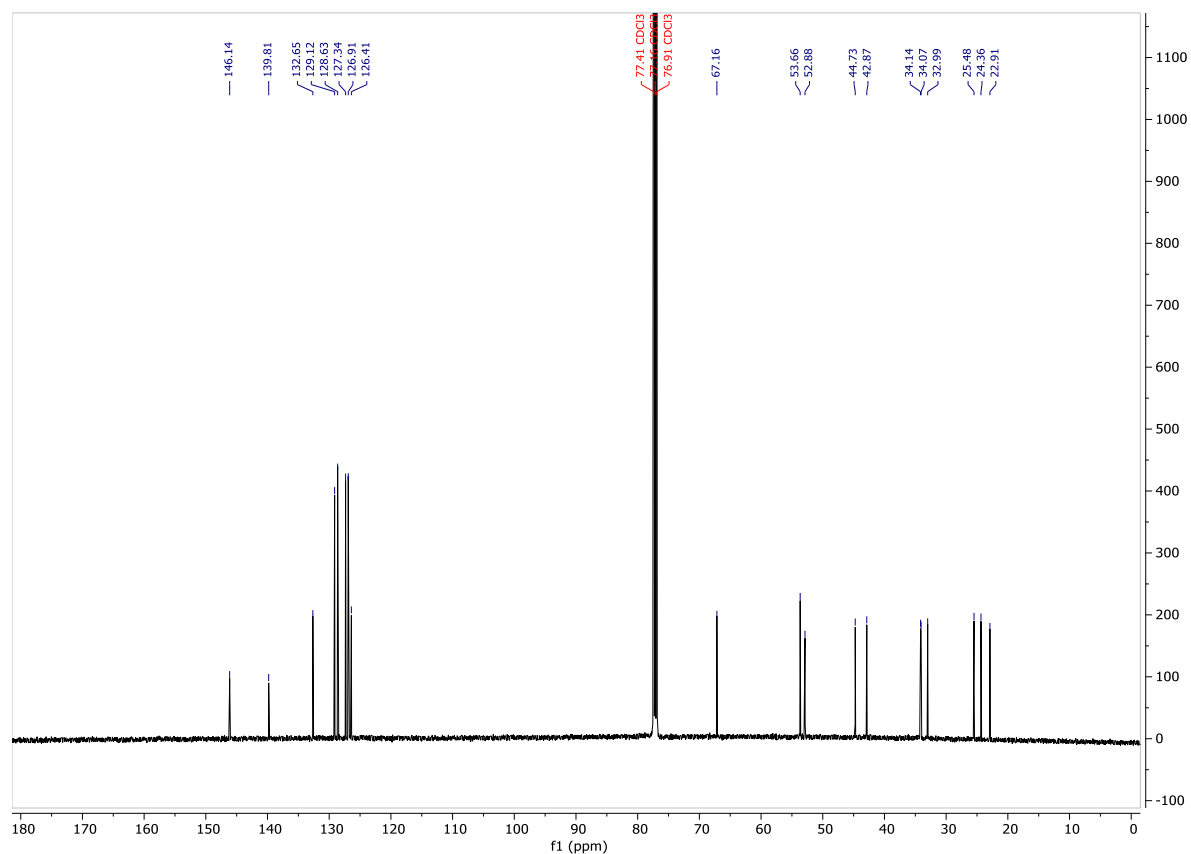
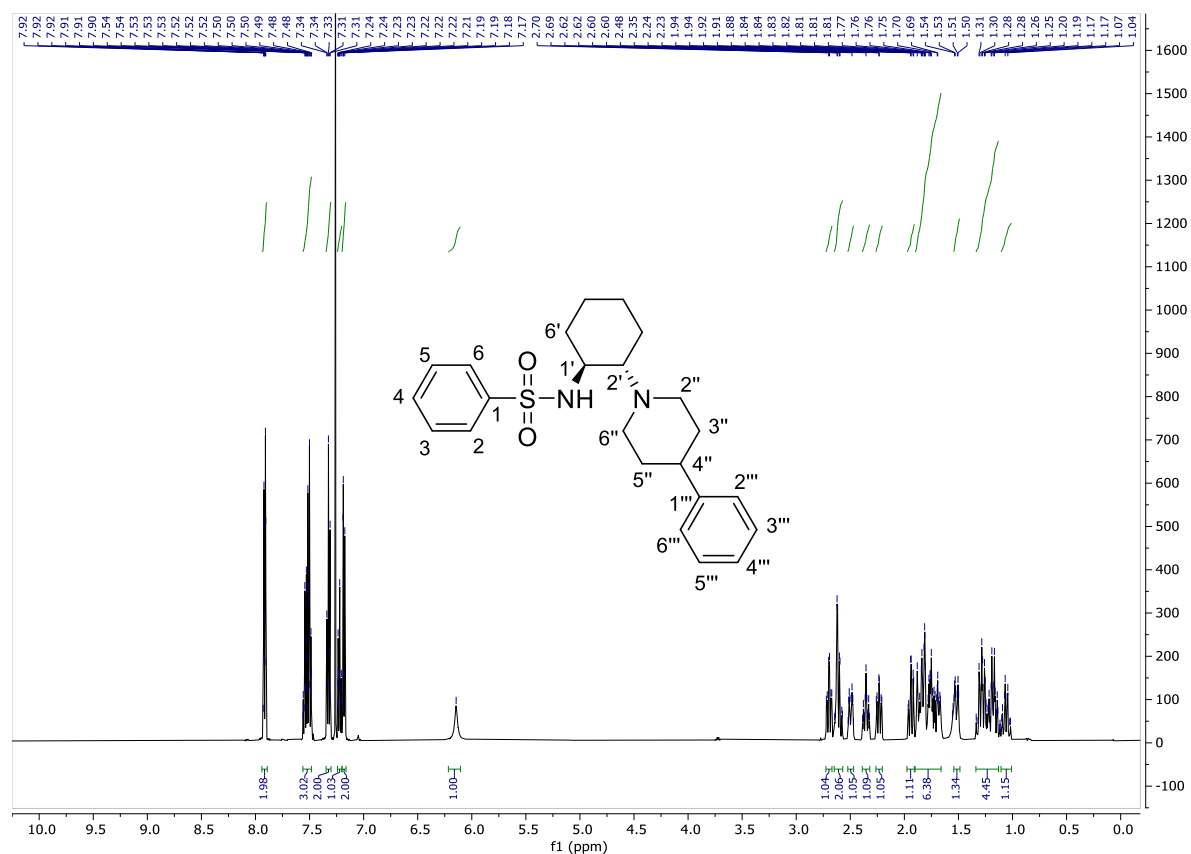
trans-N-(2-(4-phenethylpiperazin-1-yl)cyclohexyl)benzenesulfonamide (**24**)



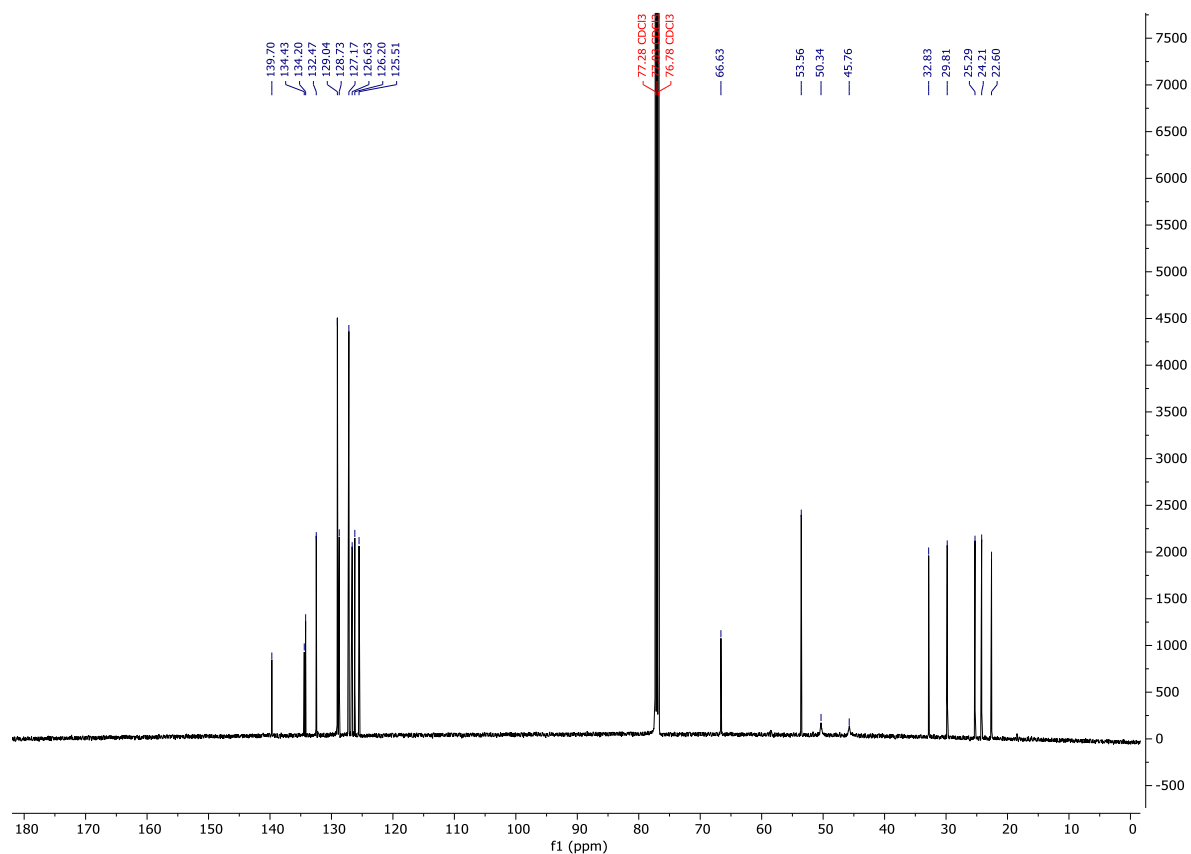
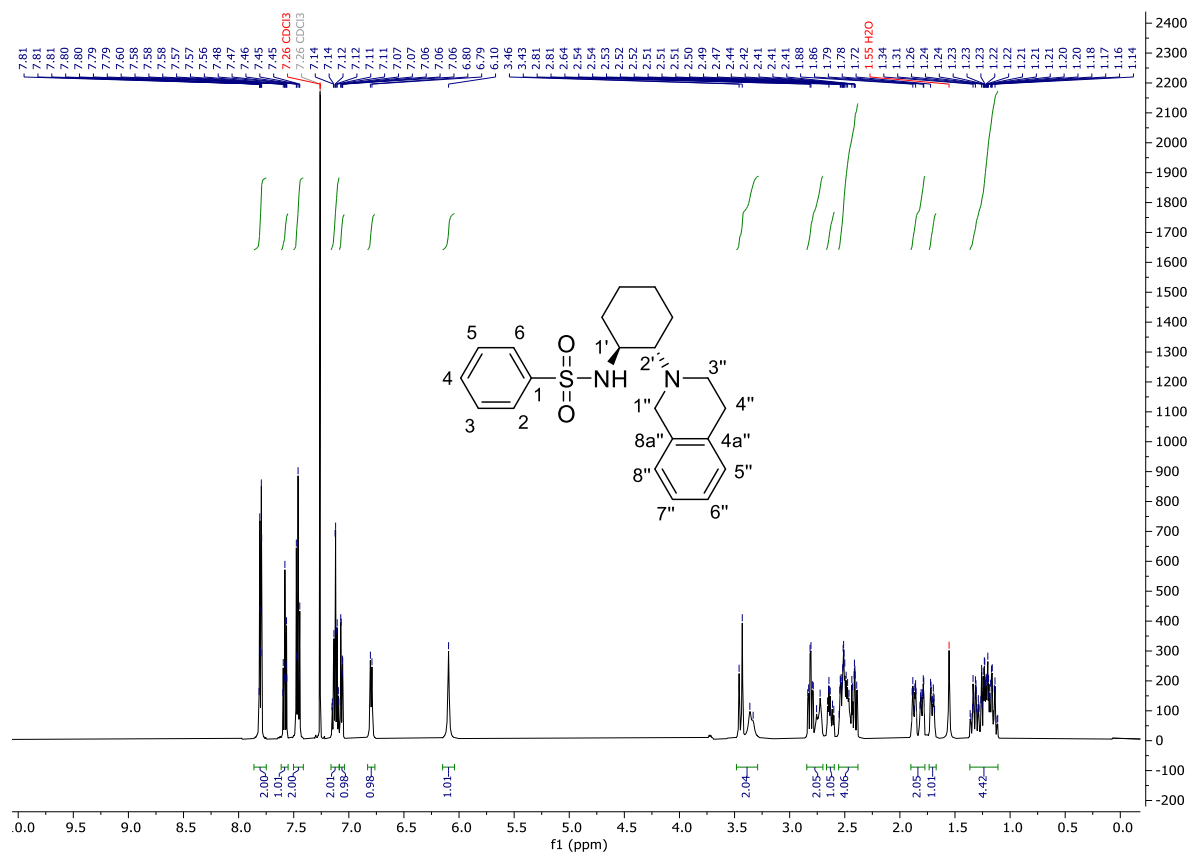
trans-N-(2-(4-methylpiperazin-1-yl)cyclohexyl)benzenesulfonamide (**25**)



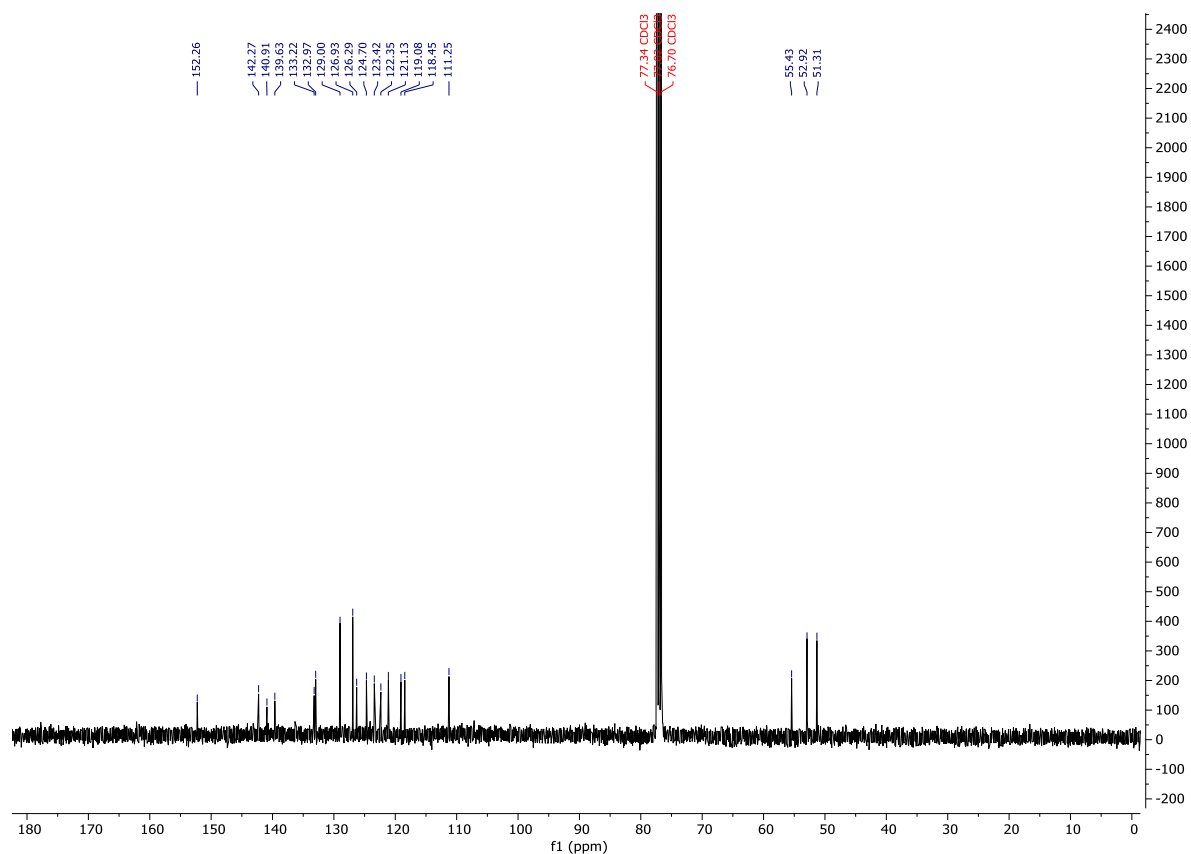
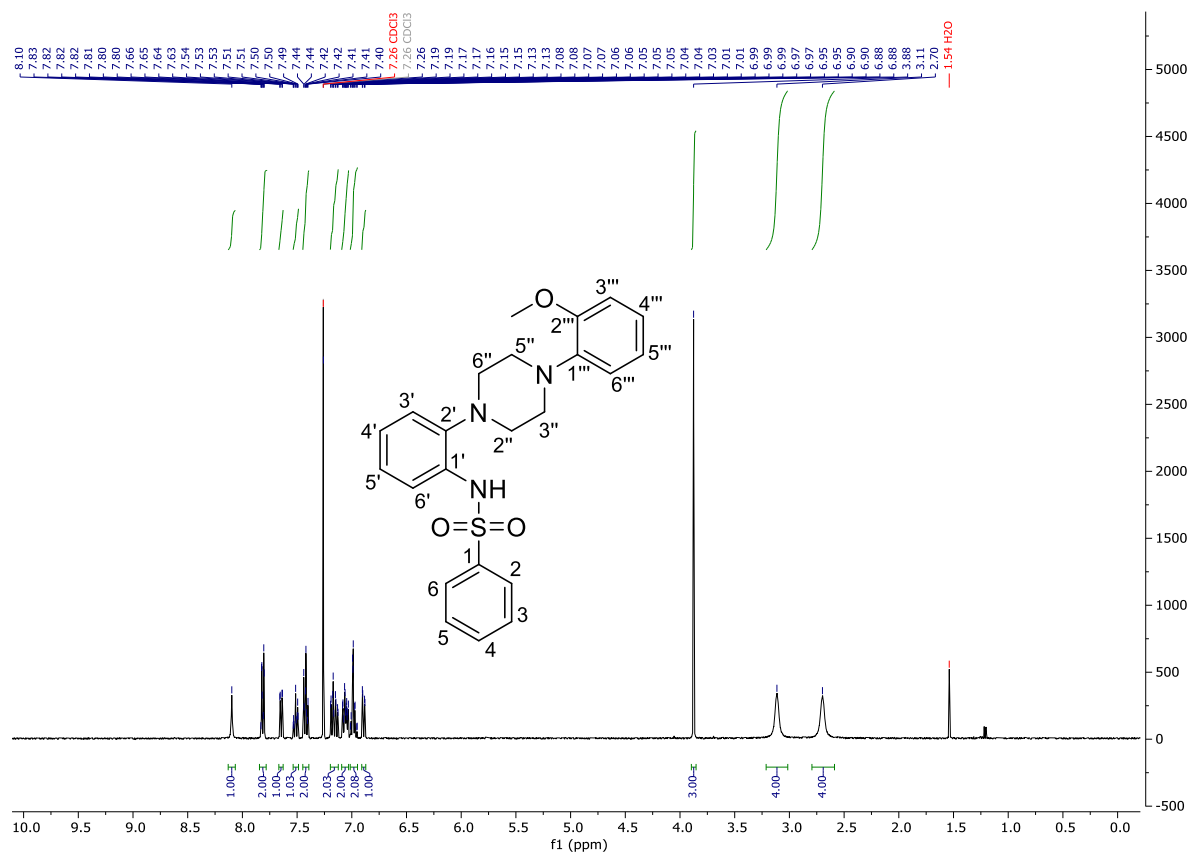
trans-*N*-(2-(4-phenylpiperidin-1-yl)cyclohexyl)benzenesulfonamide (27)



trans-N-(2-(1,2,3,4-tetrahydroisoquinolin-2-yl)cyclohexyl)benzenesulfonamide (**28**)



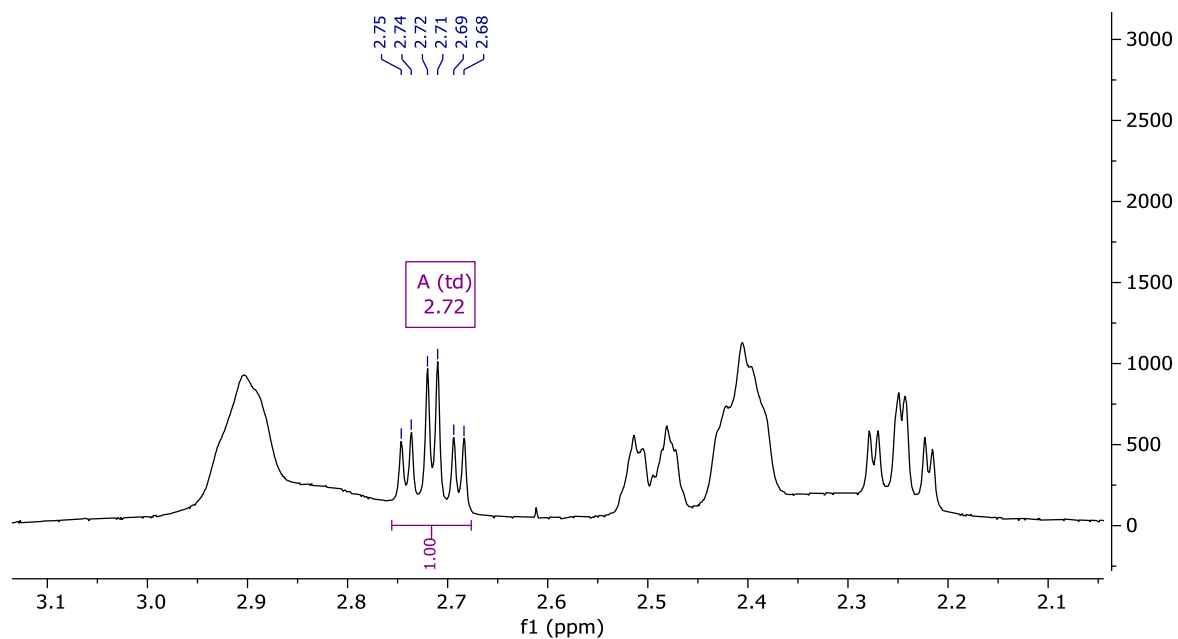
N-(2-(4-(2-methoxyphenyl)piperazin-1-yl)phenyl)benzenesulfonamide (**31**)



Details of NMR spectra for cis / trans determination

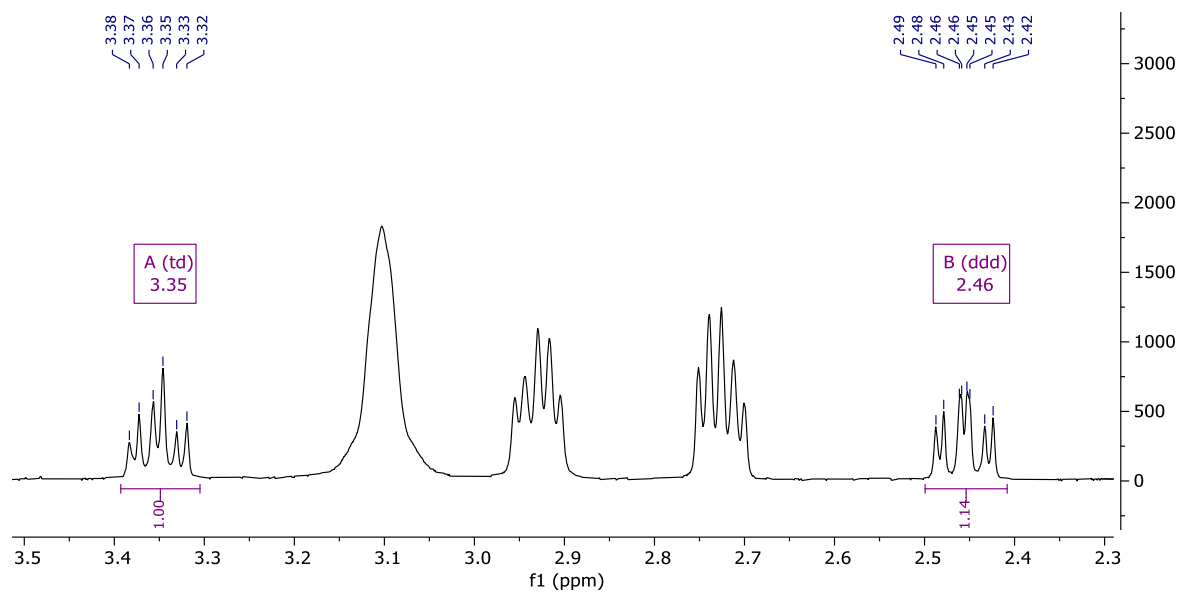
trans-*N*-(2-(4-(2-methoxyphenyl)piperazin-1-yl)cyclohexyl)benzenesulfonamide (*trans*-ML-SI3)

^1H NMR (400 MHz, Chloroform-*d*) δ 2.65 (td, $J = 10.5, 4.0$ Hz, 1H).



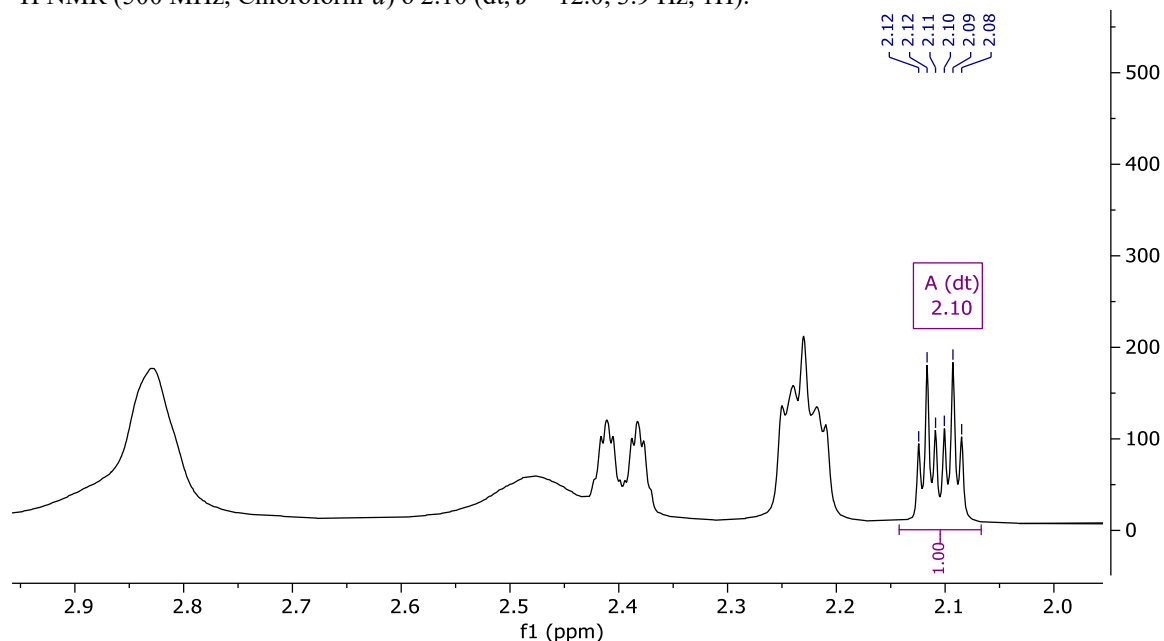
trans-1-(2-azidocyclohexyl)-4-(2-methoxyphenyl)piperazine (**11**)

^1H NMR (400 MHz, Chloroform-*d*) δ 3.28 (td, $J = 10.6, 4.4$ Hz, 1H), 2.39 (ddd, $J = 11.6, 10.4, 3.6$ Hz, 1H).



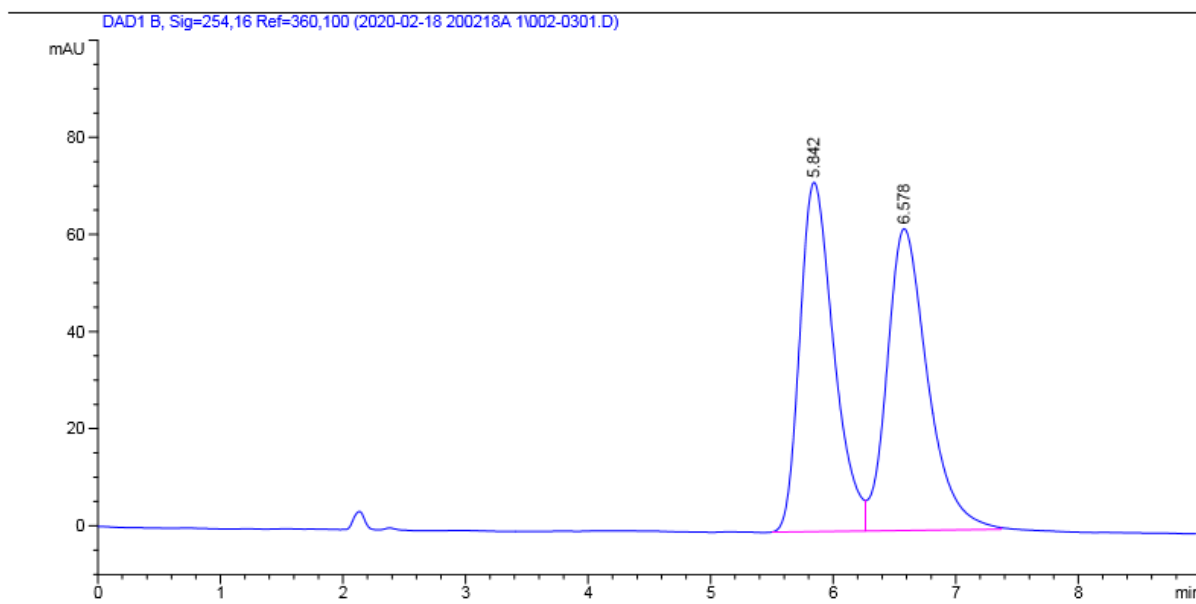
cis-N-(2-(4-(2-methoxyphenyl)piperazin-1-yl)cyclohexyl)benzenesulfonamide (*cis*- ML-SI3)

¹H NMR (500 MHz, Chloroform-*d*) δ 2.10 (dt, *J* = 12.0, 3.9 Hz, 1H).



Chromatograms of ee value determination

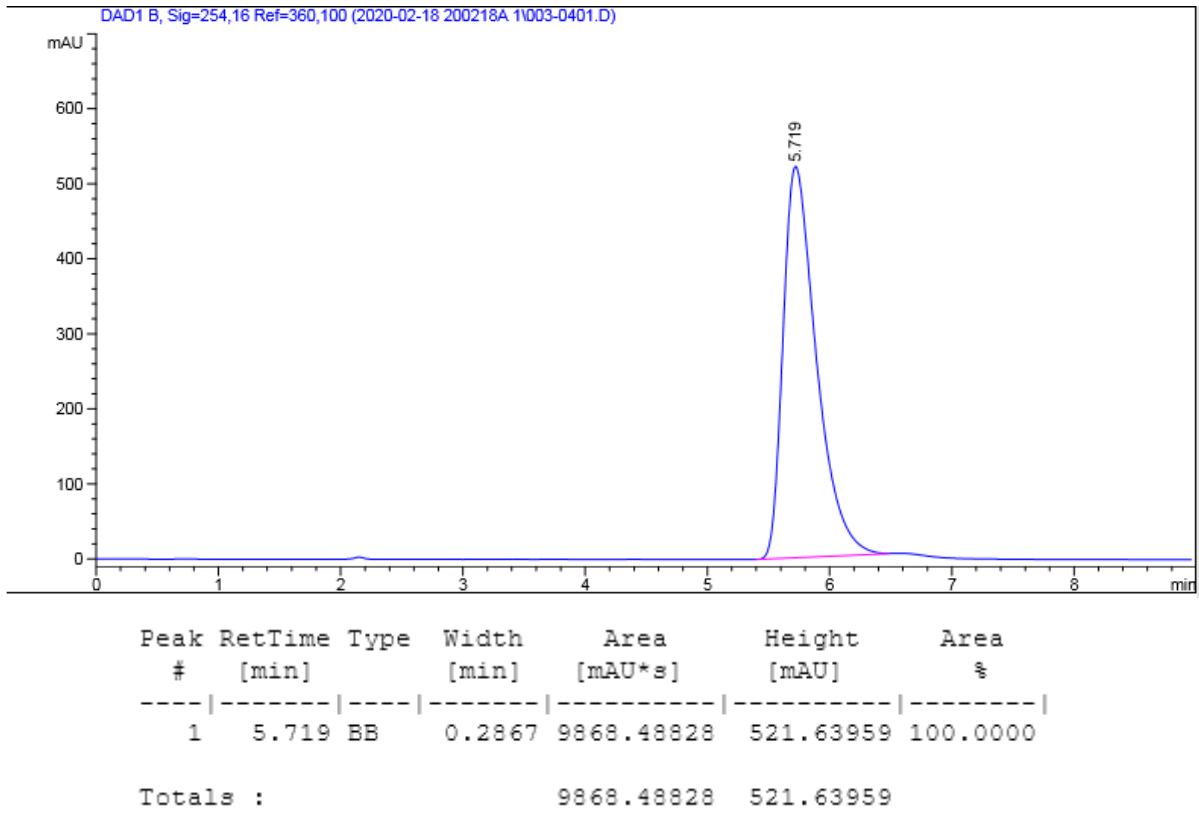
Racemic *trans*-ML-SI3



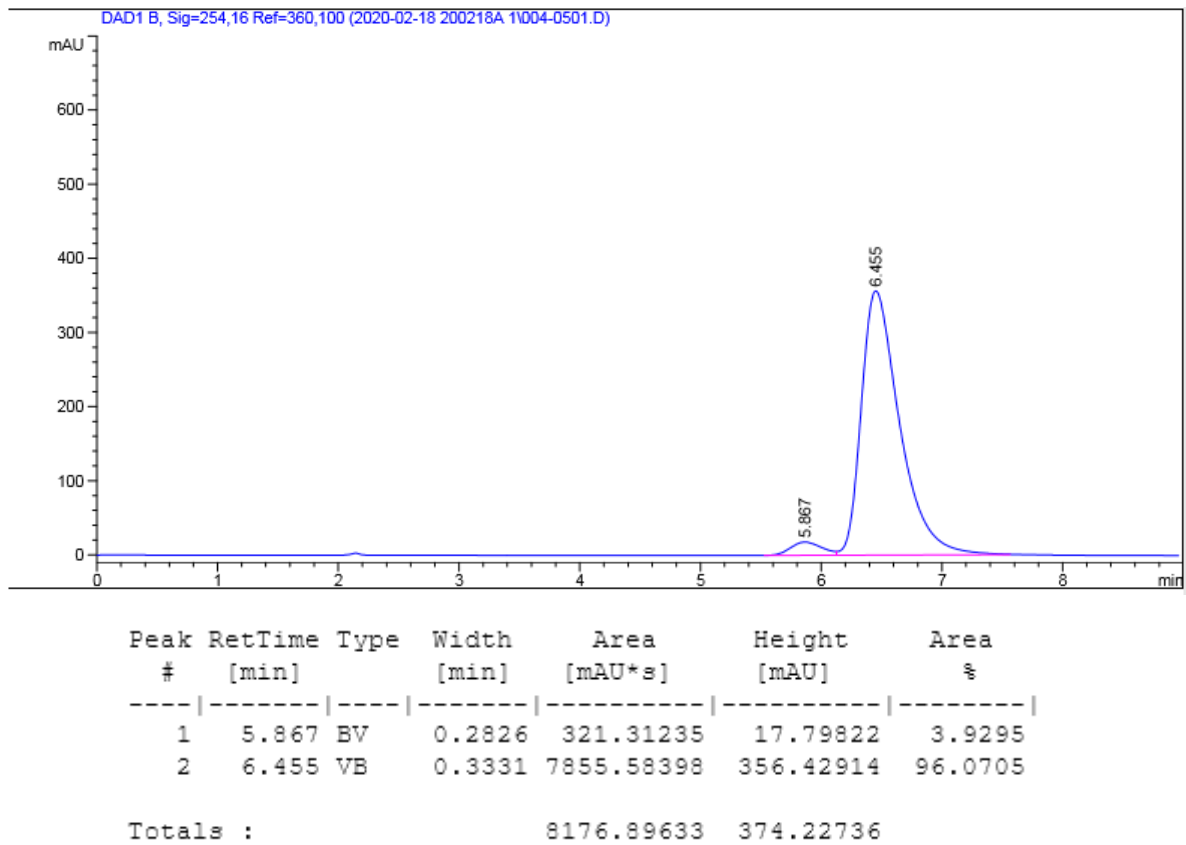
Peak #	RetTime [min]	Type	Width [min]	Area [mAU*s]	Height [mAU]	Area %
1	5.842	BV	0.2948	1385.91443	71.91606	49.1796
2	6.578	VB	0.3489	1432.15051	62.13474	50.8204

Totals : 2818.06494 134.05080

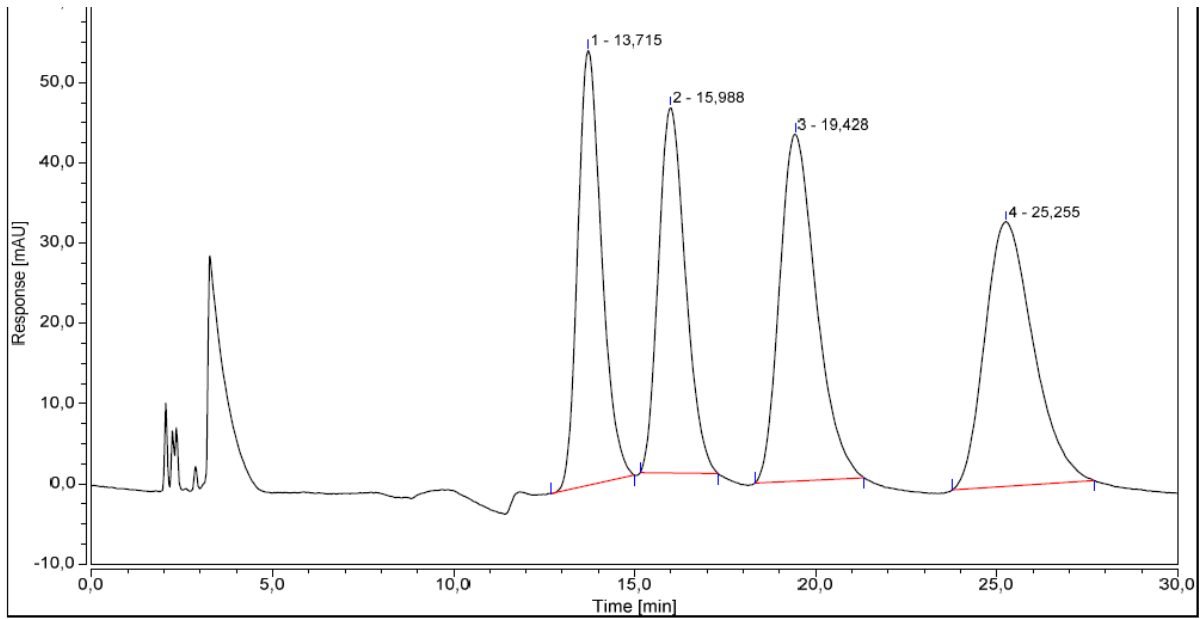
(-)-*trans*-ML-SI3



(+)-*trans*-ML-SI3



Racemic mixture of diastereomers of ML-SI1

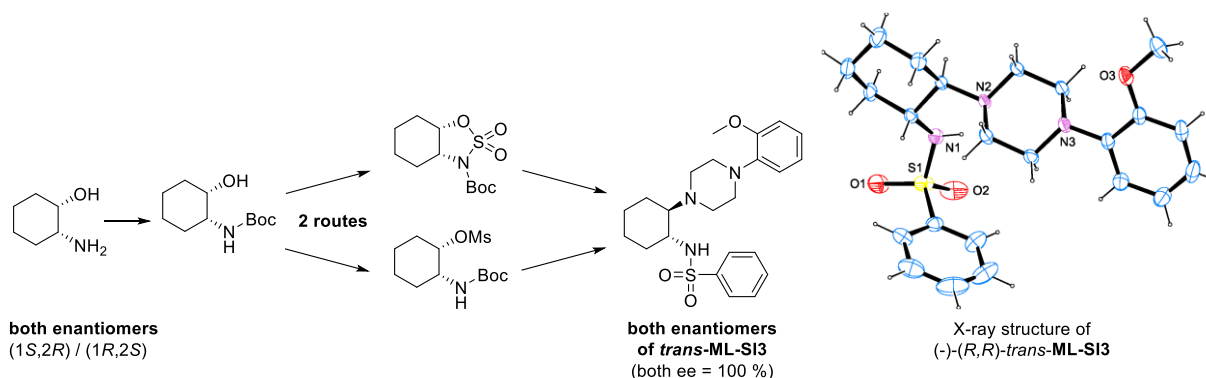


DAD1_Signal_A

No.	Retention Time min	Area mAU*min	Relative Area %
1	13,715	41,454	22,69
2	15,988	39,463	21,60
3	19,428	50,639	27,72
4	25,255	51,129	27,99
Total:		182,685	100

3.1.2 Chiral pool synthesis of enantiopure *trans*-ML-SI3

Kriegler, K.; Leser, C.; Mayer, P.; Bracher, F., *Effective chiral pool synthesis of both enantiomers of the TRPML inhibitor trans-ML-SI3*. *Arch Pharm (Weinheim)* 2021, e2100362.



3.1.2.1 Summary

From the previous study it was evident, that for the use of **ML-SI3** as a chemical tool, it is crucial to use it in its enantiopure form. If used as racemate, ambiguous results could be obtained due to the very different behaviour towards TRPML channels of the two enantiomers. The aim of this study was thus, to develop a reliable method to synthesise both enantiomers in a pure form in larger scale. Starting from commercially available enantiopure *cis*-aminohexanol, two methods were developed. After protection of the primary amino group, the first route, *via* a cyclic intermediate, starts with the creation of a sulfamidite intermediate by reaction with thionyl chloride. This conserves the *cis*-configuration because at the esters of the sulfurous acid aren't as good leaving groups as the esters of sulfuric acid. Once the configuration is locked, the sulfamidite is oxidized to the sulfamidate, whereby the oxygen containing residue is transformed into a leaving group. The following S_N2 reaction with the envisaged amino component as nucleophile, creates the desired *trans*-configuration by inversion. Because the oxidation of the sulfamidite is a problematic reaction due to the needed ruthenium catalyst, a second method was developed. Here, after the protection of the primary amino group, the secondary alcohol is directly transformed into a good leaving group by O-mesylation. The resulting mesylate is stable enough, so that the *cis*-configuration is maintained at this step. The following S_N2 reaction with the desired amino component yields the *trans*-configured diamino cyclohexane. The final steps for both routes are then deprotection of the primary amino group and subsequent N-sulfonylation. Both routes deliver the enantiomers in a predictable and reliable manner. The absolute configuration can be determined by the configuration of the used starting material, since the only stereochemistry

alternating step at one single stereocenter happens in a controlled way by inversion during the S_N2 reaction. Additionally, X-ray analysis of a single crystal confirmed the predicted absolute configuration. Combined, the results allow the (previously unknown) assignment of the *R,R*-configuration to (-)-*trans*-ML-SI3 and the *S,S*-configuration to (+)-*trans*-ML-SI3.

3.1.2.2 Personal contribution

The method development for the chiral pool synthesis was done by KATHARINA KRIEGLER during her Master thesis. She also contributed to writing of the manuscript.

My contribution to this article was the supervision of KATHARINA KRIEGLER during her Master thesis. Further, I synthesized all compounds of this publication for complete analytical data and closed missing gaps in the development of the sulfamidate route. The analytical chiral HPLC method was developed by me. Crystallization of the two enantiomers for X-ray analysis was done by me and I contributed to writing, reviewing, and editing of the manuscript.

PETER MAYER performed the X-ray analysis.

FRANZ BRACHER supervised the experiments and designed the project. He also contributed to writing, reviewing, and editing of the manuscript.

3.1.2.3 Article

The following article is printed in the original wording. Formatting may vary slightly compared to the original article.



Received: 15 September 2021 | Revised: 10 October 2021 | Accepted: 12 October 2021

DOI: 10.1002/ardp.202100362

FULL PAPER

ARCH PHARM DPhG
Archiv der Pharmazie

Effective chiral pool synthesis of both enantiomers of the TRPML inhibitor *trans*-ML-SI3

Katharina Kriegler¹ | Charlotte Leser¹ | Peter Mayer² | Franz Bracher¹ ¹Department of Pharmacy, Center for Drug Research, Ludwig-Maximilians University of Munich, Munich, Germany²Department of Chemistry, Ludwig-Maximilians University of Munich, Munich, Germany**Correspondence**

Franz Bracher, Department of Pharmacy, Center for Drug Research, Ludwig-Maximilians University of Munich, Butenandtstr. 5-13, 81377 Munich, Germany. Email: franz.bracher@cup.uni-muenchen.de

Funding information

Deutsche Forschungsgemeinschaft, Grant/Award Number: BR-1034/7-1

Abstract

Two independent chiral pool syntheses of both enantiomers of the TRPML inhibitor, *trans*-ML-SI3, were developed, starting from commercially available (1*S*,2*R*)- and (1*R*,2*S*)-configured *cis*-2-aminocyclohexanols. Both routes lead to the target compounds in excellent enantiomeric purity and good overall yields. For the most attractive (–)-*trans*-enantiomer, the *R,R*-configuration was identified by these unambiguous syntheses, and the results were confirmed by single-crystal X-ray structure analysis. These effective synthetic approaches further allow flexible variation of prominent residues in ML-SI3 for future in-depth analysis of structure–activity relationships as both the piperazine and the *N*-sulfonyl residues are introduced into the molecule at late stages of the synthesis.

KEYWORDS

arylpiperazine, chiral pool synthesis, enantiomers, sulfamidate, TRPML cation channels

1 | INTRODUCTION

The family of transient receptor potential (TRP) ion channels comprises a group of cation permeable ion channels, which encloses 28 genes in mammals. On the basis of their sequence homology they are grouped into six subfamilies (TRPC, TRPV, TRPM, TRPML, TRPP, TRPA).^[1] The TRPML subfamily consists out of three members, namely TRPML1–3 (Mucopolipins 1–3).^[1–3] In contrast to most TRPCs that are widely expressed and found in the plasma membrane, TRPMLs are predominantly expressed in intracellular vesicles of the endolysosomal system.^[3–5] The different subtypes are diversely located within the compartments of the endolysosomal system, whereby all subtypes are found in lysosomes and late endosomes, whereas TRPML2 is mainly found in recycling endosomes, and TRPML3 is localized to early endosomes and the plasma membrane.^[4–9] Mutations in the gene encoding for the TRPML1 channel are associated with the hereditary channelopathy mucopolipidosis type IV, a rare neurodegenerative

lysosomal storage disorder, which manifests in infancy and exhibits slow progression.^[10–12] Patients exhibit increased lysosomal storage due to abnormal endocytic processes and the disease is characterized by severe psychomotor retardation and visual impairment.^[10–13] TRPML subtypes 2 and 3 have not been linked to any diseases in humans yet^[3]; however, gain-of-function mutations in the TRPML3 gene in mice cause the varitint-waddler phenotype, which features dilute coat color due to pigmentation defects, deafness, and circling behavior due to vestibular defects.^[14–18] Further, TRPMLs have been shown to play a crucial role in the progression of viral infections and immune responses.^[19] Recently, it has been shown that TRPML2 is able to promote viral infections in the early stages by enhancing the vesicular trafficking and escape from endosomal compartments for viruses that require transport to the late endosomes for infection, including the yellow fever virus, influenza A virus, and Dengue virus.^[20] Additionally, TRPML2 has been shown to be involved in the regulation of the innate immune response, as macrophages exhibit an increased TRPML2

Katharina Kriegler and Charlotte Leser contributed equally to this study.

This is an open access article under the terms of the Creative Commons Attribution-NonCommercial-NoDerivs License, which permits use and distribution in any medium, provided the original work is properly cited, the use is non-commercial and no modifications or adaptations are made.

© 2021 The Authors. *Archiv der Pharmazie* published by Wiley-VCH Verlag GmbH on behalf of Deutsche Pharmazeutische Gesellschaft.

Arch. Pharm. 2022;355:e2100362.
<https://doi.org/10.1002/ardp.202100362>

wileyonlinelibrary.com/journal/ardp | 1 of 9

expression upon TLR (Toll-like receptor) activation.^[21] Moreover, altered expression levels of all TRPML subtypes have been linked to cancer, whereby the majority exhibits an involvement of TRPML1, which has among others been shown in cancer cells with activating HRAS-mutations or triple-negative breast cancer cells.^[22–24]

Although various synthetic TRPML activators with improving selectivity and potency profiles have been developed over the past decade (e.g., the unselective TRPML activator ML-SA1, TRPML2-specific ML2-SA1, or TRPML1 activator MK6-83),^[25–27] potent and selective inhibitors for TRPML channels are still missing. Hitherto only a few synthetic inhibitors of TRPML channels (ML-SI1, ML-SI2, ML-SI3, and the TRPML1-selective inhibitor EDME) were identified.^[28–30] Of the ML-SIs, merely the structures of ML-SI1 and ML-SI3 are known, although the relative and absolute configuration of these inhibitors were published without any stereochemical details (Figure 1).^[28,29] A recent characterization of both inhibitors by our group identified ML-SI3 as the more potent inhibitor and resolved some stereochemical details, revealing that the racemic *trans*-isomer shows an enhanced inhibitory activity compared to the racemic *cis*-isomer. Separation of the enantiomers of *trans*-ML-SI3 by preparative chiral high-performance liquid chromatography (HPLC) enabled us to show that the enantiomers exhibit distinct effects on the TRPML channel subtypes. The (–)-*trans*-enantiomer showed pronounced inhibitory efficacy on all three subtypes, whereas the (+)-*trans*-enantiomer acts as an inhibitor only on TRPML1 and interacts with TRPML2 and TRPML3 as an activator.^[31] However, this previous work did not permit the assignment of absolute configurations to the separated enantiomers.

Consequently, there was an urgent need for elucidation of the absolute configurations of the enantiomers of *trans*-ML-SI3 for a profound analysis of structure–activity relationships of these and future compounds from this chemotype. Further, an enantioselective synthesis should be worked out for being able to provide sufficient amounts of these enantiomerically pure chemical tools for further pharmacological investigations.

2 | RESULTS

To determine the absolute configurations of both *trans*-ML-SI3 enantiomers and provide effective access to both enantiomers, we attempted a short chiral pool synthesis, providing predictable

stereochemistry and high enantiomeric purity, starting from commercially available enantiomerically pure starting materials. Due to their commercial availability in high enantiomeric purity and at a reasonable price, the *cis*-2-aminocyclohexanols **1a** and **1b** (either in (1*S*,2*R*) or (1*R*,2*S*)-configuration) were estimated to be suitable starting materials for the planned chiral pool synthesis. The success of our approach depended on the development of a synthesis protocol that would allow us to obtain the desired *trans*-configuration of the target compounds through a controlled inversion of the stereocenter of the secondary alcohol group using an appropriate *N*-arylpiperazine building block.

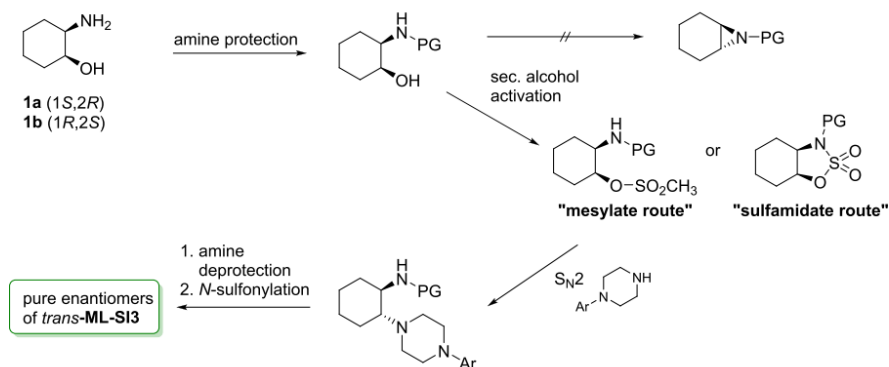
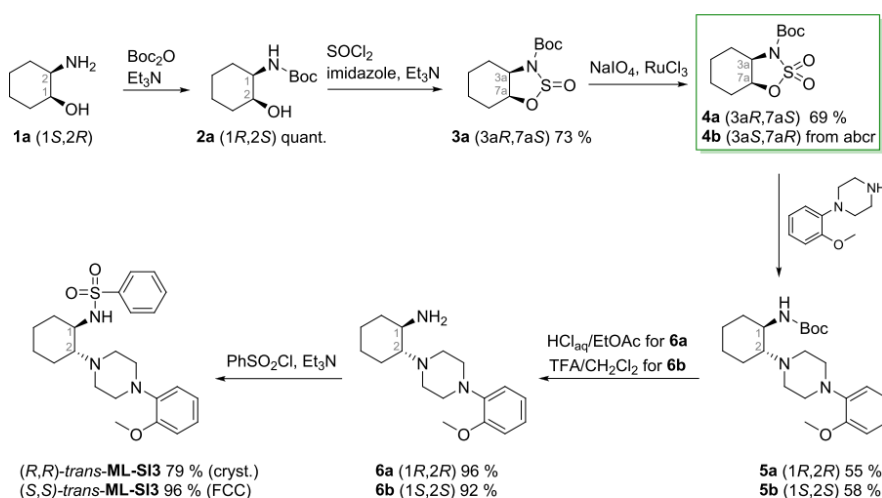
This intended clean inversion (following an S_N2 mechanism) required conversion of the secondary alcohol function into an appropriate leaving group while retaining the *cis*-configuration at this step. Literature data suggested to either convert the alcohol into a sulfonate (like mesylate), alternatively—as here, we had the special case of a vicinal aminoalcohol building block—a cyclic sulfamidate was considered. Both approaches required the protection of the primary amino group, for which the Boc, as well as an arenesulfonyl group, were considered.

At the first glance, it appeared tempting to use the phenylsulfonyl residue (which is an integral part of the target molecules) as a protective group for the amine. However, literature data and pilot experiments revealed that the obtained sulfonamide exerts, due to its noteworthy NH-acidity, considerable reactivity, and can undergo *N*-sulfonylaziridine ring formation (under undesired inversion) with the newly generated electrophile formed in the course of the conversion of the neighboring secondary alcohol into a leaving group.^[31,32] For this reason, we examined suitable protection of the amino group, which provides a less reactive derivative, and selected Boc protection. The resulting carbamate does not show undesirable NH-acidity, further, both introduction and removal of Boc groups are well documented and typically give high yields (Scheme 1).

N-Boc-protected cyclic sulfamidates **4a/4b** derived from *cis*-2-aminocyclohexanols **1a/1b** have been previously described by Guo et al.^[33] Moreover, both of these enantiomers are commercially available. This prompted us to focus on these intermediates first. Following the general procedure of Atfani et al.,^[34] the nucleophilic ring opening of purchased sulfamidates **4a** and **4b** was carried out in CH₃CN with excess 1-(2-methoxyphenyl)piperazine at 75°C to



FIGURE 1 Structures of published TRPML inhibitors: ML-SI1 and racemic *cis*- and *trans*-ML-SI3


 SCHEME 1 Strategies for the chiral pool synthesis of pure enantiomers of *trans*-ML-SI3

 SCHEME 2 Synthesis of (*R,R*)-*trans*-ML-SI3 and (*S,S*)-*trans*-ML-SI3 via the "sulfamidate route"

obtain, after acidic aqueous workup, the *trans*-configured products **5a** and **5b** in moderate yields (55% and 58%). Yields could not be improved by prolonged reaction times. Subsequent Boc-deprotection under standard acidic conditions (TFA/DCM or HCl_{aq}/EtOAc) gave primary amines **6a** and **6b** in yields of 96% and 92%. Finally, *N*-sulfonylation of these amines with benzenesulfonyl chloride in the presence of Et₃N gave (*R,R*)-*trans*-ML-SI3 and (*S,S*)-*trans*-ML-SI3 in high yields (79% [cryst.] and 96% [flash column chromatography {FCC}]). Subsequent analysis of both products by an improved analytical chiral HPLC, based on the method of Leser et al.,^[31] revealed that the (+)-enantiomer (*S,S*)-*trans*-ML-SI3 was obtained with a perfect enantiomeric excess (ee) of >99%, whereas the synthesized (–)-enantiomer (*R,R*)-*trans*-ML-SI3 had an ee of only 34%. These deviating results are likely attributable to the applied starting

materials, as both Boc-protected sulfamidates **4a** and **4b** were purchased from different commercial sources and were supplied without any information about their enantiomeric purities. To further confirm that the sulfamidate strategy generally renders both enantiomers in high enantiomeric purity, we conducted the synthesis of (*R,R*)-*trans*-ML-SI3 from the beginning, starting with the Boc-protection of (1*S*,2*R*)-2-aminocyclohexanol (**1a**) under basic conditions. Boc-protected sulfamidate **4a** was synthesized following the protocol of Rönholm et al.^[35] in a two-step procedure via formation of a cyclic sulfamidite intermediate through conversion with SOCl₂ in presence of imidazole and NEt₃ at 0°C in CH₂Cl₂. Consecutive ruthenium-catalyzed oxidation gave the sulfamidate **4a**. All further steps were conducted as described above (Scheme 2). Analysis of the so-obtained product (*R,R*)-*trans*-ML-SI3 by analytical chiral HPLC

confirmed the expected ee of >99% (see the Supporting Information for the respective chromatograms).

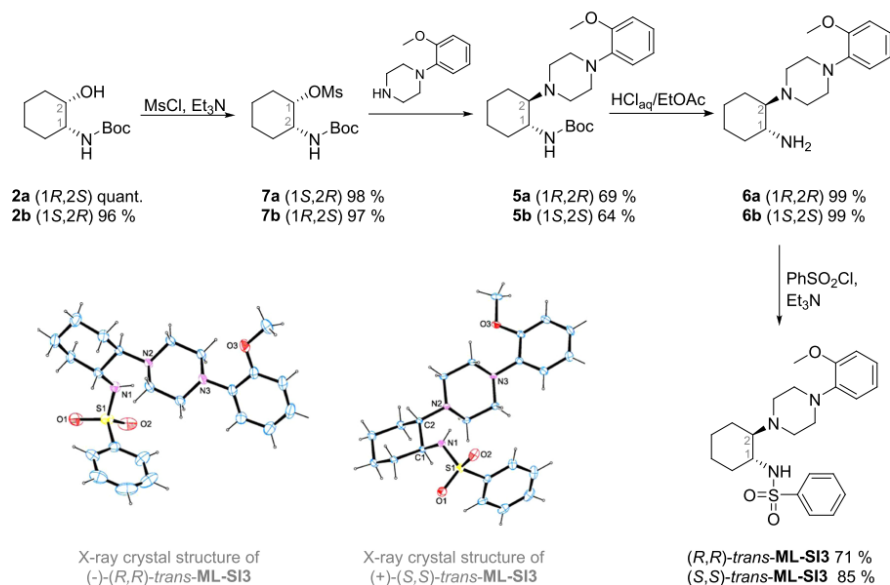
Despite the pleasing successful synthesis of both enantiomers of *trans*-ML-SI3 via the "sulfamidate route," we investigated the alternative "mesylate route" as well. The Boc-protected sulfamidates **4a/4b** are very expensive if purchased, and self-performed synthesis requires the use of a heavy metal catalyst. Following the method described above, both enantiomeric *cis*-aminocyclohexanols (**1a**, **1b**) were converted into the Boc-protected derivatives (**2a**, **2b**) in almost quantitative yields. Subsequently, the secondary alcohol functionality was converted into a mesylate (**7a**, **7b**) leaving group following a protocol of Pendem et al.,^[36] again in virtually quantitative yields. The nucleophilic displacement of the mesylate group was performed by melting **7a/7b** in excess 1-(2-methoxyphenyl)piperazine (mp 35–40°C) at 60°C, based on similar conditions described in a patent of Sutherland et al.,^[37] providing **5a** and **5b** in moderate yields (69% and 64%). The following Boc-deprotection was performed here with an even more convenient method, using a hydrochloric acid/ethyl acetate two-phase system, giving excellent yields of primary amines **6a** and **6b**. *N*-Sulfonylation was performed in the same manner as described above to give (*R,R*)-*trans*-ML-SI3 and (*S,S*)-*trans*-ML-SI3 in high overall yields (Scheme 3). Analytical chiral HPLC analysis confirmed that both enantiomers of the target compound were obtained with an ee of >99% via this route.

For both enantiomerically pure target compounds, the absolute configuration was further confirmed by X-ray crystal structure analysis (for details, see the Supporting Information).

3 | DISCUSSION

In the previous work, we highlighted the structure-activity relationships of the TRPML cation channel blocker ML-SI3 and found that the racemic *trans*-isomer shows significantly enhanced inhibitory activity compared to the racemic *cis*-isomer (Figure 1). Semipreparative HPLC separation of the enantiomers of *trans*-ML-SI3 enabled us to show that the (–)-*trans*-enantiomer showed pronounced inhibitory efficacy on all three TRPML subtypes, and represents the up to now most attractive chemical tool for further investigations of these ion channels.^[31] Further, it was evident that chirality plays an outstanding role in this chemotype of TRPML inhibitors, and only pure enantiomers should be considered as chemical tools or drug candidates here. However, this assignment of absolute configurations of the separated enantiomers of *trans*-ML-SI3 was not possible at that time.

Here, we present two chiral pool syntheses of both enantiomers of *trans*-ML-SI3 starting from commercially available (1*S*,2*R*)- and (1*R*,2*S*)-configured *cis*-2-aminocyclohexanols **1a** and **1b**, which lead to the target compounds in excellent enantiomeric purity and good overall yields. For the most attractive (–)-*trans*-enantiomer, an



SCHEME 3 Synthesis of (*R,R*)-*trans*-ML-SI3 and (*S,S*)-*trans*-ML-SI3 via the "mesylate route". The X-ray crystal structures are shown for both enantiomers

R,R-configuration was found by unambiguous enantioselective synthesis and confirmed by X-ray crystal structure analysis.

The "sulfamidate route" was hampered by the uncertain purity of purchased intermediates, but reliably provided target products of high purity when performing the entire synthetic sequence shown in Scheme 2 in our own lab.

Both the "sulfamidate route" and the "mesylate route" (Scheme 3) further allow flexible variation of prominent residues in **ML-SI3**, as both the piperazine residue and the *N*-sulfonyl group are introduced into the molecule at the late stages of the synthesis. This allows for the synthesis of a broad spectrum of enantiomerically pure analogs of this lead structure for in-depth analysis of structure–activity relationships.

4 | EXPERIMENTAL

4.1 | Chemistry

4.1.1 | General

All chemicals used were of analytical grade and were obtained from abcr, Fisher Scientific, Sigma-Aldrich (now Merck), TCI, or Th. Geyer. The cyclic sulfamidate building blocks were obtained from Sigma-Aldrich/Merck (3aR,7aS) and abcr (3aS,7aR). HPLC-grade and dry solvents were purchased from VWR or Sigma-Aldrich; all other solvents were purified by distillation. All reactions were monitored by thin-layer chromatography using precoated plastic sheets POLYGRAM® SIL G/UV254 from Macherey–Nagel and detected by irradiation with UV light (254 nm) or by staining with appropriate reagents. FCC was performed on Macherey–Nagel silica gel Si 60 (0.015–0.040 mm).

Nuclear magnetic resonance (NMR) spectra (¹H, ¹³C, DEPT, H-H-COSY, HSQC/HMQC, HMBC) were recorded at 23°C on an Avance III 400 MHz Bruker BioSpin or Avance III 500 MHz Bruker BioSpin instrument. Chemical shifts δ are stated in parts per million (ppm) and are calibrated using residual protic solvent as an internal reference for proton (CDCl₃: δ = 7.26 ppm, deuterated dimethyl sulfoxide [DMSO-*d*₆]: δ = 2.50 ppm), and for carbon, the central carbon resonance of the solvent (CDCl₃: δ = 77.16 ppm, DMSO-*d*₆: δ = 39.52 ppm). Multiplicity is defined as s = singlet, d = doublet, t = triplet, and m = multiplet. NMR spectra were analyzed with NMR software MestReNova, version 12.0.1-20560 (Mestrelab Research S.L.). High-resolution mass spectra were performed by the LMU Mass Spectrometry Service applying a Thermo Finnigan LTQ FT Ultra Fourier Transform Ion Cyclotron Resonance device at 250°C for electrospray ionization (ESI) and a Thermo Q Exactive GC Orbitrap device at 250°C and electron energy of 70 eV for electron ionization (EI). Infrared spectra were recorded from 4000–650 cm⁻¹ on a Perkin Elmer Spectrum BX-59343 FT-IR instrument. For detection, a Smiths Detection DuraSamp IR II Diamond ATR sensor was used. The absorption bands are reported in wavenumbers (cm⁻¹). Melting points were determined by the open tube capillary method on a Büchi melting

point B-540 apparatus and are uncorrected. HPLC purities were determined using an Agilent 1100 HPLC with a diode array detector and an Agilent Zorbax Eclipse plus C18 column (150 × 4.6 mm, 5 μ m) with methanol/water 80:20 adjusted to pH 9 with NaOH as mobile phase. Determination of ee values was performed using a Daicel Chiralpak IE-3 column (150 × 4.6 mm, 3 μ m). Values for specific rotation (α) were measured at 23°C at a wavelength of λ = 589 nm (Na-D-line) using a Perkin Elmer 241 Polarimeter instrument. All samples were dissolved in chloroform (layer thickness *l* = 10 cm), the concentration is stated in g/100 ml.

The InChI codes of the investigated compounds are provided as Supporting Information.

4.1.2 | Crystallography

All X-ray intensity data were measured on a Bruker D8 Venture TXS system equipped with a multilayer mirror monochromator and an Mo K α rotating anode X-ray tube (λ = 0.71073 Å). The frames were integrated with the Bruker SAINT software package.^[38] Data were corrected for absorption effects using the Multi-Scan method (SADABS).^[39] The structure was solved and refined using the Bruker SHELXTL Software Package.^[40] All C-bound hydrogen atoms have been calculated in ideal geometry riding on their parent atoms while the N-bound hydrogen atoms have been refined freely. The N–H distances have been constrained to be equal within 0.01 Å. Crystallographic data have been deposited with the Cambridge Crystallographic Data Centre, CCDC, 12 Union Road, Cambridge CB21EZ, UK. Copies of the data can be obtained free of charge on quoting the depository numbers CCDC-2109888 ((-)-(R,R)-*trans*-ML-SI3) and 2109889 ((+)-(S,S)-*trans*-ML-SI3) (<https://www.ccdc.cam.ac.uk/structures/>).

4.1.3 | Synthesis and characterization

tert-Butyl [(1*R*,2*S*)-2-hydroxycyclohexyl]carbamate (**2a**) (1*S*,2*R*)-2-Aminocyclohexan-1-ol hydrochloride (3.87 g, 25.0 mmol) was suspended in CH₂Cl₂ (70 ml) and a solution of Boc₂O in CH₂Cl₂ (2 M, 15 ml, 30 mmol) was added. The mixture was cooled to 0°C and Et₃N (7.0 ml, 50 mmol) was added dropwise. The resulting solution was stirred for 16 h while warming up to room temperature (rt). The reaction mixture was washed with brine (50 ml) and the aqueous layer extracted with CH₂Cl₂ (2 × 50 ml). The combined organic layers were dried using a hydrophobic filter and the solvent removed in vacuo. The residue was purified by FCC (petrol ether/ethyl acetate 7:3) to give **2a** (5.4 g, 25 mmol, quant.) as colorless solid. mp.: 62–63°C. [α]_D²³: +32.2 (*c* = 0.5, CHCl₃). IR (ATR): $\tilde{\nu}$ (cm⁻¹) = 3503 (OH), 3369 (NH), 2930 (m), 1663 (C=O), and 1522 (vs). ¹H NMR (400 MHz, DMSO-*d*₆) δ (ppm) = 6.14 (d, *J* = 8.2 Hz, 1H, NH), 4.44 (d, *J* = 3.8 Hz, 1H, OH), 3.72–3.67 (m, 1H, CHOH), 3.31–3.26 (m, 1H, CHNHBoc), 1.69–1.60 (m, 1H, CH₂), 1.37 (m, 14H, CH₂ and tBu), and 1.28–1.15 (m, 2H, CH₂). ¹³C NMR (101 MHz, DMSO-*d*₆) δ (ppm) = 154.8 (C=O),

77.5 (C_q-tBu), 67.0 (CHOH), 52.3 (CHNHoc), 31.7 (CH₂), 28.2 (CH₃-tBu), 26.8 (CH₂), 23.9 (CH₂), and 19.4 (CH₂). HRMS (ESI): calcd. for C₁₁H₂₀NO₃⁻ [M-H]⁻: 214.1449, found: 214.1449.

tert-Butyl [(1*S*,2*R*)-2-hydroxycyclohexyl]carbamate (**2b**)^[36]

Following the procedure described for **2a**, (1*R*,2*S*)-2-aminocyclohexan-1-ol hydrochloride (0.76 g, 5.0 mmol) was converted into Boc-protected **2b** (1.03 g, 4.48 mmol, 96%) as colorless solid. mp.: 62–63°C. [α]_D²³: –32.5 (c = 0.5, CHCl₃). IR (ATR): $\tilde{\nu}$ (cm⁻¹) = 3503 (OH), 3369 (NH), 2931 (m), 1663 (C=O), and 1522 (vs). ¹H NMR (400 MHz, DMSO-*d*₆) δ (ppm) = 6.14 (d, *J* = 8.2 Hz, 1H, NH), 4.43 (d, *J* = 3.8 Hz, 1H, OH), 3.72–3.67 (m, 1H, CHOH), 3.31–3.26 (m, 1H, CHNHoc), 1.63 (dt, *J* = 12.6, 4.3 Hz, 1H, CH₂), 1.59–1.31 (m, 14H, CH₂ and tBu), and 1.29–1.16 (m, 2H, CH₂). ¹³C NMR (101 MHz, DMSO-*d*₆) δ (ppm) = 154.8 (C=O), 77.5 (C_q-tBu), 67.0 (CHOH), 52.3 (CHNHoc), 31.7 (CH₂), 28.2 (CH₃-tBu), 26.8 (CH₂), 23.9 (CH₂), and 19.4 (CH₂). HRMS (ESI): calcd. for C₁₁H₂₀NO₃⁻ [M-H]⁻: 214.1449, found: 214.1449.

(1*S*,2*R*)-2-[(*tert*-Butoxycarbonyl)amino]cyclohexyl methanesulfonate (**7a**)

tert-Butyl [(1*R*,2*S*)-2-hydroxycyclohexyl]carbamate (**2a**) (2.19 g, 10.2 mmol) was dissolved in dry CH₂Cl₂ (70 ml) under N₂ atmosphere and Et₃N (2.1 ml, 15 mmol) was added. The solution was cooled to 0°C and methanesulfonyl chloride (1.20 ml, 15.5 mmol) was added dropwise. The reaction mixture was stirred for 2 h at 0°C. The reaction mixture was diluted with CH₂Cl₂ to 100 ml, then washed with water (50 ml), 1 M KHSO₄ solution (50 ml), and saturated NaHCO₃ solution (50 ml). The organic layer was dried using a hydrophobic filter and the solvent removed in vacuo to give **7a** (2.92 g, 9.95 mmol, 98%) as colorless solid, which was used without further purification. mp.: 122–124°C. [α]_D²³: +64.8 (c = 0.5, CHCl₃). IR (ATR): $\tilde{\nu}$ (cm⁻¹) = 3368 (NH), 2934 (m), 1687 (C=O), 1520 (vs), 1340 (s), 1169 (vs), and 899 (vs). ¹H NMR (400 MHz, CDCl₃) δ (ppm) = 4.98 (s, 1H, CHOMs), 4.75 (d, *J* = 8.1 Hz, 1H, NH), 3.66 (s, 1H, CHNHoc), 3.02 (s, 3H, Ms-CH₃), 2.20–2.10 (m, 1H, CH₂), and 1.81–1.31 (m, 16H, CH₂ and tBu). ¹³C NMR (101 MHz, CDCl₃) δ (ppm) = 155.1 (C=O), 80.7 (CHOMs), 79.8 (C_q-tBu), 51.0 (CHNHoc), 38.1 (CH₂), 30.1 (CH₂), 28.4 (CH₃-tBu), 27.1 (CH₂), 24.0 (CH₂), and 19.2 (CH₂). HRMS (ESI): calcd. for C₁₂H₂₂NO₅S⁻ [M-H]⁻: 292.1224, found: 292.1227.

(1*R*,2*S*)-2-[(*tert*-Butoxycarbonyl)amino]cyclohexyl methanesulfonate (**7b**)^[36]

Following the procedure described for **7a**, *tert*-butyl [(1*S*,2*R*)-2-hydroxycyclohexyl]carbamate (**2b**) (820 mg, 3.81 mmol) was mesylated to give **7b** (1.08 g, 3.68 mmol, 97%) as colorless solid. mp.: 122–124°C. [α]_D²³: –65.2 (c = 0.5, CHCl₃). IR (ATR): $\tilde{\nu}$ (cm⁻¹) = 3369 (NH), 2933 (m), 1689 (C=O), 1520 (vs), 1340 (s), 1170 (vs), and 899 (vs). ¹H NMR (400 MHz, CDCl₃) δ (ppm) = 4.98 (s, 1H, CHOMs), 4.75 (d, *J* = 8.1 Hz, 1H, NH), 3.66 (s, 1H, CHNHoc), 3.02 (s, 3H, Ms-CH₃), 2.19–2.09 (m, 1H, CH₂), and 1.80–1.37 (m, 16H, CH₂ and tBu). ¹³C NMR (101 MHz, CDCl₃) δ (ppm) = 155.1 (C=O),

80.7 (CHOMs), 79.8 (C_q-tBu), 51.0 (CHNHoc), 38.1 (CH₂), 30.1 (CH₂), 28.4 (CH₃-tBu), 27.1 (CH₂), 24.0 (CH₂), and 19.2 (CH₂). HRMS (ESI): calcd. for C₁₂H₂₂NO₅S⁻ [M-H]⁻: 292.1224, found: 292.1226.

tert-Butyl (3*aR*,7*aS*)-hexahydro-3*H*-benzo[*d*][1,2,3]oxathiazole-3-carboxylate-2,2-dioxide (**4a**)

tert-Butyl [(1*R*,2*S*)-2-hydroxycyclohexyl]carbamate (**2a**) (1.08 g, 5.00 mmol), imidazole (1.43 g, 21.0 mmol), and Et₃N (1.39 ml, 10.0 mmol) were dissolved in dry CH₂Cl₂ (15 ml) under nitrogen atmosphere and the resulting solution was cooled to 0°C (ice bath). To this solution was added thionyl chloride (547 μl, 7.50 mmol) dropwise at 0°C. After complete addition, the ice bath was removed and the reaction mixture was stirred at rt for 2.5 h. The mixture was filtered through a short pad of silica and the silica was washed with CH₂Cl₂ (100 ml). The filtrate was washed with brine (50 ml), dried using a hydrophobic filter, and the solvent was removed in vacuo to give the cyclic sulfamidite **3a** (953 mg, 73%), which was used in the next step without further purification. For oxidation, ruthenium chloride (7.0 mg) was dissolved in water (1.0 ml) and 100 μl of this ruthenium chloride solution (0.70 mg, 0.15 mol%) was diluted with water to 1.25 ml. To this solution was added in small portions NaIO₄ (1.19 g, 5.55 mmol), but only the amount that dissolved. The solution turned from black to yellow and was added to silica gel (2.5 g) together with the remaining NaIO₄. The wetted silica gel was stirred until the powder became homogenous again. Ethyl acetate (9 ml) was added and the slurry was cooled to 0°C on an ice bath. The sulfamidite (580 mg, 2.22 mmol) was dissolved in ethyl acetate (9 ml) and was added dropwise to the slurry. Upon complete addition, the ice bath was removed and the mixture was stirred for 30 min at rt. The slurry was filtered through a short pad of silica and the filtrate dried using a hydrophobic filter. The solvent was removed in vacuo and the residue crystallized from CH₂Cl₂ and petrol ether to give **4a** (424 mg, 1.53 mmol, 69%) as white crystals. mp.: 137–138°C (lit.^[33]: 126.9–127.6°C). [α]_D²³: +4.1° (c = 0.5, CHCl₃). IR (ATR): $\tilde{\nu}$ (cm⁻¹) = 2944 (w), 1714 (C=O), 1331 (s), 1151 (s), 826 (s), and 718 (s). ¹H NMR (400 MHz, CDCl₃) δ (ppm) = 4.95 (q, *J* = 3.4 Hz, 1H, CH), 4.14 (ddd, *J* = 10.6, 6.3, 4.3 Hz, 1H, CH), 2.41–2.23 (m, 2H, CH₂), 1.88–1.45 (m, 14H, CH₂ and tBu), and 1.27–1.14 (m, 1H, CH₂). ¹³C NMR (101 MHz, CDCl₃) δ (ppm) = 148.6 (C=O), 85.2 (C_q-tBu), 79.2 (CH), 57.7 (CH), 28.1 (CH₃-tBu), 27.4 (CH₂), 27.2 (CH₂), 22.0 (CH₂), and 19.1 (CH₂). HRMS (EI): calcd. for C₁₁H₁₉NO₅S [M]⁺: 277.0984, found: 277.0984.

tert-Butyl [(1*R*,2*R*)-2-[4-(2-methoxyphenyl)piperazin-1-yl]-cyclohexyl]carbamate (**5a**)

Procedure A: (1*S*,2*R*)-2-[(*tert*-Butoxycarbonyl)amino]cyclohexyl methanesulfonate (**7a**) (295 mg, 1.01 mmol) and 1-(2-methoxyphenyl)piperazine (0.96 g, 5.0 mmol) were heated under N₂ atmosphere to 60°C. The resulting molten mass was stirred at 60°C for 24 h, then cooled to rt. The mixture was dissolved in ethyl acetate (20 ml) and washed with 2 M NaOH. The aqueous layer was extracted with ethyl acetate (2 × 10 ml) and the combined organic layers dried using a

hydrophobic filter. The solvent was removed in vacuo and the residue purified by FCC (petrol ether/ethyl acetate/Et₃N 9:1:0.2) to give **5a** (274 mg, 0.701 mmol, 69%) as colorless solid.

Procedure B: *tert*-Butyl (3*aR*,7*aS*)-hexahydro-3*H*-benzo[*d*][1,2,3]oxathiazole-3-carboxylate-2,2-dioxide (**4a**) was dissolved in CH₃CN under nitrogen atmosphere and 1-(2-methoxyphenyl)piperazine in 5 ml CH₃CN was added. The solution was stirred for 24 h at 75°C. Then CH₃CN was removed in vacuo, the residue was taken up in ethyl acetate (50 ml), and washed with 1 M KH₂PO₄ solution (50 ml). The aqueous layer was extracted with ethyl acetate (2 × 30 ml), the combined organic layers were dried using a hydrophobic filter and the solvent was removed in vacuo. The residue was purified by FCC (petrol ether/ethyl acetate/Et₃N 9:1:0.2) to give **5a** (213 mg, 0.547 mmol, 55%) as colorless solid.

Mp.: 167–169°C. [α]_D²³: –35.4 (*c* = 0.5, CHCl₃). IR (ATR): $\tilde{\nu}$ (cm⁻¹) = 3427 (NH), 2929 (m), 2818 (OCH₃), 1700 (C=O), 1497 (vs), 1235 (s), 1025 (s), and 755 (vs). ¹H NMR (400 MHz, CDCl₃) δ (ppm) = 7.02–6.89 (m, 3H, Ar-H), 6.85 (dd, *J* = 7.8, 1.4 Hz, 1H, Ar-H), 5.20 (d, *J* = 4.7 Hz, 1H, NH), 3.86 (s, 3H, OCH₃), 3.29 (dt, *J* = 10.4, 5.1 Hz, 1H, CHNH(Boc)), 3.17–2.79 (m, 6H, CH₂ piperazine), 2.55 (dt, *J* = 10.1, 4.3 Hz, CH₂ piperazine), 2.46–2.38 f (m, 1H, CH₂), 2.24 (dt, *J* = 10.8, 3.3 Hz, 1H, CHNR₁R₂), 1.94 (d, *J* = 10.8 Hz, 1H, CH₂), 1.80 (d, *J* = 10.3 Hz, 1H, CH₂), 1.67 (d, *J* = 12.4 Hz, 1H, CH₂), 1.45 (s, 9H, *t*Bu), and 1.30–1.05 (m, 4H, CH₂). ¹³C NMR (101 MHz, CDCl₃) δ (ppm) = 156.4 (C=O), 152.2 (C_q-Ar), 141.6 (C_q-Ar), 122.8 (C-Ar), 120.9 (C-Ar), 118.2 (C-Ar), 111.1 (C-Ar), 78.8 (C_q-*t*Bu), 67.4 (CHNR₁R₂), 55.3 (OCH₃), 51.3 (CH₂ piperazine), 51.2 (CHNH(Boc)), 48.0 (CH₂ piperazine), 33.4 (CH₂), 28.5 (CH₃-*t*Bu), 25.6 (CH₂), 24.7 (CH₂), and 23.3 (CH₂). HRMS (ESI): calcd. for C₂₂H₃₆N₃O₃⁺ [M+H]⁺: 390.2751, found: 390.2758. Purity (HPLC): >96%.

tert-Butyl ((1*S*,2*S*)-2-[4-(2-methoxyphenyl)piperazin-1-yl]-cyclohexyl)carbamate (**5b**)

Following the procedure A described for **5a**, (1*R*,2*S*)-2-[(*tert*-butoxycarbonyl)amino]cyclohexyl methanesulfonate (**7b**) (294 mg, 1.00 mmol) was reacted with 1-(2-methoxyphenyl)piperazine (0.96 g, 5.0 mmol) for 40 h to give **5b** (250 mg, 0.642 mmol, 64%) as colorless solid.

Procedure B: To a solution of 1-(2-methoxyphenyl)piperazine (1.21 g, 6.29 mmol) in CH₃CN (70 ml) was added *tert*-butyl (3*aS*,7*aR*)-hexahydro-3*H*-benzo[*d*][1,2,3]oxathiazole-3-carboxylate-2,2-dioxide (**4b**) (356 mg, 1.28 mmol) and the reaction mixture was stirred at 75°C for 44 h. After cooling to rt, 1 M NaH₂PO₄ (140 ml) was added and the mixture was extracted with ethyl acetate (3 × 100 ml). The combined organic layers were washed with brine (2 × 100 ml), dried over Na₂SO₄, filtered and the solvent was removed in vacuo. The crude product was purified by column chromatography (petrol ether/ethyl acetate gradient 50:1 to 20:1 + 5% Et₃N) to yield **5b** as colorless solid (287 mg, 0.738 mmol, 58%).

Mp.: 166–168°C. [α]_D²³: +34.3 (*c* = 0.5, CHCl₃). IR (ATR): $\tilde{\nu}$ (cm⁻¹) = 3427 (NH), 2929 (m), 2818 (OCH₃), 1701 (C=O), 1497 (vs), 1235 (s), 1025 (s), and 755 (vs). ¹H NMR (400 MHz, CDCl₃) δ (ppm) = 7.03–6.88 (m, 3H, Ar-H), 6.85 (dd, *J* = 7.9, 1.4 Hz, 1H, Ar-H),

5.21 (d, *J* = 4.7 Hz, 1H, NH), 3.86 (s, 3H, OCH₃), 3.30 (dt, *J* = 10.8, 6.0 Hz, 1H, CHNH(Boc)), 3.17–2.79 (m, 6H, CH₂ piperazine), 2.55 (dt, *J* = 10.3, 4.6 Hz, 2H, CH₂ piperazine), 2.46–2.38 (m, 1H, CH₂), 2.24 (dt, *J* = 10.8, 3.3 Hz, CHNR₁R₂), 1.94 (d, *J* = 11.1 Hz, 1H, CH₂), 1.80 (d, *J* = 10.5 Hz, 1H, CH₂), 1.67 (d, *J* = 11.3 Hz, 1H, CH₂), 1.45 (s, 9H, *t*Bu), and 1.29–1.04 (m, 4H, CH₂). ¹³C NMR (101 MHz, CDCl₃) δ (ppm) = 156.5 (C=O), 152.3 (C_q-Ar), 141.6 (C_q-Ar), 122.8 (C-Ar), 120.9 (C-Ar), 118.2 (C-Ar), 111.1 (C-Ar), 78.8 (C_q-*t*Bu), 67.4 (CHNR₁R₂), 55.3 (OCH₃), 51.3 (CH₂ piperazine), 51.2 (CHNH(Boc)), 47.9 (CH₂ piperazine), 33.4 (CH₂), 28.5 (CH₃-*t*Bu), 25.6 (CH₂), 24.7 (CH₂), and 23.3 (CH₂). HRMS (ESI): calcd. for C₂₂H₃₆N₃O₃⁺ [M+H]⁺: 390.2751, found: 390.2757. Purity (HPLC): >96%.

(1*R*,2*R*)-2-[4-(2-Methoxyphenyl)piperazin-1-yl]cyclohexan-1-amine (**6a**)

tert-Butyl ((1*R*,2*R*)-2-[4-(2-methoxyphenyl)piperazin-1-yl]cyclohexyl)carbamate (**5a**) (130 mg, 0.334 mmol) was dispersed in a mixture of 4 M HCl in water and ethyl acetate (1:1, 3 ml) and stirred vigorously for 30 min. The aqueous layer was separated, alkalinized with 2 M NaOH (4 ml) and extracted with ethyl acetate (3 × 10 ml). The combined organic layers were dried using a hydrophobic filter and the solvent removed in vacuo to give **6a** (96 mg, 0.33 mmol, 99%) as colorless solid. mp.: 94–96°C. [α]_D²³: –30.5 (*c* = 0.5, CHCl₃). IR (ATR): $\tilde{\nu}$ (cm⁻¹) = 3367 (NH₂), 2926 (s), 2817 (OCH₃), 1592 (m), 1497 (s), 1236 (vs), 1012 (s), and 757 (vs). ¹H NMR (400 MHz, CDCl₃) δ (ppm) = 7.02–6.89 (m, 3H, Ar-H), 6.85 (dd, *J* = 7.9, 1.4 Hz, 1H, Ar-H), 3.86 (s, 3H, OCH₃), 3.18–2.81 (m, 6H, CH₂ piperazine), 2.71–2.56 (m, 3H, CH and CH₂ piperazine), 2.10 (td, *J* = 10.3, 3.6 Hz, 1H, CH), 2.03–1.94 (m, 1H, CH₂), 1.87f (dd, *J* = 9.5, 3.6 Hz, 1H, CH₂), 1.83–1.77 (m, 1H, CH₂), 1.70 (s, 3H, NH₂ and CH₂), and 1.31–1.06 (m, 4H, CH₂). ¹³C NMR (101 MHz, CDCl₃) δ (ppm) = 152.3 (C_q-Ar), 141.6 (C_q-Ar), 122.8 (C-Ar), 120.9 (C-Ar), 118.2 (C-Ar), 111.0 (C-Ar), 70.6 (CH), 55.3 (OCH₃), 51.5 (CH₂ piperazine), 50.7 (CH), 48.3 (CH₂ piperazine), 35.2 (CH₂), 25.9 (CH₂), 25.1 (CH₂), and 22.9 (CH₂). HRMS (ESI): calcd. for C₁₇H₂₈N₃O⁺ [M+H]⁺: 290.2227, found: 290.2228. Purity (HPLC): >96%.

(1*S*,2*S*)-2-[4-(2-Methoxyphenyl)piperazin-1-yl]cyclohexan-1-amine (**6b**)

Following the procedure described for **6a**, *tert*-butyl ((1*S*,2*S*)-2-[4-(2-methoxyphenyl)piperazin-1-yl]cyclohexyl)carbamate (**5b**) (150 mg, 0.385 mmol) was deprotected to give **6b** (110 mg, 0.380 mmol, 99%) as colorless solid. mp.: 95–97°C. [α]_D²³: +33.9 (*c* = 0.5, CHCl₃). IR (ATR): $\tilde{\nu}$ (cm⁻¹) = 3367 (NH₂), 2929 (s), 2818 (OCH₃), 1592 (m), 1497 (s), 1236 (vs), 1013 (s), and 757 (vs). ¹H NMR (400 MHz, CDCl₃) δ (ppm) = 7.02–6.88 (m, 3H, Ar-H), 6.85 (dd, *J* = 7.9, 1.4 Hz, 1H, Ar-H), 3.86 (s, 3H, OCH₃), 3.18–2.84 (m, 6H, CH₂ piperazine), 2.71–2.57 (m, 3H, CH and CH₂ piperazine), 2.15–2.07 (m, 1H, CH), 2.03–1.95 (m, 1H, CH₂), 1.87 (dd, *J* = 9.3, 3.6 Hz, 1H, CH₂), 1.83–1.76 (m, 1H, CH₂), 1.67 (s, 3H, NH₂ and CH₂), and 1.31–1.07 (m, 4H, CH₂). ¹³C NMR (101 MHz, CDCl₃) δ (ppm) = 152.3 (C_q-Ar), 141.6 (C_q-Ar), 122.8 (C-Ar), 120.9 (C-Ar), 118.2 (C-Ar), 111.0 (C-Ar), 70.6 (CH), 55.3 (OCH₃), 51.5 (CH₂ piperazine), 50.7 (CH), 48.4 (CH₂ piperazine), 35.2 (CH₂),

25.9 (CH₂), 25.1 (CH₂), and 22.9 (CH₂). HRMS (ESI): calcd. C₁₇H₂₈N₃O⁺ [M+H]⁺: 290.2227, found: 290.2228. Purity (HPLC): >96%.

N-[(1*R*,2*R*)-2-[4-(2-Methoxyphenyl)piperazin-1-yl]cyclohexyl]-benzenesulfonamide (*R,R*-*trans*-ML-SI3)

To a solution of (1*R*,2*R*)-2-[4-(2-methoxyphenyl)piperazin-1-yl]cyclohexan-1-amine (**6a**) (148 mg, 0.511 mmol) and Et₃N (1.1 ml, 0.77 mmol) in CH₂Cl₂ (5 ml) was added benzenesulfonyl chloride (72 μl, 0.56 mmol) at 0°C. The reaction mixture was stirred for 1 h, then diluted with CH₂Cl₂ to 20 ml and washed with 2 M NaOH (20 ml). The aqueous layer was extracted with CH₂Cl₂ (20 ml), the combined organic layers were dried using a hydrophobic filter, and the solvent was removed in vacuo. The residue was recrystallized from 2-propanol to give *R,R*-*trans*-ML-SI3 (173 mg, 0.403 mmol, 79%) as white crystals. mp.: 119–120°C. ee Value (chiral HPLC): >99%. [α]_D²⁵: -20.5 (c = 0.5, CHCl₃). IR (ATR): $\tilde{\nu}$ (cm⁻¹) = 3181 (NH), 2939 (m), 2822 (OCH₃), 1593 (m), 1498 (s), 1446 (s), 1343 (m), 1239 (s), 1155 (vs), and 751 (vs). ¹H NMR (400 MHz, CDCl₃) δ (ppm) = 7.94–7.87 (m, 2H, Ar-H), 7.61–7.50 (m, 3H, Ar-H), 7.06–6.98 (m, 1H, Ar-H), 6.97–6.83 (m, 3H, Ar-H), 6.11 (s, 1H, NH), 3.83 (s, 3H, OCH₃), 3.00–2.66 (m, 5H, CH₂ piperazine and CH), 2.57–2.18 (m, 6H, CH₂, CH₂ piperazine and CH), 1.87 (d, *J* = 12.5 Hz, 1H, CH₂), 1.78 (d, *J* = 10.6 Hz, 1H, CH₂), 1.68 (d, *J* = 11.1 Hz, 1H, CH₂), and 1.35–1.04 (m, 4H, CH₂). ¹³C NMR (101 MHz, CDCl₃) δ (ppm) = 152.2 (C_q-Ar), 141.0 (C_q-Ar), 139.7 (C_q-Ar), 132.6 (C-Ar), 129.0 (C-Ar), 127.3 (C-Ar), 123.2 (C-Ar), 121.0 (C-Ar), 118.3 (C-Ar), 111.1 (C-Ar), 66.7 (CHNR₁R₂), 55.4 (CH₃), 53.4 (CHNHSO₂R), 51.1 (CH₂ piperazine), 32.9 (CH₂), 25.3 (CH₂), 24.2 (CH₂), and 23.0 (CH₂). HRMS (ESI): calcd. for C₂₃H₃₂N₃O₃S⁺ [M+H]⁺: 430.2159, found: 430.2158. Purity (HPLC): >96%.

N-[(1*S*,2*S*)-2-[4-(2-Methoxyphenyl)piperazin-1-yl]cyclohexyl]-benzenesulfonamide (*S,S*-*trans*-ML-SI3)

Following the procedure described for *R,R*-*trans*-ML-SI3, (1*S*,2*S*)-2-[4-(2-methoxyphenyl)piperazin-1-yl]cyclohexan-1-amine (**6b**) (41 mg, 0.14 mmol) was reacted with benzenesulfonyl chloride (20 μl, 0.16 mmol) to give *S,S*-*trans*-ML-SI3 (52 mg, 0.12 mmol, 85%) as white crystals. mp.: 119–120°C. ee Value (chiral HPLC): >99%. [α]_D²⁵: +20.3 (c = 0.5, CHCl₃). IR (ATR): $\tilde{\nu}$ (cm⁻¹) = 3180 (NH), 2939 (m), 2823 (OCH₃), 1593 (m), 1499 (s), 1446 (s), 1343 (m), 1239 (s), 1155 (vs), and 751 (vs). ¹H NMR (400 MHz, CDCl₃) δ (ppm) = 7.98–7.88 (m, 2H, Ar-H), 7.61–7.50 (m, 3H, Ar-H), 7.05–6.84 (m, 4H, Ar-H), 6.11 (s, 1H, NH), 3.83 (s, 3H, OCH₃), 3.00–2.67 (m, 5H, CH₂ piperazine and CH), 2.55–2.20 (m, 6H, CH₂, CH₂ piperazine and CH), 1.87 (d, *J* = 12.5 Hz, 1H, CH₂), 1.78 (d, *J* = 10.5 Hz, 1H, CH₂), 1.68 (d, *J* = 11.0 Hz, 1H, CH₂), and 1.33–1.05 (m, 4H, CH₂). ¹³C NMR (101 MHz, CDCl₃) δ (ppm) = 152.2 (C_q-Ar), 141.0 (C_q-Ar), 139.7 (C_q-Ar), 132.6 (C-Ar), 129.0 (C-Ar), 127.3 (C-Ar), 123.2 (C-Ar), 121.0 (C-Ar), 118.3 (C-Ar), 111.1 (C-Ar), 66.7 (CHNR₁R₂), 55.4 (CH₃), 53.4 (CHNHSO₂R), 51.1 (CH₂ piperazine), 32.9 (CH₂), 25.3 (CH₂), 24.2 (CH₂), and 23.0 (CH₂). HRMS (ESI): calcd. for C₂₃H₃₂N₃O₃S⁺ [M+H]⁺: 430.2159, found: 430.2159. Purity (HPLC): >96%.

ACKNOWLEDGMENTS

This study was supported by Deutsche Forschungsgemeinschaft, project BR-1034/7-1 to Franz Bracher. Open Access funding enabled and organized by Projekt DEAL.

CONFLICT OF INTERESTS

The authors declare that there are no conflicts of interests.

AUTHOR CONTRIBUTIONS

Katharina Krieglér and Charlotte Leser: experimental work, collection and analysis of data, and writing of the manuscript; Peter Mayer: X-ray analysis; Franz Bracher: design of the project, supervision of experiments, and writing of the manuscript.

ORCID

Charlotte Leser  <https://orcid.org/0000-0002-4489-1787>

Franz Bracher  <http://orcid.org/0000-0003-0009-8629>

REFERENCES

- [1] D. E. Clapham, *Nature* **2003**, 426, 517.
- [2] I. S. Ramsey, M. Delling, D. E. Clapham, *Annu. Rev. Physiol.* **2006**, 68, 619.
- [3] M. Gees, G. Owsianik, B. Nilius, T. Voets, *Compr. Physiol.* **2012**, 2, 563.
- [4] X. Cheng, D. Shen, M. Samie, H. Xu, *FEBS Lett.* **2010**, 584, 2013.
- [5] H. Xu, D. Ren, *Annu. Rev. Physiol.* **2015**, 77, 57.
- [6] H. J. Kim, A. A. Soyombo, S. Tjon-Kon-Sang, I. So, S. Muallem, *Traffic* **2009**, 10, 1157.
- [7] C. Karacsonyi, A. S. Miguel, R. Puertollano, *Traffic* **2007**, 8, 1404.
- [8] X.-P. Dong, X. Cheng, E. Mills, M. Delling, F. Wang, T. Kurz, H. Xu, *Nature* **2008**, 455, 992.
- [9] K. Venkatachalam, C. O. Wong, M. X. Zhu, *Cell Calcium* **2015**, 58, 48.
- [10] R. Bargal, N. Avidan, E. Ben-Asher, Z. Olender, M. Zeigler, A. Frumkin, A. Raas-Rothschild, G. Glusman, D. Lancet, G. Bach, *Nat. Genet.* **2000**, 26, 118.
- [11] G. Bach, *Pfluegers Arch.* **2005**, 451, 313.
- [12] G. Altarescu, M. Sun, D. F. Moore, J. A. Smith, E. A. Wiggins, B. I. Solomon, N. J. Patronas, K. P. Frei, S. Gupta, C. R. Kaneski, O. W. Quarrell, S. A. Slaugenhaupt, E. Goldin, R. Schiffmann, *Neurology* **2002**, 59, 306.
- [13] M. Sun, E. Goldin, S. Stahl, J. L. Falardeau, J. C. Kennedy, J. S. Acierno, Jr., C. Bove, C. R. Kaneski, J. Nagle, M. C. Bromley, M. Colman, R. Schiffmann, S. A. Slaugenhaupt, *Hum. Mol. Genet.* **2000**, 9, 2471.
- [14] F. Di Palma, I. A. Belyantseva, H. J. Kim, T. F. Vogt, B. Kachar, K. Noben-Trauth, *Proc. Natl. Acad. Sci. U. S. A.* **2002**, 99, 14994.
- [15] K. Nagata, L. Zheng, T. Madathany, A. J. Castiglioni, J. R. Bartles, J. Garcia-Añoveros, *Proc. Natl. Acad. Sci. U. S. A.* **2008**, 105, 353.
- [16] C. Grimm, M. P. Cuajungco, A. F. J. van Aken, M. Schnee, S. Jörs, C. J. Kros, A. J. Ricci, S. Heller, *Proc. Natl. Acad. Sci. U. S. A.* **2007**, 104, 19583.
- [17] H. J. Kim, Q. Li, S. Tjon-Kon-Sang, I. So, K. Kiselyov, S. Muallem, *J. Biol. Chem.* **2007**, 282, 36138.
- [18] H. Xu, M. Delling, L. Li, X. Dong, D. E. Clapham, *Proc. Natl. Acad. Sci. U. S. A.* **2007**, 104, 18321.
- [19] G. Santoni, M. B. Morelli, C. Amantini, M. Nabissi, M. Santoni, A. Santoni, *Front. Immunol.* **2020**, 11, 739.
- [20] N. Rinkenberger, J. W. Schoggins, *mBio* **2018**, 9, e02314.
- [21] L. Sun, Y. Hua, S. Vergarajaregui, H. I. Diab, R. Puertollano, *J. Immunol.* **2015**, 195, 4922.

- [22] G. Santoni, M. Santoni, F. Maggi, O. Marinelli, M. B. Morelli, *Front. Oncol.* **2020**, *10*, 659.
- [23] J. Jung, K.-J. Cho, A. K. Najji, K. N. Clemons, C. O. Wong, M. Villanueva, S. Gregory, N. E. Karagas, L. Tan, H. Liang, M. A. Rousseau, K. M. Tomasevich, A. G. Sikora, I. Levental, D. van der Hoeven, Y. Zhou, J. F. Hancock, K. Venkatachalam, *EMBO Rep.* **2019**, *20*, e46685.
- [24] M. Xu, S. Almasi, Y. Yang, C. Yan, A. M. Sterea, A. K. Rizvi Syeda, B. Shen, C. Richard Derek, P. Huang, S. Gujar, J. Wang, W.-X. Zong, M. Trebak, Y. El Hiani, X.-P. Dong, *Cell Calcium* **2019**, *79*, 80.
- [25] D. Shen, X. Wang, X. Li, X. Zhang, Z. Yao, S. Dibble, X. P. Dong, T. Yu, A. P. Lieberman, H. D. Showalter, H. Xu, *Nat. Commun.* **2012**, *3*, 731.
- [26] C.-C. Chen, M. Keller, M. Hess, R. Schiffmann, N. Urban, A. Wolfgardt, M. Schaefer, F. Bracher, M. Biel, C. Wahl-Schott, C. Grimm, *Nat. Commun.* **2014**, *5*, 4681.
- [27] E. Plesch, C. C. Chen, E. Butz, A. Scotto Rosato, E. K. Krogsaeter, H. Yinan, K. Bartel, M. Keller, D. Robaa, D. Teupser, L. M. Holdt, A. M. Vollmar, W. Sippl, R. Puertollano, D. Medina, M. Biel, C. Wahl-Schott, F. Bracher, C. Grimm, *eLife* **2018**, *7*, e3970.
- [28] M. Samie, X. Wang, X. Zhang, A. Goschka, X. Li, X. Cheng, E. Gregg, M. Azar, Y. Zhuo, A.G. Garrity, Q. Gao, S. Slangenaupt, J. Pickel, S.N. Zolov, L.S. Weisman, G.M. Lenk, S. Titus, M. Bryant-Geneviev, N. Southall, M. Juan, M. Ferrer, H. Xu, *Dev. Cell* **2013**, *26*, 511.
- [29] W. Wang, Q. Gao, M. Yang, X. Zhang, L. Yu, M. Lawas, X. Li, M. Bryant-Geneviev, N. T. Southall, J. Marugan, M. Ferrer, H. Xu, *Proc. Natl. Acad. Sci. U. S. A.* **2015**, *112*, E1373.
- [30] P. Rühl, A. S. Rosato, N. Urban, S. Gerndt, R. Tang, C. Abrahamian, C. Leser, J. Sheng, A. Jha, G. Vollmer, M. Schaefer, F. Bracher, C. Grimm, *Sci. Rep.* **2021**, *11*, 8313.
- [31] C. Leser, M. Keller, S. Gerndt, N. Urban, C.-C. Chen, M. Schaefer, C. Grimm, F. Bracher, *Eur. J. Med. Chem.* **2021**, *210*, 112966.
- [32] D. Albanese, D. Landini, M. Penso, S. Petricci, *Tetrahedron* **1999**, *55*, 6387.
- [33] R. Guo, S. Lu, X. Chen, C.-W. Tsang, W. Jia, C. Sui-Seng, D. Amoroso, K. Abdur-Rashid, *J. Org. Chem.* **2010**, *75*, 937.
- [34] M. Atfani, L. Wei, W. D. Lubell, *Org. Lett.* **2001**, *3*, 2965.
- [35] P. Rönholm, M. Södergren, G. Hillmerson, *Org. Lett.* **2007**, *9*, 3781.
- [36] N. Pendem, C. Douat, P. Claudon, M. Laguerre, S. Castano, B. Desbat, D. Cavagnat, E. Ennifar, B. Kauffmann, G. Guichard, *J. Am. Chem. Soc.* **2013**, *135*, 4884.
- [37] D. Sutherlin, M. S. Wilson, K. W. Lai, P. Bergeron, B. Zhang, R. Beveridge, J.-P. Leclerc, A. Lemire, L. Zhao & C. Sturino Genentech, WO 2018072602, 2018.
- [38] Bruker, SAINT, Bruker AXS Inc., Madison, WI **2012**.
- [39] G. M. Sheldrick, SADABS, University of Göttingen, Göttingen, Germany **1996**.
- [40] G. M. Sheldrick, *Acta Crystallogr.* **2015**, *A71*, 3.

SUPPORTING INFORMATION

Additional supporting information may be found in the online version of the article at the publisher's website.

How to cite this article: K. Krieglér, C. Leser, P. Mayer, F. Bracher. Effective chiral pool synthesis of both enantiomers of the TRPML inhibitor *trans*-ML-SI3. *Arch. Pharm.* **2022**;355:e2100362.
<https://doi.org/10.1002/ardp.202100362>

3.1.2.4 Supplemental material and supporting information

Supplemental Material: Novel Compounds and Biological Screening Results**Effective chiral pool synthesis of both enantiomers of the TRPML inhibitor *trans*-ML-SI3**Katharina Kriegler,¹ Charlotte Leser,¹ Peter Mayer² and Franz Bracher¹¹Ludwig-Maximilians University of Munich, Department of Pharmacy - Center for Drug Research²Ludwig-Maximilians University of Munich, Department of Chemistry

Corresponding author:

Franz Bracher, Ludwig-Maximilians University of Munich, Department of Pharmacy - Center for Drug Research, Butenandtstr. 5-13, 81377 Munich, Germany

Compound No.	InChI
5a	InChI=1S/C22H35N3O3/c1-22(2,3)28-21(26)23-17-9-5-6-10-18(17)24-13-15-25(16-14-24)19-11-7-8-12-20(19)27-4/h7-8,11-12,17-18H,5-6,9-10,13-16H2,1-4H3,(H,23,26)/t17-,18-/m1/s1
5b	InChI=1S/C22H35N3O3/c1-22(2,3)28-21(26)23-17-9-5-6-10-18(17)24-13-15-25(16-14-24)19-11-7-8-12-20(19)27-4/h7-8,11-12,17-18H,5-6,9-10,13-16H2,1-4H3,(H,23,26)/t17-,18-/m0/s1
6a	InChI=1S/C17H27N3O/c1-21-17-9-5-4-8-16(17)20-12-10-19(11-13-20)15-7-3-2-6-14(15)18/h4-5,8-9,14-15H,2-3,6-7,10-13,18H2,1H3/t14-,15-/m1/s1
6b	InChI=1S/C17H27N3O/c1-21-17-9-5-4-8-16(17)20-12-10-19(11-13-20)15-7-3-2-6-14(15)18/h4-5,8-9,14-15H,2-3,6-7,10-13,18H2,1H3/t14-,15-/m0/s1
7a	InChI=1S/C12H23NO5S/c1-12(2,3)17-11(14)13-9-7-5-6-8-10(9)18-19(4,15)16/h9-10H,5-8H2,1-4H3,(H,13,14)/t9-,10+/m1/s1
7b	InChI=1S/C12H23NO5S/c1-12(2,3)17-11(14)13-9-7-5-6-8-10(9)18-19(4,15)16/h9-10H,5-8H2,1-4H3,(H,13,14)/t9-,10+/m0/s1
(<i>R,R</i>)-<i>trans</i>-ML-SI3	InChI=1S/C23H31N3O3S/c1-29-23-14-8-7-13-22(23)26-17-15-25(16-18-26)21-12-6-5-11-20(21)24-30(27,28)19-9-3-2-4-10-19/h2-4,7-10,13-14,20-21,24H,5-6,11-12,15-18H2,1H3/t20-,21-/m1/s1
(<i>S,S</i>)-<i>trans</i>-ML-SI3	InChI=1S/C23H31N3O3S/c1-29-23-14-8-7-13-22(23)26-17-15-25(16-18-26)21-12-6-5-11-20(21)24-30(27,28)19-9-3-2-4-10-19/h2-4,7-10,13-14,20-21,24H,5-6,11-12,15-18H2,1H3/t20-,21-/m0/s1

Supporting Information

Content:

- 1 Analytical chiral HPLC
- 2 Crystallographic data
- 3 NMR spectra

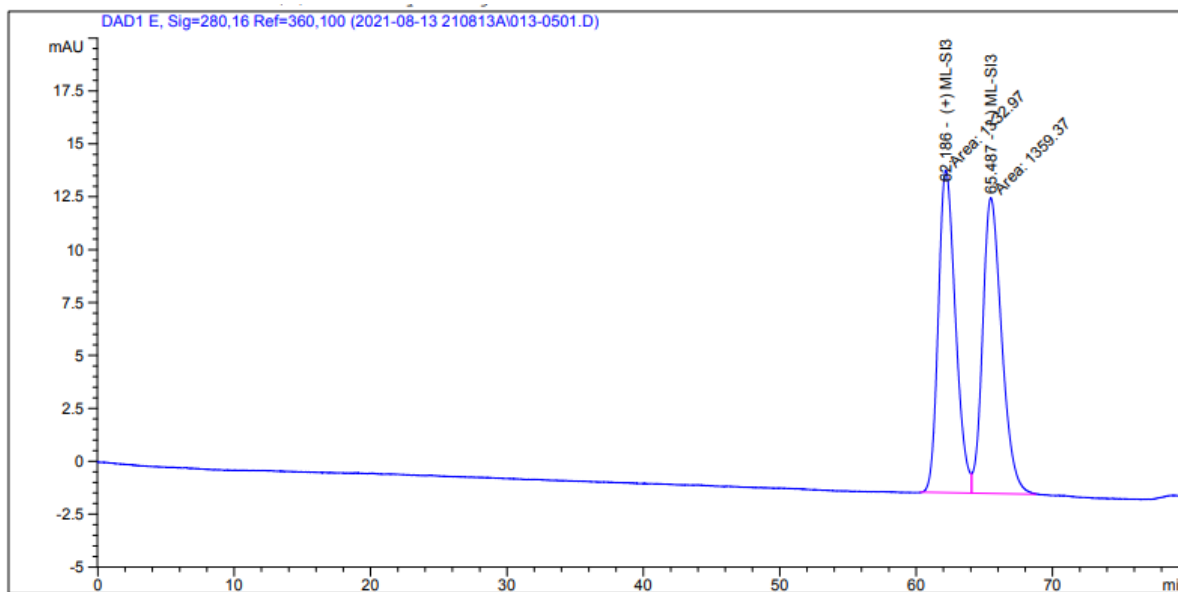
1 Analytical chiral HPLC

1.1 Method

Stationary phase: Daicel Chiralpak-IE-3 column (150 × 4.6 mm, 3 μm); mobile phase: heptane/methyl *tert*-butyl ether/2-propanol/ethanolamine (80/18/2/0.1); sample solution: approx. 1.0 mg/mL for racemic ML-SI3, approx. 0.5 mg/mL for pure enantiomers in mobile phase; injection volume: 2 μL; flow: 0.3 mL/min, column temperature: 40°C.

1.2 Chromatograms

Racemic ML-SI3



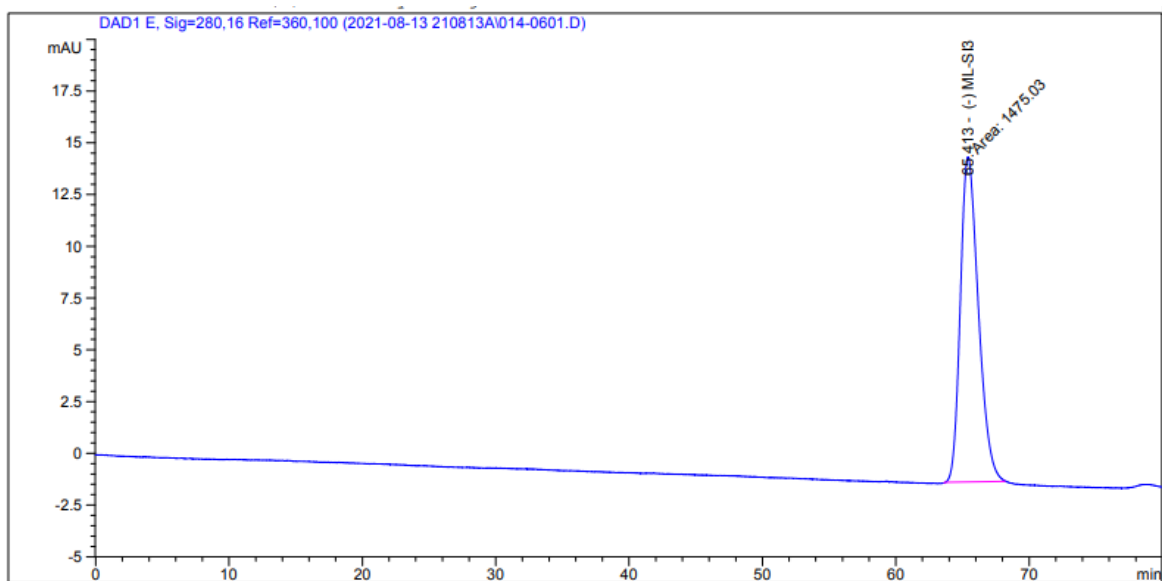
Signal 1: DAD1 E, Sig=280,16 Ref=360,100

Peak #	RetTime [min]	Type	Width [min]	Area [mAU*s]	Area %	Name
1	62.186	MF	1.4568	1332.96912	49.5098	(+) ML-SI3
2	65.487	FM	1.6211	1359.36682	50.4902	(-) ML-SI3

Totals : 2692.33594

Chiral pool synthesis of enantiopure *trans*-ML-SI3

(-)-(*R,R*)-*trans*-ML-SI3 (from mesylate route)

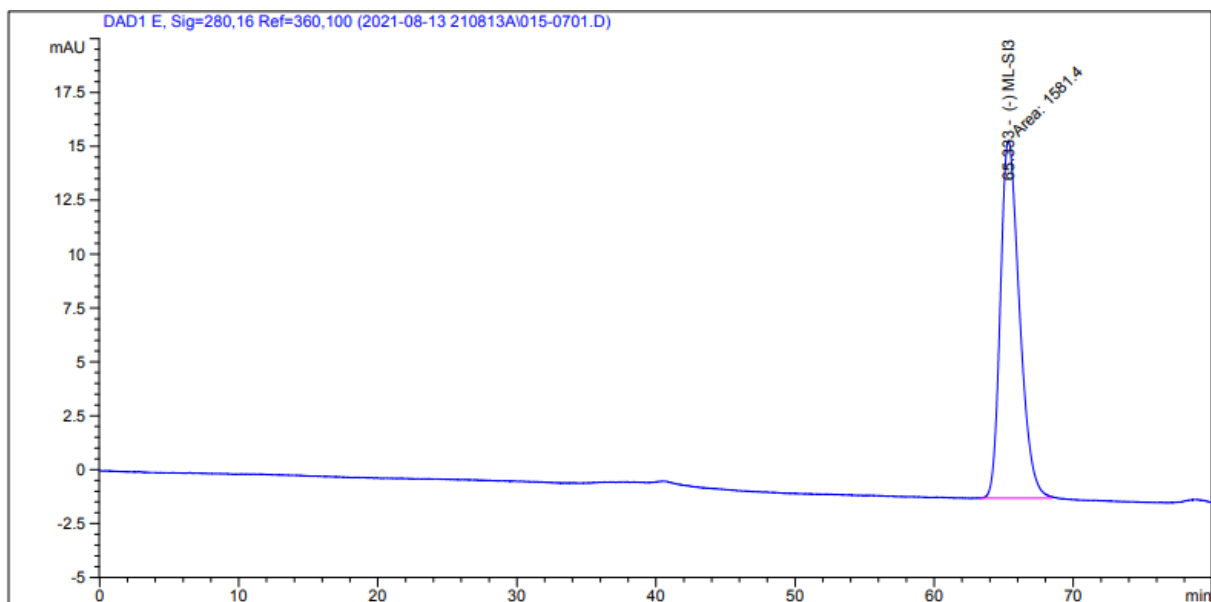


Signal 1: DAD1 E, Sig=280,16 Ref=360,100

Peak #	RetTime [min]	Type	Width [min]	Area [mAU*s]	Area %	Name
1	62.186		0.0000	0.00000	0.0000	(+) ML-SI3
2	65.413 MM		1.5654	1475.03308	100.0000	(-) ML-SI3

Totals : 1475.03308

(-)-(*R,R*)-*trans*-ML-SI3 (from sulfamidate route)



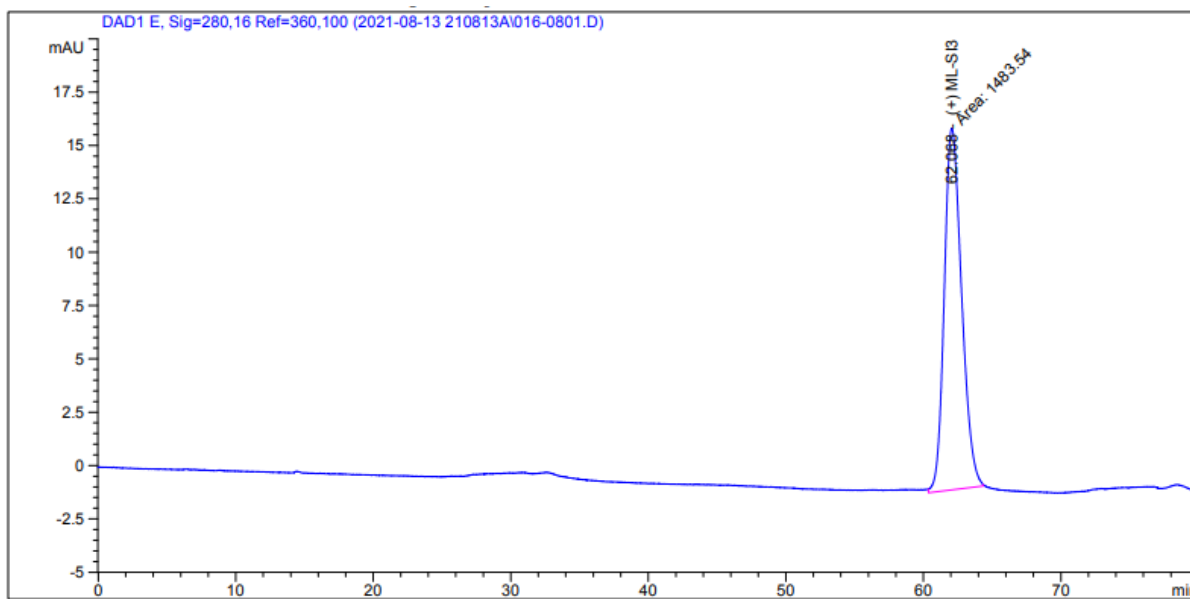
Signal 1: DAD1 E, Sig=280,16 Ref=360,100

Peak #	RetTime [min]	Type	Width [min]	Area [mAU*s]	Area %	Name
1	62.186		0.0000	0.00000	0.0000	(+) ML-SI3
2	65.333 MM		1.5880	1581.39587	100.0000	(-) ML-SI3

Totals : 1581.39587

Chiral pool synthesis of enantiopure *trans*-ML-SI3

(+)-(S,S)-*trans*-ML-SI3 (from mesylate route)

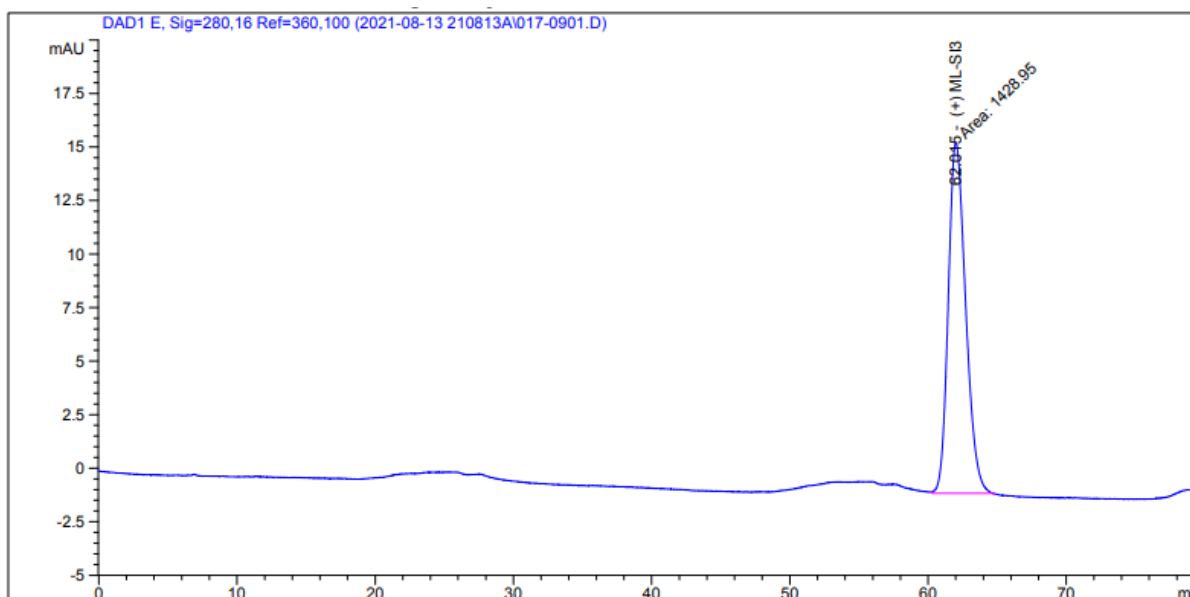


Signal 1: DAD1 E, Sig=280,16 Ref=360,100

Peak #	RetTime [min]	Type	Width [min]	Area [mAU*s]	Area %	Name
1	62.068	MM	1.4590	1483.54175	100.0000	(+) ML-SI3
2	65.487		0.0000	0.00000	0.0000	(-) ML-SI3

Totals : 1483.54175

(+)-(S,S)-*trans*-ML-SI3 (from sulfamidate route)



Signal 1: DAD1 E, Sig=280,16 Ref=360,100

Peak #	RetTime [min]	Type	Width [min]	Area [mAU*s]	Area %	Name
1	62.015	MM	1.4539	1428.94507	100.0000	(+) ML-SI3
2	65.487		0.0000	0.00000	0.0000	(-) ML-SI3

Totals : 1428.94507

2 Crystallographic data

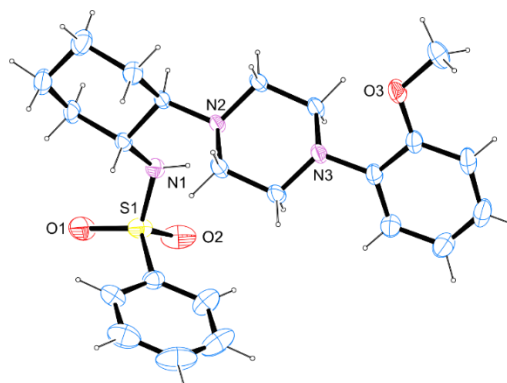
2.1 Sample preparation

To receive single crystals, the pure compounds were recrystallized from methanol, letting the crystals grow for several days at rt. The figures have been drawn at the 50% ellipsoid probability level.^[68] Crystallographic data have been deposited with the Cambridge Crystallographic Data Centre, CCDC, 12 Union Road, Cambridge CB21EZ, UK. Copies of the data can be obtained free of charge on quoting the depository numbers CCDC-2109888 ((-)-(*R,R*)-*trans*-ML-SI3) and 2109889 ((+)-(*S,S*)-*trans*-ML-SI3) (<https://www.ccdc.cam.ac.uk/structures/>).

2.2 Crystallographic information

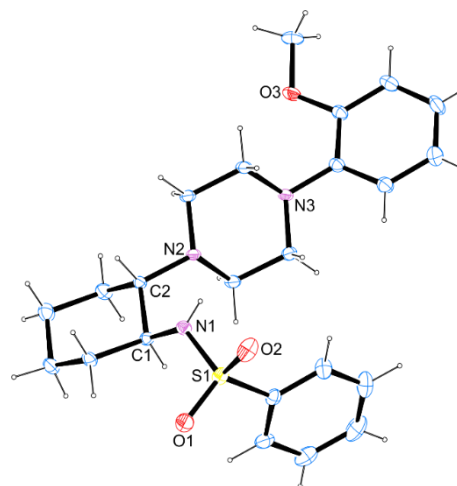
2.2.1 (-)-(*R,R*)-*trans*-ML-SI3

net formula	C ₂₃ H ₃₁ N ₃ O ₃ S
Mr/g mol ⁻¹	429.57
crystal size/mm	0.130 × 0.090 × 0.070
T/K	298.(2)
radiation	MoKα
diffractometer	'Bruker D8 Venture TXS'
crystal system	orthorhombic
space group	'P 21 21 21'
a/Å	8.8314(3)
b/Å	14.1297(5)
c/Å	37.6800(13)
α/°	90
β/°	90
γ/°	90
V/Å ³	4701.9(3)
Z	8
calc. density/g cm ⁻³	1.214
μ/mm ⁻¹	0.165
absorption correction	Multi-Scan
transmission factor range	0.94–0.99
refls. measured	77362
R _{int}	0.0496
mean σ(I)/I	0.0290
θ range	2.720–26.371
observed refls.	8120
x, y (weighting scheme)	0.0470, 2.1100
hydrogen refinement	mixed
Flack parameter	0.00(2)
refls in refinement	9586
parameters	551
restraints	1
R(F _{obs})	0.0537
R _w (F ²)	0.1301
S	1.097
shift/error _{max}	0.001
max electron density/e Å ⁻³	0.228
min electron density/e Å ⁻³	-0.273

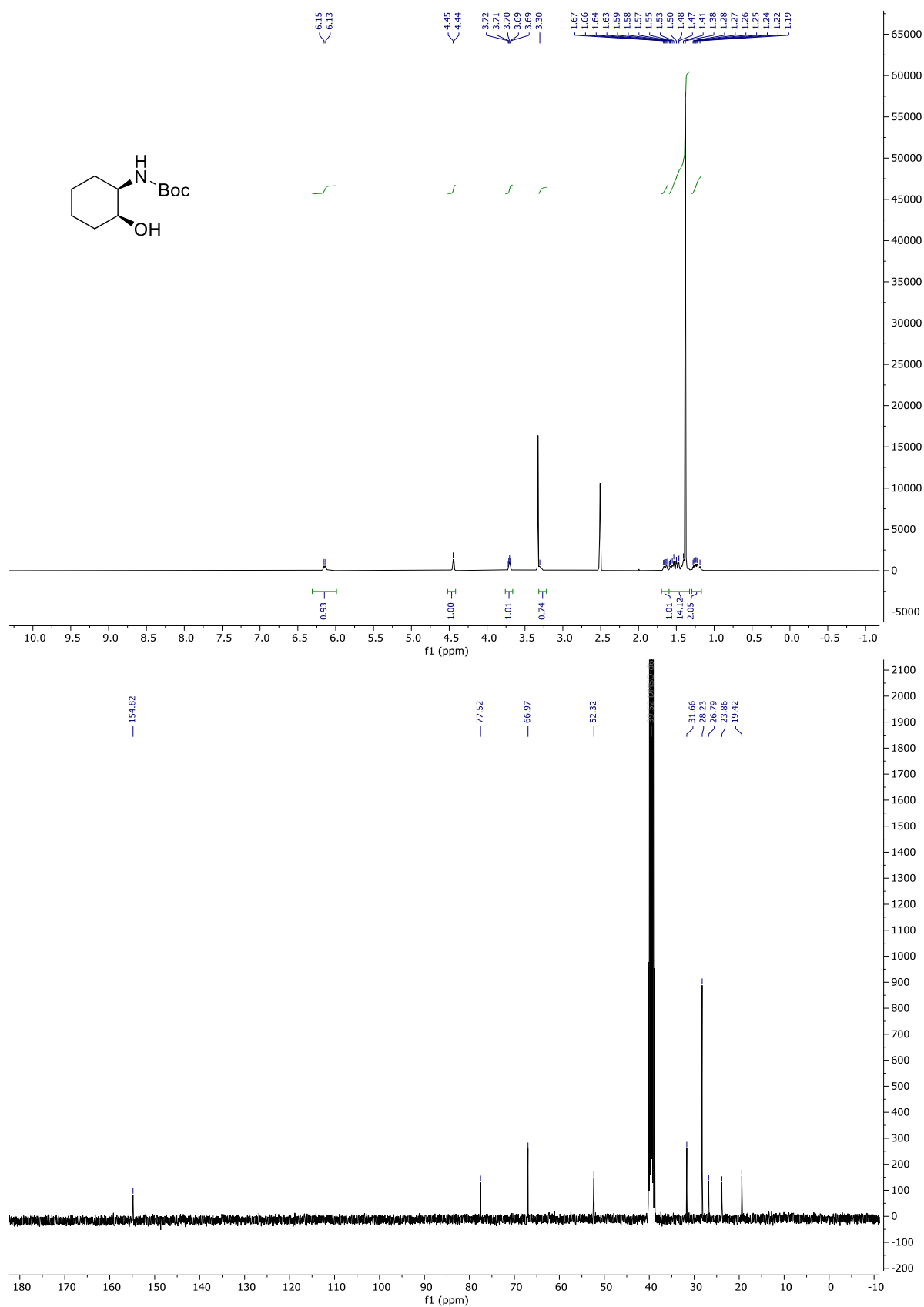


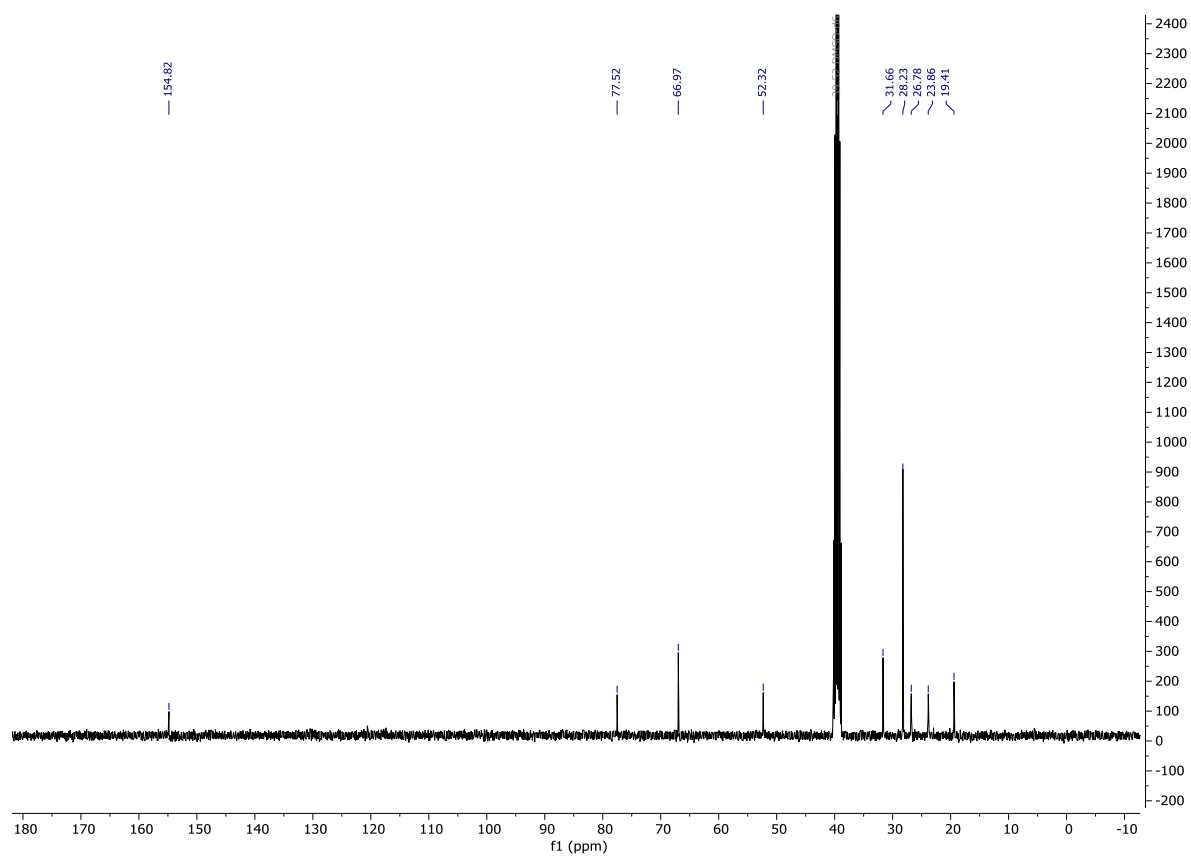
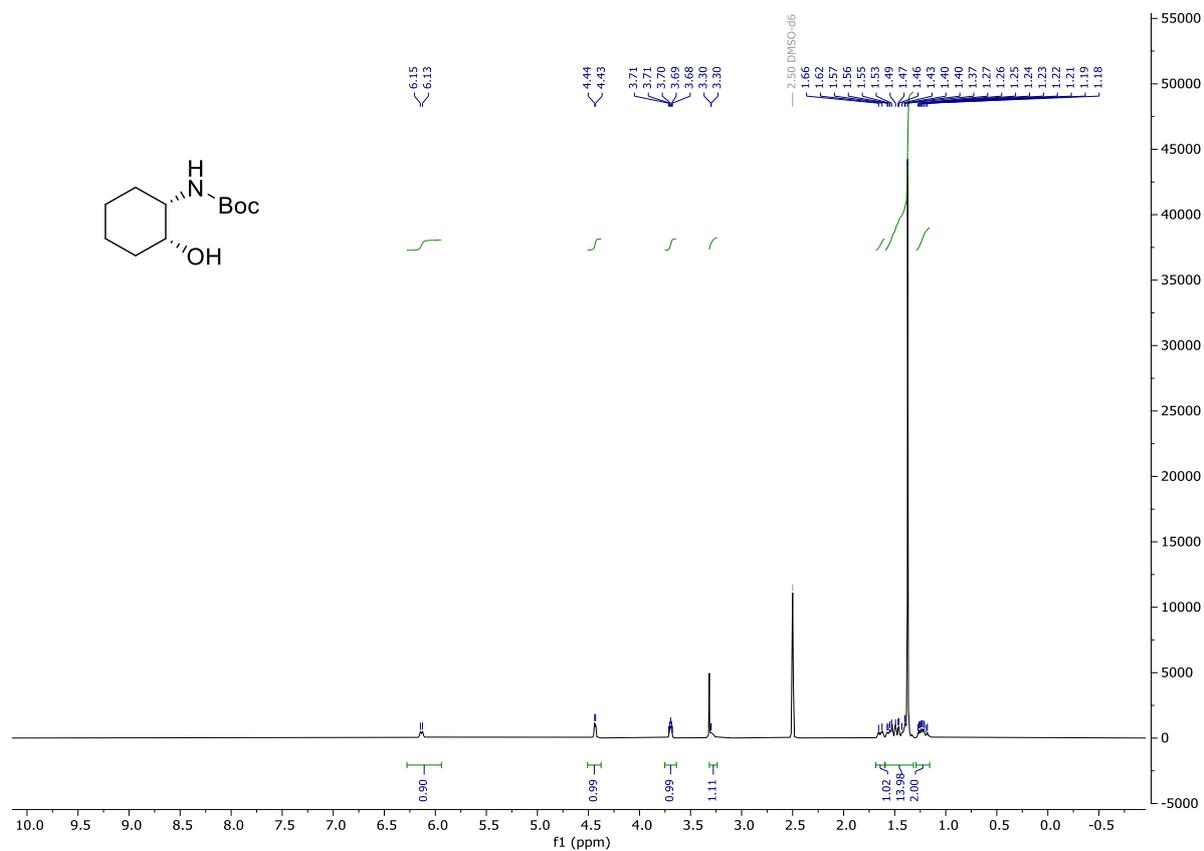
2.2.2 (+)-(S,S)-*trans*-ML-SI3

net formula	C ₉₃ H ₁₂₈ N ₁₂ O ₁₃ S ₄
M _r /g mol ⁻¹	1750.31
crystal size/mm	0.110 × 0.070 × 0.060
T/K	173.(2)
radiation	MoKα
diffractometer	'Bruker D8 Venture TXS'
crystal system	orthorhombic
space group	'P 21 21 21'
a/Å	8.7491(7)
b/Å	14.0415(11)
c/Å	37.726(3)
α/°	90
β/°	90
γ/°	90
V/Å ³	4634.7(6)
Z	2
calc. density/g cm ⁻³	1.254
μ/mm	-1 0.170
absorption correction	Multi-Scan
transmission factor range	0.96–0.99
refls. measured	74165
R _{int}	0.0684
mean σ(I)/I	0.0373
θ range	2.948–25.350
observed refls.	7454
x, y (weighting scheme)	0.0400, 1.9413
hydrogen refinement	mixed
Flack parameter	-0.02(3)
refls in refinement	8469
parameters	561
restraints	0
R(F _{obs})	0.0426
Rw(F ²)	0.1013
S	1.076
shift/errormax	0.001
max electron density/e Å ⁻³	0.310
min electron density/e Å ⁻³	-0.352



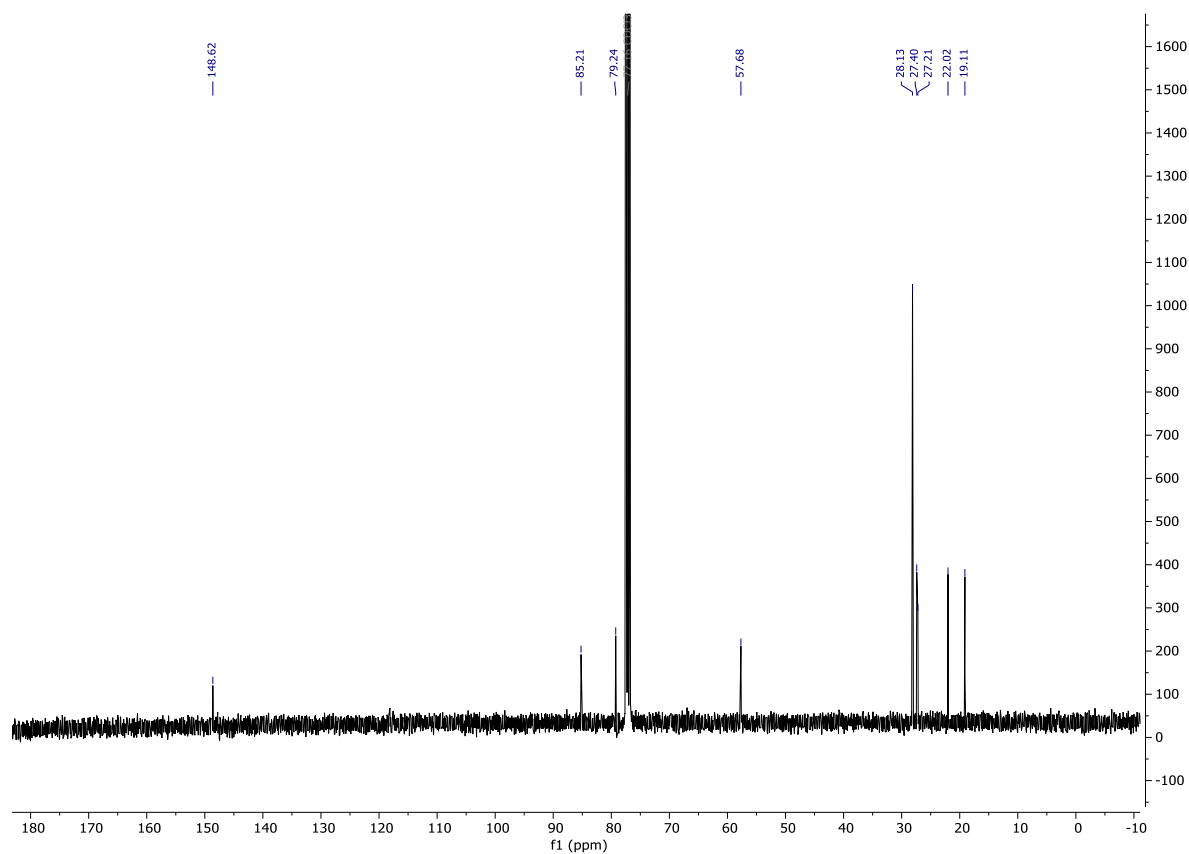
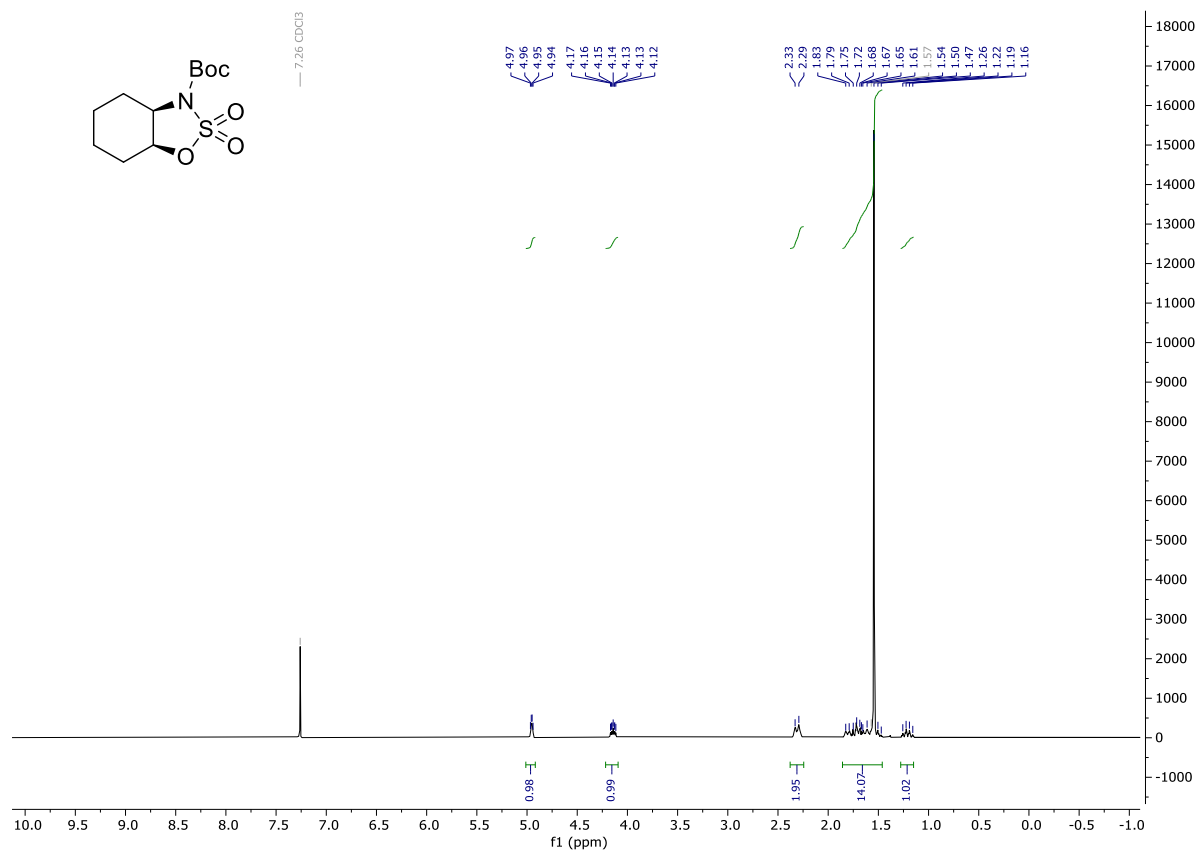
3 NMR spectra

3.1 *tert*-Butyl [(1*R*,2*S*)-2-hydroxycyclohexyl]carbamate (**2a**)

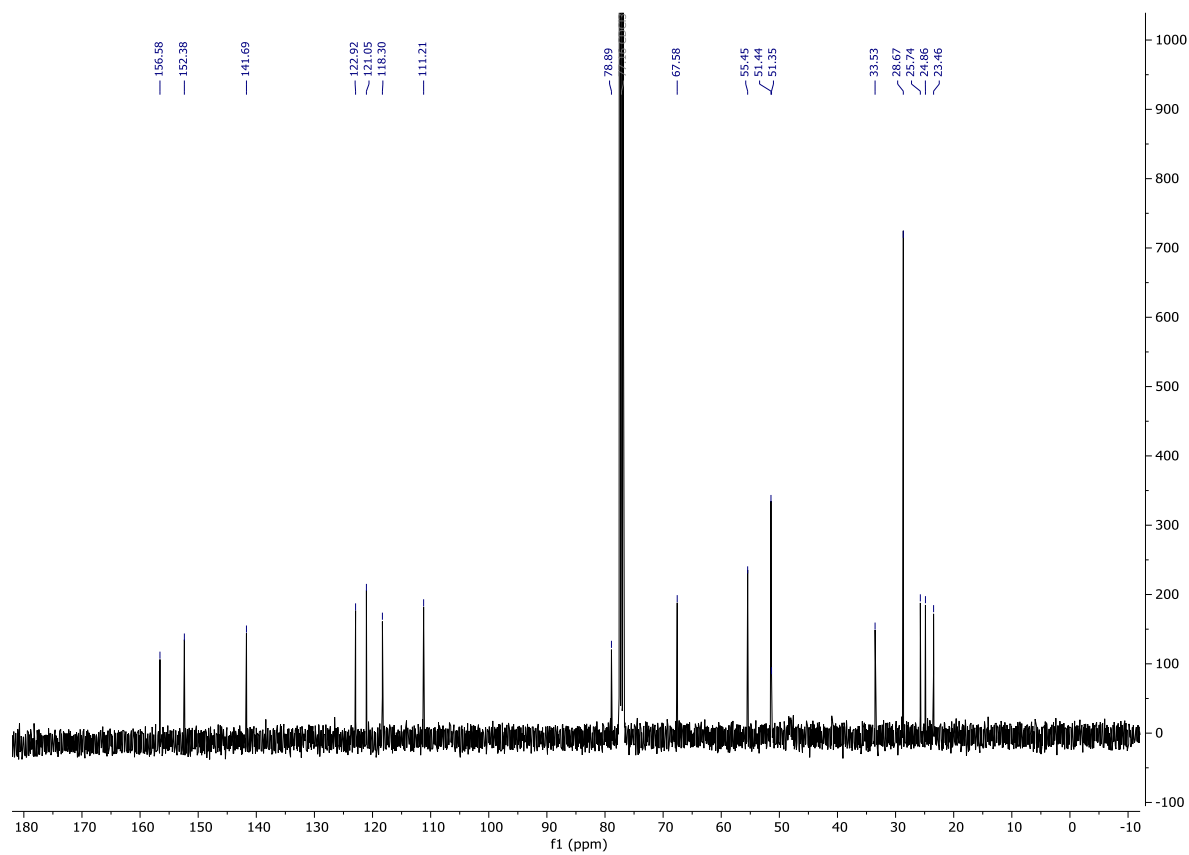
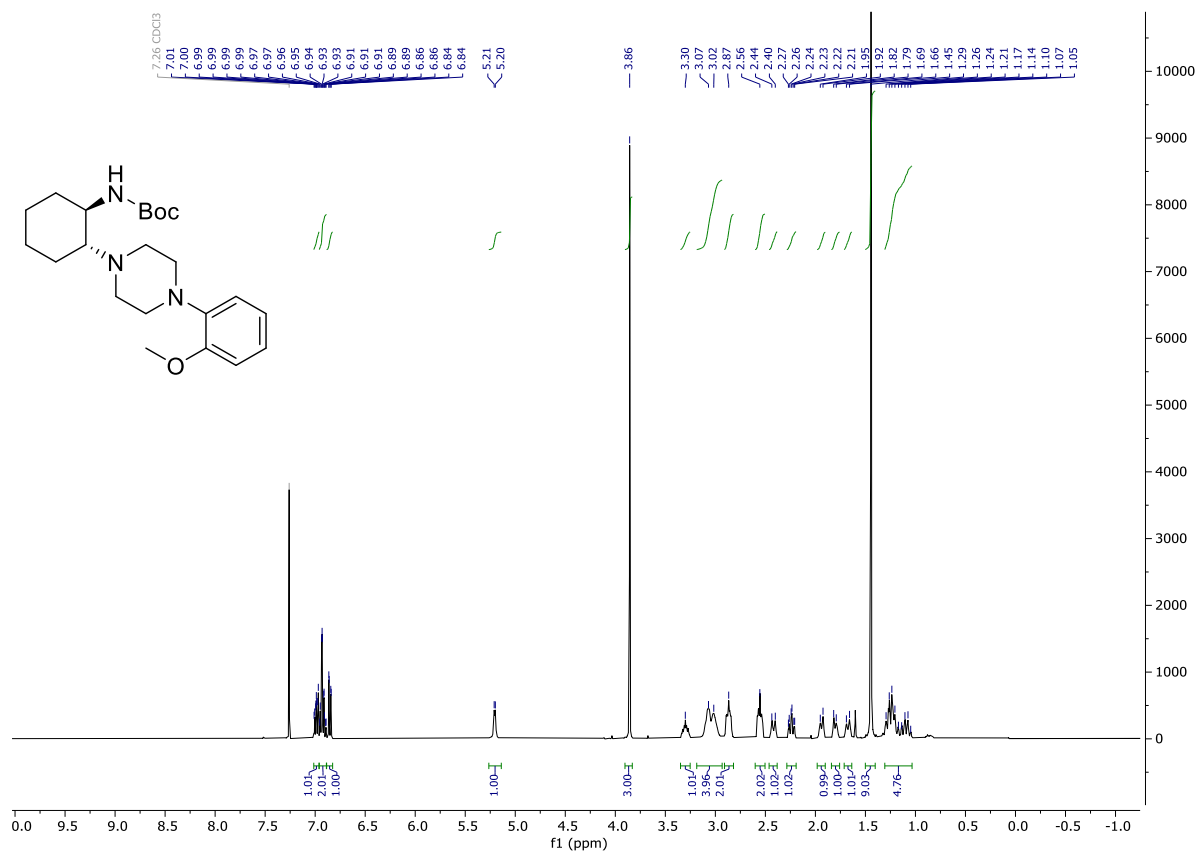
3.2 *tert*-Butyl [(1*S*,2*R*)-2-hydroxycyclohexyl]carbamate (**2b**)

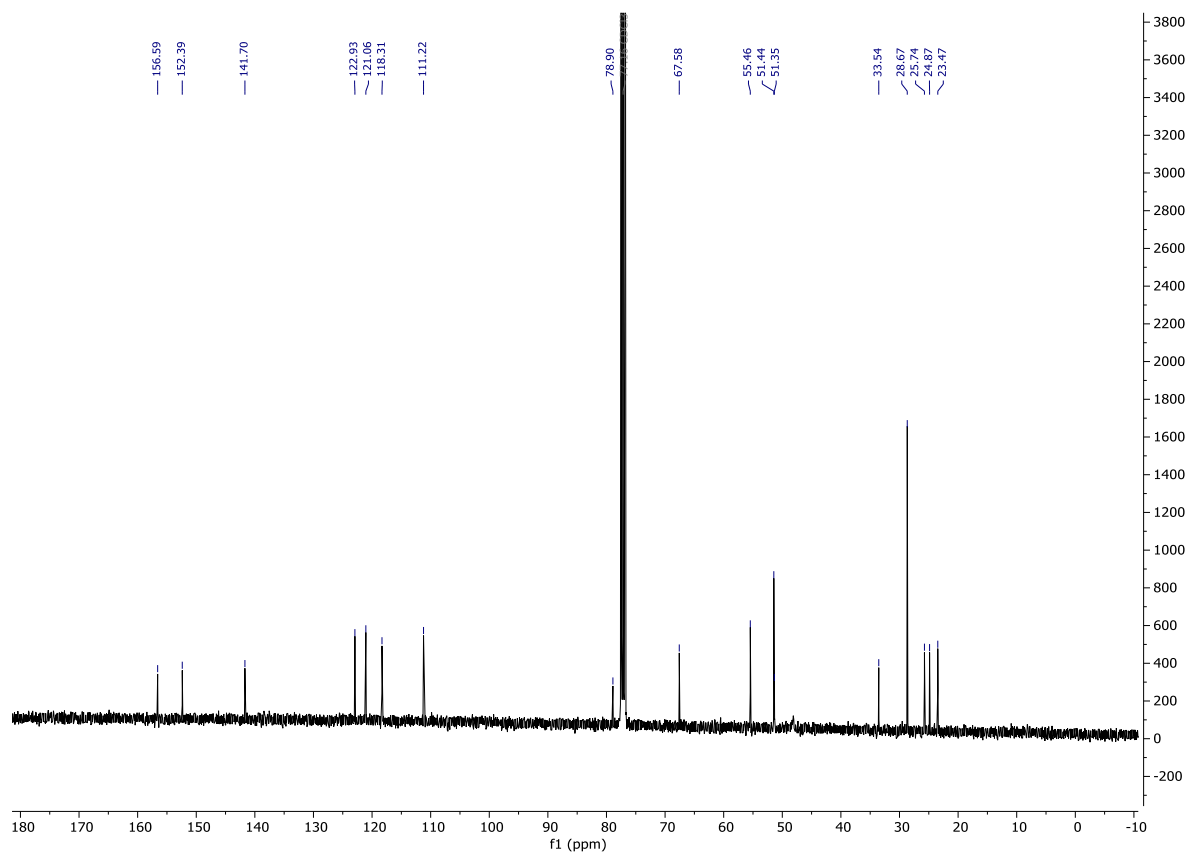
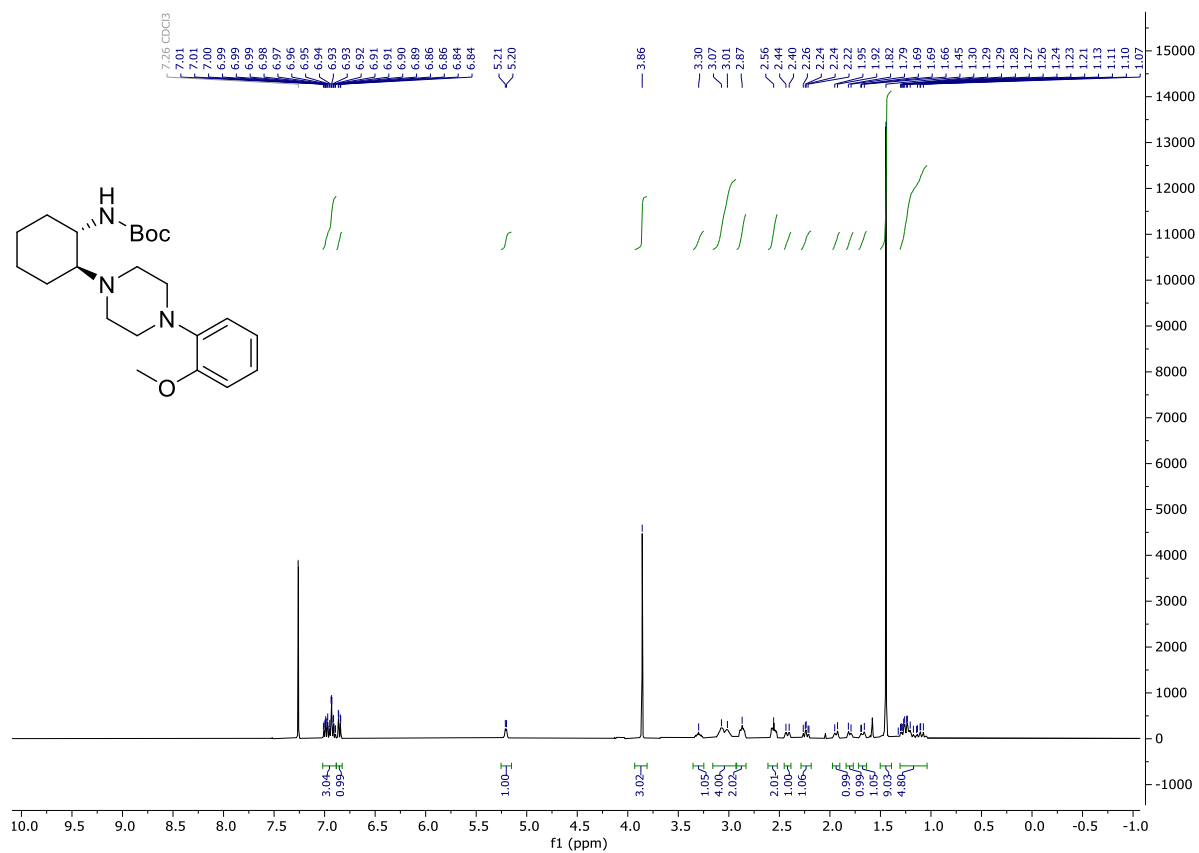
Chiral pool synthesis of enantiopure *trans*-ML-SI3

3.3 *tert*-Butyl (3*aR*,7*aS*)-hexahydro-3*H*-benzo[*d*][1,2,3]oxathiazole-3-carboxylate-2,2-dioxide (4a)

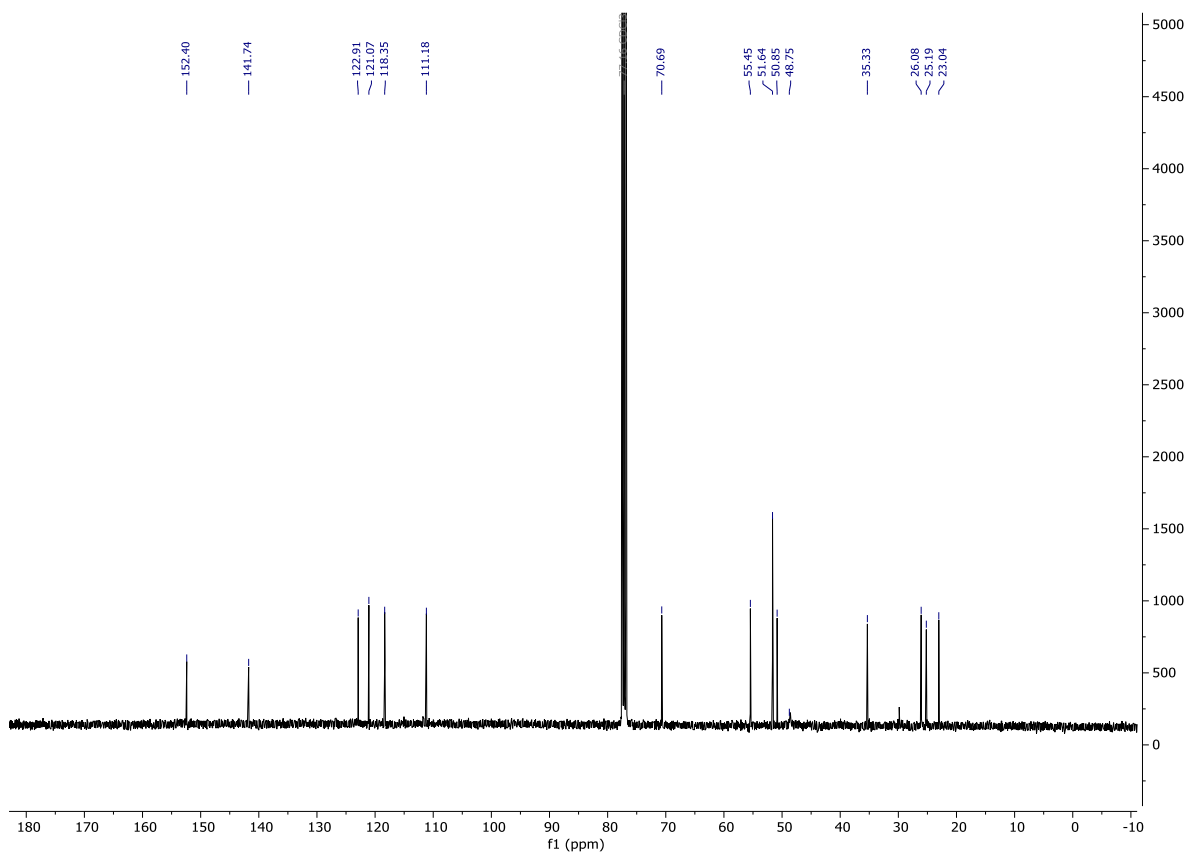
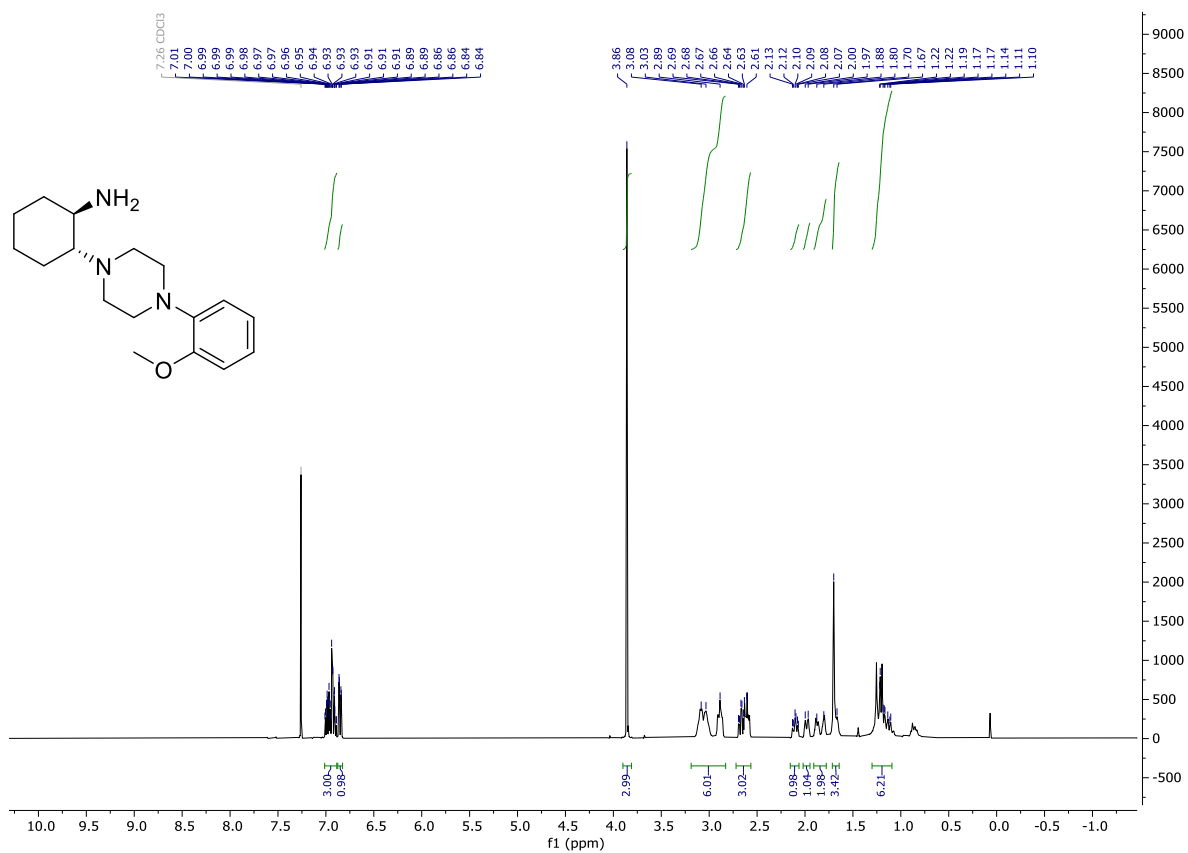


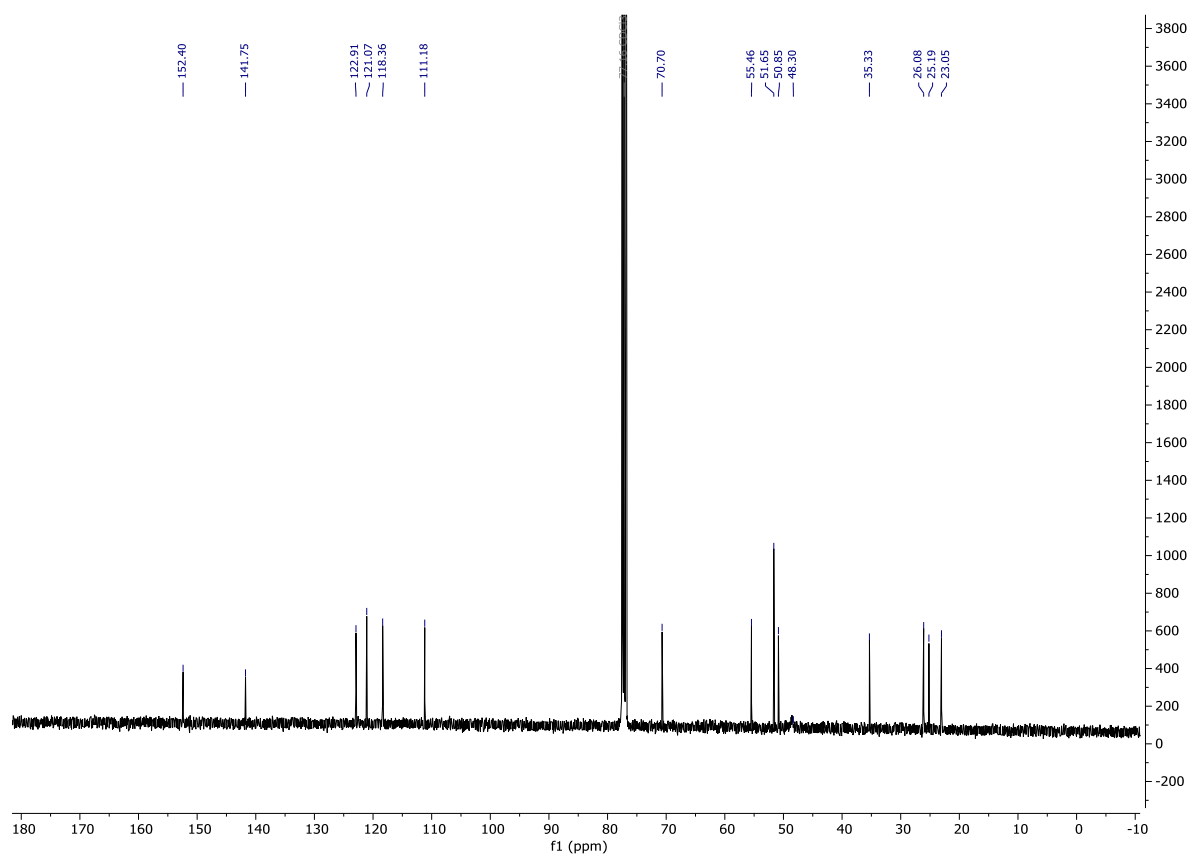
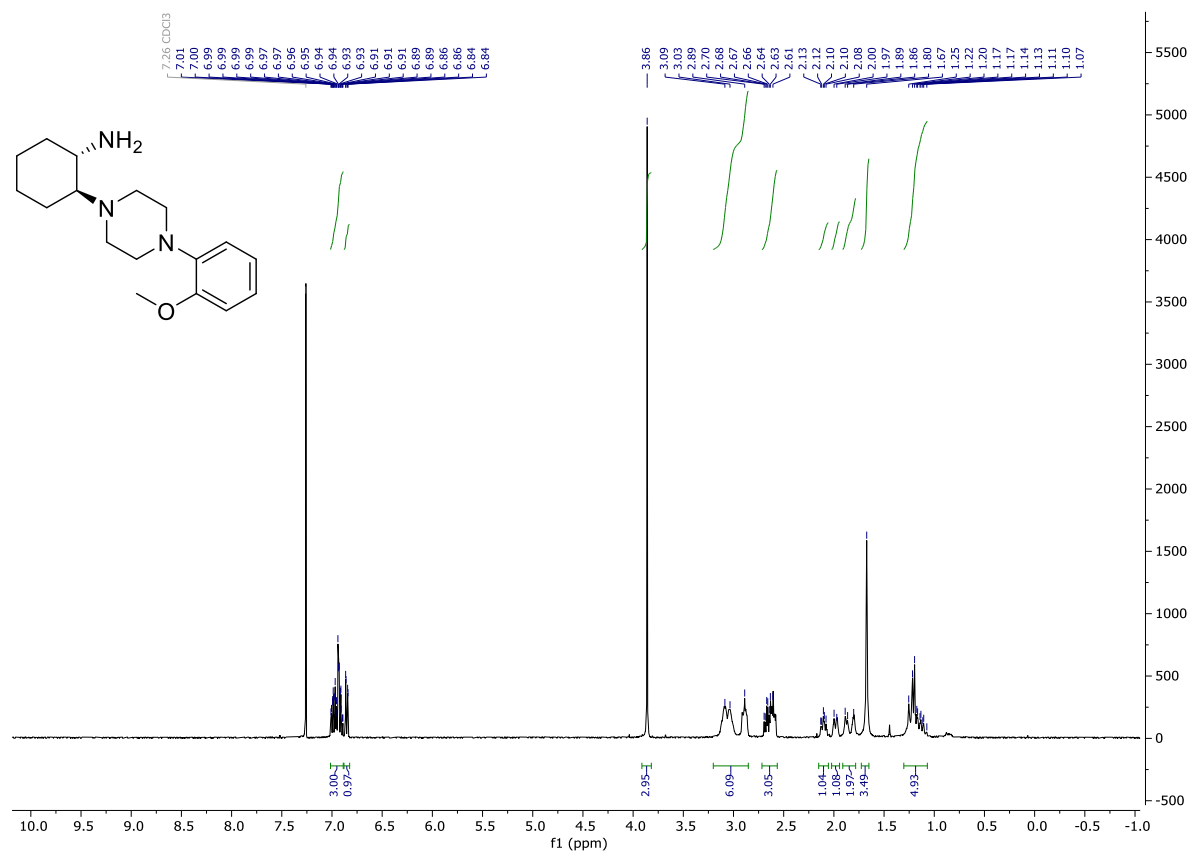
3.4 *tert*-Butyl {(1*R*,2*R*)-2-[4-(2-methoxyphenyl)piperazin-1-yl]cyclohexyl}carbamate (**5a**)



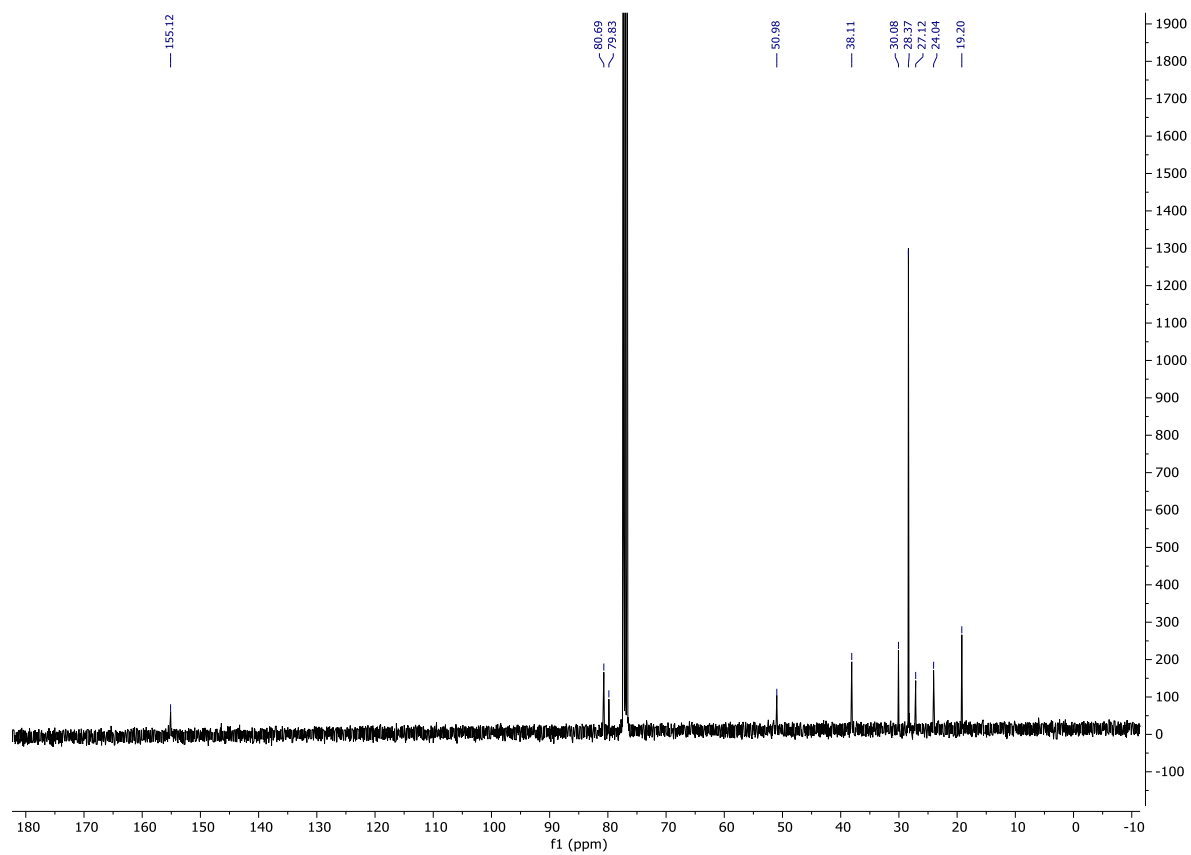
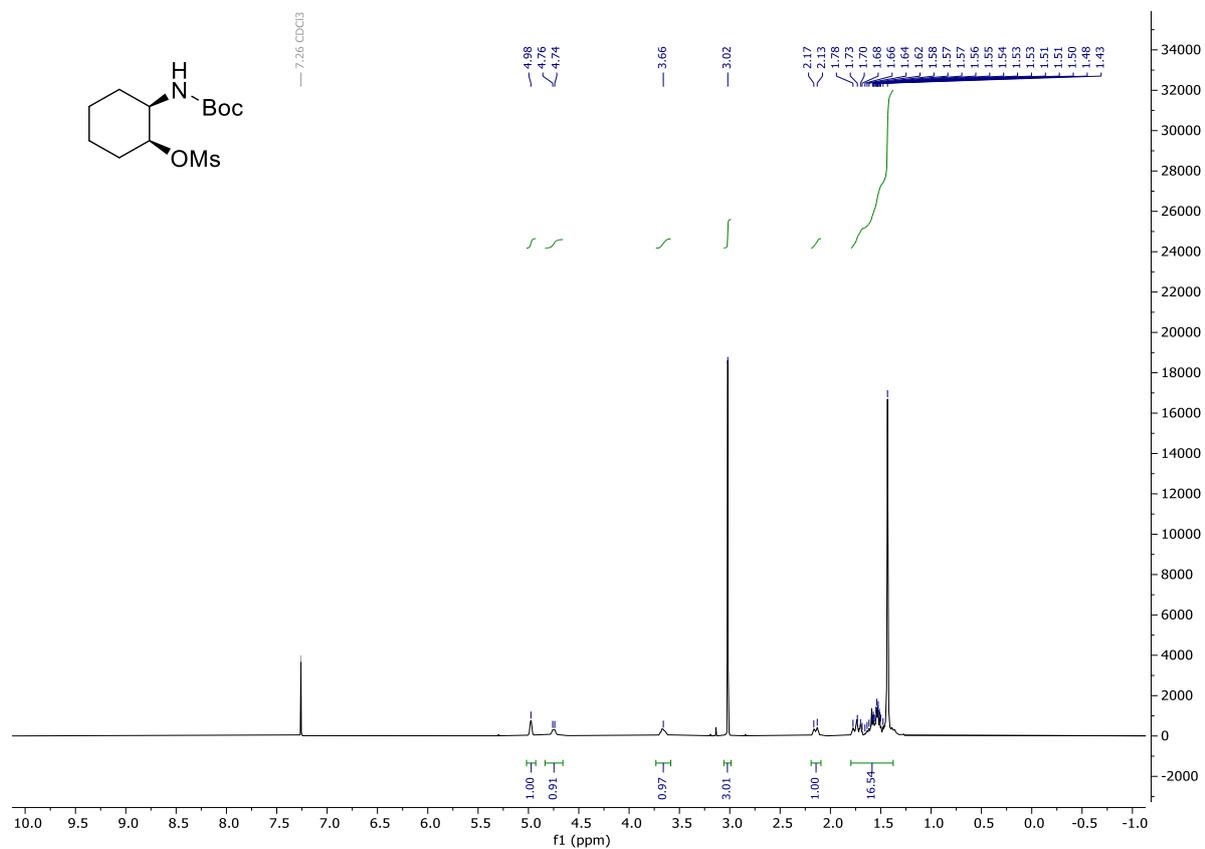
3.5 *tert*-Butyl {(1*S*,2*S*)-2-[4-(2-methoxyphenyl)piperazin-1-yl]cyclohexyl}carbamate (**5b**)

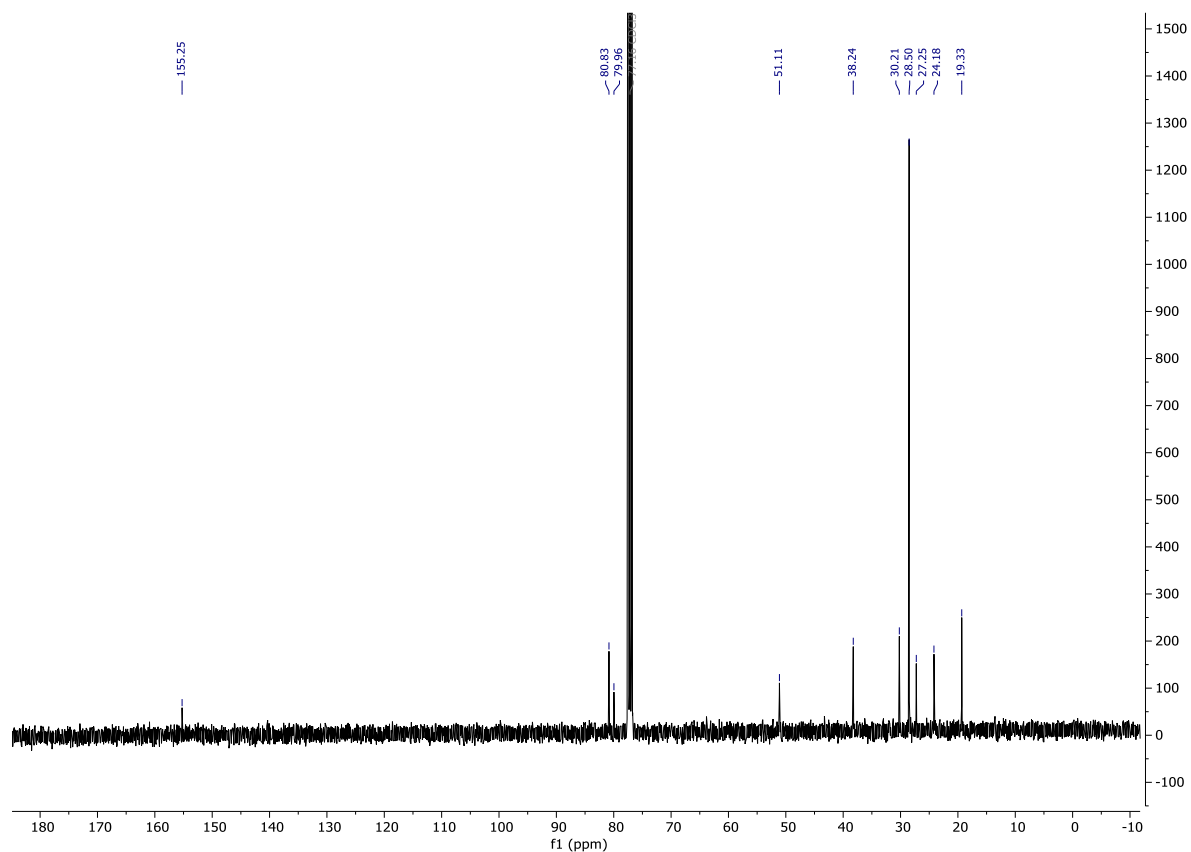
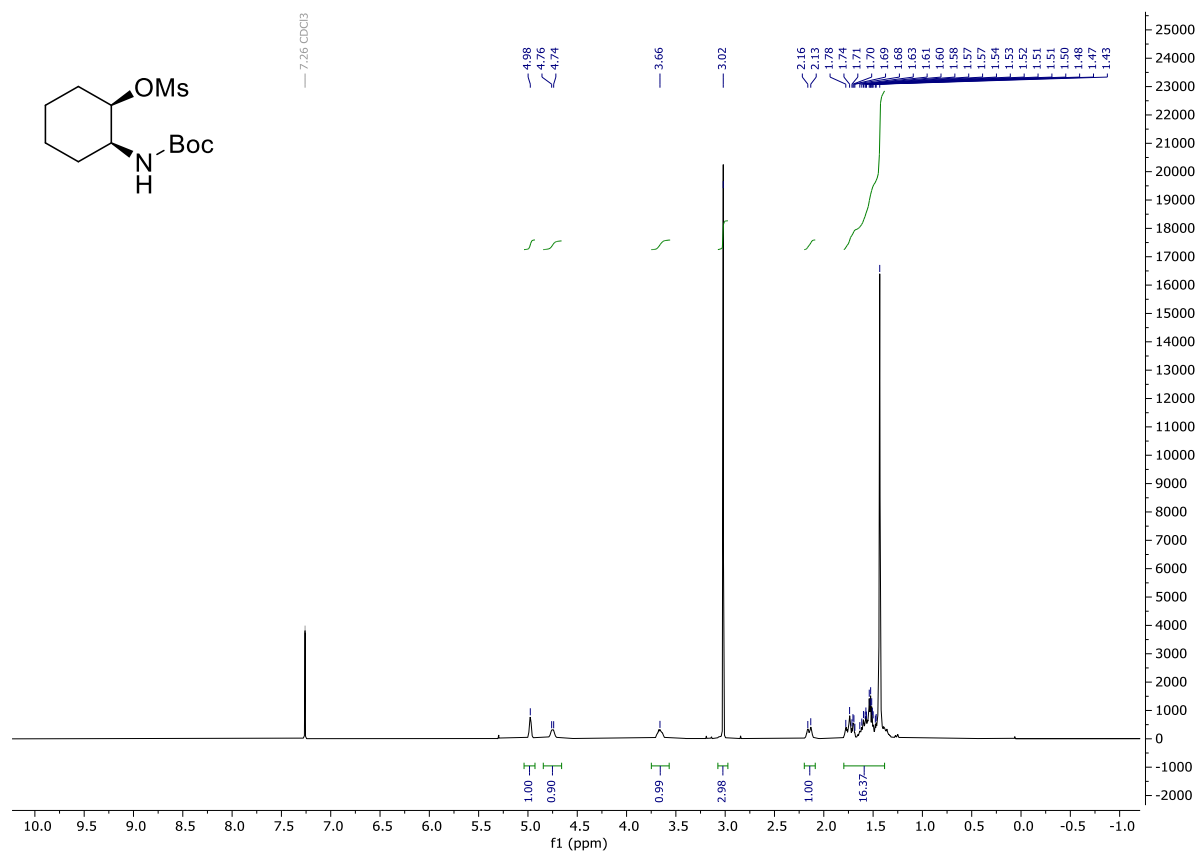
3.6 (1*R*,2*R*)-2-[4-(2-Methoxyphenyl)piperazin-1-yl]cyclohexan-1-amine (**6a**)



3.7 (1*S*,2*S*)-2-[4-(2-Methoxyphenyl)piperazin-1-yl]cyclohexan-1-amine (**6b**)

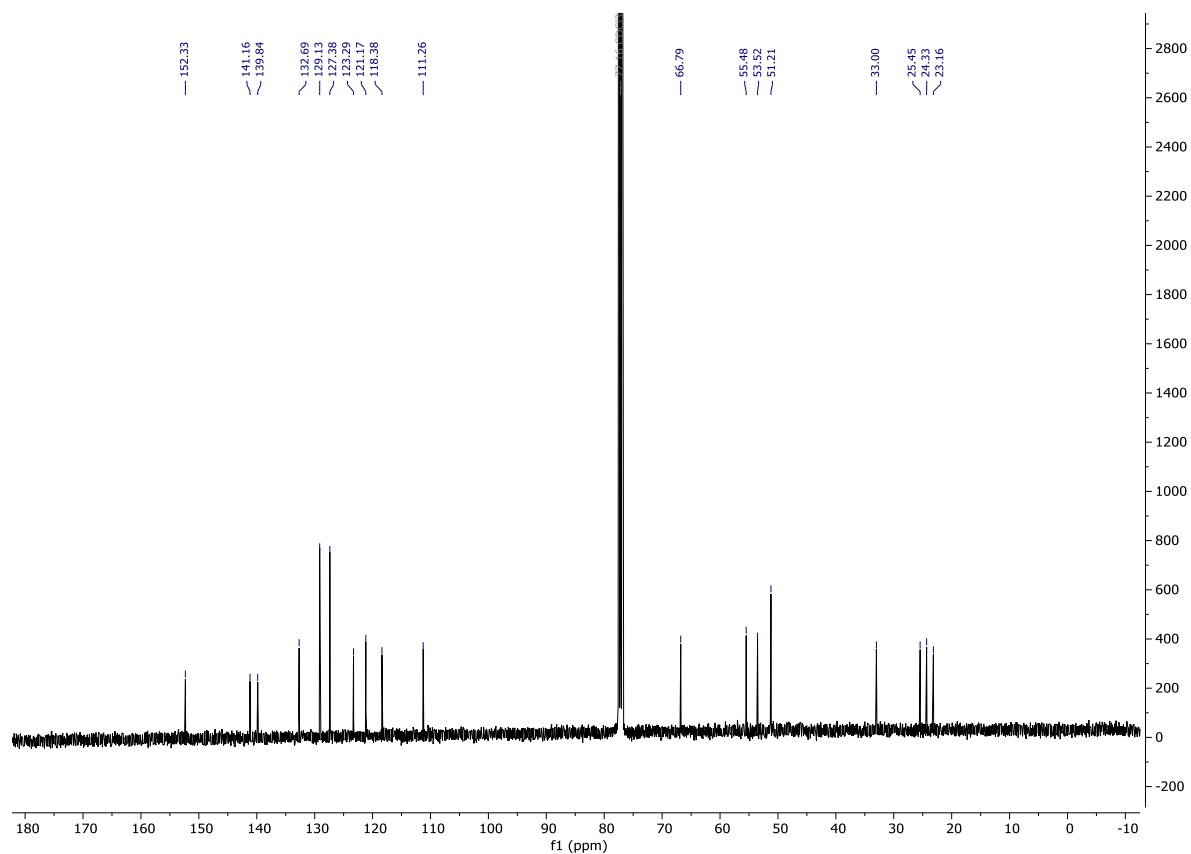
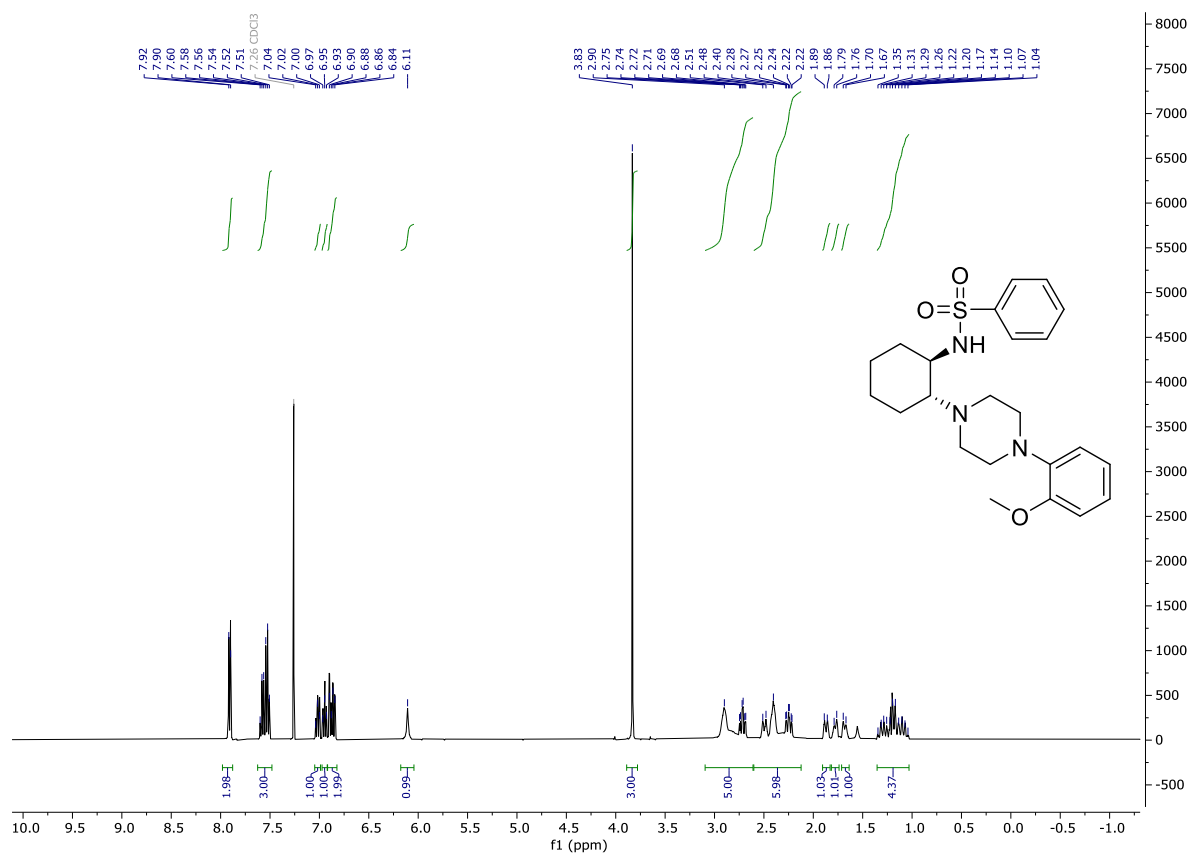
3.8 (1*S*,2*R*)-2-[(*tert*-Butoxycarbonyl)amino]cyclohexyl methanesulfonate (**7a**)



3.9 (1*R*,2*S*)-2-[(*tert*-Butoxycarbonyl)amino]cyclohexyl methanesulfonate (**7b**)

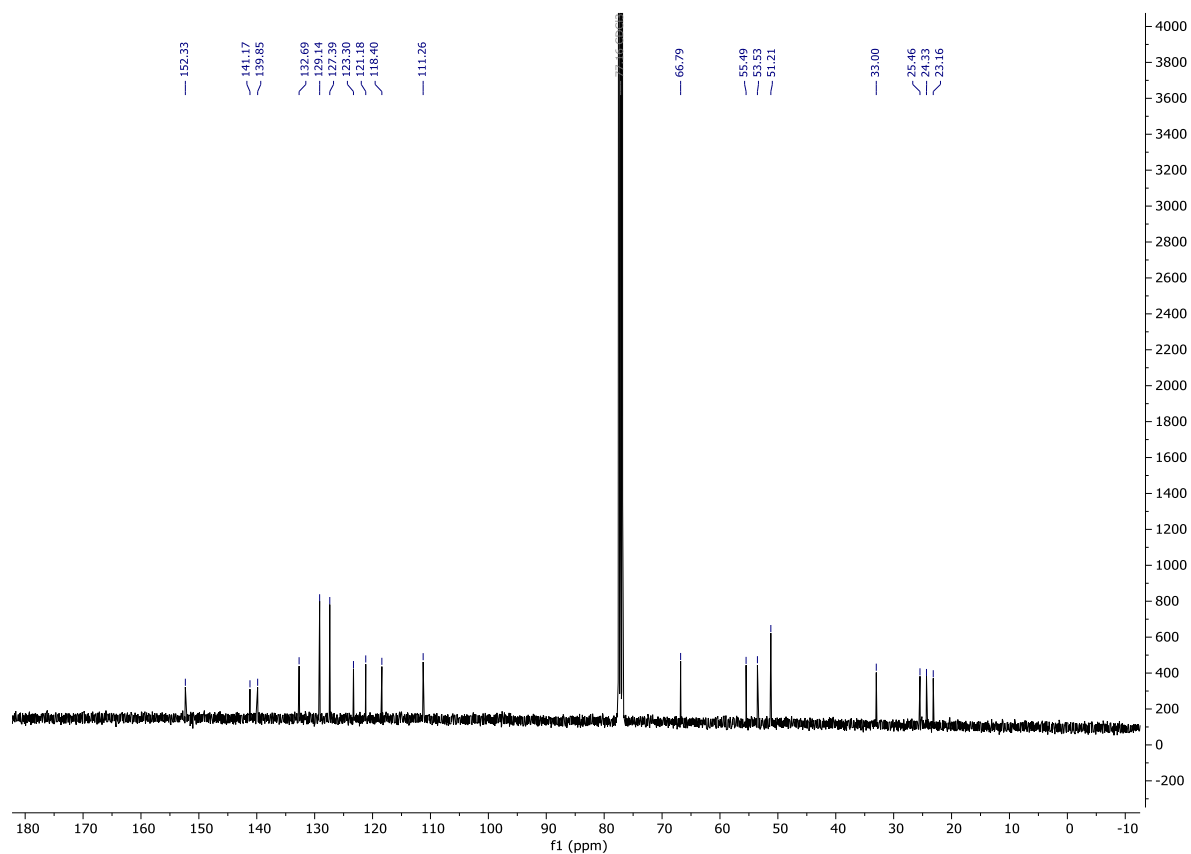
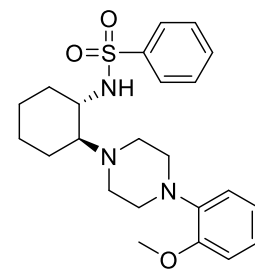
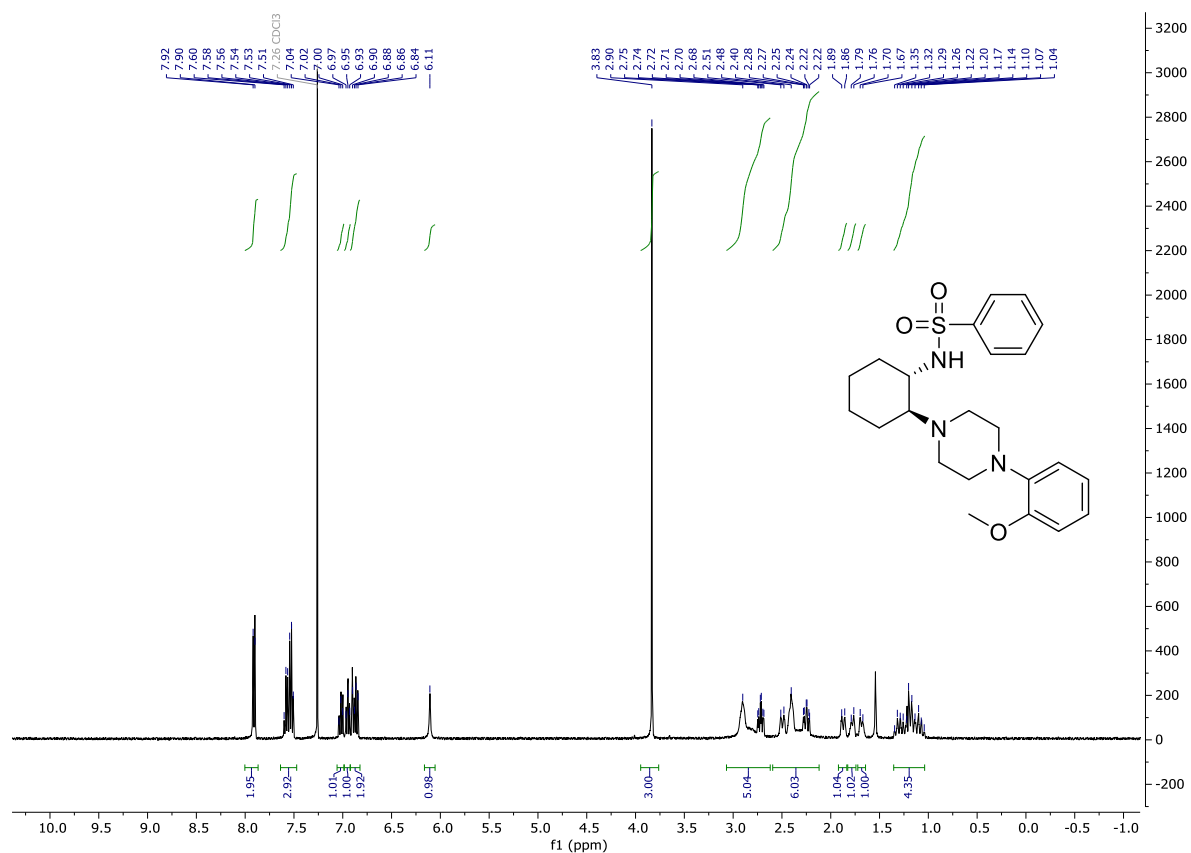
Chiral pool synthesis of enantiopure *trans*-ML-SI3

3.10 *N*-{(1*R*,2*R*)-2-[4-(2-Methoxyphenyl)piperazin-1-yl]cyclohexyl}benzenesulfonamide, (*R,R*)-*trans*-ML-SI3



Chiral pool synthesis of enantiopure *trans*-ML-SI3

3.11 *N*-{(1*S*,2*S*)-2-[4-(2-Methoxyphenyl)piperazin-1-yl]cyclohexyl}benzenesulfonamide, (*S,S*)-*trans*-ML-SI3



4 References

- [1] L.J. Farrugia, *J. Appl. Crystallogr.* **2012**, 45, 849-854.

3.1.3 Enantiopure variations of *trans*-ML-SI3

3.1.3.1 Synthesis of enantiopure *trans*-ML-SI3 variations

After the successful development of a synthesis for enantiopure *trans*-ML-SI3, the same method was applied in a next step to generate enantiopure variations. This project was the basis of DOMINIK EBERT'S Bachelor thesis. All compounds in this chapter were synthesized by him under my supervision. Synthesis of variations included the most promising alterations from the first SAR study^[69], together with two other structure motives known from the development of MK6-83^[22] (Figure 14).

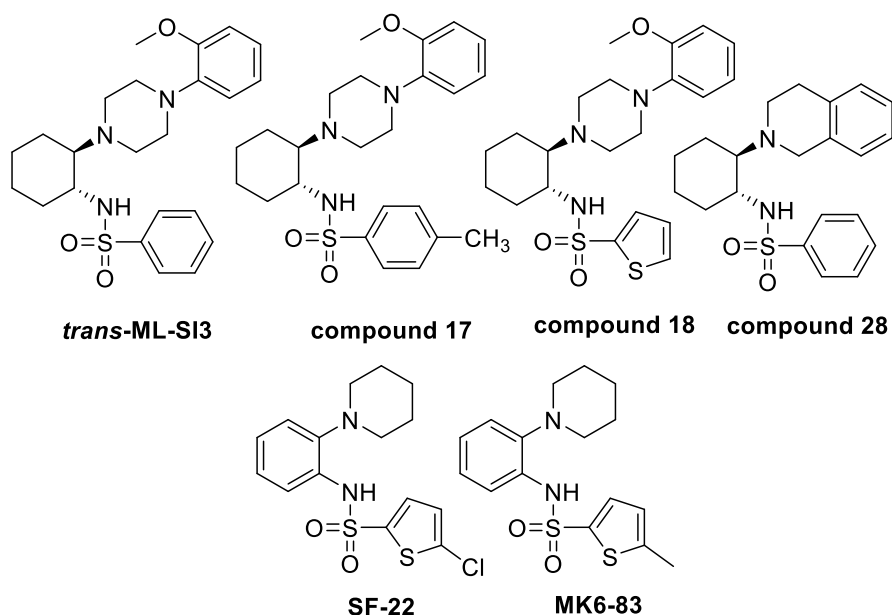


Figure 14 Chemical structures of compounds serving as model for the development of new enantiopure TRPML modulators. Compounds **17**, **18** and **28** originating from Leser *et al.*^[69] and TRMPL activators **SF-22** and **MK6-83**^[22].

The planned variations are shown in Figure 15. Only the (*R,R*)-configured target compounds are shown, however synthesis was of course planned and executed for both enantiomers respectively.

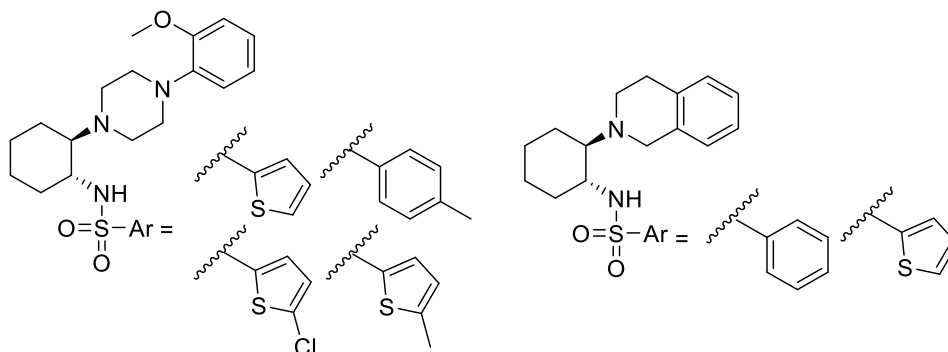
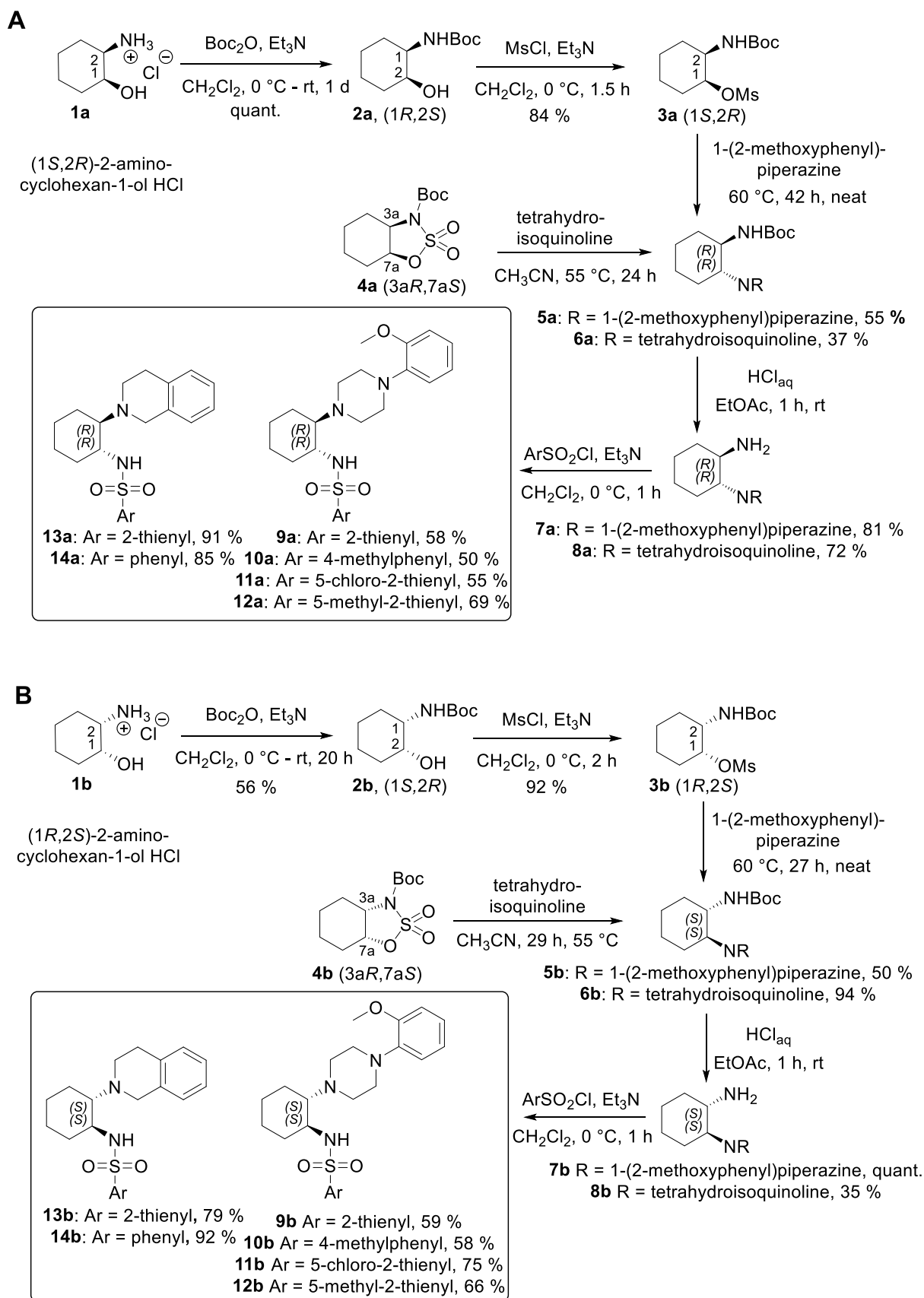


Figure 15 Envisaged structures for the synthesis of enantiopure *trans*-ML-SI3 variations. Shown are only (*R,R*)-configured target structures.

Synthesis followed the previously developed and described method^[70] (Chapter 3.1.2). Compounds with 1-(2-methoxyphenyl)piperazine as amino component (**9a/b**, **10a/b**, **11a/b**, and **12a/b**), were synthesized by the mesylate route, as the required starting materials **3a** and **3b** were easily accessible in larger amounts. For compounds with a tetrahydroisoquinoline residue (**13a/b** and **14a/b**) the sulfamidate route was used, starting from small amounts of commercially available intermediates **4a** and **4b**, purchased from abcr. Introduction of the different sulfonamide residues proceeded without complications by N-sulfonylation with the respective sulfonylchlorides. Compounds with piperazine residue were purified by crystallization from isopropanol. Tetrahydroisoquinoline compounds did not crystallize and were thus purified by column chromatography. All compounds were tested for enantiopurity by chiral HPLC and an ee value of > 99% was confirmed for all piperazine compounds, which were synthesized from mesylate intermediates **3a** and **3b**. Unfortunately, the tetrahydroisoquinoline compounds could not be analysed with the existing HPLC method and thus no ee value could be determined. Specific rotation of the tetrahydroisoquinoline derivatives **13a/b** and **14a/b** are not exactly opposing. The enantiomeric purity status therefore is uncertain and it can't be ruled out, that the purchased sulfamidate materials **4a** and **4b** might not have been completely enantiopure. This issue was already observed for material purchased from Sigma Aldrich^[70]. However the specific rotation indicates at least reasonable enantiomeric excess. Synthesis scheme and yields are given in Scheme 2.

Enantiopure variations of *trans*-ML-SI3



Scheme 2 Synthesis of enantiopure variations of *trans*-ML-SI3. **A** (*R,R*)-configured variations. **B** (*S,S*)-configured variations.

3.1.3.2 Biological evaluation of enantiopure *trans*-ML-SI3 variations

All compounds were tested in a first screening with the previously described FLIPR method^[69] by NICOLE URBAN from the SCHAEFER group, University of Leipzig. During analysis, a solubility problem of the new compounds in the thus far used HBS buffer was observed. To solve the issue, the buffer system was changed to HBS + 0.1% BSA. The improved solubility enhanced the activity of all compounds, including the **ML-SI3** enantiomers. The results of this first n=1 screening are given in Table 1.

Table 1 EC₅₀ and IC₅₀ values of the enantiopure variations of *trans*-ML-SI3 for TRPML1-3.

	TRPML1		TRPML2		TRPML3	
	EC ₅₀	IC ₅₀	EC ₅₀	IC ₅₀	EC ₅₀	IC ₅₀
(R,R)-ML-SI3	-	74 nM	-	126 nM	-	1.14 μM
(S,S)-ML-SI3	5.3 μM	-	609 nM	-	16.8 μM	-
9a	-	67 nM	-	157 nM	-	353 nM
9b	-	8.0 μM	1.4 μM	-	>100 μM	-
10a	-	106 nM	1.3 μM	-	1.6 μM	-
10b	1.3 μM	-	53 nM	-	675 nM	-
11a	-	126 nM	4.2 μM	-	-	5.9 μM
11b	1.48 μM	-	223 nM	-	2.0 μM	-
12a	-	85 nM	1.2 μM	-	-	1.2 μM
12b	1.6 μM	-	116 nM	-	1.5 μM	-
13a	-	1,7 μM	-	988 nM	-	28 μM
13b	-	8.9 μM	5.5 μM	-	> 100 μM	66 μM
14a	-	2.24 μM	-	2.62 μM	-	36 μM
14b	-	9.64 μM	11.8 μM	-	> 100 μM	62 μM

Even though the screening was only done as single determination, it is evident once more, what a crucial role the stereochemistry plays. In general compounds with *R,R*-configuration (**a** series) favour rather the inhibition of TRPML channels (Table 1, orange), while compounds with *S,S*-configuration (**b** series) tend to activate TRPML channels. The most interesting compounds from this screening (compounds **10b**, **11a**, and **12a**) were sent to PROF. DR. CHENG-CHANG CHEN at the National Taiwan University, to be tested by the lysosomal patch-clamp technique, to verify their activity against respective TRPML channel. Compound **10b** is evaluated as potent TRPML2 activator, while compounds **11a** and **12a** are verified as potent and selective TRPML1 inhibitors.

3.1.3.3 Experimental part for enantiopure variations of *trans*-ML-SI3

All chemicals used were obtained from abcr (Karlsruhe, Germany), Fisher Scientific (Schwerte, Germany), Sigma-Aldrich (now Merck, Darmstadt, Germany), TCI (Eschborn, Germany) or Th. Geyer (Renningen, Germany). Sulfamidates **4a** and **4b** were purchased from abcr. HPLC grade and dry solvents were purchased from VWR (Darmstadt, Germany) or Sigma-Aldrich, all other solvents were purified by distillation. All reactions were monitored by thin-layer chromatography (TLC) using pre-coated plastic sheets POLYGRAM® SIL G/UV254 from Macherey-Nagel and detected by irradiation with UV light (254 nm) or by staining with appropriate reagents. Flash column chromatography (FCC) was performed on Macherey-Nagel silica gel Si 60 (0.015 – 0.040 mm). NMR spectra (¹H, ¹³C, DEPT, H-H-COSY, HSQC, HMBC) were recorded at 23 °C on an Avance III 400 MHz Bruker BioSpin or Avance III 500 MHz Bruker BioSpin instrument. Chemical shifts δ are stated in parts per million (ppm) and are calibrated using residual protic solvent as an internal reference for proton (CDCl₃: δ = 7.26 ppm) and for carbon the central carbon resonance of the solvent (CDCl₃: δ = 77.16 ppm). Multiplicity is defined as s = singlet, d = doublet, t = triplet, m = multiplet. NMR spectra were analysed with NMR software MestReNova, version 12.0.1-20560 (Mestrelab Research S.L.). High resolution mass spectra were performed by the LMU Mass Spectrometry Service applying a Thermo Finnigan LTQ FT Ultra Fourier Transform Ion Cyclotron Resonance device at 250 °C. IR spectra were recorded on a Perkin Elmer FT-IR Paragon 1000 instrument as neat materials. Absorption bands were reported in wave number (cm⁻¹) with ATR PRO450-S. Melting points were determined by the open tube capillary method on a Büchi melting point B-540 apparatus and are uncorrected. Specific rotation [α] was measured at 23 °C at a wavelength of λ = 589 nm (Na-D line) using a Perkin Elmer 241 Polarimeter instrument and samples were dissolved in chloroform (layer thickness l = 10 cm), concentrations are stated in g/100 mL. Chiral HPLC analytical measurements were carried out using the following method. Stationary phase: Daicel Chiralcel-OD column (250 x 4.6 mm, 10 μ m); mobile phase: heptane/methyl *tert*-butyl ether/2-propanol/ethanolamine (50:48:2:0.1); sample concentration: 1 mg/mL in TBME or MeOH.

Biological evaluation was done by a Fluo-4/AM assay like previously described^[69]. The assay was performed by using a custom-made fluorescence imaging plate reader (FLIPR) built into a robotic liquid handling station (Freedom Evo 150, Tecan, Männedorf, Switzerland). All imaging experiments were done in a HEPES buffered solution (HBS), containing 132 mM NaCl, 6 mM KCl, 1 mM MgCl₂, 1 mM CaCl₂, 5.5 mM D-glucose, 10 mM HEPES, pH 7.4 + 0.1% bovine serum albumine. Compounds dissolved in DMSO (10 mM) were serially prediluted in assay buffer (0.98 μ M⁻¹ mM). HEK293 cells stably expressing plasma membrane-targeted human TRPML1, TRPML2 or TRPML3 were trypsinized and resuspended in cell culture medium supplemented with 4 μ M Fluo-4/AM (Invitrogen, Thermo Fisher Scientific, Waltham,

MA, U.S.A.). After incubation at 37 °C for 30 min, the cell suspension was briefly centrifuged, resuspended in assay buffer and dispensed into black pigmented, clear-bottom 384-well microwell plates (Greiner μ Clear, Frickenhausen, Germany). Then plates were placed into the FLIPR and fluorescence signals (excitation 470 nm, emission 515 nm) were recorded with a Zyla 5.5 camera (Andor, Belfast, UK) and the μ Manager software.

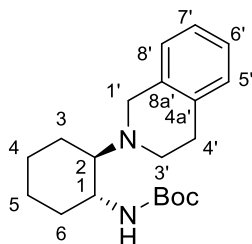
Synthesis and analytical data of previously not described compounds

General Procedure 1: Boc deprotection

The respective Boc-protected compound (1.0 eq) was dissolved in EtOAc (0.04M) until a clear solution was formed. Aqueous hydrochloric acid (4M, 20 eq) was added and the biphasic mixture was stirred for 1 h. The reaction mixture was neutralized with the quadruple amount of aqueous NaOH-solution (2M) and the aqueous layer was extracted twice with the same amount of EtOAc. The combined organic layers were filtrated through a hydrophobic filter and the solvent was removed *in vacuo*.

General Procedure 2: Synthesis of sulfonamides

The respective amine (1.0 eq) was dissolved in CH₂Cl₂ to a concentration of 0.1M and Et₃N (1.5 eq) was added. The solution was cooled down to 0 °C and the sulfonyl chloride (1.1 eq) was added. After stirring for 1 h at 0 °C, the mixture was diluted with CH₂Cl₂ and washed with the same amount of aqueous NaOH-solution (2M). The aqueous layer was extracted twice with CH₂Cl₂ (10 mL) and the combined organic layers were dried using a hydrophobic filter. The product was purified *via* recrystallization from *i*PrOH for the piperazine species or *via* FCC (CH₂Cl₂/MeOH 96:4) for the tetrahydroisoquinoline species.

***tert*-Butyl ((1*R*,2*R*)-2-(3,4-dihydroisoquinolin-2(1*H*)-yl)cyclohexyl)carbamate (6a)**

 $C_{20}H_{30}N_2O_2$

330.47 g/mol

(*R,S*)-Hexahydro-3*H*-1,2,3-benzoxthiazole-2,2-dioxide-3-carboxylic acid *t*-butyl ester **4a** (556 mg, 2.00 mmol, 1.00 eq) was dissolved in CH₃CN under N₂-atmosphere. 1,2,3,4-Tetrahydroisoquinoline (750 μL, 6.00 mmol, 3.00 eq) was added to the solution and it was stirred at 60 °C for 24 h. The solvent was removed *in vacuo* and the crude was taken up in EtOAc (75 mL). After washing the solution with KH₂PO₄-solution (1M, 75 mL) and extracting the aqueous phase twice with EtOAc (50 mL), the combined organic layers were dried through a hydrophobic filter. The solvent was removed *in vacuo* and the resulting crude was purified *via* FCC (petrol ether/EtOAc/Et₃N 9:1:0.2), to give carbamate **6a** as a colorless solid (247 mg, 0.747 mmol, 37 %).

mp.: 94 – 97 °C.

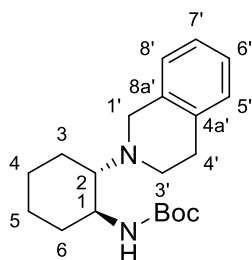
$[\alpha]_D^{23}$: -34.2 (c = 0.5, CHCl₃).

¹H NMR: (400 MHz, CDCl₃): δ (ppm) = 7.14 – 7.08 (m, 3H, 5'-H, 6'-H and 7'-H), 7.05 – 7.01 (m, 1H, 8'-H), 5.25 (s, 1H, NH), 3.89 (d, *J* = 14.7 Hz, 1H, 1'-H), 3.61 (d, *J* = 14.9 Hz, 1H, 1'-H), 3.43 – 3.34 (m, 1H, 1-H), 2.96 (dt, *J* = 11.2, 5.4 Hz, 1H, CH₂ THIQ), 2.83 (q, *J* = 4.7 Hz, 2H, CH₂ THIQ), 2.57 – 2.37 (m, 3H, CH₂ THIQ, CH₂ cyclohexane and 2-H), 1.98 – 1.93 (m, 1H, CH₂ cyclohexane), 1.85 – 1.79 (m, 1H, CH₂ cyclohexane), 1.70 (d, *J* = 10.8 Hz, 1H, CH₂ cyclohexane), 1.39 (s, 9H, *t*Bu), 1.30 (t, *J* = 3.0 Hz, 1H, CH₂ cyclohexane), 1.28 – 1.23 (m, 2H, CH₂ cyclohexane), 1.15 – 1.08 (m, 1H, CH₂ cyclohexane).

¹³C NMR: (101 MHz, CDCl₃): δ (ppm) = 156.5 (C=O), 135.9 (C-4a' or C-8a'), 135.2 (C-4a' or C-8a'), 128.9 (C-5'), 126.7 (C-8'), 126.0 (C-6' or C-7'), 125.6 (C-6' or C-7'), 79.0 (C-*t*Bu), 67.0 (C-2), 51.6 (C-1), 51.4 (CH₂ THIQ), 45.2 (CH₂ THIQ), 33.4 (CH₂ cyclohexane), 30.3 (CH₂ THIQ), 28.6 (CH₃-*t*Bu), 25.7 (CH₂ cyclohexane), 24.8 (CH₂ cyclohexane), 23.0 (CH₂ cyclohexane).

IR (ATR): $\tilde{\nu}$ (cm⁻¹) = 3381 (NH), 2925 (m), 1702 (C=O), 1480 (s), 1157 (s), 1094 (s), 749 (vs).

HRMS (ESI): *m/z* [M+H]⁺ calcd. for C₂₀H₃₁N₂O₂⁺: 331.2380, found 331.2380.

***tert*-Butyl ((1*S*,2*S*)-2-(3,4-dihydroisoquinolin-2(1*H*)-yl)cyclohexyl)carbamate (**6b**)**C₂₀H₃₀N₂O₂

330.47 g/mol

Using the same procedure as for carbamate **6a**, (*S,R*)-hexahydro-3*H*-1,2,3-benzoxthiazole-2,2-dioxide-3-carboxylic acid *t*-butyl ester **4b** (554 mg, 2.00 mmol) was reacted with 1,2,3,4-tetrahydroisoquinoline (0.751 mL, 6.00 mmol, 3.00 eq) to give carbamate **6b** as a colorless solid (622 mg, 1.88 mmol, 94 %).

mp.: 87 – 90 °C.

$[\alpha]_D^{23}$: +41.5 (c = 0.5, CHCl₃).

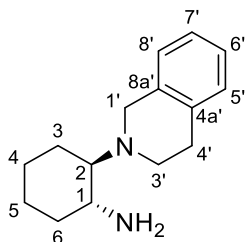
¹H NMR (400 MHz, CDCl₃): δ (ppm) = 7.14 – 7.08 (m, 3H, 5'-H, 6'-H and 7'-H), 7.05 – 7.00 (m, 1H, 8'-H), 5.25 (s, 1H, NH), 3.89 (d, *J* = 14.7 Hz, 1H, 1'-H), 3.61 (d, *J* = 14.5 Hz, 1H, 1'-H), 3.39 (ddd, *J* = 14.6, 10.5, 3.8 Hz, 1H, 1-H), 2.96 (dt, *J* = 11.1, 5.8 Hz, 1H, CH₂ THIQ), 2.83 (q, *J* = 5.0 Hz, 2H, CH₂ THIQ), 2.57 – 2.46 (m, 2H, CH₂ THIQ and CH₂ cyclohexane), 2.41 (td, *J* = 10.6, 3.0 Hz, 1H, 2-H), 1.99 – 1.93 (m, 1H, CH₂ cyclohexane), 1.85 – 1.79 (m, 1H, CH₂ cyclohexane), 1.70 (d, *J* = 11.0 Hz, 1H, CH₂ cyclohexane), 1.39 (s, 9H, *t*Bu), 1.35 – 1.20 (m, 4H, CH₂ cyclohexane).

¹³C NMR (101 MHz, CDCl₃): δ (ppm) = 156.5 (C=O), 135.9 (C-4a' or C-8a'), 135.2 (C-4a' or C-8a'), 128.9 (C-5'), 126.7 (C-8'), 126.0 (C-6' or C-7'), 125.6 (C-6' or C-7'), 79.0 (C-*q*-*t*Bu), 67.0 (C-2), 51.6 (C-1), 51.4 (C-1'), 45.2 (CH₂ THIQ), 33.4 (CH₂ cyclohexane), 30.3 (CH₂ THIQ), 28.6 (CH₃-*t*Bu), 25.7 (CH₂ cyclohexane), 24.8 (CH₂ cyclohexane), 23.03 (CH₂ cyclohexane).

IR (ATR): $\tilde{\nu}$ (cm⁻¹) = 3382 (NH), 2927 (m), 1704 (C=O), 1480 (s), 1158 (vs), 1094 (s), 749 (vs).

HRMS (ESI): *m/z* [M+H]⁺ calcd. for C₂₀H₃₁N₂O₂⁺: 331.2380, found 331.2379.

(1*R*,2*R*)-2-(3,4-Dihydroisoquinolin-2(1*H*)-yl)cyclohexan-1-amine (8a)



C₁₅H₂₂N₂
230.36 g/mol

Carbamate **6a** (253 mg, 0.766 mmol) was deprotonated using General Procedure 1 to give amine **8a** as a brownish solid (129 mg, 0.560 mmol, 72 %)

mp.: 87 – 90 °C.

$[\alpha]_D^{23}$: -25.0 (c = 0.5, CHCl₃).

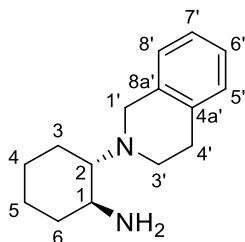
¹H NMR (400 MHz, CDCl₃): δ (ppm) = 7.16 – 7.07 (m, 3H, 5'-H, 6'-H and 7'-H), 7.05 – 6.99 (m, 1H, 8'-H), 3.90 (d, *J* = 14.9 Hz, 1H, 1'-H), 3.65 (d, *J* = 14.6 Hz, 1H, 1'-H), 2.97 (dt, *J* = 11.0, 5.7 Hz, 1H, CH₂ THIQ), 2.87 (t, *J* = 5.8 Hz, 2H, CH₂ THIQ), 2.76 (td, *J* = 10.3, 4.1 Hz, 1H, 1-H), 2.61 (dt, *J* = 11.8, 6.1 Hz, 1H, CH₂ THIQ), 2.26 (td, *J* = 10.6, 10.1, 3.3 Hz, 1H, 2-H), 2.05 – 1.97 (m, 1H, CH₂ cyclohexane), 1.92 – 1.85 (m, 1H, CH₂ cyclohexane), 1.84 – 1.77 (m, 3H, NH₂ and CH₂ cyclohexane), 1.74 – 1.66 (m, 1H, CH₂ cyclohexane), 1.27 – 1.13 (m, 4H, CH₂ cyclohexane).

¹³C NMR (101 MHz, CDCl₃): δ (ppm) = 136.2 (C-4a' or C-8a'), 135.2 (C-4a' or C-8a'), 128.9 (C-5'), 126.7 (C-8'), 126.0 (C-6' or C-7'), 125.5 (C-6' or C-7'), 70.4 (C-2), 51.5 (C-1'), 51.1 (C-1), 46.2 (CH₂ THIQ), 35.3 (CH₂ cyclohexane), 30.5 (CH₂ THIQ), 26.0 (CH₂ cyclohexane), 25.2 (CH₂ cyclohexane), 22.6 (CH₂ cyclohexane).

IR (ATR): $\tilde{\nu}$ (cm⁻¹) = 3338 (NH), 2922 (vs), 1447 (m), 1094 (s), 911 (m), 862 (s), 740 (vs).

HRMS (ESI): *m/z* [M+H]⁺ calcd. for C₁₅H₂₃N₂⁺: 231.1856, found 231.1855.

(1*S*,2*S*)-2-(3,4-Dihydroisoquinolin-2(1*H*)-yl)cyclohexan-1-amine (8b)



C₁₅H₂₂N₂
230.36 g/mol

Following General Procedure 1, carbamate **6b** (525 mg, 1.59 mmol) was deprotected to give amine **8b** as a brownish solid (129 mg, 0.560 mmol, 35 %).

mp.: 87 – 90 °C.

$[\alpha]_D^{23}$: +40.0 (c = 0.5, CHCl₃).

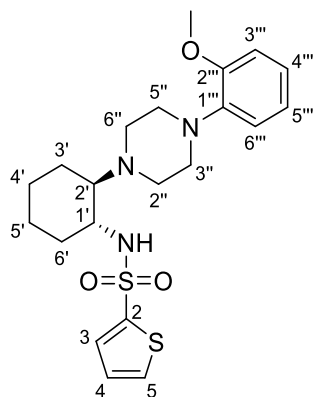
¹H NMR (400 MHz, CDCl₃): δ (ppm) = 7.15 – 7.06 (m, 3H, 5'-H, 6'-H and 7'-H), 7.05 – 6.99 (m, 1H), 3.90 (d, *J* = 14.6 Hz, 1H, 1'-H), 3.65 (d, *J* = 14.9 Hz, 1H, 1'-H), 3.01 – 2.92 (m, 1H, CH₂ THIQ), 2.87 (t, *J* = 5.8 Hz, 2H, CH₂ THIQ), 2.76 (td, *J* = 10.3, 4.2 Hz, 1H, 1-H), 2.61 (dt, *J* = 11.8, 6.1 Hz, 1H, CH₂ THIQ), 2.25 (td, *J* = 10.7, 10.1, 3.3 Hz, 1H, 2-H), 2.04 – 1.97 (m, 1H, CH₂ cyclohexane), 1.91 – 1.65 (m, 5H, CH₂ cyclohexane and NH₂), 1.31 – 1.10 (m, 4H, CH₂ cyclohexane).

¹³C NMR (101 MHz, CDCl₃): δ (ppm) = 136.2 (C-4a' or C-8a'), 135.2 (C-4a' or C-8a'), 128.9 (C-5'), 126.7 (C-8'), 126.0 (C-6' or C-7'), 125.5 (C-6' or C-7'), 70.5 (C-2), 51.5 (C-1'), 51.1 (C-1), 46.2 (CH₂ THIQ), 35.3 (CH₂ cyclohexane), 30.5 (CH₂ THIQ), 26.0 (CH₂ cyclohexane), 25.2 (CH₂ cyclohexane), 22.5 (CH₂ cyclohexane).

IR (ATR): $\tilde{\nu}$ (cm⁻¹) = 3338 (NH), 2922 (vs), 1448 (m), 1095 (s), 911 (m), 861 (s), 740 (vs).

HRMS (ESI): *m/z* [M+H]⁺ calcd. for C₁₅H₂₃N₂⁺: 231.1856, found 231.1855.

***N*-((1*R*,2*R*)-2-(4-(2-Methoxyphenyl)piperazin-1-yl)cyclohexyl)thiophene-2-sulfonamide
(9a)**



C₂₁H₂₉N₃O₃S₂
435.60 g/mol

Sulfonamide **9a** was synthesized according to General Procedure 2, using (*1R,2R*)-2-(4-(2-methoxyphenyl)piperazin-1-yl)cyclohexan-1-amine **7a** (50 mg, 0.17 mmol, 1.0 eq) and 2-thiophenesulfonyl chloride (35 mg, 0.19 mmol, 1.1 eq) giving sulfonamide **9a** as colorless crystals (47.6 mg, 0.109 mmol, 58 %), after recrystallization from ethanol.

mp.: 142 – 144 °C.

$[\alpha]_D^{23}$: -34.8 (c = 0.5, CHCl₃).

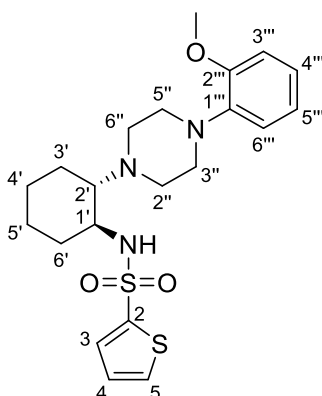
¹H NMR (400 MHz, CDCl₃): δ (ppm) = 7.62 (dd, *J* = 3.7, 1.3 Hz, 1H, 3-H), 7.58 (dd, *J* = 5.0, 1.3 Hz, 1H, 5-H), 7.11 (dd, *J* = 5.1, 3.7 Hz, 1H, 4-H), 7.04 – 6.99 (m, 1H, 4'''-H), 6.94 (td, *J* = 7.5, 1.5 Hz, 1H, 5'''-H), 6.89 (dd, *J* = 7.8, 1.9 Hz, 1H, 6'''-H), 6.85 (dd, *J* = 8.0, 1.5 Hz, 1H, 3'''-H), 6.21 (s, 1H, NH), 3.84 (s, 3H, OCH₃), 3.05 – 2.73 (m, 5H, CH₂ piperazine and 1'-H), 2.55 (d, *J* = 13.1 Hz, 1H, CH₂ cyclohexane), 2.49 – 2.23 (m, 5H, CH₂ piperazine and 2'-H), 1.94 – 1.67 (m, 3H, CH₂ cyclohexane), 1.42 – 1.27 (m, 1H, CH₂ cyclohexane), 1.27 – 1.09 (m, 3H, CH₂ cyclohexane).

¹³C NMR (101 MHz, CDCl₃): δ (ppm) = 152.3 (C-2'''), 141.2 (C-1'''), 140.9 (C-2), 132.0 (C-3), 131.7 (C-5), 127.6 (C-4), 123.3 (C-4'''), 121.2 (C-5'''), 118.4 (C-6'''), 111.2 (C-3'''), 66.7 (C-2'), 55.5 (OCH₃), 54.0 (C-1'), 51.2 (CH₂ piperazine), 33.0 (CH₂ cyclohexane), 25.5 (CH₂ cyclohexane), 24.4 (CH₂ cyclohexane), 23.2 (CH₂ cyclohexane).

IR (ATR): $\tilde{\nu}$ (cm⁻¹) = 3147 (NH), 2928 (w), 2830 (OCH₃), 1500 (m), 1240 (s), 1160 (s), 1022 (s), 734 (vs), 695 (vs).

HRMS (ESI): *m/z* [M+H]⁺ calcd. for C₂₁H₃₀N₃O₃S₂⁺: 436.1723, found 436.1722.

***N*-((1*S*,2*S*)-2-(4-(2-Methoxyphenyl)piperazin-1-yl)cyclohexyl)thiophene-2-sulfonamide
(9b)**



C₂₁H₂₉N₃O₃S₂
435.60 g/mol

Sulfonamide **9b** was synthesized according to General Procedure 2, using amine **7b** (76 mg, 0.26 mmol, 1.0 eq) and 2-thiophenesulfonyl chloride (54 mg, 0.29 mmol, 1.1 eq) giving sulfonamide **9b** as colorless crystals (75 mg, 0.17 mmol, 59 %), after recrystallization from ethanol.

mp. : 142 – 144 °C.

$[\alpha]_D^{23}$: +35.7 (c = 0.5, CHCl₃).

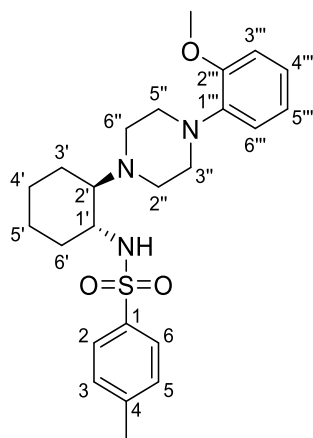
¹H NMR (400 MHz, CDCl₃): δ (ppm) = 7.62 (dd, *J* = 3.7, 1.3 Hz, 1H, 3-H), 7.58 (dd, *J* = 5.0, 1.3 Hz, 1H, 5-H), 7.11 (dd, *J* = 5.1, 3.7 Hz, 1H, 4-H), 7.04 – 6.99 (m, 1H, 4'''-H), 6.94 (td, *J* = 7.5, 1.5 Hz, 1H, 5'''-H), 6.89 (dd, *J* = 7.8, 1.8 Hz, 1H, 6'''-H), 6.85 (dd, *J* = 8.0, 1.5 Hz, 1H, 3'''-H), 6.21 (s, 1H, NH), 3.84 (s, 3H, OCH₃), 3.11 – 2.72 (m, 5H, CH₂ piperazine and 1'-H), 2.55 (d, *J* = 12.8 Hz, 1H, CH₂ cyclohexane), 2.49 – 2.23 (m, 5H, 4H CH₂ piperazine and 2'-H), 1.94 – 1.66 (m, 3H, CH₂ cyclohexane), 1.41 – 1.08 (m, 4H, CH₂ cyclohexane).

¹³C NMR (101 MHz, CDCl₃): δ (ppm) = 152.3 (C-2'''), 141.2 (C-1'''), 140.9 (C-2), 132.0 (C-3), 131.7 (C-5), 127.6 (C-4), 123.3 (C-4'''), 121.2 (C-5'''), 118.4 (C-6'''), 111.2 (C-3'''), 66.7 (C-2'), 55.5 (OCH₃), 54.0 (C-1'), 51.2 (CH₂ piperazine), 33.0 (CH₂ cyclohexane), 25.5 (CH₂ cyclohexane), 24.4 (CH₂ cyclohexane), 23.2 (CH₂ cyclohexane).

IR (ATR): $\tilde{\nu}$ (cm⁻¹) = 3149 (NH), 2929 (w), 2830 (OCH₃), 1500 (m), 1240 (s), 1160 (s), 1022 (s), 734 (vs), 695 (vs).

HRMS (ESI): *m/z* [M+H]⁺ calcd. for C₂₁H₃₀N₃O₃S₂⁺: 436.1723, found 436.1722.

***N*-((1*R*,2*R*)-2-(4-(2-Methoxyphenyl)piperazin-1-yl)cyclohexyl)-4-methyl
benzenesulfonamide (**10a**)**



C₂₄H₃₃N₃O₃S

443.61 g/mol

Using General Procedure 2, (1*R*,2*R*)-2-(4-(2-methoxyphenyl)piperazin-1-yl)cyclohexan-1-amine **7a** (51 mg, 0.18 mmol, 1.0 eq) and *p*-toluenesulfonyl chloride (36 mg, 0.19 mmol, 1.1 eq) were converted to the product. Recrystallization from isopropanol gave sulfonamide **10a** as colorless crystals (39 mg, 0.087 mmol, 50 %).

mp.: 125 – 127 °C.

$[\alpha]_D^{23}$: -5.7 (c = 0.5, CHCl₃).

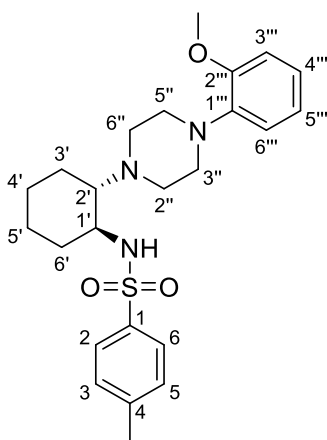
¹H NMR (400 MHz, CDCl₃): δ (ppm) = 7.78 (d, *J* = 8.3 Hz, 2H, 2-H and 6-H), 7.31 (d, *J* = 7.9 Hz, 2H, 3-H and 5-H), 7.02 (td, *J* = 7.7, 1.8 Hz, 1H, 4'''-H), 6.95 (td, *J* = 7.5, 1.5 Hz, 1H, 5'''-H), 6.90 (dd, *J* = 7.8, 1.8 Hz, 1H, 6'''-H), 6.86 (dd, *J* = 8.0, 1.5 Hz, 1H, 3'''-H), 6.07 (s, 1H, NH), 3.84 (s, 3H, OCH₃), 2.91 (s, 4H, CH₂ piperazine), 2.71 (td, *J* = 10.5, 4.1 Hz, 1H, 1'-H), 2.51 – 2.20 (m, 9H, 3H CH₃, 4H CH₂ piperazine, 1H CH₂ cyclohexane and 2'-H), 1.90 – 1.62 (m, 3H, CH₂ cyclohexane), 1.34 – 1.22 (m, 1H, CH₂ cyclohexane), 1.22 – 1.03 (m, 3H, CH₂ cyclohexane).

¹³C NMR (101 MHz, CDCl₃): δ (ppm) = 152.3 (C-2'''), 143.4 (C-4), 141.2 (C-1'''), 137.0 (C-1), 129.7 (C-3 and C-5), 127.4 (C-2 and C-6), 123.3 (C-4'''), 121.2 (C-5'''), 118.4 (C-6'''), 111.3 (C-3'''), 66.8 (C-2'), 55.5 (OCH₃), 53.5 (C-1'), 51.2 (CH₂ piperazine), 33.0 (CH₂ cyclohexane), 25.5 (CH₂ cyclohexane), 24.3 (CH₂ cyclohexane), 23.2 (CH₂ cyclohexane), 21.7 (CH₃).

IR (ATR): $\tilde{\nu}$ (cm⁻¹) = 3179 (NH), 2932 (w), 2821 (OCH₃), 1496 (m), 1340 (m), 1240 (s), 1162 (vs), 1022 (s), 818 (s), 752 (vs), 696 (vs).

HRMS (ESI): *m/z* [M+H]⁺ calcd. for C₂₄H₃₄N₃O₃S⁺: 444.2315, found 444.2314.

***N*-((1*S*,2*S*)-2-(4-(2-Methoxyphenyl)piperazin-1-yl)cyclohexyl)-4-methyl benzenesulfonamide (**10b**)**



C₂₄H₃₃N₃O₃S

443.61 g/mol

Sulfonamide **10b** was synthesized according to General Procedure 2, using (1*S*,2*S*)-2-(4-(2-methoxyphenyl)piperazin-1-yl)cyclohexan-1-amine **7b** (76 mg, 0.26 mmol) and *p*-toluenesulfonyl chloride (56 mg, 0.30 mmol, 1.1 eq) giving sulfonamide **10b** as colorless crystals (74 mg, 0.17 mmol, 58 %), after recrystallization from isopropanol.

mp.: 125 – 127 °C.

$[\alpha]_D^{23}$: +6.1 (c = 0.5, CHCl₃).

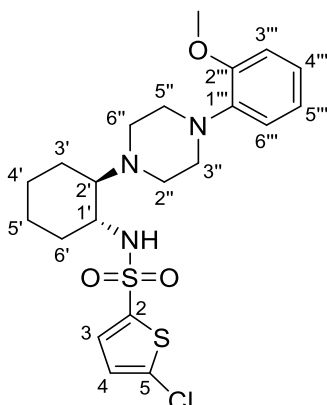
¹H NMR (400 MHz, CDCl₃): δ (ppm) = 7.78 (d, *J* = 8.4 Hz, 2H, 2-H and 6-H), 7.31 (d, *J* = 7.9 Hz, 2H, 3-H and 5-H), 7.02 (td, *J* = 7.7, 1.8 Hz, 1H, 4'''-H), 6.95 (td, *J* = 7.5, 1.5 Hz, 1H, 5'''-H), 6.90 (dd, *J* = 7.9, 1.9 Hz, 1H, 6'''-H), 6.86 (dd, *J* = 8.0, 1.5 Hz, 1H, 3'''-H), 6.07 (s, 1H, NH), 3.84 (s, 3H, OCH₃), 2.91 (s, 4H, CH₂ piperazine), 2.71 (td, *J* = 10.3, 3.9 Hz, 1H, 1'-H), 2.52 – 2.21 (m, 9H, 3H CH₃, 4H CH₂ piperazine, 1H CH₂ cyclohexane and 2'-H), 1.91 – 1.63 (m, 3H, CH₂ cyclohexane), 1.34 – 1.22 (m, 1H, CH₂ cyclohexane), 1.22 – 1.03 (m, 3H, CH₂ cyclohexane).

¹³C NMR (101 MHz, CDCl₃): δ (ppm) = 152.3 (C-2'''), 143.4 (C-4), 141.2 (C-1'''), 137.0 (C-1), 129.7 (C-3 and C-5), 127.4 (C-2 and C-6), 123.3 (C-4'''), 121.2 (C-5'''), 118.4 (C-6'''), 111.3 (C-3'''), 66.8 (C-2'), 55.47 (OCH₃), 53.5 (C-1'), 51.2 (CH₂ piperazine), 33.0 (CH₂ cyclohexane), 25.5 (CH₂ cyclohexane), 24.3 (CH₂ cyclohexane), 23.2 (CH₂ cyclohexane), 21.7 (CH₃).

IR (ATR): $\tilde{\nu}$ (cm⁻¹) = 3203 (NH), 2933 (w), 2820 (OCH₃), 1494 (m), 1340 (m), 1240 (s), 1160 (vs), 1021 (s), 818 (s), 752 (vs), 694 (vs).

HRMS (ESI): *m/z* [M+H]⁺ calcd. for C₂₄H₃₄N₃O₃S⁺: 444.2315, found 444.2314.

5-Chloro-*N*-((1*R*,2*R*)-2-(4-(2-methoxyphenyl)piperazin-1-yl)cyclohexyl)thiophene-2-sulfonamide (11a)



$C_{21}H_{28}ClN_3O_3S_2$

470.04 g/mol

Following General Procedure 2, amine **7a** (80 mg, 0.28 mmol, 1.0 eq) and 5-chloro-2-thiophenesulfonyl chloride (41 μ L, 0.30 mmol, 1.1 eq) were converted to the product. FCC ($CH_2Cl_2/MeOH$, 95:5) and recrystallization from isopropanol gave sulfonamide **11a** as brownish crystals (72 mg, 0.15 mmol, 55 %).

mp.: 126 – 128 °C.

$[\alpha]_D^{23}$: -19.7 (c = 0.5, $CHCl_3$).

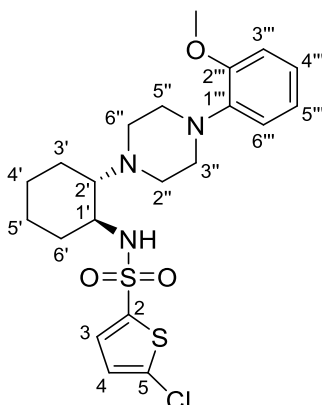
1H NMR (400 MHz, $CDCl_3$): δ (ppm) = 7.40 (d, J = 3.9 Hz, 1H, Ar-H thiophene), 7.05 – 6.99 (m, 1H, 4'''-H), 6.97 – 6.89 (m, 3H, 5'''-H, 6'''-H and Ar-H thiophene), 6.86 (dd, J = 8.0, 1.5 Hz, 1H, 3'''-H), 6.25 (s, 1H, NH), 3.85 (s, 3H, OCH_3), 3.18 – 2.82 (m, 5H, 4H CH_2 piperazine and 1'-H), 2.60 – 2.22 (m, 6H, 4H CH_2 piperazine, 1H CH_2 cyclohexane and 2'-H), 1.93 (d, J = 11.3 Hz, 1H, CH_2 cyclohexane), 1.82 (dd, J = 8.5, 2.6 Hz, 1H, CH_2 cyclohexane), 1.75 – 1.67 (m, 1H, CH_2 cyclohexane), 1.39 – 1.28 (m, 1H, CH_2 cyclohexane), 1.28 – 1.16 (m, 3H, CH_2 cyclohexane).

^{13}C NMR (101 MHz, $CDCl_3$): δ (ppm) = 152.3 (C-2'''), 141.1 (C-1'''), 139.2 (C-2 or C-5), 137.1 (C-2 or C-5), 131.3 (C-3 or C-4), 126.9 (C-3 or C-4), 123.4 (C-4'''), 121.2 (C-5'''), 118.4 (C-6'''), 111.3 (C-3'''), 66.7 (C-2'), 55.5 (OCH_3), 54.0, 51.1, 32.9, 25.4, 24.3, 23.3.

IR (ATR): $\tilde{\nu}(cm^{-1})$ = 3167 (NH), 2943 (w), 2826 (OCH_3), 1499 (s), 1412 (s), 1346 (s), 1238 (s), 1154 (vs), 1023 (vs), 988 (s), 750 (vs).

HRMS (ESI): m/z $[M+H]^+$ calcd. for $C_{21}H_{29}ClN_3O_3S_2^+$: 470.1333, found 470.1335.

5-Chloro-*N*-((1*S*,2*S*)-2-(4-(2-methoxyphenyl)piperazin-1-yl)cyclohexyl)thiophene-2-sulfonamide (11b)



C₂₁H₂₈ClN₃O₃S₂

470.04 g/mol

Sulfonamide **11b** was synthesized according to General Procedure 2, using amine **7b** (75 mg, 0.26 mmol, 1.0 eq) and 5-chloro-2-thiophenesulfonyl chloride (38 μ L, 0.29 mmol, 1.1 eq), giving sulfonamide **11b** as brownish crystals (98 mg, 0.21 mmol, 75 %), after recrystallization from isopropanol.

mp.: 129 – 131 °C.

$[\alpha]_D^{23}$: +19.0 (c = 0.5, CHCl₃).

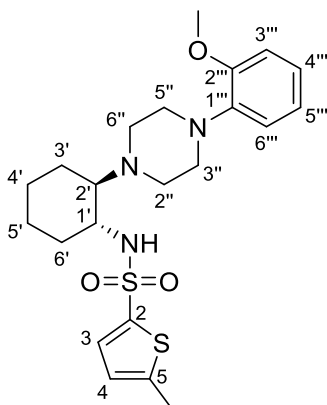
¹H NMR (400 MHz, CDCl₃): δ (ppm) = 7.40 (d, J = 3.9 Hz, 1H, Ar-H thiophene), 7.02 (ddd, J = 8.0, 6.9, 2.2 Hz, 1H, 4'''-H), 6.97 – 6.89 (m, 3H, 5'''-H, 6'''-H and Ar-thiophene), 6.86 (dd, J = 8.0, 1.5 Hz, 1H, Ar-H), 6.26 (s, 1H, NH), 3.85 (s, 3H, OCH₃), 3.11 – 2.80 (m, 5H, 4H CH₂ piperazine and 1'-H), 2.60 – 2.24 (m, 6H, 4H piperazine, 1H CH₂ cyclohexane and 2'-H), 1.93 (d, J = 11.4 Hz, 1H, CH₂ cyclohexane), 1.85 – 1.79 (m, 1H, CH₂ cyclohexane), 1.71 (d, J = 9.4 Hz, 1H, CH₂ cyclohexane), 1.39 – 1.28 (m, 1H, CH₂ cyclohexane), 1.27 – 1.16 (m, 3H, CH₂ cyclohexane).

¹³C NMR (101 MHz, CDCl₃): δ (ppm) = 152.3 (C-2'''), 141.1 (C-1'''), 139.2 (C-2 or C-5), 137.0 (C-2 or C-5), 131.3 (C-3 or C-4), 126.9 (C-3 or C-4), 123.4 (C-4'''), 121.2 (C-5'''), 118.4 (C-6'''), 111.3 (C-3'''), 66.7 (C-2'), 55.5 (OCH₃), 54.0 (C-1'), 51.1 (CH₂ piperazine), 32.9 (CH₂ cyclohexane), 25.4 (CH₂ cyclohexane), 24.3 (CH₂ cyclohexane), 23.3 (CH₂ cyclohexane).

IR (ATR): $\tilde{\nu}$ (cm⁻¹) = 3168 (NH), 2943 (w), 2826 (OCH₃), 1498 (s), 1412 (s), 1346 (s), 1238 (s), 1154 (vs), 1023 (s), 988 (s), 750 (vs).

HRMS (ESI): m/z [M+H]⁺ calcd. for C₂₁H₂₉ClN₃O₃S₂⁺: 470.1333, found 470.1336.

***N*-((1*R*,2*R*)-2-(4-(2-Methoxyphenyl)piperazin-1-yl)cyclohexyl)-5-methylthiophene-2-sulfonamide (**12a**)**



$$\text{C}_{22}\text{H}_{31}\text{N}_3\text{O}_3\text{S}_2$$

$$449.63 \text{ g/mol}$$

Sulfonamide **12a** was synthesized following General Procedure 2, using amine **7a** (81 mg, 0.28 mmol, 1.0 eq) and 5-methylthiophene-2-sulfonyl chloride (42 μL , 0.30 mmol, 1.1 eq) giving sulfonamide **12a** as brownish crystals (87 mg, 0.19 mmol, 69 %), after recrystallization from isopropanol.

mp.: 122 – 124 °C.

$[\alpha]_D^{23}$: -25.5 ($c = 0.5$, CHCl_3).

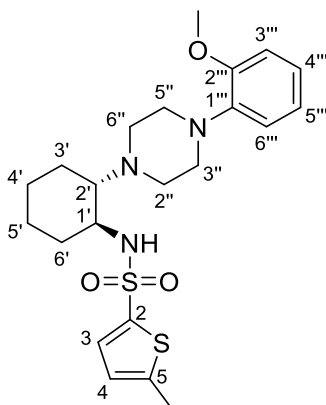
$^1\text{H NMR}$ (400 MHz, CDCl_3): δ (ppm) = 7.42 (d, $J = 3.7$ Hz, 1H, 3-H), 7.04 – 6.98 (m, 1H, 4'''-H), 6.94 (td, $J = 7.5, 1.5$ Hz, 1H, 5'''-H), 6.90 (dd, $J = 7.8, 1.9$ Hz, 1H, 6'''-H), 6.86 (dd, $J = 8.0, 1.5$ Hz, 1H, 3'''-H), 6.76 (dd, $J = 3.8, 1.1$ Hz, 1H, 4-H), 6.16 (s, 1H, NH), 3.84 (s, 3H, OCH_3), 3.05 – 2.79 (m, 5H, CH_2 piperazine and 1'-H), 2.59 – 2.23 (m, 9H, 3H CH_3 toluene, 4H CH_2 piperazine, 1H CH_2 cyclohexane and 2'-H), 1.91 (d, $J = 11.7$ Hz, 1H, CH_2 cyclohexane), 1.80 (d, $J = 8.8$ Hz, 1H, CH_2 cyclohexane), 1.70 (d, $J = 9.0$ Hz, 1H, CH_2 cyclohexane), 1.39 – 1.27 (m, 1H, CH_2 cyclohexane), 1.27 – 1.13 (m, 3H, CH_2 cyclohexane).

$^{13}\text{C NMR}$ (101 MHz, CDCl_3): δ (ppm) = 152.3 (C-2'''), 147.4 (C-5), 141.2 (C-1'''), 137.7 (C-2), 132.4 (C-3), 125.9 (C-4), 123.3 (C-4'''), 121.2 (C-5'''), 118.4 (C-6'''), 111.3 (C-3'''), 66.8 (C-2'), 55.5 (OCH_3), 53.9 (C-1'), 51.2 (CH_2 piperazine), 33.0 (CH_2 cyclohexane), 25.5 (CH_2 cyclohexane), 24.4 (CH_2 cyclohexane), 23.2 (CH_2 cyclohexane), 15.8 (CH_3).

IR (ATR): $\tilde{\nu}(\text{cm}^{-1}) = 3185$ (NH), 2941 (w), 2821 (OCH_3), 1499 (s), 1344 (s), 1238 (s), 1154 (vs), 1116 (s), 1021 (vs), 962 (s), 816 (s), 753 (vs), 707 (s).

HRMS (ESI): m/z $[\text{M}+\text{H}]^+$ calcd. for $\text{C}_{22}\text{H}_{32}\text{N}_3\text{O}_3\text{S}_2^+$: 450.1880, found 450.1879.

***N*-((1*S*,2*S*)-2-(4-(2-Methoxyphenyl)piperazin-1-yl)cyclohexyl)-5-methylthiophene-2-sulfonamide (**12b**)**



C₂₂H₃₁N₃O₃S₂

449.63 g/mol

Using General Procedure 2, amine **7b** (75 mg, 0.26 mmol, 1.0 eq) and 5-methylthiophene-2-sulfonyl chloride (39 μ L, 0.29 mmol, 1.1 eq) were converted to the product. Recrystallization from isopropanol lead to sulfonamide **12b** as brownish crystals (76 mg, 0.17 mmol, 66 %).

mp. = 122 – 124 °C.

$[\alpha]_D^{23}$ = +25.1 (c = 0.5, CHCl₃).

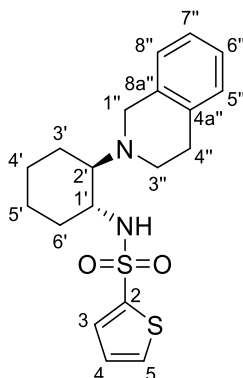
¹H NMR (400 MHz, CDCl₃): δ (ppm) = 7.42 (d, *J* = 3.5 Hz, 1H, 3-H), 7.05 – 6.98 (m, 1H, 4'''-H), 6.94 (td, *J* = 7.5, 1.5 Hz, 5'''-H), 6.90 (dd, *J* = 7.9, 1.9 Hz, 1H, 6'''-H), 6.86 (dd, *J* = 7.9, 1.5 Hz, 1H, 3'''-H), 6.76 (dd, *J* = 3.7, 1.0 Hz, 1H, 4-H), 6.16 (s, 1H, NH), 3.84 (s, 3H, OCH₃), 3.10 – 2.76 (m, 5H, CH₂ piperazine and 1'-H), 2.57 – 2.23 (m, 9H, 3H CH₃ toluene, 4H CH₂ piperazine, 1H CH₂ cyclohexane and 2'-H), 1.91 (d, *J* = 11.0 Hz, 1H, CH₂ cyclohexane), 1.80 (d, *J* = 8.5 Hz, 1H, CH₂ cyclohexane), 1.71 (d, *J* = 9.4 Hz, 1H, CH₂ cyclohexane), 1.34 (q, *J* = 12.1, 11.2 Hz, 1H, CH₂ cyclohexane), 1.26 – 1.13 (m, 3H, CH₂ cyclohexane).

¹³C NMR (101 MHz, CDCl₃): δ (ppm) = 152.3 (C-2'''), 147.4 (C-5), 141.2 (C-1'''), 137.8 (C-2), 132.4 (C-3), 125.9 (C-4), 123.3 (C-4'''), 121.2 (C-5'''), 118.4 (C-6'''), 111.3 (C-3'''), 66.8 (C-2'), 55.5 (OCH₃), 53.9 (C-1'), 51.2 (CH₂ piperazine), 33.0 (CH₂ cyclohexane), 25.5 (CH₂ cyclohexane), 24.4 (CH₂ cyclohexane), 23.2 (CH₂ cyclohexane), 15.8 (CH₃).

IR (ATR): $\tilde{\nu}$ (cm⁻¹) = 3184 (NH), 2941 (w), 2820 (OCH₃), 1499 (s), 1344 (s), 1238 (s), 1153 (vs), 1116 (s), 1021 (vs), 962 (s), 816 (s), 752 (vs), 706 (s).

HRMS (ESI): *m/z* [M+H]⁺ calcd. for C₂₂H₃₂N₃O₃S₂⁺: 450.1880, found 450.1880.

***N*-((1*R*,2*R*)-2-(3,4-Dihydroisoquinolin-2(1*H*)-yl)cyclohexyl)thiophene-2-sulfonamide
(13a)**



C₁₉H₂₄N₂O₂S₂

376.53 g/mol

Sulfonamide **13a** was synthesized according to General Procedure 2, using amine **8a** (40 mg, 0.17 mmol, 1.0 eq) and 2-thiophenesulfonyl chloride (35 mg, 0.19 mmol, 1.1 eq). FCC (CH₂Cl₂/MeOH 96:4) gave sulfonamide **13a** as a brownish oil (58 mg, 0.16 mmol, 91 %).

$[\alpha]_D^{23} = -65.6$ (c = 0.5, CHCl₃).

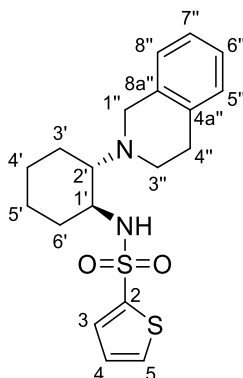
¹H NMR (400 MHz, CDCl₃): δ (ppm) = 7.56 (dd, *J* = 5.0, 1.3 Hz, 1H, 3-H), 7.52 (dd, *J* = 3.7, 1.4 Hz, 1H, 5-H), 7.16 – 7.03 (m, 4H, Ar-H, 5''-H, 6''-H, 7''H and 4-H), 6.83 (d, *J* = 6.3 Hz, 1H, 8''-H), 6.19 (s, 1H, NH), 3.53 – 3.34 (m, 2H, 1''-H), 2.95 (td, *J* = 10.7, 4.1 Hz, 1H, 1'-H), 2.76 (d, *J* = 16.3 Hz, 1H, CH₂ THIQ), 2.69 – 2.54 (m, 3H, 2H CH₂ THIQ and 1H CH₂ cyclohexane), 2.54 – 2.39 (m, 2H, CH₂ THIQ and 2'-H), 1.90 (d, *J* = 12.7 Hz, 1H, CH₂ cyclohexane), 1.87 – 1.80 (m, 1H, CH₂ cyclohexane), 1.77 – 1.69 (m, 1H, CH₂ cyclohexane), 1.43 – 1.32 (m, 1H, CH₂ cyclohexane), 1.28 – 1.17 (m, 3H, CH₂ cyclohexane).

¹³C NMR (101 MHz, CDCl₃): δ (ppm) = 141.0 (C-2), 134.6 (C-4a'' or C-8a''), 134.3 (C-4a'' or C-8a''), 132.0 (C-5), 131.8 (C-3), 128.9 (C-5''), 127.6 (C-4), 126.7 (C-8''), 126.3 (C-6'' or C-7''), 125.7 (C-6'' or C-7''), 66.7 (C-2'), 54.2 (C-1'), 50.6 (C-1''), 45.9 (CH₂ THIQ), 33.0 (CH₂ cyclohexane), 29.9 (CH₂ THIQ), 25.4 (CH₂ cyclohexane), 24.4 (CH₂ cyclohexane), 22.8 (CH₂ cyclohexane).

IR (ATR): $\tilde{\nu}$ (cm⁻¹) = 3190 (NH), 2929 (m), 1343 (s), 1159 (vs), 1092 (s), 1014 (s), 907 (s), 720 (vs), 666 (vs).

HRMS (ESI): *m/z* [M+H]⁺ calcd. for C₁₉H₂₅N₂O₂S₂⁺: 377.1352, found 377.1350.

***N*-((1*S*,2*S*)-2-(3,4-Dihydroisoquinolin-2(1*H*)-yl)cyclohexyl)thiophene-2-sulfonamide
(13b)**



C₁₉H₂₄N₂O₂S₂

376.53 g/mol

Using General Procedure 2, amine **8b** (31 mg, 0.13 mmol, 1.0 eq) and 2-thiophenesulfonyl chloride (27 mg, 0.15 mmol, 1.1 eq) were reacted. FCC (CH₂Cl₂/MeOH 96:4) gave sulfonamide **13b** as a brownish oil (40 mg, 0.11 mmol, 79 %)

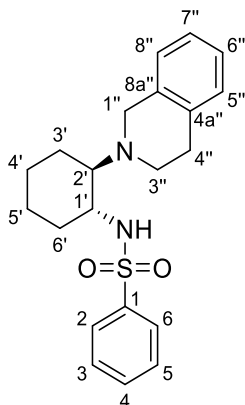
$[\alpha]_D^{23} = +108.7$ (c = 0.5, CHCl₃).

¹H NMR (500 MHz, CDCl₃): δ (ppm) = 7.56 (dd, *J* = 5.0, 1.3 Hz, 1H, 3-H), 7.52 (dd, *J* = 3.7, 1.4 Hz, 1H, 5-H), 7.15 – 7.04 (m, 4H, Ar-H, 5''-H, 6''-H, 7''-H and 4-H), 6.83 (d, *J* = 7.0 Hz, 1H, 8''-H), 6.18 (s, 1H, NH), 3.50 – 3.35 (m, 2H, 1''-H), 2.94 (td, *J* = 10.6, 4.1 Hz, 1H, 1'-H), 2.82 – 2.39 (m, 6H, 4H CH₂ THIQ, 1H CH₂ cyclohexane and 2'-H), 1.93 – 1.88 (m, 1H, CH₂ cyclohexane), 1.86 – 1.80 (m, 1H, CH₂ cyclohexane), 1.76 – 1.71 (m, 1H, CH₂ cyclohexane), 1.42 – 1.33 (m, 1H, CH₂ cyclohexane), 1.29 – 1.18 (m, 3H, CH₂ cyclohexane).

¹³C NMR (126 MHz, CDCl₃): δ (ppm) = 141.0 (C-2), 134.6 (C-4a'' or C-8a''), 134.3 (C-4a'' or C-8a''), 132.0 (C-5), 131.8 (C-3), 128.9 (C-5''), 127.6 (C-4), 126.7 (C-8''), 126.3 (C-6'' or C-7''), 125.7 (C-6'' or C-7''), 66.7 (C-2'), 54.2 (C-1'), 45.8 (CH₂ THIQ), 33.0 (CH₂ THIQ), 30.0 (CH₂ cyclohexane), 25.4 (CH₂ cyclohexane), 24.4 (CH₂ cyclohexane), 22.8 (CH₂ cyclohexane).

IR (ATR): $\tilde{\nu}$ (cm⁻¹) = 3191 (NH), 2929 (m), 1343 (s), 1158 (vs), 1090 (s), 1013 (s), 906 (m), 715 (vs), 665 (vs).

HRMS (ESI): *m/z* [M+H]⁺ calcd. for C₁₉H₂₅N₂O₂S₂⁺: 377.1352, found 377.1350.

***N*-((1*R*,2*R*)-2-(3,4-Dihydroisoquinolin-2(1*H*)-yl)cyclohexyl)benzenesulfonamide (14a)**

 $C_{21}H_{26}N_2O_2S$

370.51 g/mol

Following General Procedure 2, amine **8a** (40 mg, 0.17 mmol, 1.0 eq) and benzenesulfonyl chloride (24 μ L, 0.19 mmol, 1.1 eq) were reacted. FCC (CH₂Cl₂/MeOH 96:4) gave sulfonamide **14a** as a brownish oil (53 mg, 0.14 mmol, 85 %).

$[\alpha]_D^{23} = -52.7$ (c = 0.5, CHCl₃).

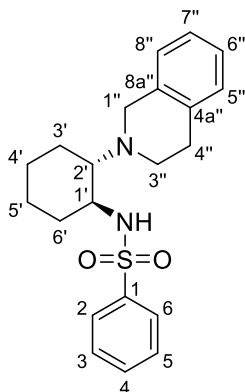
¹H NMR (500 MHz, CDCl₃): δ (ppm) = 7.82 – 7.78 (m, 2H, 2-H and 6-H), 7.61 – 7.55 (m, 1H, 4-H), 7.46 (t, *J* = 7.9 Hz, 2H, 3-H and 5-H), 7.12 (pd, *J* = 7.2, 1.8 Hz, 2H, 6''-H and 7''-H), 7.08 – 7.04 (m, 1H, 5''-H), 6.80 (d, *J* = 7.2 Hz, 1H, 8''-H), 6.11 (s, 1H, NH), 3.49 – 3.30 (m, 2H, 1''-H), 2.86 – 2.70 (m, 2H, 1'-H and CH₂ THIQ), 2.68 – 2.59 (m, 1H, CH₂ THIQ), 2.47 (dd, *J* = 38.3, 10.7 Hz, 4H, CH₂ THIQ, CH₂ cyclohexane and 2'-H), 1.88 (dd, *J* = 12.6, 3.1 Hz, 1H, CH₂ cyclohexane), 1.80 (dd, *J* = 9.6, 2.4 Hz, 1H, CH₂ cyclohexane), 1.73 – 1.67 (m, 1H, CH₂ cyclohexane), 1.37 – 1.27 (m, 1H, CH₂ cyclohexane), 1.25 – 1.11 (m, 3H, CH₂ cyclohexane).

¹³C NMR (126 MHz, CDCl₃): δ (ppm) = 139.9 (C-1), 134.5 (C-4a'' or C-8a''), 134.3 (C-4a'' or C-8a''), 132.6 (C-4), 129.2 (C-3 and C-5), 128.9 (C-5''), 127.3 (C-2 and C-6), 126.8 (C-8''), 126.4 (C-6'' or C-7''), 125.7 (C-6'' or C-7''), 66.8 (C-2'), 53.7 (C-1'), 50.5 (C-1''), 45.9 (CH₂ THIQ), 33.0 (CH₂ cyclohexane), 29.9 (CH₂ THIQ), 25.4 (CH₂ cyclohexane), 24.3 (CH₂ cyclohexane), 22.7 (CH₂ cyclohexane).

IR (ATR): $\tilde{\nu}$ (cm⁻¹) = 3202 (NH), 2928 (m), 1446 (s), 1308 (s), 1158 (vs), 1091 (vs), 906 (s), 725 (vs), 689 (vs).

HRMS (ESI): *m/z* [M+H]⁺ calcd. for C₂₁H₂₇N₂O₂S⁺: 371.1788, found 371.1786.

***N*-((1*S*,2*S*)-2-(3,4-Dihydroisoquinolin-2(1*H*)-yl)cyclohexyl)benzenesulfonamide (14b)**



C₂₁H₂₆N₂O₂S

370.51 g/mol

Sulfonamide **14b** was synthesized according to General Procedure 2, using amine **8b** (30 mg, 0.13 mmol, 1.0 eq) and benzenesulfonyl chloride (18 μ L, 0.14 mmol, 1.1 eq). FCC (CH₂Cl₂/MeOH 96:4) gave sulfonamide **14b** as a brownish oil (45 mg, 0.12 mmol, 92 %).

$[\alpha]_D^{23} = +69.6$ (c = 0.5, CHCl₃).

¹H NMR (400 MHz, CDCl₃): δ (ppm) = 7.82 – 7.78 (m, 2H, 2-H and 6-H), 7.60 – 7.55 (m, 1H, 4-H), 7.49 – 7.43 (m, 2H, 3-H and 5-H), 7.17 – 7.08 (m, 2H 6''-H and 7''-H), 7.08 – 7.05 (m, 1H, 5''-H), 6.80 (d, *J* = 6.6 Hz, 1H, 8''-H), 6.10 (s, 1H, NH), 3.43 (s, 2H, 1''-H), 2.86 – 2.37 (m, 7H, 4H CH₂ THIQ, 1H CH₂ cyclohexane, 1'-H and 2'-H), 1.87 (d, *J* = 12.3 Hz, 1H, CH₂ cyclohexane), 1.80 (d, *J* = 9.5 Hz, 1H, CH₂ cyclohexane), 1.71 (d, *J* = 10.6 Hz, 1H, CH₂ cyclohexane), 1.38 – 1.28 (m, 1H, CH₂ cyclohexane), 1.24 – 1.09 (m, 3H, CH₂ cyclohexane).

¹³C NMR (101 MHz, CDCl₃): δ (ppm) = 139.9 (C-1), 134.5 (C-4a'' or C-8a''), 134.3 (C-4a'' or C-8a''), 132.6 (C-4), 129.2 (C-3 and C-5), 128.9 (C-5''), 127.3 (C-2 and C-6), 126.8 (C-8''), 126.3 (C-6'' or C-7''), 125.7 (C-6'' or C-7''), 66.8 (C-2'), 53.7 (C-1'), 50.5 (C-1''), 45.8 (CH₂ THIQ), 33.0 (CH₂ cyclohexane), 29.9 (CH₂ THIQ), 25.4 (CH₂ cyclohexane), 24.3 (CH₂ cyclohexane), 22.7 (CH₂ cyclohexane).

IR (ATR): $\tilde{\nu}$ (cm⁻¹) = 3204 (NH), 2930 (m), 1446 (s), 1308 (s), 1159 (vs), 1091 (vs), 906 (s), 726 (vs), 689 (vs).

HRMS (ESI): *m/z* [M+H]⁺ calcd. for C₂₁H₂₇N₂O₂S⁺: 371.1788, found 371.1787

3.2 Sirtuin 6 Modulators

3.2.1 Co-crystallization of KV-30 and synthesis planning

Once **KV-30** was identified as Sirtuin 6 inhibitor, the next step was to plan reasonable modifications of the molecule, to obtain selective and potent new modulators of this functionally diverse epigenetic enzyme. The structure of **KV-30** can be broken down to three major parts, the phenanthridine scaffold (blue) to which the hydroxamate (orange) is connected *via* a phenyl linker (green), shown in Figure 16.

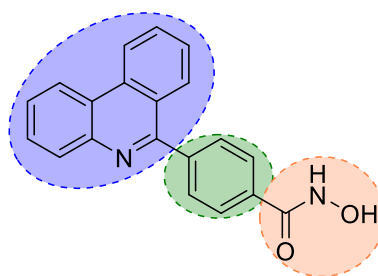
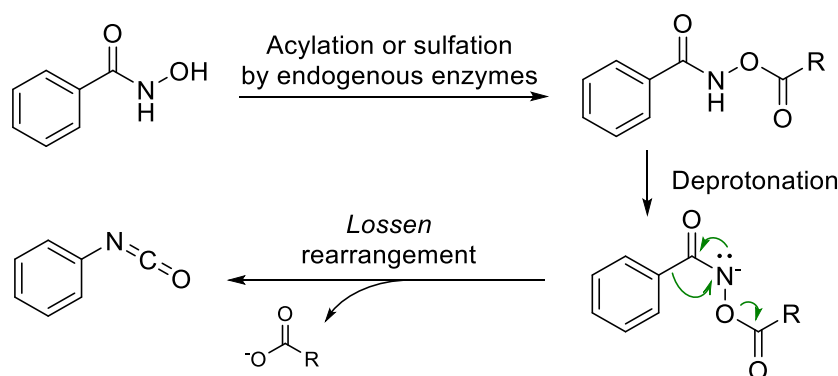


Figure 16 Chemical structure of **KV-30** with phenanthridine scaffold (blue), phenyl linker (green) and hydroxamate group (orange).

Since hydroxamic acids are known to be cytotoxic, they are undesirable for drug development, unless the hydroxamic acid is crucial for the mode of action. Hydroxamates unselectively complex multivalent metal ions, especially iron and zinc, and can thus interfere with several enzymes in the body and with cation homeostasis in general. Aside from that, they are also suspected to be mutagenic. Upon OH acylation or sulfation by endogenous enzymes, they can undergo LOSSEN rearrangement to form isocyanates (Scheme 3). These isocyanates can act as electrophiles and carbamoylate the DNA or nucleophilic proteins^[71].



Scheme 3 LOSSEN rearrangement of hydroxamic acids *in vivo*.

Hydroxamates are however found in approved drugs like for example the HDAC inhibitor Vorinostat. Their mode of action is based on the complexation of a zinc ion, and the hydroxamate can therefore not be replaced easily. These molecules are used in cancer therapy, where more severe side effects are tolerated compared to drugs with other

hope for the possibility of developing selective Sirtuin 6 modulators. The other good news revealed by the co-crystal structure was, that the hydroxamic acid does not interact with any metal ions but is involved in a network of water mediated polar interactions in the binding pocket. Thus, other polar functional groups should be able to build a similar network of interactions. The path for the first set of modifications was clear. Priority had the replacement of the hydroxamate. A set of bioisosters and other polar groups should be introduced to the molecule and their ability to build the same network of polar interactions and hydrogen bonds should be evaluated. Planned replacements of the hydroxamate and their synthesis are presented in Chapter 3.2.4.

Another peculiarity of the binding pocket is the bound water molecule. It is known that the replacement or displacement of water molecules can be beneficial in drug development^[73]. This should be exploited in the attempt of creating more selective and potent Sirtuin 6 modulators. To assess this, an additional hydroxyethyl residue at the polar group should be introduced to place a hydroxyl group at the position covered by the water molecule in the **KV-30**-Sirtuin 6 co-crystal. Planned structure motifs and their synthesis are discussed in Chapter 3.2.5.

Around the phenanthridine moiety the crystal indicates free space, which could enable additional residues at this position, aimed to strengthen interactions with the target. In fact, around the ring C of the phenanthridine is located the myristoylated substrate of Sirtuin 6, e.g., TNF α (Figure 19). Mimicking the acyl moiety of the substrate, by a heteroaromatic ring or an amido group, could enhance potency. These ideas were supported by docking experiments from DR. WEIJIE YOU. The results from the docking, with the arising most promising structure motifs and their respective syntheses, are outlined in Chapter 3.2.6.

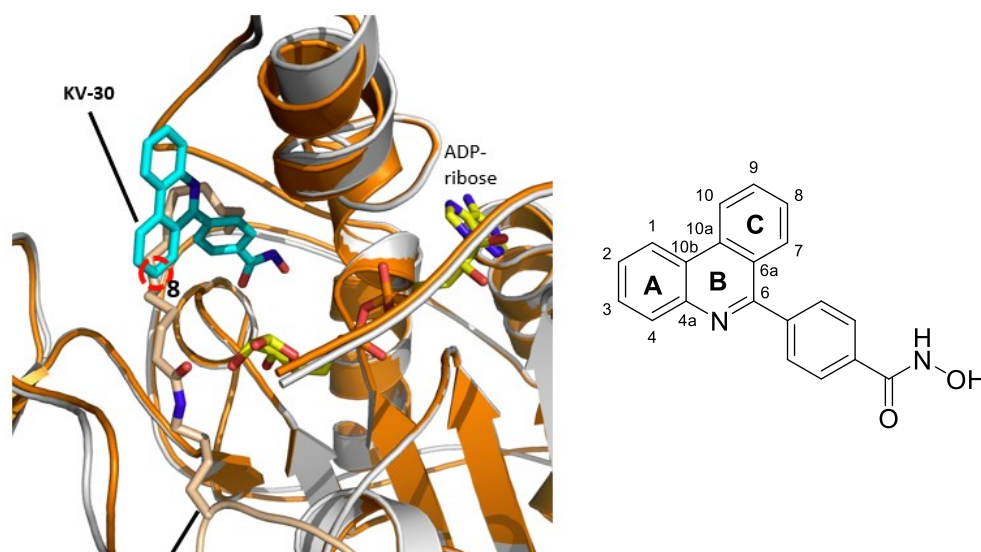


Figure 19 Left: Overlay of the co-crystal of Sirtuin 6 and **KV-30** (blue) with the co-crystal of Sirtuin 6 and myristoylated TNF α (light orange). Right: Numbering and ring assignment of the phenanthridine scaffold in **KV-30**.

In total, the analysis of the co-crystal data gave three main classes of variations, which were in scope of this project: Replacing the hydroxamate by other polar functional groups, addition of a hydroxyethyl (or similar) residue for re- or displacement of the water molecule and the addition of residues to ring C of the phenanthridine scaffold to enhance interactions at the hydrophobic binding site by mimicking the endogenous substrates of Sirtuin 6. Retrosyntheses are shown in the respective chapters. Figure 20 gives an overview of the attempted modifications.

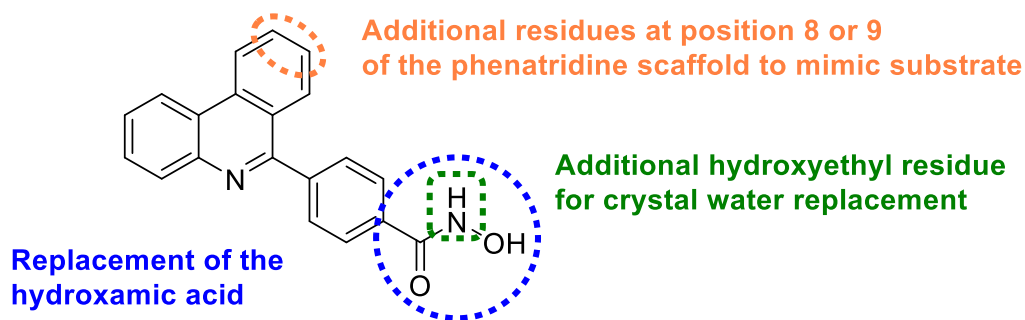
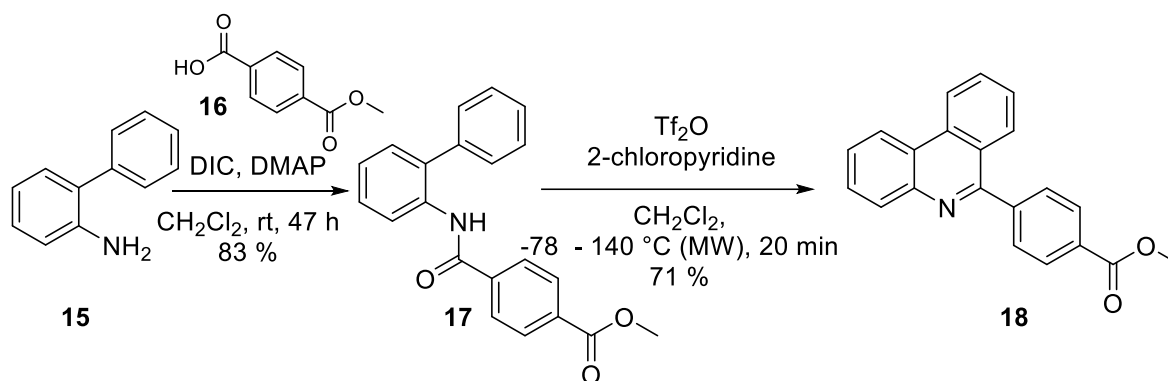


Figure 20 Planned variations of KV-30.

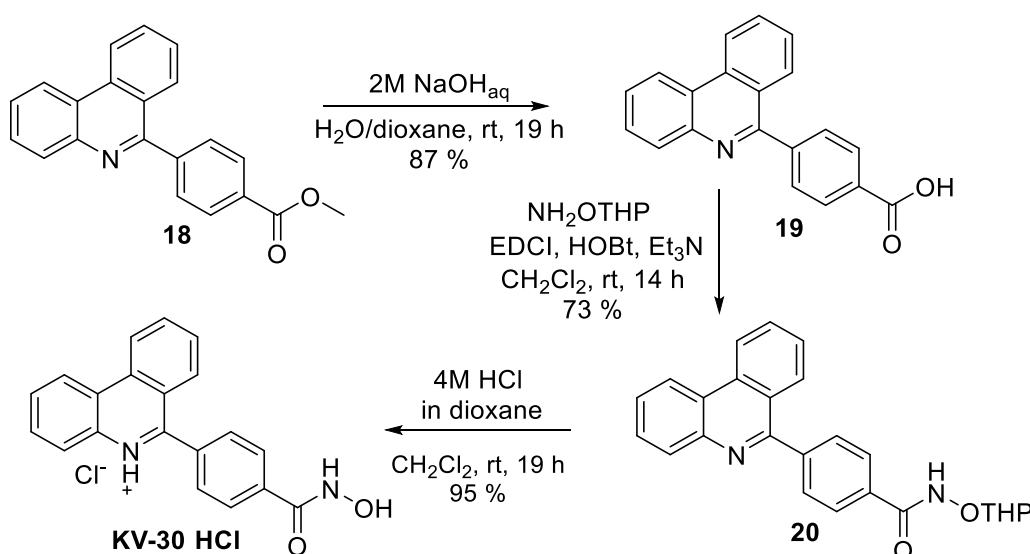
3.2.2 Synthesis of KV-30 by VÖGERL

KV-30 was first synthesized by KATHARINA VÖGERL for her dissertation^[74]. The synthesis starts with an amide coupling of amino biphenyl (**15**) with 4-(methoxycarbonyl)benzoic acid (**16**) using DIC and DMAP in methylene chloride. The resulting amide **17** is cyclized by a BISCHLER-NAPIERALSKI type reaction reported by MOVASSAGHI *et al.*^[75], with Tf_2O and 2-chloropyridine in methylene chloride, to give the desired phenanthridine **18** (Scheme 4).



Scheme 4 Construction of the phenanthridine scaffold in the synthesis of **KV-30** by VÖGERL^[74].

After the successful construction of the phenanthridine scaffold, methyl ester **18** is hydrolysed with NaOH in water/dioxane to give the free carboxylic acid **19**, which undergoes, in the next step, another amide coupling with THP-protected hydroxylamine. This time, the amide coupling is facilitated by EDCI, HOBt and triethylamine and affords the THP-protected hydroxamic acid **20**. After acidic cleavage of the THP protecting group in methylene chloride with 4M HCl in dioxane, **KV-30** is obtained as hydrochloride salt, which precipitates from the reaction mixture and can be collected through filtration (Scheme 5).



Scheme 5 Construction of the hydroxamate moiety in the synthesis of **KV-30** by VÖGERL^[74].

3.2.3 Excursus: Bischler-Napieralski reaction

Many biologically active natural products belong to the class of alkaloids. Alkaloids are basic, nitrogen containing compounds derived from the secondary metabolism of plants. Among the most famous subclasses of alkaloids are quinoline and isoquinoline alkaloids. Many representatives of these classes, like morphine (isoquinoline alkaloid, Figure 21, left) or quinine (quinoline alkaloid, Figure 21, right), are still widely used in the modern times.

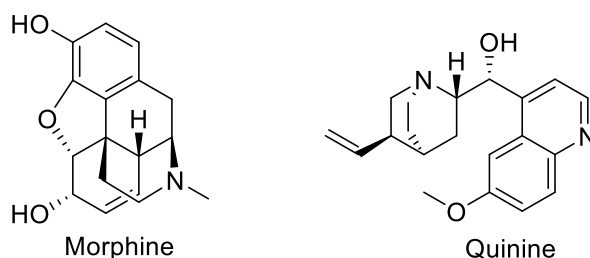
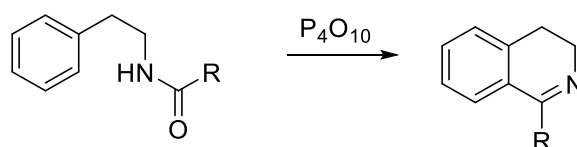


Figure 21 Chemical structures of the quinoline and isoquinoline alkaloids morphine and quinine.

Back in the days, these compounds were often the only available drugs for the treatment of severe illnesses and thus sparked very early on the interests of chemical and pharmaceutical research. This is the reason why today many famous old name reactions are known for the construction of these heterocyclic scaffolds. One of these reactions is the BISCHLER-NAPIERALSKI reaction for the construction of isoquinolines, which was published in 1893. AUGUST BISCHLER and BERNARD NAPIERALSKI were heating phenethyl amides with phosphorus pentoxide and obtained 3,4-dihydroisoquinolines (Scheme 6)^[76].



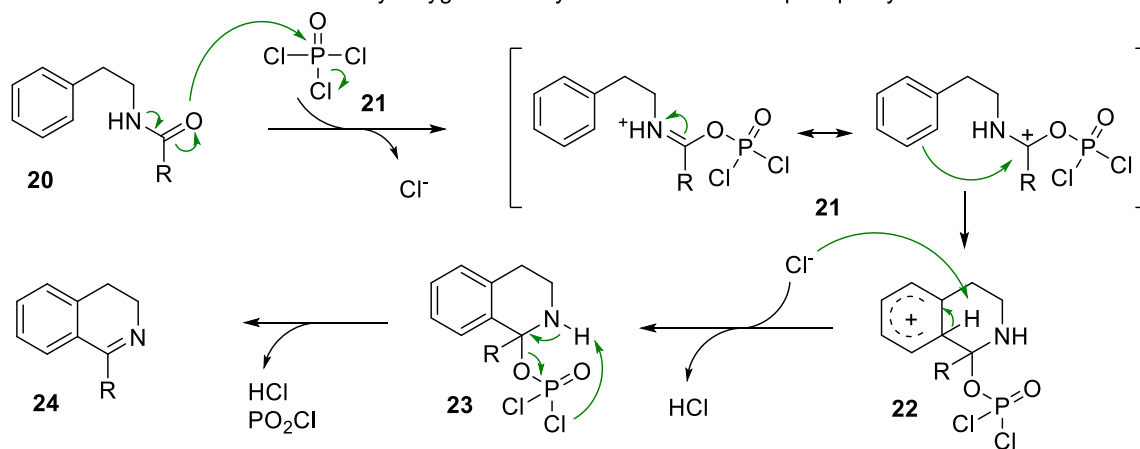
Scheme 6 Original BISCHLER-NAPIERALSKI reaction^[76].

Since then, many research groups have studied this reaction and found that several other Lewis acids can also be used for this reaction. Today, phosphorus oxychloride is the most prominent and widest used reagent. It was also shown, that the obtained 3,4-dihydroisoquinolines can easily be dehydrogenated to the corresponding, fully aromatic isoquinolines^[77].

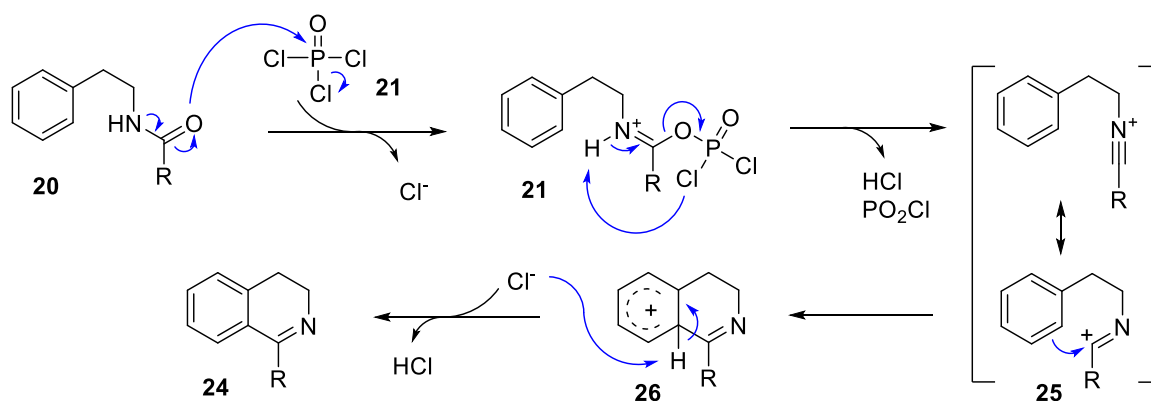
The mechanism of this reaction was under investigation for quite a long time and today there are mainly two possible mechanisms described in the literature, which are depicted in Scheme 7. Both mechanisms start with the activation of the amide (**20**) with phosphorus oxychloride, by a nucleophilic attack of the amide carbonyl to the phosphorus, which leads to the elimination of one chloride and the formation of a dichlorophosphoryl imine-ester (**21**). Upon this step, the two mechanisms follow different paths. For the first mechanism, cyclization

occurs directly in the next step. The resonance of the positive charge of the imine can create a positive charge at the former carbonyl carbon, which is the electrophile for the electrophilic substitution of the benzene ring. After deprotonation of intermediate **22**, tetrahydroisoquinoline intermediate **23** is formed, which eventually gives the dihydroisoquinoline **24** after elimination of phosphenic chloride (Scheme 7, top). In the second mechanism, the phosphoric ester species is eliminated directly after dichlorophosphoryl imine-ester (**21**) formation, resulting in nitrilium ion **25**. The resonance of the nitrilium ion can also deliver the positive charge on the former carbonyl carbon, which again is the electrophile for the S_EAr reaction. After deprotonation of intermediate **26**, dihydroisoquinoline **24** is released (Scheme 7, bottom).^[77]

Mechanism I: Elimination of carbonyl oxygen *after* cyclization *via* dichlorophosphoryl imine-ester.



Mechanism II: Elimination of carbonyl oxygen *before* cyclization *via* nitrilium ion.

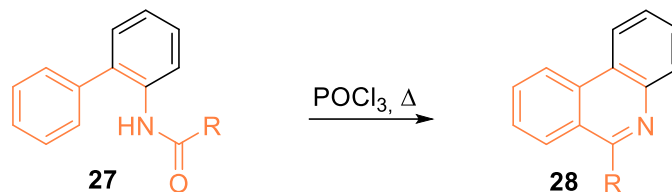


Scheme 7 Possible mechanisms of the BISCHLER-NAPIERALSKI reaction^[77].

Pictet-Hubert and Morgan-Walls reaction

Already in 1896, the Swiss chemists PICTET, known from the PICTET-SPENGLER reaction, an alternative reaction for the construction of isoquinolines and β -carboline, and HUBERT reported a method for the synthesis of phenanthridines. The phenanthridine in their report was synthesized by a condensation reaction of an *N*-acyl 2-aminobiphenyl in the presence of

ZnCl₂^[78]. This study was the starting point for the British chemists MORGAN and WALLS, who reported in 1932 a more versatile method with the same underlying principle. Instead of ZnCl₂, which had several disadvantages, such as incompatibilities with certain reactive functional groups or difficult work-up and purification, they used phosphorus oxychloride for the cyclization reaction^[79]. The reaction conditions are the same as the conditions in modern applications of the BISCHLER-NAPIERALSKI reaction. Scheme 8 shows the phenylethyl moiety of amide **27** and phenanthridine **28** in orange.



Scheme 8 The MORGAN-WALLS reaction^[79].

This reaction and its application in modern chemistry is still under investigation and further development. The method from MOVASSAGHI, published in 2008, for example replaced the harsh conditions of refluxing the respective amide over prolonged time in phosphorus oxychloride by the use of trifluoromethanesulfonic anhydride and 2-chloropyridine in combination with a short microwave irradiation^[75]. Under these conditions even acid sensitive starting materials can be cyclized, and the method proved to be very versatile and effective in the construction of the phenanthridine scaffold of the **KV-30** analogues synthesized for this project.

3.2.4 Synthesis of KV-30 analogues with replaced hydroxamic acid

The main objective of this project was the replacement of the undesired hydroxamic acid in **KV-30**. Therefore, a set of alternative polar groups should be introduced to the molecule. The envisaged structures are given in Figure 22.

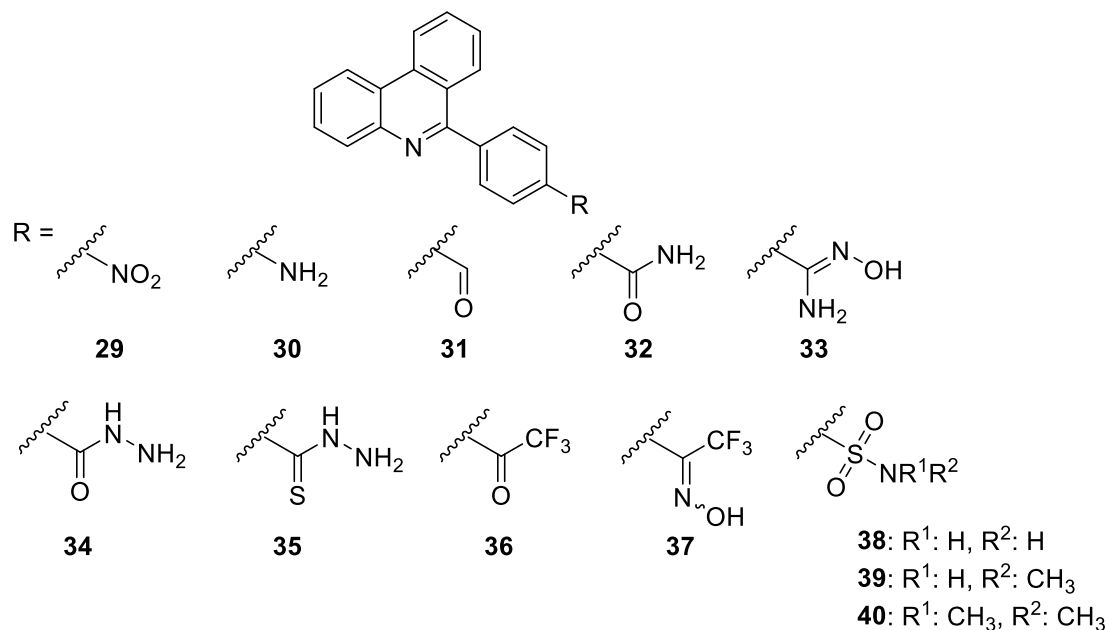
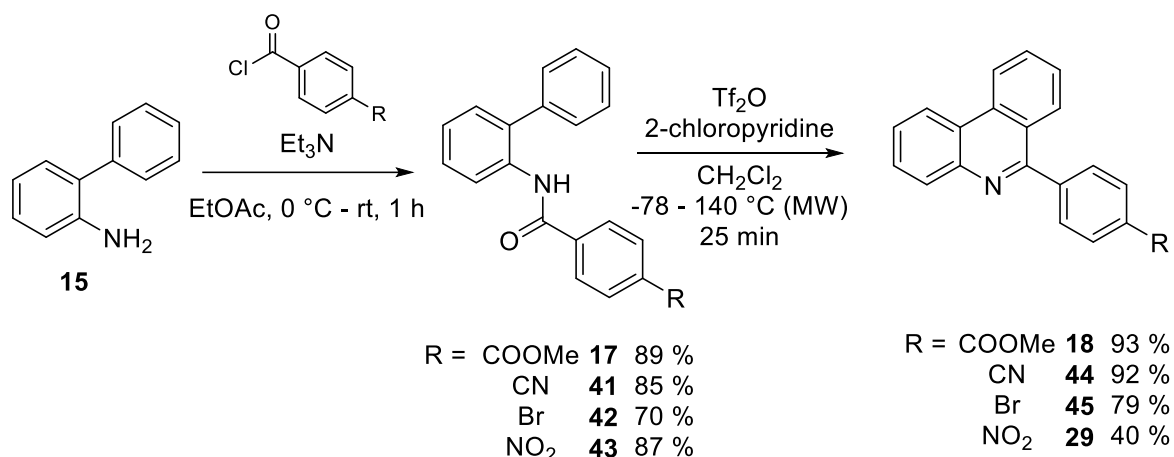


Figure 22 Envisaged structures for the first generation of **KV-30** variations.

Synthesis of target compound precursors

Synthesis of the variations with alternative polar residues was planned to start from different useful and easily available precursors. These precursors with a bromine, nitro, nitrile, or methyl ester group in position 4 of the phenyl linker should further also give access to more complex structure motifs like hydroxyethylated hydroxamic acid. As a first step towards the synthesis of the alternative polar head groups, those precursors were synthesized. The syntheses of the phenyl phenanthridine building blocks with methyl ester (**18**), nitrile (**44**), bromine (**45**), and a nitro (**29**) are shown in Scheme 9. Analogous to the synthesis of **KV-30**, the first step is the amide coupling. Unlike the synthesis of **KV-30**, 2-aminobiphenyl (**15**) was reacted with the respective benzoyl chlorides in the presence of triethylamine in ethyl acetate. Those benzoyl chlorides are cheap and readily commercially available. The alternative procedure for the amide coupling allowed a simple work-up and purification by crystallization. Hence, scale-up of the synthesis was facilitated. The following cyclization to the phenanthridines by MOVASSAGHI's method^[75] proceeded without further complications. The lower yield of the nitro compound **29** can be explained by the fact that the conditions for crystallization were not optimized for this compound. Nevertheless, compound **29** was obtained in sufficient quantity

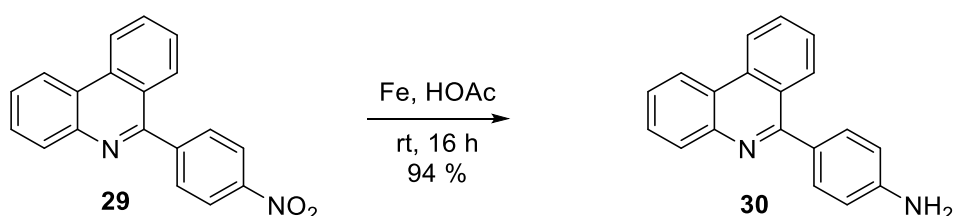
to allow its testing and the following reduction. Since compound **29** was the first target compound to be tested for Sirtuin 6 inhibition, crystallization was focussed on purity rather than yield.



Scheme 9 Synthesis of precursors for **KV-30** variations.

Synthesis of aniline **30**

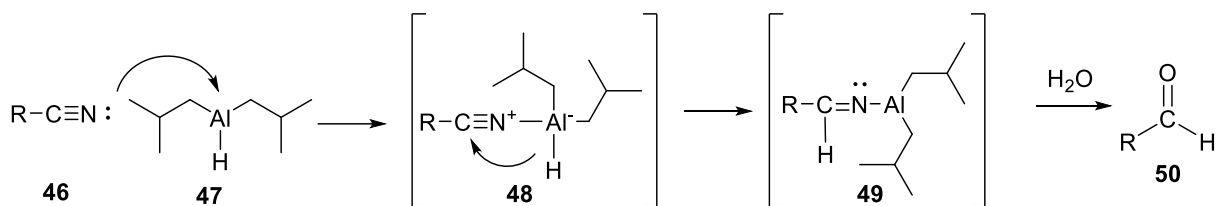
Nitrobenzene **29** was used for the synthesis of the next target compound aniline **30**. Reduction of the nitro group was carried out with iron powder in acetic acid. After neutralisation of the acetic acid, the product could be extracted with ethyl acetate. Filtration through a pad of silica afforded, without any further purification needed, aniline **30** in excellent yield (Scheme 10).



Scheme 10 Synthesis of aniline **30**.

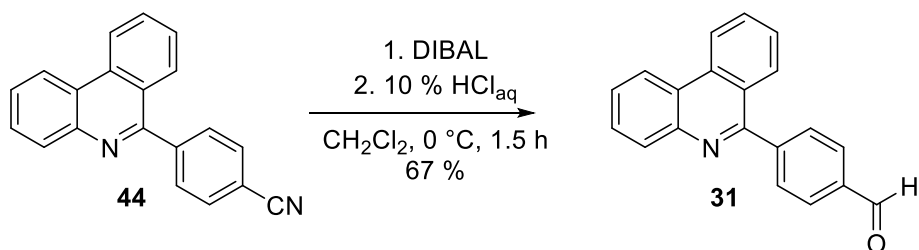
Synthesis of aldehyde **31**

Aldehydes can be synthesized starting from nitriles by selective reduction with diisobutyl aluminium hydride (DIBAL, **47**). The bulky residues of this reducing agent ensure that only one hydride is transferred to the nitrile **46**, thus after the addition of the complex hydride to the nitrile (intermediate **48**), the reduction stops after the transfer of the single hydride with the formation of imine **49**. Upon aqueous work up, aldehyde **50** is released. The mechanism of this reaction is depicted in Scheme 11.



Scheme 11 Mechanism of the reduction of nitriles with DIBAL.

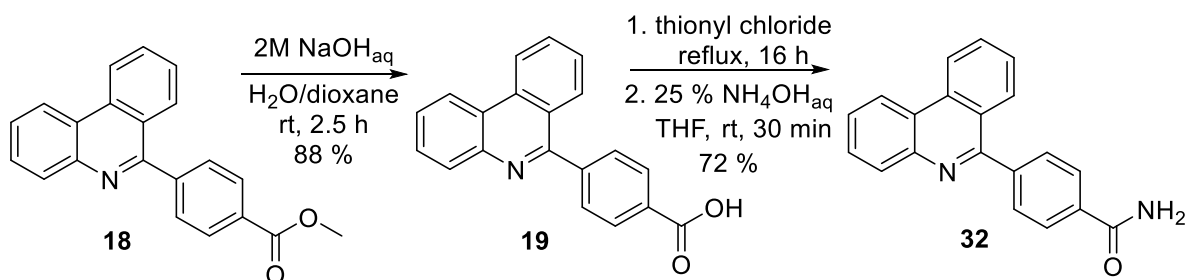
For the synthesis of the desired benzaldehyde **31**, a method from WEN *et al.*^[80] was used. A first attempt was carried out with 1.4 eq of DIBAL, considering that because of the specific steric nature of DIBAL, the excess of reducing agent should not be problematic. However, a small amount of side product was formed under these conditions. HRMS revealed it to be the primary alcohol. Therefore, the amount of DIBAL was reduced to 1.2 eq and aldehyde **31** was obtained in good yield (Scheme 12).



Scheme 12 Synthesis of aldehyde **31**.

Synthesis of primary carboxamide **32**

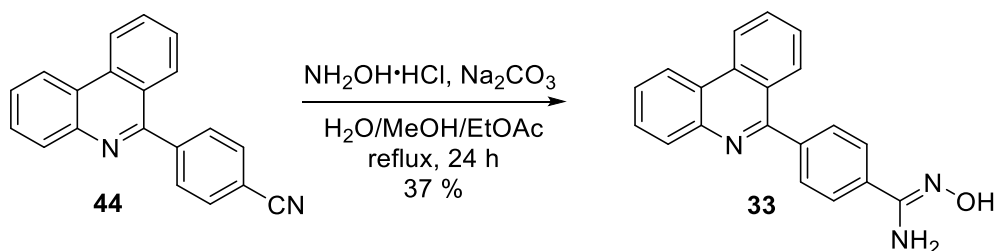
To start with the synthesis of carboxamide **32**, methyl ester **18** was converted to the free carboxylic acid by saponification with aqueous NaOH, like previously described by VÖGERL^[74]. The carboxylic acid **19** was then activated by refluxing in neat thionyl chloride. After the removal of excess thionyl chloride by azeotropic distillation with toluene, the resulting crude acid chloride was taken up in THF and treated with aqueous ammonium hydroxide solution, which gave carboxamide **32** in good yield (Scheme 13).



Scheme 13 Synthesis of primary carboxamide **32**.

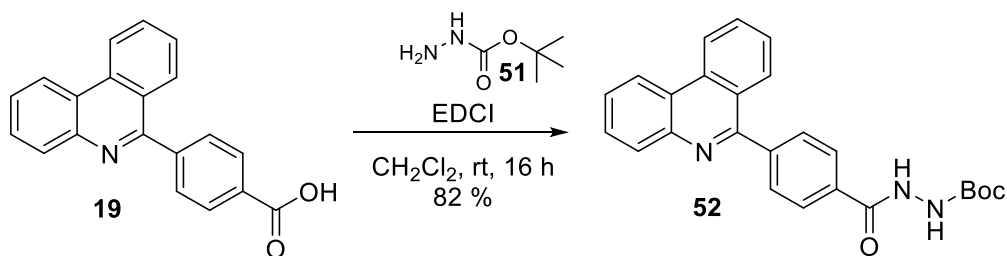
Synthesis of amidoxime **33**

The synthesis of amidoxime **33** should follow the method of HAZELDINE *et al.*^[81]. Usually, the transformation of nitriles into amidoximes using hydroxylamine proceeds without any further complications. In this case though, a very basic problem hampered the synthesis, and it wouldn't be the last time during this project. The very poor solubility properties of this class of compounds have complicated not only this synthetic procedure. The reaction is normally carried out in a mixture of water and methanol, to ensure release of hydroxylamine from the hydrochloride salt by Na_2CO_3 . Under these conditions though, nitrile **44** is not soluble and therefore even under reflux no reaction could be observed. To, literally, solve this problem, ethyl acetate was added to the reaction mixture, which at least partially dissolved the starting material at room temperature. A mixture of methanol and ethyl acetate (1:1) was used in the end to pre-suspend nitrile **44**, which was then added to the solution of hydroxylamine hydrochloride and Na_2CO_3 in water/methanol. Additionally the resulting reaction mixture was refluxed to enhance solubility and under these conditions, the reaction was finally successful. Equally for purification by FCC poor solubility was an issue. This is why amidoxime **33** was obtained only in moderate yield (Scheme 14).



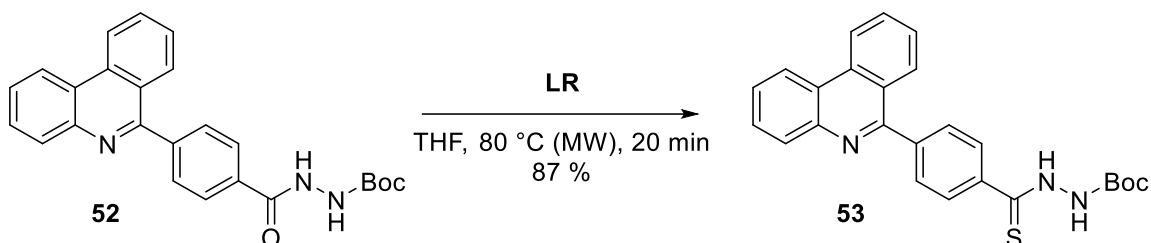
Scheme 14 Synthesis of amidoxime **33**.

The configuration of the obtained amidoxime **33** was verified by a NOE NMR experiment. A resonance between the OH and the NH_2 protons was observed, which means those protons are close in space. The experiment showed, that amidoxime **33** was obtained as Z-isomer (Figure 18).



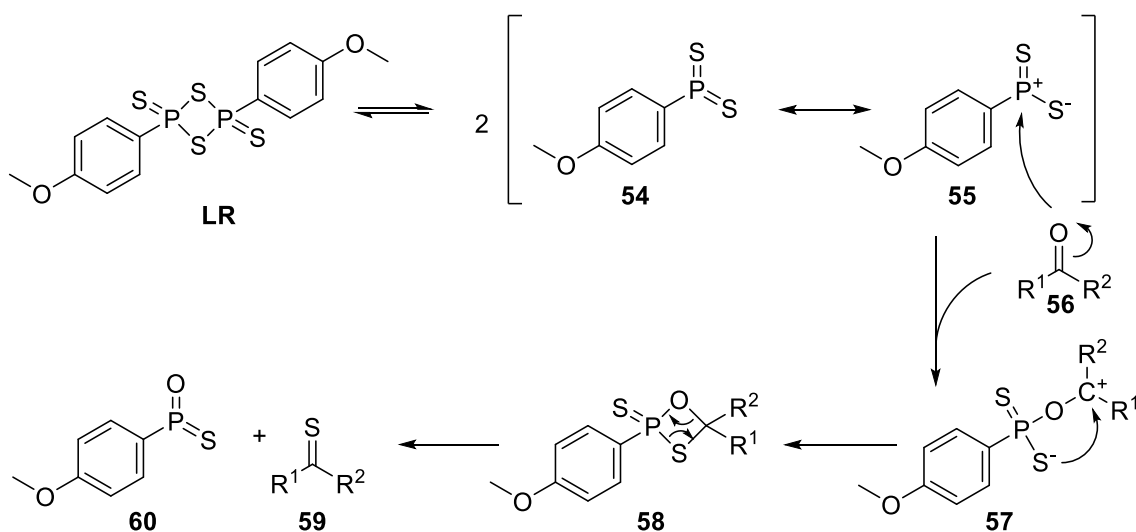
Scheme 15 Synthesis of Boc-protected hydrazide **52**.

For the envisaged thiohydrazine **35**, Boc-protected hydrazide **52** was converted to Boc-protected thiohydrazide **53** following a method of MOLTENI *et al.*^[83], using LAWESSON's reagent (**LR**). The thionation of hydrazide **52** proceeded with selectivity for the hydrazide carbonyl, the Boc carbonyl remained unthionated (Scheme 16).



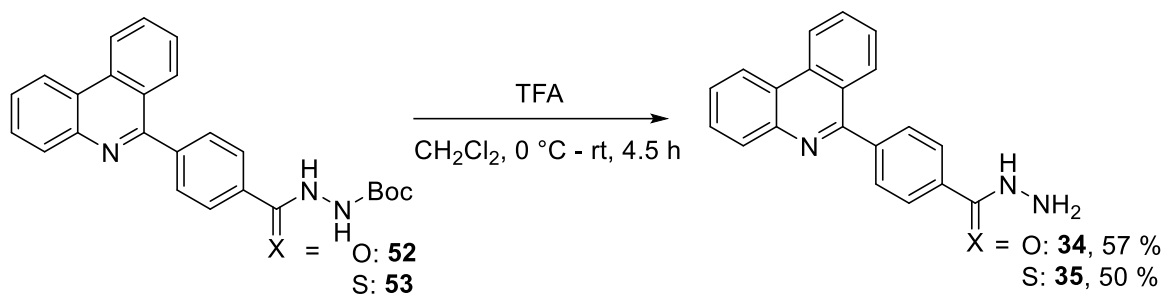
Scheme 16 Thionation with LAWESSON's reagent.

The thionation of carbonyl groups with Lawesson's reagent (**54**) is a widely used approach to obtain thiocarbonyls. The reaction begins with the dissociation of **LR** to dithiophosphine ylide **55**, which reacts with the carbonyl by nucleophilic attack of the carbonyl carbon to the phosphorus. Then cyclic thioxaphosphetan intermediate **58** is formed, similar to the WITTIG reaction. Driving force of the reaction is the release of thioxophosphine oxide **60**. The mechanism of thionation by LAWESSON's reagent is depicted in Scheme 17.^[84]



Scheme 17 Mechanism of the thionation of a carbonyl group with LAWESSON's reagent^[84].

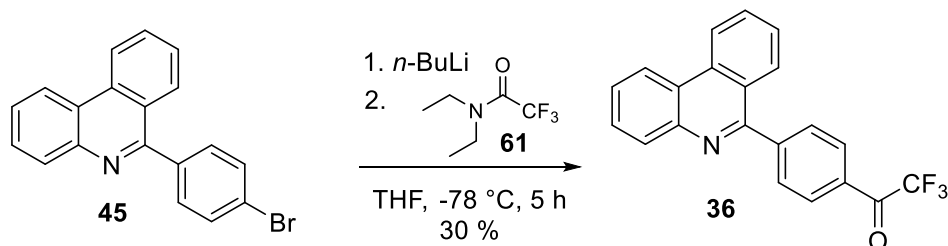
Boc deprotection for both, compound **52** and **53**, was carried out with TFA in methylene chloride and gave the free hydrazide **34** and thiohydrazide **35** in moderate yields (Scheme 18).



Scheme 18 Synthesis of hydrazide **34** and thiohydrazide **35**.

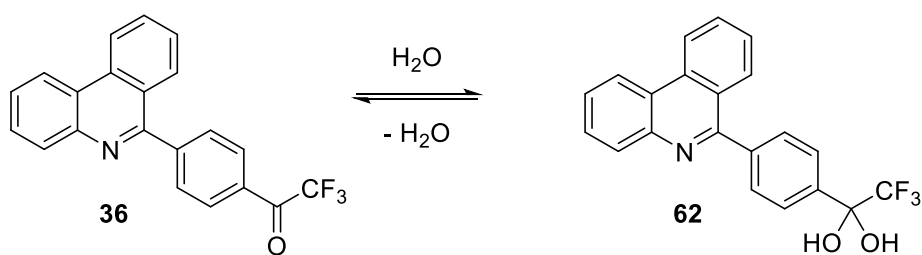
Synthesis of trifluoromethyl ketone **36** and trifluoromethyl oxime **37**

Trifluoromethyl ketone **36** was synthesized using an organometallic reaction approach described by FISHWICK *et al.*^[85], where a bromine-lithium exchange of bromo derivative **45** with *n*-butyllithium is the first step and the obtained lithiated intermediate is subsequently reacted with *N,N*-diethyl-2,2,2-trifluoroacetamide (**61**). After aqueous work-up, the crude trifluoromethyl ketone **36** is released (Scheme 19).



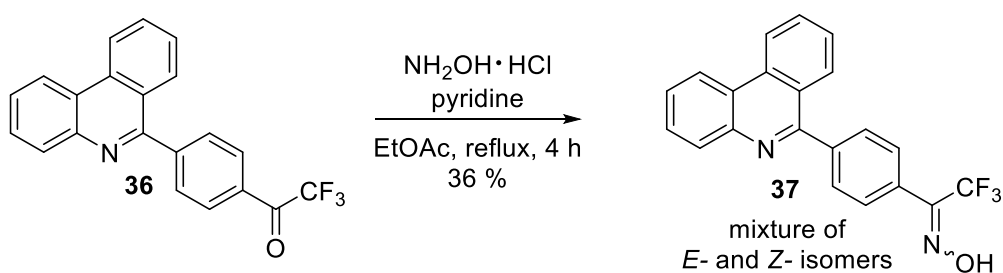
Scheme 19 Synthesis of trifluoromethyl ketone **36**.

Due to the high electronegative properties of fluorine, trifluoromethyl ketones can form stable hydrates. Normally a carbon with two hydroxy groups (geminal diol **62**) is not stable, but under these extreme electron withdrawing conditions, stable hydrate formation is possible (Scheme 20). This phenomenon is also observed in other examples known in pharmaceutical chemistry, like ninhydrin or chloralhydrate.



Scheme 20 Equilibrium of trifluoromethyl ketone **36** and its respective hydrate **62**.

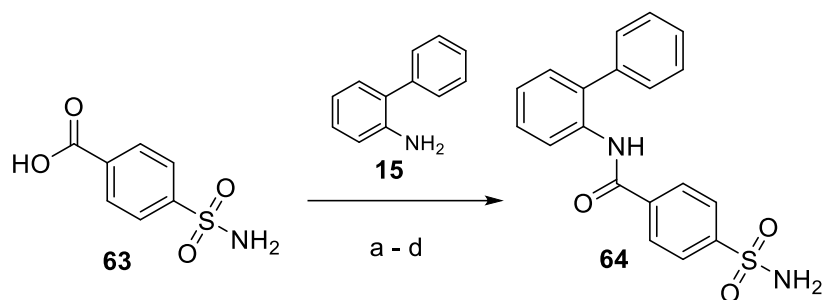
This feature of trifluoromethyl ketones explains the very poor chromatographic behaviour on silica gel, as this addition of OH-groups to the carbonyl is also possible with the free OH-groups of the silica gel. This compound could thus not be purified by FCC, but an alternative method for purification had to be found. Crystallization gave only 30 % pure trifluoromethyl ketone **36**, despite complete conversion of the starting material. Removal of the solvent from the mother liquor yielded the remaining approx. 70 % of product, which wasn't completely pure, but could be used for the synthesis of the corresponding oxime. Trifluoromethyl ketone **36** was reacted with hydroxylamine hydrochloride in pyridine and ethyl acetate. Purification was also achieved through crystallization and trifluoromethyl oxime **37** was obtained as a mixture of *E*- and *Z*-isomers (Scheme 21).



Scheme 21 Synthesis of trifluoromethyl oxime **37**.

Synthesis of sulfonamides **38**, **39** and **40**

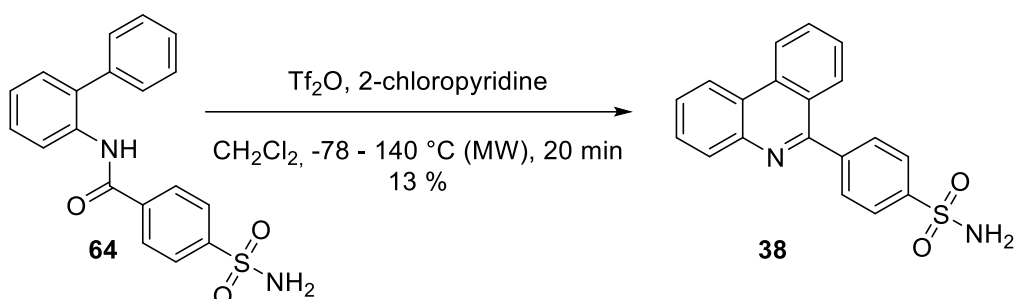
The synthesis of primary sulfonamide **38** was first attempted as described before, starting with the amide coupling to benzamide **64**, bearing the desired primary sulfonamide in position 4 of the phenyl ring. Already the amide coupling turned out to be challenging. Activation of carboxylic acid **63** by chlorination with thionyl chloride and subsequent treatment with 2-aminobiphenyl (**15**) gave only trace amounts of the desired amide. Activation with oxalyl chloride in the presence of catalytic amounts of DMF failed completely. Activation by EDCI yielded only 10 % crude product when DIPEA was used as base. The desired benzamide **64** was finally obtained at least in moderate yield, when using the method of YANG *et al.*^[86], where DMAP is used (Scheme 22).



	conditions	yield
a	1. 63 , thionyl chloride, reflux, 24 h 2. 15 , Et ₃ N	6 %
b	1. 63 , oxalyl chloride, DMF/CH ₂ Cl ₂ , 40 °C, 48 h 2. 15 , Et ₃ N	-
c	63 , 15 , EDCI, HOBT, DIPEA, DMF, rt, 12 h	< 10 % (crude product)
d	63 , 15 , EDCI, HOBT, DMAP, DMF, rt, 12 h	46 %

Scheme 22 Conditions for the synthesis of benzamide **64**.

For cyclization, the standard method from MOVASSAGHI^[75] was employed, but gave poor results for this specific compound. TLC indicated degradation and indeed, sulfonamide **38** was obtained after purification in only 13 % yield (Scheme 23).

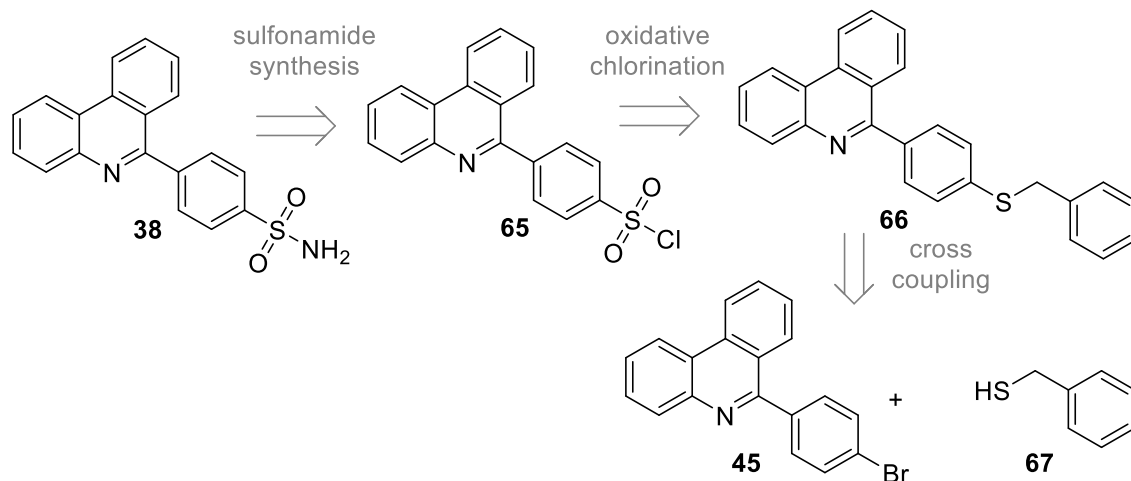


Scheme 23 First approach for the synthesis of sulfonamide **38**.

Nevertheless, the few milligrams obtained from this synthesis could be used for a first screening of biological activity against Sirtuin 6. The results from this screening indicated, that sulfonamide **38** was a very promising compound for finding highly active, drug-like Sirtuin 6 inhibitors (details of the biological activity will be discussed in Chapter 3.2.7). Thus, a more efficient synthesis pathway had to be worked out.

Literature research brought forth a method by GÖBEL *et al.*^[87], where the precursor of the aromatic primary sulfonamide is an aryl bromide. This bromide is coupled with benzyl mercaptan to the respective thioether. This thioether can then be subjected to oxidative chlorination, giving access to an aryl sulfonyl chloride. Bromophenyl phenanthridine **45** was

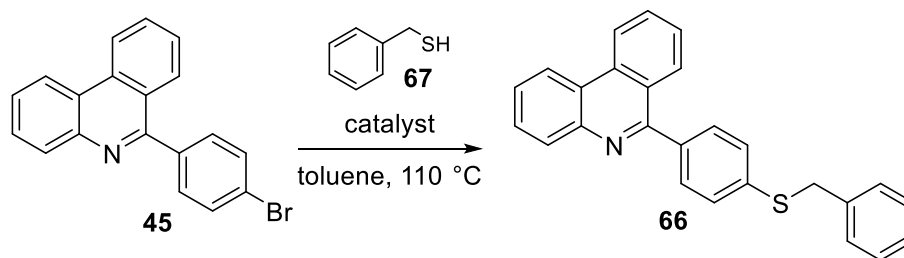
already available from the synthesis of trifluoromethyl ketone **36**, thus this method seemed very promising. Retrosynthesis for this route is shown in Scheme 24. Besides bromophenyl bromide **45**, benzyl mercaptan (**67**) was required for this approach *via* the benzyl thioether intermediate **66**. Benzyl mercaptan is a cheap compound with relatively low toxicity, having the only disadvantage of possessing a very unpleasant odour, which might in turn create some solitude in the lab. An advantage of this method is, that with the sulfonyl chloride intermediate **65**, various sulfonamides, other than the primary, are accessible.



Scheme 24 Retrosynthesis for the second synthetic approach for sulfonamide **38**.

The first step of this synthetic route is the cross-coupling reaction of bromophenyl phenanthridine **45** and benzyl mercaptan (**67**). GÖBEL *et al.* used tris(dibenzylideneacetone)-dipalladium(0) ($\text{Pd}_2(\text{dba})_3$) with 1,1'-bis(diphenylphosphanyl)ferrocene (dppf) as catalyst and DIPEA as base in refluxing toluene for this sulfur-carbon cross coupling reaction^[87]. In order to simplify the preparation of the catalyst, the first synthesis attempt of benzyl thioether **66** was done with commercially available [1,1'-bis-(diphenylphosphino)-ferrocen]-dichloro-palladium(II) ($\text{Pd}(\text{dppf})\text{Cl}_2$). However, no complete conversion occurred, even after 4 days. Upon work-up and purification, benzyl thioether **66** was obtained in 23 % yield. As this was just the very first step in the planned synthetic route, 23 % yield were not sufficient. Doubling the amount of catalyst still didn't lead to complete conversion. It led to the conclusion, that the preparation of the catalyst couldn't be simplified, and thus the next attempt was carried out with the catalyst originally used by GÖBEL^[87], where the palladium is in oxidation state zero. After three hours, the starting material was fully consumed, but still the yield remained too low with 47 %. Finally, when doubling the amount of catalyst, benzyl thioether **66** was obtained in 84 % yield. All attempts are summarized in Scheme 25.

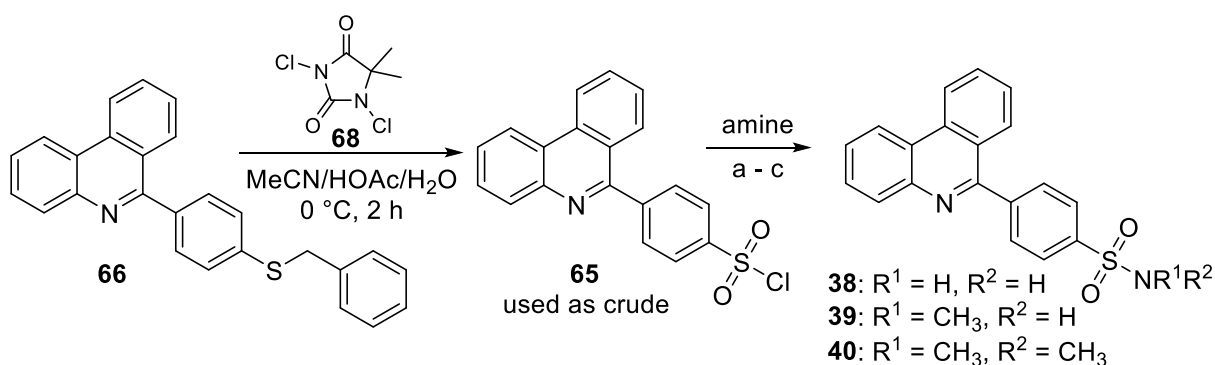
Synthesis of Sirtuin 6 modulators



entry	conditons	yield
1	Pd(dppf)Cl ₂ 0.02 eq, DIPEA, 4 days	23 % no complete conversion
2	Pd(dppf)Cl ₂ 0.05 eq, DIPEA, 24 h	not determined no complete conversion
3	Pd ₂ (dba) ₃ 0.02 eq, dppf 0.04 eq, DIPEA, 3 h	47 % complete conversion
4	Pd ₂ (dba) ₃ 0.04 eq, dppf 0.08 eq, DIPEA, 3 h	84 % complete conversion

Scheme 25 Conditions for the cross-coupling reaction of bromophenyl phenanthridine **45** with benzyl mercaptan (**67**).

After benzyl thioether **66** had been obtained in sufficient quantity, the next steps towards the synthesis of sulfonamide **38** were carried out following the procedure of GÖBEL^[87]. Oxidative chlorination of thioether **66** with 1,3-dichloro-5,5-dimethylhydantoin (**68**) in a mixture of acetonitrile, acetic acid and water gave sulfonyl chloride **65**. Because sulfonyl chlorides are very reactive and might degrade during FCC, sulfonyl chloride **65** was used as crude and directly reacted with the corresponding amines. The syntheses of primary sulfonamide **38**, *N*-methyl sulfonamide **39**, and *N,N*-dimethyl sulfonamide **40** are summarized in Scheme 26.



	product	amine	conditions	yield over 2 steps
a	38	NH ₃	MeCN, 0 °C - rt, 15 min	74 %
b	39	NH ₂ CH ₃	THF, 0 °C - rt, 15 min	89 %
c	40	NH(CH ₃) ₂	THF, 0 °C - rt, 15 min	84 %

Scheme 26 Synthesis of sulfonamides **38**, **39**, and **40**.

3.2.5 Synthesis of variations aimed at the replacement of water

Trapped water molecules can play an active role in the binding of a small molecule modulator. Especially if they have a high energy level, replacement or displacement can result in a decreased total energy level and thus more favourable binding and higher potency of the modulator^[73]. The aim of the structures synthesized in this chapter, was to address the trapped water molecule at the polar binding site of **KV-30** in Sirtuin 6 (Figure 24, marked in orange).

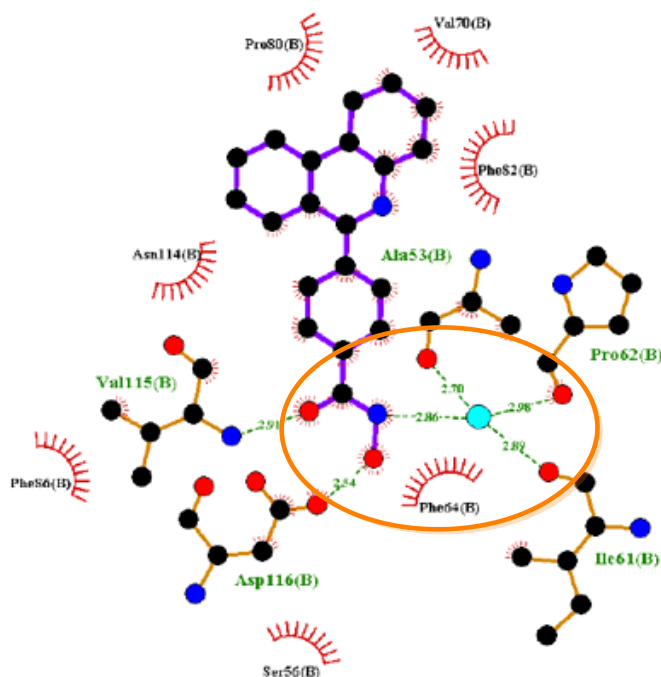


Figure 24 Co-crystal of Sirtuin 6 and **KV-30** showing the water molecule in close proximity to the hydroxamate.

Proof of concept should be achieved by adding a hydroxyethyl residue to the polar head group. A hydroxymethyl residue was not considered due to the expectable instability of the resulting hemiaminal structure. The primary alcohol should be able to build the same network of polar interactions as the trapped water and should thus be able to replace it. Planned variations are shown in Figure 25.

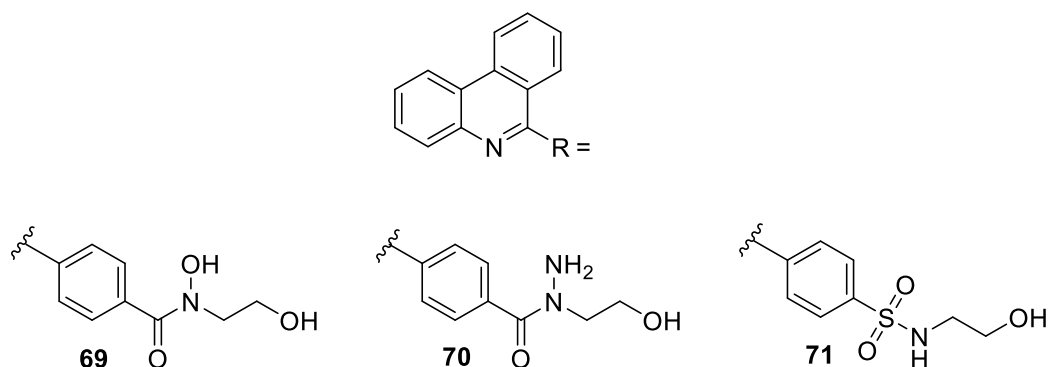
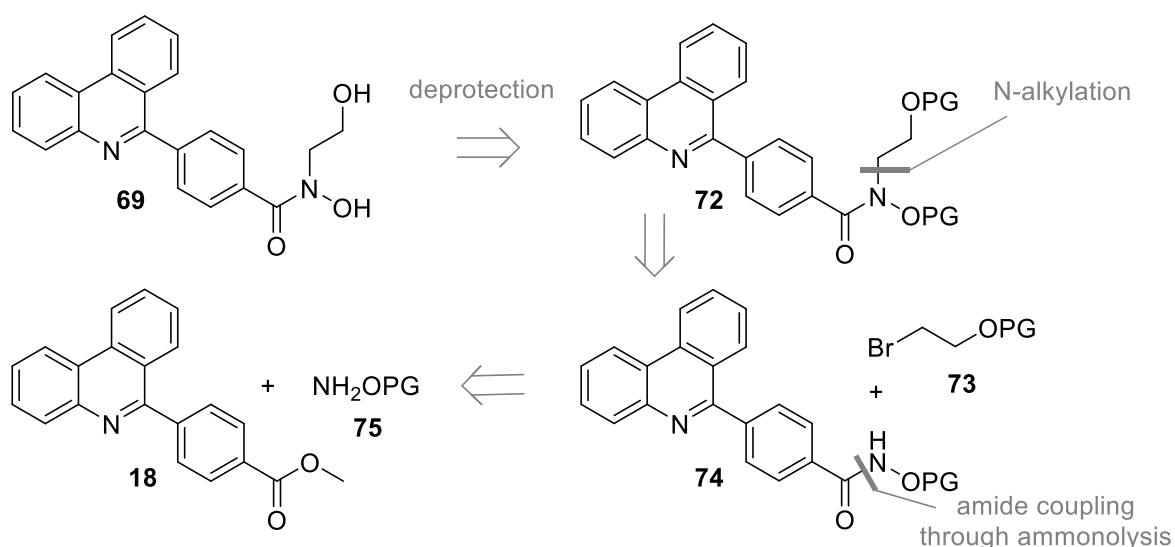


Figure 25 Structures of planned hydroxyethyl variations **69**, **70**, and **71** for the replacement of the water molecule.

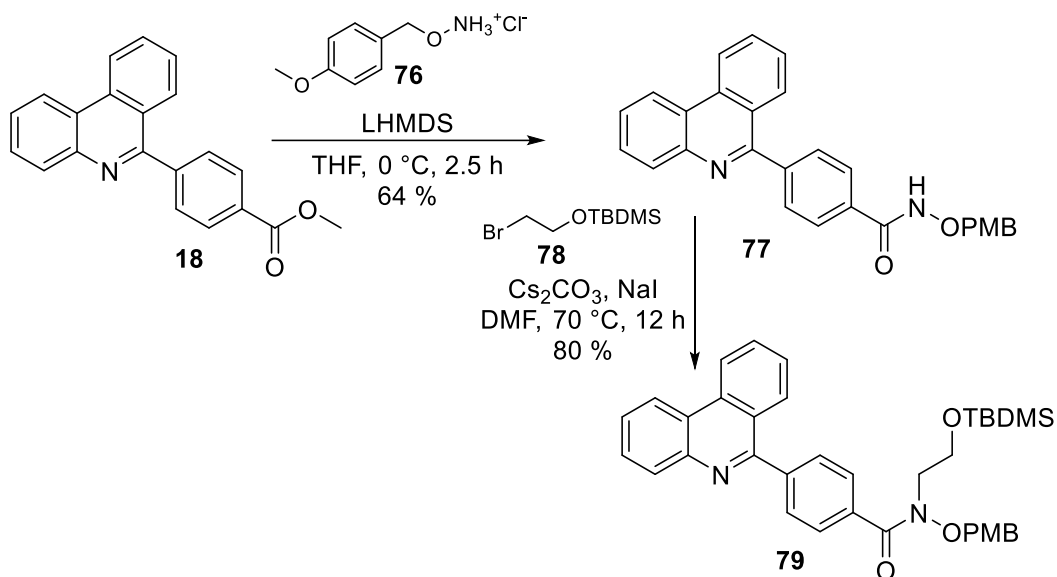
Synthesis of *N*-hydroxyethyl hydroxamic acid **69**

Literature search revealed, that for the planned motif of hydroxyethylated hydroxamic acid, only very few examples are known. A similar substructure was published by LEE *et al.* in BIOORGANIC MEDICINAL CHEMISTRY LETTERS^[88], but unfortunately, this journal does not provide detailed information about synthetic procedures. Inspired by the synthetic sequence from this publication, a synthesis plan was worked out. Evidently, to ensure selective reactions, all amine and alcohol groups had to be suitably protected. Retrosynthesis for the *N*-hydroxyethyl hydroxamic acid **69** is shown in Scheme 27. The hydroxyethyl residue should be introduced via *N*-alkylation with protected 2-bromoethanol **73** of the before constructed, protected hydroxamic acid **74**. Starting material for this purpose should be again methyl ester **18**, but the amide coupling was planned to be done in one step via ammonolysis with an *O*-protected hydroxylamine species (**75**).



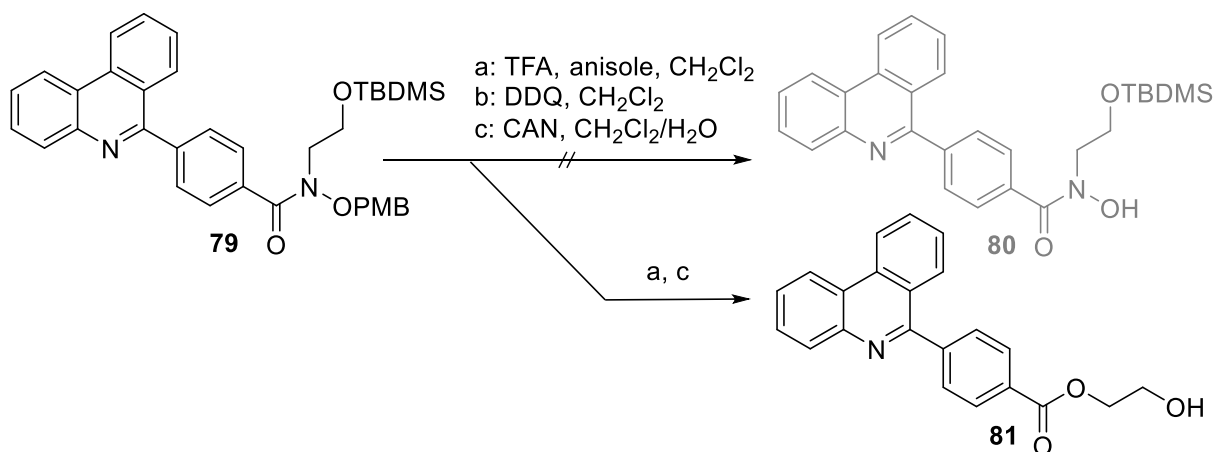
Scheme 27 Retrosynthesis of *N*-hydroxyethyl hydroxamate **69**.

In a first attempt, *O*-PMB-protected hydroxylamine **76** and *O*-TBDMS-protected bromoethanol **78** were used, the same protecting groups as used by LEE. Amide coupling was achieved by a method published by BOSCH *et al.*^[89], which allowed the direct base-mediated (LHMDS) ammonolysis of methyl ester **18** with *O*-PMB-protected hydroxylamine hydrochloride (**76**) which gave intermediate **77** in good yield. For the subsequent *N*-alkylation a method by LU *et al.*^[90], additionally using catalytic amounts of sodium iodide to facilitate the substitution reaction, was used to synthesise di-protected *N*-hydroxyethyl hydroxamate **79** in good yield (Scheme 28).



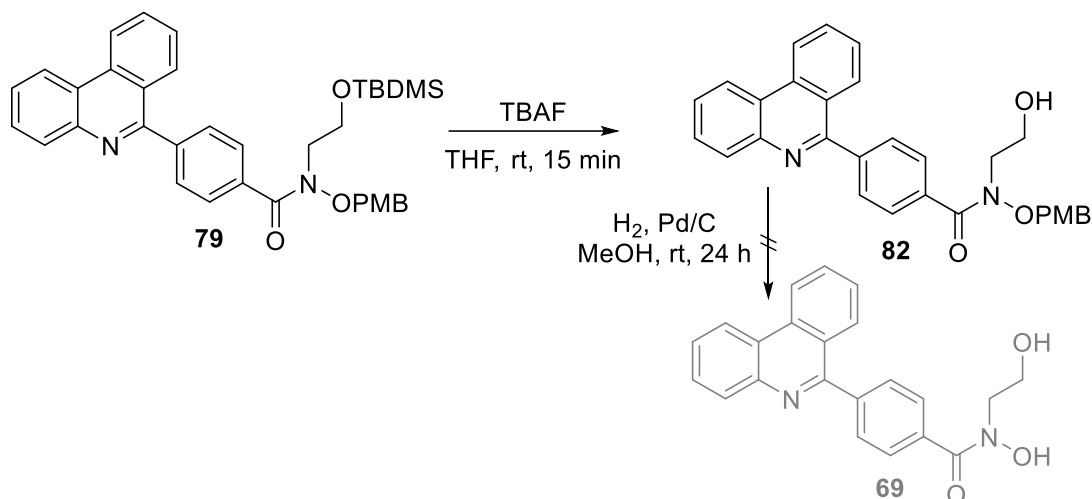
Scheme 28 Synthesis of PMB and TBDMS protected *N*-hydroxyethyl hydroxamate **79**.

A problem with this synthetic route occurred during deprotection. PMB-deprotection was not successful with either TFA/anisole, DDQ or CAN. With DDQ, even after several days, only starting material was observed in TLC analysis. TFA/anisole and CAN deprotection led to the formation of a side product, which was identified by HRMS and NMR as hydroxyethyl ester **81** (Scheme 29).



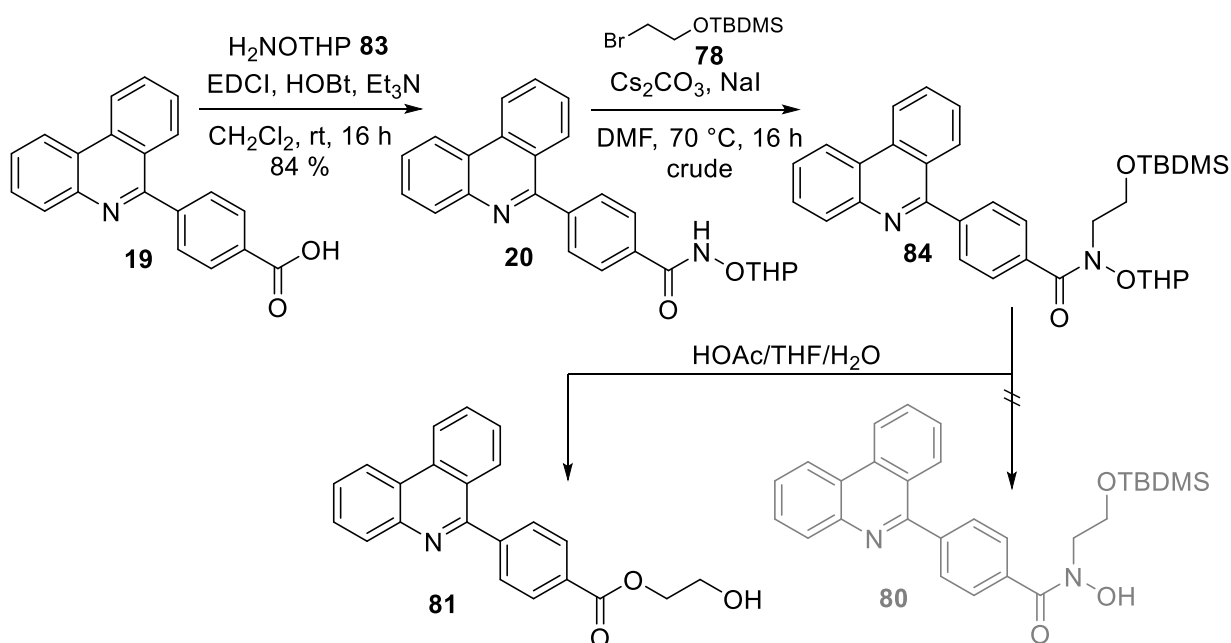
Scheme 29 Attempted deprotections of PMB and TBDMS protected *N*-hydroxyethyl hydroxamate **79**.

In a next attempt, di-protected *N*-hydroxyethyl hydroxamate **79** was first TBDMS-deprotected with TBAF and subsequently subjected to catalytic hydrogenation, to cleave the PMB-group. TBDMS-deprotection proceeded without further complications (TLC-MS control showed intermediate **82**) but the subsequent hydrogenation was not successful, as TLC indicated, that no reaction had occurred (Scheme 30).



Scheme 30 Attempted PMB deprotection by catalytic hydrogenation.

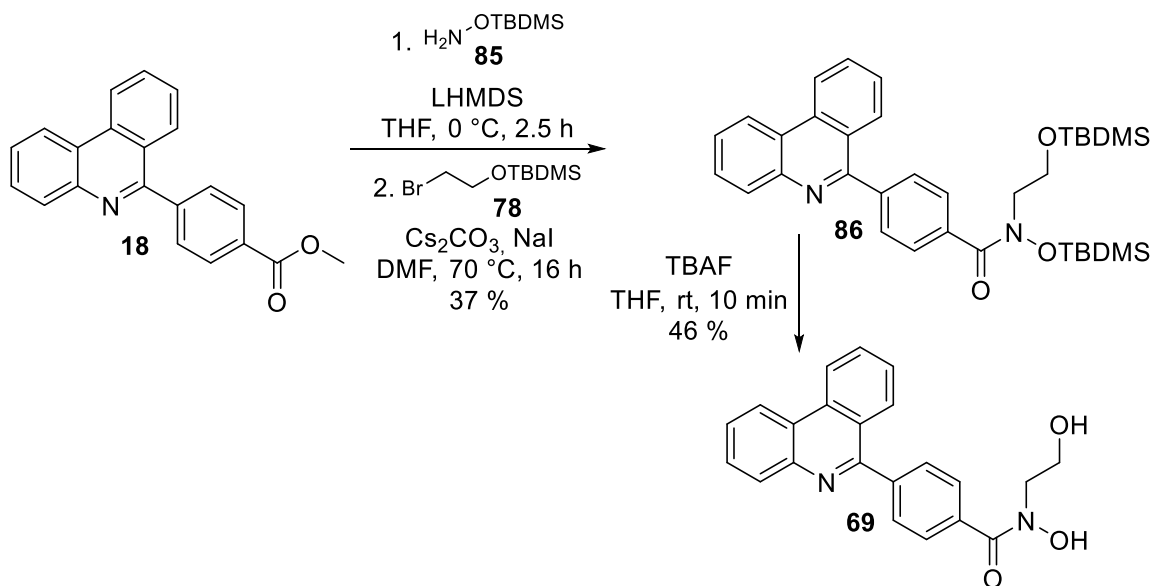
Since all attempts for PMB-deprotection failed, different protecting groups for the hydroxamic acid were assessed. Starting with *O*-THP-protected hydroxylamine (**83**), as previously described by VÖGERL^[74] for the synthesis of **KV-30**. Applying VÖGERL's method, where the amide coupling is facilitated by EDCI, provided THP-protected hydroxamate **20** in good yield. The subsequent *N*-alkylation equally worked without difficulty with the THP-group. The acidic conditions however, which are necessary to cleave the THP-group, unfortunately yielded again the undesired hydroxyethyl ester side product **81**. The synthetic attempt is summarized in Scheme 31.



Scheme 31 Alternative synthetic attempt for *N*-hydroxyethyl hydroxamate via THP protected intermediate **84**.

Because the deprotection of the TBDMS-group with TBAF had worked for this type of molecule without any undesired side reactions, the next idea was to equally use the TBDMS protecting group for the hydroxamate. Following the same synthetic route as described above with *O*-

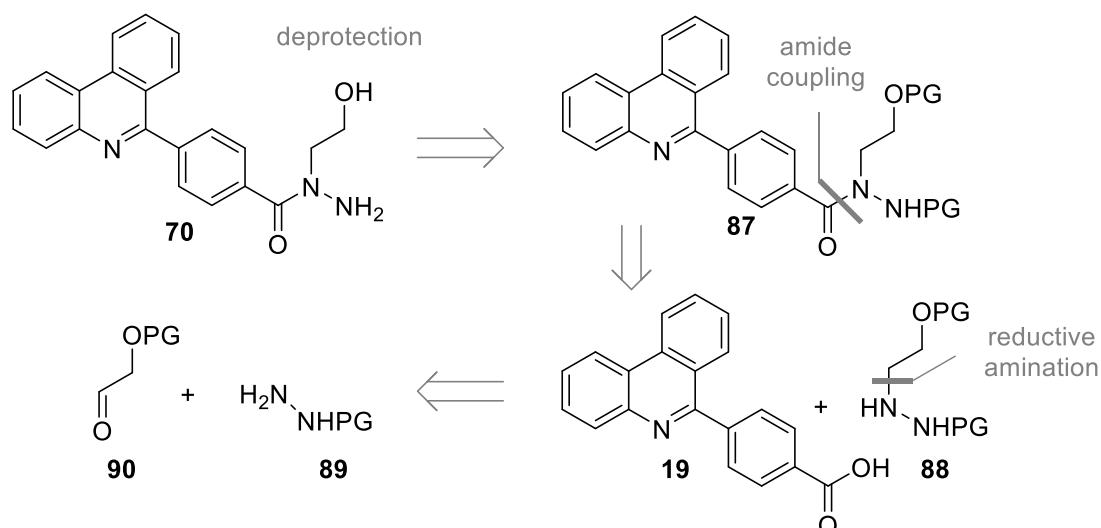
TBDMS-protected hydroxylamine (**85**), finally gave the desired *N*-hydroxyethyl hydroxamate **69** after dual TBDMS deprotection with TBAF (Scheme 32).



Scheme 32 Successful synthetic approach for the construction of *N*-hydroxyethyl hydroxamate **69**.

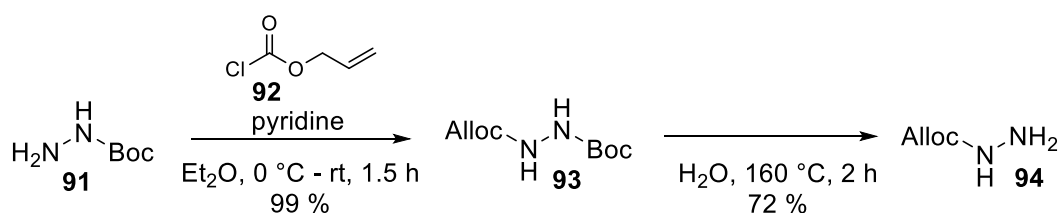
Synthesis of *N*-hydroxyethyl hydrazide **70**

Like for the synthesis of the *N*-hydroxyethyl hydroxamate, only very few reports of a similar substructure could be found for *N*-hydroxyethyl hydrazide. KAWANISHI *et al.* reported a *N*-Alloc-*O*-TBDMS-protected *N*-hydroxyethyl hydrazide intermediate for the construction of a 1,2-dihydro-3H-indazol-3-one structure motif^[91]. Again, this synthesis was published in BIOORGANIC MEDICINAL CHEMISTRY LETTERS. In this case though, the authors had published the synthesis with experimental details additionally in a patent^[92]. The central building block of the synthesis is the di-protected hydroxyethyl hydrazine **88**, which can be synthesized by reductive amination protected 2-hydroxyacetaldehyde **90** with *N*'-protected hydrazine **89**. The resulting hydrazine intermediate **100** can then be coupled to phenanthridinylbenzoic acid **19**. After deprotection, the envisaged *N*-hydroxyethyl hydrazide **70** should be obtained. Retrosynthesis is shown in Scheme 33.



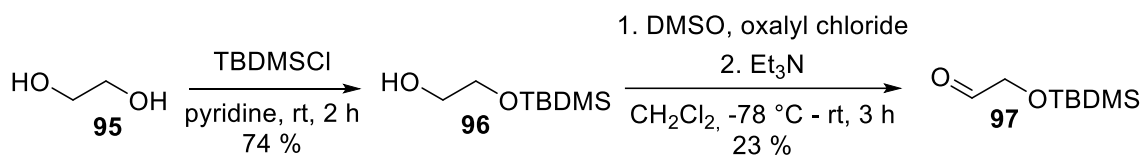
Scheme 33 Retrosynthesis of *N*-hydroxyethyl hydrazide **70**.

KAWANISHI *et al.* used TBDMS for hydroxy protection and Alloc for hydrazine protection. First step of the assembly of the central building block **100** was the synthesis of Alloc-protected hydrazine (**94**) by a two-step procedure from SAMMIS *et al.*, where originally Boc-protected hydrazine (**91**) is transformed to the desired Alloc-protected hydrazine (**94**)^[93]. The obtained product is purified by distillation (Scheme 34).



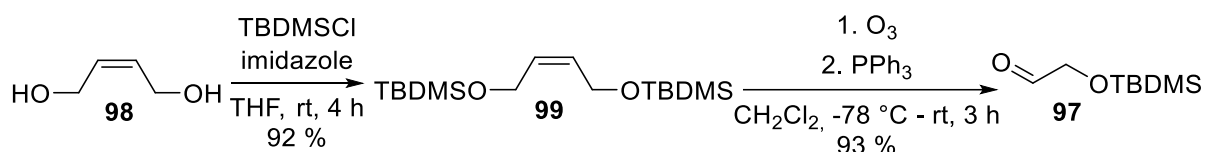
Scheme 34 Synthesis of Alloc protected hydrazine **94**.

For the synthesis of TBDMS-protected 2-hydroxyacetaldehyde (**97**), a method from CORNIL *et al.* was tried in a first attempt^[94]. This method starts with mono-TBDMS-protection of ethylene glycol and should give the desired aldehyde after SWERN oxidation of the remaining unprotected alcohol. The TBDMS-monoprotection step proceeded smoothly, however the following SWERN oxidation gave aldehyde **97** only in low yield (Scheme 35). Because the aldehyde is needed in larger amounts, an alternative, higher yielding method had to be found.



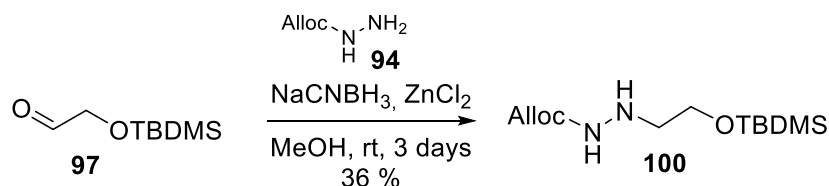
Scheme 35 First, low yielding approach to the synthesis of TBDMS protected 2-hydroxyacetaldehyde (**97**) by SWERN oxidation.

Alternative synthesis of aldehyde **97** followed a method described by LAFONTAINE *et al.*, where 2-butene-1,4-diol is TBDMS-protected and subsequently subjected to ozonolysis^[95]. Because of the symmetric nature of 2-butene-1,4-diol, one equivalent of the alkene gives two equivalents of the desired aldehyde. This method proved to be fit for purpose, as it delivered aldehyde **97** with an overall yield of 86 % (Scheme 36). Purification was achieved by FCC with PE/EtOAc, and because of the high volatility of the TBDMS-protected hydroxy acetaldehyde, complete removal of the solvent was impossible. If the synthesis were to be repeated, either the mobile phase of FCC would need to be switched to lower boiling solvents, or purification would need to be achieved by distillation with carefully applied vacuum.



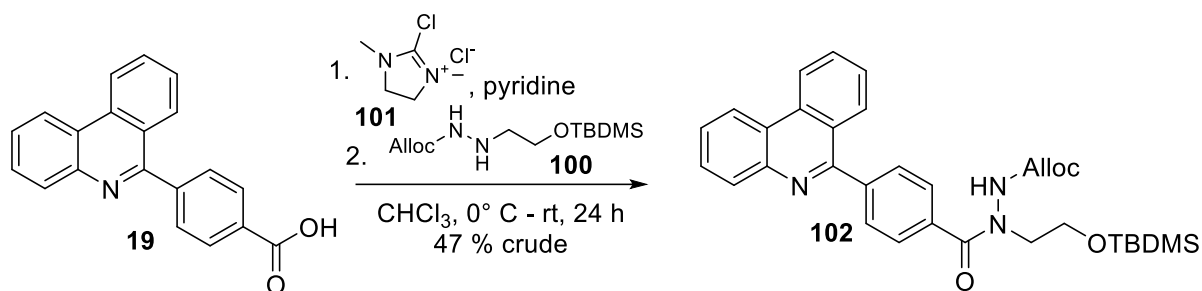
Scheme 36 Second approach to the synthesis of TBDMS protected 2-hydroxyacetaldehyde (**97**) *via* ozonolysis.

The subsequent reductive amination followed the procedure from the beforementioned patent, but gave the desired hydrazine intermediate **100** only in low yield (Scheme 37)^[92].



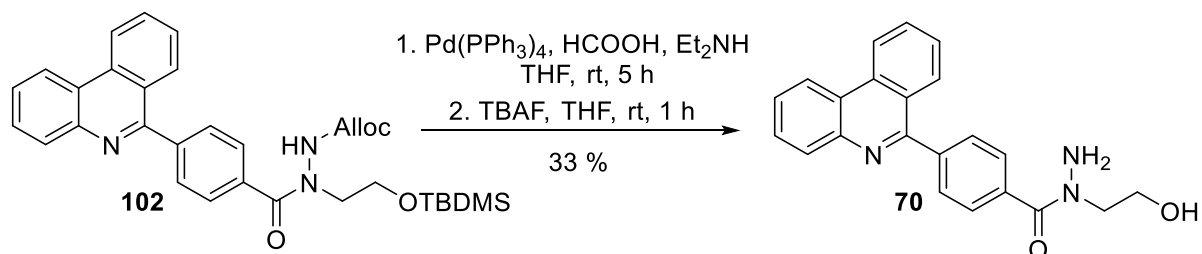
Scheme 37 Synthesis of Alloc and TBDMS protected *N*-hydroxyethyl hydrazine **100**.

The low yield was mainly due to the fact, that the reaction did not reach completion, but stopped mostly with the formation of the imine. The imine in this case is very stable and can even be isolated. All attempts to further reduce the imine to the desired hydrazine **100** failed. The use of other hydride reagents for the reductive amination, like sodium triacetoxy borohydride, equally failed to improve the yield. Nevertheless, the above obtained hydrazine intermediate **100** was enough, to proceed to the following amide coupling. Again, the described synthetic method from the patent was used. Activation of carboxylic acid **19** was achieved by 2-chloro-1,3-dimethylimidazolium chloride (**101**) and subsequent treatment with the protected *N*-hydroxyethyl hydrazine intermediate **100** gave di-protected *N*-hydroxyethyl hydrazide **102** in moderate yield as a pale-yellow oil (Scheme 38). Because the handling of sticky oils is quite difficult, the obtained product was directly subjected to deprotection, without intermediate characterization.



Scheme 38 Synthesis of Alloc and TBDMS protected *N*-hydroxyethyl hydrazide **102**.

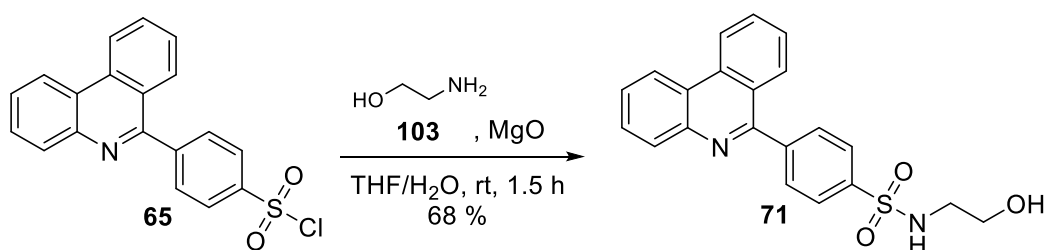
Alloc-deprotection was achieved by tetrakis(triphenylphosphan)palladium(0) in the presence of diethylamine and formic acid, followed by TBDMS-deprotection with TBAF. The deprotection sequence was carried out without intermediate isolation, only the palladium catalyst was removed by filtration through a pad of silica, before TBDMS deprotection. The desired *N*-hydroxyethyl hydrazide **70** was obtained in moderate yield over two steps (Scheme 39).



Scheme 39 Deprotection to give the *N*-hydroxyethyl hydroxamate **70**.

Synthesis of *N*-hydroxyethyl sulfonamide **71**

Synthesis of the *N*-hydroxyethyl sulfonamide could be achieved by sulfonylation of ethanolamine (**103**) with sulfonyl chloride **65**, originating from the synthesis of the primary sulfonamide **38**. KANG *et al.*^[96] described a synthetic procedure using magnesium oxide, which should result in selectivity for *N*-sulfonylation over *O*-sulfonylation. Even though the procedure was not completely selective, and some sulfonate by-product was found, *N*-hydroxyethyl sulfonamide **71** was still obtained in adequate yield (Scheme 40).



Scheme 40 Synthesis of *N*-hydroxyethyl sulfonamide **71**.

3.2.6 Synthesis of potential substrate mimetic analogues

To further enhance potency of this class of inhibitors, analogues, that could potentially mimic the endogenous substrate of Sirtuin 6 should be synthesized. The endogenous substrates of Sirtuin 6 are proteins with an *N*-acylated lysine residue. The overlay of the co-crystal of Sirtuin 6 with **KV-30** and Sirtuin 6 with myristoylated TNF α , obtained by DR. WEIJE YOU at the University of Bayreuth showed, that the phenanthridine ring is in the same position as the end of the long chain fatty acid (Figure 26). The position of the respective amide bond of the substrate is located at the exit of the lipophilic acyl channel of Sirtuin 6. Therefore, introducing a residue at ring C of the phenanthridine, that mimics this amide bond, could further enhance potency and selectivity. Especially since this lipophilic acyl channel is a unique feature of Sirtuin 6.

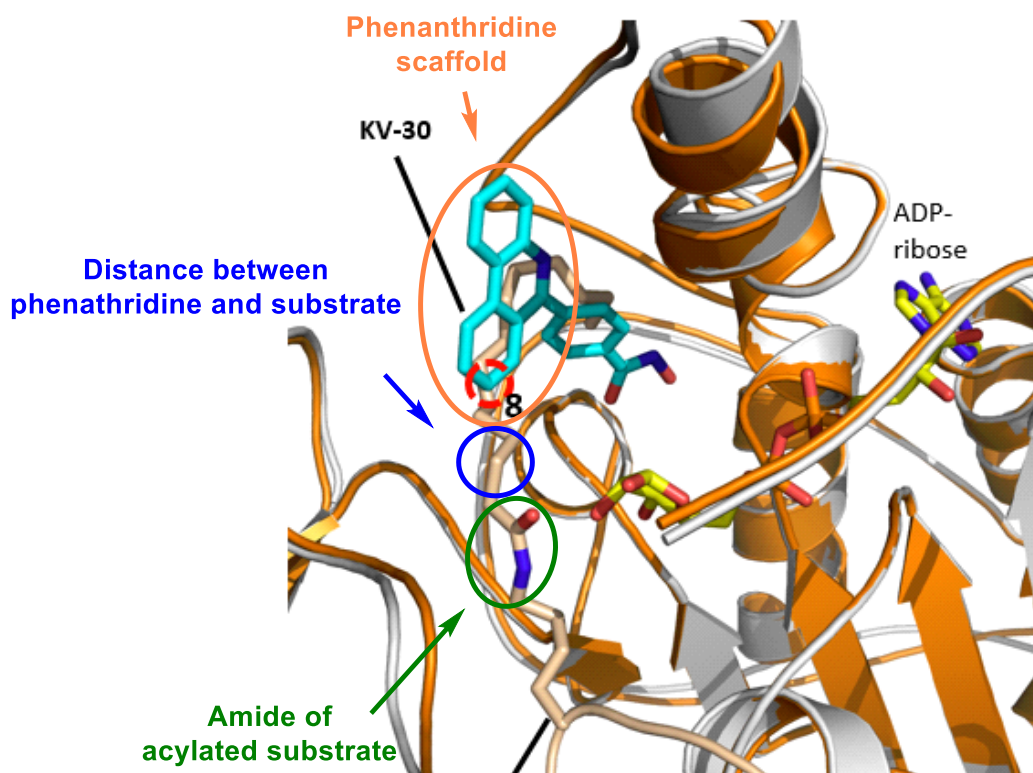
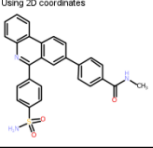
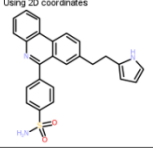
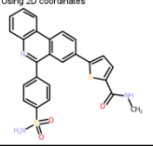
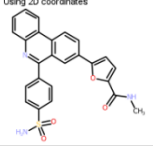
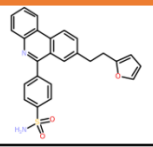
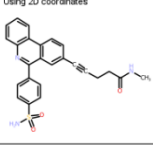
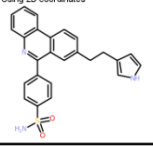
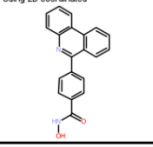
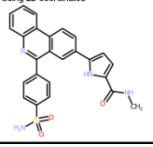
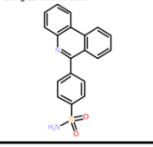
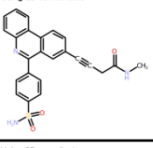
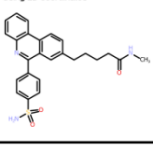
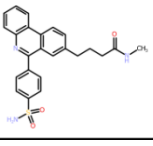


Figure 26 Overlay of the co-crystals of Sirtuin 6 with **KV-30** (blue) and myristoylated-TNF α (light-orange) showing the relative position of **KV-30** to the endogenous substrate and identifying position 8 of the phenanthridine as promising position for the substrate mimicking residue.

The planning of such potential substrate mimetic compounds was supported by docking studies carried out by DR. WEIJE YOU. Proposed structures and the respective docking results are shown in Table 2. The top compounds from this docking study (Table 2, orange box) were then considered for synthesis.

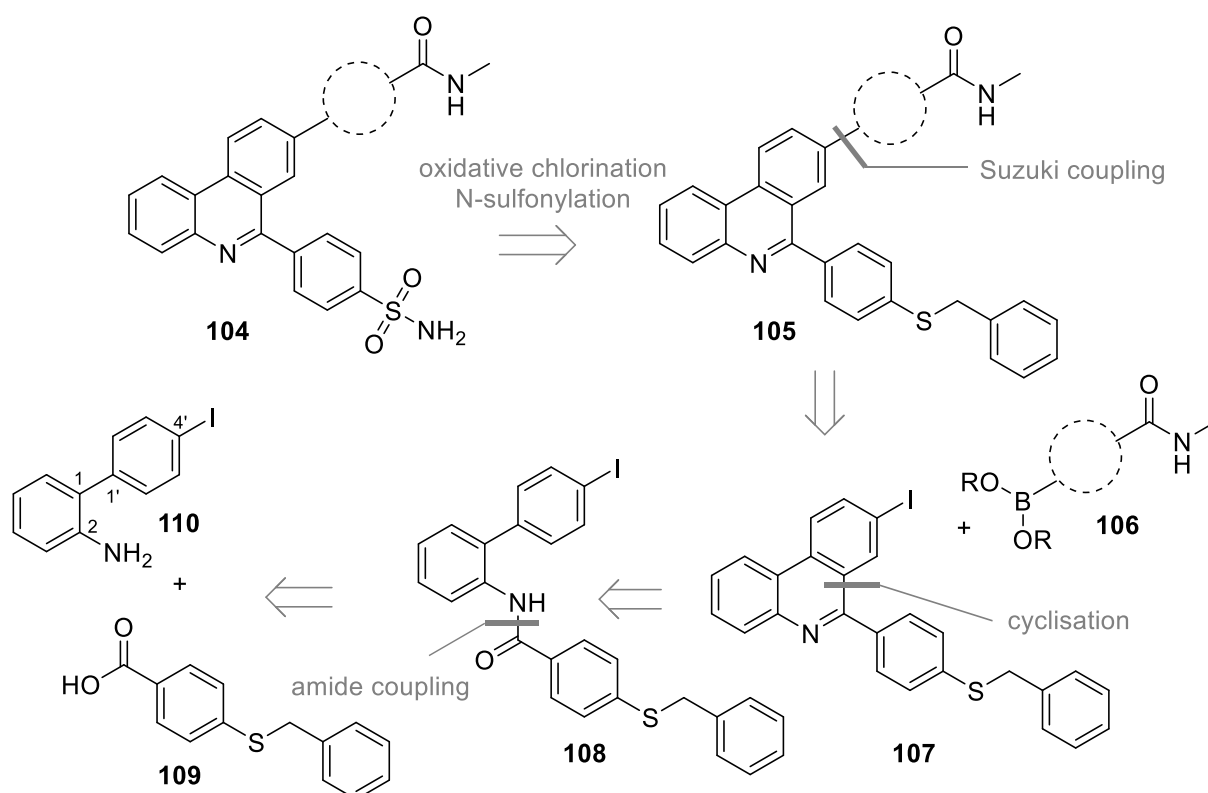
Synthesis of Sirtuin 6 modulators

Table 2 Docking results for structures with additional moiety at the phenanthridine. Two compounds with best score and highest rank were envisaged for synthesis (orange box).

	<table border="1"> <tr><td>Type</td><td>3</td><td>Name</td><td>CLE121-phenyl</td></tr> <tr><td>Rank</td><td>1</td><td>Score</td><td>27.11-</td></tr> <tr><td>XLogP</td><td>5.224</td><td>Mol. weight</td><td>467.130</td></tr> <tr><td>No. of Rot. Bonds</td><td>6</td><td>No. of Bonds</td><td>38</td></tr> <tr><td>H acceptor</td><td>6</td><td>H donor</td><td>2</td></tr> <tr><td>Comment</td><td colspan="3"></td></tr> </table>	Type	3	Name	CLE121-phenyl	Rank	1	Score	27.11-	XLogP	5.224	Mol. weight	467.130	No. of Rot. Bonds	6	No. of Bonds	38	H acceptor	6	H donor	2	Comment					<table border="1"> <tr><td>Type</td><td>1</td><td>Name</td><td>CLE121-2-pyrrolyl</td></tr> <tr><td>Rank</td><td>8</td><td>Score</td><td>23.6-</td></tr> <tr><td>XLogP</td><td>4.610</td><td>Mol. weight</td><td>427.135</td></tr> <tr><td>No. of Rot. Bonds</td><td>6</td><td>No. of Bonds</td><td>35</td></tr> <tr><td>H acceptor</td><td>4</td><td>H donor</td><td>2</td></tr> <tr><td>Comment</td><td colspan="3"></td></tr> </table>	Type	1	Name	CLE121-2-pyrrolyl	Rank	8	Score	23.6-	XLogP	4.610	Mol. weight	427.135	No. of Rot. Bonds	6	No. of Bonds	35	H acceptor	4	H donor	2	Comment			
Type	3	Name	CLE121-phenyl																																																
Rank	1	Score	27.11-																																																
XLogP	5.224	Mol. weight	467.130																																																
No. of Rot. Bonds	6	No. of Bonds	38																																																
H acceptor	6	H donor	2																																																
Comment																																																			
Type	1	Name	CLE121-2-pyrrolyl																																																
Rank	8	Score	23.6-																																																
XLogP	4.610	Mol. weight	427.135																																																
No. of Rot. Bonds	6	No. of Bonds	35																																																
H acceptor	4	H donor	2																																																
Comment																																																			
	<table border="1"> <tr><td>Type</td><td>3</td><td>Name</td><td>CLE121-Thiophene</td></tr> <tr><td>Rank</td><td>2</td><td>Score</td><td>26.67-</td></tr> <tr><td>XLogP</td><td>3.911</td><td>Mol. weight</td><td>473.087</td></tr> <tr><td>No. of Rot. Bonds</td><td>6</td><td>No. of Bonds</td><td>37</td></tr> <tr><td>H acceptor</td><td>6</td><td>H donor</td><td>2</td></tr> <tr><td>Comment</td><td colspan="3"></td></tr> </table>	Type	3	Name	CLE121-Thiophene	Rank	2	Score	26.67-	XLogP	3.911	Mol. weight	473.087	No. of Rot. Bonds	6	No. of Bonds	37	H acceptor	6	H donor	2	Comment					<table border="1"> <tr><td>Type</td><td>3</td><td>Name</td><td>CLE121-furan</td></tr> <tr><td>Rank</td><td>9</td><td>Score</td><td>23.59-</td></tr> <tr><td>XLogP</td><td>3.937</td><td>Mol. weight</td><td>457.110</td></tr> <tr><td>No. of Rot. Bonds</td><td>6</td><td>No. of Bonds</td><td>37</td></tr> <tr><td>H acceptor</td><td>6</td><td>H donor</td><td>2</td></tr> <tr><td>Comment</td><td colspan="3"></td></tr> </table>	Type	3	Name	CLE121-furan	Rank	9	Score	23.59-	XLogP	3.937	Mol. weight	457.110	No. of Rot. Bonds	6	No. of Bonds	37	H acceptor	6	H donor	2	Comment			
Type	3	Name	CLE121-Thiophene																																																
Rank	2	Score	26.67-																																																
XLogP	3.911	Mol. weight	473.087																																																
No. of Rot. Bonds	6	No. of Bonds	37																																																
H acceptor	6	H donor	2																																																
Comment																																																			
Type	3	Name	CLE121-furan																																																
Rank	9	Score	23.59-																																																
XLogP	3.937	Mol. weight	457.110																																																
No. of Rot. Bonds	6	No. of Bonds	37																																																
H acceptor	6	H donor	2																																																
Comment																																																			
	<table border="1"> <tr><td>Type</td><td>3</td><td>Name</td><td>CLE121-alkyne-c5</td></tr> <tr><td>Rank</td><td>3</td><td>Score</td><td>26.2-</td></tr> <tr><td>XLogP</td><td>4.500</td><td>Mol. weight</td><td>428.119</td></tr> <tr><td>No. of Rot. Bonds</td><td>6</td><td>No. of Bonds</td><td>35</td></tr> <tr><td>H acceptor</td><td>4</td><td>H donor</td><td>1</td></tr> <tr><td>Comment</td><td colspan="3"></td></tr> </table>	Type	3	Name	CLE121-alkyne-c5	Rank	3	Score	26.2-	XLogP	4.500	Mol. weight	428.119	No. of Rot. Bonds	6	No. of Bonds	35	H acceptor	4	H donor	1	Comment					<table border="1"> <tr><td>Type</td><td>2</td><td>Name</td><td>CLE121-alkyne-c5</td></tr> <tr><td>Rank</td><td>10</td><td>Score</td><td>23.17-</td></tr> <tr><td>XLogP</td><td>3.925</td><td>Mol. weight</td><td>443.130</td></tr> <tr><td>No. of Rot. Bonds</td><td>6</td><td>No. of Bonds</td><td>35</td></tr> <tr><td>H acceptor</td><td>6</td><td>H donor</td><td>2</td></tr> <tr><td>Comment</td><td colspan="3"></td></tr> </table>	Type	2	Name	CLE121-alkyne-c5	Rank	10	Score	23.17-	XLogP	3.925	Mol. weight	443.130	No. of Rot. Bonds	6	No. of Bonds	35	H acceptor	6	H donor	2	Comment			
Type	3	Name	CLE121-alkyne-c5																																																
Rank	3	Score	26.2-																																																
XLogP	4.500	Mol. weight	428.119																																																
No. of Rot. Bonds	6	No. of Bonds	35																																																
H acceptor	4	H donor	1																																																
Comment																																																			
Type	2	Name	CLE121-alkyne-c5																																																
Rank	10	Score	23.17-																																																
XLogP	3.925	Mol. weight	443.130																																																
No. of Rot. Bonds	6	No. of Bonds	35																																																
H acceptor	6	H donor	2																																																
Comment																																																			
	<table border="1"> <tr><td>Type</td><td>1</td><td>Name</td><td>CLE121-3-pyrrolyl</td></tr> <tr><td>Rank</td><td>4</td><td>Score</td><td>24.87-</td></tr> <tr><td>XLogP</td><td>4.766</td><td>Mol. weight</td><td>427.135</td></tr> <tr><td>No. of Rot. Bonds</td><td>6</td><td>No. of Bonds</td><td>35</td></tr> <tr><td>H acceptor</td><td>4</td><td>H donor</td><td>2</td></tr> <tr><td>Comment</td><td colspan="3"></td></tr> </table>	Type	1	Name	CLE121-3-pyrrolyl	Rank	4	Score	24.87-	XLogP	4.766	Mol. weight	427.135	No. of Rot. Bonds	6	No. of Bonds	35	H acceptor	4	H donor	2	Comment					<table border="1"> <tr><td>Type</td><td>0</td><td>Name</td><td>KV-30</td></tr> <tr><td>Rank</td><td>11</td><td>Score</td><td>23.12-</td></tr> <tr><td>XLogP</td><td>4.387</td><td>Mol. weight</td><td>314.106</td></tr> <tr><td>No. of Rot. Bonds</td><td>3</td><td>No. of Bonds</td><td>27</td></tr> <tr><td>H acceptor</td><td>2</td><td>H donor</td><td>2</td></tr> <tr><td>Comment</td><td colspan="3"></td></tr> </table>	Type	0	Name	KV-30	Rank	11	Score	23.12-	XLogP	4.387	Mol. weight	314.106	No. of Rot. Bonds	3	No. of Bonds	27	H acceptor	2	H donor	2	Comment			
Type	1	Name	CLE121-3-pyrrolyl																																																
Rank	4	Score	24.87-																																																
XLogP	4.766	Mol. weight	427.135																																																
No. of Rot. Bonds	6	No. of Bonds	35																																																
H acceptor	4	H donor	2																																																
Comment																																																			
Type	0	Name	KV-30																																																
Rank	11	Score	23.12-																																																
XLogP	4.387	Mol. weight	314.106																																																
No. of Rot. Bonds	3	No. of Bonds	27																																																
H acceptor	2	H donor	2																																																
Comment																																																			
	<table border="1"> <tr><td>Type</td><td>3</td><td>Name</td><td>CLE121-pyrrole</td></tr> <tr><td>Rank</td><td>5</td><td>Score</td><td>24.76-</td></tr> <tr><td>XLogP</td><td>4.047</td><td>Mol. weight</td><td>456.126</td></tr> <tr><td>No. of Rot. Bonds</td><td>6</td><td>No. of Bonds</td><td>37</td></tr> <tr><td>H acceptor</td><td>6</td><td>H donor</td><td>3</td></tr> <tr><td>Comment</td><td colspan="3"></td></tr> </table>	Type	3	Name	CLE121-pyrrole	Rank	5	Score	24.76-	XLogP	4.047	Mol. weight	456.126	No. of Rot. Bonds	6	No. of Bonds	37	H acceptor	6	H donor	3	Comment					<table border="1"> <tr><td>Type</td><td>0</td><td>Name</td><td>CLE121</td></tr> <tr><td>Rank</td><td>12</td><td>Score</td><td>23.04-</td></tr> <tr><td>XLogP</td><td>3.879</td><td>Mol. weight</td><td>334.078</td></tr> <tr><td>No. of Rot. Bonds</td><td>3</td><td>No. of Bonds</td><td>27</td></tr> <tr><td>H acceptor</td><td>4</td><td>H donor</td><td>1</td></tr> <tr><td>Comment</td><td colspan="3"></td></tr> </table>	Type	0	Name	CLE121	Rank	12	Score	23.04-	XLogP	3.879	Mol. weight	334.078	No. of Rot. Bonds	3	No. of Bonds	27	H acceptor	4	H donor	1	Comment			
Type	3	Name	CLE121-pyrrole																																																
Rank	5	Score	24.76-																																																
XLogP	4.047	Mol. weight	456.126																																																
No. of Rot. Bonds	6	No. of Bonds	37																																																
H acceptor	6	H donor	3																																																
Comment																																																			
Type	0	Name	CLE121																																																
Rank	12	Score	23.04-																																																
XLogP	3.879	Mol. weight	334.078																																																
No. of Rot. Bonds	3	No. of Bonds	27																																																
H acceptor	4	H donor	1																																																
Comment																																																			
	<table border="1"> <tr><td>Type</td><td>2</td><td>Name</td><td>CLE121-alkyne-c4</td></tr> <tr><td>Rank</td><td>6</td><td>Score</td><td>24.29-</td></tr> <tr><td>XLogP</td><td>3.756</td><td>Mol. weight</td><td>429.115</td></tr> <tr><td>No. of Rot. Bonds</td><td>5</td><td>No. of Bonds</td><td>34</td></tr> <tr><td>H acceptor</td><td>6</td><td>H donor</td><td>2</td></tr> <tr><td>Comment</td><td colspan="3"></td></tr> </table>	Type	2	Name	CLE121-alkyne-c4	Rank	6	Score	24.29-	XLogP	3.756	Mol. weight	429.115	No. of Rot. Bonds	5	No. of Bonds	34	H acceptor	6	H donor	2	Comment					<table border="1"> <tr><td>Type</td><td>2</td><td>Name</td><td>CLE121-pentanoic</td></tr> <tr><td>Rank</td><td>13</td><td>Score</td><td>19.8-</td></tr> <tr><td>XLogP</td><td>4.403</td><td>Mol. weight</td><td>447.162</td></tr> <tr><td>No. of Rot. Bonds</td><td>9</td><td>No. of Bonds</td><td>35</td></tr> <tr><td>H acceptor</td><td>6</td><td>H donor</td><td>2</td></tr> <tr><td>Comment</td><td colspan="3"></td></tr> </table>	Type	2	Name	CLE121-pentanoic	Rank	13	Score	19.8-	XLogP	4.403	Mol. weight	447.162	No. of Rot. Bonds	9	No. of Bonds	35	H acceptor	6	H donor	2	Comment			
Type	2	Name	CLE121-alkyne-c4																																																
Rank	6	Score	24.29-																																																
XLogP	3.756	Mol. weight	429.115																																																
No. of Rot. Bonds	5	No. of Bonds	34																																																
H acceptor	6	H donor	2																																																
Comment																																																			
Type	2	Name	CLE121-pentanoic																																																
Rank	13	Score	19.8-																																																
XLogP	4.403	Mol. weight	447.162																																																
No. of Rot. Bonds	9	No. of Bonds	35																																																
H acceptor	6	H donor	2																																																
Comment																																																			
	<table border="1"> <tr><td>Type</td><td>2</td><td>Name</td><td>CLE121-butanolic</td></tr> <tr><td>Rank</td><td>7</td><td>Score</td><td>23.83-</td></tr> <tr><td>XLogP</td><td>3.834</td><td>Mol. weight</td><td>433.146</td></tr> <tr><td>No. of Rot. Bonds</td><td>8</td><td>No. of Bonds</td><td>34</td></tr> <tr><td>H acceptor</td><td>6</td><td>H donor</td><td>2</td></tr> <tr><td>Comment</td><td colspan="3"></td></tr> </table>	Type	2	Name	CLE121-butanolic	Rank	7	Score	23.83-	XLogP	3.834	Mol. weight	433.146	No. of Rot. Bonds	8	No. of Bonds	34	H acceptor	6	H donor	2	Comment																													
Type	2	Name	CLE121-butanolic																																																
Rank	7	Score	23.83-																																																
XLogP	3.834	Mol. weight	433.146																																																
No. of Rot. Bonds	8	No. of Bonds	34																																																
H acceptor	6	H donor	2																																																
Comment																																																			

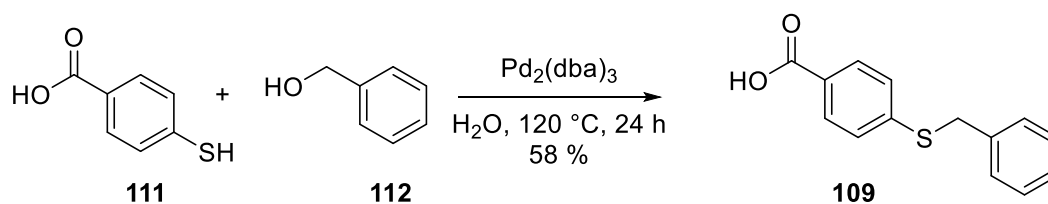
Both top compounds are supposed to mimic the amide of *N*-acyl lysine with a *N*-methyl arylcarboxamide residue at position 8 of the phenanthridine. The phenyl and thienyl ring serve as spacer unit to overcome the distance in between the phenanthridine ring and the location of the endogenous substrate. The introduction of the respective arylcarboxamide was planned late stage *via* SUZUKI cross-coupling, using the respective arylboronic acid **106**. For this cross-coupling reaction, the phenanthridine needs a suitable halogen residue at position 8. To achieve the best possible conditions for the SUZUKI cross-coupling, iodine was chosen as halogenide. Because selective halogenation of the phenanthridine is rather difficult, the residue needs to be introduced to the molecule already from the beginning. Therefore, 4'-iodo-biphenyl-2-amine **110** is needed as starting material for the amide coupling leading to amide **108**, which can then be cyclized to the required 8-iodophenanthridine **107**. Because it was already known from the previous syntheses that sulfonamides are problematic during the

cyclization reaction, it had to be “protected” or introduced after the cyclization, as already done for sulfonamides **38-40** and **70**. In this case bromine served as placeholder and the sulfur residue was introduced via cross-coupling reaction with benzyl mercaptan (**67**). However, since another cross-coupling reaction was planned, the bromine residue at the phenyl linker was not a suitable placeholder for the cyclization reaction. This time, the thioether needs to be introduced before amide coupling and cyclization. Thus, the second starting material required for this approach, was benzylthiobenzoic acid **109**. Retrosynthesis of the generic potential substrate mimetic compound **104** is shown in Scheme 41.



Scheme 41 Retrosynthesis of potential substrate mimetic compounds with an additional aryl amide moiety at position 8 of the phenanthridine.

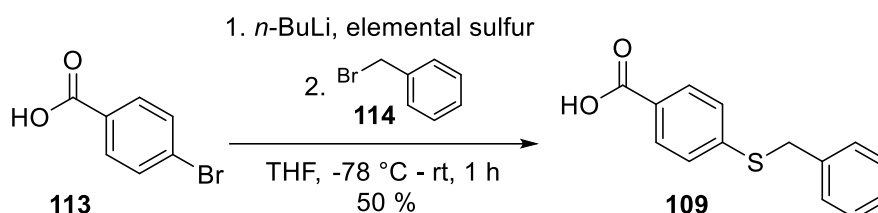
The first attempt for the synthesis of benzylthioethercarboxylic acid **109**, was the direct benzylation of 4-mercaptobenzoic acid (**111**) with benzyl alcohol (**112**) under pressure in the presence of a palladium catalyst in water, described by HIKAWA *et al.* (Scheme 42)^[97].



Scheme 42 Synthesis of thioether **109** via direct benzylation.

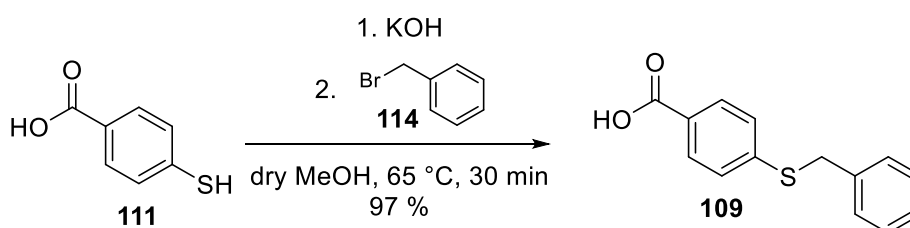
Even though the synthesis was successful, the yield was not sufficient, and the work up required to remove the palladium catalyst was extremely difficult, especially during scale-up. Thus, this approach was not suitable, as this building block was required in larger quantities.

An alternative approach followed a procedure from HAM *et al.* starting from 4-bromobenzoic acid (**113**)^[98]. After a bromo-lithium exchange with *n*-BuLi, elemental sulfur is added to the reaction mixture. The resulting thiolate is treated with benzyl bromide (**114**) to give the desired benzyl thioether (Scheme 43). The reaction worked in small scale (50 % yield at 2 mmol scale) but gave a very complex mixture of impurities during scale up which led to only 12 % yield in 10 mmol scale.



Scheme 43 Synthesis of thioether **109** via bromo-lithium exchange, addition of elemental sulfur and S-benylation with benzyl bromide (**114**).

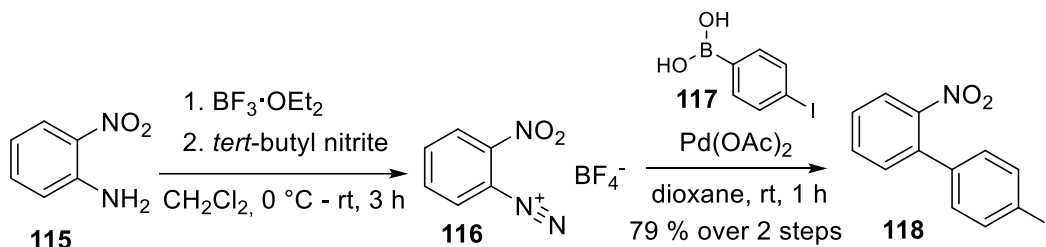
Finally successful was the synthesis of thioether **109** when preparing the thiolate by deprotonation of the before used 4-mercaptobenzoic acid (**111**) with an excess of KOH in anhydrous MeOH and subsequently adding benzyl bromide (**114**) (Scheme 44). This reaction gave the desired building block in good yield in a scale up to 20 mmol (97 % yield for 5 mmol, 80 % yield for 20 mmol).



Scheme 44 Synthesis of thioether **109** via deprotonation and S-benylation with benzyl bromide (**114**).

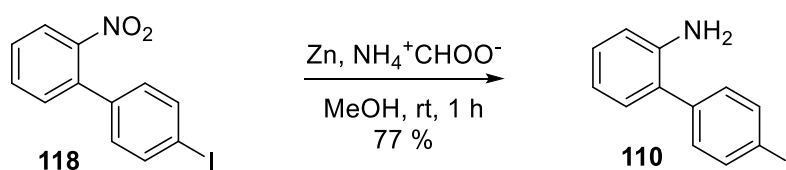
Having the first required starting material for the amide coupling in hands, the next step was finding a suitable procedure for the second starting material, iodinated biphenyl amine **110**. Biphenyls are commonly constructed via SUZUKI cross-coupling reactions, but in this case, the product itself is supposed to bear an iodine residue. This is why reaction conditions had to be found, that would prevent the iodine from either reacting or de-halogenating. A promising approach was the coupling of 4-iodophenylboronic acid **117**, which brings in the iodine for the envisaged 8-iodophenanthridine **107**, with 2-nitrophenyl diazonium salt **116**. The nitro group can later be reduced to the desired primary amine. For the coupling of arene diazonium salts with boronic acids, only palladium is required as catalyst, but no ligand nor base^[99]. These

conditions lead to a selective cross-coupling. The required 2-nitrophenyl diazonium tetrafluoroborate (**116**) was synthesized from 2-nitroaniline (**115**) with boron trifluoride etherate and *tert*-butyl nitrite, as described by KUETHE *et al.*^[100]. The following coupling reaction with 4-iodophenylboronic acid (**117**) gave the desired biphenyl **118** in 79 % yield over two steps (Scheme 45)^[100].



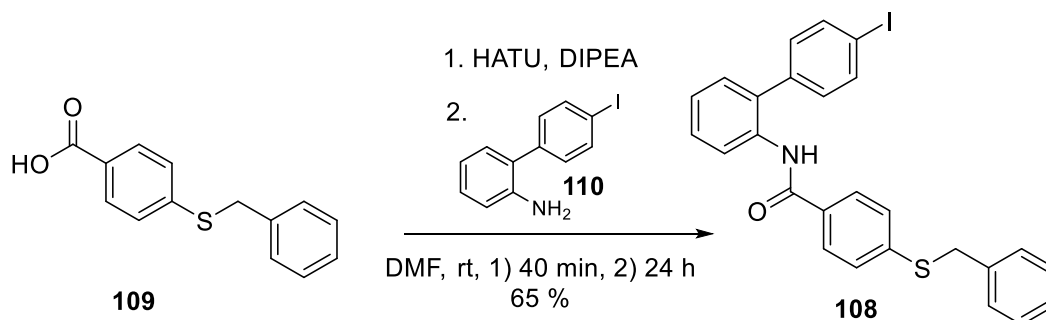
Scheme 45 Synthesis of nitrobiphenyl **118**.

The obtained 4'-iodo-2-nitro-1,1'-biphenyl (**118**) was reduced with zinc to the desired 4'-iodo-[1,1'-biphenyl]-2-amine (**110**) according to a procedure from ANNAMALAI *et al.*^[101] with 77 % yield (Scheme 46).



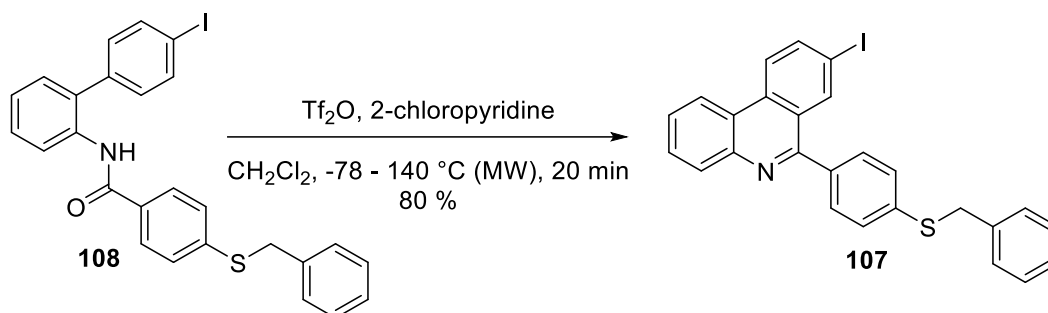
Scheme 46 Reduction of nitrobiphenyl **118** to aminobiphenyl **110**.

With benzoic acid **109** and aminobiphenyl **110** available, the next challenge was to find reaction conditions for the amide coupling. The objective was to find conditions, where no excess of the amine is required, as this starting material is more challenging and expensive to prepare. Therefore, a procedure used by CARINA GLAS^[102] from our group was chosen, where 1.5 eq carboxylic acid are activated with HATU in the presence of DIPEA in DMF, followed by the addition of the amine. Using this method, benzoic acid **109** was successfully activated and upon addition of aminobiphenyl **110** to the reaction mixture, amide **108** was obtained in sufficient yield (Scheme 47).



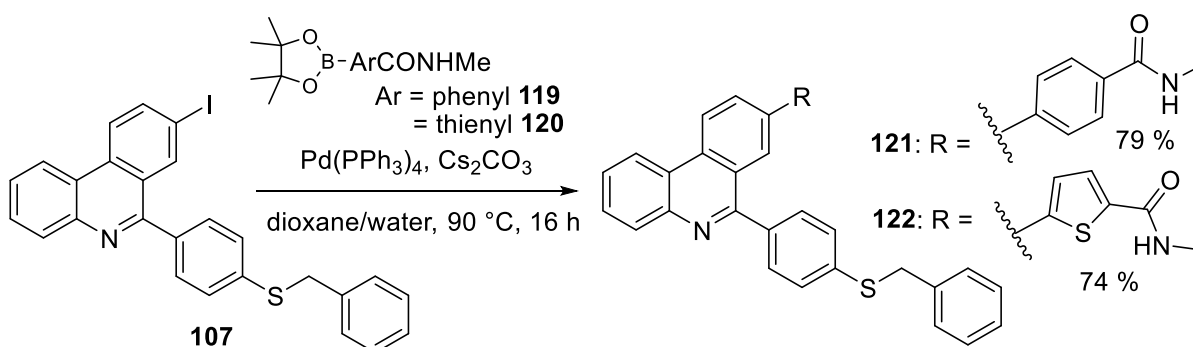
Scheme 47 Synthesis of amide **108**.

The next step was the cyclodehydration reaction, which followed the same procedure from MOVASSAGHI^[75] as described before. The key intermediate, benzylthio-substituted 8-iodophenanthridine **107** was obtained in good yield (Scheme 48).



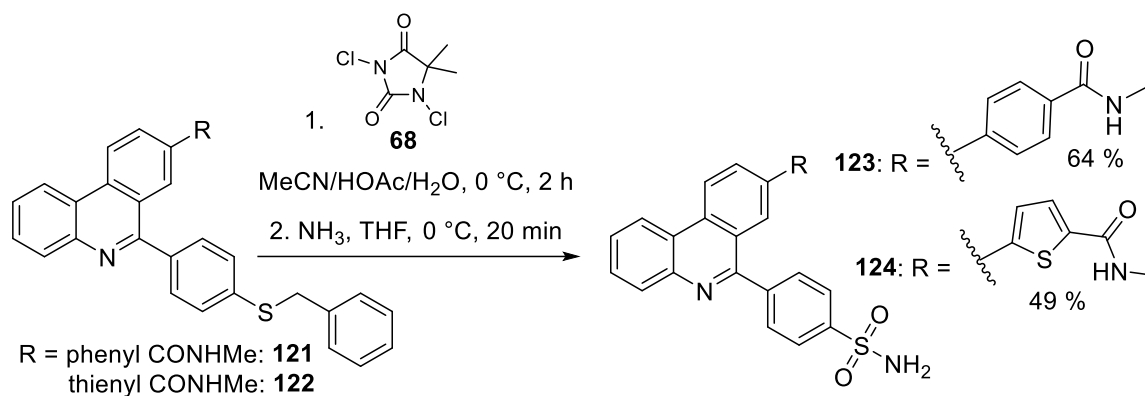
Scheme 48 Synthesis of 8-iodophenanthridine **107**.

Because poor solubility of the phenanthridine sulfonamides was already observed during the syntheses of sulfonamide **38** (Chapter 3.2.4), the SUZUKI cross-coupling for the introduction of the substrate mimicking residue was carried out with benzyl thioether **107** rather than the final sulfonamide. To purge palladium catalysts, purification by FCC is required and this is difficult to achieve with a poorly soluble compound. A procedure from BREHOVA *et al.*^[103] using pinacolboronate **119** and pinacolboronate **120** with tetrakis(triphenylphosphine)-palladium(0) as catalyst and caesium carbonate as base in dioxane/water 4:1 gave the desired phenanthridinyl arylcarboxamides **121** and **122** in good yield (Scheme 49).



Scheme 49 Introduction of the desired arylcarboxamide residues *via* SUZUKI cross-coupling.

Finally, the benzyl thioether residues in **121** and **122** had to be converted to the envisaged primary sulfonamides. The same procedure as used for the synthesis of compound **38** was used^[87]. Oxidative chlorination with dichlorohydantoin **68**, followed by treatment of the intermediate sulfonyl chloride with ammonia, gave the target compounds **123** and **124** (Scheme 50).



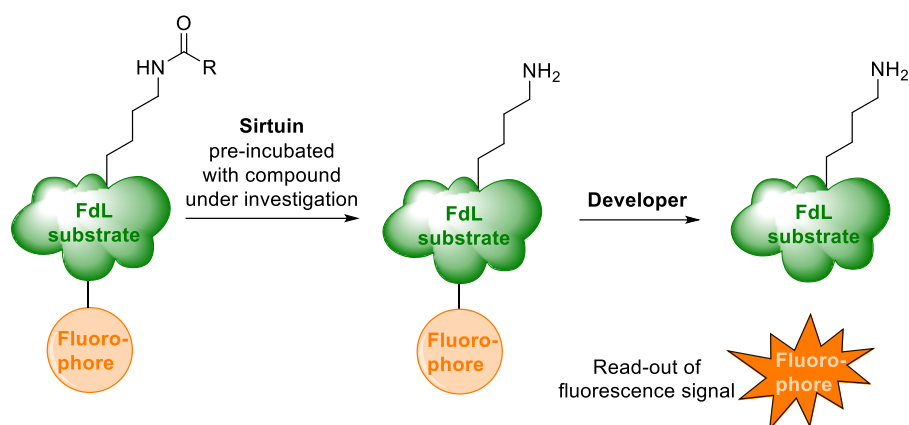
Scheme 50 Synthesis of target sulfonamide compounds **123** and **124**.

Both obtained compounds **123** and **124** showed very poor solubility, barely 3 mg/mL dissolved in DMSO for NMR analysis. Equally the high melting points (**123**: mp. = 343-345 °C, **124**: mp. = 333-335 °C) indicated very strong intermolecular interactions of these planar compounds. These unfavourable physicochemical properties not only complicated purification and chemical characterization, but also hampered the assessment of biological activity (more details in Chapter 3.2.7). Attempts to convert the phenanthridine bases into better soluble hydrochloric acid salts were unsuccessful.

3.2.7 Results from biological testing

3.2.7.1 Evaluation as Sirtuin 6 modulators

All synthesized target compounds were tested by using the Fluor de Lys (FdL) assay for their biological activity against Sirtuin 6 at University of Bayreuth by DR. WEIJE YOU in the group of PROF. DR. CLEMENS STEEGBORN. For this assay, an acylated substrate of the respective sirtuin is linked to a fluorophore. Upon addition of active sirtuin, the substrate is deacylated, which is sensitising the substrate to the developer solution. The developer solution then cleaves the fluorophore from the deacylated substrate, and the amount of free fluorophore can be measured (Scheme 51). The fluorescence signal is directly proportional to the deacylase activity of the sirtuin, which infers in turn the biological activity of a test compound.



Scheme 51 Principle of the Fluor de Lys assay (FdL).

Screening for effect on deacetylation activity of Sirtuin 6

KV-30 was initially tested at three different concentrations (1 μM , 10 μM , and 100 μM) and inhibited Sirtuin 6 to approx. 40 % at 10 μM and to approx. 80 % at 100 μM (Figure 27).

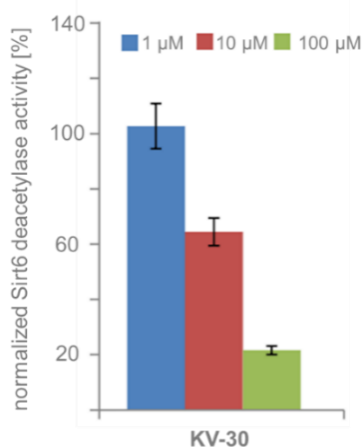


Figure 27 Effect of **KV-30** on Sirtuin 6 at 1 μM (no inhibition), 10 μM (40% inhibition) and 100 μM (80% inhibition).

Because **KV-30** inhibits Sirtuin 6 already at 10 μM , the screening of all synthesized target compounds was done at minimum 5 μM and 25 μM .

Compounds with small polar residue at the phenyl ring (nitrobenzene **29**, aniline **30** and aldehyde **31**; all structures are shown in the following Table 3, p. 151) were tested at 1 μM , 5 μM , and 25 μM had no noteworthy effect on Sirtuin 6 (Figure 28).

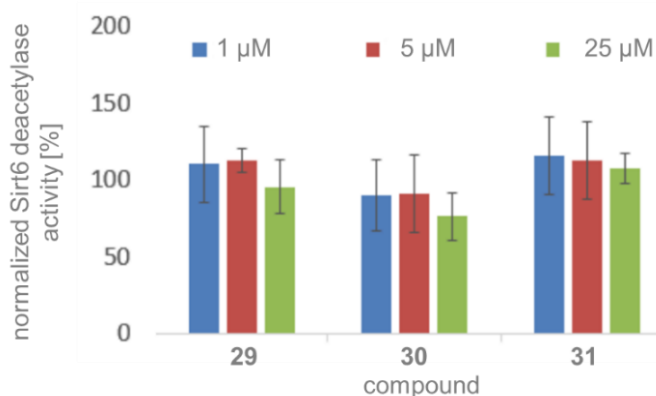


Figure 28 Screening results of compounds **29-31** at 1 μM , 5 μM , and 25 μM .

The replacement of the hydroxamic acid with bioisosters led in most cases to a loss of activity (amidoxime **33**, hydrazide **34**, thiohydrazide **35**, trifluoromethyl ketone **36** and trifluoromethyl oxime **37**). Carboxamide **32** (CLE-115) and sulfonamide **38** (CLE-121) however retained the inhibitory activity against Sirtuin 6. Sulfonamide **38** (CLE-121) inhibits Sirtuin 6 to approx. 45 % at 5 μM and 75 % at 25 μM . *N*-Monomethyl sulfonamide **39** and *N,N*-dimethyl sulfonamide **40** no longer have an inhibitory effect, showing that the primary sulfonamide group is crucial for Sirtuin 6 inhibition. The screening results of compounds **32-40** are shown in Figure 29.

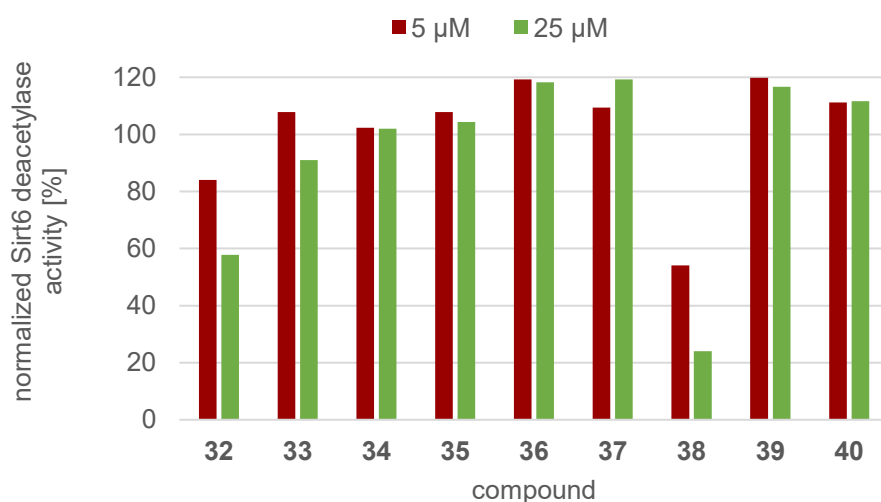


Figure 29 Screening results of bioisosteric compounds **32-40** at 5 μM and 25 μM .

Compounds with a *N*-hydroxyethyl residue, which was introduced with the intent to replace the water molecule present in the Sirtuin 6-**KV-30** co-crystal (*N*-hydroxyethyl hydroxamate **69**, *N*¹-hydroxyethyl hydrazide **70** and *N*-hydroxyethyl sulfonamide **71**), were inactive towards Sirtuin 6 (Figure 30). This is potentially due to the limited space in the binding pocket and therefore larger residues do not fit in anymore.

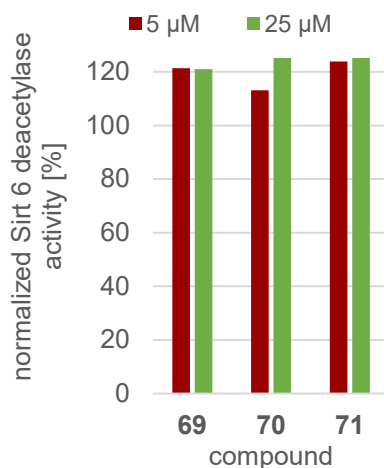


Figure 30 Screening results of *N*-hydroxyethyl compounds **69-71** at 5 μM and 25 μM.

The potential substrate mimetic compounds **123** and **124** were also tested but gave ambiguous results. Both compounds inhibit Sirtuin 6 at the 1 μM level. However, the inhibitory activity for compound **123** at 25 μM was lower than at 5 μM. Compound **124** gave a negative signal at 5 μM and 25 μM. The results are shown in Figure 31. These issues could be related to auto fluorescence of the compounds or to their poor solubility. Thus, these compounds would need further optimization for improved solubility, to be suitable for the FdL assay.

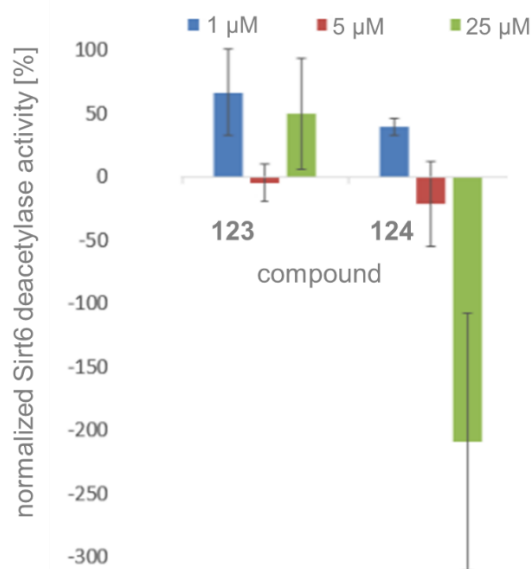


Figure 31 Screening results for potential substrate mimetic compounds **123** and **124**.

Determination of IC₅₀ values for Sirtuin 6 deacetylation

IC₅₀ values were determined for the most promising compounds from the initial screening, **KV-30** and CLE-121 (**38**), by plotting the %Sirt6 deacetylase activity against the concentration range. The IC₅₀ obtained for CLE-121 (**38**) is in the low micromolar range (2.2 μM). The concentration-effect relationship of **KV-30** (black squares) and CLE-121 (white circles) is shown in Figure 32.

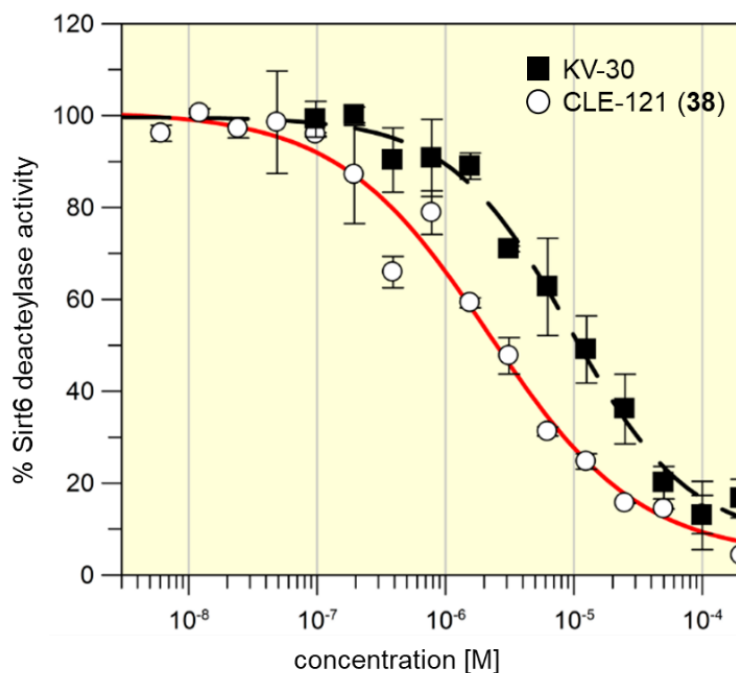


Figure 32 Concentration-effect relationship of CLE-121 (**38**) and **KV-30**.

The Sirtuin 6 deacetylation inhibitory activity of hydroxamic acid **KV-30** and the novel sulfonamide CLE-121 (**38**) are in the same order of magnitude, with the sulfonamide being even slightly more potent. Thus, the intended replacement of the hydroxamic acid by a less problematic functional group was successful. Sulfonamides are a common structure motif in biologically active compounds and possess no inherent cytotoxicity. Also there is no unwanted side effect due to the complexation with zinc ions expected.

With an IC₅₀ of 2.2 μM, sulfonamide **38** (CLE-121) is equipotent as the thus far most potent published inhibitor **JYQ-42** (IC₅₀: 2.33 μM)^[64]. However, further studies are required, to fully characterize the pharmacological profile of the newly developed phenanthridine based sulfonamide inhibitor CLE-121 (**38**).

Selectivity of deacetylation inhibition

To further characterize the activity profiles of **KV-30** and CLE-121 (**38**), they were tested on Sirtuins 1-3 and Sirtuin 5 for selectivity studies. CLE-121 (**38**) was tested at 3.125 μM and 12.5 μM showing no effect on Sirtuins 1-3 and Sirtuin 5. Sirtuin 6 was inhibited to approx. 50 % at 3.125 μM and 90 % at 12.5 μM respectively (Figure 33).

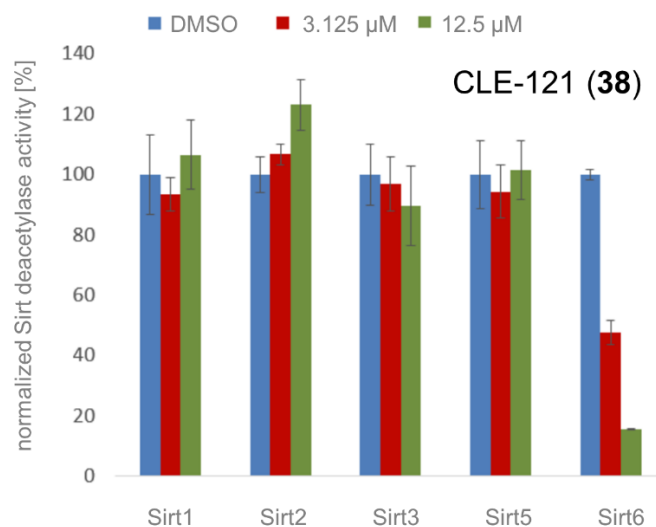


Figure 33 Selectivity screening of CLE-121 (**38**).

KV-30 was tested at 12.5 μM and 50 μM and inhibited Sirtuin 6 at these concentrations to approx. 50 % and 80 %. Sirtuin 3 was inhibited by **KV-30** to approx. 15 % at 12.5 μM and 60 % at 50 μM . The results for the **KV-30** selectivity screening are shown in Figure 34.

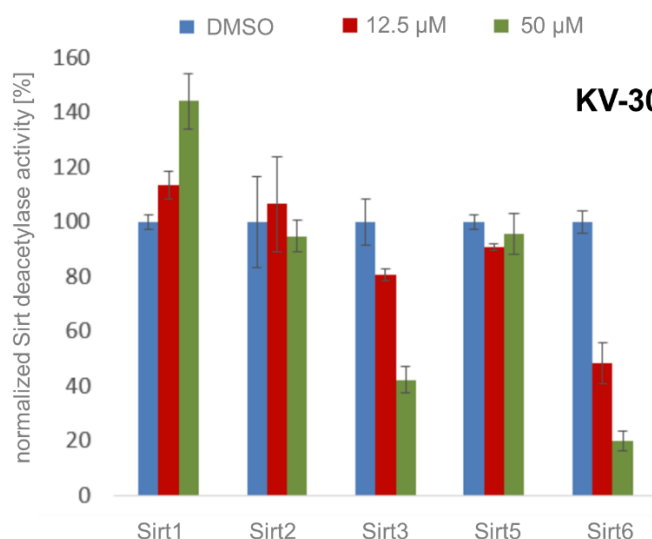


Figure 34 Selectivity screening of **KV-30**.

The results indicate that CLE-121 has a more promising selectivity profile (no inhibition at 12.5 μM) than **KV-30**, albeit testing at higher concentrations ($\geq 50 \mu\text{M}$) is still pending.

Screening for effect on demyristoylation activity of Sirtuin 6

During the time of the ongoing investigation of the compounds' biological activity, DR. WEIJE You unfortunately left the University of Bayreuth without a successor for the Sirtuin 6 project. Therefore, it wasn't possible to obtain further results nor follow up on some open points. To allow the project to proceed, compounds which showed an effect on Sirtuin 6 were additionally tested by BPS Bioscience Inc. in San Diego, using a commercially available test kit for Sirtuin 6. The commercially available test kit for Sirtuin 6 is using a myristoylated substrate. **KV-30** and CLE-121 (**38**) are both able to inhibit Sirtuin 6 demyristoylation. **KV-30** is inhibiting Sirtuin 6 demyristoylation to 33 % at 10 μ M and to 51 % at 25 μ M. CLE-121 (**38**) shows a 30 % and 35 % inhibition respectively at the same concentrations. Carboxamide **32** (CLE-115) shows no noteworthy demyristoylation inhibition. Nicotinamide (NAM) was used as a positive control at 1 μ M, 50 μ M, and 100 μ M. The results are shown in Figure 35.

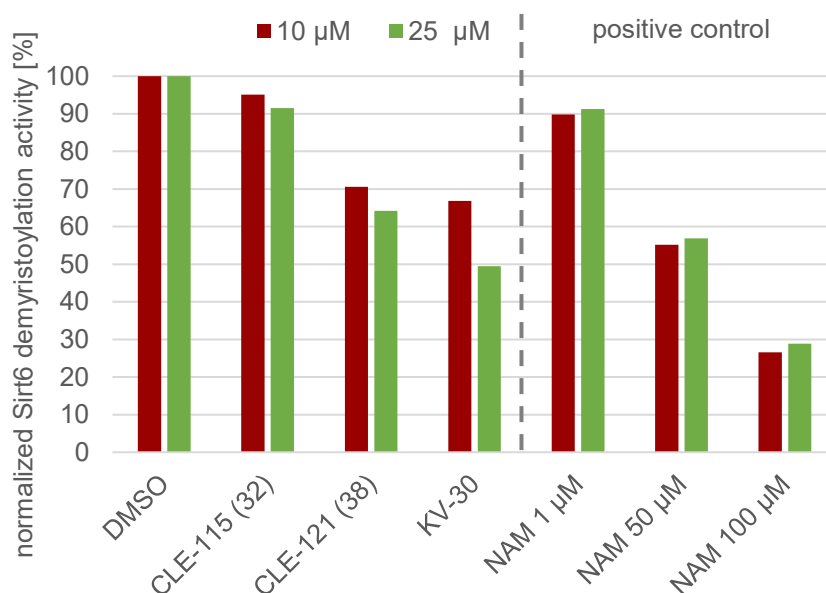
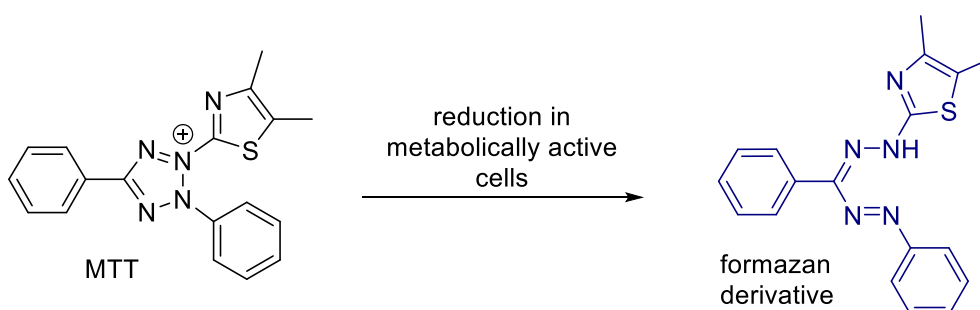


Figure 35 Results for CLE-115 (**32**), CLE-121 (**38**) and **KV 30** demyristoylation activity.

3.2.7.2 MTT assay

Before compounds are used in cellular assays, it is important to know about their cytotoxicity. Therefore, compounds are routinely tested in the MTT assay by MARTINA STADLER in our group. This assay is using humane leukemia cells (HL-60).

Basis of this assay developed by MOSMANN is the metabolic activity of living cells, which is required to reduce 3-(4,5-dimethylthiazol-2-yl)-2,5-diphenyltetrazolium bromide (MTT) to the respective formazan^[104]. This formazan derivative is intensely blue colored (Scheme 52) and therefore its concentration, which is directly proportional to the number of metabolically active living cells, can be read out photometrically.



Scheme 52 Reaction of MTT to formazan in living cells.

KV-30 was already known to exhibit moderate cytotoxicity ($IC_{50} = 8.6 \mu M$)^[74] and is therefore to be used with caution in cellular assays. In contrast, CLE-121 (**38**) can be considered non-toxic ($IC_{50} > 50 \mu M$), and its use in cellular assays is unproblematic. Most of the other compounds from this study are non-toxic as well ($IC_{50} > 50 \mu M$), only aldehyde **31**, trifluoromethyl oxime **37**, *N*-hydroxyethyl hydroxamate **69**, *N*-hydroxyethyl sulfonamide **71** and *N*-methylbenzamide derivative **123** showed some weak activity in the MTT assay (IC_{50} values $\sim 35 \mu M$). This is supporting the hypothesis, that **KV-30**'s cytotoxicity is mainly due to the hydroxamic acid functionality. The results are shown in Table 3.

Biological evaluation of Sirtuin 6 modulators

Table 3 Results from the cytotoxicity screening (MTT assay).

compound	structure	IC ₅₀ [μM]	compound	structure	IC ₅₀ [μM]
KV-30		8.6 ^[74]	37		>50
29		>50	38 (CLE-121)		>50
30		>50	39		>50
31		33	40		>50
32 (CLE-115)		>50	69		35
33		>50	70		>50
34		>50	71		35
35		>50	123		36
36		35	124		>50

3.2.7.3 Agar diffusion assay

Additionally, all final compounds were tested routinely in the BRACHER group by MARTINA STADLER for their antimicrobial and antifungal effects in a standard agar diffusion assay. This assay is based on the formation of growth inhibition zones. Test platelets are impregnated with a solution of the compound of interest and placed on agar plates, which contain appropriate growth medium. The plates are incubated with the respective bacteria or fungi and the applied compounds can then diffuse into the medium to inhibit growth of the microorganisms. As positive control, tetracycline (broad-spectrum antibiotic) and clotrimazole (broad-spectrum antifungal agent) were included in all experiments.

None of the synthesized target compounds showed any antimicrobial effect towards the investigated bacteria (*Escherichia coli*, *Pseudomonas marginalis*, *Straphylococcus equorum*, *Streptococcus entericus*) and fungi/yeasts (*Yarrowia lipolytica*, *Saccharomyces cerevisiae*).

3.2.8 Experimental part for Sirtuin 6 modulators

3.2.8.1 Chemistry

All chemicals used were of analytical grade and were obtained from abcr (Karlsruhe, Germany), Fisher Scientific (Schwerte, Germany), Sigma-Aldrich (now Merck, Darmstadt, Germany), TCI (Eschborn, Germany) or Th. Geyer (Renningen, Germany). HPLC grade and dry solvents were purchased from VWR (Darmstadt, Germany) or Sigma-Aldrich, all other solvents were purified by distillation. All reactions were monitored by thin-layer chromatography (TLC) using pre-coated plastic sheets POLYGRAM® SIL G/UV254 from Macherey-Nagel and detected by irradiation with UV light (254 nm) or by staining with appropriate reagents. Flash column chromatography (FCC) was performed on Macherey-Nagel silica gel Si 60 (0.015 – 0.040 mm). NMR spectra (¹H, ¹³C, DEPT, H-H-COSY, HSQC, HMBC) were recorded at 23 °C on an Avance III 400 MHz Bruker BioSpin or Avance III 500 MHz Bruker BioSpin instrument. Chemical shifts δ are stated in parts per million (ppm) and are calibrated using residual protic solvent as an internal reference for proton (CDCl₃: δ = 7.26 ppm, CD₂Cl₂: δ = 5.32 ppm, DMSO-*d*₆: δ = 2.50 ppm) and for carbon the central carbon resonance of the solvent (CDCl₃: δ = 77.16 ppm, CD₂Cl₂: δ = 53.84 ppm, DMSO-*d*₆: δ = 39.52 ppm). Multiplicity is defined as s = singlet, d = doublet, t = triplet, m = multiplet. NMR spectra were analysed with NMR software MestReNova, version 12.0.1-20560 (Mestrelab Research S.L.). High resolution mass spectra were performed by the LMU Mass Spectrometry Service applying a Thermo Finnigan LTQ FT Ultra Fourier Transform Ion Cyclotron Resonance device at 250 °C for ESI and a Thermo Q Exactive GC Orbitrap device at 250 °C and an electron energy of 70 eV for EI. IR spectra were recorded on a Perkin Elmer FT-IR Paragon 1000 instrument as neat materials. Absorption bands were reported in wave number (cm⁻¹) with ATR PRO450-S. Melting points were determined by the open tube capillary method on a Büchi melting point B-540 apparatus and are uncorrected. HPLC purities were determined using an Agilent 1100 HPLC with a diode array detector and an Agilent Zorbax Eclipse plus C18 column (150 × 4.6 mm; 5 μ m) with methanol/water in different ratios, neutral or pH adjusted with NaOH or triethylamine.

General procedure 1 (GP1): Amide coupling of aminobiphenyl with benzoyl chlorides

To a stirred solution of 2-aminobiphenyl in ethyl acetate (0.3M) was added triethylamine (1.1 eq), followed by portion wise addition of the appropriate benzoyl chloride (1.1 eq) at 0 °C. The resulting suspension was stirred at rt for 1h, then diluted with ethyl acetate and washed with sat. aq. NaHCO₃ solution. The aqueous layer was extracted with ethyl acetate, dried using a phase separation filter and the solvent removed *in vacuo*. The residue was crystallized either from ethyl acetate/hexanes or isopropanol.

General procedure 2 (GP2): Cyclodehydration of aryl amides

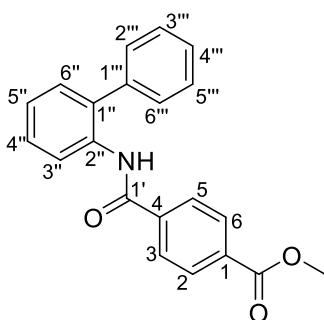
The appropriate aryl amide was dissolved in dry methylene chloride (~0.2M, depending on solubility of the starting material) in a microwave vial under nitrogen atmosphere and 2-chloropyridine (1.2 eq) was added. The solution was cooled to -78 °C and trifluoromethanesulfonic anhydride was added dropwise. The mixture was allowed to warm up to 0 °C, stirred for 5 min, warmed up to rt and stirred for an additional 5 min. Subsequently the vial was placed into the microwave and heated to 120 °C (max. pressure 145 psi) for 10 min. After cooling the mixture was poured into a mixture of ice and 2M NaOH and extracted 3 times with methylene chloride. The combined organic layers were dried using a phase separation filter, the solvent removed *in vacuo* and the residue crystallized or purified by FCC.

General procedure 3 (GP3): Hydrolysis of benzyl thioethers to sulfonamides

The benzyl thioether was suspended in a mixture of acetonitrile/acetic acid/water (40:1.5:1) (~0.1M), was cooled to 0 °C and was stirred for 15 min. Subsequently 1,3-dichloro-5,5-dimethylhydantoin was added and the mixture was stirred for 2 h. The solvent was removed *in vacuo*, the residue was taken up in methylene chloride, 5% NaHCO₃ solution was added, and the biphasic system was stirred for another 15 min. The layers were separated, and the aqueous layer was extracted twice with methylene chloride. The combined organic layers were dried using a phase separating filter, the solvent was removed *in vacuo* and the crude sulfonyl chloride was used without further purification. The crude sulfonyl chloride was dissolved in tetrahydrofuran or acetonitrile (~0.1M) and a solution of the appropriate amine in tetrahydrofuran or water was added dropwise at 0 °C. The resulting mixture was stirred at rt for 15 min, then water was added, and the solution was neutralized with hydrochloric acid. The reaction mixture was extracted with ethyl acetate three times, the combined organic layers were dried using a phase separation filter and the solvent was removed *in vacuo*. The residue was purified by trituration or crystallization from isopropanol or ethanol.

General procedure 4 (GP4): SUZUKI coupling of iodophenanthridines

Iodophenanthridine (1 eq), the appropriate boronic acid or boronic pinacol ester (3 eq), Pd(PPh₃)₄ (0.1 eq), and caesium carbonate (3 eq) were suspended in prior degassed dioxane/water (4:1, ~ 0.1M) and were heated to 90 °C. The mixture was stirred at this temperature for 16 h. Upon complete consumption of iodophenanthridine, water was added, and the mixture was extracted with ethyl acetate. The combined organic layers were washed with brine, were dried using a hydrophobic filter and the solvents were removed *in vacuo*. The residue was purified by FCC (CH₂Cl₂/MeOH 98:2) to give the desired substituted phenanthridine.

Methyl 4-([1,1'-biphenyl]-2-ylcarbamoyl) benzoate (17**)**^[105]

 $C_{21}H_{17}NO_3$

331.37 g/mol

Amide **17** was synthesized according to GP1, using 2-aminobiphenyl (1.69 g, 10.0 mmol) and 4-cyanobenzoyl chloride (2.19 g, 11.0 mmol). Purification was achieved through crystallization from ethyl acetate/petrol ether to obtain amide **17** as off-white solid (2.95 g, 8.91 mmol, 89 %).

mp.: 173 – 175 °C (lit.^[105] 181.3 – 182.0 °C).

¹H NMR (500 MHz, CDCl₃): δ (ppm) = 8.52 (d, J = 8.3 Hz, 1H, 3''-H), 8.07 – 8.03 (m, 2H, 2-, 6-H), 8.00 (s, 1H, NH), 7.67 – 7.63 (m, 2H, 3-, 5-H), 7.55 – 7.50 (m, 2H, 3'''-, 5''-H), 7.48 – 7.42 (m, 4H, 4''-, 4'''-, 2'''- 6'''-H), 7.32 (dd, J = 7.6, 1.7 Hz, 1H, 6''-H), 7.24 (dd, J = 7.5, 1.2 Hz, 1H, 5''-H), 3.93 (s, 3H, CH₃).

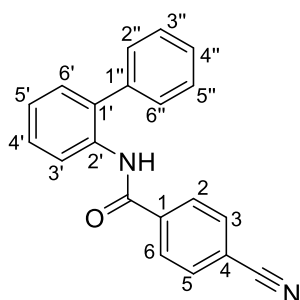
¹³C NMR (126 MHz, CDCl₃): δ (ppm) = 166.2 (COOR), 164.0 (CONH), 138.7 (C-4), 137.9 (C-1'''), 134.6 (C-2''), 132.9 (C-1), 132.5 C-1''), 130.0 (C-6''), 130.0 (C-2, -6), 129.4 (C-3'', -5''), 129.3 (C-2'', -6''), 128.7 (C-4''), 128.3 (C-4'''), 126.9 (C-3, -5), 124.7 (C-5''), 121.1 (C-3''), 52.4 (CH₃).

IR (ATR): $\tilde{\nu}$ [cm⁻¹] = 3230, 1727, 1639, 1536, 1276, 1108, 740.

HRMS (EI): m/z [M]⁺ calcd. for C₂₁H₁₇NO₃⁺: 331.1208, found: 331.1202.

Purity (HPLC): >96 % (210 nm, 254 nm).

***N*-([1,1'-Biphenyl]-2-yl)-4-cyanobenzamide (**41**)^[105]**



$C_{20}H_{14}N_2O$

298.34 g/mol

Amide **41** was synthesized according to GP1, using 2-aminobiphenyl (508 mg, 3.00 mmol) and 4-cyanobenzoyl chloride (546 mg, 3.30 mmol). Purification was achieved through crystallization from ethyl acetate/petrol ether to obtain amide **41** as off-white solid (760 mg, 2.55 mmol, 85 %).

mp.: 136 – 138 °C (lit.^[105] 134.0 – 134.5 °C)

¹H NMR (500 MHz, CDCl₃): δ (ppm) = 8.48 (d, J = 8.2 Hz, 1H, 3'-H), 7.96 (s, 1H, NH), 7.72 – 7.64 (m, 4H, 2-,3-,5-,6-H), 7.55 – 7.50 (m, 2H, 3''-, 5''-H), 7.49 – 7.41 (m, 4H, 4'-, 4''-, 2''-, 6''-H), 7.33 (dd, J = 7.6, 1.7 Hz, 1H, 6'-H), 7.28 – 7.24 (m, 2H, 5'-H).

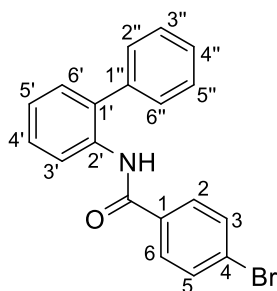
¹³C NMR (126 MHz, CDCl₃): δ (ppm) = 163.1(C=O), 138.7 (C-1), 137.8 (C-1''), 134.3 (C-2''), 132.6 (C-3,-5 and C-1'), 130.1 (C-6'), 129.4 (C-2'',-6'' or C-3'', -5''), 129.3 (C-2'',-6'' or C-3'', -5''), 128.7 (C-4'), 128.5 (C4''), 127.5 (C-2, -6), 125.0 (C-5'), 121.2 (C-3'), 117.8 (CN), 115.4 (C-4).

IR (ATR): $\tilde{\nu}$ [cm⁻¹] = 3230, 2230, 1644, 1530, 1320, 852, 745.

HRMS (EI): m/z [M]⁺ calcd. for C₂₀H₁₄N₂O⁺: 298.1106, found: 298.1101.

Purity (HPLC): >96 % (210 nm, 254 nm).

***N*-([1,1'-Biphenyl]-2-yl)-4-bromobenzamide (**42**)^[106]**



C₁₉H₁₄BrNO

352.23 g/mol

Amide **42** was synthesized according to GP1, using 2-aminobiphenyl (846 mg, 5.00 mmol) and 4-bromobenzoyl chloride (1.20 g, 5.50 mmol). Purification was achieved through crystallization to obtain amide **42** as off-white solid (1.24 g, 5.51 mmol, 70 %).

mp.: 122 – 124 °C (lit.^[106] 121 °C)

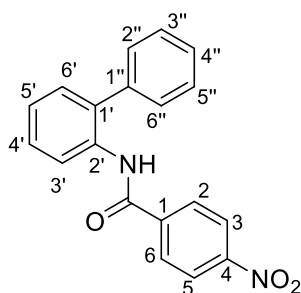
¹H NMR (500 MHz, CDCl₃): δ (ppm) = 8.52 – 8.47 (m, 1H, 3'-H), 7.92 (s, 1H, NH), 7.55 – 7.49 (m, 4H, 3-, 5-, 3''-, 5''-H), 7.47 – 7.42 (m, 6H, 2-, 6-, 2''-, 6''-, 4'-, 4''-H), 7.31 (dd, *J* = 7.6, 1.6 Hz, 1H, 6'-H), 7.23 (td, *J* = 7.5, 1.2 Hz, 1H, 5'-H).

¹³C NMR (126 MHz, CDCl₃): δ (ppm) = 164.0 (C=O), 138.0 (C-1''), 134.7 (C-2'), 133.6 (C-1), 132.4 (C-1'), 132.0 (C-3, -5), 130.0 (C-6'), 129.3 (C-2'', -6'' or C-3'', -5''), 129.3 (C-2'', -6'' or C-3'', -5''), 128.7 (C-4'), 128.4 (C-2, -6), 128.3 (C-4''), 126.5 (C-4), 124.6 (C-5'), 121.1 (C-3').

IR (ATR): $\tilde{\nu}$ [cm⁻¹] = 3304, 2657, 1645, 1518, 1485, 1471, 1310, 1069, 1009, 837, 745, 703.

HRMS (EI): *m/z* [M]⁺⁺ calcd. for C₁₉H₁₄BrNO⁺⁺: 351.0259, found: 351.0255.

Purity (HPLC): >96 % (210 nm, 254 nm).

***N*-([1,1'-Biphenyl]-2-yl)-4-nitrobenzamide (**43**)^[105]**C₁₉H₁₄N₂O₃

318.33 g/mol

Amide **43** was synthesized according to GP1 using 2-aminobiphenyl (846 mg, 5.00 mmol) and 4-nitrobenzoyl chloride (2.78 g, 15.0 mmol). Due to poor solubility the excess of benzoyl chloride was needed, and it was pre-suspended in ethyl acetate (30 mL). The reaction mixture was carefully washed with saturated NaHCO₃. Crystallization from isopropanol gave amide **43** as light-yellow solid (1.39 g, 87 %).

mp.: 156 – 158 °C (lit. ^[105]109.5 – 110.0 °C).

¹H NMR (400 MHz, CD₂Cl₂): δ (ppm) = 8.42 (d, *J* = 8.2 Hz, 1H, 3'-H), 8.27 – 8.18 (m, 2H, 3-, 5-H), 7.98 (s, 1H, NH), 7.79 – 7.73 (m, 2H, 2-, 6-H), 7.56 – 7.50 (m, 2H, 3''-, 5''-H), 7.49 – 7.42 (m, 4H, 4''-H, 2''-, 6''-H, 4'-H), 7.36 (dd, *J* = 7.7, 1.7 Hz, 1H, 6'-H), 7.28 (td, *J* = 7.5, 1.2 Hz, 1H, 5'-H).

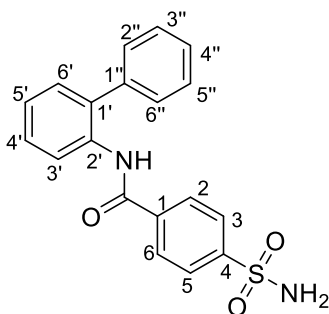
¹³C NMR (101 MHz, CD₂Cl₂): δ (ppm) = 163.4 (C=O), 150.1 (C-4), 140.8 (C-1), 138.2 (C-1''), 134.9 (C-2'), 133.5 (C-1'), 130.6 (C-6'), 129.7 (C-3'', -5''), 129.7 (C-2'', -6''), 128.9 (C-4' or C-4''), 128.8 (C-4' or C-4''), 128.4 (C-2, -6), 125.5 (C-5'), 124.3 (C-3, -5), 121.8 (C-3').

IR (ATR): $\tilde{\nu}$ [cm⁻¹] = 3231, 3052, 1644, 1600, 1535, 1521, 1344, 1325, 1308, 1011, 864, 855, 758, 704.

HRMS (ESI): *m/z* [M-H]⁻ calcd. for C₁₉H₁₃N₂O₃⁻: 317.0932, found: 317.0932.

Purity (HPLC): >96 % (210 nm, 254 nm).

***N*-([1,1'-Biphenyl]-2-yl)-4-sulfamoylbenzamide (64)**



C₁₉H₁₆N₂O₃S

352.41 g/mol

4-Sulfamoylbenzoic acid (424 mg, 2.00 mmol), EDCI (469 mg, 2.40 mmol), and HOBT (324 mg, 2.40 mmol) were dissolved in 2 mL dry DMF and were stirred at rt for 30 min. 2-Aminobiphenyl (406 mg, 2.40 mmol) and DMAP (73 mg, 0.60 mmol) were added, and the solution was stirred at 45 °C for 24 h. After cooling to rt, the mixture was diluted with ethyl acetate (30 mL) and was washed with saturated NaHCO₃ solution (2x 20 mL) and brine (1x 20 mL). The organic layer was dried using a hydrophobic filter and the solvent was removed *in vacuo*. The residue was purified by FCC (PE/EtOAc 1:1) to give amide **64** as colourless solid (327 mg, 0.928 mmol, 46 %).

mp.: 190 – 192°C.

¹H NMR (400 MHz, DMSO-*d*₆): δ (ppm) = 10.06 (s, 1H, NH), 7.89 (q, *J* = 8.5 Hz, 4H, 2-, 6-H, 3-, 5-H), 7.51 – 7.35 (m, 10H, SO₂NH₂, biphenyl-H), 7.32 – 7.27 (m, 1H, 4''-H).

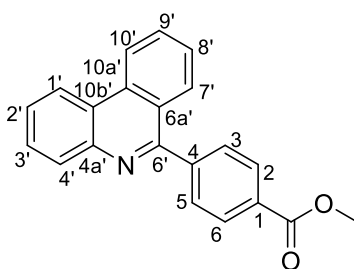
¹³C NMR (101 MHz, DMSO-*d*₆): δ (ppm) = 164.7 (C=O), 146.4 (C-4), 139.1 (C_q biphen.), 138.4 (C_q biphen.), 137.4 (C-1), 134.6 (C_q biphen.), 130.3 (CH biphen.), 128.6 (C-2'', -6''), 128.4 (CH biphen.), 128.2 (C-3'', -5''), 128.1 (C-2, -6), 127.9 (CH biphen.), 127.2 (C-4''), 127.1 (CH biphen.), 125.6 (C-3, -5).

IR (ATR): $\tilde{\nu}$ [cm⁻¹] = 3416, 3325, 3195, 3064, 2924, 1670, 1523, 1447, 1336, 1319, 1156, 914, 890, 858, 758, 749, 710.

HRMS (ESI): *m/z* [M-H]⁻ calcd. for C₁₉H₁₅N₂O₃S⁻: 351.0809, found: 351.0811.

Purity (HPLC): >96 % (210 nm, 254 nm).

Methyl 4-(phenanthridin-6-yl) benzoate (18**)**^[105]



C₂₁H₁₅NO₂

313.36 g/mol

Phenanthridine **18** was synthesized according to GP2, using amide **17** (994 mg, 3.00 mmol). Purification was achieved through crystallization from ethyl acetate/petrol ether to obtain phenanthridine **18** as off-white solid (850 mg, 2.71 mmol, 93 %).

mp.: 156 – 158 °C (lit.^[105] 158.8 – 158.9 °C).

¹H NMR (400 MHz, CDCl₃): δ (ppm) = 8.73 (ddd, *J* = 8.7, 1.1, 0.6 Hz, 1H, 10'-H), 8.64 (dd, *J* = 8.0, 1.5 Hz, 1H, 1'-H), 8.29 – 8.20 (m, 3H, 2-, 6-, 4'-H), 8.03 (ddd, *J* = 8.2, 1.3, 0.6 Hz, 1H, 7'-H), 7.89 (ddd, *J* = 8.3, 7.0, 1.3 Hz, 1H, 9'-H), 7.85 – 7.81 (m, 2H, 3-, 5-H), 7.78 (ddd, *J* = 8.2, 7.0, 1.5 Hz, 1H, 3'-H), 7.72 (ddd, *J* = 8.4, 7.1, 1.5 Hz, 1H, 2'-H), 7.64 (ddd, *J* = 8.3, 7.0, 1.2 Hz, 1H, 8'-H), 3.99 (s, 3H, CH₃).

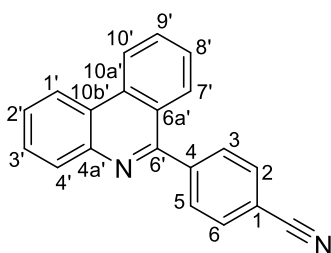
¹³C NMR (101 MHz, CDCl₃): δ (ppm) = 167.1 (COOR), 160.3 (C-6'), 144.4 (C-4), 143.9 (C-4a'), 133.6 (C-10a'), 130.9 (C-9'), 130.6 (C-4'), 130.5 (C-1), 130.0 (C-3, -5), 129.9 (C-2, -6), 129.2 (C-3'), 128.6 (C-7'), 127.5 (C-8'), 127.5 (C-2'), 125.1 (C-6a'), 124.0 (C-10b'), 122.5 (C-10'), 122.2 (C-1'), 52.4 (CH₃).

IR (ATR): $\tilde{\nu}$ [cm⁻¹] = 2949, 1724, 1609, 1430, 1274, 1102, 749, 723, 702.

HRMS (ESI): *m/z* [M+H]⁺ calcd. for C₂₁H₁₆NO₂⁺: 314.1176, found: 314.1177.

Purity (HPLC): >96 % (210 nm, 254 nm).

4-(Phenanthridin-6-yl) benzonitrile (44)^[105]



C₂₀H₁₂N₂
280.33 g/mol

Phenanthridine **44** was synthesized according to GP2, using amide **41** (149 mg, 0.500 mmol). Purification was achieved by FCC (PE/EtOAc 9:1) to obtain phenanthridine **44** as off-white solid (129 mg, 0.460 mmol, 92 %).

mp.: 177 – 179 °C. (lit.^[105] 174.9 – 175 °C)

¹H NMR (400 MHz, CDCl₃): δ (ppm) = 8.77 – 8.73 (m, 1H, 10'-H), 8.65 (dd, *J* = 8.1, 1.6 Hz, 1H, 1'-H), 8.26 – 8.21 (m, 1H, 4'-H), 7.99 (ddd, *J* = 8.3, 1.4, 0.7 Hz, 1H, 7'-H), 7.94 – 7.87 (m, 5H, 9', 2-, 3-, 5-, 6-H), 7.82 – 7.77 (m, 1H, 3'-H), 7.74 (ddd, *J* = 8.4, 7.0, 1.5 Hz, 1H, 2'-H), 7.66 (ddd, *J* = 8.2, 7.0, 1.2 Hz, 1H, 8'-H).

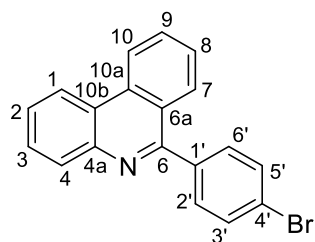
¹³C NMR (101 MHz, CDCl₃): δ (ppm) = 159.1 (C-6'), 144.3 (C-4), 143.6 (C-4'), 133.6 (C-10a'), 132.3 (C-2, -6), 131.0 (C-9'), 130.6 (C-3, -5), 130.5 (C-4'), 129.2 (C-3'), 128.0 (C-7'), 127.6 (C-2'), 127.5 (C-8'), 124.6 (C-6a'), 123.9 (C-10b'), 122.6 (C-10'), 122.1 (C-1'), 118.7 (CN), 112.6 (C-1).

IR (ATR): $\tilde{\nu}$ [cm⁻¹] = 3063, 2225, 1610, 1363, 1030, 843, 750, 723.

HRMS (ESI): *m/z* [M+H]⁺ calcd. for C₂₀H₁₃N₂⁺: 281.1073, found: 281.1072.

Purity (HPLC): >96 % (210 nm, 254 nm).

6-(4-Bromophenyl) phenanthridine (45)^[107]



C₁₉H₁₂BrN
334.22 g/mol

Phenanthridine **45** was synthesized according to GP2, using amide **42** (176 mg, 0.500 mmol). Purification was achieved by FCC (PE/EtOAc 9:1) to obtain phenanthridine **45** as off-white solid (132 mg, 0.395 mmol, 79 %).

mp.: 169 – 171 °C (lit.^[107] 164 – 165 °C)

¹H NMR (400 MHz, CDCl₃): δ (ppm) = 8.78 – 8.71 (m, 1H, 10-H), 8.69 – 8.62 (m, 1H, 1-H), 8.29 – 8.22 (m, 1H, 4-H), 8.12 – 8.06 (m, 1H, 7-H), 7.91 (ddd, *J* = 8.4, 7.0, 1.3 Hz, 1H, 9-H), 7.80 (ddd, *J* = 8.2, 7.0, 1.5 Hz, 1H, 3-H), 7.76 – 7.70 (m, 3H, 2-, 3'-, 5'-H), 7.70 – 7.63 (m, 3H, 8-, 2'-, 6'-H).

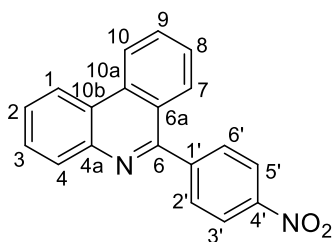
¹³C NMR (101 MHz, CDCl₃): δ (ppm) = 160.0 (C-6), 143.8 (C-4a), 138.7 (C-1'), 133.5 (C-10a), 131.7 (C-3, -5), 131.4 (C-2, -6), 130.7 (C-9), 130.4 (C-4), 129.0 (C-3), 128.5 (C-7), 127.3 (C-8), 127.2 (C-2), 125.0 (C-6a), 123.8 (C-10b), 123.2 (C-4'), 122.4 (C-10), 122.0 (C-1).

IR (ATR): $\tilde{\nu}$ [cm⁻¹] = 2922, 1481, 1390, 1011, 821, 753.

HRMS (ESI): *m/z* [M+H]⁺ calcd. for C₁₉H₁₃BrN⁺: 334.0226, found: 334.0226.

Purity (HPLC): >96 % (210 nm, 254 nm).

6-(4-Nitrophenyl)phenanthridine (29)^[105]



C₁₉H₁₂N₂O₂
300.32 g/mol

Nitrophenyl phenanthridine was synthesized according to GP2 using amide **43** (1.4 g (91 % purity), 4.0 mmol). Crystallization from isopropanol gave phenanthridine **29** as light-yellow solid (485 mg, 1.61 mmol, 40 %).

mp.: 190 – 192 °C (lit.^[105] 183.5 – 183.9 °C).

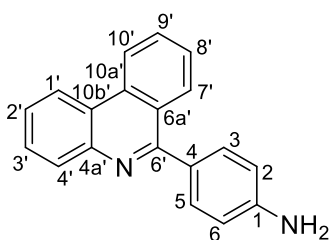
¹H NMR (400 MHz, CDCl₃): δ (ppm) = 8.76 (d, *J* = 8.3 Hz, 1H, 10-H), 8.66 (dd, *J* = 8.0, 1.6 Hz, 1H, 1-H), 8.49 – 8.40 (m, 2H, 3'-, 5'-H), 8.27 – 8.22 (m, 1H, 4-H), 8.02 – 7.97 (m, 1H, 7-H), 7.97 – 7.89 (m, 3H, 2'-, 6'-H, 9-H), 7.81 (ddd, *J* = 8.1, 7.0, 1.6 Hz, 1H, 3-H), 7.75 (ddd, *J* = 8.4, 7.0, 1.5 Hz, 1H, 2-H), 7.67 (ddd, *J* = 8.3, 7.0, 1.2 Hz, 1H, 8-H).

¹³C NMR (101 MHz, CDCl₃): δ (ppm) = 158.9 (C-6), 148.2 (C-4'), 146.3 (C-1'), 143.8 (C-4a), 133.7 (C-10a), 131.2 (C-9), 131.0 (C-2', -6'), 130.6 (C-4), 129.4 (C-3), 128.1 (C-7), 127.9 (C-2), 127.7 (C-8), 124.8 (C-6a), 124.1 (C-10b), 123.9 (C-3'-, 5'), 122.7 (C-10), 122.2 (C-1).

IR (ATR): $\tilde{\nu}$ [cm⁻¹] = 3070, 1928, 1602, 1516, 1349, 1328, 1106, 958, 854, 846, 760, 726, 696.

HRMS (ESI): *m/z* [M+H]⁺ calcd. for C₁₉H₁₃N₂O₂⁺: 301.0972, found: 301.0970.

Purity (HPLC): >96 % (210 nm, 254 nm).

4-(Phenanthridin-6-yl)aniline (30)^[79]


C₁₉H₁₄N₂
270.33 g/mol

Nitrophenyl phenanthridine **29** (455 mg, 1.52 mmol) was suspended in acetic acid (10 mL) and iron powder (423 mg, 5.00 mmol) was added portion wise. The suspension was stirred at rt for 16 h and upon complete reduction, the acetic acid was neutralized by dropwise addition of the suspension to 2M aqueous NaOH (100 mL). The resulting black suspension was extracted with ethyl acetate (1x 100 mL, 2x 50 mL). The combined organic layers were dried using a hydrophobic filter and the solvent was removed *in vacuo* to give aniline **30** as beige solid (384 mg, 1.42 mmol, 94 %).

mp.: 196 – 198 °C (lit.^[79] 197 – 199 °C).

¹H NMR (500 MHz, CDCl₃): δ (ppm) = 8.69 (d, *J* = 8.3 Hz, 1H, 10'-H), 8.60 (d, *J* = 8.2 Hz, 1H, 1'-H), 8.22 (t, *J* = 7.0 Hz, 2H, 7'-H, 4'-H), 7.84 (t, *J* = 7.6 Hz, 1H, 9'-H), 7.74 (t, *J* = 7.4 Hz, 1H, 3'-H), 7.69 – 7.55 (m, 4H, 2'-H, 3-, 5-H, 8'-H), 6.86 (dd, *J* = 8.4, 2.5 Hz, 2H, 2-, 6-H), 3.88 (s, 2H, NH₂).

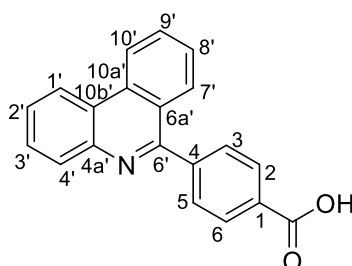
¹³C NMR (126 MHz, CDCl₃): δ (ppm) = 161.4 (C-6'), 147.2 (C-1), 144.2 (C-4a'), 133.7 (C-10a'), 131.3 (C-3, -5), 130.5 (C-9'), 130.4 (C-4'), 130.2 (C-4), 129.2 (C-7'), 128.8 (C-3'), 127.1 (C-8'), 126.6 (C-2'), 125.6 (C-6a'), 123.7 (C-10b'), 122.3 (C-10'), 122.0 (C-1'), 114.9 (C-2, -6).

IR (ATR): $\tilde{\nu}$ [cm⁻¹] = 3418, 3306, 1632, 1606, 1514, 1481, 1457, 1361, 1276, 1172, 959, 820, 760, 727.

HRMS (ESI): *m/z* [M+H]⁺ calcd. for C₁₉H₁₅N₂⁺: 271.1230, found: 271.1229.

Purity (HPLC): >96 % (210 nm, 254 nm).

4-(Phenanthridin-6-yl)benzoic acid (19)^[108]



C₂₀H₁₃NO₂

299.33 g/mol

Methyl ester **18** (666 mg, 2.13 mmol) was dissolved in dioxane (12 mL) and water (10 mL) was added. To the resulting suspension was added 2M aqueous NaOH (2.66 mL) and was stirred for 2.5 h at rt. To the now clear solution was added 5 mL of aqueous HCl and the resulting suspension was stirred for 10 min. The precipitate was filtered and was washed with cold water. The solid was high vacuum dried, to give carboxylic acid **19** as light-yellow solid (559 mg, 1.87 mmol, 88 %).

mp.: 273 – 275 °C (lit.^[108] no mp. determined, VÖGERL^[74]: 287 – 288 °C).

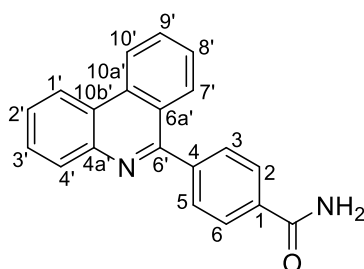
¹H NMR (400 MHz, DMSO-*d*₆): δ (ppm) = 13.16 (s, 1H, COOH), 8.97 (d, *J* = 8.4 Hz, 1H, 10'-H), 8.88 (dd, *J* = 8.1, 1.6 Hz, 1H, 1'-H), 8.20 – 8.11 (m, 3H, 2-, 6-, 4'-H), 8.00 (ddd, *J* = 9.6, 7.5, 1.7 Hz, 2H, 7'-, 9'-H), 7.87 – 7.73 (m, 5H, 3-, 5-, 3'-, 2'-, 8'-H).

¹³C NMR (101 MHz, DMSO-*d*₆): δ (ppm) = 167.1 (COOH), 159.6 (C-6'), 143.3 (C-4), 143.1 (C-4a'), 132.8 (C-10a'), 131.3 (C-9'), 131.0 (C-1), 129.9 (C-3, -5), 129.8 (C-3'), 129.3 (C-2, -6), 129.2 (C-4'), 128.0 (C-7'), 127.9 (C-8'), 127.6 (C-2'), 124.2 (C-6a'), 123.4 (C-10b'), 123.0 (C-10'), 122.8 (C-1').

IR (ATR): $\tilde{\nu}$ [cm⁻¹] = 2850, 1693, 1426, 1295, 871, 751, 725.

HRMS (ESI): *m/z* [M-H]⁻ calcd. for C₂₀H₁₂NO₂⁻: 298.0874, found: 298.0874.

Purity (HPLC): >96 % (210 nm, 254 nm).

4-(Phenanthridin-6-yl) benzamide (32)C₂₀H₁₄N₂O

298.34 g/mol

Carboxylic acid **19** (102 mg, 0.341 mmol) was dissolved in thionyl chloride (3.0 mL, 41 mmol) and was stirred at reflux (70 °C) for 16 h. After cooling to rt, the excess of thionyl chloride was removed *in vacuo* by azeotropic distillation with toluene. The residue was taken up in THF (2 mL), 25% aqueous ammonium hydroxide (1.0 mL, 7.0 mmol) was added and the mixture was stirred vividly for 30 min at rt. The reaction mixture was diluted with ethyl acetate (30 mL) and was washed with saturated aqueous NaHCO₃ solution (30 mL). The aqueous layer was extracted with ethyl acetate (3x 20 mL), the combined organic layers were dried using a hydrophobic filter and the solvent removed *in vacuo*. The residue was purified by FCC (CH₂Cl₂/MeOH 95:5) to give carboxamide **32** as colourless solid (73 mg, 0.25 mmol, 72 %).

mp.: 250 – 252 °C.

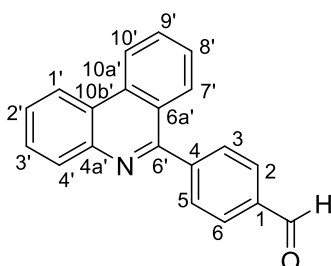
¹H NMR (400 MHz, DMSO-*d*₆): δ (ppm) = 8.98 (d, *J* = 8.3 Hz, 1H, 10'-H), 8.88 (dd, *J* = 8.2, 1.6 Hz, 1H, 1'-H), 8.18 – 8.12 (m, 2H, 1x NH₂, 4'-H), 8.12 – 8.08 (m, 2H, 2-, 6-H), 8.05 – 7.98 (m, 2H, 7'-H, 9'-H), 7.87 – 7.74 (m, 5H, 3'-H, 3-, 5-H, 2'-H, 8'-H), 7.52 (s, 1H, 1x NH₂).

¹³C NMR (101 MHz, DMSO-*d*₆): δ (ppm) = 168.0 (C=O), 160.3 (C-6'), 143.6 (C-4a'), 142.3 (C-4), 134.9 (C-1), 133.3 (C-10a'), 131.7 (C-9'), 130.3 (C-4'), 130.0 (C-3, -5), 129.7 (C-3'), 128.5 (C-7'), 128.4 (C-2', C-8'), 128.0 (C-2, -6), 124.7 (C-10b'), 123.8 (C-6a'), 123.4 (C-10'), 123.2 (C-1').

IR (ATR): $\tilde{\nu}$ [cm⁻¹] = 3376, 3190, 1646, 1616, 1406, 1363, 1134, 1124, 962, 868, 756, 728, 661.

HRMS (ESI): *m/z* [M+H]⁺ calcd. for C₂₀H₁₅N₂O⁺: 299.1179, found: 299.1181.

Purity (HPLC): >96 % (210 nm, 254 nm).

4-(Phenanthridin-6-yl) benzaldehyde (31)^[109]C₂₀H₁₃NO

283.33 g/mol

Nitrile **44** (561 mg, 2.00 mmol, 1.00 eq) was dissolved in methylene chloride (8 mL) under nitrogen atmosphere and was cooled to 0 °C. A solution of DIBAL in toluene (1 mol/L, 2.40 mL, 1.20 eq) was added dropwise and the solution was stirred for 1 h at 0 °C. Subsequently a 10 % aqueous solution of HCl (20 mL) was added and the mixture was stirred for 30 min at rt. The layers were separated, the aqueous layer was neutralized with aqueous NaOH and was extracted twice with methylene chloride (2x 20 mL). The combined organic layers were dried using a hydrophobic filter and the solvent was removed *in vacuo*. The residue was purified by FCC (CH₂Cl₂/EtOH 99:1) to give aldehyde **31** as light-yellow solid (379 mg, 1.34 mmol, 67 %)

mp.: 173 – 175 °C (lit.^[109] no mp. given)

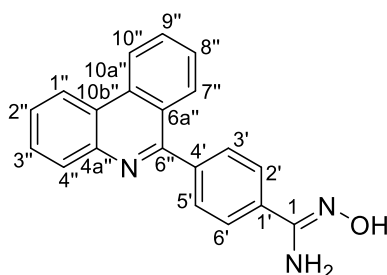
¹H NMR (400 MHz, CDCl₃): δ (ppm) = 10.17 (s, 1H, COH), 8.74 (ddd, *J* = 8.8, 1.2, 0.6 Hz, 1H, 10'-H), 8.65 (dd, *J* = 8.0, 1.5 Hz, 1H, 1'-H), 8.28 – 8.21 (m, 1H, 4'-H), 8.13 – 8.06 (m, 2H, 2-, 6-H), 8.03 (ddd, *J* = 8.3, 1.3, 0.7 Hz, 1H, 7'-H), 7.96 – 7.86 (m, 3H, 3-, 5-, 9'-H), 7.79 (ddd, *J* = 8.2, 7.0, 1.5 Hz, 1H, 3'-H), 7.73 (ddd, *J* = 8.4, 7.0, 1.5 Hz, 1H, 2'-H), 7.65 (ddd, *J* = 8.2, 7.0, 1.2 Hz, 1H, 8'-H).

¹³C NMR (101 MHz, CDCl₃): δ (ppm) = 192.2 (COH), 159.9 (C-6'), 145.9 (C-4), 143.8 (C-4a'), 136.5 (C-1), 133.7 (C-10a'), 131.0 (C-9'), 130.7 (C-3, -5), 130.6 (C-4'), 123.0 (C-2, -6), 129.2 (C-3'), 128.4 (C-7'), 127.6 (C-8'), 127.6 (C-2'), 125.0 (C-6a'), 124.0 (C-10b'), 122.6 (C-10'), 122.2 (C-1').

IR (ATR): $\tilde{\nu}$ [cm⁻¹] = 2848, 2362 1700, 1209, 827, 764, 729.

HRMS (ESI): *m/z* [M+H]⁺ calcd. for C₂₀H₁₄NO⁺: 284.1070, found: 284.1072.

Purity (HPLC): >96 % (210nm, 254 nm).

***N*'-Hydroxy-4-(phenanthridin-6-yl) benzimidamide (33)**

 $C_{20}H_{15}N_3O$

313.36 g/mol

Hydroxylamine hydrochloride (45 mg, 0.65 mmol, 3.3 eq) and $NaHCO_3$ (55 mg, 0.65 mmol, 3.3 eq) were dissolved in water (1 mL) and were diluted with MeOH (3 mL). Nitrile **44** (56 mg, 0.20 mmol, 1.0 eq) was dissolved in a mixture of MeOH/EtOAc 1:1 (10 mL) and was added to the mixture. The reaction mixture was refluxed for 24 h, after cooling to rt the reaction mixture was diluted with ethyl acetate (15 mL) and the salts were filtered off. The organic layer was washed with saturated aqueous $NaHCO_3$ (10 mL). The aqueous layer was extracted twice with ethyl acetate (10 mL). The combined organic layers were dried using a hydrophobic filter and the solvent was removed *in vacuo*. The residue was purified by FCC (PE/EtOAc/ Et_3N 2:8:0.1) to give amidoxime **33** as off-white solid (23 mg, 0.073 mmol, 37 %).

mp.: 227 – 229 °C.

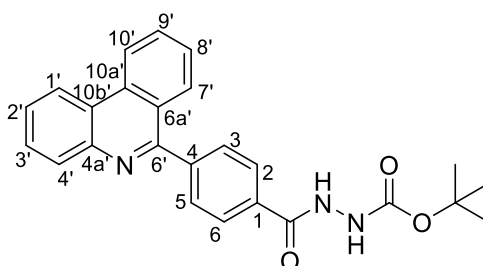
1H NMR (400 MHz, DMSO- d_6): δ (ppm) = 9.79 (s, 1H, OH), 8.96 (d, J = 8.3 Hz, 1H, 10''-H), 8.86 (dd, J = 8.1, 1.5 Hz, 1H, 1''-H), 8.13 (dd, J = 8.1, 1.5 Hz, 1H, 4''-H), 8.07 (d, J = 8.2 Hz, 1H, 7''-H), 8.02 – 7.96 (m, 1H, 9''-H), 7.93 – 7.88 (m, 2H, 2'-, 6'-H), 7.83 (td, J = 8.1, 7.5, 1.5 Hz, 1H, 3''-H), 7.80 – 7.71 (m, 4H, 3'-, 5'-, 2''-, 8''-H), 5.95 (s, 2H, NH_2).

^{13}C NMR (101 MHz, DMSO- d_6): δ (ppm) = 160.5 (C-6''), 151.0 (C-1), 143.7 (C-4a''), 140.1 (C-4'), 134.2 (C-1'), 133.3 (C-10a''), 131.6 (C-9''), 130.2 (C-4''), 130.0 (C-3', -5'), 129.6 (C-3''), 128.5 (C-8''), 128.4 (C-7''), 127.8 (C-2''), 125.8 (C-2', -6'), 124.8 (C-6a''), 123.7 (C-10b''), 123.4 (C-10''), 123.2 (C-1'').

IR (ATR): $\tilde{\nu}$ [cm^{-1}] = 3479, 3142, 1634, 1579, 1460, 1362, 1142, 1084, 926, 836, 760, 728.

HRMS (EI): m/z [M] $^{+}$ calcd. for $C_{20}H_{15}N_3O$ $^{+}$: 313.1215, found: 313.1204.

Purity (HPLC): >96 % (210 nm, 254 nm).

***tert*-Butyl 2-(4-(phenanthridin-6-yl)benzoyl)hydrazine-1-carboxylate (**52**)**C₂₅H₂₃N₃O₃

413.48 g/mol

Carboxylic acid **19** (898 mg, 3.00 mmol) was suspended in methylene chloride (30 mL), then *tert*-butyl carbazate and EDCI were added to the mixture. The resulting clear solution was stirred for 16 h at rt, then was diluted with CH₂Cl₂ (30 mL) and was washed with saturated NaHCO₃ solution (3x 50 mL) and brine (1x 50 mL). The combined aqueous layers were extracted with CH₂Cl₂ (3x 50 mL), then the combined organic layers were dried using a hydrophobic filter and the solvent was removed *in vacuo*. The residue was purified by FCC (petrol ether/ethyl acetate 3:7) to give Boc-hydrazide **52** as colourless solid (1.02 g, 2.47 mmol, 82 %).

mp.: 218 – 220 °C.

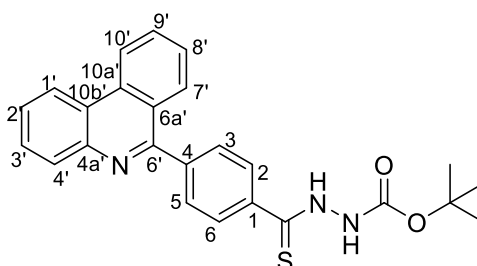
¹H NMR (400 MHz, DMSO-*d*₆): δ (ppm) = 10.38 (s, 1H, PhCONH), 9.08 – 8.94 (m, 2H, NHBoc, 10'-H), 8.88 (dd, *J* = 8.2, 1.6 Hz, 1H, 1'-H), 8.15 (dd, *J* = 8.1, 1.5 Hz, 1H, 4'-H), 8.08 (d, *J* = 7.9 Hz, 2H, 2-, 6-H), 8.04 – 7.97 (m, 2H, 7'-H, 9'-H), 7.87 – 7.73 (m, 5H, 3-, 5-H, 3'-H, 2'-H, 8'-H), 1.46 (s, 9H, CH₃).

¹³C NMR (101 MHz, DMSO-*d*₆): δ (ppm) = 165.7 (PhC=O), 159.7 (C-6'), 155.5 (C=O Boc), 143.1 (4a'), 142.3 (C-4), 132.8 (C-10a', C-1) 131.2 (C-9'), 129.8 (C-3, -5, C-4'), 129.2 (C-3'), 128.0 (C-2' or C-8'), 127.9 (C-2' or C-8'), 127.5 (C-7'), 127.4 (C-2, -6), 124.2 (C-6a'), 123.4 (C-10b'), 123.0 (C-10'), 122.8 (C-1'), 79.3 (C_q *t*Bu), 28.1 (CH₃).

IR (ATR): $\tilde{\nu}$ [cm⁻¹] = 3372, 3266, 2982, 2926, 1749, 1642, 1535, 1492, 1364, 1252, 1157, 753, 728.

HRMS (ESI): *m/z* [M+H]⁺ calcd. for C₂₅H₂₄N₃O₃⁺: 414.1812, found: 414.1813.

Purity (HPLC): >96 % (210 nm, 254 nm).

tert-Butyl 2-(4-(phenanthridin-6-yl)phenylcarbonothioyl)hydrazine-1-carboxylate (53)

 $C_{25}H_{23}N_3O_2S$

429.54 g/mol

To Boc-hydrazide **52** (413 mg, 1.00 mmol) in 2 mL dry THF was added LAWESSON's reagent (404 mg, 1.00 mmol). The mixture was heated in a microwave at 80 °C for 20 min (max pressure 140 psi) and was allowed to cool to rt. The solvent was removed *in vacuo* and the residue was purified by FCC (CH₂Cl₂/MeOH 98:2) to give Boc-thiohydrazide **53** as yellow solid (373 mg, 0.868 mmol, 87 %).

mp.: 147 – 149 °C.

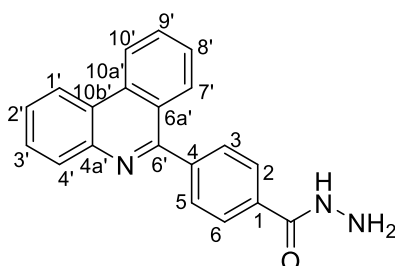
¹H NMR (500 MHz, DMSO-*d*₆): δ (ppm) = 11.92 (s, 1H, S=CNH), 9.57 (s, 1H, NHBoc), 8.97 (d, *J* = 8.4 Hz, 1H, 10'-H), 8.87 (dd, *J* = 8.2, 1.5 Hz, 1H, 1'-H), 8.14 (dd, *J* = 8.1, 1.4 Hz, 1H, 4'-H), 8.07 – 7.89 (m, 4H, 7'-H, 9'-H, 2-, 6-H), 7.87 – 7.73 (m, 5H, 3'-H, 3-, 5-H, 2'-H, 8'-H), 1.46 (s, 9H, CH₃).

¹³C NMR (126 MHz, DMSO-*d*₆): δ (ppm) = 197.7 (C=S), 159.6 (C-6'), 154.1 (C=O), 143.1 (C-4a'), 141.6 (C-4), 139.0 (C-1), 132.9 (C-10a'), 131.3 (C-9'), 129.8 (C-4'), 129.5 (C-3, -5), 129.2 (C-3'), 128.0 (C-7' or C-8'), 127.9 (C-7' or C-8'), 127.5 (C-2,-6), 127.5 (C-2'), 124.2 (C-6a'), 123.3 (C-10b'), 123.0 (C-10'), 122.8 (C-1'), 79.9 (C_q *t*Bu), 28.1 (CH₃ *t*Bu).

IR (ATR): $\tilde{\nu}$ [cm⁻¹] = 3176, 2929, 2364, 1712, 1410, 1365, 1241, 1150, 961, 838, 759, 725.

HRMS (ESI): *m/z* [M+H]⁺ calcd. for C₂₅H₂₄N₃O₂S⁺: 430.1584, found: 430.1584.

Purity (HPLC): >96 % (210 nm, 254 nm).

4-(Phenanthridin-6-yl)benzohydrazide (34)

 $C_{20}H_{15}N_3O$

313.36 g/mol

Boc-hydrazide **52** (124 mg, 0.300 mmol) was dissolved in methylene chloride (2 mL) and was cooled to 0 °C. TFA (675 μ L, 9.00 mmol) was added dropwise and the mixture was stirred for 10 min at 0 °C then an additional 4 h at rt. The volatiles were removed *in vacuo* and the residue was purified by FCC ($CH_2Cl_2/MeOH$ 95:5) to give hydrazide **34** as colourless solid (54 mg, 0.17 mmol, 57 %).

mp.: 232 – 234 °C.

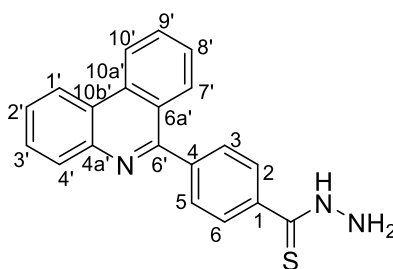
1H NMR (400 MHz, $CDCl_3$): δ (ppm) = 8.73 (d, J = 8.3 Hz, 1H, 10'-H), 8.64 (dd, J = 8.2, 1.5 Hz, 1H, 1'-H), 8.24 (dd, J = 8.1, 1.5 Hz, 1H, 4'-H), 8.03 (dt, J = 8.4, 0.8 Hz, 1H, 7'-H), 7.98 – 7.92 (m, 2H, 2-, 6-H), 7.89 (ddd, J = 8.3, 7.0, 1.3 Hz, 1H, 9'-H), 7.87 – 7.82 (m, 2H, 3-, 5-H), 7.78 (ddd, J = 8.3, 7.1, 1.5 Hz, 1H, 3'-H), 7.72 (ddd, J = 8.3, 7.0, 1.5 Hz, 1H, 2'-H), 7.64 (ddd, J = 8.2, 7.0, 1.1 Hz, 1H, 8'-H), 7.48 (s, 1H, NH), 4.18 (s, 2H, NH_2).

^{13}C NMR (101 MHz, $CDCl_3$): δ (ppm) = 168.5 (C=O), 160.1 (C-6'), 143.9 (C-4a'), 143.5 (C-4), 133.7 (C-10a'), 133.0 (C-1), 131.0 (C-9'), 130.6 (C-4'), 130.4 (C-3, -5), 129.2 (C-3'), 128.6 (C-7'), 127.5 (C-8'), 127.5 (C-2'), 127.2 (C-2, -6), 125.1 (C-6a'), 124.0 (C-10b'), 122.5 (C-10'), 122.2 (C-1').

IR (ATR): $\tilde{\nu}$ [cm^{-1}] = 3292, 2926, 1640, 1608, 1524, 1329, 1115, 952, 863, 838, 758, 727.

HRMS (ESI): m/z [$M+H$]⁺ calcd. for $C_{20}H_{16}N_3O^+$: 314.1288, found: 314.1291.

Purity (HPLC): >96 % (210 nm, 254 nm).

4-(Phenanthridin-6-yl)benzothiohydrazide (35)C₂₀H₁₅N₃S

329.43 g/mol

Boc-thiohydrazide **53** (129 mg, 0.300 mmol) was dissolved in methylene chloride (2 mL) and cooled to 0 °C. TFA (675 μL, 9.00 mmol) was added dropwise and the mixture was stirred for 10 min at 0 °C then an additional 4 h at rt. The volatiles were removed *in vacuo* and the residue was purified by FCC (CH₂Cl₂/MeOH 98:2) to give thiohydrazide **35** as green solid (49 mg, 0.15 mmol, 50 %).

mp.: 302 – 304 °C.

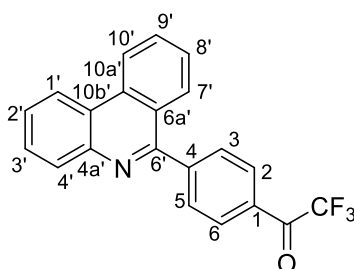
¹H NMR (500 MHz, DMSO-*d*₆): δ (ppm) = 12.32 (s, 1H, NH), 9.00 – 8.93 (m, 1H, 10'-H), 8.87 (dd, *J* = 8.2, 1.5 Hz, 1H, 1'-H), 8.14 (dd, *J* = 8.1, 1.5 Hz, 1H, 4'-H), 8.06 (dd, *J* = 8.3, 1.3 Hz, 1H, 7'-H), 8.03 – 7.88 (m, 3H, 9'-H, 2-, 6-H), 7.84 (ddd, *J* = 8.2, 6.9, 1.5 Hz, 1H, 3'-H), 7.80 – 7.74 (m, 4H, 3'-H, 3-, 5-H, 8'-H), 6.35 (s, 2H, NH₂).

¹³C NMR (126 MHz, DMSO-*d*₆): δ (ppm) = 182.0 (C=S), 160.2 (C-6'), 143.7 (C-4a'), 141.2 (C-4), 139.2 (C-1), 133.3 (C-10a'), 131.7 (C-9'), 130.2 (C-4'), 129.9 (C-8'), 129.7 (C-3'), 128.5 (C-7'), 128.4 (C-3, -5), 127.9 (C-2'), 127.7 (C-2, -6), 124.7 (C-6a'), 123.8 (C-10b'), 123.4 (C-10'), 123.2 (C-1').

IR (ATR): $\tilde{\nu}$ [cm⁻¹] = 3166, 2854, 1558, 1524, 1401, 1368, 1300, 1224, 981, 966, 920, 838, 753, 724.

HRMS (ESI): *m/z* [M+H]⁺ calcd. for C₂₀H₁₆N₃S⁺: 330.1059, found: 330.1062.

Purity (HPLC): >96 % (210 nm, 254 nm).

2,2,2-Trifluoro-1-(4-(phenanthridin-6-yl)phenyl)ethan-1-one (36)C₂₁H₁₂F₃NO

351.33 g/mol

4-Bromophenyl phenanthridine **45** (334 mg, 1.00 mmol) was dissolved in dry THF (5 mL) under nitrogen atmosphere and was cooled to -78 °C. *n*-BuLi (2.5M in hexanes, 480 μL, 1.20 mmol) was added dropwise over 10 min and the solution was stirred for 1.5 h at -78 °C. Then a solution of *N,N*-diethyl-2,2,2-trifluoroacetamide (197 μL, 1.40 mmol) in dry THF (0.5 mL) was added dropwise over 10 min and the solution was stirred another 3.5 h at -78 °C. The reaction mixture was quenched with saturated NH₄Cl solution (10 mL). After warming up to rt the mixture was diluted with ethyl acetate (15 mL), the layers were separated, and the organic layer was washed with saturated NH₄Cl solution (20 mL) and water (20 mL). The combined aqueous layers were extracted with ethyl acetate (2x 30 mL), the combined organic layers were dried using a hydrophobic filter and the solvent was removed *in vacuo*. The residue was purified by crystallization from isopropanol yielding trifluoromethyl ketone **36** as colourless crystals (104 mg, 0.296 mmol, 30 %). Removing the solvent of the mother liquor yielded additional crude trifluoromethyl ketone **36** as off-white solid (255 mg, ~0.726 mmol, ~73 %), which was used as obtained for the synthesis of trifluoromethyl oxime **37**.

mp.: 160 – 162 °C.

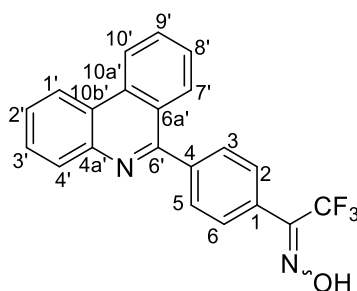
¹H NMR (500 MHz, CDCl₃): δ (ppm) = 8.77 – 8.74 (m, 1H, 10'-H), 8.66 (dd, *J* = 8.1, 1.5 Hz, 1H, 1'-H), 8.29 (dq, *J* = 7.8, 1.0 Hz, 2H, 2-, 6-H), 8.27 – 8.23 (m, 1H, 4'-H), 8.03 (ddd, *J* = 8.2, 1.3, 0.6 Hz, 1H, 7'-H), 7.97 – 7.94 (m, 2H, 3-, 5-H), 7.91 (ddd, *J* = 8.4, 7.0, 1.3 Hz, 1H, 9'-H), 7.80 (ddd, *J* = 8.3, 7.0, 1.5 Hz, 1H, 3'-H), 7.75 (ddd, *J* = 8.3, 7.0, 1.4 Hz, 1H, 2'-H), 7.66 (ddd, *J* = 8.3, 7.0, 1.2 Hz, 1H, 8'-H).

¹³C NMR (126 MHz, CDCl₃): δ (ppm) = 180.3 (q, *J* = 35.2 Hz, C=O), 159.2 (C-6'), 146.9 (C-4), 143.7 (C-4a'), 133.6 (C-10a'), 131.0 (C-9'), 130.6 (C-3-, 5-C), 130.5 (C-4'), 130.3 (q, *J* = 2.2 Hz (C-2, -6), 129.9 (C-1), 129.2 (C-3'), 128.1 (C-7'), 127.6 (C-2'), 127.5 (C-8'), 124.6 (C-6a'), 123.9 (C-10b'), 122.5 (C-10'), 122.1 (C-1'), 116.7 (q, *J* = 291.5 Hz, CF₃).

IR (ATR): $\tilde{\nu}$ [cm⁻¹] = 3072, 1714, 1606, 1581, 1367, 1330, 1199, 1173, 1133, 939, 868, 755, 728, 707.

HRMS (ESI): m/z $[M+H_2O+H]^+$ calcd. for $C_{21}H_{15}F_3NO_2^+$: 370.1049, found: 370.1051.

Purity (HPLC): crystals: >96 % (210 nm, 254 nm).

(E,Z)-2,2,2-Trifluoro-1-(4-(phenanthridin-6-yl)phenyl)ethan-1-one oxime (37)

 $C_{21}H_{13}F_3N_2O$

366.34 g/mol

Crude trifluoromethyl ketone **36** (250 mg, 0.712 mmol), hydroxylamine HCl (200 mg, 2.88 mmol) and pyridine (230 μ L, 2.84 mmol) were suspended in a mixture of EtOAc/MeOH (1:1, 7 mL). The mixture was stirred at reflux (70 °C) for 4 h, was diluted with ethyl acetate (50 mL) and was washed with water (30 mL) and brine (30 mL). The combined aqueous layers were extracted with ethyl acetate (2x 40 mL), the combined organic layers were dried using a hydrophobic filter and the solvent was removed *in vacuo*. Purification of the residue by crystallization from isopropanol gave trifluoromethyl oxime **37** as off-white crystals, a mixture of *E*- and *Z*-isomers (94 mg, 0.26 mmol, 36 %).

mp.: 255 – 257 °C.

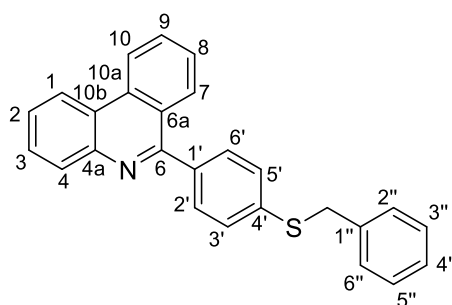
¹H NMR (500 MHz, DMSO-*d*₆): δ (ppm) = 13.26 (s, 0.45H, NOH, *E,Z*), 12.94 (s, 0.55H, NOH, *E,Z*), 8.98 (dt, J = 8.6, 1.4 Hz, 1H, 10'-H), 8.88 (dt, J = 8.2, 1.7 Hz, 1H, 1'-H), 8.14 (dt, J = 8.1, 1.5 Hz, 1H, 4'-H), 8.06 (dd, J = 8.2, 1.3 Hz, 1H, 7'-H), 8.00 (ddt, J = 8.6, 7.0, 1.7 Hz, 1H, 9'-H), 7.91 – 7.69 (m, 7H, 3-, 5-H, 3'-H, 2'-H, 8'-H, 2-, 6-H).

¹³C NMR (126 MHz, DMSO-*d*₆): δ (ppm) = 1160.0 (C-6' *E,Z*), 160.0 (C-6' *E,Z*), 145.82 – 144.19 (m, C=NOH), 143.6 (4a', *E,Z*), 143.6 (4a', *E,Z*), 141.4 (C-4, *E,Z*), 141.1 (C-4, *E,Z*), 133.3 (C-10a'), 131.7 (C-9', *E,Z*), 131.7 (C-9', *E,Z*), 131.2 (C-1, *E,Z*), 130.4 (C-3, -5, *E,Z*), 130.4 (C-3, -5, *E,Z*), 130.3 (C-4'), 129.7 (C-3', *E,Z*), 129.7 (C-3', *E,Z*), 129.0 (C-2, -6, *E,Z*), 128.6 (C-2, -6, *E,Z*), 128.5 (C-2' or C-8', or C-7', *E,Z*), 128.5 (C-2' or C-8', or C-7', *E,Z*), 128.4 (C-2' or C-8', or C-7', *E,Z*), 128.4 (C-2' or C-8', or C-7', *E,Z*), 128.0 (C-2' or C-8' *E,Z*), 128.0 (C-2' or C-8', *E,Z*), 127.4 (C-1, *E,Z*), 124.6 (C-6a', *E,Z*), 124.6 (C-6a', *E,Z*), 123.8 (C-10b', *E,Z*), 123.8 (C-10b', *E,Z*), 123.4 (C-10'), 123.2 (C-1'), 121.7 (q, J = 273.8 Hz, CF₃, *E,Z*), 119.0 (q, J = 282.9 Hz, CF₃, *E,Z*).

IR (ATR): $\tilde{\nu}$ [cm⁻¹] = 2786, 1611, 1572, 1486, 1457, 1442, 1340, 1211, 1170, 1117, 1038, 1017, 959, 836, 758, 727.

HRMS (ESI): m/z [M+H]⁺ calcd. for C₂₁H₁₄F₃N₂O⁺: 367.1053, found: 367.1056.

Purity (HPLC): >96 % (210 nm, 254 nm).

6-(4-(Benzylthio)phenyl)phenanthridine (66)

 $C_{26}H_{19}NS$

377.51 g/mol

$Pd_2(dba)_3$ (41 mg, 0.040 mmol) and dppf (44 mg, 0.080 mmol) were suspended in prior degassed toluene (40 mL) under nitrogen atmosphere, then bromophenyl phenanthridine **45** (1.34 g, 4.00 mmol), benzyl mercaptan (517 μ L, 4.40 mmol) and DIPEA (760 μ L, 4.40 mmol) were added. The mixture was heated to reflux (110 $^{\circ}C$) and was stirred at this temperature for 3 h. After cooling to rt the mixture was diluted with ethyl acetate (60 mL) and was washed with water (80 mL). The aqueous layer was extracted with ethyl acetate (2x 50 mL), the combined organic layers were washed with brine (100 mL) and were dried using a hydrophobic filter. The solvent was removed *in vacuo* and the residue purified by FCC (CH_2Cl_2) followed by crystallization from acetone to give benzyl thioether **66** as light-yellow solid (1.27 g, 3.37 mmol, 84 %).

mp.: 158 – 160 $^{\circ}C$.

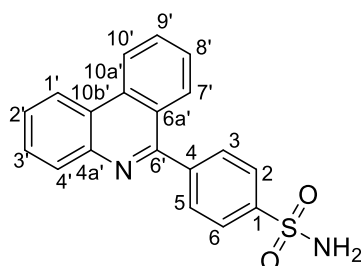
1H NMR (400 MHz, $CDCl_3$): δ (ppm) = 8.73 – 8.69 (m, 1H, 10-H), 8.62 (dd, J = 8.1, 1.4 Hz, 1H, 1-H), 8.25 – 8.20 (m, 1H, 4-H), 8.09 (ddd, J = 8.3, 1.3, 0.6 Hz, 1H, 7-H), 7.87 (ddd, J = 8.3, 6.9, 1.3 Hz, 1H, 9-H), 7.76 (ddd, J = 8.2, 7.0, 1.5 Hz, 1H, 7-H), 7.72 – 7.60 (m, 4H, 2-H, 2'-, 6'-H, 8-H), 7.52 – 7.47 (m, 2H, 3'-, 5'-H), 7.43 – 7.38 (m, 2H, 2''-, 6''-H), 7.37 – 7.30 (m, 2H, 3''-, 5''-H), 7.31 – 7.26 (m, 1H, 4''-H), 4.24 (s, 2H, CH_2).

^{13}C NMR (126 MHz, $CDCl_3$): δ (ppm) = 160.7 (C-6), 144.0 (C-4a'), 137.8 (C-1' or C-4'), 137.7 (C-1' or C-4'), 137.4 (C-1''), 133.6 (C-10a), 130.7 (C-9'), 130.5 (C-10'), 130.4 (C-2', -6'), 129.2 (C-3', -5'), 129.0 (C-7), 129.0 (C-2'', -6''), 128.9 (C-3), 128.8 (C-3'', -5''), 127.5 (C-4''), 127.3 (C-8), 127.1 (C-2), 125.3 (C-6a), 123.9 (C-10b), 122.4 (C-10), 122.1 (C-1), 38.8 (CH_2).

IR (ATR): $\tilde{\nu}$ [cm^{-1}] = 3030, 1738, 1596, 1564, 1482, 1454, 1358, 1218, 1133, 1082, 1068, 958, 859, 818, 755, 726, 716.

HRMS (ESI): m/z [$M+H$] $^+$ calcd. for $C_{26}H_{20}NS^+$: 378.1311, found: 378.1313.

Purity (HPLC): >96 % (210 nm, 254 nm).

4-(Phenanthridin-6-yl)benzenesulfonamide (38)

 $C_{19}H_{14}N_2O_2S$

334.39 g/mol

Method A: Synthesis according to GP2 using amide **64** (176 mg, 0.500 mmol). Purification by FCC ($CH_2Cl_2/MeOH$ 97:3) gave sulfonamide **38** as beige solid (22 mg, 0.066 mmol, 13 %).

Method B: Synthesis according to GP3. Benzyl thioether **66** (1.27 g, 3.36 mmol) was converted to crude sulfonyl chloride **65** (1.51 g). A part of the obtained crude 4-(phenanthridin-6-yl)benzenesulfonyl chloride (**65**) (227 mg, ~0.500 mmol) and aqueous ammonium hydroxide solution (25%, 341 μ L, 5.00 mmol) were used. Trituration in isopropanol gave sulfonamide **38** as colourless solid (123 mg, 0.368 mmol, 74 %).

mp.: 259 – 261 °C.

1H NMR (400 MHz, DMSO- d_6): δ (ppm) = 8.98 (d, J = 8.3 Hz, 1H, 10'-H), 8.89 (dd, J = 8.1, 1.6 Hz, 1H, 1'-H), 8.14 (dd, J = 8.0, 1.5 Hz, 1H, 4'-H), 8.07 – 7.98 (m, 4H, 2-, -6-H, 9'-H, 7'-H), 7.95 – 7.90 (m, 2H, 3-H, -5), 7.87 – 7.75 (m, 3H, 3'-H, 2'-H, 8'-H), 7.54 (s, 2H, SO_2NH_2).

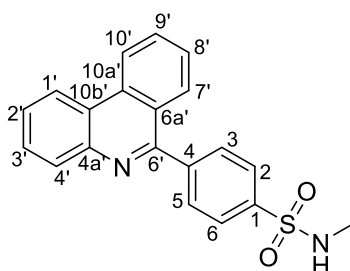
^{13}C NMR (101 MHz, DMSO- d_6): δ (ppm) = 159.7 (C-6'), 144.8 (C-1), 143.6 (C-4a'), 142.9 (C-4), 133.3 (C-10a'), 131.8 (C-9'), 130.8 (C-3, -5), 130.3 (C-4'), 129.7 (C-3'), 128.5 (C-7' or C-2' or C-8'), 128.3 (C-7' or C-2' or C-8'), 128.1 (C-7' or C-2' or C-8'), 126.2 (C-2, -6), 124.6 (C-6a'), 123.9 (C-10b'), 123.5 (C-1'), 123.3 (C-10').

IR (ATR): $\tilde{\nu}$ [cm^{-1}] = 3302, 3058, 1569, 1339, 1155, 1091, 920, 827, 759, 724.

HRMS (ESI): m/z [$M+H$] $^+$ calcd. for $C_{19}H_{15}N_2O_2S^+$: 335.0849, found: 335.0850.

Purity (HPLC): >96 % (210 nm, 254 nm).

***N*-Methyl-4-(phenanthridin-6-yl)benzenesulfonamide (39)**



C₂₀H₁₆N₂O₂S

348.43 g/mol

Methyl sulfonamide **39** was synthesized according to GP3, using crude sulfonyl chloride **65** (136 mg, ~0.300 mmol) and a solution of methylamine (33 % in ethanol, 187 μ L, 1.50 mmol). Trituration in isopropanol gave methyl sulfonamide **39** as off-white solid (93 mg, 0.27 mmol, 89 %).

mp.: 254 – 256 °C.

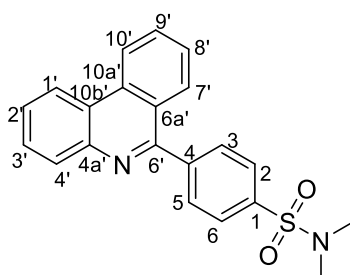
¹H NMR (400 MHz, DMSO-*d*₆): δ (ppm) = 8.99 (dd, J = 8.7, 1.1 Hz, 1H, 10'-H), 8.89 (dd, J = 8.2, 1.6 Hz, 1H, 1'-H), 8.14 (dd, J = 7.9, 1.5 Hz, 1H, 4'-H), 8.04 – 7.94 (m, 6H, 7'-H, 9'-H, 2-, 6-H, 3-, 5-H), 7.87 – 7.75 (m, 3H, 3'-H, 2'-H, 8'-H), 7.63 (q, J = 5.0 Hz, 1H, NH), 2.54 (s, 3H, CH₃).

¹³C NMR (101 MHz, DMSO-*d*₆): δ (ppm) = 159.1 (C-6'), 143.1 (C-4a'), 142.9 (C-4), 139.4 (C-1), 132.8 (C-10a'), 131.3 (C-9'), 130.5 (C-3, -5), 129.8 (C-4'), 129.3 (C-3'), 128.1 (C-8'), 127.9 (C-2'), 127.7 (C-7'), 126.7 (C-2, -6), 124.1 (C-6a'), 123.4 (C-10b'), 123.0 (C-10'), 122.8 (C-1'), 28.8 (CH₃).

IR (ATR): $\tilde{\nu}$ [cm⁻¹] = 3283, 3065, 1609, 1570, 1457, 1394, 1322, 1306, 1159, 1087, 956, 830, 767, 728.

HRMS (ESI): m/z [M+H]⁺ calcd. for C₂₀H₁₇N₂O₂S⁺: 349.1005, found: 349.1006.

Purity (HPLC): >96 % (210 nm, 254 nm).

***N,N*-Dimethyl-4-(phenanthridin-6-yl)benzenesulfonamide (40)**C₂₁H₁₈N₂O₂S

362.45 g/mol

Dimethyl sulfonamide **40** was synthesized according to GP3, using crude sulfonyl chloride **65** (136 mg, ~0.300 mmol) and a solution of dimethylamine (2M in THF, 750 μ L, 1.50 mmol). Trituration in isopropanol gave dimethyl sulfonamide **40** as off-white solid (91 mg, 0.25 mmol, 84 %).

mp.: 239 – 241 °C.

¹H NMR (400 MHz, DMSO-*d*₆): δ (ppm) = 9.02 – 8.96 (m, 1H, 10'-H), 8.93 – 8.86 (m, 1H, 1'-H), 8.18 – 8.12 (m, 1H, 4'-H), 8.10 – 7.94 (m, 6H, 7'-H, 3-, 5-H, 2-, 6-H, 9'-H), 7.88 – 7.76 (m, 3H, 3'-H, 2'-H, 8'-H), 2.73 (s, 6H, CH₃).

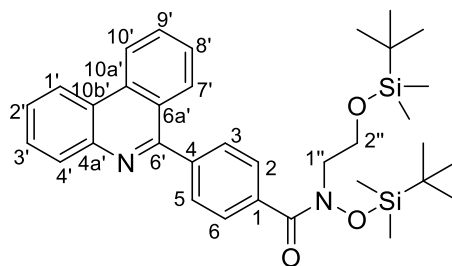
¹³C NMR (101 MHz, DMSO-*d*₆): δ (ppm) = 159.0 (C-6'), 143.5 (C-4), 143.1 (C-4a'), 134.9 (C-10a'), 132.9 (C-1), 131.4 (C-9'), 130.6 (C-3, -5), 129.8 (C-4'), 129.3 (C-3'), 128.1 (C-8'), 127.9 (C-2'), 127.7 (C-7'), 127.6 (C-2, -6), 124.1 (C-6a'), 123.4 (C-10b'), 123.0 (C-10'), 122.8 (C-1'), 37.7 (CH₃).

IR (ATR): $\tilde{\nu}$ [cm⁻¹] = 1608, 1578, 1558, 1458, 1397, 1336, 1159, 1136, 1088, 942, 841, 766, 732.

HRMS (ESI): *m/z* [M+H]⁺ calcd. for C₂₁H₁₉N₂O₂S⁺: 363.1162, found: 363.1164.

Purity (HPLC): >96 % (210 nm, 254 nm).

***N*-((*tert*-Butyldimethylsilyloxy)-*N*-(2-((*tert*-butyldimethylsilyloxy)ethyl)-4-(phenanthridin-6-yl)benzamide (86)**



$C_{34}H_{46}N_2O_3Si_2$

586.92 g/mol

Methyl ester **18** (160 mg, 0.511 mmol) and *O*-TBDMS-hydroxylamine (119 mg, 0.766 mmol) were dissolved in dry THF (10 mL) under N_2 atmosphere and was cooled to 0 °C. A solution of LHMDS (1M in THF, 1.79 mL, 1.79 mmol) was added dropwise and the solution was stirred for 1 h at 0 °C. Then water (15 mL) was added to quench the LHMDS, and the mixture was diluted with ethyl acetate (20 mL). The layers were separated, and the aqueous layer was extracted twice with ethyl acetate (2x 20 mL). The combined organic layers were dried using a hydrophobic filter and the solvent was removed *in vacuo*. The residue was dissolved in DMF (1 mL), together with Cs_2CO_3 (228 mg, 0.7 mmol) and NaI (8 mg, 0.05 mmol) under N_2 atmosphere. (2-Bromoethoxy)-*tert*-butyldimethylsilane (322 μ L, 1.50 mmol) was added and the suspension was heated to 70 °C and was stirred at this temperature for 3 h. Then water (10 mL) and ethyl acetate (10 mL) were added to the mixture and the layers were separated. The aqueous layer was extracted twice with ethyl acetate (2x 15 mL). The combined organic layers were washed twice with water (2x 20 mL) and once with brine (20 mL), then were dried using a hydrophobic filter. The solvent was removed *in vacuo* and the residue was purified by FCC (PE/EtOAc 9:1) to give di-TBDMS-*N*-hydroxyethylhydroxamic acid **86** as colourless oil (108 mg, 0.184 mmol, 36 %).

1H NMR (400 MHz, $CDCl_3$) δ (ppm): = 8.71 (d, J = 8.3 Hz, 1H, 10'-H), 8.63 (dd, J = 8.2, 1.5 Hz, 1H, 1'-H), 8.25 (dd, J = 8.1, 1.4 Hz, 1H, 4'-H), 8.10 (d, J = 9.2 Hz, 1H, 7'-H), 8.07 – 8.02 (m, 2H, 2-, 6-H), 7.87 (ddd, J = 8.3, 7.0, 1.3 Hz, 1H, 9'-H), 7.80 – 7.67 (m, 4H, 3'-H, 3-, 5-H, 2'-H), 7.62 (ddd, J = 8.2, 7.0, 1.2 Hz, 1H, 8'-H), 4.59 – 4.52 (m, 2H, 1''-H), 3.99 – 3.94 (m, 2H, 2''-H), 1.03 (s, 9H, CH_3 *t*Bu), 0.92 (s, 9H, CH_3 *t*Bu), 0.28 (s, 6H, $Si(CH_3)_2$), 0.10 (s, 6H, $Si(CH_3)_2$).

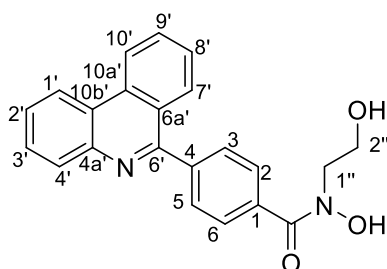
^{13}C NMR (101 MHz, $CDCl_3$) δ (ppm): = 160.9 (C-6'), 156.7 (C=O), 144.0 (C-4a'), 141.3 (C-4), 133.6 (C-10a'), 132.7 (C-1), 130.7 (C-9'), 130.6 (C-4'), 129.7 (C-3, -5), 129.0 (C-3'), 128.9 (C-7'), 127.3 (C-8'), 127.2 (C-2, -6), 127.2 (C-2'), 125.3 (C-6a'), 123.9 (C-10b'), 122.4 (C-10'),

Experimental for Sirtuin 6 modulators

122.1 (C-1'), 73.8 (C-1''), 62.8 (C-2''), 26.4 (CH₃ tBu), 26.1 (CH₃ tBu), 18.5 (C_q tBu), 18.4 (C_q tBu), -5.1 (Si(CH₃)₂), -5.2 (Si(CH₃)₂).

IR (ATR): $\tilde{\nu}$ [cm⁻¹] = 2954, 2928, 2856, 1611, 1581, 1569, 1472, 1461, 1311, 1250, 1136, 1093, 948, 831, 776, 760, 726.

HRMS (ESI): m/z [M+H]⁺ calcd. for C₃₄H₄₇N₂O₃Si₂⁺: 587.3120, found: 587.3124.

***N*-hydroxy-*N*-(2-hydroxyethyl)-4-(phenanthridin-6-yl)benzamide (69)**C₂₂H₁₈N₂O₃

358.4 g/mol

Di-TBDMS-*N*-hydroxyethylhydroxamic acid **86** (88 mg, 0.15 mmol) was dissolved in dry THF under nitrogen atmosphere and a solution of TBAF (1M in THF, 0.6 mL, 0.60 mmol) was added dropwise. The solution was stirred for 30 min at rt subsequently the solvent was removed *in vacuo*. The residue was purified by FCC (CH₂Cl₂/MeOH 98:2) to give *N*-hydroxyethylhydroxamic acid **69** as colourless solid (25 mg, 0.070 mmol, 47 %).

mp.: 162 – 164 °C.

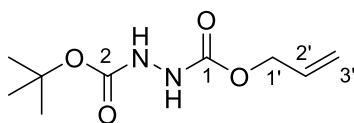
¹H NMR (500 MHz, DMSO-*d*₆): δ (ppm) = 10.68 (s, 0.74H, NOH), 10.09 (s, 0.26H, NOH rot.), 8.99 – 8.94 (m, 1H, 10'-H), 8.89 – 8.82 (m, 1H, 1'-H), 8.16 – 8.11 (m, 1H, 4'-H), 8.08 – 7.96 (m, 4H, 7'-H, 9'-H, 2-, 6-H), 7.88 – 7.71 (m, 5H, 3'-H, 2'-H, 8'-H, 3-, 5-H), 4.92 – 4.84 (m, 1H, OH), 4.39 – 4.34 (m, 1.45H, 1''-H), 4.14 (dd, *J* = 5.7, 4.3 Hz, 0.55H, 1''-H rot.), 3.79 – 3.69 (m, 2H, 2''-H).

¹³C NMR (126 MHz, DMSO-*d*₆): δ (ppm) = 159.9 (C-6'), 159.9 (C-6' rot.), 156.6 (C=O rot.), 153.0 (C=O), 143.2 (C-4a'), 143.2 (C-4a' rot.), 140.4 (C-10a' rot.), 140.2 (C-10a'), 132.8 (C-4), 132.5 (C-1), 131.2 (C-9' rot.), 131.2 (C-9'), 129.8 (C-4' rot.), 129.8 (C-4'), 129.7 (C-3, -5), 129.2 (C-3' rot.), 129.2 (C-3'), 128.7 (C-8' rot.), 128.1 (C-8'), 127.9 (C-7' rot.), 127.9 (C-7'), 127.4 (C-2' rot.), 127.4 (C-2'), 126.1 (C-2, -6), 124.3 (C-6a'), 123.3 (C-10b' rot.), 123.3 (C-10b'), 122.9 (C-10'), 122.7 (C-1'), 73.1 (C-1''), 68.5 (C-1'' rot.), 60.4 (C-2''), 59.4 (C-2'' rot.).

IR (ATR): $\tilde{\nu}$ [cm⁻¹] = 3175, 3056, 2854, 1638, 1571, 1460, 1398, 1368, 1294, 1260, 1102, 1073, 961, 836, 756, 727.

HRMS (ESI): *m/z* [M+H]⁺ calcd. for C₂₂H₁₉N₂O₃⁺: 359.1390, found: 359.1393.

Purity (HPLC): >96 % (double peak, both rotamers together) (210 nm, 254 nm).

1-Allyl 2-(*tert*-butyl) hydrazine-1,2-dicarboxylate (93)^[93]

 $C_9H_{16}N_2O_4$

216.24 g/mol

tert-Butyl carbazate (3.97 g, 30.0 mmol, 1.00 eq) and pyridine (2.67 mL, 33.0 mmol, 1.10 mmol) were dissolved in diethyl ether (120 mL) under nitrogen atmosphere and were cooled to 0 °C. Allyl chloroformate was added dropwise and the solution was stirred for 45 min at 0 °C and 45 min at rt. The reaction mixture was washed with 5 % aqueous HCl and 5 % NaHCO₃ solution. The organic layer was dried using a hydrophobic filter and the solvent was removed *in vacuo* to give Boc-Alloc-hydrazine **93** as white solid (6.40 g, 29.6 mmol, 99 %).

mp.: 87 – 89 °C (lit. no mp. determined).

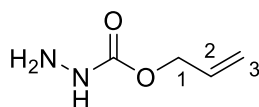
¹H NMR (400 MHz, CDCl₃): δ (ppm) = 6.37 (d, *J* = 62.7 Hz, 2H, NH), 5.91 (ddt, *J* = 17.2, 10.4, 5.7 Hz, 1H, 2'-H), 5.33 (dq, *J* = 17.1, 1.5 Hz, 1H, 3'-H), 5.24 (dq, *J* = 10.5, 1.3 Hz, 1H, 3'-H), 4.64 (dt, *J* = 5.7, 1.4 Hz, 2H, 1'-H), 1.47 (s, 9H, CH₃ *t*Bu).

¹³C NMR (101 MHz, CDCl₃): δ (ppm) = 156.6 (C=O), 132.1 (C-2'), 118.6 (C-3'), 82.0 (C_q *t*Bu), 66.8 (C-1'), 28.3 (CH₃ *t*Bu).

IR (ATR): $\tilde{\nu}$ [cm⁻¹] = 3289, 2981, 1746, 1733, 1694, 1516, 1367, 1265, 1243, 1225, 1158, 1057, 992, 935.

HRMS (EI): *m/z* [M]⁺ calcd. for C₉H₁₆N₂O₄⁺: 216.1110, found: 216.1099.

Allyl hydrazinecarboxylate (94)^[93]



C₄H₈N₂O₂

116.12 g/mol

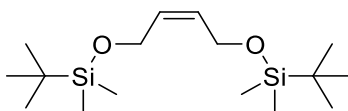
Boc-Alloc-hydrazine **93** (4.97 g, 23.0 mmol) was suspended in 30 mL water and was heated to 160 °C for 1.5 h. Water was removed by rotary evaporation and the product was purified by distillation (bp. ~56 °C at 0.1 mbar) to give Alloc-hydrazine **94** as colourless oil (1.98 g, 17.1 mmol, 74 %).

¹H NMR (400 MHz, CDCl₃): δ (ppm) = 6.01 (s, 1H, NH), 5.92 (ddt, *J* = 16.4, 10.9, 5.7 Hz, 1H, 2-H), 5.32 (dd, *J* = 17.2, 1.6 Hz, 1H, 3-H), 5.24 (dd, *J* = 10.4, 1.4 Hz, 1H, 3-H), 4.61 (dt, *J* = 5.8, 1.4 Hz, 2H, 1-H), 3.76 (d, *J* = 4.1 Hz, 2H, NH₂).

¹³C NMR (101 MHz, CDCl₃): δ (ppm) = 158.8 (C=O), 132.6 (C-2), 118.4 (C-3), 66.3 (C-1).

IR (ATR): $\tilde{\nu}$ [cm⁻¹] = 3333, 2363, 1702, 1631, 1502, 1269, 1178, 1057, 925.

HRMS (EI): *m/z* [M]⁺⁺ calcd. for C₄H₈N₂O₂⁺⁺: 116.0586, found: 116.0581.

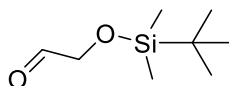
(Z)-2,2,3,3,10,10,11,11-octamethyl-4,9-dioxa-3,10-disiladodec-6-ene (99)^[95]C₁₆H₃₆O₂Si₂

316.63 g/mol

2-Butene-1,4-diol (1.76 g, 20.0 mmol) and imidazole (6.00 g, 88.0 mmol) were dissolved in THF (80 mL) and a solution of TBDMSCl (6.63 g, 44.0 mmol) in THF (20 mL) was added dropwise. The solution was stirred at rt for 2.5 h. THF was removed *in vacuo*, the residue was taken up in diethyl ether and was washed with ice-cold aqueous 1M HCl (40 mL), saturated NaHCO₃ solution (40 mL) and water (40 mL). The organic layer was dried using a hydrophobic filter and the solvent was removed *in vacuo*. The residue was purified by FCC (petrol ether/ethyl acetate 8:2) to give the di-TBDMS-butenediol **99** as colourless oil (5.80 g, 18.3 mmol, 92 %) ¹H NMR (400 MHz, CDCl₃): δ (ppm) = 5.55 (ddd, *J* = 4.1, 3.2, 0.8 Hz, 2H, CH), 4.26 – 4.20 (m, 4H, CH₂), 0.90 (s, 18H, CH₃ *t*Bu), 0.07 (s, 12H Si(CH₃)₂).

¹³C NMR (101 MHz, CDCl₃): δ (ppm) = 130.3 (CH), 59.8 (CH₂), 26.1 (CH₃ *t*Bu), 18.5 (C_q *t*Bu), -5.0 (Si(CH₃)₂).

IR (ATR): $\tilde{\nu}$ [cm⁻¹] = 2928, 2855, 1472, 1463, 1252, 1076, 832, 772.

2-((*tert*-Butyldimethylsilyl)oxy)acetaldehyde (97**)^[95]**

C₈H₁₈O₂Si
174.31 g/mol

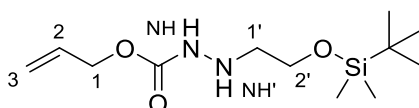
Di-TBDMS-butenediol **99** (4.75 g, 15.0 mmol) was dissolved in CH₂Cl₂ (80 mL) and was cooled to -78 °C. Ozone was bubbled through the solution until a blue colour appeared. Subsequently O₂ was bubbled through the solution until the blue colour disappeared (removal of residual ozone), then N₂ for an additional 10 min. Triphenylphosphine (4.77 g, 18.0 mmol) was added at -78 °C, the solution was allowed to warm up to rt and stirred for another 2 h at rt. Then a mixture of ethyl acetate/petrol ether (1:1, 100 mL) was added and the reaction mixture was filtered through a pad of celite. The solvents of the filtrate were removed *in vacuo* and the residue was purified by FCC (petrol ether/ethyl acetate 8:2). Because of the high volatility of acetaldehyde **97**, the product was obtained with residual ethyl acetate as colourless oil (4.86 g, ~27.9 mmol, ~93 %).

¹H NMR (400 MHz, CDCl₃): δ (ppm) = 9.70 (t, *J* = 0.9 Hz, 1H, O=CH), 4.21 (d, *J* = 0.9 Hz, 2H, CH₂), 0.93 (s, 9H, CH₃, *t*Bu), 0.10 (s, 6H, Si(CH₃)₂).

¹³C NMR (101 MHz, CDCl₃): δ (ppm) = 202.5 (O=CH), 69.8 (CH₂), 25.9 (CH₃ *t*Bu), 18.5 (C_q *t*Bu), -5.3 (Si(CH₃)₂).

IR (ATR): $\tilde{\nu}$ [cm⁻¹] = 2928, 2857, 1739, 1472, 1253, 1122, 833, 776.

HRMS (EI): *m/z* [M]⁺ calcd. for C₈H₁₈O₂Si⁺: 174.1076, calcd. for [M-CH₃]⁺: 159.0841, found: 159.0832.

Allyl 2-(2-((*tert*-butyldimethylsilyl)oxy)ethyl)hydrazine-1-carboxylate (100**)^[92]**C₁₂H₂₆N₂O₃Si

274.44 g/mol

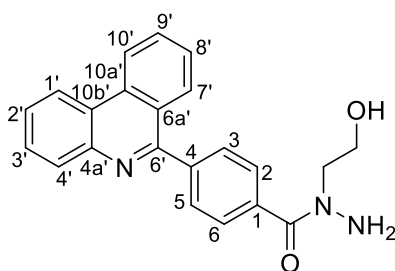
Acetaldehyde **97** (1.74 g, 10.0 mmol) and Alloc-hydrazine **94** were dissolved in CHCl₃ (15 mL) and stirred at rt for 19 h. Subsequently, the reaction mixture was dried by filtration through a hydrophobic filter, to remove any water formed during the imine formation. CHCl₃ was removed *in vacuo*. The residue together with zinc chloride (409 mg, 3.00 mmol) was dissolved in dry MeOH (25 mL) under N₂ atmosphere and a solution of NaCNBH₃ (529 mg, 8.00 mmol) in dry MeOH (25 mL) was added dropwise. The mixture was stirred for 3 days at rt. Then a mixture of ethyl acetate/petrol ether (1:1, 60 mL) was added, the reaction mixture was filtered through a pad of celite, and the filtrate was washed with water (50 mL) and saturated brine (50 mL). The organic layer was dried using a hydrophobic filter and the solvents were removed *in vacuo*. The residue was purified by FCC (petrol ether/ethyl acetate 7:3) to give *N*-Alloc-*O*-TBDMS-hydroxyethylhydrazine **100** as colourless oil (730 mg, 2.66 mmol, 27 %).

¹H NMR (400 MHz, CDCl₃): δ (ppm) = 6.30 (s, 1H, NH), 5.92 (ddt, *J* = 16.4, 10.8, 5.6 Hz, 1H, 2-H), 5.31 (d, *J* = 17.1 Hz, 1H, 3-H), 5.22 (dq, *J* = 10.4, 1.3 Hz, 1H, 3-H), 4.61 (d, *J* = 5.7 Hz, 2H, 1-H), 4.19 (s, 1H, NH'), 3.77 – 3.72 (m, 2H, 2'-H), 2.98 (q, *J* = 5.5 Hz, 2H, 1'-H), 0.90 (s, 9H, CH₃ *t*Bu), 0.07 (s, 6H, Si(CH₃)₂).

¹³C NMR (101 MHz, CDCl₃): δ (ppm) = 157.1 (NHCOOR), 132.7 (C-2), 118.1 (C-3), 66.0 (C-1), 61.8 (C-2'), 53.9 (C-1'), 26.1 (CH₃ *t*Bu), 18.4 (C_q *t*Bu), -5.2 (Si(CH₃)₂).

IR (ATR): $\tilde{\nu}$ [cm⁻¹] = 3312, 2928, 2856, 1712, 1471, 1463, 1253, 1095, 832, 774.

HRMS (ESI): *m/z* [M+H]⁺ calcd. for C₁₂H₂₇N₂O₃Si⁺: 275,1785, found: 275.1785.

***N*-(2-Hydroxyethyl)-4-(phenanthridin-6-yl)benzohydrazide (70)**C₂₂H₁₉N₃O₂

357.41 g/mol

Carboxylic acid **19** (398 mg, 1.33 mmol) and pyridine (645 μ L, 7.98 mmol) were dissolved in CHCl₃ (20 mL) and were cooled to 0°C. Then a solution of 2-chloro-1,3-dimethylimidazolium chloride (450 mg, 2.66 mmol) in CHCl₃ (5 mL) was added dropwise. The resulting solution was allowed to warm up to rt and was stirred for another 15 min. Then a solution of *N*-Alloc-*O*-TBDMS-hydroxyethylhydrazine **100** (730 mg, 2.66 mmol) in CHCl₃ (5 mL) was added and the reaction mixture was stirred over night at rt. Water was added to the mixture, the layers were separated, and the aqueous layer was extracted twice with ethyl acetate (2x 30 mL). The combined organic layers were washed with brine and were dried using a hydrophobic filter and the solvent was removed *in vacuo*. Purification by FCC (CH₂Cl₂/MeOH 98:2) gave Alloc and TBDMS protected hydrazide **102** (350 mg, ~0.630 mmol, ~47 %) as a pale-yellow oil, that was used for the next steps without further characterization. For Alloc deprotection compound **102** (300 mg, 0.540 mmol), formic acid (113 μ L, 2.70 mmol), diethyl amine (279 μ L, 2.70 mmol) and Pd(PPh₃)₄ (62 mg, 0.054 mmol) were dissolved in THF (5 mL) and N₂ atmosphere and were stirred at rt for 5h. Upon complete deprotection, the reaction mixture was diluted with ethyl acetate (20 mL) and was filtrated through a pad of silica. Removing the solvent of the filtrate *in vacuo* gave the crude Alloc deprotected derivative as beige solid (142 mg, ~0.30 mmol, ~56 %). A part of this crude product (124 mg, ~0.263 mmol) was used for TBDMS deprotection. Therefore, it was dissolved in dry THF (2.5 mL) under N₂ atmosphere and a solution of TBAF (1M in THF, 526 μ L, 0.526 mmol) was added. The resulting mixture was stirred for 1 h at rt, then was diluted with ethyl acetate (15 mL) and was washed with brine (15 mL). The aqueous layer was extracted twice with ethyl acetate (10 mL), the combined organic layers were dried using a hydrophobic filter and the solvent was removed *in vacuo*. The residue was purified by FCC (CH₂Cl₂/MeOH 92:8) to give *N*'-hydroxyethylhydrazide **70** as off-white solid (54 mg, 0.151 mmol, 32 % over two deprotection steps).

¹H NMR (500 MHz, DMSO-*d*₆): δ (ppm) = 8.96 (d, *J* = 8.3 Hz, 1H, 10'-H), 8.87 (dd, *J* = 8.2, 1.5 Hz, 1H, 1'-H), 8.13 (dd, *J* = 8.1, 1.5 Hz, 1H, 4'-H), 8.07 (dd, *J* = 8.2, 1.3 Hz, 1H, 7'-H), 7.99

Experimental for Sirtuin 6 modulators

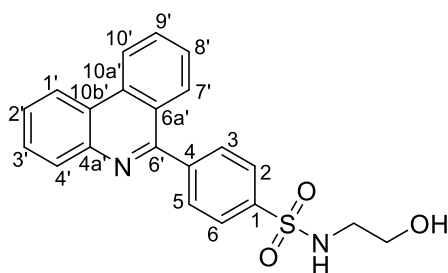
(ddd, $J = 8.4, 7.0, 1.3$ Hz, 1H, 9'-H), 7.85 – 7.64 (m, 7H, 3'-H, 3-, 5-H, 2'-H, 8'-H, 2-, 6-H), 5.05 – 4.80 (m, 3H, NH₂, OH), 3.78 – 3.43 (m, 4H, CH₂).

¹³C NMR (101 MHz, CDCl₃): δ (ppm) = 170.4 (C=O), 168.9 (C=O, rot.), 160.1 (C-6'), 159.8 (C-6', rot.), 143.2 (C-4a'), 140.0 (C-1 or C-4), 139.6 (C-1 or C-4, rot.), 137.28 (C-1 or C-4), 136.4 (C-1 or C-4, rot.), 132.8 (C-10a'), 131.2 (C-9'), 129.8 (C-4'), 129.5 (prop. C-2, -6, rot.), 129.2 (C-3'), 128.5 (C-3, -5), 128.4 (C-3, -5, rot.), 128.1 (C-2' or C-8'), 127.9 (C-7', C2' or C-8'), 127.4 (C-2, -6), 124.3 (C-6a'), 123.3 (C-10b'), 122.9 (C-10'), 122.7 (C-1'), 58.0 (CH₂), 57.5 (CH₂, rot.), 53.8 (CH₂), 52.1 (CH₂, rot.).

IR (ATR): $\tilde{\nu}$ [cm⁻¹] = 3202, 2924, 1626, 1607, 1458, 1424, 1365, 1323, 1056, 927, 843, 756, 727.

HRMS (ESI): m/z [M+H]⁺ calcd. for C₂₂H₂₀N₃O₂⁺: 358.1550, found: 358.1555.

Purity (HPLC): >96% (210 nm, 254 nm).

***N*-(2-Hydroxyethyl)-4-(phenanthridin-6-yl)benzenesulfonamide (71)**C₂₁H₁₈N₂O₃S

378.45 g/mol

Ethanolamine (60 μ L, 1.0 mmol) was dissolved in water (400 μ L), then MgO (207 mg, 5.00 mmol) and THF (400 μ L) were added. The resulting mixture was stirred vividly at rt for 30 min. Crude sulfonyl chloride **65** (454 mg, ~1.00 mmol) and THF (400 μ L) were added portion wise, and the mixture was stirred for 1.5 h. Subsequently the mixture was diluted with ethyl acetate and was filtered, leaving a bulky residue in the filter. The filtrate was washed with brine and the aqueous layer was extracted twice with ethyl acetate (2x 50 mL). The combined organic layers were dried using a hydrophobic filter and the solvent was removed *in vacuo*. Purification by FCC (CH₂Cl₂/MeOH 96:4) yielded only low amounts of hydroxyethyl sulfonamide **71** (40 mg, 0.11 mmol, 11 %), probably due to the low solubility in ethyl acetate. To recover more product, the filter residue from the first filtration was boiled in a mixture of CH₂Cl₂/MeOH (1:1, 150 mL) and was filtered hot. The solvent of the filtrate was removed *in vacuo* and the residue was purified by FCC, yielding additional hydroxyethyl sulfonamide **71** (212 mg, 0.56 mmol, 56 %).

mp.: 209 – 211 °C.

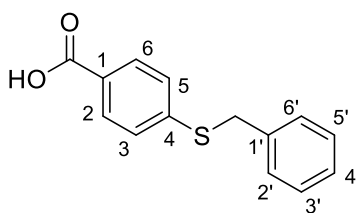
¹H NMR (400 MHz, DMSO-*d*₆): δ (ppm) = 9.01 – 8.96 (m, 1H, 10'-H), 8.89 (dd, *J* = 8.0, 1.6 Hz, 1H, 1'-H), 8.14 (dd, *J* = 8.0, 1.5 Hz, 1H, 4'-H), 8.05 – 7.98 (m, 4H, 2-, 6-H, 7'-H, 9'-H), 7.97 – 7.92 (m, 2H, 3-, 5-H), 7.88 – 7.75 (m, 4H, 3'-H, 2'-H, 8'-H, SO₂NH), 4.75 (t, *J* = 5.6 Hz, 1H, OH), 3.44 (q, *J* = 6.1 Hz, 2H, CH₂OH), 2.91 (q, *J* = 5.5 Hz, 2H, SO₂NHCH₂).

¹³C NMR (101 MHz, DMSO-*d*₆): δ (ppm) = 159.6 (C-6'), 143.6 (C-4a'), 143.3 (C-4), 141.2 (C-1), 133.3 (C-10a'), 131.8 (C-9'), 131.0 (C-3, -5), 130.3 (C-4'), 129.8 (C-3'), 128.6 (C-8'), 128.4 (C-2'), 128.1 (C-7'), 127.1 (C-2, -6), 124.6 (C-6a'), 123.9 (C-10b'), 123.5 (C-10'), 123.3 (C-1'), 60.4 (CH₂OH), 45.7 (SO₂NHCH₂).

IR (ATR): $\tilde{\nu}$ [cm⁻¹] = 3157, 2920, 2848, 1609, 1562, 1432, 1326, 1174, 1068, 961, 846, 837, 766, 722.

HRMS (ESI): *m/z* [M+H]⁺ calcd. for C₂₁H₁₉N₂O₃S⁺: 379.1111, found: 379.1113.

Purity (HPLC): >96 % (210 nm, 254 nm).

4-(Benzylthio)benzoic acid (109)^[110]C₁₄H₁₂O₂S

244.31 g/mol

4-Mercaptobenzoic acid (771 mg, 5.00 mmol) and KOH (842 mg, 15.0 mmol) were dissolved in 25 mL dry MeOH (approx. 5 min until complete dissolution) then benzyl bromide (624 μ L, 5.25 mmol) was added dropwise. The resulting suspension was heated to 65 °C and was stirred under reflux for 30 min. The mixture was allowed to cool down to rt, then was diluted with water (20 mL) and 2M aqueous HCl (20 mL). The mixture was extracted three times with ethyl acetate (1x 100, 2x 50 mL), the combined organic layers were dried using a hydrophobic filter and the solvent removed *in vacuo* to give benzylthioether **109** (1.19 g, 4.85 mmol, 97 %) as light-yellow crystals.

mp.: 188 – 190 °C (lit.^[110] 189 – 190 °C)

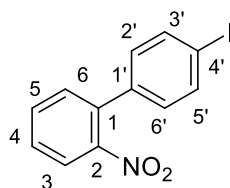
¹H NMR (400 MHz, DMSO-*d*₆): δ (ppm) = 12.86 (s, 1H, COOH), 7.85 – 7.79 (m, 2H, 2-H, 6-H), 7.45 – 7.38 (m, 4H, 3-H, 5-H, 2'-H, 6'-H), 7.35 – 7.29 (m, 2H, 3'-H, 5'-H), 7.27 – 7.22 (m, 1H, 4'-H), 4.34 (s, 2H, CH₂).

¹³C NMR (101 MHz, DMSO-*d*₆): δ (ppm) = 166.9 (COOH), 143.0 (C-4), 136.8 (C-1'), 129.7 (C-2, C-6), 128.9 (C-2', C-6'), 128.5 (C-3', C-5'), 127.4 (C-1), 127.2 (C-4'), 126.4 (C-3, C-5), 35.3 (CH₂).

IR (ATR): $\tilde{\nu}$ [cm⁻¹] = 3854, 3746, 3648, 3612, 2540, 1778, 1588, 14,17, 1281, 953, 840, 763, 717.

HRMS (ESI): *m/z* [M-H]⁻ calcd. for C₁₄H₁₂O₂S: 243.0485, found: 243.0486.

Purity (HPLC): >96 % (210 nm, 254 nm).

4'-Iodo-2-nitro-1,1'-biphenyl (118)^[100]

325.11 g/mol

To a solution of 2-nitroaniline (1.38 g, 10.0 mmol) in 100 mL CH₂Cl₂ was added BF₃·OEt₂ (1.48 mL, 12.0 mmol) at 0 °C, followed by very slow, dropwise addition of *tert*-butyl nitrite (1.98 mL, 15.0 mmol). The resulting suspension was allowed to warm up to rt and was stirred for 3 h, then filtered to collect 2-nitrobenzenediazonium tetrafluoroborate salt (**116**) as light brown solid (2.08 g, 8.78 mmol, 88 %, ¹H NMR (400 MHz, CD₃CN) δ (ppm) = 8.86 (dd, *J* = 8.2, 1.4 Hz, 1H), 8.71 (dd, *J* = 8.4, 1.2 Hz, 1H), 8.52 (ddd, *J* = 8.4, 7.7, 1.4 Hz, 1H), 8.33 (td, *J* = 7.9, 1.2 Hz, 1H), ¹³C NMR (101 MHz, CD₃CN) δ (ppm) = 144.4, 138.0, 137.8, 129.6.), which was used directly in the next step. For the following Suzuki type reaction, the diazonium tetrafluoroborate salt **116** (2.61 g, 11.0 mmol) was dissolved together with 4-iodophenylboronic acid (2.56 g, 10.0 mmol) in dioxane (25 mL) under a nitrogen atmosphere. A suspension of palladium acetate (67 mg, 0.30 mmol) in dioxane (5 mL) was prepared separately under nitrogen atmosphere and was added to the reaction mixture. After approx. 5 min the mixture started boiling and was cooled to rt by a water bath. The mixture was stirred for 1 h at rt. Then water (20 mL) was added, and the mixture was extracted three times with ethyl acetate (3x 50 mL). The combined organic layers were dried using a hydrophobic filter and the solvent was removed *in vacuo*. The residue was purified by FCC (PE/EtOAc 9:1) to give nitrobiphenyl **118** as light-yellow solid (2.58 g, 7.92 mmol, 79 %).

mp.: 91 – 93 °C (lit.^[100] 81 – 82 °C).

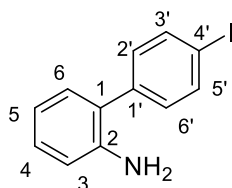
¹H NMR (400 MHz, CDCl₃): δ (ppm) = 7.89 (dd, *J* = 8.1, 1.4 Hz, 1H, 3-H), 7.80 – 7.73 (m, 2H, 3'-, 5'-H), 7.63 (td, *J* = 7.6, 1.3 Hz, 1H, 5-H), 7.51 (ddd, *J* = 8.1, 7.4, 1.4 Hz, 1H, 4-H), 7.40 (dd, *J* = 7.7, 1.5 Hz, 1H, 6-H), 7.09 – 7.03 (m, 2H, 2'-, 6'-H).

¹³C NMR (101 MHz, CDCl₃): δ (ppm) = 149.1 (C-2), 138.0 (C-3', -5'), 137.2 (C-1'), 135.5 (C-1), 132.7 (C-5), 131.9 (C-6), 129.9 (C-2', -6'), 128.7 (C-4), 124.5 (C-3), 94.4 (C-4').

IR (ATR): $\tilde{\nu}$ [cm⁻¹] = 2923, 1518, 1355, 1001, 854, 820, 745.

HRMS (EI): *m/z* [M]⁺ calcd. for C₁₂H₉INO₂⁺: 324.9600, found: 324.9593.

Purity (HPLC): >96 % (210 nm, 254 nm).

4'-iodo-[1,1'-biphenyl]-2-amine (110) $C_{12}H_{10}IN$

295.12 g/mol

Nitrobiphenyl **118** (2.57 g, 7.90 mmol), ammonium formate (2.5 g, 40 mmol) and zinc (4.3 g, 65 mmol) were dissolved in dry methanol under nitrogen atmosphere and were stirred at rt for 1 h. The reaction mixture was filtered through a pad of celite, and the solvent of the filtrate was removed *in vacuo*. The residue was taken up in CH_2Cl_2 to precipitate the ammonium formate and was filtered. The solvent of the filtrate was removed *in vacuo* and the residue was purified by FCC (CH_2Cl_2) to give amine **110** as yellow solid (1.78 g, 6.04 mmol, 77 %).

mp.: 64 – 66 °C.

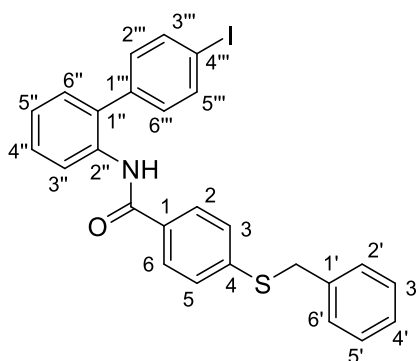
1H NMR (400 MHz, $CDCl_3$): δ (ppm) = 7.81 – 7.75 (m, 2H, 3'-, 5'-H), 7.24 – 7.19 (m, 2H, 2'-, 6'-H), 7.17 (ddd, J = 8.1, 7.3, 1.6 Hz, 1H, 4-H), 7.08 (dd, J = 7.6, 1.6 Hz, 1H, 6-H), 6.82 (td, J = 7.4, 1.2 Hz, 1H, 5-H), 6.76 (dd, J = 8.0, 1.2 Hz, 1H, 3-H), 3.72 (s, 2H, NH_2).

^{13}C NMR (101 MHz, $CDCl_3$): δ (ppm) = 143.5 (C-2), 139.2 (C-1'), 138.1 (C-3', -5'), 131.2 (C-2', -6') 130.4 (C-6), 129.0 (C-4), 126.5 (C-1), 118.9 (C-5), 115.9 (C-3), 92.9 (C-4').

IR (ATR): $\tilde{\nu}$ [cm^{-1}] = 3459, 3378, 1611, 1476, 1450, 1292, 1158, 997, 821, 751.

HRMS (ESI): m/z [$M+H$] $^+$ calcd. for $C_{12}H_{11}IN^+$: 295.9931, found: 295.9930.

Purity (HPLC): >96 % (210 nm, 254 nm).

4-(Benzylthio)-N-(4'-iodo-[1,1'-biphenyl]-2-yl) benzamide (108)C₂₆H₂₀INOS

521.42 g/mol

Thioether **109** (2.20 g, 9.00 mmol) was dissolved in 18 mL DMF, then DIPEA (3.0 mL, 17 mmol) and HATU (3.30 g, 8.69 mmol) were added, and the mixture was stirred for 40 min at rt. Then amine **110** (1.71 g, 5.79 mmol) was added and the mixture was stirred at rt for 24 h. The mixture was diluted with ethyl acetate (200 mL) then was washed twice with water (2x 100 mL), once with 10 % aqueous K₂CO₃ solution (100 mL) and once with brine (50 mL). The organic layer was dried using a hydrophobic filter and the solvent was removed *in vacuo*. The residue was purified by FCC (CH₂Cl₂) and subsequently crystallized from ethanol to give amide **108** as colourless solid (1.95 g, 3.74 mmol, 65 %).

mp.: 159 – 161 °C.

¹H NMR (500 MHz, CDCl₃): δ (ppm) = 8.41 (dd, *J* = 8.3, 1.2 Hz, 1H, 3''-H), 7.85 – 7.81 (m, 2H, 3'''-, 5'''-H), 7.77 (s, 1H, NH), 7.52 – 7.48 (m, 2H, 2-, 6-H), 7.43 (ddd, *J* = 8.5, 7.1, 1.9 Hz, 1H, 4''-H), 7.37 – 7.26 (m, 7H, 3-, 5-H, Ar-H benzyl), 7.22 (ddd, *J* = 14.8, 7.4, 1.6 Hz, 2H, 6''-H, 5''-H), 7.19 – 7.15 (m, 2H, 2'''-, 6'''-H), 4.19 (s, 2H, CH₂).

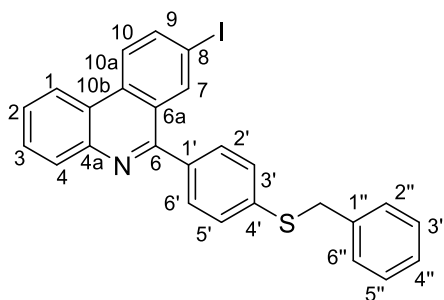
¹³C NMR (126 MHz, CDCl₃): δ (ppm) = 164.7 (C=O), 142.6 (C-4), 138.5 (C-3''', -5'''), 137.8 (C-1'''), 136.5 (C-1'), 134.7 (C-2''), 131.6 (C-1''), 131.6 (C-1), 131.3 (C-2''', -6'''), 130.1 (C-6'''), 129.1 (C-4''), 128.9 (C-2', -6' or C-3', -5'), 128.8 (C-2', -6' or C-3', -5'), 127.9 (C-3, -5), 127.7 (C-4'), 127.4 (C-2, -6), 124.9 (C-5''), 122.1 (C-3''), 94.2 (C-4'''), 37.7 (CH₂).

IR (ATR): $\tilde{\nu}$ [cm⁻¹] = 3318, 1656, 1645, 1510, 1486, 1476, 1304, 1291, 829, 756, 718.

HRMS (ESI): *m/z* [M+H]⁺ calcd. for C₂₆H₂₁INOS⁺: 522.0383, found: 522.0386.

Purity (HPLC): >96 % (210 nm, 254 nm).

6-(4-(Benzylthio)phenyl)-8-iodo phenanthridine (107)



$C_{26}H_{18}INS$

503.41 g/mol

Phenanthridine **107** was synthesized according to GP2 using amide **108** (0.26 g, 0.50 mmol). Purification by FCC (CH_2Cl_2) gave phenanthridine **107** as light-yellow solid (0.20 g, 0.40 mmol 80 %).

mp.: 183 – 185 °C.

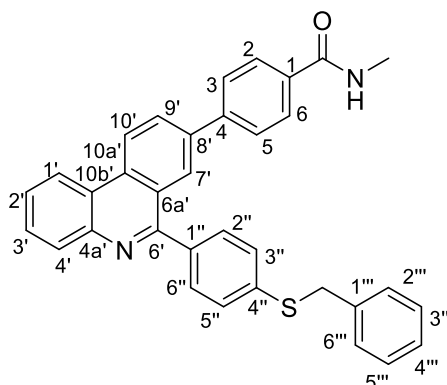
1H NMR (500 MHz, $CDCl_3$): δ (ppm) = 8.56 (dd, J = 8.2, 1.4 Hz, 1H, 1-H), 8.45 – 8.39 (m, 2H, 10-H, 7-H), 8.24 – 8.19 (m, 1H, 4-H), 8.12 (dd, J = 8.7, 1.8 Hz, 1H, 9-H), 7.78 (ddd, J = 8.3, 7.0, 1.4 Hz, 1H, 3-H), 7.69 (ddd, J = 8.3, 7.0, 1.4 Hz, 1H, 2-H), 7.64 – 7.58 (m, 2H, 2'-, 6'-H), 7.53 – 7.47 (m, 2H, 3'-, 5'-H), 7.43 – 7.37 (m, 2H, 2''-, 6''-H), 7.37 – 7.32 (m, 2H, 3''-, 5''-H), 7.31 – 7.26 (m, 1H, 4''-H), 4.25 (s, 2H, CH_2).

^{13}C NMR (126 MHz, $CDCl_3$): δ (ppm) = 159.3 (C-6), 143.9 (C-4a), 139.4 (C-9), 138.2 (C-1'), 137.4 (C-7), 137.2 (C-1''), 137.0 (C-4'), 132.8 (C-10a), 130.6 (C-4), 130.3 (C-2', -6'), 129.6 (C-3), 129.3 (C-3', -5'), 129.0 (C-2'', -6''), 128.8 (C-3'', -5''), 127.5 (C-2, C-4''), 126.9 (C-6a), 124.3 (C-10), 123.3 (C-10b), 121.9 (C-1), 92.9 (C-8), 38.7 (CH_2).

IR (ATR): $\tilde{\nu}$ [cm^{-1}] = 2920, 2852, 1594, 1562, 1493, 1452, 1354, 1184, 1086, 1066, 960, 823, 813, 760, 731, 716.

HRMS (ESI): m/z [$M+H$] $^+$ calcd. for $C_{26}H_{19}INS^+$: 504.0277, found: 504.0279.

Purity (HPLC): >96 % (210 nm, 254 nm).

4-(6-(4-(Benzylthio)phenyl)phenanthridin-8-yl)-N-methyl benzamide (121)

 $C_{34}H_{26}N_2OS$

510.66 g/mol

Substituted phenanthridine **121** was synthesized according to GP5 using 8-iodophenanthridine **107** (101 mg, 0.200 mmol), boronic acid pinacol ester **119** (107 mg, 0.600 mmol), Pd(PPh₃)₄ (23 mg, 0.020 mmol) and Cs₂CO₃ (195 mg, 0.600 mmol). The product was obtained after purification by FCC (CH₂Cl₂/MeOH 98:2) as light-yellow foam (81 mg, 0.16 mmol, 79 %).

mp.: 95 – 105 °C (amorph).

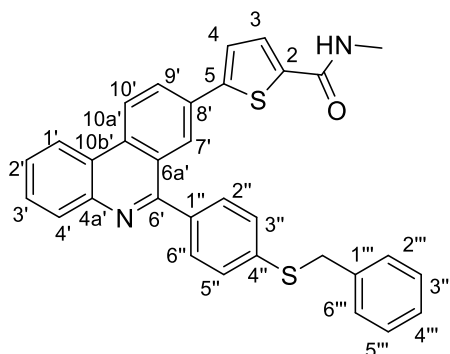
¹H NMR (400 MHz, CDCl₃): δ (ppm) = 8.77 (d, *J* = 8.7 Hz, 1H, 10'-H), 8.65 – 8.60 (m, 1H, 1'-H), 8.30 (d, *J* = 1.9 Hz, 1H, 7'-H), 8.24 (dd, *J* = 8.3, 1.3 Hz, 1H, 4'-H), 8.11 (dd, *J* = 8.6, 1.9 Hz, 1H, 9'-H), 7.89 – 7.84 (m, 2H, 2-, 6-H), 7.78 (ddd, *J* = 8.2, 7.0, 1.4 Hz, 1H, 3'-H), 7.74 – 7.65 (m, 5H, 2''-, 6''-H, 3-, 5-H, 2'-H), 7.53 – 7.48 (m, 2H, 3'''-, 5''-H), 7.44 – 7.36 (m, 2H, 2'''-, 6'''-H), 7.36 – 7.29 (m, 2H, 3'''-, 5'''-H), 7.28 – 7.23 (m, 1H, 4'''-H), 6.19 (d, *J* = 5.3 Hz, 1H, NH), 4.24 (s, 2H, CH₂), 3.06 (d, *J* = 4.8 Hz, 3H, CH₃).

¹³C NMR (126 MHz, CDCl₃): δ (ppm) = 167.8 (C=O), 160.7 (C-6'), 144.1 (C-4a'), 143.2 (C-4), 138.9 (C-8'), 138.0 (C-4''), 137.5 (C-1''), 137.3 (C-1'''), 134.0 (C-1), 133.2 (C-10a'), 130.5 (C-4'), 130.4 (C-2'', -6''), 129.7 (C-9'), 129.3 (C-3'), 129.2 (C-3'', -5''), 129.0 (C-2''', -6'''), 128.8 (C-3''', -5'''), 127.7 (C-2, -6), 127.6, (C-3, -5) 127.5 (C-4'''), 127.4 (C-2'), 127.0 (C-7'), 125.6 (C-6a'), 123.6 (C-10b'), 123.3 (C-10'), 122.2 (C-1'), 38.7 (CH₂), 27.1 (CH₃).

IR (ATR): $\tilde{\nu}$ [cm⁻¹] = 3302, 3029, 2928, 1641, 1546, 1494, 1307, 1142, 1087, 965, 827, 760, 738, 696.

HRMS (ESI): *m/z* [M+H]⁺ calcd. for C₃₄H₂₇N₂OS⁺: 511.1839, found: 511.1841.

Purity (HPLC): >96 % (210 nm, 254 nm).

5-(6-(4-(Benzylthio)phenyl)phenanthridin-8-yl)-N-methylthiophene-2-carboxamide (122)C₃₂H₂₄N₂OS₂

516.69 g/mol

For the required boronic acid pinacol ester **120**, 5-(4,4,5,5-tetramethyl-1,3,2-dioxaborolan-2-yl)thiophene-2-carboxylic acid (508 mg, 2.00 mmol) EDCI (469 mg, 2.40 mmol) and HOBt (324 mg, 2.40 mmol) were dissolved in DMF (2 mL) and was stirred at rt for 30 min. Methylamine (2M in THF, 3.0 mL, 6.0 mmol) was added and the mixture was stirred at rt for 16 h. The mixture was diluted with ethyl acetate (20 mL) and was washed twice with water (2x 20 mL), 5% aqueous LiCl solution (1x 20 mL) and brine (1x 20 mL). The organic layer was dried using a hydrophobic filter and the solvent was removed *in vacuo*. The crude pinacol ester **120** (396 mg, 1.48 mmol, 74%, ¹H NMR (400 MHz, DMSO-*d*₆) δ (ppm) = 8.52 (d, *J* = 4.8 Hz, 1H, NH), 7.72 (d, *J* = 3.7 Hz, 1H, H-Ar), 7.52 (d, *J* = 3.7 Hz, 1H, H-Ar), 2.76 (d, *J* = 4.6 Hz, 3H, NHCH₃), 1.29 (s, 12H, CH₃.) was used without further purification. For the following Suzuki coupling according to GP4, the crude boronic acid pinacol ester **120** (198 mg, ~0.741 mmol), 8-iodophenanthridine **107** (124 mg, 0.247 mmol), Pd(PPh₃)₄ (29 mg, 0.025 mmol) and Cs₂CO₃ (241 mg, 0.741 mmol) were used. After purification by FCC (CH₂Cl₂/MeOH 98:2) and crystallization from ethanol, the product was obtained as light-yellow solid (95 mg, 0.18 mmol, 74 %).

mp.: 226 – 228 °C.

¹H NMR (400 MHz, CDCl₃): δ (ppm) = 8.71 (d, *J* = 8.7 Hz, 1H, 10'-H), 8.61 – 8.56 (m, 1H, 1'-H), 8.32 (d, *J* = 1.9 Hz, 1H, 7'-H), 8.22 (dd, *J* = 8.0, 1.4 Hz, 1H, 4'-H), 8.09 (dd, *J* = 8.6, 1.9 Hz, 1H, 9'-H), 7.80 – 7.74 (m, 1H, 3'-H), 7.73 – 7.65 (m, 3H, 2'-H, 2''-, 6''-H), 7.54 – 7.50 (m, 2H, 3''-, 5''-H), 7.48 (dd, *J* = 3.9, 0.6 Hz, 1H, 3-H), 7.44 – 7.39 (m, 2H, 2'''-, 6'''-H), 7.37 – 7.27 (m, 4H, 3'''-, 5'''-H, 4-H, 4'''-H), 6.03 – 5.96 (m, 1H, NH), 4.27 (s, 2H, CH₂), 3.03 (d, *J* = 4.8 Hz, 3H, CH₃).

¹³C NMR (101 MHz, CDCl₃): δ (ppm) = 162.4 (C=O), 160.5 (C-6'), 147.6 (C-5), 144.1 (C-4a'), 138.5 (C-2), 138.2 (C-4''), 137.3 (C-1'' or C-1'''), 137.2 (C-1'' or C-1'''), 133.4 (C-10a'), 132.4

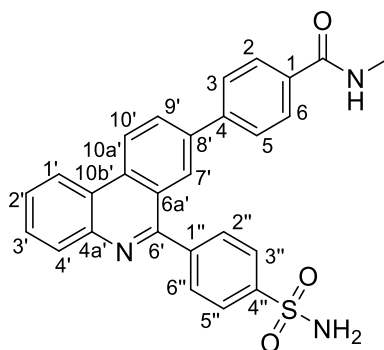
Experimental for Sirtuin 6 modulators

(C-6a'), 130.6 (C-4'), 130.4 (C-2'', -6''), 129.4 (C-3'), 129.2 (C-3'', -5''), 129.1 (C-3), 129.1 (C-2''', -6'''), 128.8 (C-3''', -5'''), 128.5 (C-9'), 127.5 (C-4'''), 127.5 (C-2'), 125.6 (C-7'), 125.5 (C-10b'), 124.4 (C-4), 123.5 (C-10'), 122.2 (C-1'), 38.6 (CH₂), 26.9 (CH₃).

IR (ATR): $\tilde{\nu}$ [cm⁻¹] = 3311, 3030, 1629, 1552, 1519, 1453, 1323, 1308, 1142, 1084, 951, 826, 811, 764, 698.

HRMS (ESI): m/z [M+H]⁺ calcd. for C₃₂H₂₅N₂OS₂⁺: 517.1403, found: 517.1407.

Purity (HPLC): >96 % (210 nm, 254 nm).

N-Methyl-4-(6-(4-sulfamoylphenyl)phenanthridin-8-yl)benzamide (123)C₂₇H₂₁N₃O₃S

467.55 g/mol

Sulfonamide **123** was synthesized according to GP3 using benzyl thioether **121** (70 mg, 0.14 mmol), 1,3-dichloro-5,5-dimethylhydantoin (54 mg, 0.27 mmol) and subsequently 25 % aqueous ammonium hydroxide (120 μ L, 1.39 mmol). After removal of the volatiles *in vacuo* and trituration of the crude product in methanol, sulfonamide **123** was obtained as light-pink solid (64 mg, 0.088 mmol, 64 %).

mp.: 343 – 345 °C.

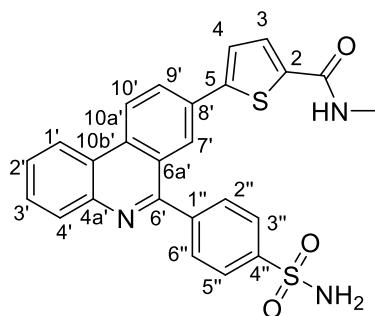
¹H NMR (500 MHz, DMSO-*d*₆): δ (ppm) = 9.10 (d, J = 8.8 Hz, 1H, 10'-H), 8.93 (dd, J = 8.3, 1.6 Hz, 1H, 1'-H), 8.50 (q, J = 4.5 Hz, 1H, NH), 8.36 (dd, J = 8.6, 1.9 Hz, 1H, 9'-H), 8.23 (d, J = 1.9 Hz, 1H, 7'-H), 8.16 (dd, J = 8.1, 1.5 Hz, 1H, 4'-H), 8.10 – 8.01 (m, 4H, 3''-, 5''-H, 2''-, 6''-H), 7.98 – 7.93 (m, 2H, 2-, 6-H), 7.87 (ddd, J = 8.1, 6.9, 1.5 Hz, 1H, 3'-H), 7.84 – 7.80 (m, 3H, 3-, 5-H, 2'-H), 7.53 (s, 2H, SO₂NH₂), 2.81 (d, J = 4.5 Hz, 3H, CH₃).

¹³C NMR (126 MHz, DMSO-*d*₆): δ (ppm) = 166.1 (C=O), 159.2 (C-6'), 144.4 (C-4'), 143.2 (C-4a'), 142.2 (C-1''), 141.7 (C-4), 138.7 (C-8'), 133.9 (C-1), 132.4 (C-10a'), 130.5 (C-2'', -6''), 130.2 (C-9'), 129.9 (C-4'), 129.5 (C-3'), 128.0 (C-2, -6), 127.9 (C-2'), 127.1 (C-3, -5), 125.8 (C-3'', -5''), 125.7 (C-7'), 124.4 (C-6a'), 124.0 (C-10'), 123.1 (C-10b'), 123.0 (C-1'), 26.3 (CH₃).

IR (ATR): $\tilde{\nu}$ [cm⁻¹] = 3405, 3311, 3062, 2360, 1645, 1610, 1546, 1505, 1458, 1336, 1155, 1140, 828, 757, 735.

HRMS (ESI): m/z [M+H]⁺ calcd. for C₂₇H₂₂N₃O₃S⁺: 468.1376, found: 468.1378.

Purity (HPLC): >96 % (210 nm, 254 nm).

***N*-Methyl-5-(6-(4-sulfamoylphenyl)phenanthridin-8-yl)thiophene-2-carboxamide (124)**

 $C_{25}H_{19}N_3O_3S_2$

473.58 g/mol

Sulfonamide **124** was synthesized according to GP3 using benzyl thioether **121** (67 mg, 0.13 mmol), 1,3-dichloro-5,5-dimethylhydantoin (51 mg, 0.26 mmol) and subsequently 25 % aqueous ammonium hydroxide (250 μ L, 2.89 mmol). After removal of the volatiles *in vacuo* and trituration of the crude product in methanol sulfonamide **124** was obtained as light-yellow solid (32 mg, 0.068 mmol, 49 %).

mp.: 333 – 335 °C.

^1H NMR (500 MHz, DMSO- d_6): δ (ppm) = 9.06 (d, J = 8.8 Hz, 1H, 10'-H), 8.91 (dd, J = 8.2, 1.6 Hz, 1H, 1'-H), 8.56 (q, J = 4.6 Hz, 1H, NH), 8.37 (dd, J = 8.7, 2.0 Hz, 1H, 9'-H), 8.21 (d, J = 1.9 Hz, 1H, 7'-H), 8.16 (dd, J = 8.1, 1.5 Hz, 1H, 4'-H), 8.12 – 8.07 (m, 2H, 3''-, 5''-H), 8.05 – 7.99 (m, 2H, 2''-, 6''-H), 7.87 (ddd, J = 8.2, 6.9, 1.5 Hz, 1H, 3'-H), 7.82 (ddd, J = 8.4, 7.0, 1.5 Hz, 1H, 2'-H), 7.75 (d, J = 4.0 Hz, 1H, 3-H), 7.68 (d, J = 4.0 Hz, 1H, 4-H), 7.58 (s, 2H, SO₂NH₂), 2.78 (d, J = 4.6 Hz, 3H, CH₃).

^{13}C NMR (126 MHz, DMSO- d_6): δ (ppm) = 161.2 (C=O), 159.0 (C-6'), 145.7 (C-5), 144.5 (C-4''), 143.2 (C-4a'), 142.0 (C-1''), 140.1 (C-2), 132.6 (C-6a'), 132.5 (C-10a'), 130.4 (C-2'', -6''), 129.9 (C-4'), 129.6 (C-3'), 129.0 (C-3), 128.6 (C-9'), 127.9 (C-2'), 125.8 (C-3'', -5''), 125.7 (C-4), 124.5 (C-8'), 124.3 (C-10'), 123.9 (C-7'), 123.1 (C-10b'), 123.0 (C-1'), 26.1 (CH₃).

IR (ATR): 3394, 3327, 1630, 1550, 1325, 1301, 1161, 1139, 806, 762, 734.

HRMS (ESI): m/z [M+H]⁺ calcd. for C₂₅H₂₀N₃O₃S₂⁺: 474.0941, found: 474.0942.

Purity (HPLC): >96 % (210 nm, 254 nm)

3.2.8.2 Biological testing

Fluor de Lys Assay

University of Bayreuth:

Fluor de Lys experiments by DR. WEIJE YOU as previously described^[111].

In brief the conditions of the assay:

Component	Concentration
Sirt6-FL	2 μ M
NAD ⁺	500 μ M
Acetylated FdL peptide	100 μ M
DMSO	1 %
Buffer	20 mM Hepes pH 7.5, 100 mM NaCl, 2 mM DTT

- Steps**
1. Incubate @ 37 °C for 1.5 hours
 2. Mix with developer solution @ room temperature for 0.5 h
 3. Fluorescence emission is detected with 460 nm light

BPS Bioscience Inc.:

SIRT6 Fluorogenic Assay Kit (BPS catalog number 50022) was used for the test. All of the compounds were dissolved in DMSO. A series of dilutions of the compounds were prepared with 10 % DMSO in assay buffer and 5 μ L of the dilution was added to a 50 μ L reaction so that the final concentration of DMSO is 1 % in all of reactions. The compounds were pre-incubated in duplicate at RT for 30 minutes in a mixture containing assay buffer, 5 μ g BSA, SIRT6 enzyme and a test compound. After 30 minutes, the enzymatic reactions were initiated by the addition of SIRT substrate to a final concentration of 10 μ M. The enzymatic reaction proceeded for 60 minutes at 37 °C.

After enzymatic reactions, 50 μ L of 2x SIRT Developer was added to each well for the SIRT enzymes and the plate was incubated at room temperature for an additional 15 minutes.

Fluorescence intensity was measured at an excitation of 360 nm and an emission of 460 nm using a Tecan Infinite M1000 microplate reader.

MTT assay

HL-60 cells (DSM number: ACC 3) were purchased from the German Collection of Microorganisms and Cell Cultures GmbH (DSMZ, Braunschweig) and cultivated in RPMI 1640 medium supplemented with 10 % fetal bovine serum (FBS). For the MTT assay, cell density was adjusted to roughly 9×10^5 cells/mL. Cells were then seeded in 96-well plates by transferring 99 μ L into each well and incubating for 24 h at 37 °C with 5 % CO₂. The test compounds were used as 10 mM solutions in DMSO or, if IC₅₀ values were determined, as a dilution series thereof (1:2, at least 5 dilution steps). 1.0 μ L of test compound solution or Triton X-100 (0.1 mg/mL) as positive control or DMSO alone as negative control were transferred to each well and incubated for additional 24 h. Then 10 μ L MTT solution (5.0 mg/mL in PBS) were added to each well and incubated for 2 h. After this time, 190 μ L DMSO was added and the plate was shaken for 1 h in the dark. The absorbance of each well was measured at 570 nm with a MRX Microplate Reader (Dynex Technologies). The software Prism 4 (GraphPad) was used to analyze all data and calculate IC₅₀ values.

Agar diffusion assay

All tested germs were also purchased from the DSMZ and cultivated following their instructions in liquid culture. The agar plates were filled with suitable culture media as follows. For *E. coli* (DSM number: 426), *P. marginalis* (DSM number: 7527) and *Y. lipolytica* (DSM number: 1345) a mixture of 35.2 g all-culture agar (AC-agar) and 20 g agar in 1.0 L water was used. For *S. cerevisiae* (DSM number: 1333) 35.2 g AC agar in 1.0 L water was used. For *S. equorum* (DSM number: 20675) and *S. entericus* (DSM number: 14446) a mixture of 10 g casein peptone, 5.0 g yeast extract, 5.0 g glucose, 5.0 g sodium chloride and 15 g agar in 1.0 L water was used. All agar media were autoclaved and filled in petri dishes under aseptic conditions, while still hot and liquid. After cooling for at least 1 h at 8 °C, the agar plates were ready to use. The test platelets (d = 6.0 mm, Macherey-Nagel) were impregnated with 3.0 μ L of a 1 % (m/V) solution of the respective compounds or the positive control tetracycline (as antibacterial) or clotrimazole (as antifungal agent) in DMSO. As negative control DMSO (3.0 μ L) alone was used. All platelets were dried for 24 h at room temperature, then six were placed onto each agar plate, onto which germs were transferred before with cotton swabs: 4 test platelets impregnated with compounds, as well as 1 suitable positive and 1 negative control. The agar plates were sealed and incubated for 36 h at 32 °C (bacteria) or 28 °C (fungi). Then the antimicrobial effect was assessed by manually measuring the diameters of the zones of inhibition.

4 Summary

The aim of this thesis was to develop and characterize small molecule modulators of TRPML lysosomal ion channels and the epigenetic enzyme Sirtuin 6.

For the TRPML modulators the starting point was the inhibitor **ML-S13** which was published with ambiguous structure regarding its stereochemical configuration. Therefore, the first objective was to clarify the optimal stereochemistry and conduct a structure-activity relationship analysis. The results from this study have been published in the EUROPEAN JOURNAL OF MEDICINAL CHEMISTRY^[69]. During this study, enantiopure (-)-*trans*-**ML-S13** was identified as eutomer and the most potent TRPML1 inhibitor. It was also shown that the absolute configuration plays a crucial role in the biological activity profile of the compounds, as the stereoisomers (±)-*cis*-**ML-S13** and (+)-*trans*-**ML-S13** are potent activators of TRPML2. To enable further studies of the biological activity of the enantiomers, a method was developed, that allowed a larger scale synthesis. This method was published in the journal ARCHIV DER PHARMAZIE^[70]. Compounds from the **ML-S13** series are state of the art TRPML inhibitors and are extensively used as chemical tools, for example as benchmark compounds by our own group^[27] or other research groups^[112].

For the Sirtuin 6 project, **KV-30**, a compound synthesized previously in the BRACHER group, which was originally designed as HDAC 6 (histone deacetylase 6) inhibitor, was identified as agent against *Toxoplasma gondii*. It was inactive towards HDAC 6 but was found to inhibit Sirtuin 6. **KV-30** is bearing a hydroxamic acid as zinc chelator, because of its original design intent as HDAC inhibitor. Since sirtuins are NAD⁺-, not zinc-dependent, the hydroxamic acid group is not crucial for the activity and should thus be replaced. This structure motif brings undesirable properties such as unspecific metal ion complexation and cytotoxicity. The replacement was successfully achieved with the innocuous sulfonamide group of compound **38** (CLE121). This compound serves as lead structure for the development of new chemotype Sirtuin 6 inhibitors, which is the basis of the SFB 1309 “Chemical Biology of Epigenetic Modifications” project C06. This project will be continued in the group of PROF. DR. FRANZ BRACHER.

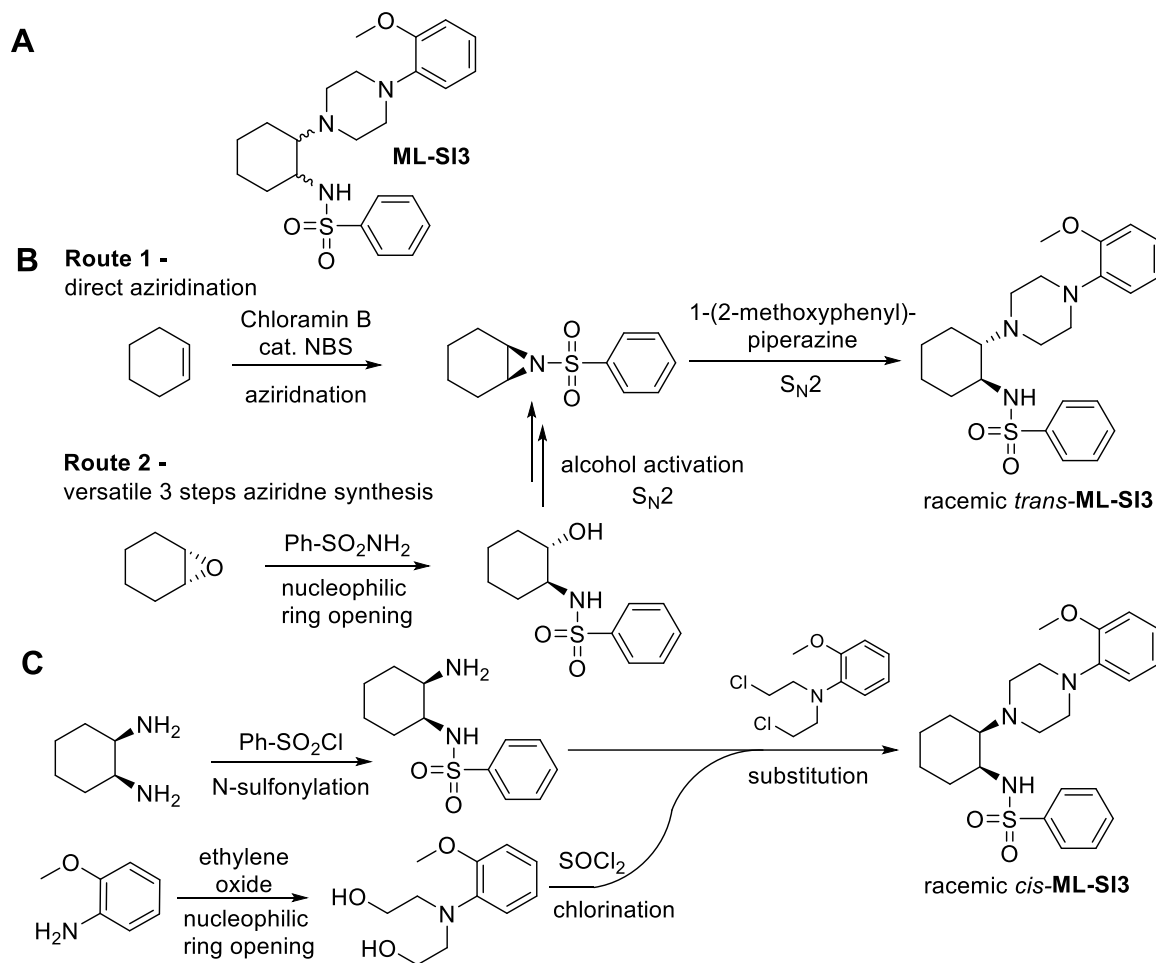
4.1 TRPML modulators

To achieve the first objective, the elucidation of the exact stereochemistry of **ML-SI3**, which was published with ambiguous chemical structure (Scheme 53, **A**) synthetic routes towards *trans*- and *cis*-**ML-SI3** were developed.

trans-**ML-SI3** can be synthesized by a convenient 2-step procedure, with a *cis*-aziridine derivative as intermediate. This aziridine can be synthesized by two different approaches. The first option is the direct aziridination of an olefine with N-chloramines under NBS catalysis. For the synthesis of the required aziridine for **ML-SI3**, cyclohexene and commercially available chloramine B were used. Drawback of this method is, that the finally desired aryl sulfonamide moiety needs to be available as *N*-chloramine. If other aryl sulfonamide moieties should be introduced as variation, there is a need for an alternative synthesis approach to the required aziridine. This can be achieved by a three-step procedure, starting from cyclohexene oxide, which can be versatilely opened with any primary aryl sulfonamide. The resulting *trans*-alcohol is activated by conversion to a sulfonic ester, and the following intramolecular nucleophilic substitution reaction gives the desired *cis*-aziridine. The aziridine ring can in turn be opened by nucleophiles, in the case of **ML-SI3** by 1-(2-methoxyphenyl)-piperazine. For variations of the amino component of **ML-SI3**, the used amine can easily be exchanged. This S_N2 reaction leads to the desired *trans*-configuration (Scheme 53, **B**).

The synthesis of *cis*-**ML-SI3** was more challenging since this configuration is energetically less favoured. During the first synthesis attempts, which included nucleophilic substitution reactions at the stereocenters, undesired inversions towards the more stable *trans*-configuration have been observed. Therefore, the synthesis of *cis*-**ML-SI3** needs to start directly with an already correctly configured starting material like *cis*-diamino cyclohexane and conditions, that could lead to an unwanted inversion reaction must be avoided. As first step, the sulfonamide moiety is added to the *cis*-diamino cyclohexane scaffold by N-sulfonylation with benzenesulfonyl chloride. Subsequently, the amino moiety is constructed by *de-novo* piperazine synthesis *via* substitution reaction of an N-Lost derivative (obtained in two steps from 2-methoxyaniline), which then leads to racemic *cis*-**ML-SI3** (Scheme 53, **C**).

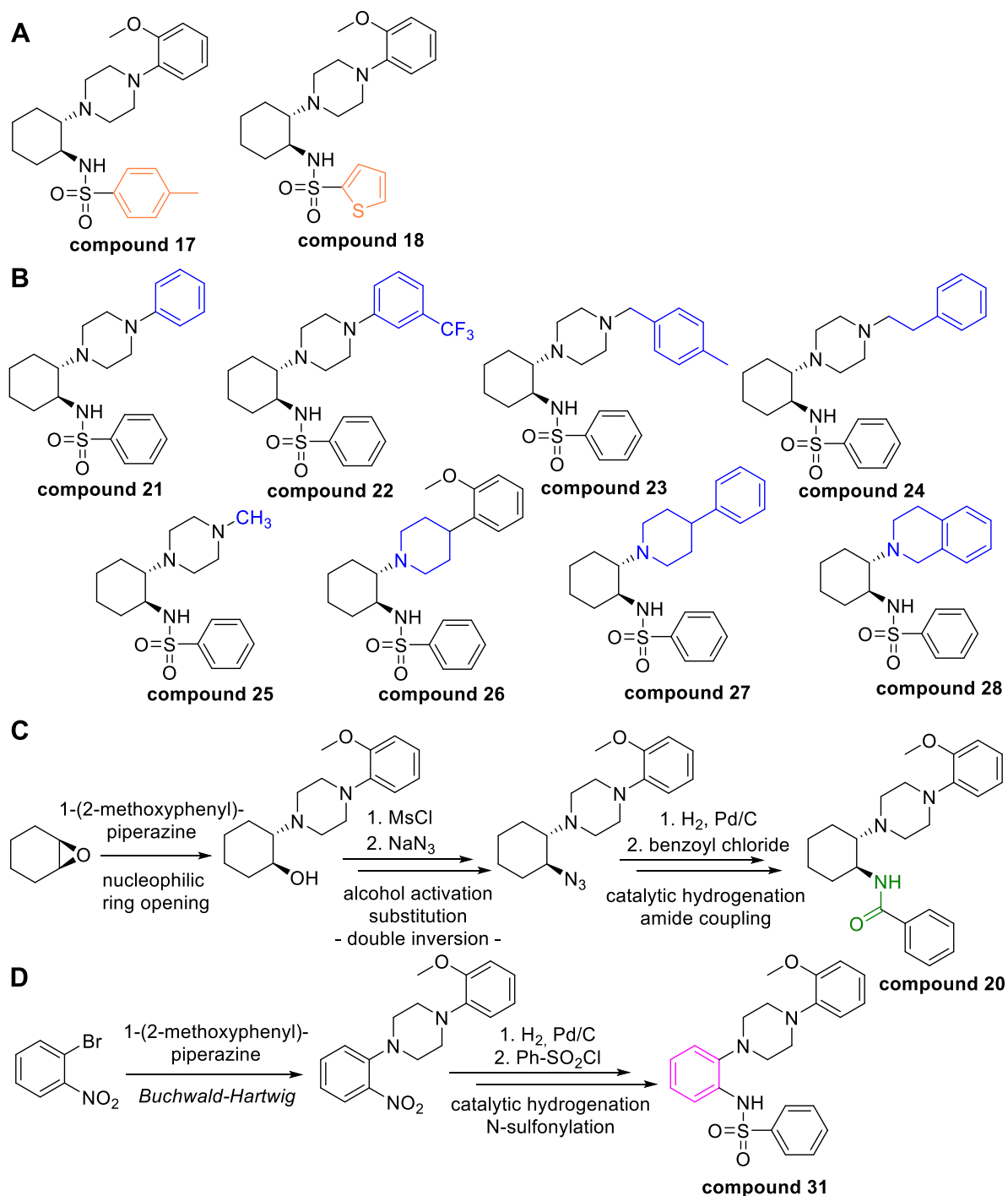
Since during the syntheses of racemic *trans*- and *cis*-**ML-SI3** *meso*-compounds are used as intermediates (*N*-sulfonyl aziridine for *trans*-**ML-SI3**) or starting materials (*cis*-diamino cyclohexane for *cis*-**ML-SI3**), these approaches can only lead to the racemic form of the respective diastereomers.



Scheme 53 Syntheses of *trans*- and *cis*-**ML-SI3** for stereochemistry elucidation. **A** **ML-SI3** as depicted by Wang *et al.*^[26]. **B** Synthesis of racemic *trans*-**ML-SI3**. **C** Synthesis of racemic *cis*-**ML-SI3**.

For a structure-activity relationship study, a series of variations of **ML-SI3** was synthesized. Since the *trans*-configuration was shown to be superior, only *trans*-variations have been synthesized by using the above-described methods for *trans*-**ML-SI3**. Two compounds with alternative aryl sulfonamide component (Scheme 54, **A**) and eight compounds with alternative aliphatic amino component (Scheme 54, **B**) have been synthesized. The role of the sulfonamide was investigated by replacement of the sulfonamide with a carboxamide. For this compound, an alternative synthesis method was used, as the carboxamide is not a suitable nucleophile for the nucleophilic epoxide ring opening reaction due to insufficient NH-acidity. Therefore, cyclohexene oxide was opened with 1-(2-methoxyphenyl)piperazine instead and the resulting alcohol substituted after activation with an azide group. During this reaction, only the *trans*-configured azide is formed, which indicates that a double inversion must have occurred during this substitution reaction. This is possible because of the neighbouring piperazine nitrogen. This nitrogen can act as nucleophile for a first S_N2 reaction to the corresponding cyclic *cis*-configured quaternary ammonium, which is then reacting with the azide ion in a second S_N2 . The double inversion leads to the retention of the original *trans*-configuration. After catalytic hydrogenation of the azide, the resulting primary amine is acylated

with benzoyl chloride, delivering the desired **compound 20** (Scheme 54, **C**). Additional to the racemic variations of *trans*-**ML-SI3**, an achiral variation with a benzene instead of the cyclohexane ring was synthesized. Starting with a BUCHWALD-HARTWIG cross-coupling of 1-bromo-2-nitrobenzene with 1-(2-methoxyphenyl) piperazine, subsequent reduction of the nitro group by catalytic hydrogenation and following N-sulfonylation gave the desired achiral aromatic **compound 31** (Scheme 54, **D**).



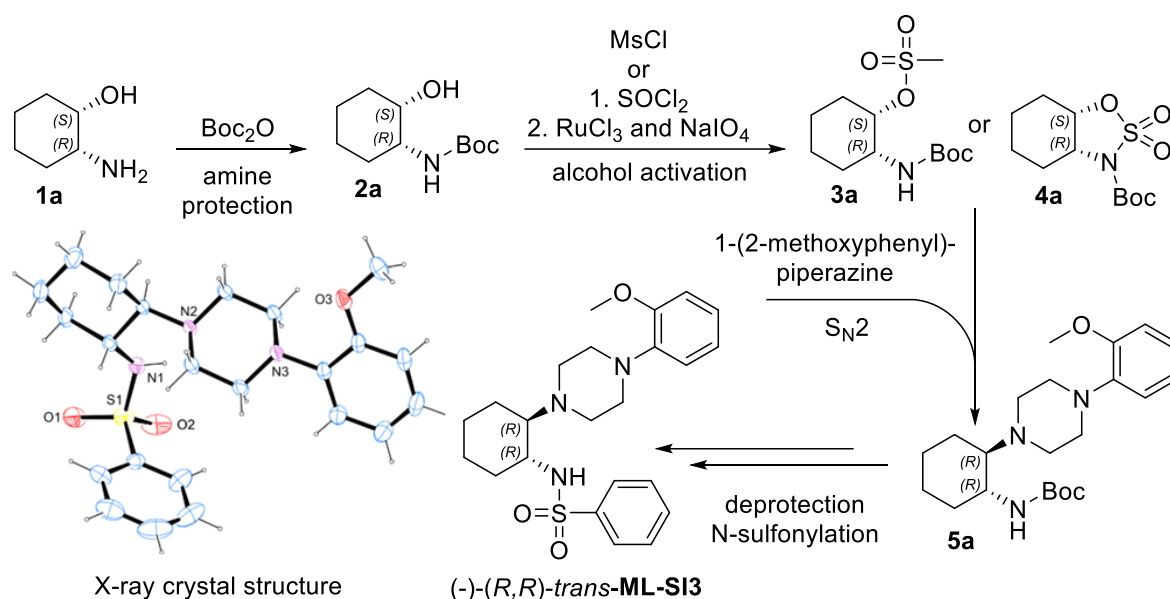
Scheme 54 Variations of **ML-SI3**. **A** Chemical structures of **compounds 17-18** with alternative aryl sulfonamide moiety. **B** Chemical structures of **compounds 21-28** with alternative amino component. **C** Synthesis of **compound 20** with carboxamide instead of sulfonamide. **D** Synthesis of achiral, aromatic **compound 31**.
Numbering of compounds taken from Leser *et al.*^[69].

Racemic *trans*-**ML-SI3** was separated by chiral semi-preparative HPLC, and specific rotation of the enantiomers was measured. This allowed the assignment of (-) and (+)-*trans*-**ML-SI3**. However, the absolute configuration cannot be determined by chiral HPLC or specific rotation.

All obtained compounds were tested by a Fura-2-AM based single cell calcium imaging assay at 10 μM for their effect towards TRPML1, -2 and -3. Additionally, the concentration-effect relationship was determined by a Fluo-4-AM based FLIPR screening in the group of PROF. DR. MICHAEL SCHAEFER by NICOLE URBAN at the University of Leipzig. From these tests it became apparent, that most influential to the biological activity is indeed the stereochemical configuration. Except **compound 24**, all variations of **ML-SI3** act as TRPML1 inhibitors, with the most potent being (-)-*trans*-**ML-SI3** with an IC_{50} of 1.6 μM . Achiral **compound 31** with an IC_{50} of 1.8 μM and racemic **compound 18** with an IC_{50} of 2.3 μM are next in line with regards to potent TRPML1 inhibitor. Those three compounds are also the only ones who show noteworthy inhibition of TRPML3 ((-)-*trans*-**ML-SI3** IC_{50} : 12.5 μM , **compound 18** IC_{50} : 15.9 μM and **compound 31** IC_{50} : 21.7 μM). For TRPML2, almost all compounds act as activators, only **compound 20**, **compound 25** and **compound 28** inhibit TRPML2. The most potent and efficient TRPML2 activators are (+)-*trans*-**ML-SI3** (EC_{50} : 2.7 μM) and **compound 17** (EC_{50} : 4.0 μM), while the best inhibitor of TRPML2 is (-)-*trans*-**ML-SI3** with an IC_{50} of 2.3 μM .

To make the enantiomers of this series easily available, which hitherto they weren't since separation by semi-preparative HPLC was required, a highly efficient chiral pool synthesis was developed. This method was developed together with KATHARINA KRIEGLER, who worked on her Master's thesis under my supervision. Commercially available enantiopure *cis*-2-amino cyclohexanol was used as chiral pool starting material. While the configuration of the amino group is retained throughout the synthesis, the stereocenter of the secondary alcohol is inverted in a controlled manner ($\text{S}_{\text{N}}2$ -reaction after alcohol activation). This approach allows the assignment of the absolute configuration based on retrosynthesis. If (1*S*,2*R*)-2-aminocyclohexan-1-ol (**1a**) is used, the (-)-*trans*-**ML-SI3** enantiomer is obtained. Therefore it was proven that the stereocenters of (-)-*trans*-**ML-SI3** are (*R,R*) configured. This was additionally confirmed by X-ray crystal structure analysis. Scheme 55 shows the synthetic sequence for the (*R,R*) enantiomer. All steps were equally done for the (*S,S*)-enantiomer starting from the enantiomeric *cis*-2-amino cyclohexanol.

Summary



Scheme 55 Chiral pool synthesis and X-ray crystal structure of enantiopure $(-)-(R,R)\text{-trans-ML-SI3}$.

Next, this versatile method was applied to synthesise enantiopure variations of *trans-ML-SI3*, which was done by DOMINIK EBERT for his Bachelor's thesis under my supervision. The resulting compounds are shown in Figure 36. In total six pairs of enantiomers with alternative sulfonamide and alternative amino component were synthesized. The residues were chosen based on the most promising candidates from the SAR study (best selectivity and potency)^[69] and from other compounds which are known to be highly active towards TRPML1 (**SF-22** and **MK-6-83**)^[22].

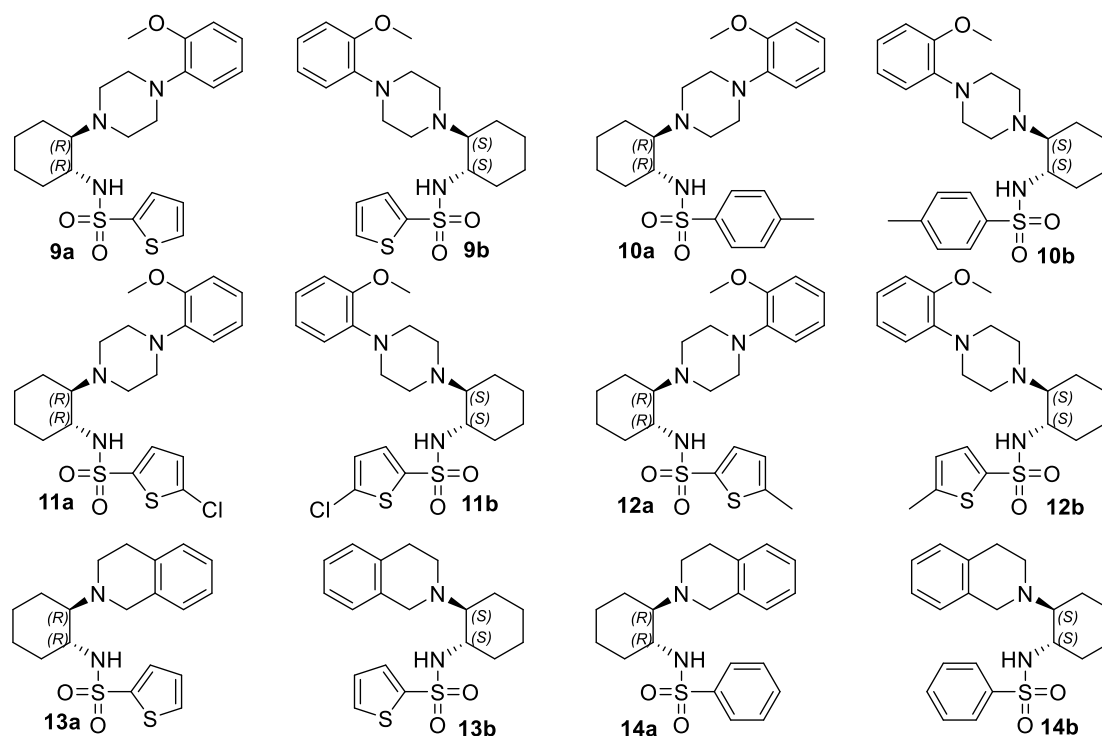


Figure 36 Chemical structures of synthesized enantiopure **ML-SI3** variations.

Summary

The enantiopure variations were tested in the group of PROF. DR. MICHAEL SCHAEFER at the University of Leipzig by NICOLE URBAN for their activity against TRPML1, TRPML2 and TRPML3 by a Fluo-4/AM based FLIPR screening. (-)-(R,R)- and (+)-(S,S)-*trans*-**ML-SI3** were included in the screening as benchmark. During this study, a solubility issue of some of the variations was observed, which could be solved by the addition of 0.1% bovine serum albumin to the HBS assay buffer. With this improved solubility conditions, the potency of (-)-(R,R)-*trans*-**ML-SI3** was improved by a factor of 20, from an IC₅₀ of 1.6 μM to 74 nM, revealing the full potential of this compound. All (R,R)-enantiomers are inhibitors of TRPML1. While compounds **9a**, **13a** and **14a** inhibit all three TRPML subtypes, compound **10a** activates TRPML2 and TRPML3. Compounds **11a** and **12a** activate TRPML2 but inhibit TRPML3. Compounds **9a**, **10a**, **11a** and **12a** have a similar potency for TRPML1 inhibition as (R,R)-**ML-SI3**, but compound **11a** shows a more promising selectivity profile (IC₅₀^{TRPML1}: 126 nM, EC₅₀^{TRPML2}: 4.2 μM, IC₅₀^{TRPML3}: 5.9 μM). Compound **13a** is slightly more active on TRPML2 (IC₅₀: 988 nM) than on TRPML1 (IC₅₀: 1.7 μM). The (S,S) enantiomers **10b**, **11b** and **12b** are activators of all TRPMLs with **10b** being the most potent (EC₅₀: 53 nM), showing a selectivity factor of 20 over TRPML1 (EC₅₀: 1.3 μM) and 10 over TRPML3 (EC₅₀: 675 nM). Since this testing was only intended as a pre-screening and the experiments only done as single determination, the results need to be taken with a grain of salt. Nevertheless, they give very important hints towards the future development and characterization of these TRPML modulators. Compounds **11a**, **12a** and **10b** are currently under evaluation and confirmation of activity by patch clamp experiments in the group of PROF. DR. CHENG-CHANG CHEN at the National Taiwan University.

4.2 Sirtuin 6 modulators

The hit compounds of this project **KV-30** consists of a phenanthridine scaffold with a phenyl linker unit which is bearing a hydroxamic acid as a polar head group. A co-crystal, solved by DR. WEIJE YOU in the group of PROF. DR. CLEMENS STEEGBORN at the University of Bayreuth, revealed that the hydroxamic acid moiety is building a network of polar interactions, involving a water molecule. The most important information from the co-crystal was, that the hydroxamic acid does not interact with any metal ions. The phenanthridine scaffold itself shows no polar interactions with the target. Schematic representation of the co-crystal of Sirtuin 6 and **KV-30** is shown in Figure 37.

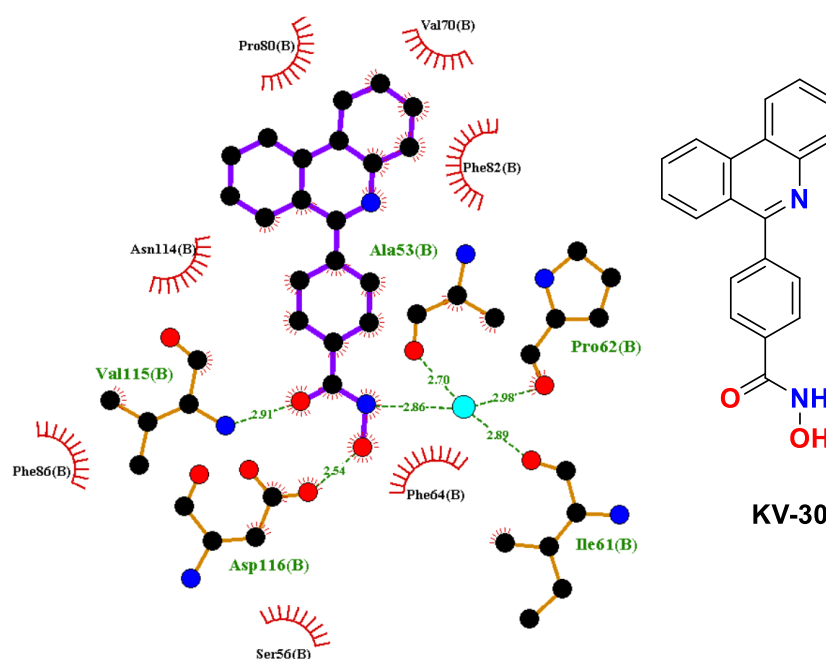
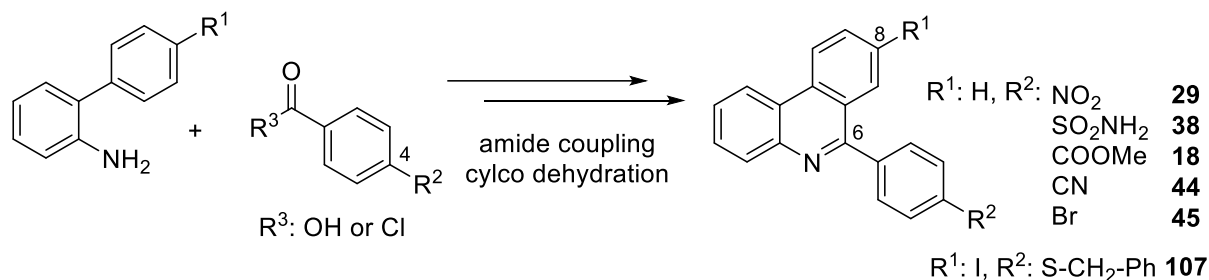


Figure 37 Left: Schematic representation of the Sirtuin 6 and **KV-30** co-crystal. A bound water molecule is represented by a light blue ball. Right: Chemical structure of **KV-30**.

To achieve the primary objective, the replacement of the problematic hydroxamic acid moiety, the focus was the introduction of alternative polar head groups while retaining the phenanthridine scaffold and the phenyl linker. Additionally, the information regarding the water molecule and the space around the phenanthridine ring provided by the co-crystal structure were exploited by addition of residues to the hydroxamic acid (hydroxyethyl) and the phenanthridine ring (aryl *N*-methyl amides) that could potentially improve potency and selectivity.

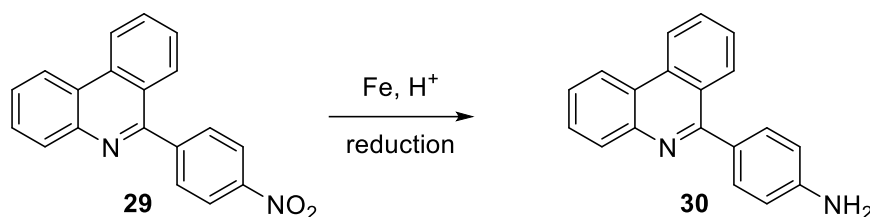
As first step towards the planned variations, a couple of useful 6-phenylphenanthridine precursors were synthesized by a versatile BISCHLER-NAPIERALSKI type cyclodehydration reaction. The *N*-([1,1'-biphenyl]-2-yl)benzamide derivatives, which are required as starting materials for this reaction, can easily be synthesized from 2-aminobiphenyl and a carboxylic

acid derivative, already bearing the desired precursor or placeholder in position 4 (Scheme 56).



Scheme 56 Generic synthesis of the 6-arylphenanthridine scaffold.

Methyl ester-, nitrile- and bromo-intermediates **18**, **44**, and **45** were synthesized in variable scale and with good yields following this procedure. Benzyl thioether **107**, with an iodine at position 8 of the phenanthridine ring, was successfully synthesized by this generic method as well. The envisaged polar groups of nitrobenzene **29** and sulfonamide **38** were directly obtained by this reaction. Nitrobenzene **29** was additionally reduced to the corresponding aniline **30** (Scheme 57).

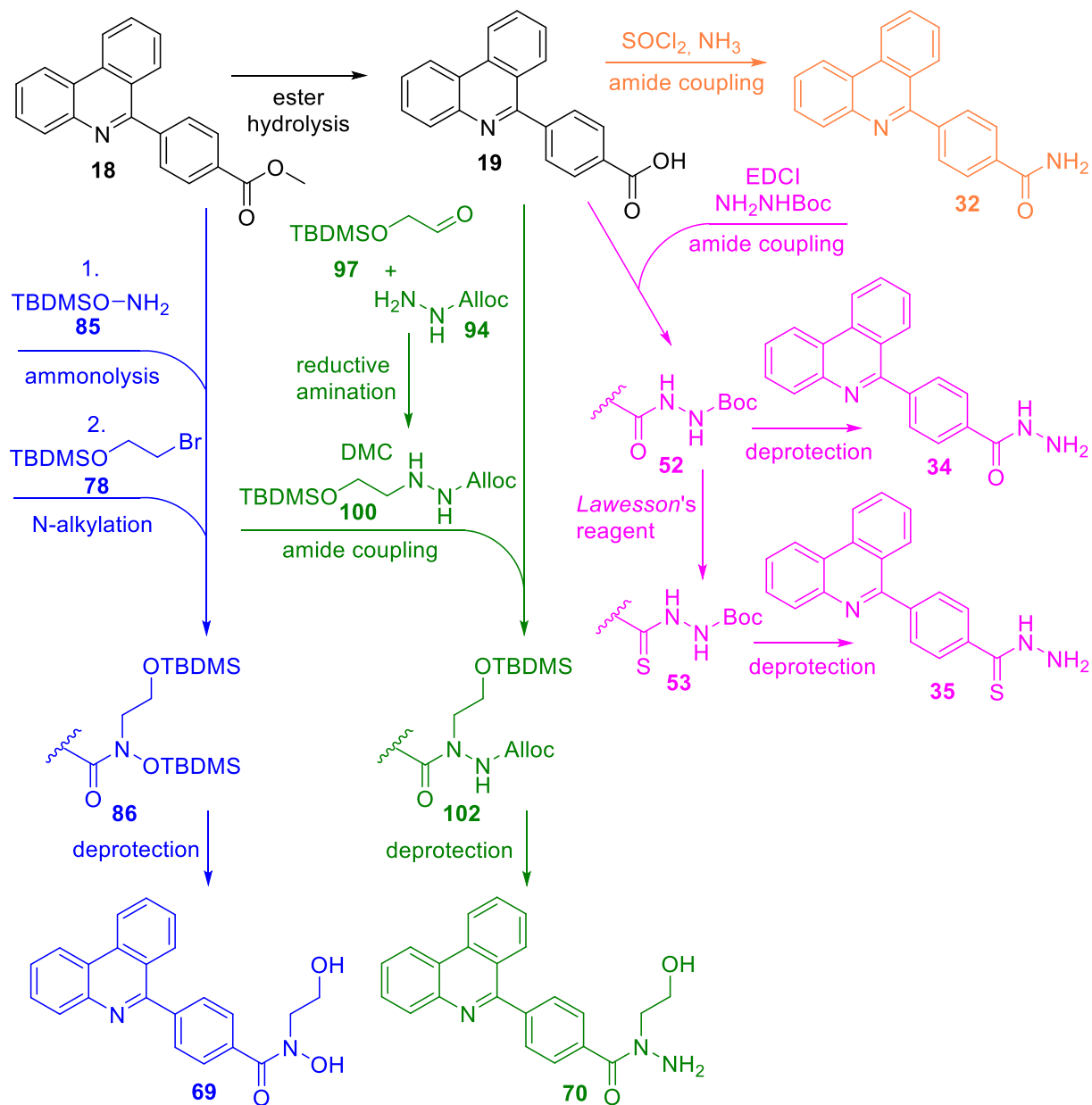


Scheme 57 Synthesis of aniline **30**.

Starting from methyl ester **18**, five target compounds were synthesized. First, carboxamide **32** by activation of carboxylic acid **19** with thionyl chloride after ester hydrolysis and subsequent addition of ammonia. Next, the two hydrazide compounds **34** and **35**, which were obtained through coupling of Boc protected hydrazine to carboxylic acid **19**. For thiohydrazide **35**, Boc-protected hydrazide **52** was thionated with LAWESSON's reagent, giving the Boc-protected thiohydrazide intermediate **53**. Boc deprotection delivered hydrazide **34** and thiohydrazide **35**. Syntheses of the more complex compounds *N*-hydroxyethylhydroxamic acid **69** and *N*¹-hydroxyethyl hydrazide **70** with hydroxyethyl residue aimed at the replacement of the water molecule, equally started from methyl ester **18**. The hydroxamic acid moiety of compound **69** was introduced *via* direct ammonolysis of methyl ester **18** with *O*-TBDMS protected hydroxylamine (**85**). The resulting *O*-TBDMS protected hydroxamic acid was *N*-alkylated with TBDMS protected 2-bromoethanol (**78**). Removal of the TBDMS protecting groups released the target compound *N*-hydroxyethyl-hydroxamic acid **69**. For *N*¹-hydroxyethyl hydrazide **70**, the required hydroxyethyl hydrazine **100** derivative was built up by reductive amination of TBDMS protected 2-hydroxyacetaldehyde (**97**) with Alloc protected hydrazine (**94**). The

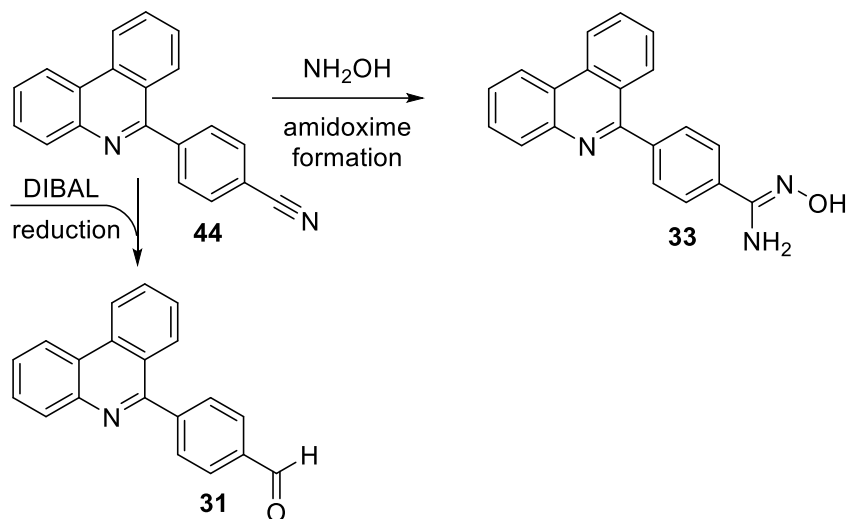
Summary

resulting alkylated hydrazine intermediate **100** was then coupled with carboxylic acid **19**, which had been activated by 2-chloro-1,3-dimethylimidazolium chloride (DMC), which gave the di-protected *N*¹-hydroxyethyl hydrazide intermediate **102**. After first Alloc, then TBDMS deprotection, the envisaged *N*¹-hydroxyethyl hydrazide **70** was obtained. Syntheses of compounds **32**, **34**, **35**, **69**, and **70** with methyl ester **18** as starting material are shown in Scheme 58.



Scheme 58 Syntheses starting from methyl ester intermediate **18**. Orange: amide **32**, Pink: hydrazide **34** and thiohydrazide **35**, Blue: *N*-hydroxyethyl hydroxamic acid **69**, Green: *N*¹-hydroxyethyl hydrazide **70**.

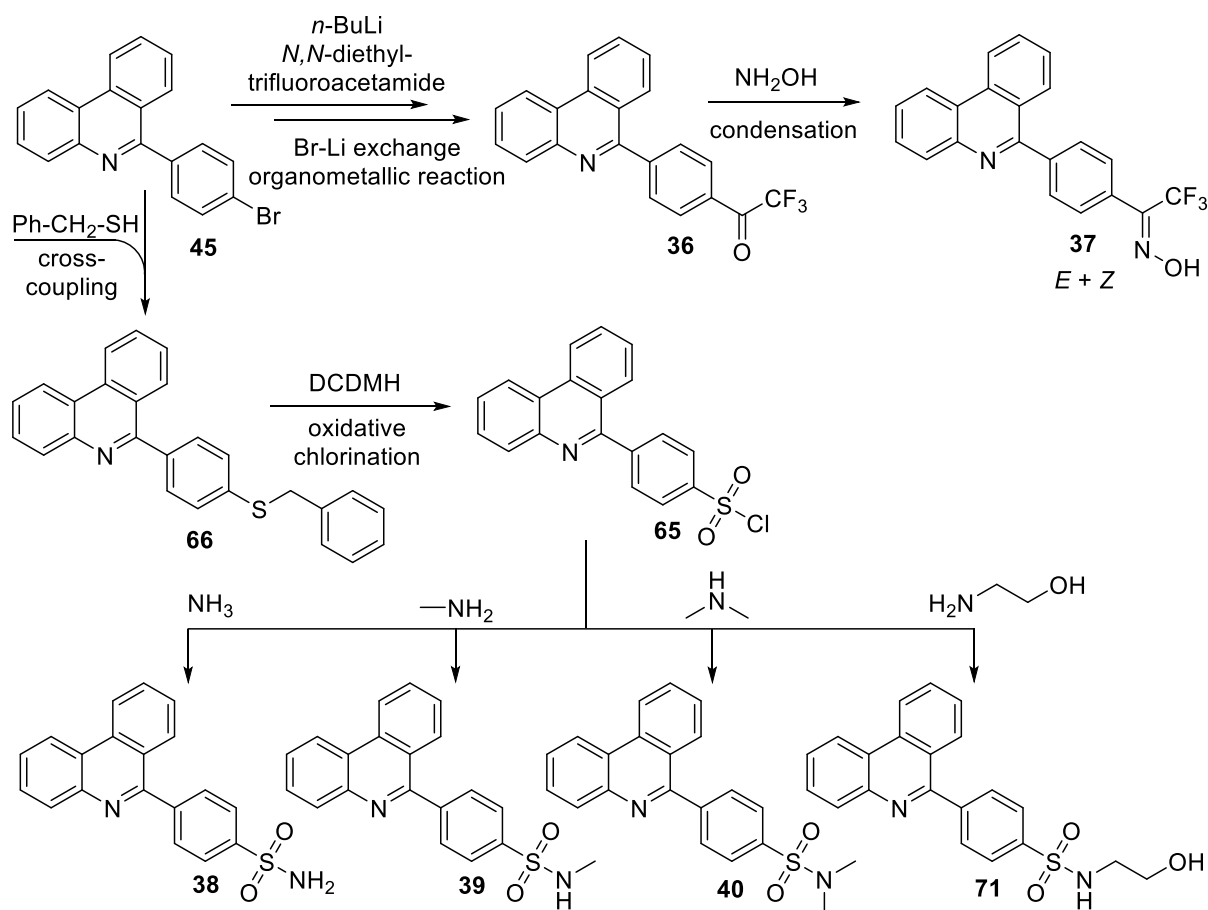
Nitrile intermediate **44** afforded amidoxime **33** upon reaction with hydroxylamine, and aldehyde **31** upon reduction with the complex hydride DIBAL (Scheme 59).



Scheme 59 Aldehyde **31** and amidoxime **33** synthesized from nitrile intermediate **44**.

Bromo-intermediate **45** served as starting material for the synthesis of trifluoromethyl ketone **36** and the corresponding trifluoromethyl oxime **37**. A bromo-lithium exchange allowed the organometallic reaction of the lithiated species with *N,N*-diethyl trifluoroacetamide. After aqueous work-up trifluoromethyl ketone **36** was obtained. This compound was subsequently additionally reacted with hydroxylamine to give trifluoromethyl oxime **37**. The bromo intermediate further served as starting material for an alternative synthesis of sulfonamide **38**. Here, the sulfur was introduced *via* a palladium catalyzed cross-coupling reaction of bromo-intermediate **45** with benzyl mercaptan (**67**). The resulting benzyl thioether **66** was subjected to oxidative chlorination with 1,3-dichloro-5,5-dimethylhydantoin (DCDMH), which gave sulfonyl chloride **65**. Reaction with different amines (ammonia, methylamine, dimethylamine and 2-aminoethanol) allowed the synthesis of primary sulfonamide **38**, mono-methyl sulfonamide **39**, dimethyl sulfonamide **40** and *N*-hydroxyethyl sulfonamide **71**. Syntheses of compounds **36**, **37**, **38**, **39**, **40**, and **71**, synthesized from bromo-intermediate **45**, are shown in Scheme 60.

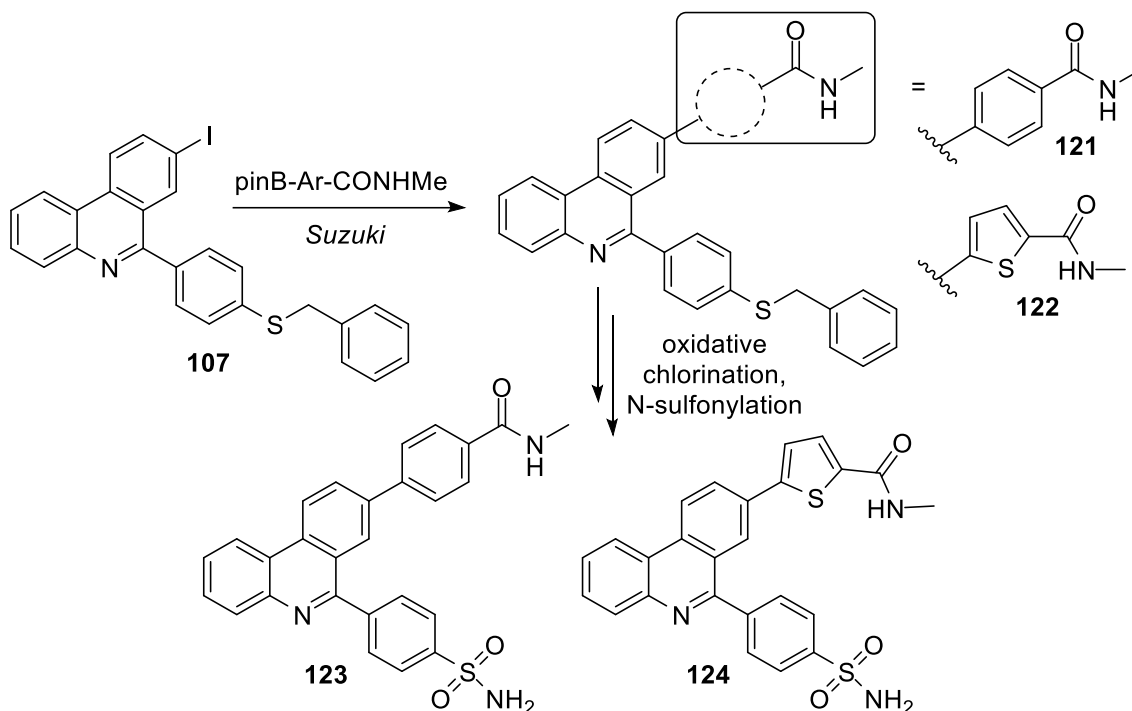
Summary



Scheme 60 Syntheses starting from bromo intermediate 45. Trifluoromethyl ketone **36** and oxime **37**. Sulfonamides **38**, **39**, **40**, and **71**.

Since the endogenous substrates of Sirtuin 6 are proteins with *N*-acylated lysine residues (e.g myristoylated TNF α), compounds bearing a potential substrate mimetic *N*-methyl amide residue were synthesized. Docking studies performed by DR. WEIJE YOU indicated that the position 8 of the phenanthridine ring would place the residue most beneficially towards the substrate binding site of Sirtuin 6. As linker unit to bring the *N*-methyl amide in the correct position, phenyl and thiophene were chosen. For this type of compounds, the primary sulfonamide was selected as polar head group. Since the envisaged compounds are biaryls, the substrate mimetic residue was introduced *via* SUZUKI cross-coupling reactions. The required halogenated phenanthridine was successfully obtained by the generic cyclodehydration protocol (Scheme 46). The iodine residue was introduced by using 4'-iodo-[1,1'-biphenyl]-2-amine as starting material. Because of the poor solubility of the sulfonamides and potential negative influence on coupling efficiency, the benzyl thioether moiety was used as placeholder for the final sulfonamide. The SUZUKI cross-coupling of intermediate **107** with the respective boronic acid pinacol esters of *N*-methyl benzamide and *N*-methyl-2-thiophene carboxamide gave the benzyl thioether intermediates **121** and **122**. These were subjected to the same oxidative chlorination and subsequent *N*-sulfonylation as the "naked"

phenanthridinebenzyl thioether **66**, which afforded the potential substrate mimetic target compounds **123** and **124**. (Scheme 61).



Scheme 61 Synthesis of potential substrate mimetic compounds **123** and **124**.

The synthesized compounds were tested in the group of PROF. DR. CLEMENS STEEGBORN at the University of Bayreuth by DR. WEIJE YOU, using a Fluor de Lys (FdL) assay. The screening at 5 μM and 25 μM showed that carboxamide **32** (CLE-115) and primary sulfonamide **38** (CLE-121) are Sirtuin 6 inhibitors. All other compounds were inactive towards Sirtuin 6, or in the case of the substrate mimetic compounds **123** and **124**, gave ambiguous screening results, probably due to poor solubility. Since CLE-121 showed very promising results with an approximate 50% inhibition of Sirtuin 6 at 5 μM , the concentration-effect relationship for this compound was determined. CLE-121 has an IC_{50} towards Sirtuin 6 of 2.2 μM . Therefore, CLE-121 is equipotent as the thus far most potent published allosteric noncompetitive Sirtuin 6 inhibitor **JYQ-42** with an IC_{50} of 2.33 μM ^[64] and more potent than the competitive salicylate (DAMONTE *et al.* compound 11: IC_{50} = 22 μM ^[57]) and quinazolidinedione (SOCIALI *et al.* compound 3: IC_{50} = 37 μM ^[58]) inhibitors. Additionally, **KV-30** and CLE-121 were tested on Sirtuins 1-3 and 5. At 3.125 μM and 12.5 μM . At these concentrations CLE-121 had no effect on the other sirtuins. **KV-30** is inhibiting Sirtuin 3 at higher concentrations (approx. 50% inhibition at 50 μM). CLE-121 showed no cytotoxicity in the MTT assay (IC_{50} >50 μM) in contrast to KV-30 with an IC_{50} of 8.6 μM . With CLE-121 a new, non-toxic, potent and selective Sirtuin 6 inhibitor has been identified. This compound serves as lead structure for further development of this new chemotype of Sirtuin 6 inhibitors, with a focus to improve potency towards the target and physicochemical properties.

5 Appendix

5.1 Abbreviations

(TF)EB	transcription factor EB
Å	Angström
ADP	adenosine diphosphate
Alloc	allyloxy carbonyl
AMPK	5' AMP-activated protein kinase
approx.	approximately
aq	aqueous
Ar	aryl
ATR	attenuated total reflexion
Boc	<i>tert</i> -butyloxy carbonyl
BSA	bovine serum albumine
c	concentration
calcd.	calculated
CAN	cer ammonium nitrate
CCDC	Cambridge crystallographic data centre
CMA	chaperone mediated autophagy
d (NMR)	duplett
DAD	diode array detector
DCDMH	1,3-dichloro-5,5-dimethylhydantoin
DDQ	2,3,-Dichloro-5,6-dicynao-1,4-benzochinon
DEPT	distortionless enhancement by polarization transfer
DIBAL	diisobutylaluminium hydride
DIC	<i>N,N'</i> -diisopropylcarbodiimide
DIPEA	diisopropylethylamine
DMAP	4-(dimethylamino)pyridine
DMC	coupling hydroxyethylhydrazide
DMF	dimethylformamide
DMSO	dimethylsulfoxide
DNA	desoxyribonucleic acid
dppf	1-1'-bis(diphenylphosphino)ferrocene
DTT	dithiothreitol
e.g.	exempli gratia, for example
EC ₅₀	half maximal effective concentration
EDCI	1-ethyl-3-(3-dimethylaminopropyl)carbodiimide
EDME	estradiolmethylether
ee	enantiomeric excess
eq	equivalent
ER	endoplasmic reticulum
ESI	electrospray ionization
<i>et al.</i>	et alii
Et ₃ N	triethylamine

Abbreviations

EtOAc	ethyl acetate
eV	electron volt
FBS	fetal bovine serum
FCC	flash column chromatography
FdL	Fluor de Lys
FFA	free fatty acids
FLIPR	fluorescence imaging plate reader
Fluo-4/AM	fluo-4 acetoxymethylester
FT-IR	fourrier transformation infrared
Fura-2/AM	fura-2 acetoxymethylester
H2A	histone 2 A
H2B	histone 2 B
H3	histone 3
H3K56	histone 3 lysine 56
H3K9	histone 3 lysine 9
H4	histone 4
HAT	histone acetyl transferase
HATU	1-[bis(dimethylamino)methylene]-1H-1,2,3-triazolo[4,5-b]pyridinium 3-oxide hexafluorophosphate
HBS	HEPES buffered saline
HDAC	histone deacetylase
HEK293 cells	human embryonic kidney 293 cells
HEPES	2-[4-(2-hydroxyethyl)piperazin-1-yl]ethane-1-sulfonic acid
H-H-COSY	H-H-correlation spectroscopy
HL-60 cell line	human leukemia 60 cell line
HMBC	heteronuclear multiple bond correlation
HMG-CoA	3-hydroxy-3-methylglutaryl coenzyme A
HOAc	acetic acid
HOBt	hydroxybenzothiazole
HPLC	high pressure liquid chromatography
HRMS	high resolution mass spectrometry
HSQC	heteronuclear single quantum correlation
HTS	High throughput screening
IC ₅₀	half maximal inhibitory concentration
<i>i</i> PrOH	2-propylalcohol
IR	infrared spectroscopy
<i>J</i>	coupling constant NMR
KDAC	lysine deacteylase
LHMDS	lithium hexamethyldisilazide
lit.	literature
LR	Lawesson's reagent
m (IR)	medium
M (molar)	mole per liter
m (NMR)	multiplett
<i>m/z</i>	mass per charge
MeOH	methanol
MHz	mega hertz

Abbreviations

min	minutes
mp	melting point
Mr	relative molecular mass
MsCl	mesyl chloride
mTOR	mammalian target of rapamycin
MTT	(4,5-dimethylthiazol-2-yl)-2,5-diphenyltetrazolium bromide
MW	microwave
Na-D	sodium-D-spectral line
NAD ⁺	nicotinamide adenine dinucleotide
NAM	nicotine amide
<i>n</i> -BuLi	<i>n</i> -butyllithium
NMR	nuclear magnetic resonance spectroscopy
No.	number
NOE NMR	nuclear overhauser effect nuclear magnetic resonance
p.	page
PARP1	poly [ADP-ribose] polymerase 1
Pd(dppf)Cl ₂	[1,1'-bis(diphenylphosphino)ferrocene]palladium(II) dichloride
Pd(OAc) ₂	palladium acetate
Pd(PPh ₃) ₄	tetrakis(triphenylphosphine)palladium(0)
Pd ₂ (dba) ₃	tris(dibenzylideneacetone)dipalladium(0)
PE	petrol ether
PG	protecting group
PI(3,5)P ₂	phosphatidylinositol 3,5-bisphosphate
PI(4,5)P ₂	phosphatidylinositol 4,5-bisphosphate
pinB	boronic acid pinacol ester
PMB	<i>p</i> -methoxybenzyl
ppm	parts per million
prop.	proportionally
quant.	quantitative
RetTime	retention time
ROS	reactive oxygen species
rot.	rotamer
rt	room temperature
s (IR)	strong
s (NMR)	singulett
SAR	structure activity relationship
S _E Ar	electrophilic aromatic substitution
Sir2	silent regulator 2
S _N 2	bimolecular nucleophilic substitution
<i>t</i>	tert
t (NMR)	triplett
TBAF	<i>tert</i> -butylammonium fluoride
TBDMS	<i>tert</i> -butyldimethylsilyl
TBME	tert-Butylmethyl ether
<i>t</i> Bu	tert-Butyl

Abbreviations

TC ₅₀	median toxic dose
Tf ₂ O	trifluoromethanesulfonic anhydride
TFA	trifluoroacetic acid
THF	tetrahydrofuran
THIQ	tetrahydroisoquinoline
THP	tetrahydropyrane
TLC	thin layer chromatography
TNF α	tumor necrosis factor alpha
TPC	two pore channel
TRP	transient receptor potential
TRPA	transient receptor potential ankyrin
TRPC	transient receptor potential canonical
TRPM	transient receptor potential melastatin
TRPML	transient receptor potential mucolipin
TRPP	transient receptor potential polycystic
TRPV	transient receptor potential vanilloid
TSA	trichostatin A
TsCl	tosyl chloride
$\tilde{\nu}$	wavenumber
V-ATPase	vacuolar type ATPase
vs (IR)	very strong
w (IR)	weak

5.2 References

- [1] D. J. Klionsky, *Autophagy* **2008**, *4*, 740-743.
- [2] M. L. Schultz, L. Tecedor, M. Chang, B. L. Davidson, *Trends Neurosci* **2011**, *34*, 401-410.
- [3] Y. Feng, D. He, Z. Yao, D. J. Klionsky, *Cell Res* **2014**, *24*, 24-41.
- [4] W. W. Yim, N. Mizushima, *Cell Discov* **2020**, *6*, 6.
- [5] R. A. Saxton, D. M. Sabatini, *Cell* **2017**, *168*, 960-976.
- [6] R. Scherz-Shouval, Z. Elazar, *Trends Biochem Sci* **2011**, *36*, 30-38.
- [7] D. J. Puleston, A. K. Simon, *Immunology* **2014**, *141*, 1-8.
- [8] C. He, D. J. Klionsky, *Annu Rev Genet* **2009**, *43*, 67-93.
- [9] L. R. Lapierre, C. Kumsta, M. Sandri, A. Ballabio, M. Hansen, *Autophagy* **2015**, *11*, 867-880.
- [10] X. Zhang, X. Cheng, L. Yu, J. Yang, R. Calvo, S. Patnaik, X. Hu, Q. Gao, M. Yang, M. Lawas, M. Dellling, J. Marugan, M. Ferrer, H. Xu, *Nat Commun* **2016**, *7*, 12109.
- [11] A. Scotto Rosato, S. Montefusco, C. Soldati, S. Di Paola, A. Capuozzo, J. Monfregola, E. Polishchuk, A. Amabile, C. Grimm, A. Lombardo, M. A. De Matteis, A. Ballabio, D. L. Medina, *Nat Commun* **2019**, *10*, 5630.
- [12] N. Takasaka, J. Araya, H. Hara, S. Ito, K. Kobayashi, Y. Kurita, H. Wakui, Y. Yoshii, Y. Yumino, S. Fujii, S. Minagawa, C. Tsurushige, J. Kojima, T. Numata, K. Shimizu, M. Kawaishi, Y. Kaneko, N. Kamiya, J. Hirano, M. Odaka, T. Morikawa, S. L. Nishimura, K. Nakayama, K. Kuwano, *J Immunol* **2014**, *192*, 958-968.
- [13] J. Shao, X. Yang, T. Liu, T. Zhang, Q. R. Xie, W. Xia, *Protein Cell* **2016**, *7*, 281-290.
- [14] N. Huang, Z. Liu, J. Zhu, Z. Cui, Y. Li, Y. Yu, F. Sun, Q. Pan, Q. Yang, *Tumour Biol* **2017**, *39*, 1010428317708532.
- [15] L. Wang, W. Guo, J. Ma, W. Dai, L. Liu, S. Guo, J. Chen, H. Wang, Y. Yang, X. Yi, G. Wang, T. Gao, G. Zhu, C. Li, *Autophagy* **2018**, *14*, 518-533.
- [16] S. Iachettini, D. Trisciuglio, D. Rotili, A. Lucidi, E. Salvati, P. Zizza, L. Di Leo, D. Del Bufalo, M. R. Ciriolo, C. Leonetti, C. Steegborn, A. Mai, A. Rizzo, A. Biroccio, *Cell Death Dis* **2018**, *9*, 996.
- [17] P. Li, M. Gu, H. Xu, *Trends Biochem Sci* **2019**, *44*, 110-124.
- [18] R. Bargal, N. Avidan, E. Ben-Asher, Z. Olender, M. Zeigler, A. Frumkin, A. Raas-Rothschild, G. Glusman, D. Lancet, G. Bach, *Nat Genet* **2000**, *26*, 118-123.
- [19] N. Rinkenberger, J. W. Schoggins, *mBio* **2018**, *9*.
- [20] M. P. Cuajungco, M. A. Samie, *Pflugers Arch* **2008**, *457*, 463-473.
- [21] X. Li, X. Wang, X. Zhang, M. Zhao, W. L. Tsang, Y. Zhang, R. G. Yau, L. S. Weisman, H. Xu, *Proc Natl Acad Sci U S A* **2013**, *110*, 21165-21170.
- [22] C. C. Chen, M. Keller, M. Hess, R. Schiffmann, N. Urban, A. Wolfgardt, M. Schaefer, F. Bracher, M. Biel, C. Wahl-Schott, C. Grimm, *Nat Commun* **2014**, *5*, 4681.
- [23] D. Shen, X. Wang, X. Li, X. Zhang, Z. Yao, S. Dibble, X. P. Dong, T. Yu, A. P. Lieberman, H. D. Showalter, H. Xu, *Nat Commun* **2012**, *3*, 731.
- [24] E. Plesch, C. C. Chen, E. Butz, A. Scotto Rosato, E. K. Krogsaeter, H. Yinan, K. Bartel, M. Keller, D. Robaa, D. Teupser, L. M. Holdt, A. M. Vollmar, W. Sippl, R. Puertollano, D. Medina, M. Biel, C. Wahl-Schott, F. Bracher, C. Grimm, *Elife* **2018**, *7*.

References

- [25] M. Samie, X. Wang, X. Zhang, A. Goschka, X. Li, X. Cheng, E. Gregg, M. Azar, Y. Zhuo, A. G. Garrity, Q. Gao, S. Slaugenhaupt, J. Pickel, S. N. Zolov, L. S. Weisman, G. M. Lenk, S. Titus, M. Bryant-Geneviev, N. Southall, M. Juan, M. Ferrer, H. Xu, *Dev Cell* **2013**, *26*, 511-524.
- [26] W. Wang, Q. Gao, M. Yang, X. Zhang, L. Yu, M. Lawas, X. Li, M. Bryant-Geneviev, N. T. Southall, J. Marugan, M. Ferrer, H. Xu, *Proc Natl Acad Sci U S A* **2015**, *112*, E1373-1381.
- [27] P. Ruhl, A. S. Rosato, N. Urban, S. Gerndt, R. Tang, C. Abrahamian, C. Leser, J. Sheng, A. Jha, G. Vollmer, M. Schaefer, F. Bracher, C. Grimm, *Sci Rep* **2021**, *11*, 8313.
- [28] D. Noble, *J Exp Biol* **2015**, *218*, 816-818.
- [29] C. D. Allis, T. Jenuwein, *Nat Rev Genet* **2016**, *17*, 487-500.
- [30] C. H. Arrowsmith, C. Bountra, P. V. Fish, K. Lee, M. Schapira, *Nat Rev Drug Discov* **2012**, *11*, 384-400.
- [31] Y. Wang, J. He, M. Liao, M. Hu, W. Li, H. Ouyang, X. Wang, T. Ye, Y. Zhang, L. Ouyang, *Eur J Med Chem* **2019**, *161*, 48-77.
- [32] A. R. Chang, C. M. Ferrer, R. Mostoslavsky, *Physiol Rev* **2020**, *100*, 145-169.
- [33] L. Tasselli, W. Zheng, K. F. Chua, *Trends Endocrinol Metab* **2017**, *28*, 168-185.
- [34] F. Fiorentino, A. Mai, D. Rotili, *J Med Chem* **2021**, *64*, 9732-9758.
- [35] M. A. Klein, J. M. Denu, *J Biol Chem* **2020**, *295*, 11021-11041.
- [36] P. W. Pan, J. L. Feldman, M. K. Devries, A. Dong, A. M. Edwards, J. M. Denu, *J Biol Chem* **2011**, *286*, 14575-14587.
- [37] S. Masri, P. Rigor, M. Cervantes, N. Ceglia, C. Sebastian, C. Xiao, M. Roqueta-Rivera, C. Deng, T. F. Osborne, R. Mostoslavsky, P. Baldi, P. Sassone-Corsi, *Cell* **2014**, *158*, 659-672.
- [38] J. L. Feldman, J. Baeza, J. M. Denu, *J Biol Chem* **2013**, *288*, 31350-31356.
- [39] M. Rahnasto-Rilla, T. Kokkola, E. Jarho, M. Lahtela-Kakkonen, R. Moaddel, *Chembiochem* **2016**, *17*, 77-81.
- [40] M. Yasuda, D. R. Wilson, S. D. Fugmann, R. Moaddel, *Anal Chem* **2011**, *83*, 7400-7407.
- [41] M. Rahnasto-Rilla, J. Tyni, M. Huovinen, E. Jarho, T. Kulikowicz, S. Ravichandran, A. B. V. L. Ferrucci, M. Lahtela-Kakkonen, R. Moaddel, *Sci Rep* **2018**, *8*, 4163.
- [42] W. You, W. Zheng, S. Weiss, K. F. Chua, C. Steegborn, *Sci Rep* **2019**, *9*, 19176.
- [43] W. You, D. Rotili, T. M. Li, C. Kambach, M. Meleshin, M. Schutkowski, K. F. Chua, A. Mai, C. Steegborn, *Angew Chem Int Ed Engl* **2017**, *56*, 1007-1011.
- [44] J. Xu, S. Shi, G. Liu, X. Xie, J. Li, A. A. Bolinger, H. Chen, W. Zhang, P. Y. Shi, H. Liu, J. Zhou, *Eur J Med Chem* **2023**, *246*, 114998.
- [45] Z. Zhang, W. Sun, G. Zhang, Z. Fang, X. Chen, L. Li, *Eur J Pharm Sci* **2023**, *185*, 106424.
- [46] Z. Huang, J. Zhao, W. Deng, Y. Chen, J. Shang, K. Song, L. Zhang, C. Wang, S. Lu, X. Yang, B. He, J. Min, H. Hu, M. Tan, J. Xu, Q. Zhang, J. Zhong, X. Sun, Z. Mao, H. Lin, M. Xiao, Y. E. Chin, H. Jiang, Y. Xu, G. Chen, J. Zhang, *Nat Chem Biol* **2018**, *14*, 1118-1126.
- [47] J. H. Kim, J. M. Lee, J. H. Kim, K. R. Kim, *Biochem Biophys Res Commun* **2018**, *503*, 1415-1421.
- [48] W. You, C. Steegborn, *ACS Med Chem Lett* **2020**, *11*, 2285-2289.
- [49] M. A. Klein, C. Liu, V. I. Kuznetsov, J. B. Feltenberger, W. Tang, J. M. Denu, *J Biol Chem* **2020**, *295*, 1385-1399.

References

- [50] X. Chen, W. Sun, S. Huang, H. Zhang, G. Lin, H. Li, J. Qiao, L. Li, S. Yang, *J Med Chem* **2020**, *63*, 10474-10495.
- [51] J. Tenhunen, T. Kucera, M. Huovinen, J. Kublbeck, E. Bisenieks, B. Vigante, Z. Ogle, G. Duburs, M. Dolezal, R. Moaddel, M. Lahtela-Kakkonen, M. Rahnasto-Rilla, *Biomed Pharmacother* **2021**, *138*, 111452.
- [52] B. He, J. Hu, X. Zhang, H. Lin, *Org Biomol Chem* **2014**, *12*, 7498-7502.
- [53] J. Liu, W. Zheng, *Org Biomol Chem* **2016**, *14*, 5928-5935.
- [54] Y. Huang, J. Zhang, D. Xu, Y. Peng, Y. Jin, L. Zhang, *Mol Med Rep* **2021**, *23*.
- [55] M. D. Parenti, A. Grozio, I. Bauer, L. Galeno, P. Damonte, E. Millo, G. Sociali, C. Franceschi, A. Ballestrero, S. Bruzzone, A. Del Rio, A. Nencioni, *J Med Chem* **2014**, *57*, 4796-4804.
- [56] G. Sociali, L. Galeno, M. D. Parenti, A. Grozio, I. Bauer, M. Passalacqua, S. Boero, A. Donadini, E. Millo, M. Bellotti, L. Sturla, P. Damonte, A. Puddu, C. Ferroni, G. Varchi, C. Franceschi, A. Ballestrero, A. Poggi, S. Bruzzone, A. Nencioni, A. Del Rio, *Eur J Med Chem* **2015**, *102*, 530-539.
- [57] P. Damonte, G. Sociali, M. D. Parenti, D. Soncini, I. Bauer, S. Boero, A. Grozio, M. V. Holtey, F. Piacente, P. Becherini, R. Sanguineti, A. Salis, G. Damonte, M. Cea, M. Murone, A. Poggi, A. Nencioni, A. Del Rio, S. Bruzzone, *Bioorg Med Chem* **2017**, *25*, 5849-5858.
- [58] G. Sociali, M. Magnone, S. Ravera, P. Damonte, T. Vigliarolo, M. Von Holtey, V. G. Vellone, E. Millo, I. Caffa, M. Cea, M. D. Parenti, A. Del Rio, M. Murone, R. Mostoslavsky, A. Grozio, A. Nencioni, S. Bruzzone, *FASEB J* **2017**, *31*, 3138-3149.
- [59] B. E. Bolivar, J. T. Welch, *Chembiochem* **2017**, *18*, 931-940.
- [60] L. H. Yuen, S. Dana, Y. Liu, S. I. Bloom, A. G. Thorsell, D. Neri, A. J. Donato, D. Kireev, H. Schuler, R. M. Franzini, *J Am Chem Soc* **2019**, *141*, 5169-5181.
- [61] W. Sun, X. Chen, S. Huang, W. Li, C. Tian, S. Yang, L. Li, *Bioorg Med Chem Lett* **2020**, *30*, 127215.
- [62] M. Wood, S. Rymarchyk, S. Zheng, Y. Cen, *Arch Biochem Biophys* **2018**, *638*, 8-17.
- [63] W. You, C. Steegborn, *J Med Chem* **2018**, *61*, 10922-10928.
- [64] Q. Zhang, Y. Chen, D. Ni, Z. Huang, J. Wei, L. Feng, J. C. Su, Y. Wei, S. Ning, X. Yang, M. Zhao, Y. Qiu, K. Song, Z. Yu, J. Xu, X. Li, H. Lin, S. Lu, J. Zhang, *Acta Pharm Sin B* **2022**, *12*, 876-889.
- [65] C. C. Chen, E. Krogsaeter, C. Y. Kuo, M. C. Huang, S. Y. Chang, M. Biel, *Biomed Pharmacother* **2022**, *148*, 112751.
- [66] A. D. Bondarev, M. M. Attwood, J. Jonsson, V. N. Chubarev, V. V. Tarasov, H. B. Schioth, *Br J Clin Pharmacol* **2021**, *87*, 4577-4597.
- [67] K. Vogerl, N. Ong, J. Senger, D. Herp, K. Schmidtkunz, M. Marek, M. Muller, K. Bartel, T. B. Shaik, N. J. Porter, D. Robaa, D. W. Christianson, C. Romier, W. Sippl, M. Jung, F. Bracher, *J Med Chem* **2019**, *62*, 1138-1166.
- [68] L. J. Farrugia, *Journal of Applied Crystallography* **2012**, *45*, 849-854.
- [69] C. Leser, M. Keller, S. Gerndt, N. Urban, C. C. Chen, M. Schaefer, C. Grimm, F. Bracher, *Eur J Med Chem* **2021**, *210*, 112966.
- [70] K. Kriegler, C. Leser, P. Mayer, F. Bracher, *Arch Pharm (Weinheim)* **2021**, e2100362.

References

- [71] G. F. Smith, *Prog Med Chem* **2011**, *50*, 1-47.
- [72] Bundesinstitut für Arzneimittel und Medizinprodukte, Bufexamac-haltige Arzneimittel zur topischen Anwendung: Widerruf der Zulassungen in der EU wegen ungünstigen Nutzen-Risiko-Verhältnisses
(<https://www.bfarm.de/SharedDocs/Risikoinformationen/Pharmakovigilanz/DE/RI/2010/RI-bufexamac.html>; accessed 19.07.2024).
- [73] S. Andreev, T. Pantsar, R. Tesch, N. Kahlke, A. El-Gokha, F. Ansideri, L. Gratz, J. Romasco, G. Sita, C. Geibel, M. Lammerhofer, A. Tarozzi, S. Knapp, S. A. Laufer, P. Koch, *J Med Chem* **2022**, *65*, 1283-1301.
- [74] K. Vögerl, dissertation, Ludwig-Maximilians-Universität (München), **2018**.
- [75] M. Movassaghi, M. D. Hill, *Org Lett* **2008**, *10*, 3485-3488.
- [76] A. Bischler, B. Napieralski, *Berichte der deutschen chemischen Gesellschaft* **1893**, *26*, 1903-1908.
- [77] M. M. Heravi, S. Khaghaninejad, N. Nazari, in *Advances in Heterocyclic Chemistry, Vol. 112* (Ed.: A. R. Katritzky), Academic Press, **2014**, pp. 183-234.
- [78] A. Pictet, A. Hubert, *Berichte der deutschen chemischen Gesellschaft* **2006**, *29*, 1182-1189.
- [79] G. T. Morgan, L. P. Walls, *J. Chem. Soc.* **1931**, *0*, 2447-2456.
- [80] L. Wen, M. Li, J. B. Schlenoff, *Journal of the American Chemical Society* **1997**, *119*, 7726-7733.
- [81] S. Hazeldine, B. Pachaiyappan, N. Steinbergs, S. Nowotarski, A. S. Hanson, R. A. Casero, Jr., P. M. Woster, *J Med Chem* **2012**, *55*, 7378-7391.
- [82] R. Braslau, M. O. Anderson, F. Rivera, A. Jimenez, T. Haddad, J. R. Axon, *Tetrahedron* **2002**, *58*, 5513-5523.
- [83] V. Molteni, X. Li, J. Nabakka, F. Liang, J. Wityak, A. Koder, L. Vargas, R. Romeo, N. Mitro, P. A. Mak, H. M. Seidel, J. A. Haslam, D. Chow, T. Tuntland, T. A. Spalding, A. Brock, M. Bradley, A. Castrillo, P. Tontonoz, E. Saez, *J Med Chem* **2007**, *50*, 4255-4259.
- [84] T. Ozturk, E. Ertas, O. Mert, *Chem Rev* **2007**, *107*, 5210-5278.
- [85] C. W. G. Fishwick, J. M. Sanderson, J. B. C. Findlay, *Tetrahedron Letters* **1994**, *35*, 4611-4614.
- [86] C. Yang, J. Wang, Y. Cheng, X. Yang, Y. Feng, X. Zhuang, Z. Li, W. Zhao, J. Zhang, X. Sun, X. He, *Bioorg Chem* **2020**, *100*, 103931.
- [87] P. Göbel, F. Ritterbusch, M. Helms, M. Bischof, K. Harms, M. Jung, E. Meggers, *European Journal of Inorganic Chemistry* **2015**, *2015*, 1654-1659.
- [88] J. Lee, S. U. Kang, S. Y. Kim, S. E. Kim, Y. J. Jo, S. Kim, *Bioorganic & Medicinal Chemistry Letters* **2001**, *11*, 965-968.
- [89] L. Bosch, J.-F. Mouscadet, X.-J. Ni, J. Vilarrasa, *Tetrahedron Letters* **2011**, *52*, 753-756.
- [90] D. Lu, A. Shen, Y. Liu, X. Peng, W. Xing, J. Ai, M. Geng, Y. Hu, *Eur J Med Chem* **2016**, *115*, 191-200.
- [91] N. Kawanishi, T. Sugimoto, J. Shibata, K. Nakamura, K. Masutani, M. Ikuta, H. Hirai, *Bioorg Med Chem Lett* **2006**, *16*, 5122-5126.
- [92] H. Hirai, N. Kawanishi, M. Hirose, T. Sugimoto, K. Kamijyo, J. Shibata, K. Masutani, *US 2009/0137597 A1*, **2009**.

References

- [93] G. M. Sammis, E. M. Flamme, H. Xie, D. M. Ho, E. J. Sorensen, *J Am Chem Soc* **2005**, *127*, 8612-8613.
- [94] J. Cornil, P. G. Echeverria, S. Reymond, P. Phansavath, V. Ratovelomanana-Vidal, A. Guerinot, J. Cossy, *Org Lett* **2016**, *18*, 4534-4537.
- [95] J. A. Lafontaine, D. P. Provencal, C. Gardelli, J. W. Leahy, *J Org Chem* **2003**, *68*, 4215-4234.
- [96] H. H. Kang, H. S. Rho, D. H. Kim, S.-G. Oh, *Tetrahedron Letters* **2003**, *44*, 7225-7227.
- [97] H. Hikawa, I. Azumaya, *Org Biomol Chem* **2014**, *12*, 5964-5972.
- [98] J. Ham, I. Yang, H. Kang, *J Org Chem* **2004**, *69*, 3236-3239.
- [99] A. Roglans, A. Pla-Quintana, M. Moreno-Manas, *Chem Rev* **2006**, *106*, 4622-4643.
- [100] J. T. Kuethe, K. G. Childers, *Advanced Synthesis & Catalysis* **2008**, *350*, 1577-1586.
- [101] P. Annamalai, H.-C. Hsiao, S. Raju, Y.-H. Fu, P.-L. Chen, J.-C. Horng, Y.-H. Liu, S.-C. Chuang, *Organic Letters* **2019**, *21*, 1182-1186.
- [102] C. Glas, E. Naydenova, S. Lechner, N. Wossner, L. Yang, J. C. B. Dietschreit, H. Sun, M. Jung, B. Kuster, C. Ochsenfeld, F. Bracher, *Eur J Med Chem* **2022**, *240*, 114594.
- [103] P. Brehova, E. Chaloupecka, M. Cesnek, J. Skacel, M. Dracinsky, E. Tloustova, H. Mertlikova-Kaiserova, M. P. Soto-Velasquez, V. J. Watts, Z. Janeba, *Eur J Med Chem* **2021**, *222*, 113581.
- [104] T. Mosmann, *J Immunol Methods* **1983**, *65*, 55-63.
- [105] P.-Q. Huang, X.-Y. Su, *Synthesis* **2022**, *55*, 877-891.
- [106] C. Lion, J. P. Boukou-Poba, C. Charvy, *Bulletin des Sociétés Chimiques Belges* **2010**, *98*, 557-566.
- [107] K. Yanai, H. Togo, *Tetrahedron* **2020**, *76*.
- [108] C. J. Evoniuk, G. d. P. Gomes, S. P. Hill, S. Fujita, K. Hanson, I. V. Alabugin, *Journal of the American Chemical Society* **2017**, *139*, 16210-16221.
- [109] K. H. Lee, S. Oh, S. J. Lee, Y. K. Kim, S. S. Yoon, *Molecular Crystals and Liquid Crystals* **2012**, *563*, 206-214.
- [110] D. F. Elliott, C. Harington, *Journal of the Chemical Society (Resumed)* **1949**.
- [111] C. Schlicker, G. Boanca, M. Lakshminarasimhan, C. Steegborn, *Aging (Albany NY)* **2011**, *3*, 852-872.
- [112] J. Goretzko, I. Pauels, N. Heitzig, K. Thomas, M. Kardell, J. Nass, E. K. Krogsaeter, S. Schloer, B. Spix, A. L. Linard Matos, C. Leser, T. Wegner, F. Glorius, F. Bracher, V. Gerke, J. Rossaint, C. Grimm, U. Rescher, *Cell Rep* **2023**, *42*, 113501.